DTIC
ELECTE
NOV 2 1 1995
S D
F

1994 ANNUAL TROPICAL CYCLONE REPORT

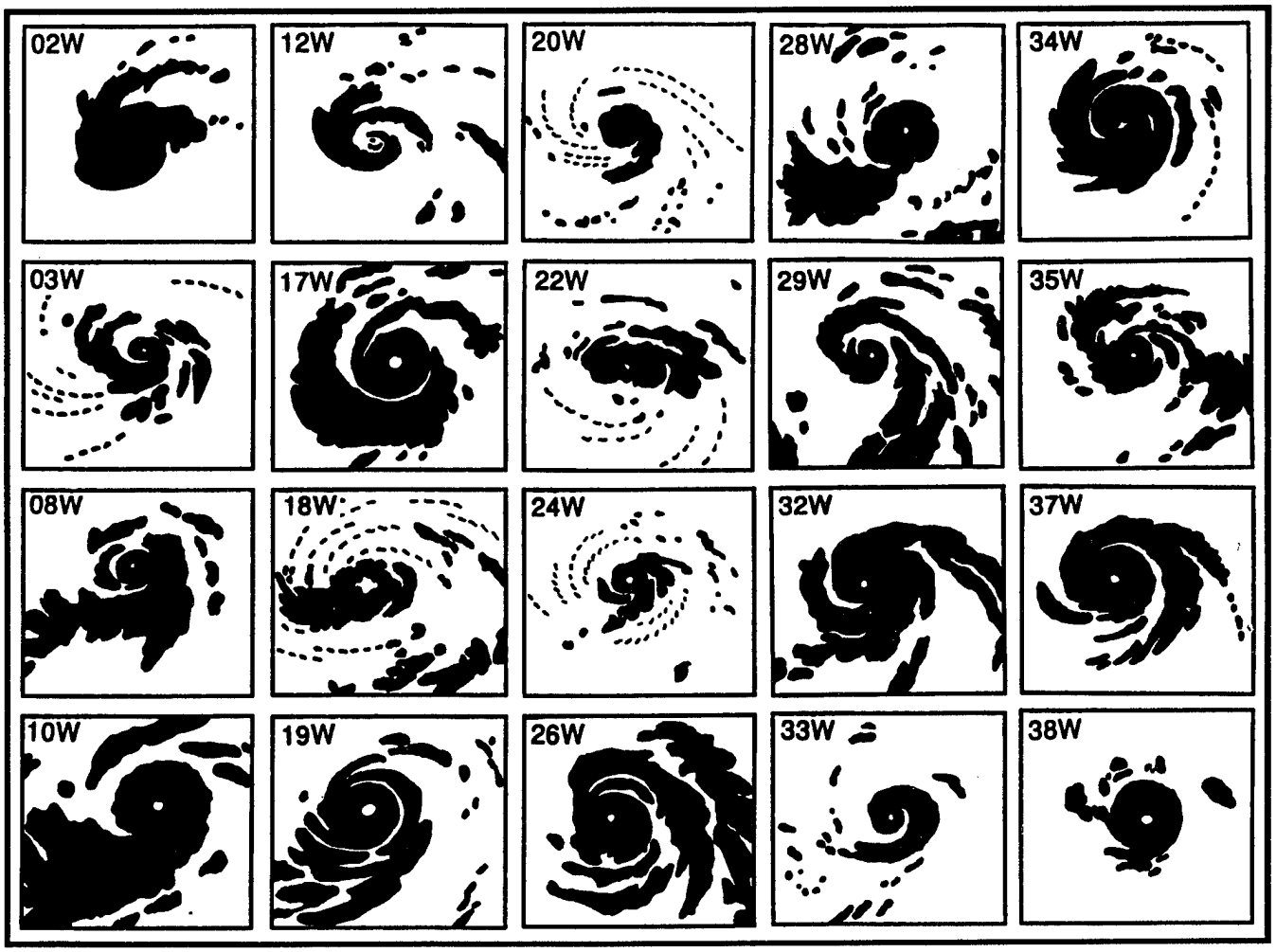

JOINT TYPHOON WARNING CENTER
GUAM, MARIANA ISLANDS

19951120 004

DTIC QUALITY INSPECTED 5

DISTRIBUTION STATEMENT A
Approved for public release
Distribution Unlimited

FRONT COVER: All twenty of the typhoons that formed in the western North Pacific Ocean in 1994 appear in this mosaic of cloud silhouettes to show the variability of cloud pattern size and shape of these typhoons at, or near, their peak intensity. All the boxes within the mosaic are of the same scale (10° of latitude by 10° of longitude) and, for reference, each typhoon's alphanumeric designator appears in the upper left corner of its respective box. (Cloud silhouettes courtesy of Dr. M. A. Lander.)

ERRATA SHEET FOR THE 1994 ANNUAL TROPICAL CYCLONE REPORT

1. Page iii - last line of the first paragraph: "3140.1W" should read "3140.1V"

2. Page 21 - Section 3.1, first paragraph, first line: "included five super" should read "included six super".

3. Pages 88 and 89 - The imagery on page 88 should appear over the caption "Figure 3-14-3 As a hybrid...." on page 89; and, the imagery on page 89 should appear over the caption "Figure 3-14-2 Brendan exhibits....." on page 88.

4. Page 184 - Table 3-32-1, The heading for column 3 "Best Track intensity (kt)" should read "Current Intensity Estimate (kt)";and, the heading for column 4 "Intensity (kt)" should read "Best Track Intensity (kt)"...

5. Page 187 - Figures 3-33-1 (a), (b) and (c): For each of the three images, the label "10°N" should read "EQ" indicating the location of the equator. The remaining labels for latitude should be adjusted accordingly.

U. S. NAVAL PACIFIC METEOROLOGY AND OCEANOGRAPHY CENTER WEST
JOINT TYPHOON WARNING CENTER
COMNAVMARIANAS
PSC 489, BOX 12
FPO AP 96536-0051

Accesion For
NTIS CRA&I ☑
DTIC TAB ☐
Unannounced ☐
Justification .....
By .....
Distribution /
Availability Codes
Dist | Avail and / or Special
A-1

JAMES F. ETRO

CAPTAIN, UNITED STATES NAVY
COMMANDING OFFICER

JOSEPH P. BASSI

LIEUTENANT COLONEL, UNITED STATES AIR FORCE
DIRECTOR, JOINT TYPHOON WARNING CENTER

Work on this report was supported in part by funds provided by the Office of Naval Research Grant N00014-91-J1721

STAFF

JOINT TYPHOON WARNING CENTER

LCDR	ERNEST P. PETZRICK	USN	TDO, DEPUTY DIRECTOR
* LCDR	TERESA M. GOBEL	USN	TDO, DEPUTY DIRECTOR
LCDR	ALEX J. DECARIA	USN	TDO
** LCDR	STACY R. STEWART	USNR	TDO
* CAPT	JOHN S. SHATTUCK	USAF	TDO,
* LT	GREGORY SALVATO	USN	TDO
* LT	PAUL E. MATTHEWS	USN	TDO
AG1	SHISHMON D. BAILEY	USN	LPO, SAT FORECASTER, TDA
* AG2	BONNIE J. CAMPBELL	USN	LPO, TDA
* AG2	SCOTT E. McKEE	USN	LPO, TDA
AG2	GARY M. VINES	USN	TDA
* AG3	DAVID L. HAZEL	USN	TDA
SRA	DAVID J. CORREA, JR.	USAF	TDA
SRA	JORDAN S. KELLY	USAF	TDA
SRA	VINCENT L. PETRASEK	USAF	TDA
* SRA	LESLEY R. ROUELL	USAF	TDA
SRA	TIMOTHY C. WILLIAMS	USAF	TDA
A1C	SHAWN L. PETERSON	USAF	TDA
* A1C	SEAN R. VOLOM	USAF	TDA

36 OSS/OSJ

CAPT	ELIZABETH B. BORELLI	USAF	TDO, OIC USPACOM SAT NETWORK, TECHNIQUE DEVELOPMENT
* CAPT	CHRISTOPHER K. BROOKS	USAF	OIC USPACOM SAT NETWORK
MSGT	KARL H. STEVENS	USAF	SAT FORECASTER, NCOIC
TSGT	VINCENT T. AGUON	USAF	CHIEF INFORMATION MANAGEMENT
* TSGT	THEODORE V. MUSTAIKES, JR.	USAF	SAT FORECASTER
TSGT	SCOTT C. COPELAND	USAF	SAT FORECASTER
TSGT	RICHARD J. CONKLIN	USAF	DATA DEVELOPMENT
TSGT	HAROLD D. EIFERT	USAF	SAT FORECASTER
TSGT	MICHAEL S. GREHAN	USAF	SAT FORECASTER
SSGT	RICHARD D. JACOBSEN	USAF	SAT FORECASTER
SSGT	JEWEL K. TAPPY	USAF	SAT FORECASTER

ATCR STAFF

LT	MICHAEL D. ANGOVE	USN	TDO, EDITOR
CAPT	DAN B. MUNDELL	USAF	TDO, BEST TRACK OFFICER
CAPT	JOHN A. RUPP	USAF	TDO, STATISTICS OFFICER
MR	FRANK H. WELLS	USN	TECHNICAL EDITOR
AG3	JASON E. ECCLES	USN	GRAPHICS, TDA
AG3	ROBERT M. GIGUERE	USN	GRAPHICS, STATISTICS, TDA
AG3	ANDRES G. GRANT	USN	GRAPHICS, TDA

UNIVERSITY OF GUAM / JTWC RESEARCH LIAISON

DR	MARK A. LANDER	TROPICAL CYCLONE RESEARCH, TECHNICAL WRITING
MR	CHARLES P. GUARD	TROPICAL CYCLONE RESEARCH, TECHNICAL WRITING

* TRANSFERRED DURING 1994
** ACTIVE DUTY TRAINING

FOREWORD

The Annual Tropical Cyclone Report is prepared by the staff of the Joint Typhoon Warning Center (JTWC), a combined Air Force/Navy organization operating under the command of the Commanding Officer, U.S. Naval Pacific Meteorology and Oceanography Center West (NAVPACMETOCCEN WEST)/Joint Typhoon Warning Center, Guam. The JTWC was founded 1 May 1959 when the U.S. Commander-in-Chief Pacific (USCINCPAC) forces directed that a single tropical cyclone warning center be established for the western North Pacific region. The operations of JTWC are guided by USCINCPAC Instruction 3140.1W.

The mission of JTWC is multifaceted and includes:

1. Continuous monitoring of all tropical weather activity in the Northern and Southern Hemispheres, from 180° east longitude westward to the east coast of Africa, and the prompt issuance of appropriate advisories and alerts when tropical cyclone development is anticipated.

2. Issuance of warnings on all significant tropical cyclones in the above area of responsibility.

3. Determination of requirements for tropical cyclone reconnaissance and assignment of appropriate priorities.

4. Post-storm analysis of significant tropical cyclones occurring within the western North Pacific and North Indian Oceans.

5. Cooperation with the Naval Research Laboratory, Monterey, California on operational evaluation of tropical cyclone models and forecast aids, and the development of new techniques to support operational forecast requirements.

Special thanks to: Lieutenant Colonel Peter A. Morse for his support as the Director, JTWC for the past year and a half; the men and women of the Alternate Joint Typhoon Warning Center for standing in for JTWC as needed; Fleet Numerical Meteorology and Oceanography Center (FLENUMETOCCEN) for their operational support; the Naval Research Laboratory for its dedicated research; the Air Force Global Weather Central for continued satellite support; the 36th Communications Squadron's Defense Meteorological Satellite Program (DMSP) Site 18 at Nimitz Hill, Guam; and the Operations and Equipment Support departments of NAVPACMETOCCEN WEST, Guam for their high quality support; all the men and women of the ships and facilities ashore throughout the JTWC area of responsibility (AOR), and especially on Guam, who took the observations that became the basis for our analyses, forecasts and post analyses; the staff at National Oceanic and Atmospheric Administration (NOAA) National Environmental Satellite, Data, and Information Service (NESDIS) for their tropical cyclone position and intensity estimates; CDR. Lester E. Carr III and Dr. Russell L. Elsberry for their efforts at the Naval Postgraduate School and publication of the *Systematic and Integrated Approach to Tropical Cyclone Track Forecasting Part 1* ; the personnel at the Navy Publications and Printing Service Branch Office, Guam; Dr. Robert F. Abbey Jr. and the Office of Naval Research for their support to the University of Guam for the JTWC Research Liaisons to JTWC; the University of Guam Research Liaisons for their important contributions to this publication; Dr. Mark Lander for his training efforts, suggestions and valuable insights; and, AG3 Andres G. Grant, AG3 Robert M. Giguere and AG3 Jason E. Eccles for their excellent desktop publishing and graphics assistance.

EXECUTIVE SUMMARY

1994 was notable for the Joint Typhoon Warning Center (JTWC) in many respects. We witnessed the two longest-lived tropical cyclones on record; Typhoon John, which lasted for 30 days over the North Pacific Ocean and Tropical Cyclone Rewa (05P) which lasted for 21 days in the southwestern Pacific Ocean. We also, for the first time in history, recorded the binary interaction between Typhoon Pat and Tropical Storm Ruth and through eventual merger.

The Northwest Pacific (NWPAC) was especially active in 1994, with several long lived, slow-moving typhoons that dramatically increased the workload for the men and women of the JTWC. For the first time in our 36-year history, the JTWC issued more than 1000 warnings in NWPAC, on a total of 41 significant tropical cyclones. The DMSP Tropical Cyclone Reconnaissance Network (DMSP Network) logged over 5000 fixes during the year; also a record high. In spite of the very heavy workload, the JTWC continued to improve its forecast accuracy. Track forecast errors at 48- and 72-hours were the lowest ever, and intensity forecast errors were among the lowest in 20 years.

Sixty warnings were issued on the five tropical cyclones which occurred in the North Indian Ocean during 1994, and a record total of 390 warnings on 30 tropical cyclones in the Southern Hemisphere, 27 of which were within JTWC's area of responsibility. JTWC forecast errors were better than the long-term averages for 19 years in the North Indian Ocean, and among the lowest ever for the 14 years in the Southern Hemisphere.

During the past year, the JTWC has refined its forecast methods by applying a "systematic and integrated approach to tropical cyclone forecasting" developed by CDR Lester Carr and Dr. Russell Elsberry at the Naval Postgraduate School. This approach helps the forecaster improve upon dynamical track forecasts generated by the numerical models by fostering a more analytical view of the environmental influences on tropical cyclone motion, size and intensity.

When we consider JTWC forecasting performance over the past 20 years, it is important to note that the seven "best" years in NWPAC have occurred in the 8-year period since the loss of dedicated aircraft reconnaissance in 1987. Our results in 1994 underscore the value of actions taken by the center and supporting agencies to upgrade our computer systems, develop state-of-the-art satellite processing equipment, and better utilize the data from remote sensing platforms. The time savings afforded us by version 2.76 of the Automated Tropical Cyclone Forecast (ATCF) system, improved data retrieval capabilities of the Automated Weather Distribution System (AWDS) and integration of the Mark IVB into the Meteorological Imagery, Data Display, and Analysis System (MIDDAS) contributed to better forecast time management. The task of issuing 1058 high-quality warnings over the course of 168 tropical cyclone days (94 of which had multiple tropical cyclones), would have been very difficult if not impossible in the grease-pencil and acetate world we operated in less than 10 years ago.

TABLE OF CONTENTS

Page

FOREWORD iii
EXECUTIVE SUMMARY iv
1. OPERATIONAL PROCEDURES 1
1.1 General 1
1.2 Data Sources 1
1.3 Communications 2
1.4 Data Displays 5
1.5 Analyses 6
1.6 Forecast Procedures 6
1.7 Warnings 9
1.8 Prognostic Reasoning Messages 10
1.9 Tropical Cyclone Formation Alerts 10
1.10 Significant Tropical Weather Advisories 10

2. RECONNAISSANCE AND FIXES 13
2.1 General 13
2.2 Reconnaissance Availability 13
2.3 Satellite Reconnaissance Summary 13
2.4 Radar Reconnaissance Summary 16
2.5 Tropical Cyclone Fix Data 17

3. SUMMARY OF WESTERN NORTH PACIFIC AND NORTH INDIAN OCEAN TROPICAL CYCLONES 21
3.1 Western North Pacific Tropical Cyclones 21

Individual Tropical Cyclone Narratives

Tropical Cyclone	Author	Page	Tropical Cyclone	Author	Page
01W TD	Lander	40	21W TS Harry	Guard	121
02W TY Owen	Lander	44	22W TY Ivy	Lander	123
03W TY Page	Lander	47	10E TY John	Lander	128
04W TD	Lander	52	23W TS Joel	Guard	133
05W TS Russ	Guard	54	24W TY Kinna	Guard	135
06W TS Sharon	Guard	56	25W TS Luke	Guard	139
07W TD	Guard	58	26W STY Melissa	Guard	142
08W TY Tim	Guard	60	27W TS Nat	Lander	149
09W TS Vanessa	Lander	64	28W STY Orchid	Guard	156
10W STY Walt	Lander	69	29W TY Pat	Lander	162
11W TS Yunya	Lander	75	30W TS Ruth	Lander	171
12W TY Zeke	Lander	79	31W TD	Lander	174
13W TD	Guard	84	32W TY Seth	Lander	178
14W TS Brendan	Guard	86	33W TY Verne	Lander	185
15W TS Amy	Lander	90	34W TY Teresa	Lander	193
16W TS Caitlin	Guard	92	35W TY Wilda	Lander	197
17W STY Doug	Guard	94	36W TS Yuri	Lander	204
18W TY Ellie	Lander	100	37W STY Zelda	Lander	209
08E TS Li	Guard	105	38W TY Axel	Lander	217
19W STY Fred	Guard	107	39W TS Bobbie	Lander	223
20W TY Gladys	Lander	113			

Page

3.2 North Indian Ocean Tropical Cyclones 231

Individual Tropical Cyclone Narratives

Tropical Cyclone	Author	Page	Tropical Cyclone	Author	Page
TC 01B	Staff	234	TC 04B	Staff	241
TC 02B	Angove	236	TC 05A	Staff	243
TC 03A	Staff	239			

4. SUMMARY OF SOUTH PACIFIC AND SOUTH INDIAN OCEAN TROPICAL CYCLONES 245
   4.1 General 245
   4.2 South Pacific and South Indian Ocean Tropical Cyclones 245

5. SUMMARY OF FORECAST VERIFICATION 251
   5.1 Annual Forecast Verification 251
   5.2 Comparison of Objective Techniques 266
   5.3 Testing and Results 269

6. TROPICAL CYCLONE WARNING VERIFICATION STATISTICS 275
   6.1 General 275
   6.2 Warning Verification Statistics 275

7. TROPICAL CYCLONE SUPPORT SUMMARY 317
   7.1 Tropical Cyclone Forecaster's Reference Guide 317
   7.2 Automated Tropical Cyclone Forecasting System (ATCF) 3.0 317
   7.3 Prototype Automated Tropical Cyclone Handbook (PATCH) 317
   7.4 New Tropical Cyclone Related Wind Data Sets 317
   7.5 Satellite Imagery Analyses Upgrades 318
   7.6 Satellite Multi-Sensor Structure and Intensity Applications 318
   7.7 Development of the Systematic Approach to TC Track Forecasting 319
   7.8 Development of a High Confidence TC Intensity Data Base 320
   7.9 An Investigation of the Relationships between Cyclonic Cells in the TUTT and the Intensity Change of Tropical Cyclones 321
   7.10 The Natural Variation in the Relationship between Maximum Wind and Minimum Central Pressure in Tropical Cyclones 321
   7.11 A Study of the Characteristics of Very Small (Midget) TCs 321
   7.12 A Saffir-Simpson-Like Hurricane Scale for the Tropical W.Pacific 321
   7.13 NOGAPS Tropical Cyclone Forecast Performance 322

BIBLIOGRAPHY 323
APPENDIX A - Definitions 326
APPENDIX B - Names for Tropical Cyclones in the Western North Pacific Ocean and South China Sea 329
APPENDIX C - Contractions 331
APPENDIX D - Past Annual Tropical Cyclone Reports 335
APPENDIX E - Distribution List 336

1. OPERATIONAL PROCEDURES

1.1 GENERAL

The Joint Typhoon Warning Center (JTWC) provides a variety of routine products and services to the organizations within its area of responsibility (AOR), including:

1.1.1 SIGNIFICANT TROPICAL WEATHER ADVISORY — Issued daily or more frequently as needed, to describe all tropical disturbances and their potential for further development during the advisory period. A separate bulletin is issued for the western Pacific and the Indian Ocean.

1.1.2 TROPICAL CYCLONE FORMATION ALERT — Issued in a specified area when synoptic, satellite, or other germane data indicate that the development of a significant tropical cyclone is likely within 12 to 24 hours.

1.1.3 TROPICAL CYCLONE/ TROPICAL DEPRESSION WARNING — Issued periodically throughout each day to provide forecasts of position, intensity, and wind distribution for tropical cyclones in JTWC's AOR.

1.1.4 PROGNOSTIC REASONING MESSAGE — Issued with warnings for tropical storms, typhoons and super typhoons in the western North Pacific to discuss the rationale for the content of the specific JTWC warning.

1.1.5 PRODUCT CHANGES — The contents and availability of the above JTWC products are set forth in USCINCPACINST 3140.1V. Changes to USCINCPACINST 3140.1V and JTWC products and services are proposed and discussed at the annual U.S. Pacific Command (PACOM) Tropical Cyclone Conference.

1.2 DATA SOURCES

1.2.1 COMPUTER PRODUCTS — Numerical and statistical guidance are available from the USN Fleet Numerical Meteorology and Oceanography Center (FLENUMETOCCEN) at Monterey, California. These products along with selected ones from the National Meteorological Center (NMC) Suitland Maryland are received by microcomputer dial-up connections using military and commercial telephone lines. Numerical model guidance is also received from international sources as well.

1.2.2 CONVENTIONAL DATA — These data sets are comprised of land and shipboard surface observations, and enroute meteorological observations from commercial and military aircraft (AIREPS) recorded within six hours of synoptic times, and cloud-motion winds derived from satellite data. The conventional data are hand- and computer-plotted, and hand-analyzed in the tropics for the surface/gradient and 200-mb levels. These analyses are prepared twice daily from 0000Z and 1200Z synoptic data. Also, FLENUMETOCCEN supplies JTWC with computer generated analyses and prognoses, from 0000Z and 1200Z synoptic data, at the surface, 850-mb, 700-mb, 500-mb, 400-mb, and 200-mb levels, deep-layer-mean winds, wind shear, and geopotential height-change charts.

1.2.3 SATELLITE RECONNAISSANCE — Meteorological satellite imagery recorded at USAF/USN ground sites and USN ships supply day and night coverage in JTWC's AOR. Interpretation of these satellite data provides tropical cyclone positions and estimates of current and forecast intensities (Dvorak, 1984). The USAF tactical satellite sites and Air Force

Global Weather Central (AFGWC) currently receive and analyze special sensor microwave/imager (SSM/I) data to provide locations of tropical cyclones of which the center is obscured by cirrus clouds, and estimates of 35-kt (18 m/sec) wind radii near tropical cyclones. In addition, the Naval Oceanographic Office forwards scatterometer data. Use of satellite reconnaissance is discussed further in section 2.3 Satellite Reconnaissance Summary.

1.2.4 RADAR RECONNAISSANCE — Land-based radar observations are used to position tropical cyclones. Once a well-defined tropical cyclone moves within the range of land-based radar sites, radar reports are invaluable for determination of position, movement, and, in the case of Doppler radar, storm structure and wind information. JTWC's use of radar reports during 1994 is discussed in Section 2.4 Radar Reconnaissance Summary.

1.2.5 AIRCRAFT RECONNAISSANCE — Until the summer of 1987, dedicated aircraft reconnaissance was used routinely to locate and determine the wind structure of tropical cyclones. Now, aircraft fixes are only rarely available from transiting jet aircraft or from weather reconnaissance aircraft involved in research missions.

1.2.6 DRIFTING METEOROLOGICAL BUOYS — In 1989, the Commander, Naval Meteorology and Oceanography Command (COMNAVMETOCCOM) put its Integrated Drifting Buoy Plan (1989-1994) into action to meet USCINCPACFLT requirements that included tropical cyclone warning support. In 1994, 30 drifting buoys were deployed in the western North Pacific by a Naval Oceanographic Office-contracted C-130 aircraft. Of the 30 buoys, 24 were Compact Meteorological and Oceanographic Drifters (CMOD) with temperature and pressure sensors and six were Wind Speed and Direction (WSD) drifters with wind speed and direction, temperature and pressure. The drifters were evenly split by type over two deployments - the first in June followed by the second in August. The purpose of the split deployment was to overlap the expected three month lifespans of the CMOD buoys in order to provide continuous coverage during the peak of the western North Pacific tropical cyclone season.

1.2.7 AUTOMATED METEOROLOGICAL OBSERVING STATIONS (AMOS) — Through a cooperative effort between the COMNAVMETOCCOM, the Department of the Interior, and NOAA/NWS to increase data available for tropical analysis and forecasting, a network of 20 AMOS stations is being installed in the Micronesian Islands (see Tables 1-1 and 1-2). Previous to this effort, two sites were installed in the Northern Mariana Islands at Saipan and Rota through a joint venture between the Navy and NOAA/NWS. The site at Saipan relocated to Tinian in 1992. Since September of 1991, the capability to transmit data via Service ARGOS and NOAA polar orbiting satellites has been available as a backup to regular data transmission to the Geostationary Operational Environmental Satellite (GOES) West, and more recently for sites to the west of Guam, to the Japanese Geostationary Meteorological Satellite (GMS). Upgrades to existing sites are also being accomplished as the opportunity arises to enable access to the ARGOS-system. JTWC receives data from all AMOS sites via the AWN under the KWBC bulletin headers SMPW01, SIPW01 and SNPW01 (SXMY10 for Tinian and Rota).

1.3 COMMUNICATIONS

Primary telecommunications support is being provided by the Naval Telecommunications Center (NTCC), Nimitz Hill, a component of the Naval Computers and Telecommunications Area Master Stations,

Table 1-1 AUTOMATED METEOROLOGICAL OBSERVING STATIONS SUMMARY

Site	Location	Call sign	ID#	System	Installed
Rota	14.2°N, 145.2°E	15D16448	91221	ARC	1987
Enewetak	11.4°N, 162.3°E	ENIP2	91251	C-MAN/ARGOS	1989
Pagan	18.1°N, 145.8°E	PAGP2	91222	C-MAN/ARGOS	1990
Kosrae	5.3°N, 163.0°E	KOSP2	91355	C-MAN/ARGOS	1990
Mili	6.1°N, 171.8°E	MILP2	91377	C-MAN	1990
Oroluk	7.6°N, 155.1°E	ORKP2	91343	C-MAN	1991
Pingelap	6.3°N, 160.7°E	PIGP2	91352	C-MAN/ARGOS	1991
Ulul	8.7°N, 149.7°E	-----	91328	C-MAN/ARGOS	1992
Tinian	15.0°N, 145.6°E	15D151D2	91231	ARC	1992
Satawan	5.3°N, 153.7°E	SATP2	91338	C-MAN/ARGOS	1993

ARC = Automated Remote Collection system (via GOES West)
C-MAN = Coastal-Marine Automated Network (via GOES West or GMS)
ARGOS = Service ARGOS data collection (via NOAA's TIROS-N)

Table 1-2 PROPOSED AUTOMATED METEOROLOGICAL OBSERVING STATIONS

Site	Location	Installation	Delayed
Pulusuk	6.5°N, 149.5°E	1993	Yes*
Ulithi	10.1°N, 139.8°E	1993	Yes**
Ngulu	8.3°N, 137.5°E	1993	Yes**
Faraulep	8.1°N, 144.6°E	1994	Yes**
Eauripik	6.7°N, 143.0°E	1994	Yes**
Maloelap	8.7°N, 171.2°E	1994	Yes
Utirik	11.2°N, 169.8°E	1994	Yes
Satawal	7.3°N, 147.0°E	1995	Yes
Ujelang	9.8°N, 160.9°E	1995	Yes
Ebon	4.6°N, 168.7°E	1995	Yes
Maug	20.0°N, 145.2°E	1996	No

* Runway construction
** Testing of GMS transmission packages

Western Pacific (NCTAMS WESTPAC). NPMOCW/JTWC recently transitioned from a circuit limiting microwave configuration to a fully expandable fiber optic based system. In the future this new configuration will expand to eliminate the Nimitz Hill NTCC from the path between NPMOCW/JTWC and NCTAMS WESTPAC and streamline each circuit in the process. Systems and their configurations which are available to JTWC follow.

1.3.1 AUTOMATED DIGITAL NETWORK (AUTODIN) — AUTODIN is in the process of transitioning to the Defense Messaging System (DMS). The Gateguard system changed from using a long-haul dedicated circuit to Camp Smith, Hawaii to a dedicated STU-III (Secure Telephone Unit) dial-up operating at a 4800 baud rate via the Defense Switched Network (DSN) with NCTAMS WESTPAC. AUTODIN/DMS is used for dissemination of warnings, alerts, other related bulletins plus messages to Department of Defense (DOD) and other U.S. Government installations. These messages are relayed for further transmission over Navy Fleet Broadcasts, and Coast Guard continuous wave Morse code and voice broadcasts. AUTODIN/DMS messages can be relayed to commercial telecommunications for delivery to non-DOD users. Inbound message traffic for JTWC is received via AUTODIN/DMS addressed to NAVPACMETOCCEN WEST GU//JTWC//.

1.3.2 AUTOMATED WEATHER NETWORK (AWN) — The AWN provides weather data over the Pacific Meteorological Data System (PACMEDS). The PACMEDS, operational at JTWC since April 1988, allows Pacific-Theater agencies to receive weather information at a 1200 baud rate. JTWC uses the WINDS/AWNCOM software application package on a microcomputer to send and receive data via the PACMEDS. This system provides effective storage and manipulation of the large volume of meteorological reports available from throughout JTWC's vast AOR. Through the AWN, JTWC has access to data available on the Global Telecommunications System (GTS). JTWC's AWN station identifier is PGTW.

1.3.3 AUTOMATED WEATHER DISTRIBUTION SYSTEM (AWDS) - The AWDS has two dual monitor workstations that are networked to a communications and weather data computer server. Data are provided to the server by two 9600 baud rate circuits. Alphanumeric AWN data are supplied by Tinker AFB via one circuit, and satellite imagery and computer graphics are supplied by Air Force Global Weather Center (AFGWC) on the other. The AWDS provides JTWC with an additional source of AWN data and satellite data.

1.3.4 DEFENSE SWITCHED NETWORK (DSN) - DSN, formerly AUTOVON, is a worldwide, general purpose, switched telecommunications network for the DOD. The network provides a rapid and vital voice and data link for JTWC to communicate tropical cyclone information with DOD installations and civilian agencies. JTWC uses DSN to access, FTS2000, SprintNET networks, and commercial carriers for voice and data requirements. These requirements include the Naval Oceanography Data Distribution System (NODDS), Air Force Dial-In System (AFDIS), TELEFAX, and fallback dial-up for the Automated Tropical Cyclone Forecast (ATCF) system. The DSN telephone numbers for JTWC are 349-5240 or 349-4224.

1.3.5 TACTICAL ENVIRONMENTAL SUPPORT SYSTEM (3) (TESS(3)) - The TESS(3) has replaced the NAVAL ENVIRONMENTAL DATA NETWORK (NEDN). The TESS(3) has a primary dedicated packet switched data link to FLENUMETOCCEN and receives super-computer-generated world master-grid gridded fields, allowing for local value added tailoring of analyses and prognoses. The TESS(3) pro-

vides connectivity via the Defense Data Network (DDN) with all of COMNAVMETOCCOM Centers world-wide.

1.3.6 SPRINTNET - PUBLIC DATA NETWORK (PDN) - A commercial packet switching network that provides low-speed interactive transmission to users of FLENUMETOCCEN products. The PDN serves as a backup to the direct DDN MILNET connectivity. JTWC can request and receive FLENUMETOCCEN produced objective tropical cyclone forecast aids via SprintNET if DDN services are disrupted. SprintNET allows direct access of FLENUMETOCCEN products via the Automated Tropical Cyclone Forecast (ATCF) system. SprintNET also serves as an alternate methods of obtaining FLENUMETOCCEN analyses and forecast fields from the NODDS system.

1.3.7 DEFENSE DATA NETWORK (DDN) - The DDN is a DOD computer communications network utilized to exchange data files. Because the DDN has links, or gateways, to military information networks, it is frequently used to exchange data with the research community. JTWC's INTERNET address is 192.231.128.1 and its E-mail account is jtops@npmocw.navy.mil. The 36 OSS/OSJ address is admin@npmocw.navy.mil.

1.3.8 TELEPHONE FACSIMILE - TELEFAX provides the capability to rapidly scan and transmit, or receive, documents over commercial telephone lines or DSN. TELEFAX is used to disseminate tropical cyclone advisories and warnings to key agencies on Guam and, in special situations, to DOD, other U.S. Government agencies, and the other Micronesian Islands. Inbound documents for JTWC are received at (671) 349-6143, (671) 349-6101, or (671) 349-4032. (DSN area code for Pacific is 315.)

1.3.9 LOCAL USER TERMINAL (LUT) - JTWC uses a LUT, provided by the Naval Oceanographic Office, as the primary means of receiving real-time data from drifting meteorological buoys and ARGOS-equipped AMOS via the polar orbiting TIROS-N satellites.

1.4 DATA DISPLAYS

1.4.1 AUTOMATED TROPICAL CYCLONE FORECAST (ATCF) SYSTEM — The ATCF is an advanced software program that assists the Typhoon Duty Officer (TDO) in the preparation, formatting, and dissemination of JTWC's products. It cuts message preparation time and reduces the number of corrections. The ATCF automatically displays: the working and objective best tracks; forecasts of track, intensity, and wind distribution; and, information from computer generated forecast aids and products from other agencies. It also computes the myriad of statistics calculated by JTWC. A module permits satellite reconnaissance fixes to be input from 36 OSS/OSJ into the LAN. The ATCF is also used to transmit the Tropical Cyclone bogus for FLENUMETOCCEN for use in NOGAPS

1.4.2 TESS(3) receives, processes, stores, displays and prints copies of FLENUMETOCCEN data and environmental products. It also ingests and displays satellite imagery from the Naval Meteorological Data Receiver-Recorder Set (SMQ-11) and other TESS(3) sets worldwide.

1.4.3 AWDS functions are similar manner to that of the TESS(3), but the environmental products and satellite global data base imagery are produced by AFGWC.

1.4.4 NAVAL OCEANOGRAPHIC DATA DISTRIBUTION SYSTEM (NODDS) — NODDS is a personal computer (PC)-based system that uses a telephone modem to download, store and display environmental and satellite data base products from FLENUMETOCCEN.

1.4.5 NAVAL SATELLITE DISPLAY SYSTEM - GEOSTATIONARY (NSDS-G) — The NSDS-G is NAVPACMETOCCEN WEST's primary geostationary imagery processing and display system. It can be used to process high resolution geostationary imagery for analysis of tropical cyclone positions and intensity estimates for the western Pacific Ocean should the the Meteorological Imagery, Data Display, and Analysis System (MIDDAS) fail.

1.4.6 PC-BASED WEATHER FACSIMILE (PCGRAFAX) SYSTEM — PCGRAFAX is a microcomputer-based system that receives, stores and displays analog and digital facsimile products that are transmitted over high frequency (HF) radio.

1.4.7 SATELLITE WEATHER DATA IMAGING SYSTEM (SWDIS) — The SWDIS (also known as the M-1000) is a PC-based system that interfaces with the LAN to retrieve, store, and display various products such as: geostationary satellite imagery from other NSDS-G sites at Rota (Spain), Pearl Harbor (Hawaii), or Norfolk (Virginia), scatterometer data from NAVOCEANO, and composites of global geostationary satellite imagery from the Internet. The SWDIS has proven instrumental in providing METEOSAT reduced-resolution coverage of tropical cyclones over the western Indian Ocean.

1.5 ANALYSES

The JTWC TDO routinely performs manual streamline analyses of composite surface/gradient-level (3000 ft (914 m)) and upper-tropospheric (centered on the 200-mb level) data for 0000Z and 1200Z daily. Computer analyses of the surface, 925-, 850-, 700-, 500-, 400-, and 200-mb levels, deep-layer-mean winds, frontal boundaries depiction, 1000-200 mb/400-200 mb/and 700-400 mb wind shear, 500 mb and 700 mb 24-hour height change, and a variety of other meteorological displays come from the 0000Z and 1200Z FLENUMETOCCEN data bases. Additional sectional charts at intermediate synoptic times and auxiliary charts, such as station-time plot diagrams, time-height cross section charts and pressure-change charts, are analyzed during periods of significant tropical cyclone activity.

1.6 FORECAST PROCEDURES

1.6.1 INITIAL POSITIONING — The warning position is the best estimate of the center of the surface circulation at synoptic time. It is estimated from an analysis of all fix information received from one hour before to one and one-half hours after that synoptic time. The analysis is aided by a computer-generated objective best track scheme that weights fix information based on its statistical accuracy. The TDO includes synoptic observations and other information to adjust the position, testing consistency with the past direction, speed of movement and the influence of the different scales of motion. If the fix data are not available due to reconnaissance platform malfunction or communication problems, or are considered unrepresentative, synoptic data and/or extrapolation from previous fixes are used.

1.6.2 TRACK FORECASTING — In preparing the JTWC official forecast, the TDO evaluates a wide variety of information, and employs a number of objective and subjective techniques. Because tropical cyclone track forecasting has and continues to require a significant amount of subjective input from the TDO, detailed aspects of the forecast-development process will vary somewhat from TDO to TDO, particularly with respect to the weight given to any of the available guidance. JTWC uses a standardized, three-phase tropical cyclone motion forecasting process to improve not only

track forecast accuracy, but also intensity forecast accuracy and forecast-to-forecast consistency.

1.6.2.1 Field Analysis Phase — Navy Operational Global Atmospheric Prediction System (NOGAPS) analyses and prognoses at various levels are evaluated for position, development, and movement of not only the tropical cyclone, but also relevant synoptic features such as: 1) subtropical ridge circulations, 2) mid-latitude short/long-wave troughs and associated weaknesses in the subtropical ridge, 3) monsoon surges, 4) cyclonic cells in the Tropical Upper-Tropospheric Trough (TUTT), 5) other tropical cyclones, and 6) the distribution of sea surface temperature. This process permits the TDO to develop an initial impression of the environmental steering influences to which the tropical cyclone is and will be subjected to as depicted by NOGAPS. The NOGAPS analyses are then compared to the hand-plotted and analyzed charts prepared by the TDO and to the latest satellite imagery in order to determine how well the NOGAPS-initialization process has conformed to the available synoptic data, and how well the resultant analysis fields agree with the synoptic situation inferred from the imagery. Finally, the TDO compares both the computer and hand-analyzed charts to monthly climatology in order to make a preliminary determination of to what degree the tropical cyclone is, and will continue to be, subjected to a climatological or nonclimatological synoptic environment. Noting latitudinal and longitudinal displacements of the subtropical ridge and long-wave midlatitude features is of particular importance, and will partially determine the relative weights given to climatologically- or dynamically-based objective forecast guidance.

1.6.2.2 Objective Techniques Analysis Phase — By applying the guidance of the "Systematic and Integrated Approach,"(Carr and Elsberry, 1994) the TDO can relate the latest set of guidance given by JTWC's suite of objective techniques with the NOGAPS model prognoses and currently observed meteorological conditions. This allows the TDO to evaluate the objective techniques guidance to the following principles. First, the degree to which the current situation is considered to be, and will continue to be, climatological is further refined by comparing the forecasts of the climatology-based objective techniques, dynamically-based techniques, and past motion of the present storm. This assessment partially determines the relative weighting given the different classes of objective techniques. Second, the spread of the set of objective forecasts, when plotted, is used to provide a measure of the predictability of subsequent motion, and the advisability of including a moderate probability alternate forecast scenario in the prognostic reasoning message or warning (outside the western North Pacific). The directional spread of the plotted objective techniques is typically small well-before or well-after recurvature (providing high forecast confidence), and is typically large near the decision-point of recurvature or non-recurvature, or during a quasi-stationary or erratic movement phase. A large spread increases the likelihood of alternate forecast scenarios.

1.6.2.3 Construct Forecast Phase — The TDO then constructs the JTWC official forecast giving due consideration to the: 1) extent to which the synoptic situation is, and is expected to remain, climatological; 2) past statistical performance of the various objective techniques on the current storm; and, 3) known properties of individual objective techniques given the present synoptic situation or geographic location. The following guidance for weighting the objective techniques is applied:

a) Weight persistence strongly in the first 12 to 24 hours of the forecast period.

b) Give significant weight to the last JTWC forecast at all forecast times, unless there is sig-

nificant evidence to warrant a departure. (Also consider the latest forecasts from regional warning centers, if applicable.)

c) Give more weight to the techniques that have been performing well on the current tropical cyclone and/or are expected to perform well in the current and anticipated synoptic situations.

d) Stay within the "envelope" determined by the spread of objective techniques forecasts unless there is a strong specific reason for not doing so (e.g., all objective forecasts start out at a significant angle relative to past motion of the current tropical cyclone).

e) Apply the "Systematic and Integrated Approach," (Carr and Elsberry, 1994) using conceptual models of recurving, dynamically-related meteorological patterns with the traits of the numerical and objective aid guidance associated with the specific synoptic situation.

1.6.3 INTENSITY FORECASTING — The empirically derived Dvorak (1984) technique is used as a first guess for the intensity forecast. The TDO then adjusts the forecast after evaluating climatology and the synoptic situation. An interactive conditional climatology scheme allows the TDO to define a situation similar to the system being forecast in terms of location, time of year, current intensity, and intensity trend. Synoptic influences such as the location of major troughs and ridges, and the position and intensity of the TUTT all play a large part in intensifying or weakening a tropical cyclone. JTWC incorporates a checklist into the intensity forecast procedure. Such criteria as upper-level outflow patterns, neutral points, sea-surface temperatures, enhanced monsoonal or cross-equatorial flow, and vertical wind shear are evaluated for their tendency to enhance or inhibit normal development, and are incorporated into the intensity forecast process through locally developed thumb rules. In addition to climatology and synoptic influences, the first guess is modified for interactions with land, with other tropical cyclones, and with extratropical features. Climatological and statistical methods are also used to assess the potential for rapid intensification (Mundell, 1990).

1.6.4 WIND-RADII FORECASTING — Since the loss of dedicated aircraft reconnaissance in 1987, JTWC has turned to other data sources for determining the radii of winds around tropical cyclones. The determination of wind radii forecasts is a three-step process:

a) First, low-level satellite drift winds, microwave imager 35-kt wind speed analysis (See Chapter 2), and synoptic data are used to derive the current wind distribution.

b) Next the first guess of the radii is determined from statistically-derived empirical wind radii models. JTWC currently used three models: the Tsui model, the Huntley model, and the Martin-Holland model. The latter model uses satellite-derived parameters to determine the size and shape of the wind profile associated with a particular tropical cyclone. The Martin-Holland model also incorporates latitude and speed of motion to produce an asymmetrical wind distribution. These models provide wind distribution analyses and forecasts that are primarily influenced by the intensity forecasts. The analyses are then adjusted based on the actual analysis from step a), and the forecasts are adjusted appropriately.

c) Finally, synoptic considerations, such as the interaction of the cyclone with mid-latitude high pressure cells, are used to fine-tune the forecast wind radii.

1.6.5 EXTRATROPICAL TRANSITION — When a tropical cyclone moves into the mid-latitudes, if often enters an environment that is detrimental to the maintenance of the tropical cyclone's structure and energy-producing mechanisms. The effects of cooler sea surface temperatures, cooler and dryer environmental air, and strong vertical wind shear all act to convert the tropical cyclone into an extratropical

cyclone. JTWC indicates that this conversion process is occurring by stating that the tropical cyclone is "becoming extratropical." JTWC will indicate that the conversion is expected to be complete by stating that the system has become "extratropical." When a tropical cyclone is forecast to become extratropical, JTWC coordinates the transfer of responsibility with the appropriate regional NAVPACMETOCCEN, which assumes warning responsibility for the extratropical system.

1.6.6 TRANSFER OF WARNING RESPONSIBILITY — JTWC coordinates the transfer of warning responsibility for tropical cyclones entering or exiting its AOR. For tropical cyclones crossing 180° E longitude in the North Pacific Ocean, JTWC coordinates with the Central Pacific Hurricane Center (CPHC), Honolulu via the Naval Western Oceanography Center (NAVPACMETOCCEN), Pearl Harbor, Hawaii. For tropical cyclones crossing 180° E longitude in the South Pacific Ocean, JTWC coordinates with the NAVPACMETOCCEN, which has responsibility for the eastern South Pacific. Whenever a tropical cyclone threatens Guam, files are electronically transferred from JTWC to the Alternate Joint Typhoon Warning Center (AJTWC) collocated with NAVPACMETOCCEN. In the event that JTWC should become incapacitated, the AJTWC assumes JTWC's functions. Assistance in determining satellite reconnaissance requirements, and in obtaining the resultant data, is provided by the weather unit supporting the 15th Air Base Wing, Hickam AFB, Hawaii.

1.7 WARNINGS

JTWC issues two types of warnings: Tropical Cyclone Warnings and Tropical Depression Warnings.

1.7.1 TROPICAL CYCLONE WARNINGS — These are issued when a closed circulation is evident and maximum sustained 1-minute winds are forecast to reach 34 kt (18 m/sec) within 48 hours, or when the tropical cyclone is in such a position that life or property may be endangered within 72 hours.

Each Tropical Cyclone Warning is numbered sequentially and includes the following information: the current position of the surface center; an estimate of the position accuracy and the supporting reconnaissance (fix) platform(s); the direction and speed of movement during the past six hours (past 12 hours in the Southern Hemisphere); and the intensity and radial extent of over 35-, 50-, and 100-kt (18-, 26-, and 51 m/sec) surface winds, when applicable. At forecast intervals of 12, 24, 36, 48, and 72 hours (12, 24, 36 and 48 hours in the Southern Hemisphere), information on the tropical cyclone's anticipated position, intensity and wind radii is provided. Vectors indicating the mean direction and mean speed between forecast positions are included in all warnings. In addition, a 3-hour extrapolated position is provided in the remarks section.

Warnings in the western North Pacific and North Indian Oceans are issued every six hours (unless an amendment is required), valid at standard times: 0000Z, 0600Z, 1200Z and 1800Z (at a minimum every 12 hours: 0000Z, 1200Z or 0600Z, 1800Z in the Southern Hemisphere). All warnings are released to the communications network no earlier than synoptic time and no later than synoptic time plus two and one-half hours, so that recipients are assured of having all warnings in hand by synoptic time plus three hours (0300Z, 0900Z, 1500Z and 2100Z). By area, the warning bulletin headers are: WTIO31-35 PGTW for northern latitudes from 35° to 100° east longitude, WTPN31-36 PGTW for northern latitudes from 100° to 180° east longitude, WTXS31-36 PGTW for southern latitudes from 35° to 135° east longitude, and WTPS31-35 PGTW for

southern latitudes from 135° to 180° east longitude.

1.7.2 TROPICAL DEPRESSION WARNINGS — These are issued only for western North Pacific tropical depressions that are not expected to reach the criteria for Tropical Cyclone Warnings, as mentioned above. The depression warning contains the same information as a Tropical Cyclone Warning except that the Tropical Depression Warning is issued every 12 hours (unless an amendment is required) at standard synoptic times and extends in 12-hour increments only through 36 hours.

Both Tropical Cyclone and Tropical Depression Warning forecast positions are later verified against the corresponding best track positions (obtained during detailed post-storm analyses) to determine the most probable path and intensity of the cyclone. A summary of the verification results for 1994 is presented in Chapter 5, Summary of Forecast Verification.

1.8 PROGNOSTIC REASONING MESSAGES

These plain language messages provide meteorologists with the rationale for the JTWC forecasts for tropical cyclones in the western North Pacific Ocean. They also discuss alternate forecast scenarios, if changing conditions indicate such potential. Prognostic reasoning messages (WDPN31-36 PGTW) are prepared to complement tropical cyclone (but not tropical depression) warnings. In addition to these messages, prognostic reasoning information may be provided in the remark section of a tropical cyclone warning.

1.9 TROPICAL CYCLONE FORMATION ALERTS

Tropical Cyclone Formation Alerts are issued whenever interpretation of satellite imagery and other meteorological data indicates that the formation of a significant tropical cyclone is likely. These alerts will specify a valid period, usually not exceeding 24 hours, and must either be canceled, reissued, or superseded by a warning prior to expiration. By area, the Alert bulletin headers are: WTIO21-25 PGTW for northern latitudes from 35° to 100°E longitude, WTPN21-26 PGTW for northern latitudes from 100° to 180°E longitude, WTXS21-26 PGTW for southern latitudes from 35° to 135°E longitude, and WTPS21-25 PGTW for southern latitudes from 135° to 180°E longitude.

1.10 SIGNIFICANT TROPICAL WEATHER ADVISORIES

This product contains a description of all tropical disturbances in JTWC's AOR and their potential for further (tropical cyclone) development. In addition, all tropical cyclones in warning status are briefly discussed and referenced.

Two separate messages are issued daily, and each is valid for a 24-hour period. The Significant Tropical Weather Advisory for the Western Pacific Ocean is issued by 0600Z. The Significant Tropical Weather Advisory for the Indian Ocean is issued by 1800Z. These are reissued whenever the situation warrants. For each suspect area, the words "poor", "fair", or "good" are used to describe the potential for development. "Poor" will be used to describe a tropical disturbance in which the meteorological conditions are currently unfavorable for development. "Fair" will be used to describe a tropical disturbance in which the meteorological conditions are favorable for development, but 1significant development has not commenced or is not expected to occur in the next 24 hours. "Good" will be used to describe the potential for development of a disturbance covered by an Alert. By area, the advisory bulletin headers are: ABPW10 PGTW for northern latitudes from 100° to 180°E longitude and southern latitudes from 135° to 180°E longitude and

ABIO10 PGTW for northern latitudes from 35° to 100°E longitude and southern latitudes from 35° to 135°E longitude.

Intentionally left blank

2. RECONNAISSANCE AND FIXES

2.1 GENERAL

JTWC depends primarily on two reconnaissance platforms, satellite and radar, to provide necessary, accurate and timely meteorological information in support of advisories, alerts and warnings. When available, synoptic and aircraft reconnaissance data are also used to supplement the above. As in past years, the optimal use of all available reconnaissance resources to support JTWC's products remains a primary concern. Weighing the specific capabilities and limitations of each reconnaissance platform, and the tropical cyclone's threat to life and property, both afloat and ashore, continues to be an important factor in careful product preparation.

2.2 RECONNAISSANCE AVAILABILITY

2.2.1 SATELLITE — Interpretation of satellite imagery by analysts at Air Force/Navy ground sites and on Navy ships yields tropical cyclone positions, estimates of the current intensity, and forecast intensity. Additional positioning and surface wind estimation information is available for analysis where the DMSP SSM/I data are received and displayed.

2.2.2 RADAR — Interpretation of land-based radar, which remotely senses and maps precipitation within tropical cyclones, provides positions in the proximity (usually within 175 nm (325 km) of radar sites in the Kwajalein, Guam, Japan, South Korea, China, Taiwan, Philippine Islands, Hong Kong, Thailand, India and Australia. Where Doppler radars are located, such as the new NEXRAD installation on Guam, measurements of radial velocity are also available, and observations of the tropical cyclone's horizontal velocity field and wind structure integrated in the vertical are possible within the radar volume.

2.2.3 AIRCRAFT — No weather reconnaissance aircraft fixes were received at JTWC in 1994.

2.2.4 SYNOPTIC — JTWC also determines tropical cyclone positions based on the analysis of surface/gradient-level synoptic data. These positions are an important supplement to fixes provided by analysts using data from remote sensing platforms, and become most valuable in situations where neither satellite, radar nor aircraft fixes are available or representative.

2.3 SATELLITE RECONNAISSANCE SUMMARY

The Air Force provides satellite reconnaissance support to JTWC through the DMSP Tropical Cyclone Reporting Network (DMSP Network), which consists of several tactical sites and a centralized facility. The personnel of the Satellite Operations (hereafter referred to as Sat Ops) at 36 OSS/OSJ, collocated with JTWC at Nimitz Hill, Guam, coordinate required tropical cyclone reconnaissance support with the following units:

Unit	Call sign
15 ABW/WE, Hickam AFB, Hawaii	PHIK
18 OSS/WE, Kadena AB, Japan	RODN
603 ACCS/DOW, Osan AB, Republic of Korea	RKWU
Air Force Global Weather Central, Offutt AFB, Nebraska	KGWC

The DMSP Network sites provide a combined coverage from polar orbiting satellites that includes most of the western North Pacific, from near the international date line westward into the South China Sea. The Naval Pacific Meteorology and Oceanography Detachment at Diego Garcia furnishes fixes through interpretation of low resolution NOAA polar orbiting satellite imagery that covers the central Indian

Ocean, and Navy ships equipped for direct satellite readout contribute supplementary support. Also, civilian contractors with the U.S. Army at Kwajalein Atoll supplement Sat Ops satellite coverage with fixes on tropical cyclones in the Marshall Islands and east of the date line.

Additionally, mosaics developed from DMSP satellite imagery are available from the FLENUMETOCCEN via the DDN. These mosaics are used to metwatch the areas not included in the coverage of DMSP Network tactical sites. They provide JTWC forecasters with the time-delayed capability to "see" what AFGWC's satellite image analysts have been fixing.

Sat Ops also uses high resolution geostationary imagery to support the reconnaissance mission. Animation of images is invaluable for determining the location and motion of cloud system centers, particularly in the formative stages. Animation is also valuable in assessing changes in the environment that affect tropical cyclone behavior. Sat Ops is able to process high resolution digital geostationary data through its MIDDAS, and the Navy's Geostationary Satellite Receiving System (GSRS). The MIDDAS consists of a network of three microcomputers, advanced graphics software, and large screen work stations that process and display geostationary imagery, NOAA High Resolution Picture Transmission (HRPT) and TIROS Operational Vertical Sounder (TOVS) data, and DMSP imagery.

In support of JTWC, AFGWC analyzes stored imagery from both the DMSP and NOAA spacecraft. These imagery are recorded and stored onboard the spacecraft for later relay to a command readout site which in turn passes the data via a communication satellite to AFGWC. This enables AFGWC to obtain the global coverage needed to monitor all tropical cyclones worldwide several times a day.

The hub of the DMSP Network is Sat Ops, which is responsible for coordinating satellite reconnaissance requirements with JTWC and tasking the individual network sites for the necessary tropical cyclone fixes, current intensity estimates, and SSM/I-derived surface winds. When a particular satellite pass is selected to support JTWC's next tropical cyclone warning, two sites are tasked to fix the tropical cyclone from the same pass. This "dual-site" concept provides the necessary redundancy that virtually guarantees JTWC a satellite fix to support each warning. It also supplies independent assessments of the same data to provide TDOs a measure of confidence in the location and intensity information.

The DMSP Network provides JTWC with several products and services. The main service is to monitor the AOR for indications of tropical cyclone development. If development is suspected, JTWC is notified. Once JTWC issues either a TCFA or a warning, the DMSP Network provides tropical cyclone positions and current intensity estimates, with a forecast intensity estimate implied from the code (Dvorak 1975, 1984) shown in Figure 2-1. Each satellite-derived tropical cyclone position is assigned a Position Code Number (PCN), which is a measure of positioning confidence. The PCN is determined by a combination of 1) the availability of visible landmarks in the image that can be used as references for precise gridding, and 2) the degree of organization of the tropical cyclone's cloud system (Table 2-1). Once the tropical cyclone's intensity reaches 50 kt (26 m/sec), the DMSP Network analyzes the distribution of SSM/I-derived 35-kt (18-m/sec) winds in the rain-free areas near the tropical cyclone.

Sat Ops provides at least one estimate of the tropical cyclone's current intensity every 6 hours once JTWC is in alert or warning status. Current intensity estimates are made using the Dvorak technique for both visible and enhanced infrared imagery. For the intensity analysis of mature tropical cyclones, the enhanced infrared technique is preferred due to its objectivity;

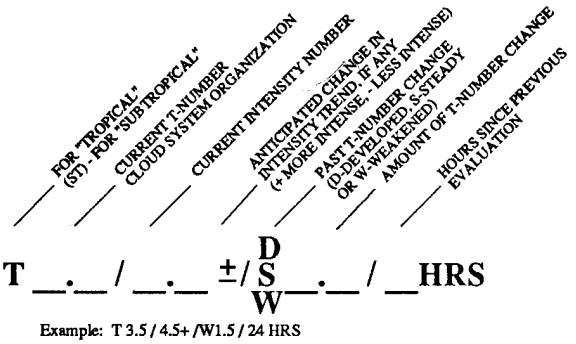

Figure 2-1 Dvorak code for communicating estimates of current and forecast intensity derived from satellite data. In the example, the current "T-number" is 3.5, but the current intensity is 4.5. The cloud system has weakened by 1.5 "T-numbers" since the evaluation conducted 24-hours earlier. The plus (+) symbol indicates an expected reversal of the weakening trend or very little further weakening of the tropical cyclone during the next 24-hour period.

however, daily use of the visible technique adds a measure of consistency and helps resolve ambiguities in the enhanced infrared techniques. The standard relationship between tropical cyclone "T-number", maximum sustained surface wind speed, and minimum sea-level pressure (Atkinson and Holliday, 1977) for the Pacific is shown in Table 2-2. For subtropical cyclones, intensity estimates are made using the Hebert and Poteat (1975) technique.

Table 2-1 POSITION CODE NUMBER (PCN)

PCN	METHOD FOR CENTER DETERMINATION/GRIDDING
1	EYE/GEOGRAPHY
2	EYE/EPHEMERIS
3	WELL DEFINED CIRCULATION CENTER/GEOGRAPHY
4	WELL DEFINED CIRCULATION CENTER/EPHEMERIS
5	POORLY DEFINED CIRCULATION CENTER/GEOGRAPHY
6	POORLY DEFINED CIRCULATION CENTER/EPHEMERIS

2.3.1 SATELLITE PLATFORM SUMMARY

Figure 2-2 shows the operational status of polar orbiting spacecraft. Data were received from four DMSP spacecraft during 1994. Of these, F8 was limited to only one channel of SSM/I data until it was placed in a standby status in April 94. F10 was operational until September when the Operational Line Scan (OLS) instrument failed, however F10 SSM/I data transmissions continued. F11 performed well throughout 1994 and F12, which didn't include a SSM/I instrument, became operational in August. Of the five TIROS-N spacecraft, NOAA9 remained in standby. NOAA10 and NOAA12 were operational throughout the year. NOAA 11 died January 1995. NOAA14, which was launched in December, later became operational in early 1995.

Table 2-2 ESTIMATED MAXIMUM SUSTAINED WIND SPEED (KT) AS A FUNCTION OF DVORAK CURRENT AND FORECAST INTENSITY NUMBER AND MINIMUM SEA-LEVEL PRESSURE (MSLP)

T-NUMBER	ESTIMATED WIND SPEED-KT	(M/SEC)	MSLP (MB) (PACIFIC)
0.0	<25	<(13)	- - - -
0.5	25	(13)	- - - -
1.0	25	(13)	- - - -
1.5	25	(13)	- - - -
2.0	30	(15)	1000
2.5	35	(18)	997
3.0	45	(23)	991
3.5	55	(28)	984
4.0	65	(33)	976
4.5	77	(40)	966
5.0	90	(46)	954
5.5	102	(53)	941
6.0	115	(59)	927
6.5	127	(65)	914
7.0	140	(72)	898
7.5	155	(80)	879
8.0	170	(87)	858

2.3.2 STATISTICAL SUMMARY

During 1994, fix and intensity information from the DMSP Network was the primary input to JTWC's warnings and post analyses. JTWC received at least 8387 satellite fixes — 4442 covered tropical cyclones in the western North Pacific, 193 in the North Indian Ocean, and 1849 in the Southern Hemisphere. The geosta-

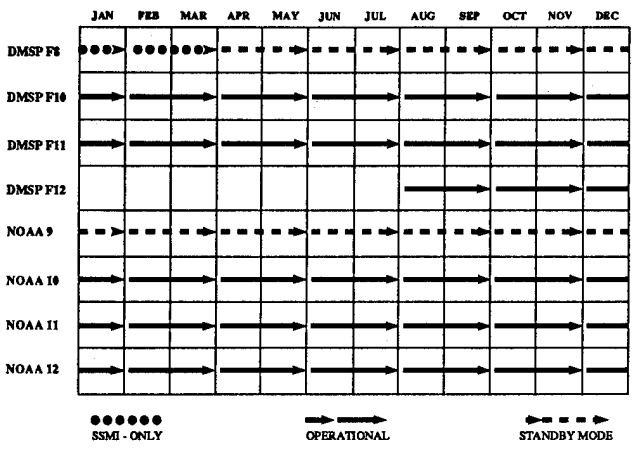

Figure 2-2 Polar orbiting spacecraft status for 1994

tionary platform was the source of 73 percent of the fixes and 27 percent were from polar orbiters. A comparison of all satellite fixes with only their corresponding best track positions is shown in Table 2-3.

2.3.3 APPLICATION OF NEW TECHNOLOGY

Sat Ops continued to make use of the real-time direct transmissions of SSM/I data received, processed and displayed by the Air Force's Mark IVB tactical terminals for surface wind speed estimation. These data were routinely used to identify areas of 35-kt winds, particularly surrounding tropical cyclones. Time-late SSM/I data, stored on board the DMSP spacecraft for later reception, processing and forwarding from FNMOC to be displayed on the MISTIC II, provided coverage over the JTWC's entire AOR. These time-late SSM/I data were used by analysts at AFGWC to develop 35-kt wind envelope bulletins for tropical cyclone warning support.

2.3.4 FUTURE OF SATELLITE RECONNAISSANCE

Sat Ops remains committed to, and strives to, improve the support to the PACOM tropical cyclone warning system. Expected in mid 1995 is the next software upgrade for the DMSP Mark IVB that will allow for the processing of water vapor channel from the geostationary meteorological satellite (GMS). Also, in 1995, the MIDDAS will be upgraded to allow for the processing and display of GMS water vapor and spit-window infrared. Near-term plans include the upgrade of the MIDDAS processing computers for quicker image processing. In addition, access to the Internet allows for receipt of mosaics of the European Space Agency (ESA) Remote Sensing satellite (ERS-1) scatterometer data which provides wind vectors to better define the tropical cyclone's surface wind envelope and surrounding environment.

2.4 RADAR RECONNAISSANCE SUMMARY

Of the 41 significant tropical cyclones in the western North Pacific during 1994, 19 passed within range of land-based radar with sufficient precipitation and organization to be fixed. A total of 661 land-based radar fixes were logged at JTWC. As defined by the World Meteorological Organization (WMO), the accuracy of these fixes falls within three categories: good [within 10 km (5 nm)], fair [within 10 - 30 km (5 - 16 nm)], and poor [within 30 - 50 km (16 - 27 nm)]. Of the 661 radar fixes encoded in this manner, 133 were good, 311 fair, and 217 poor. The radar network provided timely and accurate fixes which allowed JTWC to better track and forecast tropical cyclone movement. In addition to fixes, the Andersen AFB (Guam) NEXRAD Doppler radar supplied meteorologists with a new look into the vertical and horizontal structure of precipitation and winds in tropical cyclones passing near the island.

In the Southern Hemisphere, four radar reports were logged for tropical cyclones. No radar fixes were received for the North Indian Ocean.

2.5 TROPICAL CYCLONE FIX DATA

Table 2-4a delineates the number of fixes per platform for each individual tropical cyclone for the western North Pacific. Totals and percentages are also indicated. Similar information is provided for the North Indian Ocean in Table 2-4b, and for the South Pacific and South Indian Oceans in Table 2-4c.

Table 2-3 MEAN DEVIATION(NM) OF ALL DMSP NETWORK DERIVED TROPICAL CYCLONE POSITIONS FROM JTWC BEST TRACK POSITIONS (NUMBER OF CASES IN PARENTHESES)

NORTHWEST PACIFIC OCEAN

PCN	1984-1993 AVERAGE		1994 AVERAGE	
1&2	14.0	(6091)	13.9	(1105)
3&4	22.8	(6213)	26.8	(784)
5&6	37.9	(14557)	50.8	(2278)
Totals	29.0	(26861)	36.5	(4167)

NORTH INDIAN OCEAN

PCN	1984-1993 AVERAGE		1994 AVERAGE	
1&2	13.5	(151)	11.4	(14)
3&4	34.7	(116)	33.3	(19)
5&6	38.9	(1323)	38.7	(132)
Totals	36.2	(1590)	35.8	(165)

WESTERN SOUTH PACIFIC AND SOUTH INDIAN OCEAN

PCN	1984-1993 AVERAGE		1994 AVERAGE	
1&2	16.3	(2478)	15.7	(302)
3&4	27.2	(2160)	28.0	(216)
5&6	36.7	(9755)	46.3	(1174)
Totals	31.7	(14393)	38.5	(1692)

Table 2-4a 1994 NORTHWEST PACIFIC OCEAN FIX PLATFORM SUMMARY

TROPICAL CYCLONE			SATELLITE	RADAR	SYNOPTIC	AIRCRAFT	TOTAL
01W	TD		50	0	0	0	50
02W	TY	Owen	112	0	1	0	113
03W	TY	Page	122	0	2	0	124
04W	TD		64	0	0	0	64
05W	TS	Russ	71	42	0	0	113
06W*	TS	Sharon	64	0	3	0	67
07W	TD		35	12	0	0	47
08W	TY	Tim	99	24	0	0	123
09W	TS	Vanessa	22	0	0	0	22
10W	STY	Walt	204	144	1	0	349
11W	TS	Yunya	52	0	0	0	52
12W	TY	Zeke	78	0	0	0	78
13W	TD		14	0	1	0	15
14W	TS	Brendan	90	2	1	0	93
15W	TS	Amy	29	0	0	0	29
16W	TS	Caitlin	54	3	0	0	57
17W	STY	Doug	197	38	0	0	235
18W	TY	Ellie	186	43	0	0	229
08E	TS	Li	65	0	0	0	65
20W	TY	Gladys	163	55	0	0	218
21W	TS	Harry	73	17	0	0	90
22W	TY	Ivy	102	0	0	0	102
23W	TS	Joel	63	0	0	0	63
24W	TY	Kinna	148	21	0	0	169
25W	TY	Luke	83	2	0	0	85
26W	STY	Melissa	116	0	0	0	116
10E	TY	John	136	0	0	0	136
27W	TS	Nat	88	12	0	0	100
28W	STY	Orchid	228	106	0	0	334
29W	TY	Pat	68	0	0	0	68
30W	TS	Ruth	58	0	0	0	58
31W	TD		63	0	0	0	63
32W	TY	Seth	198	17	1	0	216
33W	TY	Verne	208	19	0	0	227
34W	TY	Teresa	126	0	0	0	126
35W	TY	Wilda	161	19	0	0	180
36W	TS	Yuri	37	0	0	0	37
37W	STY	Zelda	216	31	0	0	247
38W*	TY	Axel	147	0	5	0	152
39W	TS	Bobbie	96	0	0	0	96
		Totals	4373	661	17	0	5051
Percentage of Total			87%	13%	<1%	0%	100%

* Regenerated

Table 2-4b 1994 NORTH INDIAN OCEAN FIX PLATFORM SUMMARY

TROPICAL CYCLONE	SATELLITE	RADAR	SYNOPTIC	TOTAL
01B	54	0	0	54
02B	67	0	0	67
03A	17	0	0	17
04B	24	0	0	24
05A	32	0	0	32
Totals	194	0	0	194
Percentage of Total	100%	0%	0%	100%

Table 2-4c 1994 SOUTH PACIFIC AND SOUTH INDIAN OCEANS FIX PLATFORM SUMMARY

TROPICAL CYCLONE		SATELLITE	RADAR	SYNOPTIC	AIRCRAFT	TOTAL
01S	Alexina	68	0	0	0	68
02S	Bettina	59	0	0	0	59
03S	Cecilia	75	0	0	0	75
04S	Naomi	32	0	0	0	32
05P	Rewa	249	3	0	0	252
06S	Oscar	62	0	0	0	62
07P		6	0	0	0	6
08S	Daisy	31	0	0	0	31
09S	Pearl	98	0	0	0	98
10S	Edema	35	0	0	0	35
11P	Sarah	90	0	0	0	90
12S	Quenton	64	0	0	0	64
13S	Geralda	59	0	0	0	59
14P	Sadie	18	0	0	0	18
15S	Hollanda	10	0	0	0	10
16S	Ivy	95	0	0	0	95
17S		74	1	0	0	75
18P	Theodore	55	0	0	0	55
19S	Kelvina	15	0	0	0	15
20S	Litanne	87	0	0	0	87
21S	Mariola	107	0	0	0	107
22S	Sharon	62	0	0	0	62
23S*	Nadia	53	0	0	0	53
24P	Tomas	55	0	0	0	55
25P	Usha	59	0	3	0	84
26S	Odille	143	0	0	0	143
27S	Tim	39	0	0	0	39
28S	Vivienne	75	0	0	0	75
29P		21	0	0	0	21
30S	Willy	44	0	0	0	44
	Totals	1940	4	3	0	1947
	Percentage of Total	99.6 %	<1 %	<1 %	0 %	100 %

* Regenerated

3. SUMMARY OF WESTERN NORTH PACIFIC AND NORTH INDIAN OCEAN TROPICAL CYCLONES

3.1 WESTERN NORTH PACIFIC OCEAN TROPICAL CYCLONES

The year of 1994 included five super typhoons, 16 lesser typhoons, 15 tropical storms and five tropical depressions (Table 3-1). The calendar year total of 41 significant tropical cyclones (TCs) in the western North Pacific was the highest since 1967 when there were also 41 (Table 3-2). The year's total of six super typhoons was two above the 35-year (1960-1994) average (Figure 3-1), and the year's total of 36 named TCs was eight above the 35-year average (1960-1994) (Figure 3-2). Thirty-five of the 41 significant TCs in the western North Pacific during 1994 originated in the low-level monsoon trough or near-equatorial trough. Two — Tropical Depression 31W and Yuri (36W) — formed in direct association with cold-core

Table 3-1 WESTERN NORTH PACIFIC SIGNIFICANT TROPICAL CYCLONES FOR 1994

TROPICAL CYCLONE	PERIOD OF WARNING	NUMBER OF WARNINGS ISSUED	ESTIMATED MAXIMUM SURFACE WINDS KT (M/SEC)	ESTIMATED MSLP (MB)
01W TD	04 JAN - 06 JAN	5	25 (13)	1002
02W TY OWEN	01 MAR - 08 MAR	32	75 (39)	968
03W TY PAGE	11 MAY - 17 MAY	25	90 (46)	954
04W TD	24 MAY - 26 MAY	11	30 (15)	1000
05W TS RUSS	04 JUN - 09 JUN	20	55 (28)	984
06W TS SHARON	21-22 JUN/22-25 JUN	14	45 (23)	991
07W TD	03 JUL - 04 JUL	7	30 (15)	1000
08W TY TIM	07 JUL - 11 JUL	18	125 (64)	916
09W TS VANESSA	09 JUL - 11 JUL	10	45 (23)	991
10W STY WALT	14 JUL - 26 JUL	50	130 (67)	910
11W TS YUNYA	18 JUL - 21 JUL	14	45 (23)	991
12W TY ZEKE	18 JUL - 24 JUL	26	65 (33)	976
13W TD	25 JUL - 26 JUL	4	25 (13)	1002
14W TS BRENDAN	29 JUL - 01 AUG	15	50 (26)	987
15W TS AMY	29 JUL - 31 JUL	8	40 (21)	994
16W TS CAITLIN	02 AUG - 04 AUG	9	60 (31)	980
17W STY DOUG	02 AUG - 13 AUG	42	140 (72)	898
18W TY ELLIE	08 AUG - 16 AUG	33	80 (41)	963
08E TS LI	13 AUG - 18 AUG	21	55 (28)	984
19W STY FRED	14 AUG - 22 AUG	33	130 (67)	910
20W TY GLADYS	22 AUG - 02 SEP	45	105 (54)	938
21W TS HARRY	25 AUG - 29 AUG	15	60 (31)	980
22W TY IVY	28 AUG - 03 SEP	26	75 (39)	968
10E TY JOHN	28 AUG - 08 SEP	45	105 (54)	938
23W TS JOEL	04 SEP - 07 SEP	15	45 (23)	991
24W TY KINNA	05 SEP - 11 SEP	27	85 (44)	958
25W TS LUKE	09 SEP - 14 SEP	22	50 (26)	987
26W STY MELISSA	11 SEP - 18 SEP	29	135 (69)	904
27W TS NAT	15 SEP - 22 SEP	29	45 (23)	991
28W STY ORCHID	18 SEP - 30 SEP	48	135 (69)	904
29W TY PAT	21 SEP - 26 SEP	18	95 (49)	949
30W TS RUTH	24 SEP - 28 SEP	18	45 (23)	991
31W TD	29 SEP - 03 OCT	11	30 (15)	1000
32W TY SETH	02 OCT - 11 OCT	37	120 (62)	922
33W TY VERNE	15 OCT - 31 OCT	66	115 (59)	927
34W TY TERESA	17 OCT - 26 OCT	37	80 (41)	963
35W TY WILDA	20 OCT - 01 NOV	49	125 (64)	916
36W TS YURI	23 OCT - 25 OCT	9	35 (18)	997
37W STY ZELDA	28 OCT - 08 NOV	44	135 (69)	904
38W TY AXEL	13-14 DEC/15-25 DEC	42	115 (59)	927
39W TS BOBBIE	17 DEC - 25 DEC	29	50 (26)	987
	TOTAL:	1058		

Table 3-2 DISTRIBUTION OF WESTERN NORTH PACIFIC TROPICAL CYCLONES FOR 1959 - 1994

YEAR	JAN	FEB	MAR	APR	MAY	JUN	JUL	AUG	SEP	OCT	NOV	DEC	TOTALS
1959	0	1	1	1	0	1	3	8	9	3	2	2	31
	000	010	010	100	000	001	111	512	423	210	200	200	17 7 7
1960	1	0	1	1	1	3	3	9	5	4	1	1	30
	001	000	001	100	010	210	210	810	041	400	100	100	19 8 3
1961	1	1	1	1	4	6	5	7	6	7	2	1	42
	010	010	100	010	211	114	320	313	510	322	101	100	20 11 11
1962	0	1	0	1	3	0	8	8	7	5	4	2	39
	000	010	000	100	201	000	512	701	313	311	301	020	24 6 9
1963	0	0	1	1	0	4	5	4	4	6	0	3	28
	000	000	001	100	000	310	311	301	220	510	000	210	19 6 3
1964	0	0	0	0	3	2	8	8	8	7	6	2	44
	000	000	000	000	201	200	611	350	521	331	420	101	26 13 5
1965	2	2	1	1	2	4	6	7	9	3	2	1	40
	110	020	010	100	101	310	411	322	531	201	110	010	21 13 6
1966	0	0	0	1	2	1	4	9	10	4	5	2	38
	000	000	000	100	200	100	310	531	532	112	122	101	20 10 8
1967	1	0	2	1	1	1	8	10	8	4	4	1	41
	010	000	110	100	010	100	332	343	530	211	400	010	20 15 6
1968	0	1	0	1	0	4	3	8	4	6	4	0	31
	000	001	000	100	000	202	120	341	400	510	400	000	20 7 4
1969	1	0	1	1	0	0	3	3	6	5	2	1	23
	100	000	010	100	000	000	210	210	204	410	110	010	13 6 4
1970	0	1	0	0	0	2	3	7	4	6	4	0	27
	000	100	000	000	000	110	021	421	220	321	130	000	12 12 3
1971	1	0	1	2	5	2	8	5	7	4	2	0	37
	010	000	010	200	230	200	620	311	511	310	110	000	24 11 2
1972	1	0	1	0	0	4	5	5	6	5	2	3	32
	100	000	001	000	000	220	410	320	411	410	200	210	22 8 2
1973	0	0	0	0	0	0	7	6	3	4	3	0	23
	000	000	000	000	000	000	430	231	201	400	030	000	12 9 2
1974	1	0	1	1	1	4	5	7	5	4	4	2	35
	010	000	010	010	100	121	230	232	320	400	220	020	15 17 3
1975	1	0	0	1	0	0	1	6	5	6	3	2	25
	100	000	000	001	000	000	010	411	410	321	210	002	14 6 5
1976	1	1	0	2	2	2	4	4	5	0	2	2	25
	100	010	000	110	200	200	220	130	410	000	110	020	14 11 0
1977	0	0	1	0	1	1	4	2	5	4	2	1	21
	000	000	010	000	001	010	301	020	230	310	200	100	11 8 2
1978	1	0	0	1	0	3	4	8	4	7	4	0	32
	010	000	000	100	000	030	310	341	310	412	121	000	15 13 4
1979	1	0	1	1	2	0	5	4	6	3	2	3	28
	100	000	100	100	011	000	221	202	330	210	110	111	14 9 5
1980	0	0	1	1	4	1	5	3	7	4	1	1	28
	000	000	001	010	220	010	311	201	511	220	100	010	15 9 4
1981	0	0	1	1	1	2	5	8	4	2	3	2	29
	000	000	100	010	010	200	230	251	400	110	210	200	16 12 1
1982	0	0	3	0	1	3	4	5	6	4	1	1	28
	000	000	210	000	100	120	220	500	321	301	100	100	19 7 2
1983	0	0	0	0	0	1	3	6	3	5	5	2	25
	000	000	000	000	000	010	300	231	111	320	320	020	12 11 2
1984	0	0	0	0	0	2	5	7	4	8	3	1	30
	000	000	000	000	000	020	410	232	130	521	300	100	16 11 3
1985	2	0	0	0	1	3	1	7	5	5	1	2	27
	020	000	000	000	100	201	100	520	320	410	010	110	17 9 1
1986	0	1	0	1	2	2	2	5	2	5	4	3	27
	000	100	000	100	110	110	200	410	200	320	220	210	19 8 0
1987	1	0	0	1	0	2	4	4	7	2	3	1	25
	100	000	000	010	000	110	400	310	511	200	120	100	18 6 1

TABLE CONTINUED ON TOP OF NEXT PAGE

Table 3-2 CONTINUED FROM PREVIOUS PAGE

YEAR	JAN	FEB	MAR	APR	MAY	JUN	JUL	AUG	SEP	OCT	NOV	DEC	TOTALS	
1988	1	0	0	0	1	3	2	5	8	4	2	1	27	
	100	000	000	000	100	111	110	230	260	400	200	010	14 12	1
1989	1	0	0	1	2	2	6	8	4	6	3	2	35	
	010	000	000	100	200	110	231	332	220	600	300	101	21 10	4
1990	1	0	0	1	2	4	4	5	5	5	4	1	31	
	100	000	000	010	110	211	220	500	410	230	310	100	21 9	1
1991	0	0	2	1	1	1	4	8	6	3	6	0	32	
	000	000	110	010	100	100	400	332	420	300	330	000	20 10	2
1992	1	1	0	0	0	3	4	8	5	6	5	0	33	
	100	010	000	000	000	210	220	440	410	510	311	000	21 11	1
1993	0	0	2	2	1	2	5	8	5	6	4	3	38	
	000	000	011	002	010	101	320	611	410	321	112	300	21 9	8
1994	1	0	1	0	2	2	9	9	8	7	0	2	41	
	001	000	100	000	101	020	342	630	440	511	000	110	21 15	5
(1959-1994)														
MEAN	0.6	0.3	0.6	0.8	1.3	2.1	4.6	6.4	5.7	4.7	2.9	1.4	31.4	
CASES	21	10	23	27	45	77	165	231	205	169	105	51	1129	

The criteria used in Table 3-2 are as follows:
1) If a tropical cyclone was first warned on during the last two days of a particular month and continued into the next month for longer than two days, then that system was attributed to the second month.
2) If a tropical cyclone was warned on prior to the last two days of a month, it was attributed to the first month, regardless of how long the system lasted.
3) If a tropical cyclone began on the last day of the month and ended on the first day of the next month, that system was attributed to the first month. However, if a tropical cyclone began on the last day of the month and continued into the next month for only two days, then it was attributed to the second month.

TABLE 3-2 LEGEND

Total for the month/year → 41
Typhoons → 21 15 5
Tropical Storms
Tropical Depressions

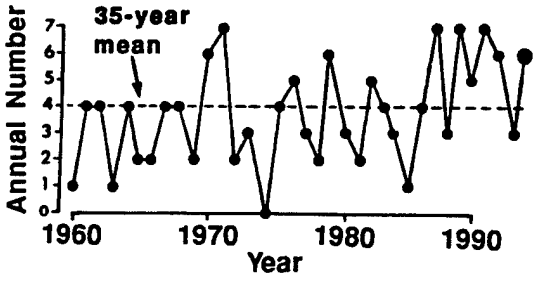

Figure 3-1 Number of western North Pacific super typhoons (1960-1994).

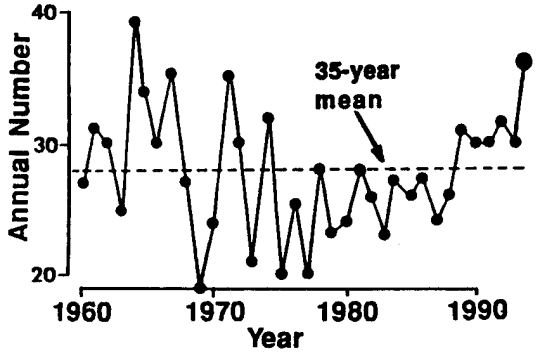

Figure 3-2 Tropical cyclones of tropical storm or greater intensity in the western North Pacific (1960-1994).

cyclonic vortices in the tropical upper tropospheric trough (TUTT). Ivy (22W) and Ellie (25W) formed in the subtropics from disturbances at the southern end of midlatitude troughs. Two of the year's named TCs — Li (06E) and John (08E) — formed in the monsoon trough of the eastern North Pacific and survived the long westward passage across the central Pacific to the western North Pacific.

Some of the large-scale atmospheric and oceanic climatic parameters continued to be indicative of El Niño conditions during most of 1994: the sea surface temperature (SST) over much of the eastern equatorial Pacific — especially near the international date line — was consistently warmer than normal, and the Southern Oscillation Index (SOI) (Climate Analysis Center, 1994) was strongly negative for most of the year (Figure 3-3). From September through the remainder of the year,

low-level westerly winds penetrated far to the east of normal (Figure 3-4). By the end of December, monsoonal low-level westerly wind flow was straddling the equator and had penetrated well-beyond the international date line to near 160°W. Based on the Pacific basin SST patterns and the distribution of wind and surface pressure in the tropics of the Pacific basin, the U.S. Climate Analysis Center (along with other international meteorological centers) officially declared that an El Niño event was under way, and predicted that it would reach its mature phase in early 1995. With the anomalous eastward push of monsoonal westerlies, several of the year's tropical cyclones formed east of 160°E and south of 20°N (Figure 3-5a). The number of tropical cyclones that form in this region is highly dependent upon El Niño, with more during El Niño years and less in other years. Unlike most El Niño years, however, there were several tropical cyclones that formed east of 160°E and north of 20°N. These tropical cyclones formed in association with TUTT cells, mid-latitude troughs, or were at the eastern end of a reverse-oriented monsoon trough. Despite a high number of tropical cyclones which formed well to the east of normal, there were a significant number of tropical cyclones that formed in the western part of the basin (including four that formed in the South China Sea); hence the 1994 annual mean genesis location was close to normal (Figure 3-5b).

The monsoon circulation of the western North Pacific (WNP) was very active during 1994 and was highlighted by three major episodes — one each during July, September and October— of reverse orientation of the trough axis. A reverse-oriented monsoon trough in the WNP is an episodic event that occurs on average about once each typhoon season sometime between mid-July and mid-October. During some years it is not seen; but during other years (such as 1989 and 1994) the monsoon trough repeatedly organizes in a reverse orientation. The distinguishing characteristics of a reverse-oriented monsoon trough are a SW-NE (i.e., reverse) orientation of the trough axis with respect to the normal NW-SE orientation of the trough axis, and the penetration of the trough axis into subtropical areas normally the province of easterly flow (Figure 3-6a,b). When the monsoon trough axis acquires a reverse orientation, tropical cyclones along it tend to move on north-oriented tracks (JMA 1976) and may undergo binary interactions with other tropical cyclones or monsoon depressions located along the trough axis (Lander 1995).

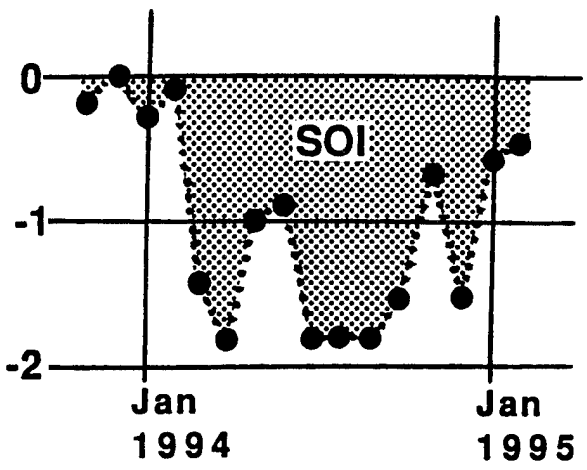

Figure 3-3 The Southern Oscillation Index (SOI) (shaded) for 1994 (adapted from Climate Analysis Center, 1994).

The first occurrence during 1994 of reverse orientation of the monsoon trough in the WNP was during July. By mid-July, an active reverse-oriented monsoon trough stretched across the tropics of the WNP from the South China Sea northeastward into sub-tropical latitudes near the international date line. Three tropical cyclones formed in this trough — Walt (10W), Yunya (11W), and Zeke (12W). Each of these tropical cyclones moved on north-oriented tracks, and each exhibited unusual eastward motion at low latitude.

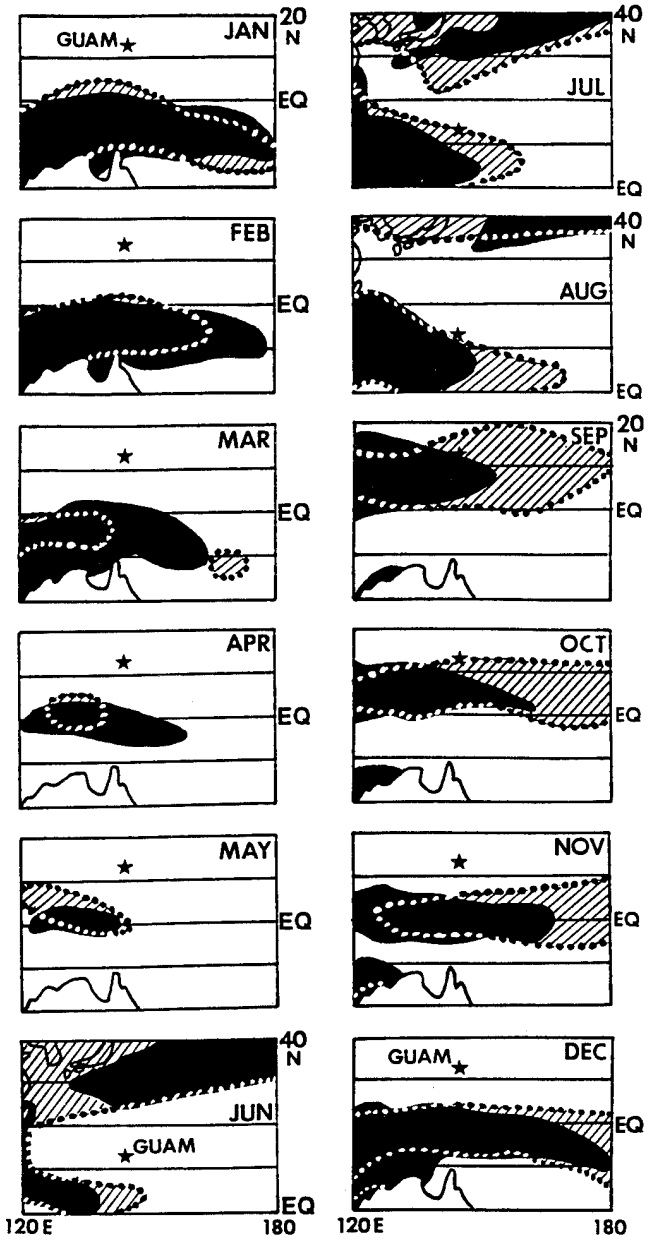

Figure 3-4 Comparison between climatological (black) and analyzed (hatched) mean monthly winds with a westerly component for the western North Pacific in 1994. For June, July, and August the area of coverage is shifted northward to include the subtropics of the North Pacific. For reference, the star indicates the location of Guam. The outline of Australia appears in the lower left of each panel except for June, July, and August where the Korean Peninsula and Japan appear in the upper left. The climatology is adapted from Sadler *et al.*, 1987. The 1994 monthly mean winds were adapted from the Climate Analysis Center, 1994.

The second occurrence during 1994 of reverse orientation of the monsoon trough in the WNP was during September. For a full two weeks in the middle of September, an active reverse-oriented monsoon trough dominated the large-scale circulation of the WNP. Five tropical cyclones formed in this trough — Melissa (26W), Nat (27W), Orchid (28W), Pat (29W), and Ruth (30W). All of them moved on north-oriented tracks. Nat, Orchid, and Ruth exhibited unusual eastward motion at low-latitude. Pat and Ruth underwent a binary interaction that resulted in the merger of the two systems into one.

The third occurrence during 1994 of reverse orientation of the monsoon trough in the WNP occurred in October. By mid-October, the monsoon trough was oriented zonally at low latitude and in the eastern portion of the basin. Three tropical cyclones — Teresa (34W), Verne (33W), and Wilda (35W) — formed in succession in this monsoon trough and initially moved westward. By the end of October, Teresa, Verne and Wilda had moved relative to each other so as to bring the axis of the monsoon trough into a reverse orientation. As soon as this occurred, the westward motion of Verne ceased, and Wilda began to move on a north-oriented "S-shaped" track.

The tracks of the TCs which formed in the WNP during 1994 indicates a high number of north-oriented tracks. Of the 39 TCs which formed in the WNP during 1994: fifteen (38%) were straight moving, only six (15%) were recurvers, thirteen (33%) moved on north-oriented tracks, and five were designated as "other" (Table 3-3). Of the 13 tropical cyclones which moved on north-oriented tracks during 1994, five underwent "S" motion. Four of the five "other" storms remained in or near the South China Sea. Ten of the thirteen tropical cyclones during 1994 which moved on north-oriented tracks occurred in association with the three episodes of reverse orientation of the monsoon trough.

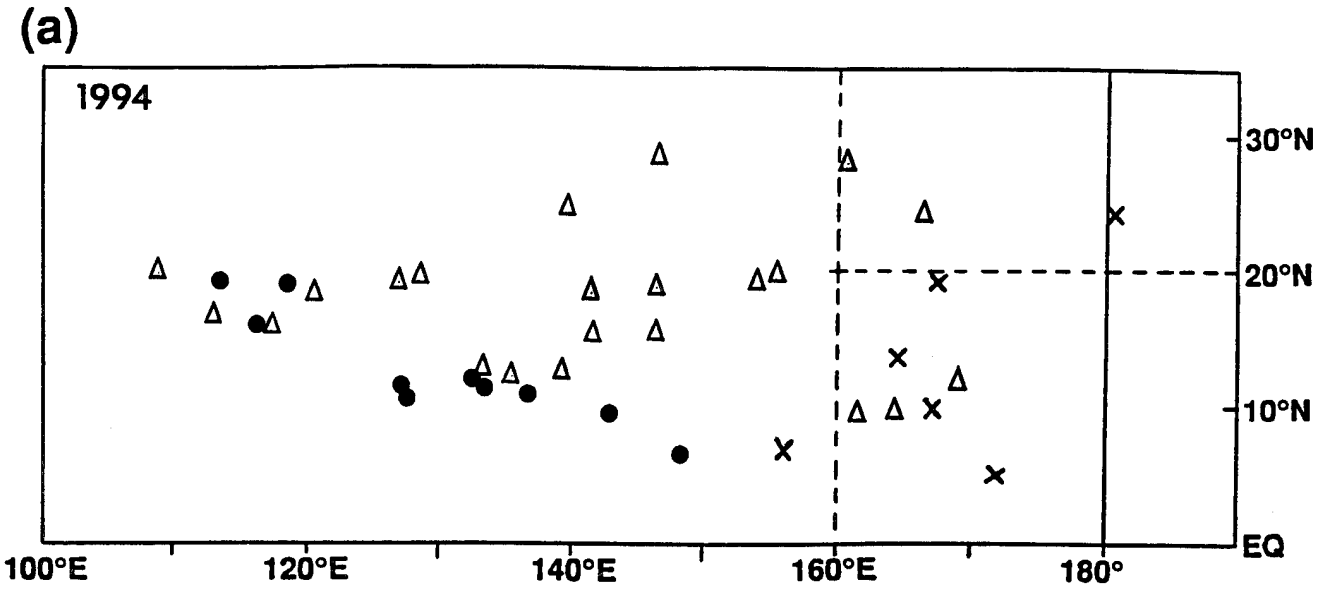

Figure 3-5a Point of formation of significant tropical cyclones in 1994 as indicated by the initial intensity of 25 kt (13 m/sec) on the best track. The symbols indicate: solid dots = 01 January to 15 July; open triangles = 16 July to 15 October; and, X = 16 October to 31 December.

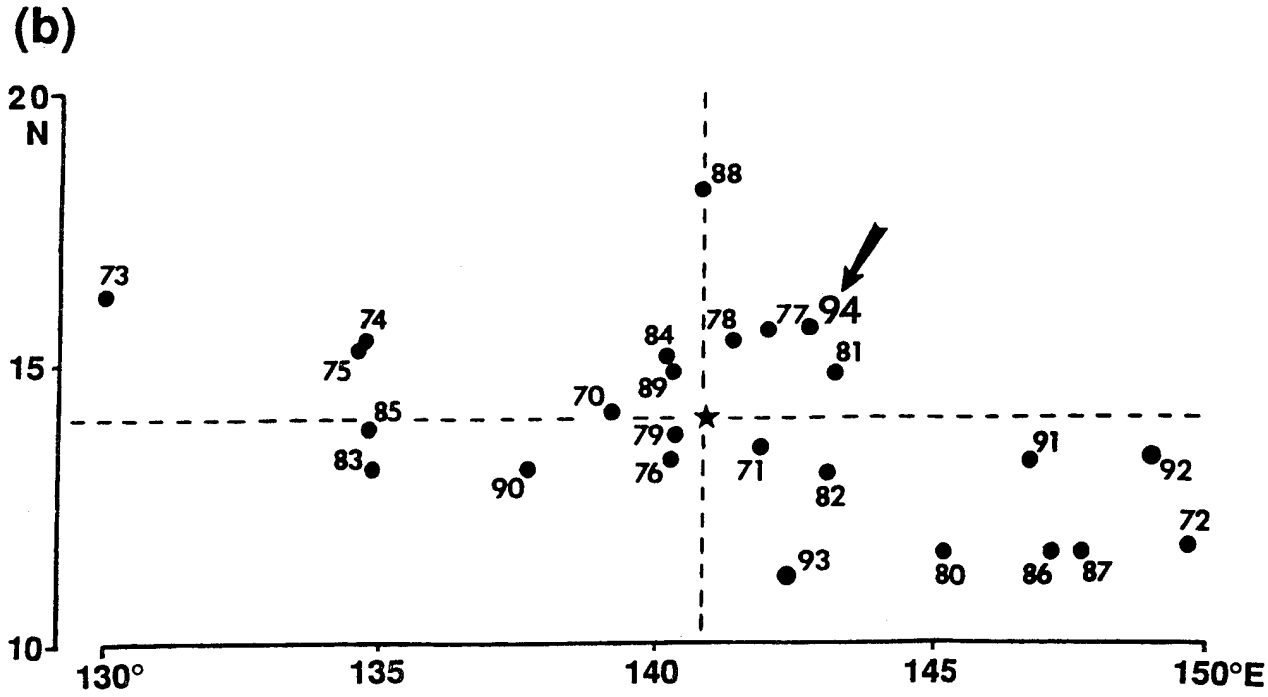

Figure 3-5b Mean annual genesis locations for the period 1970-1994. 1994's location is indicated by the arrow. The star lies at the intersection of the 25-year average latitude and longitude of genisis. For statistical puposes, genesis is defined as the first 25 kt (13 m/sec) intensity on the best track.

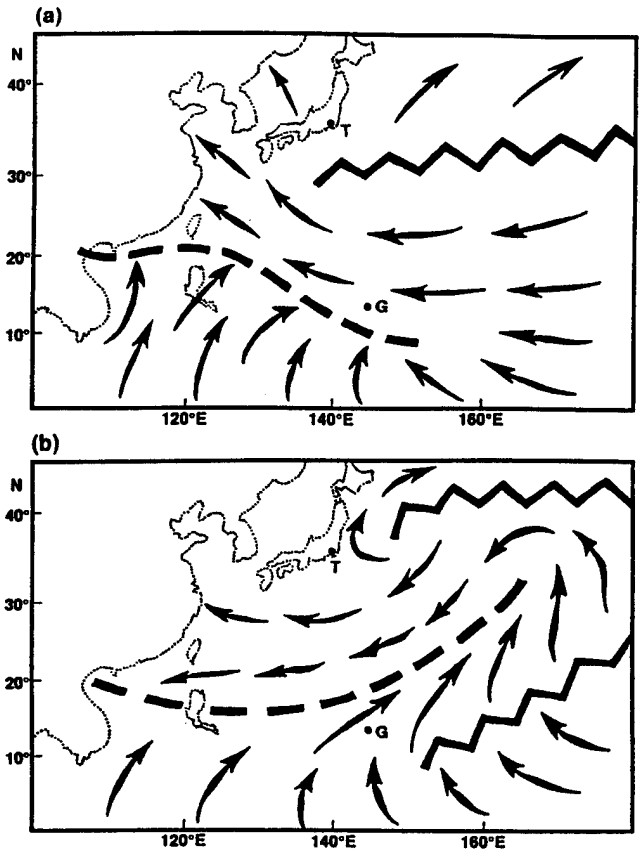

Figure 3-6 The low-level circulation during the summer in the tropics of the western North Pacific: (a) The long-term average; and (b) a schematic example of the low-level circulation associated with a reverse-oriented monsoon trough. Bold zig-zag lines indicate ridge axes, and bold dashed line indicated the axis of the monsoon trough. Arrows indicated wind direction. The locations of Guam (G) and Tokyo (T) are indicated.

In summary, an illustration of all the tropical cyclone activity in the WNP and North Indian Oceans is provided in Figure 3-7. Table 3-4 includes: a climatology of typhoons, and tropical storms and typhoons for the WNP for the period 1945-1959 and 1960-1994; and a summary of warning days. Table 3-5 is a summary of the TCFA's for the WNP for 1976-1994. Composite best tracks for the WNP Ocean tropical cyclones are provided for the periods: 01 January to 28 July (Figure 3-8), 16 July to 02 September (Figure 3-9), 20 August to 29 September (Figure 3-10), and 28 September to 26 December (Figure 3-11).

3.1.1 MONTHLY ACTIVITY SUMMARY

JANUARY

Tropical cyclone activity got off to an early start during 1994. **Tropical Depression 01W** occurred in January in the near-equatorial trough. January TCs are most properly considered to be late-season storms, born in atmospheric conditions that evolved during November and December of the previous calendar year.

FEBRUARY

The month with the lowest average number of tropical cyclones in the western North Pacific is February. In keeping with climatology, there were no significant tropical cyclones in the western North Pacific basin during February 1994.

MARCH

There were no significant tropical cyclones in the western North Pacific basin during March 1994, however, the tropical disturbance which became Typhoon Owen (02W) was first detected in late March in a near-equatorial trough in the Caroline islands.

APRIL

One tropical cyclone — **Owen (02W)** — was active during April. The tropical disturbance from which it developed formed in the Caroline islands at the end of March. Tracking westward, Owen reached peak intensity of 75 kt (39 m/sec) one day before it crossed several islands of the Philippine archipelago where three people were killed and four were reported missing. Emerging into the South China Sea, it turned northward, steadily weakened, and dissipated over water northwest of Luzon. The rest of April was quiet.

MAY

During early May, the Mei-yu front became established from Hong Kong to Japan. In the

deeper tropics, a near-equatorial trough became established across the western North Pacific between 5°N and 10°N. On 08 May, a cloud cluster in the near-equatorial trough began to organize and drift toward the northwest. Four days later, this disturbance became **Page (03W)** at a location about 300 nm (550 km) west of Guam. It continued to move northwestward and became a typhoon on 15 May. Shortly thereafter, it recurved. Page reached its peak intensity of 90 kt (46 m/sec) 30 hours after the point of recurvature. On 18 May, Page accelerated into the midlatitudes and became extratropical. The tropics then became quiet until 23 May when **Tropical Depression 04W** developed east of the Philippines. This tropical depression never became a tropical storm. It crossed the South China Sea and dissipated over Vietnam. The remainder of May was inactive as the amount of deep convection in the tropics was suppressed.

JUNE

During early June, tropical cyclone activity was focused in the South China Sea. On 04 June, **Russ (05W)** developed and moved northward toward Hong Kong. When about 100 nm (185 km) south of Hong Kong, Russ turned toward the west and went ashore in southern China just east of the Luichow peninsula on 09 June. Russ was the first of a series of tropical cyclones that hit southern China and contributed to destructive flooding. During the middle of June, deep convection increased across the western North Pacific south of 10°N to the international date line. Despite the increase of deep convection, no tropical cyclones formed until 22 June when a tropical depression formed east of the Philippines. After crossing the Philippines, this tropical depression became **Sharon (06W)** on 23 June. Sharon made landfall in central Vietnam on 28 June.

JULY

One of the busiest Julys on record, a total of nine tropical cyclones occured during the month. Tropical cyclone activity for the month began in the South China Sea with the development of **Tropical Depression 07W** south of Hong Kong on 03 July. This short-lived system moved westward and made landfall in southern China, just northeast of the Luichow Peninsula on 04 July. During the first week of July, a very intense TUTT established from the east coast of China to the international date line. South of this TUTT, large-scale deep convection increased. On 07 July, the tropical disturbance that became **Tim (08W)** appeared in the Philippine Sea. While on a northwestward track, this system rapidly reached a peak intensity of 125 kt (64 m/sec), and on 10 July, it made landfall on the east coast of Taiwan. As Tim neared the Taiwan coast, **Vanessa (09W)** formed in the South China Sea. Vanessa was short-lived, moved northeastward, and was absorbed by the circulation of the larger Tim.

On 14 July, a reverse oriented monsoon trough developed east of the Philippines. The first super typhoon of the season, **Walt (10W)** formed along the axis of this trough. Walt underwent unusual northeastward motion along the trough axis, and reached its 130 kt (67 m/sec) peak intensity on 19 July before turning back to the northwest. As Walt weakened, it slowly tracked to the west and dissipated during the early morning hours of 27 July near western Japan after a total of 50 warnings.

Along with Walt (10W), two other tropical cyclones formed along the axis of the reverse oriented monsoon trough — **Yunya (11W)**, west of Walt; and **Zeke (12W)**, northeast of Walt. Yunya developed in the South China Sea west of Luzon. It underwent unusual eastward motion and crossed Luzon from west to east on 19 July with a landfall intensity of 45 kt (23 m/sec). Heading east, Yunya dissipated over water in the Philippine Sea on 21 July. Meanwhile, Zeke (12W) developed northeast of

Walt and moved on an unusual "S-shaped" track. Zeke reached its maximum intensity of 65 kt (33 m/sec) on 22 July as it made a sharp turn toward the north. It later turned northeastward and became extratropical poleward of 40°N on 24 July.

On 24 July, the large-scale low-level circulation of the western North Pacific became organized as a monsoon gyre. **Tropical Depression 13W** developed on 25 July in a monsoon surge along the southeastern periphery of the gyre. Tropical depression 13W dissipated on 26 July. Its remnants accelerated to the north within a band of large-scale deep convection that formed a fish-hook pattern on the eastern side of the gyre.

On 28 July, the gyre that had dominated the flow gave way to a more typical monsoon cloud band stretching from the South China Sea eastward into Micronesia. On 29 July, a tropical disturbance that formed in this monsoon trough became **Brendan (14W)**. It moved rapidly to the north and was located over Korea by the end of the month. Two other tropical cyclones also formed in the monsoon trough during the last week of July — **Amy (15W)** and **Caitlin (16W)**. Amy formed in the South China Sea near Hainan Island on 28 July, and made landfall near Haiphong in northern Vietnam on 31 July. The tropical disturbance that became Caitlin formed near Guam on 29 July, and moved west-northwestward. It did not become a tropical storm until early August.

AUGUST

August 1994 was a very active month. There were a total of nine significant tropical cyclones: eight that formed during the month and one that was still active from July. On the first day of the month, Brendan, which developed in July, became extratropical in the Sea of Japan. On 02 August, Caitlin developed northeast of the Philippines and moved northwestward over Taiwan and into southeastern China. A few days later, the disturbance that became **Doug (17W)** developed east of the Philippines. It moved northwestward passing just off the northeastern tip of Taiwan. Doug then moved northward toward Korea. Close to the resort island of Cheju on 10 August, it created poor weather and gusty winds which contributed to the crash of a Korean Air Lines A-300 jet trying to land at Cheju International Airport.

On 08 August, the tropical disturbance that became **Ellie (18W)** developed in the subtropics (i.e., north of 25°N) at the base of a midlatitude trough. Ellie passed southwest of Kyushu on 13 August where wind gusts up to 87 kt (45 m/sec) were recorded. It later recurved in the Yellow Sea and dissipated over land in northeastern China. On 13 August Hurricane **Li (06E)** approached 180°E from the central Pacific, weakened as it crossed into JTWC's area of responsibility, and dissipated near Wake Island on 16 August. On 14 August, the tropical disturbance that became **Fred (19W)** became a tropical depression near 19°N ; 139°E. Fred tracked just north of Taiwan and went ashore south of Shanghai on 22 August as one of the most destructive typhoons to hit that region in decades.

On 20 August, a midlatitude trough in combination with the tropical upper tropospheric trough (TUTT) produced several areas of deep convection in the subtropics (i.e., approximately 25°N) from 160°E to the international date line. Two typhoons — **Gladys (20W)** and **Ivy (22W)** — formed in this area. Gladys was a very small tropical cyclone that had its first warning on 22 August as it moved westward. The first warning on Ivy was issued on 28 August as it moved toward the northwest.

On 25 August, a tropical disturbance in the monsoon trough became a tropical depression east of the Philippines on 25 August. This tropical depression moved across Luzon and became **Harry (21W)** on 26 August. Harry passed south of Hong Kong, crossed Hainan Island, and went ashore near Haiphong, Vietnam. It dissipated over land on 29 August.

On 28 August, **John (10E)** moved from the central Pacific across 180°E, forming and east-west chain of tropical cyclones with Gladys and Ivy. By the end of August, Gladys was approaching northern Taiwan as a typhoon, Ivy was heading northwestward near 30°N ; 159°E, and John was weakening near 29°N ; 172°E.

SEPTEMBER

September was even more active than August, with a total of 12 tropical cyclones: nine that formed during the month and three that were still active from August. On the first day of the month, Gladys, which developed in August, crossed Taiwan, and dissipated over China on 02 September. Ivy, which also developed during August, recurved far to the east of Japan and became extratropical on 03 September. John (10E), the last of the August tropical cyclones overlapping into September, weakened during the first few days of September, but on 06 September, it began to reintensify. John recurved, and on 08 September, it moved back across 180°E into the central North Pacific as a Hurricane.

During the first week of September, after Gladys (20W) moved into China, monsoon southwesterlies began to strengthen over the South China Sea and across low latitudes of the western North Pacific. **Joel (23W)**, formed in the South China Sea along the axis of the monsoon trough, moved northwestward across Hainan Island and then went ashore in Vietnam near Haiphong on 07 September. On 05 September, a large monsoon depression formed west of the Mariana island chain. A separate tropical disturbance which formed on the northeastern side of this monsoon depression broke free of it, and moved northward. This tropical disturbance became **Kinna (24W)**. Kinna recurved south of Tokyo, accelerated to the northeast, and became extratropical on 11 September. On 09 September, a tropical disturbance developed in the Philippine Sea, moved northwestward, and passed across northern Luzon. Once it entered the South China Sea, it intensified and became **Luke (25W)**. Luke moved westward and passed over Hainan Island, and then moved ashore in northern Vietnam close to where Harry (21W) and Joel (23W) had made landfall earlier.

On 10 September a monsoon depression (which later became **Melissa (26W)** formed in the Marshall Islands. The large circulation of Melissa at one point covered a substantial portion of the western North Pacific basin from 180°E to the Philippines. Melissa moved on a north-oriented "S-shaped" track. It recurved southeast of Hokkaido, Japan, on 19 September and became extratropical.

By mid-September, a reverse-oriented monsoon trough stretched from the South China Sea, east-northeastwards into the cloud bands south of Melissa's large circulation. **Nat (27W)** formed in the Philippine Sea along the axis of this monsoon trough and moved eastward. Nat followed an "S-shaped" track: initially moving eastward, it turned northward along 150°E, and recurved near 30°N. Nat dissipated over water on 22 September. On 18 September, another tropical disturbance formed in the Philippine Sea along the monsoon trough axis in approximately the same location where Nat (27W) originated. This tropical disturbance became **Orchid (28W)**. Like Nat, Orchid initially moved eastward followed by a turn to the north. On 25 September, Orchid became the fourth super typhoon of 1994. It accelerated toward the north-northeast on 28 September and made landfall on the Japanese main island of Shikoku on 29 September.

As Orchid intensified, two more tropical disturbances formed to its east along the monsoon trough axis — **Pat (29W)** and **Ruth (30W)**. Pat (29W) and Ruth (30W) underwent a binary interaction. During the night of 26 September, Pat and Ruth merged to become one tropical cyclone. The merged Pat and Ruth recurved and dissipated over open water on 28 September. On 29 September, **Tropical**

Depression 31W developed near 22°N ; 150°E in association with a TUTT cell. It dissipated over water on 03 October.

OCTOBER

The fourth consecutive month of above normal tropical cyclone activity in the western North Pacific basin had five typhoons, one of them a super typhoon, and two tropical storms. The tropical cyclones of October were notable for their longevity: three of the seven longest-lived tropical cyclones of 1994 occurred. Verne (33W), for example, persisted for more than half the month, and required 66 warnings.

On the first day of the month, the tropical disturbance that became **Seth (32W)** formed in the Marshall Islands. This disturbance moved toward the west-northwest, intensified, and passed south of Guam as a tropical storm on 05 October. Seth reached a peak intensity of 120 kt (62 m/sec) while southeast of Taiwan on 07 October. It later skirted the northeastern tip of Taiwan, recurved along the China coast south of Shanghai, and went ashore in Korea where wind gusts to near 70 kt (36 m/sec) and rainfall in excess of 300 mm (11.8 inches) were experienced. Seth became extratropical in the Sea of Japan on 11 October.

The three days 12 through 14 October were the only days during the month without a tropical cyclone active in the western North Pacific basin. During the period 15 to 20 October, three tropical cyclones — **Teresa (34W)**, **Verne (33W)**, and **Wilda (35W)** — formed in a monsoon trough which stretched east-west across Micronesia. On 21 October, the westernmost of the three, Teresa, crossed the Philippine Islands very close to Manila. Loss of life was reported. On 19 October, the middle tropical cyclone, Verne (33W), passed very close to the island of Rota in the Mariana Island chain. Verne later stalled in the Philippine Sea west of Guam before recurving and moving northeastward, well east of Japan. The easternmost tropical cyclone of these three, Wilda (35W), formed north of the Marshall Island group on 19 October. It moved westward, and then stalled for 24-hours northeast of Saipan where high winds downed trees and power lines, and pulled tin roofs from houses. Eleven people were injured in typhoon-related accidents. Wilda then moved turned north-northeastward and moved on an unusual "S-shaped" track. It was accelerating into the midlatitudes on the last day of the month.

Toward the end of the month, a tropical disturbance developed east of the international date line at relatively high latitude (25°N), in direct association with a TUTT cell. This disturbance moved rapidly westward, crossed the international date line, and became **Yuri (36W)** on 24 October. Yuri slowed, turned north, and dissipated over water on 27 October.

And finally, **Zelda (37W)** formed and spent the majority of its life in November. As Verne (33W) and Wilda (35W) were undergoing extratropical transition on the last day of October, Zelda (37W) was intensifying near 10°N ; 150°E.

NOVEMBER

Zelda (37W) was located southeast of Guam and intensifying as the month of November began. It became a typhoon on 02 November, moved west-northwestward and passed directly over Anatahan (a small island of the Northern Marianas located about 70 nm (130 km) north of Saipan). The large eye of Zelda passed over Anatahan where the homes and crops of the 39 residents were devastated. On 05 November, Zelda reached peak intensity of 135 kt (69 m/sec), making it the sixth and final super typhoon of 1994. Zelda recurved and dissipated over water south of Japan on 08 November.

Despite the presence of a near-equatorial trough, and westerly low-level winds extending to the international date line, deep convection was largely absent over most of the area, and no significant tropical cyclones formed in the western North Pacific basin during November.

DECEMBER

The first half of December was very quiet, continuing the break in tropical cyclone activity that began in early November. Amounts of deep convection began to increase in the Marshall Islands during mid-December in association with a twin-trough monsoon flow pattern. Two tropical cyclones — **Axel (38W)** and **Bobbie (39W)** — began as tropical disturbances that formed in the Marshall Islands in the near-equatorial trough of the northern hemisphere. On 16 December, Axel reached minimal tropical storm intensity while passing well south of Guam. Moving steadily westward along about 10°N, Axel crossed through the Philippine Archipelago on 21 December where at least 12 people died.

While Axel was intensifying in the Philippine Sea on 17 December, the final tropical cyclone of 1994, Bobbie (39W) was forming in the southern Marshall Islands. Bobbie moved toward the west-northwest, and reached peak intensity of 50 kt (26 m/sec) on 22 December. On 23 December, it passed north of Saipan with winds of 45 kt (23 m/sec). Bobbie had no significant impact on Saipan or on other islands of the Northern Marianas. On Christmas Day, Bobbie dissipated as a significant tropical cyclone, closing out the 1994 tropical cyclone season. The remainder of December was quiet, as deep convection and tropical cyclone activity shifted to the southern hemisphere.

3.1.2 IMPACTS OF THE TROPICAL CYCLONES OF 1994

Twenty-three of the 41 significant tropical cyclones in the western North Pacific basin during 1994 made landfall in Asia. The Philippine islands were especially hard hit with eight significant landfalling tropical cyclones. Other countries experiencing significant impacts from landfalling tropical cyclones were Taiwan (three major landfalling typhoons and two close passes), Korea (one major landfalling typhoon — Seth (32W) — one tropical storm, and a damaging close pass by Doug (17W)), China (eleven significant tropical cyclones made landfall somewhere along its extensive coastline), Japan (only one major typhoon — Orchid (28W) — and one tropical storm), the Ryukyu Islands (three major typhoons passed through the southern end of this island chain), Vietnam (four significant landfalling tropical cyclones), and the islands of Micronesia (Saipan and Anatahan of the Northern Mariana island group were severely impacted by Zelda (37W)). The greatest loss of life occurred in southern China where the landfall of three tropical cyclones — Russ (05W), Sharon (06W), and Tropical Depression 07W contributed to widespread flooding that left more than 1,400 people dead. The damage, which included the destruction of nearly one million houses in southern China, was estimated in excess of US$6 billion. Loss of life also occurred in the Philippines and Taiwan. Reports of the loss of life due to the impact of tropical cyclones in any of the other countries were not received. The greatest loss of life at sea occurred when a Maltese oil tanker, the *Thanassis A*, sank in the South China Sea in heavy seas associated with Teresa (34W) and the northeast monsoon. Seventeen people were reported to be dead or missing and nineteen other crew members were rescued. The JTWC received no additional reports indicating loss of life at sea.

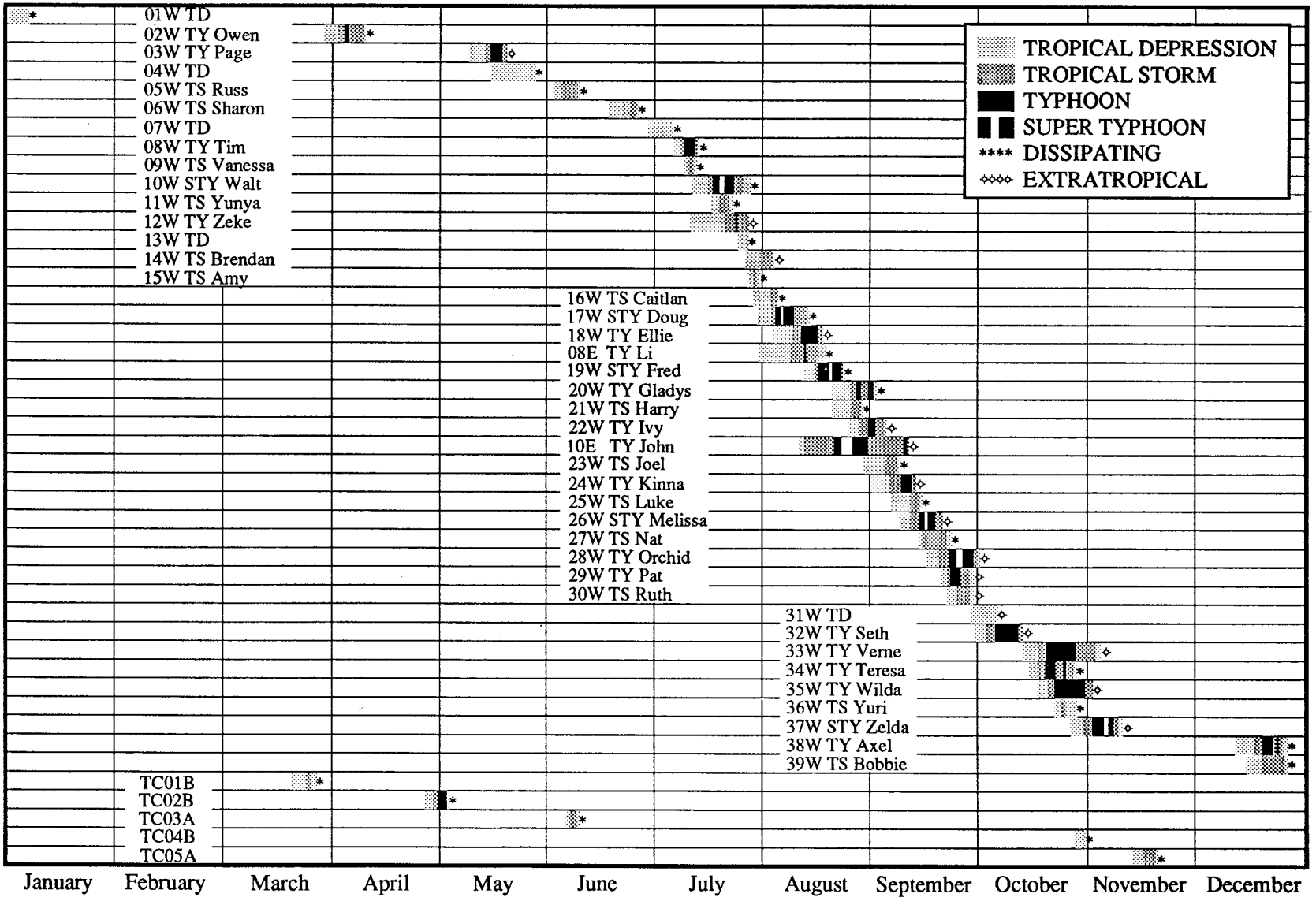

Figure 3-7 Chronology of western North Pacific and North Indian Ocean tropical cyclones for 1994.

Table 3-3 Individual 1978-1994 tropical cyclone (TC) track types. The observed track classes are defined as straight moving (SM), recurving (R), north-oriented (NO), "S"-track (S), and "other". Further subdivisions of the "other" category are indicated by icons: ■ = TC remained in or near South China Sea for its whole life; ⩘ = TC made many loops and meanders but made little overall forward progress; O = TC formed in Mei-yu cloud band and tracked rapidly to the northeast; < = TC formed over open Pacific and died over water after a short track; c = TC formed in the lee of Taiwan during conditions of monsoonal southwesterly flow and tracked northward then westward around the top of Taiwan to make landfall on the China coast.

YEAR	SM	R	NO+S	OTHER	■	<	⩘	O	c
1978	5	10	10	7	4	3	-	-	-
1979	9	12	2	5	2	2	1	1	-
1980	10	7	6	5	4	1	1	-	-
1981	11	7	5	6	2	2	1	-	1
1982	9	5	7	6	2	1	1	2	-
1983	11	5	4	5	4	1	1	-	-
1984	6	5	11	8	5	3	1	-	-
1985	7	3	9	8	5	2	1	-	-
1986	9	12	2	3	1	1	1	1	-
1987	7	2	10	5	2	3	-	-	-
1988	9	4	8	5	2	-	1	2	1
1989	15	5	9	6	3	3	-	-	-
1990	8	11	5	7	5	1	-	-	1
1991	11	14	2	4	3	1	1	-	-
1992	8	11	9	4	3	1	-	-	-
1993	15	10	4	8	2	6	-	-	-
1994	15	6	13	5	4	1	-	-	-
	165	129	116	97	53	32	10	6	3

Table 3-4 WESTERN NORTH PACIFIC TROPICAL CYCLONES

TYPHOONS

(1945 - 1959)

	JAN	FEB	MAR	APR	MAY	JUN	JUL	AUG	SEP	OCT	NOV	DEC	TOTALS
MEAN	0.3	0.1	0.3	0.4	0.7	1.0	2.9	3.1	3.3	2.4	2.0	0.9	16.4
CASES	5	1	4	6	10	15	29	46	49	36	30	14	245

(1960 - 1994)

	JAN	FEB	MAR	APR	MAY	JUN	JUL	AUG	SEP	OCT	NOV	DEC	TOTALS
MEAN	0.3	0.1	0.2	0.4	0.7	1.1	2.7	3.4	3.3	3.2	1.7	0.7	17.9
CASES	10	2	8	15	25	38	96	118	116	113	61	24	626

TROPICAL STORMS AND TYPHOONS

(1945 - 1959)

	JAN	FEB	MAR	APR	MAY	JUN	JUL	AUG	SEP	OCT	NOV	DEC	TOTALS
MEAN	0.4	0.1	0.5	0.5	0.8	1.6	2.9	4.0	4.2	3.3	2.7	1.2	22.2
CASES	6	2	7	8	11	22	44	60	64	49	41	18	332

(1960 - 1994)

	JAN	FEB	MAR	APR	MAY	JUN	JUL	AUG	SEP	OCT	NOV	DEC	TOTALS
MEAN	0.5	0.3	0.5	0.6	1.1	1.9	4.3	5.6	5.1	4.3	2.7	1.2	27.9
CASES	19	9	17	22	38	65	149	195	177	150	94	43	978

Table 3-5 TROPICAL CYCLONE FORMATION ALERTS FOR THE WESTERN NORTH PACIFIC OCEAN 1976-1994

YEAR	INITIAL TCFAS	TROPICAL CYCLONES WITH TCFAS	TOTAL TROPICAL CYCLONES	FALSE ALARM RATE*	PROBABILITY OF DETECTION
1976	34	25	25	26%	100%
1977	26	20	21	23%	95%
1978	32	27	32	16%	84%
1979	27	23	28	15%	82%
1980	37	28	28	24%	100%
1981	29	28	29	3%	96%
1982	36	26	28	28%	93%
1983	31	25	25	19%	100%
1984	37	30	30	19%	100%
1985	39	26	27	33%	96%
1986	38	27	27	29%	100%
1987	31	24	25	23%	96%
1988	33	26	27	21%	96%
1989	51	32	35	37%	91%
1990	33	30	31	9%	97%
1991	37	29	31	22%	94%
1992	36	32	32	20%	100%
1993	50	35	38	30%	92%
1994	50	40	40 **	20%	100%
(1976-1994) MEAN:	35.4	27.4	28.8	23%	95%
TOTALS:	637	493	519		

* The false alarm rate is the difference between the number of initial TCFA's and the number of tropical cyclones with TCFA's divided by the number of inital TCFA's and is expressed as a percentage.

** Note: The total of 40 tropical cyclones (TCs) results from 41 TCs minus two (TC08E and 10E), plus one for the regeneration of TC38W.

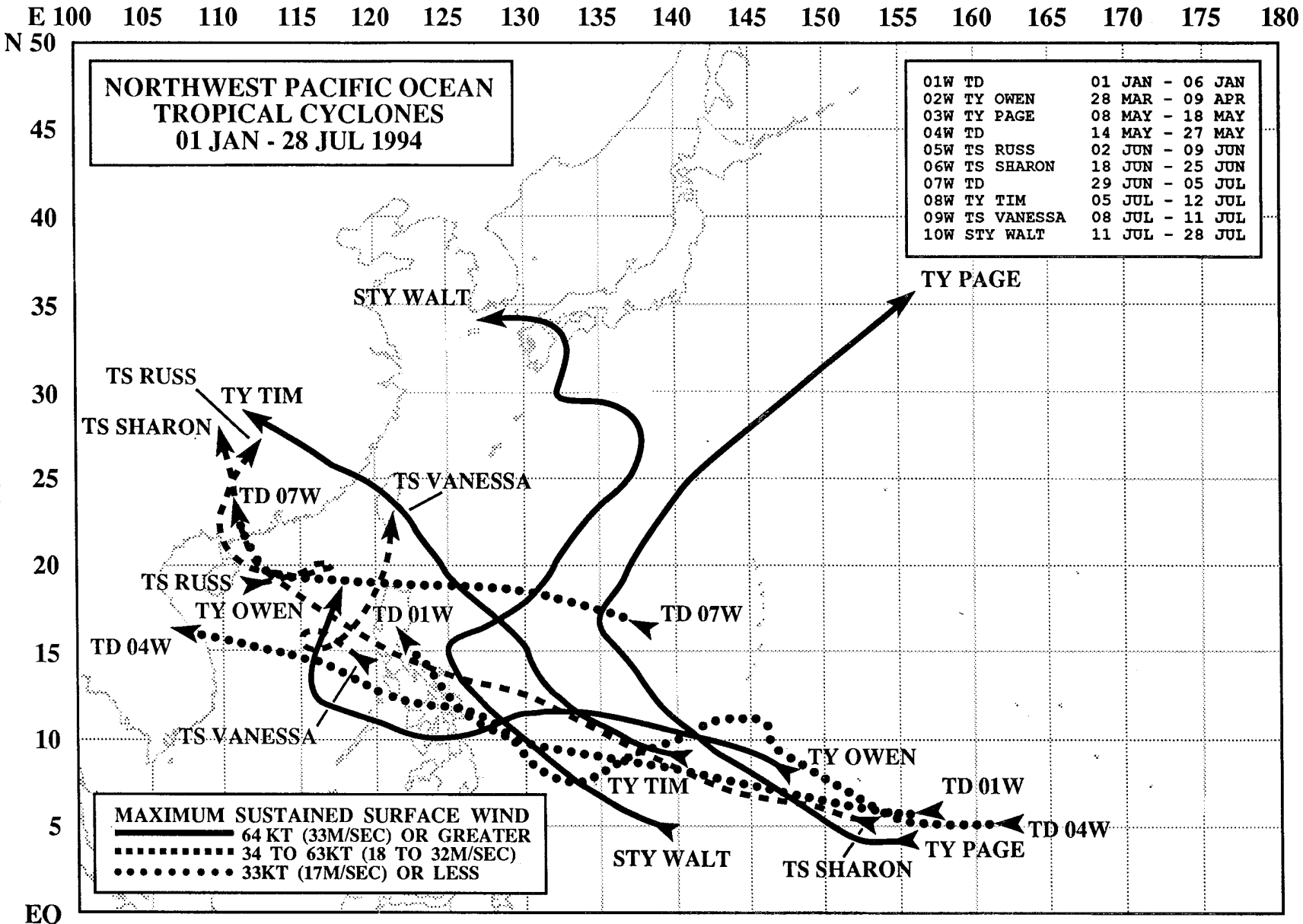

Figure 3-8 Composite best tracks for the North West Pacific Ocean tropical cyclones for the period 1 January to 28 July 1994.

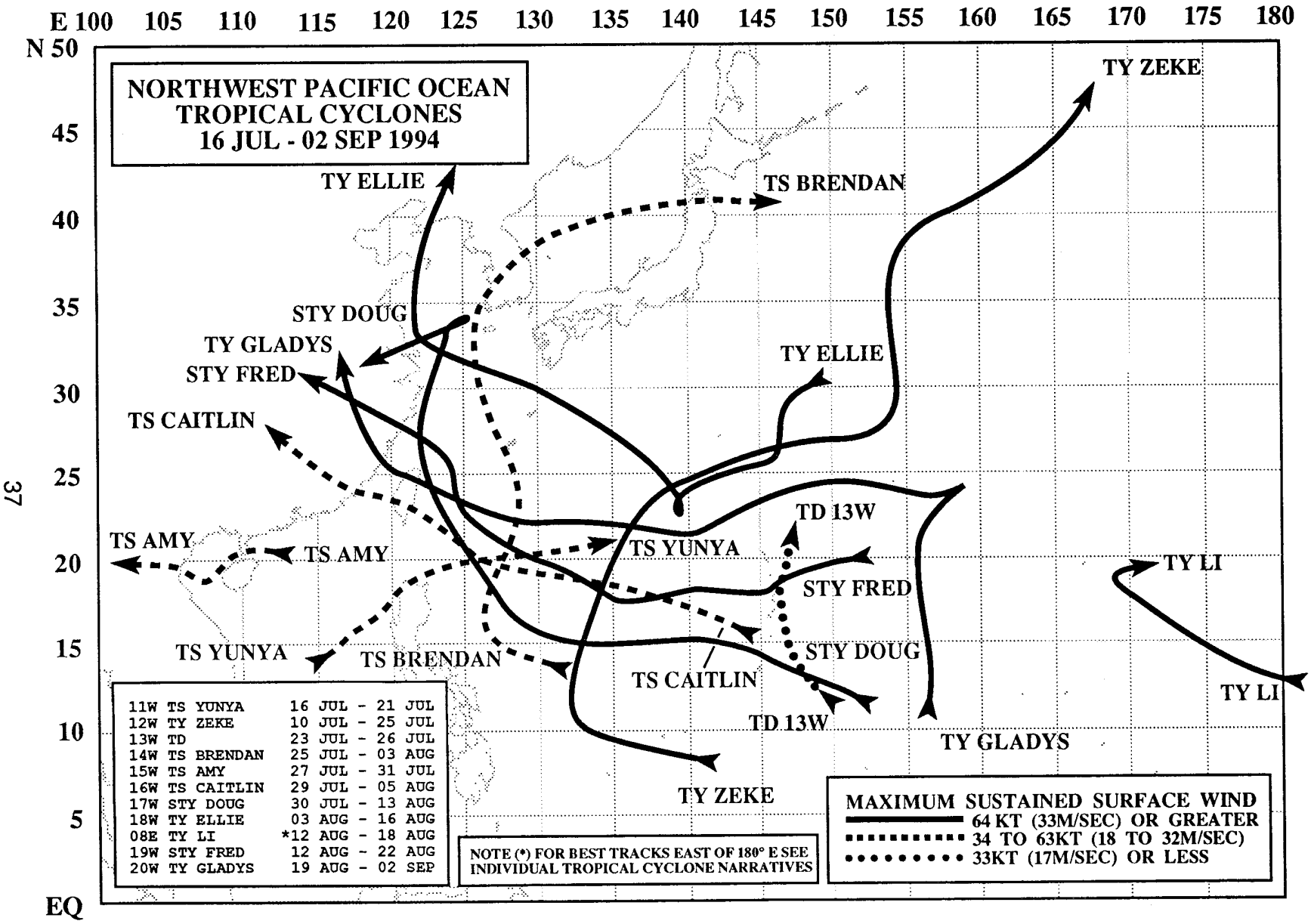

Figure 3-9 Composite best tracks for the North West Pacific Ocean tropical cyclones for the period 16 July to 02 September 1994.

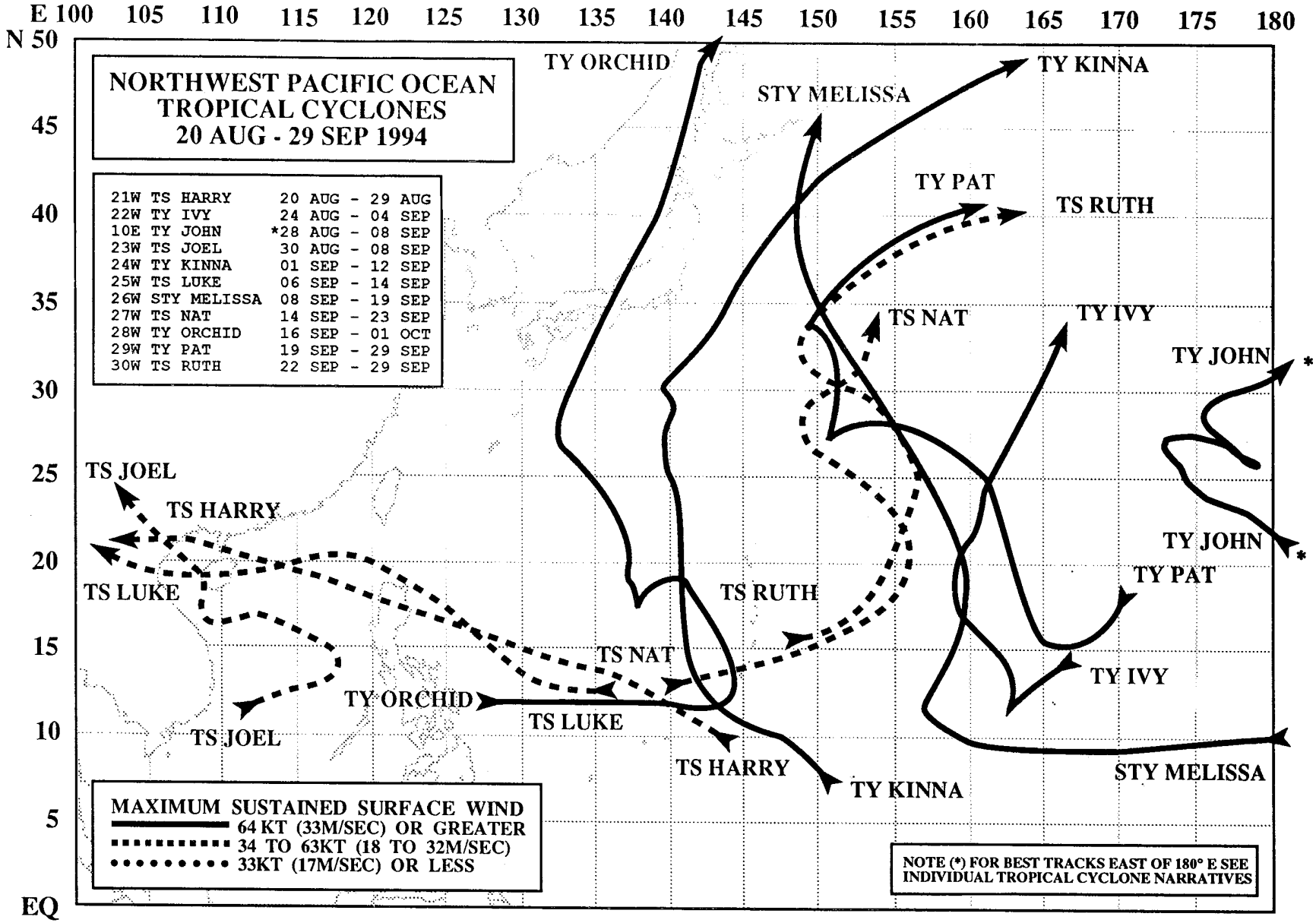

Figure 3-10 Composite best tracks for the North West Pacific Ocean tropical cyclones for the period 20 August to 29 September 1994.

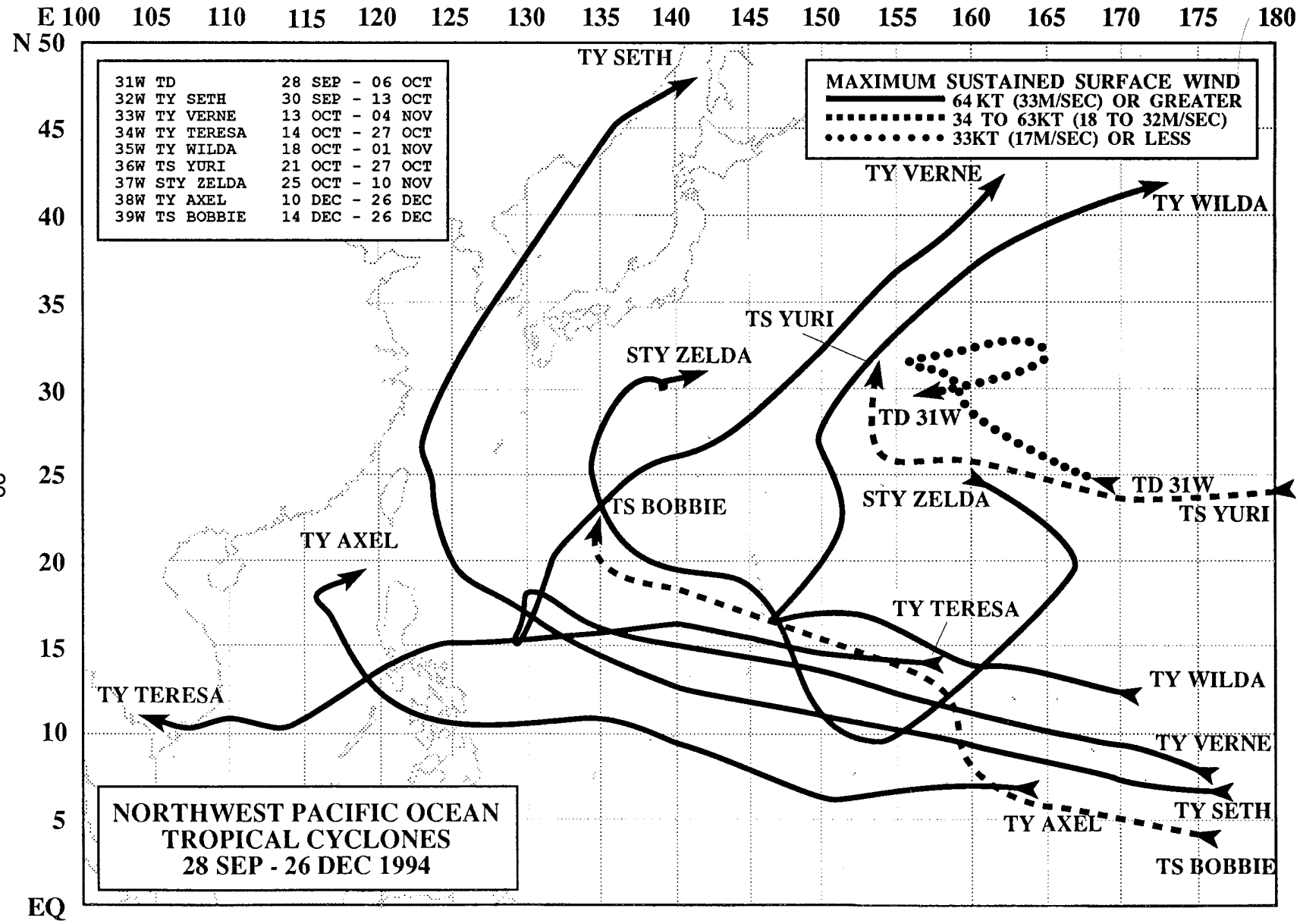

Figure 3-11 Composite best tracks for the North West Pacific Ocean tropical cyclones for the period 28 September to 26 December 1994.

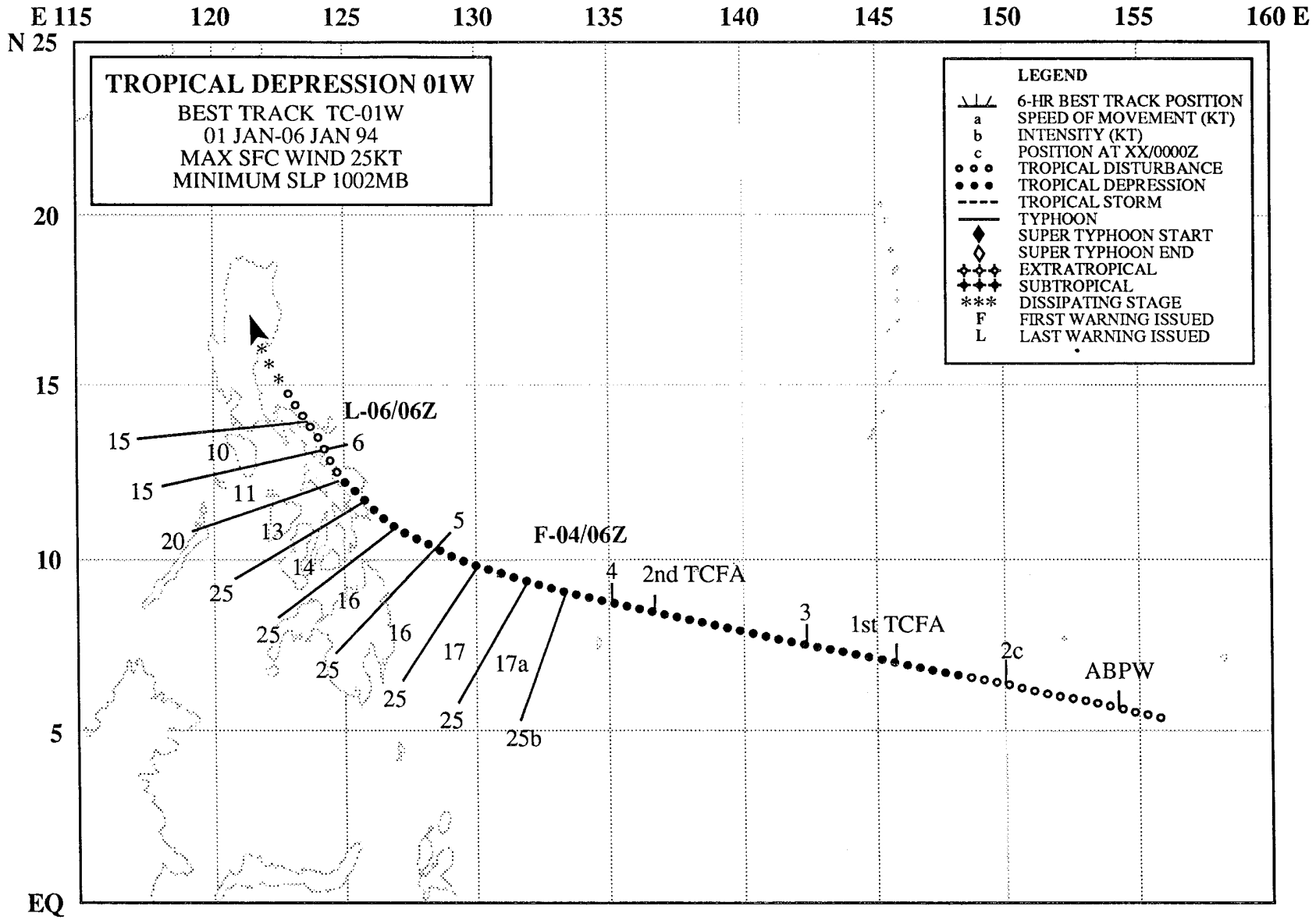
E 115
120
125
130
135
140
145
150
155
160 E
N 25
20
15
10
5
EQ
TROPICAL DEPRESSION 01W
BEST TRACK TC-01W
01 JAN-06 JAN 94
MAX SFC WIND 25KT
MINIMUM SLP 1002MB
LEGEND
6-HR BEST TRACK POSITION
a SPEED OF MOVEMENT (KT)
b INTENSITY (KT)
c POSITION AT XX/0000Z
TROPICAL DISTURBANCE
TROPICAL DEPRESSION
TROPICAL STORM
TYPHOON
SUPER TYPHOON START
SUPER TYPHOON END
EXTRATROPICAL
SUBTROPICAL
*** DISSIPATING STAGE
F FIRST WARNING ISSUED
L LAST WARNING ISSUED
L-06/06Z
F-04/06Z
2nd TCFA
1st TCFA
2c
ABPW
25b

TROPICAL DEPRESSION 01W

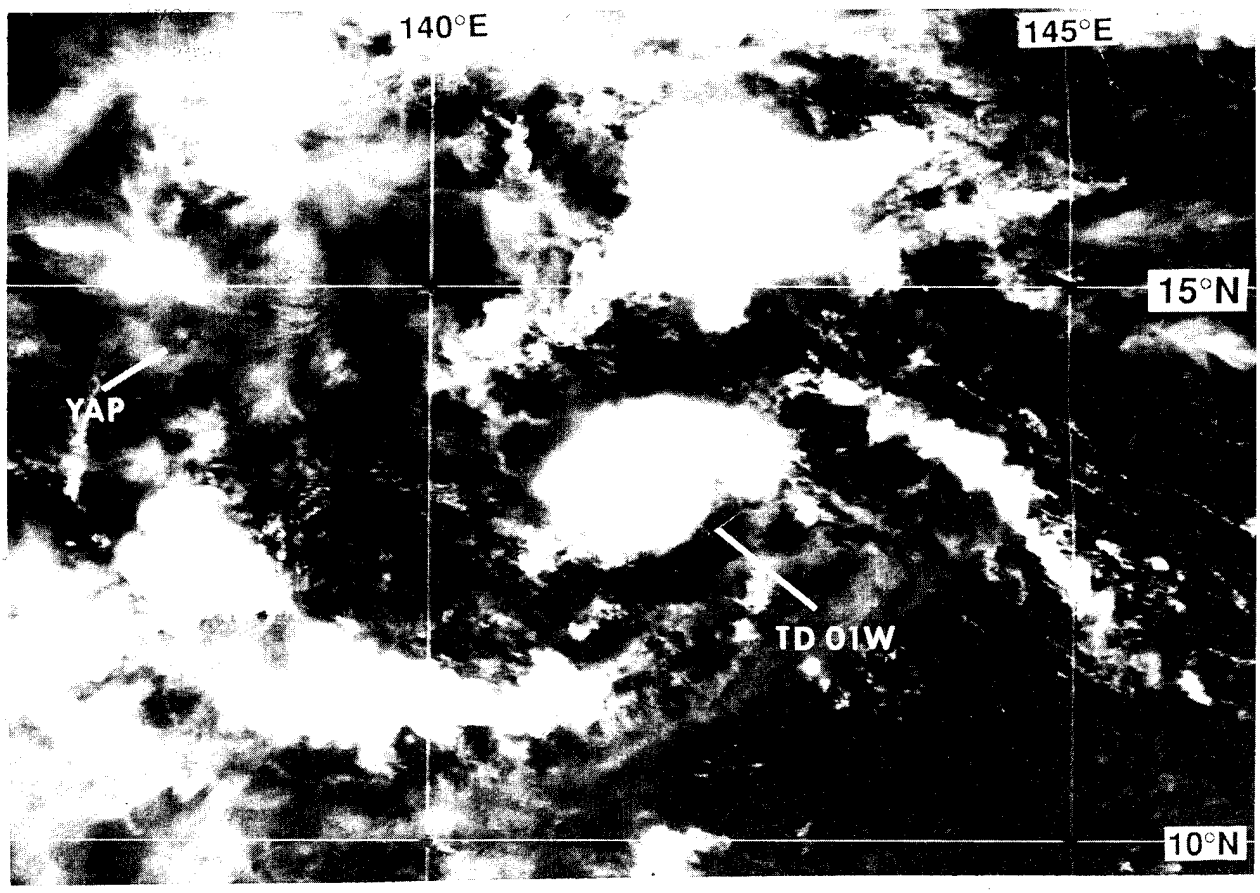

Figure 3-01-1 The disturbance which would later become TD 01W shows cyclonically curved lines of cumulonimbus clouds surrounding a small central cluster of deep convection (030231Z January visible GMS imagery).

I. HIGHLIGHTS

The first significant tropical cyclone of 1994 in the western North Pacific, Tropical Depression 01W reached a maximum intensity of only 25 kt (13 m/sec). Tropical Depression 01W formed in the near-equatorial trough of the Northern Hemisphere at a time when the monsoon trough of the Southern Hemisphere was also active.

II. TRACK AND INTENSITY

Tropical Depression 01W was first detected as a poorly organized area of cloudiness in the near-equatorial trough in the eastern Caroline islands. The disturbance was first mentioned on the 010600Z January Significant Tropical Weather Advisory. An increase in convective organization and a gradient-level wind of 30 kt (15 m/sec) at Chuuk (WMO 91334) prompted a Tropical Cyclone Formation Alert at 021400Z. During the daylight hours of 03 January (022100Z to 030800Z) the disturbance lost much of its deep convection; and, although it retained organized curved cloud lines (Figure 3-01-1), it had yet to intensify into a significant tropical cyclone. A dramatic flare-up of deep convection between 031800Z and 040000Z, that produced a large cold cirrus cloud shield with anticyclonic outflow, prompted a second Tropical Cyclone Formation Alert which was issued at 031900Z followed by the first warning at 040600Z. This first cold cloud shield collapsed by evening (040600Z), and the intensity was held at 25

kt (13 m/sec). A second flare-up of deep convection between 041800Z and 050000Z resulted in another large cold cirrus cloud shield. The system appeared to be somewhat sheared with the low-level circulation center located at the southeastern edge of this cloud shield. Synoptic wind and pressure reports and satellite intensity estimates indicated that the system had still failed to mature and the intensity was kept at 25 kt (13 m/sec). At 051200Z, Tropical depression 01W made landfall on the island of Samar in the central Philippines. Convection became disorganized and synoptic reports from land and ships indicated that the disturbance was weakening. The last warning on Tropical Depression 01W was issued at 060600Z as the system tracked along the east coast of Luzon, and lost its deep convection.

III. DISCUSSION

Tropical Depression 01W was forming in the Northern Hemisphere near-equatorial trough at the same time as the Australian Northwest Monsoon was reaching a peak of activity. When the first Tropical Cyclone Formation Alert was issued for Tropical Depression 01W, two named tropical cyclones, Rewa (05P) and Oscar (06S), and a tropical disturbance were active in the Australian region of the monsoon trough of the Southern Hemisphere (Figure 3-01-2). Tropical Depression 01W formed in a wind pattern with some similarity to the twin-trough pattern that is commonly observed during the simultaneous occurrence of tropical cyclones on both sides of the equator. In this case, however, the southern monsoon trough was clearly dominant and further from the equator than the northern near-equatorial trough.

Another interesting feature of the evolution of Tropical Depression 01W was the strong diurnal periodicity of the flare-up of large cold cirrus shields near the circulation center. On two occassions, once on the early morning of 04 January, and again during the early morning of 05 January, a large mesoscale convective system developed on the northwestern side of the circulation center and produced an extensive area of very cold dense cirrus cloud cover. During the afternoon, after both of these early morning flare-ups, the convection collapsed and the cirrus canopy thinned. Despite the increase of convection near the low-level circulation center, Tropical Depression 01W failed to intensify. A possible reason may be the presence of persistent southeasterly shear across the system. A large-scale collapse of the Australian Northwest Monsoon occurred concurrently with the dissipation of Tropical Depression 01W.

IV. IMPACT

Although Tropical Depression 01W brought heavy rains to some areas of the Philippine Islands, no reports of significant damage or fatalities were received.

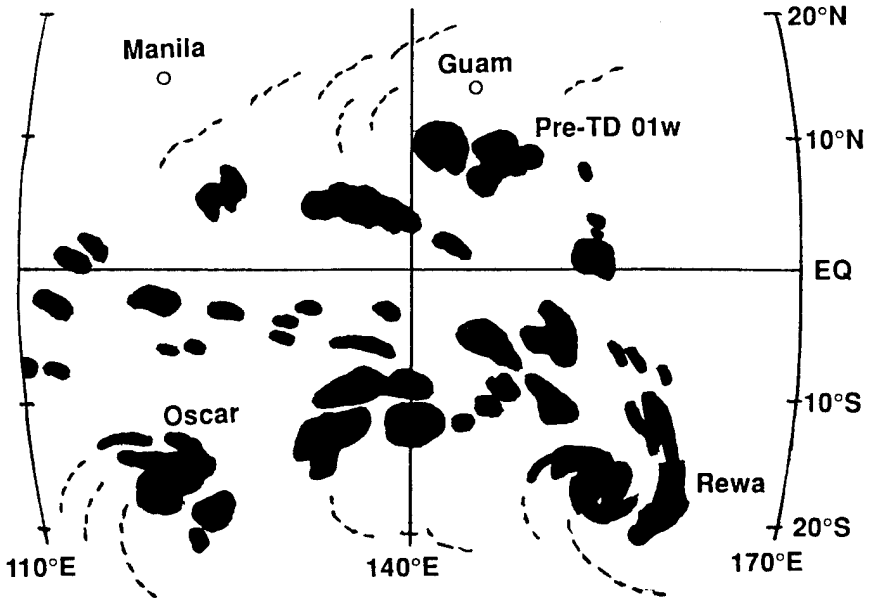

Figure 3-01-2 Cloud silhouettes adapted from the 021234Z infrared GMS imagery show two named tropical cyclones — Rewa (05P) and Oscar (06S) — along the axis of low pressure of an active Australian monsoon. The disturbance which would later intensify to become Tropical Depression 01W is seen south of Guam. Thin dashed lines show streamers of high-thin cirrus.

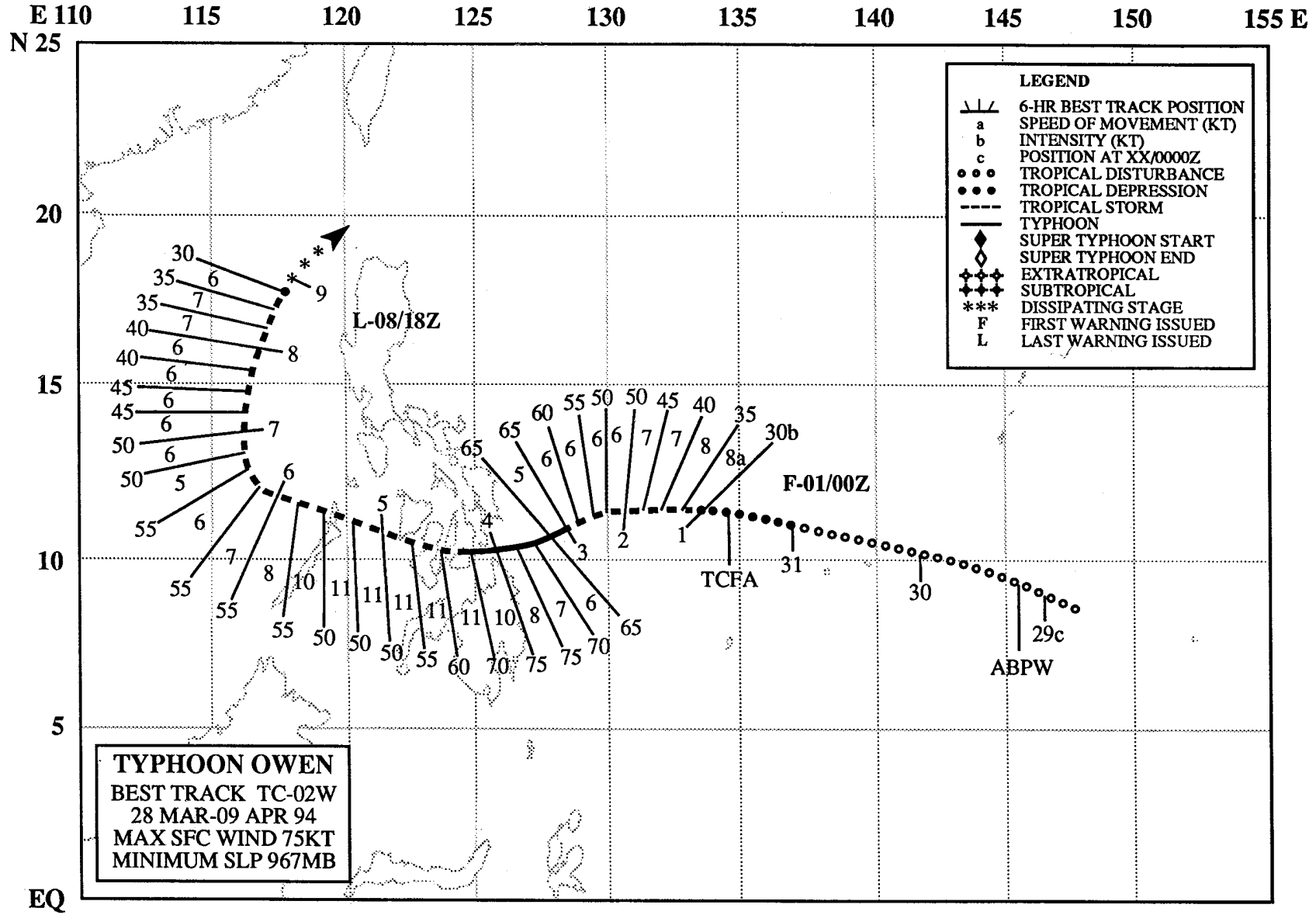
E 110
115
120
125
130
135
140
145
150
155 E
N 25
20
15
10
5
EQ
LEGEND
6-HR BEST TRACK POSITION
a SPEED OF MOVEMENT (KT)
b INTENSITY (KT)
c POSITION AT XX/0000Z
TROPICAL DISTURBANCE
TROPICAL DEPRESSION
TROPICAL STORM
TYPHOON
SUPER TYPHOON START
SUPER TYPHOON END
EXTRATROPICAL
SUBTROPICAL
*** DISSIPATING STAGE
F FIRST WARNING ISSUED
L LAST WARNING ISSUED
L-08/18Z
F-01/00Z
TCFA
ABPW
TYPHOON OWEN
BEST TRACK TC-02W
28 MAR-09 APR 94
MAX SFC WIND 75KT
MINIMUM SLP 967MB

TYPHOON OWEN (02W)

I. HIGHLIGHTS

Unusual southwestward motion brought Owen from the Philippine Sea across the southern islands of the Philippine Archipelago. Like many typhoons which track across the Philippine islands on a southwestward trajectory, Owen was small-sized. Until typhoon intensity was diagnosed, Owen was not forecast to reach typhoon intensity

II. TRACK AND INTENSITY

During the last week of March, there was extensive deep convection in Micronesia associated with a near-equatorial trough in the region. The first mention of a tropical disturbance embedded within this large-scale cloudiness over Micronesia appeared on the 290600Z March Significant Tropical Weather Advisory. On 30 March, deep convection flared along the equator in association with low-level westerly winds. The disturbance (pre-Owen) in the near-equatorial trough appeared to be shearing and losing its separate identity in the extensive cloudiness. By 31 March, the equatorial cloudiness had collapsed, and a distinct cloud cluster appeared in the near-equatorial trough that exhibited cyclonic curvature. A Tropical Cyclone Formation Alert was issued at 311800Z, followed by a warning at 010000Z.

Owen's development was contrary to expectations. It was not forecasted to become a typhoon until satellite imagery at 030000Z April indicated typhoon intensity. The presence of upper-level shear from the southeast, large diurnal fluctuations in the amount and organization of Owen's deep convection, and interaction with the Philippine Islands were considered to be factors unfavorable for intensification.

Also unanticipated was Owen's southwestward motion during the two days prior to landfall in the Philippine islands. At 020600Z, Owen began to move toward the west-southwest. By the time it passed between the islands of Leyte and Mindanao, Owen had lost nearly 1.5° of latitude. The peak intensity of 75 kt (39 m/sec) was reached shortly before passage between these two islands (Figure 3-02-1). Owen weakened to tropical storm intensity as it crossed several islands of the Philippine archipelago. Emerging into the South China Sea, it turned northward, steadily weakened, and dissipated over water northwest of Luzon. The final warning was issued at 090000Z.

III. DISCUSSION

Typhoons have occurred in the month of April for fifteen of the past 36 years. Of these, six (including Owen) have made landfall in the Philippine Islands. Four (including Owen) of these six moved into the Philippine Archipelago near the island of Samar, one struck northern Luzon, and another moved westward at very low latitude (6°N) and crossed over the southern end of Mindanao.

Owen's west-southwestward motion prior to landfall in the Philippines was somewhat unusual. Climatology for the region indicates northwestward motion. Of the six typhoons impacting the Philippines in April during the past 36 years, only two — Owen and Wanda (1971) — were moving west-southwestward at landfall. Owen's later recurvature in the South China Sea at low latitude (13°N) is about 3° south of the average latitude of recurvature for all tropical cyclones in that region during April.

IV. IMPACT

As Owen swept across the central Philippines, three people were killed and four were reported missing. On the island of Cebu, more than 7000 villagers living in the coastal areas were affected by flash

floods. Emerging into the South China Sea west of the Philippine islands, Owen passed to the south of the drilling rig, SEDCO 709 (11.6°N ; 118.9°E). Maximum sustained winds measured on the rig were 50 kt (26 m/sec) with a peak gust of 67 kt (35 m/sec). No damage or fatalities were reported on the rig.

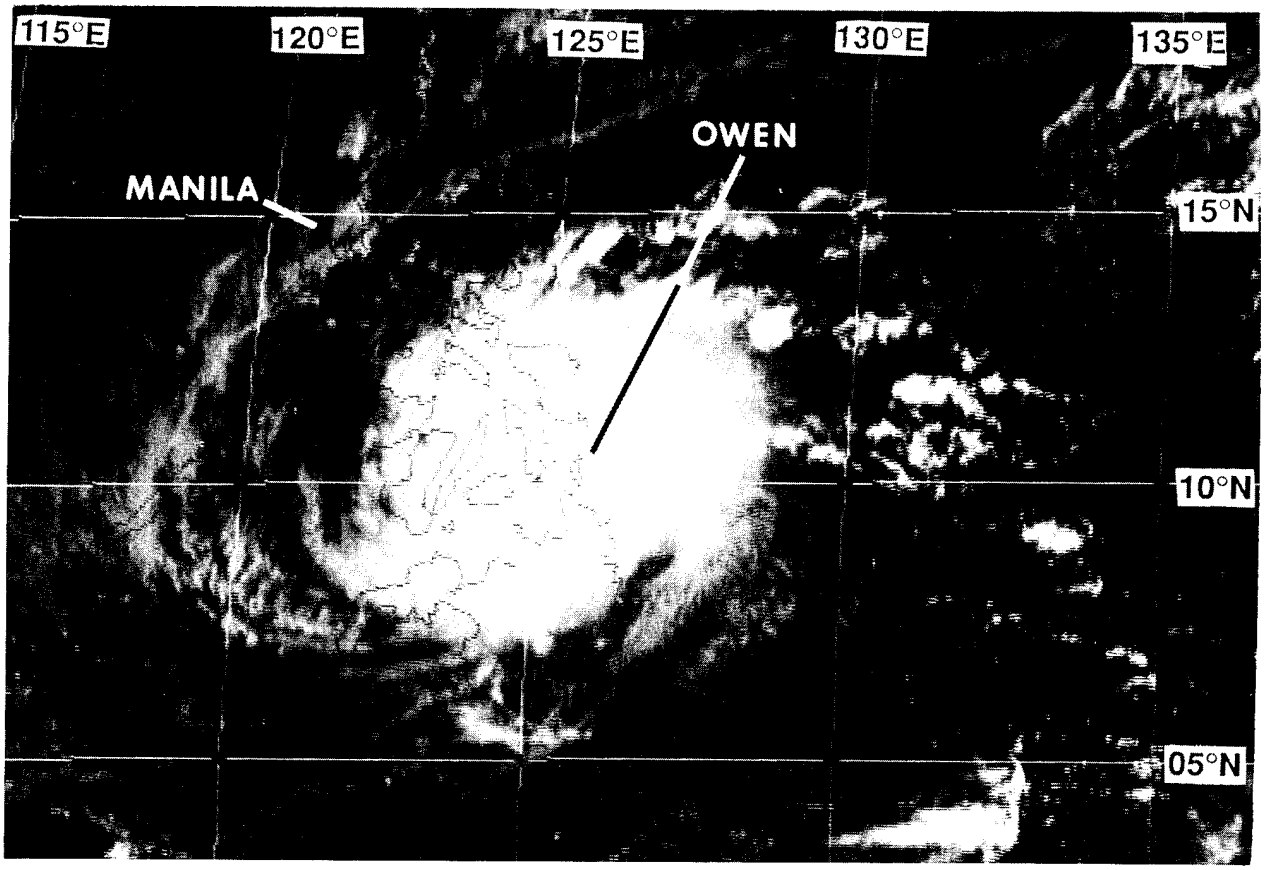

Figure 3-02-1 Owen passes between the islands of Leyte and Mindanao at its peak intensity of 75 kt (39 m/sec) (0322331Z April visible GMS imagery)

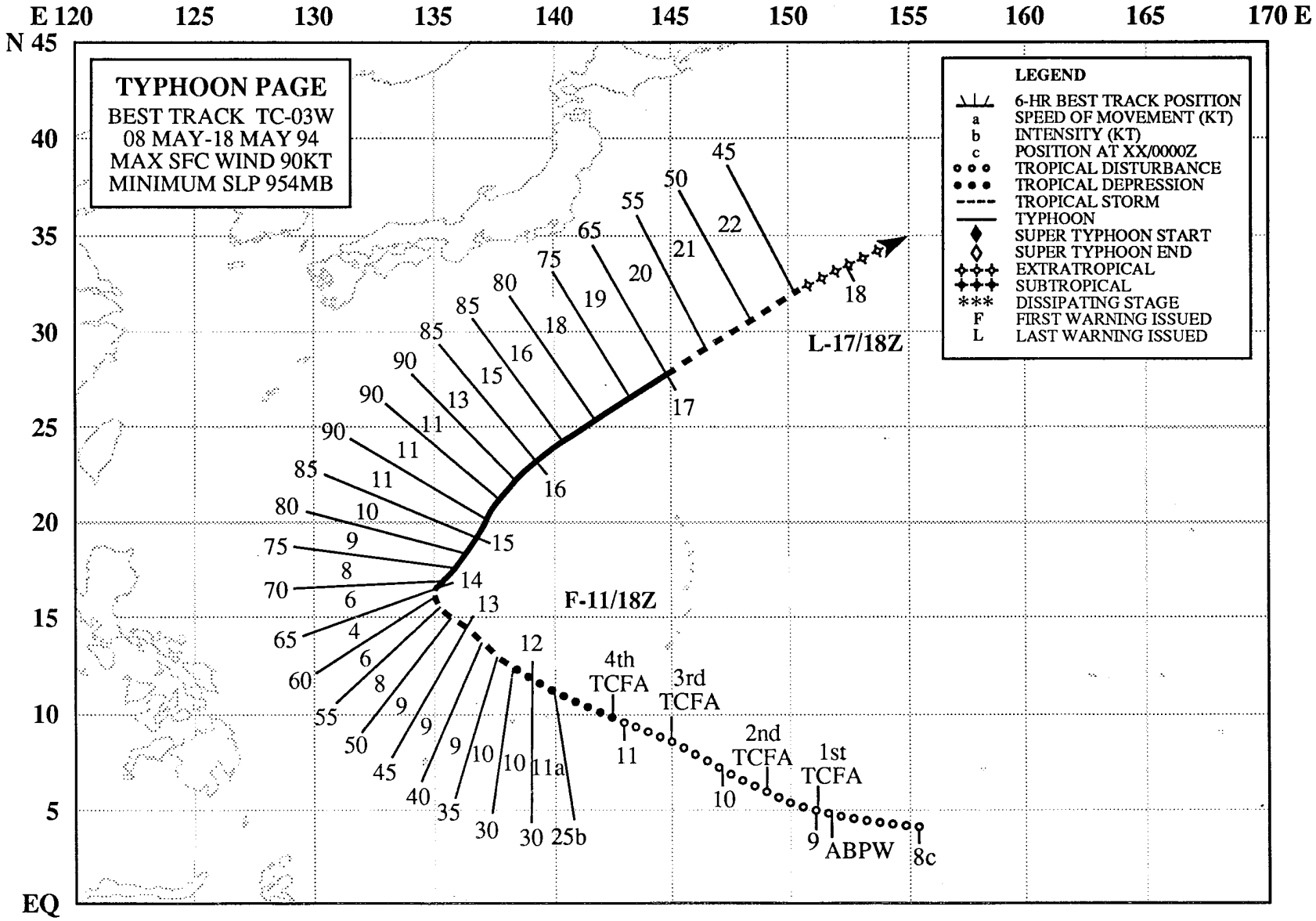
E 120
125
130
135
140
145
150
155
160
165
170 E
N 45
40
35
30
25
20
15
10
5
EQ
TYPHOON PAGE
BEST TRACK TC-03W
08 MAY-18 MAY 94
MAX SFC WIND 90KT
MINIMUM SLP 954MB
LEGEND
6-HR BEST TRACK POSITION
a SPEED OF MOVEMENT (KT)
b INTENSITY (KT)
c POSITION AT XX/0000Z
TROPICAL DISTURBANCE
TROPICAL DEPRESSION
TROPICAL STORM
TYPHOON
SUPER TYPHOON START
SUPER TYPHOON END
EXTRATROPICAL
SUBTROPICAL
*** DISSIPATING STAGE
F FIRST WARNING ISSUED
L LAST WARNING ISSUED
L-17/18Z
F-11/18Z
4th TCFA
3rd TCFA
2nd TCFA
1st TCFA
ABPW
8c
25b
11a

TYPHOON PAGE (03W)

I. HIGHLIGHTS

Forming at very low latitude in the northern of twin near-equatorial troughs (i.e., one trough north of the equator, and the other south of the equator); Page was very slow to develop, with four Tropical Cyclone Formation Alerts issued prior to the first warning. Page was one of relatively few tropical cyclones that reach peak intensity well past the point of recurvature. The recurvature of Page was not well-anticipated, and the average 72-hour forecast error of 475 nm (880 km) was the largest for any western North Pacific typhoon during 1994.

II. TRACK AND INTENSITY

During the first week of May, there was extensive deep convection in Micronesia associated with a near-equatorial trough in the region. On 08 May, a flare-up of deep convection in the eastern Caroline Islands was included as a suspect area on the 081800Z May Significant Tropical Weather Advisory. By the morning of 09 May, visible satellite imagery indicated an increase in the organization of the deep convection in this tropical disturbance, and synoptic reports confirmed the presence of a low-level circulation center located near 5°N 153°E. The first of four Tropical Cyclone Formation Alerts was issued at 082355Z. A second Tropical Cyclone Formation Alert was issued at 091330Z because the estimated location of the low-level circulation center was nearing the edge of the previous alert box. The disturbance failed to intensify, but since conditions were deemed favorable for intensification, a third Tropical Cyclone Formation Alert was issued at 101330Z. By the evening of 11 May, a large convective band formed to the north of the estimated low-level circulation center, but the overall organization of deep convection within the system still did not indicate an increased intensity, so the fourth Tropical Cyclone Formation Alert was issued at 110530Z. During the early morning hours of 12 May, the organization of the deep convection improved rapidly, and the first warning was issued at 111800Z.

Page moved steadily on a northwestward track and slowly intensified during the 42 hours following the first warning. At 131200Z, the system abruptly slowed and began its turn toward the northeast, reaching its point of recurvature at 131800Z. Page became a typhoon at 140000Z. At 150000Z, thirty hours after the point of recurvature, Page's intensity peaked at 90 kt (46 m/sec) (Figure 3-03-1). After recurvature, Page gradually accelerated to a maximum forward speed of 22 kt (41 km/hr). The final warning was issued at 171800Z as Page began its transition to an extratropical low about 600 miles east-southeast of Tokyo.

III. DISCUSSION

a. Forecast performance

The average track forecast errors for Page were the worst for any typhoon during 1994. The main factor contributing to these large average errors was a failure to anticipate the recurvature of Page (Figure 3-03-2a). The NOGAPS model and its derived track guidance (Figure 3-03-2b) gave early indications of recurvature, but the repetition of numerical forecasts of northward motion during a period of ongoing westward motion eroded the forecasters confidence in the numerical guidance. As a result, JTWC forecasters relied more on a consensus of various climatological, statistical and dynamic aids, which correctly indicated a decrease in the forward speed of motion, but were late to forecast recurvature.

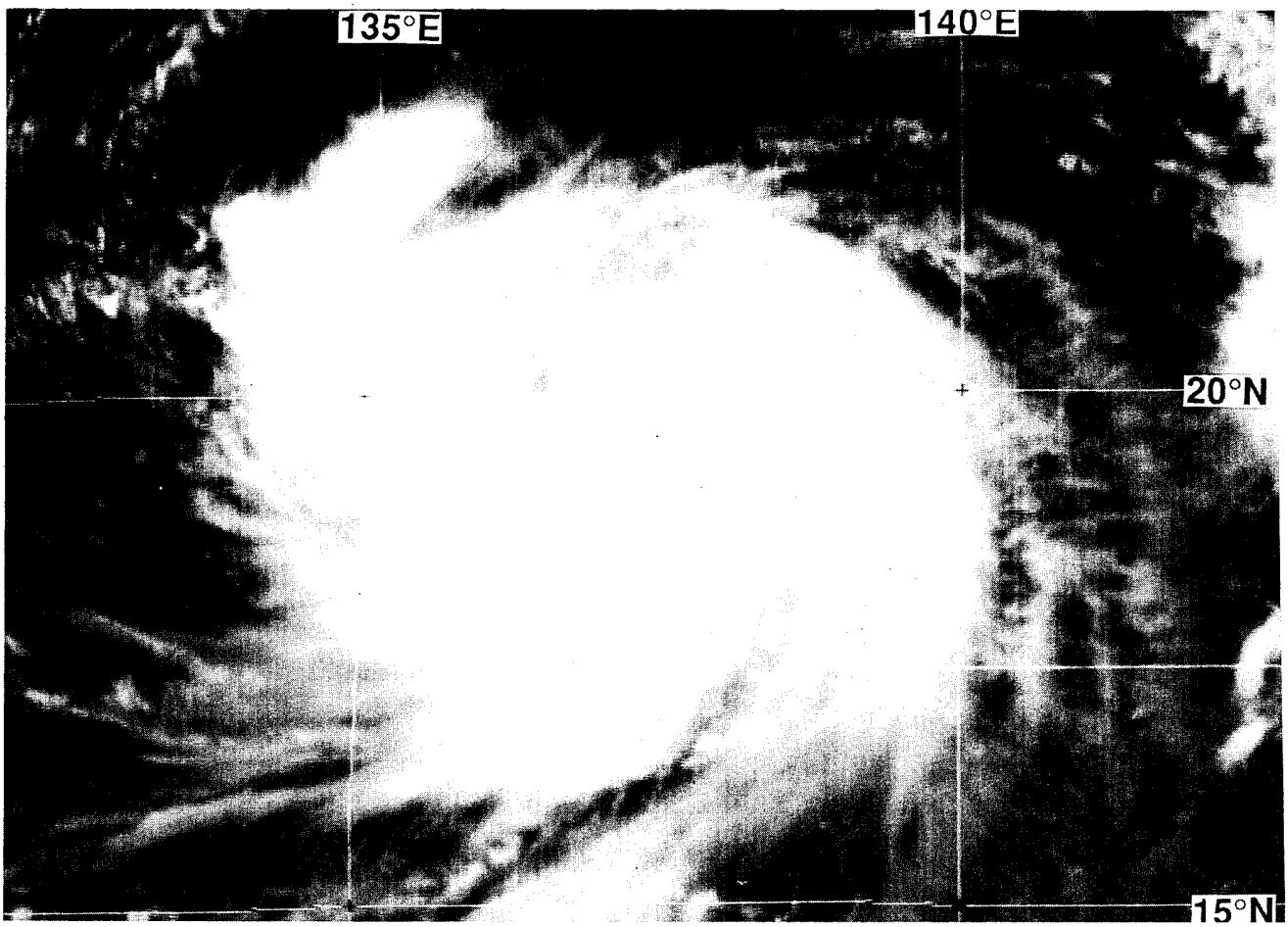

Figure 3-03-1 Page at peak intensity (150231Z May visible GMS imagery).

b. Peak intensity after recurvature

Of 77 cases of typhoons that exhibited classical recurvature (i.e., a roughly "<"-shaped track that features initial steady west-northwestward motion, then a northward turn while slowing, followed by an acceleration toward the northeast) during the period 1978 to 1993, about three-fourths (57) reached peak intensity at, or before, the point of recurvature (Figure 3-03-3); where the point of recurvature is identified as that point where the typhoon reaches its western-most longitude as it moves poleward. A much smaller group (seven) reached peak intensity 24 hours or more after the point of recurvature. Page reached its peak intensity of 90 kt (46 m/sec) 30 hours after the point of recurvature placing it in the very small group of typhoons that have waited that long. Another interesting feature of Figure 3-03-3, is an apparent relationship (represented by the best-fit curve) between typhoon peak intensity and its timing with respect to the point of recurvature. The higher the peak intensity of a recurving typhoon, the greater the delay of recurvature with respect to the timing of the peak intensity. Of the 30 recurving typhoons reaching peak intensities of 120 kt (62 m/sec) or greater during the period 1978 to 1993, only three reached peak intensity after recurvature. On average, recurving typhoons attaining peak intensities less than 120 kt (62 m/sec) reached peak intensity about 12 hours prior to the point of recurvature; recurving typhoons attaining peak intensities of 120 kt (62 m/sec) or greater reached peak intensity about 48 hours prior to the point of recurvature.

(a)

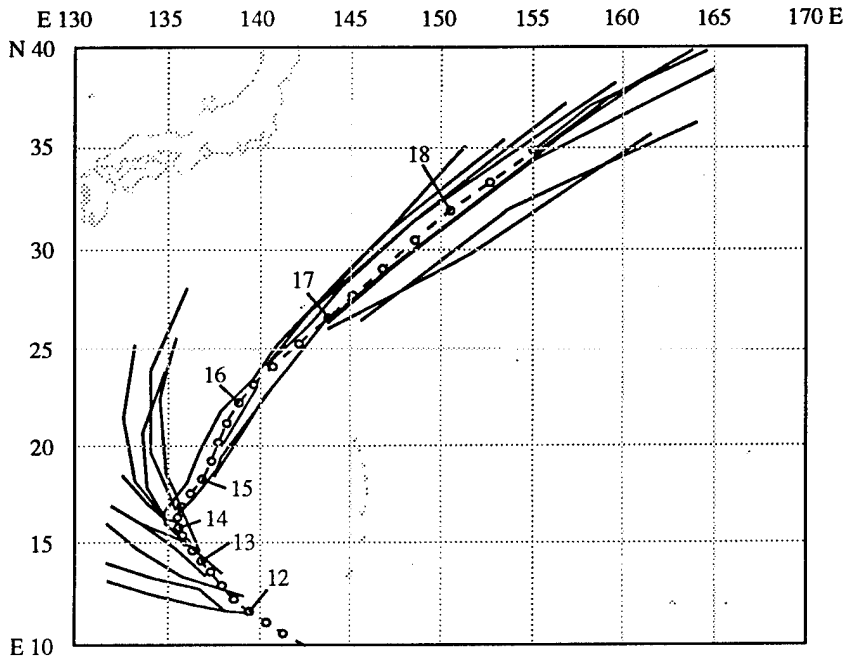

(b)

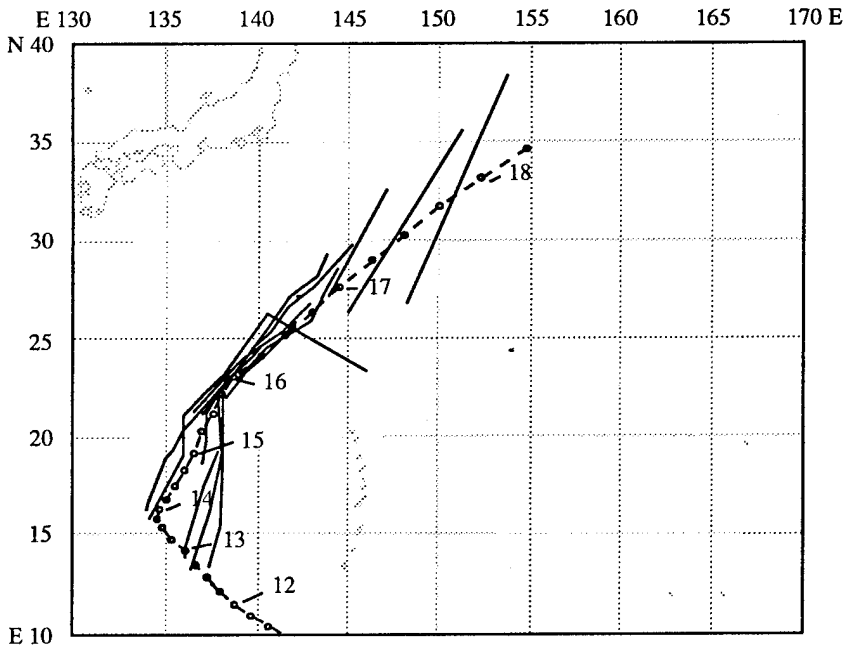

Figure 3-03-2 (a) JTWC forecast tracks prior to the point of recurvature of Page. (b) NOGAPS forecast tracks prior to the point of recurvature of Page.

IV. IMPACT

Typhoon Page remained over open ocean its entire life, and no reports of fatalities or significant damage were received. Large westerly swell generated by Page while it was in the Philippine Sea impacted the western shores of the Mariana Islands. Several tourists required rescue from high surf and strong currents along Guam's western reefs.

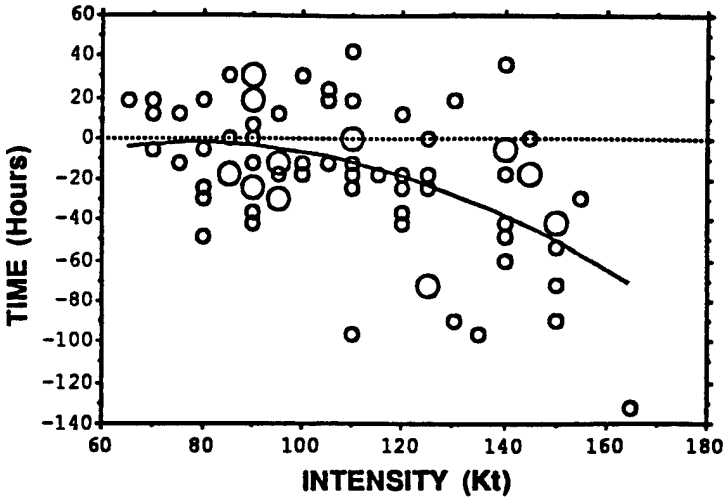

Figure 3-03-3 Timing of peak intensity (kt) with respect to the time of recurvature (+/- hours) versus peak intensity for 77 recurving typhoons during the period 1978 to 1993. Open circles indicate individual typhoons, larger open circles indicate more than one typhoon occupies that point on the graph. A circle on the dashed zero line is indicative of a typhoon that reached peak intensity at the same time that it reached its point of recurvature; typhoons reaching peak intensity after recurvature are plotted above this line, those reaching peak intensity prior to recurvature are plotted below. The best-fit second-order polynomial is indicated by the curve defined by: $Y = -58.315 + 1.453 X - .009 X2$. If the peak intensity, X, is known, this equation estimates the number of hours, Y, between the time of peak intensity and the time when the typhoon reaches its point of recurvature.

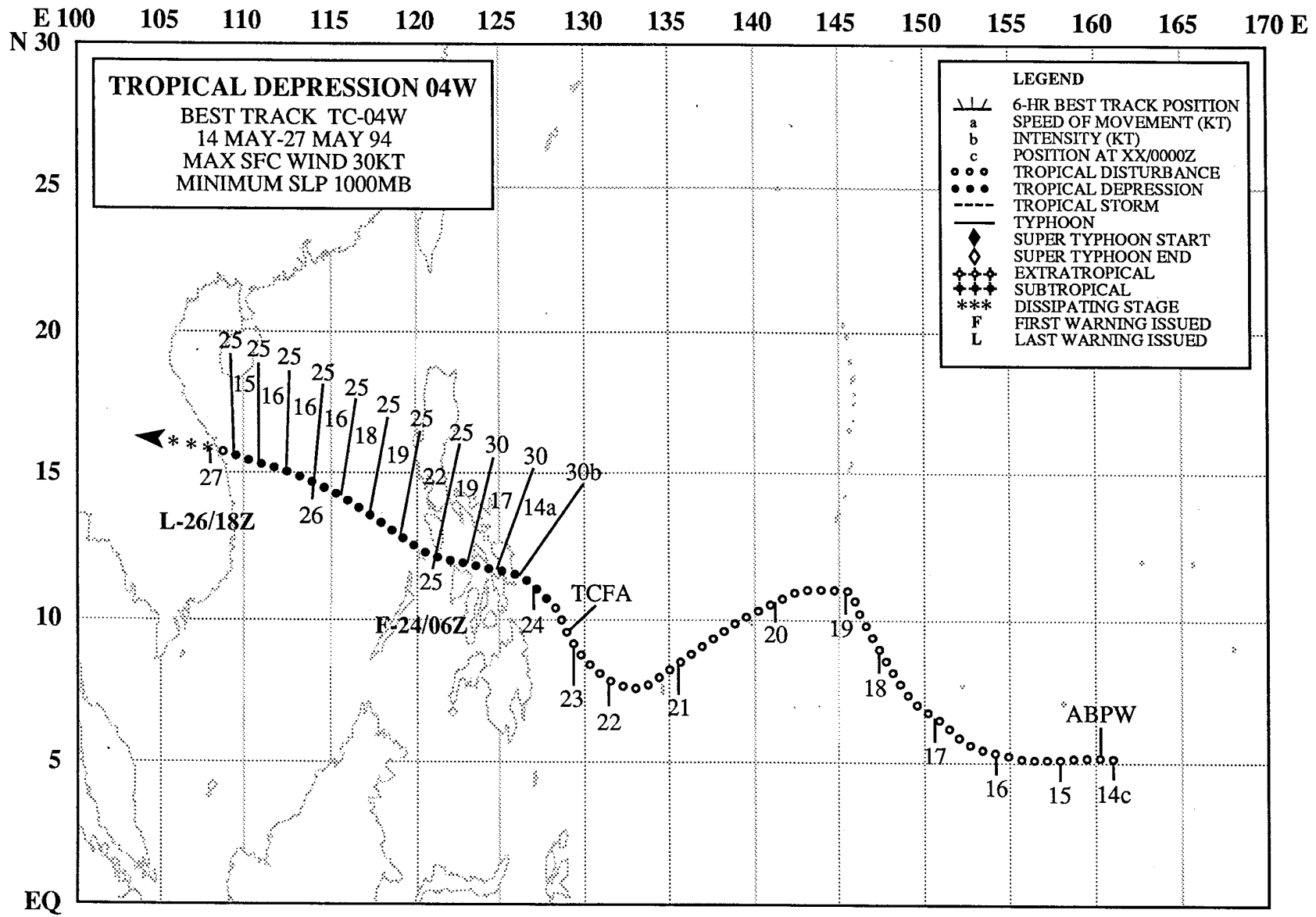
E 100 105 110 115 120 125 130 135 140 145 150 155 160 165 170 E
N 30
25
20
15
10
5
EQ
TROPICAL DEPRESSION 04W
BEST TRACK TC-04W
14 MAY-27 MAY 94
MAX SFC WIND 30KT
MINIMUM SLP 1000MB
LEGEND
6-HR BEST TRACK POSITION
a SPEED OF MOVEMENT (KT)
b INTENSITY (KT)
c POSITION AT XX/0000Z
TROPICAL DISTURBANCE
TROPICAL DEPRESSION
TROPICAL STORM
TYPHOON
SUPER TYPHOON START
SUPER TYPHOON END
EXTRATROPICAL
SUBTROPICAL
*** DISSIPATING STAGE
F FIRST WARNING ISSUED
L LAST WARNING ISSUED
L-26/18Z
F-24/06Z
TCFA
ABPW

TROPICAL DEPRESSION 04W

As Typhoon Page (03W) was undergoing its recurvature, westerly monsoonal winds extended eastward at low latitude into the eastern Caroline Islands. An area of deep convection straddled the equator which was associated with a weak cyclonic circulation near Kosrae. This weak circulation was first mentioned on the 140600Z May significant tropical weather advisory. For about five days, the weak low-level circulation moved west-northwestward toward Guam, however, convection failed to consolidate in the center. As the disturbance neared Guam it turned to the west-southwest and passed very close to Palau at 210600Z. After passing Palau, the system turned northwestward into the Philippine Sea. SSM/I imagery at 230101Z indicated a well-defined low-level circulation center. Visible and infrared satellite imagery also indicated an increase in organization of the system and a consolidation of deep convection near the low-level circulation center. These data prompted the issuance of a Tropical Cyclone Formation Alert at 230600Z. As the system neared the Philippines, the amount of deep convection near the low-level center increased, and the first warning was issued at 240600Z. Tropical Depression 04W entered the South China Sea by 250600Z. Twice, once while over the Philippine islands, and again 24 hours later over water west of Luzon, a large mesoscale convective system (MCS) formed near the center of Tropical Depression 04W and produced an extensive cold cirrus cloud shield (Figure 3-04-1a,b). On both occasions, the MCS began to grow explosively at sunset, with the maximum extent of cold cirrus observed during the pre-dawn hours. After the decay of the second large MCS during the daylight hours of 26 May, the low-level circulation center of Tropical Depression 04W moved westward and made landfall along the coast of central Vietnam. The final warning was issued at 261800Z. No reports of damage or injuries were received.

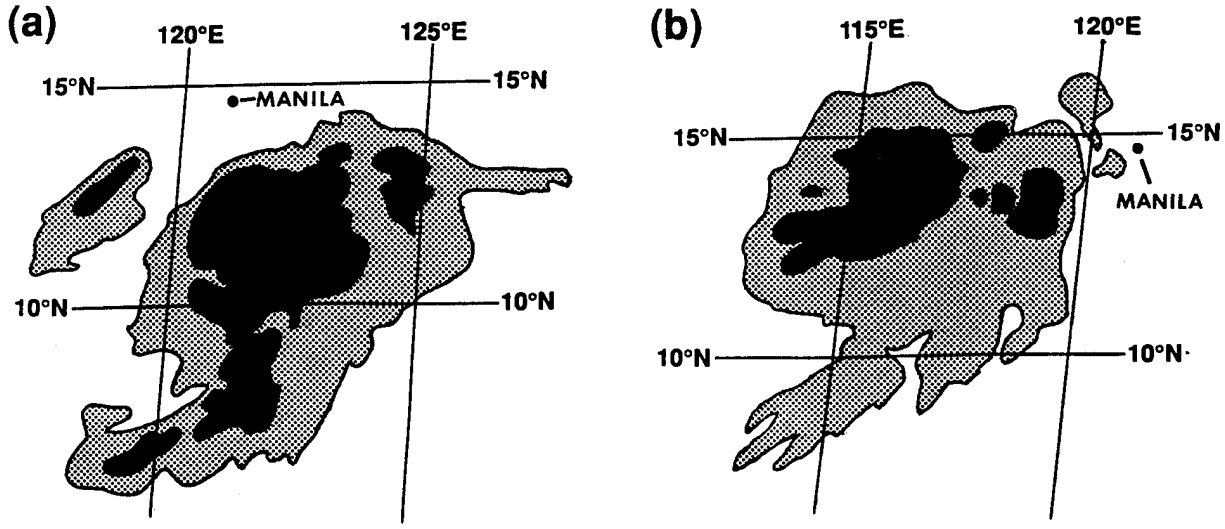

Figure 3-04-1 Schematic illustration of two episodes of early morning flare-up of the deep convection associated with Tropical Depression 04W based on: (a) 241931Z May enhanced infrared GMS imagery; and, (b) 251931Z May enhanced infrared GMS imagery. Shaded regions indicate cloud-top temperatures less than -60°C; black regions indicate cloud-top temperatures less than -75°C.

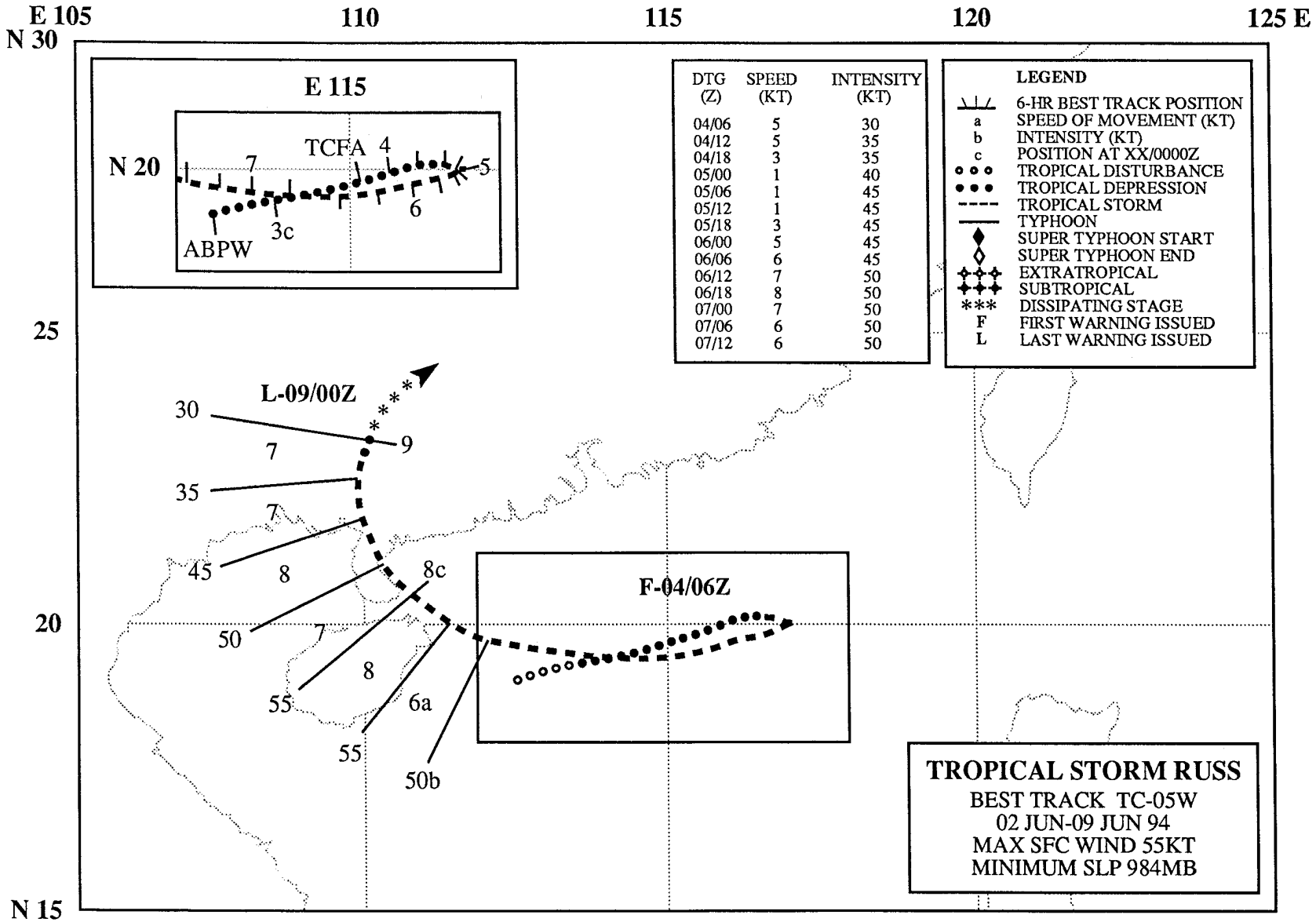
E 105
110
115
120
125 E
N 30
25
20
N 15
E 115
N 20
TCFA
ABPW
7
4
5
6
3c
DTG (Z) | SPEED (KT) | INTENSITY (KT)
04/06 5 30
04/12 5 35
04/18 3 35
05/00 1 40
05/06 1 45
05/12 1 45
05/18 3 45
06/00 5 45
06/06 6 45
06/12 7 50
06/18 8 50
07/00 7 50
07/06 6 50
07/12 6 50
LEGEND
6-HR BEST TRACK POSITION
a SPEED OF MOVEMENT (KT)
b INTENSITY (KT)
c POSITION AT XX/0000Z
TROPICAL DISTURBANCE
TROPICAL DEPRESSION
TROPICAL STORM
TYPHOON
SUPER TYPHOON START
SUPER TYPHOON END
EXTRATROPICAL
SUBTROPICAL
*** DISSIPATING STAGE
F FIRST WARNING ISSUED
L LAST WARNING ISSUED
L-09/00Z
30
7
9
35
7
45
8
8c
50
7
8
55
6a
55
50b
F-04/06Z
TROPICAL STORM RUSS
BEST TRACK TC-05W
02 JUN-09 JUN 94
MAX SFC WIND 55KT
MINIMUM SLP 984MB

TROPICAL STORM RUSS (05W)

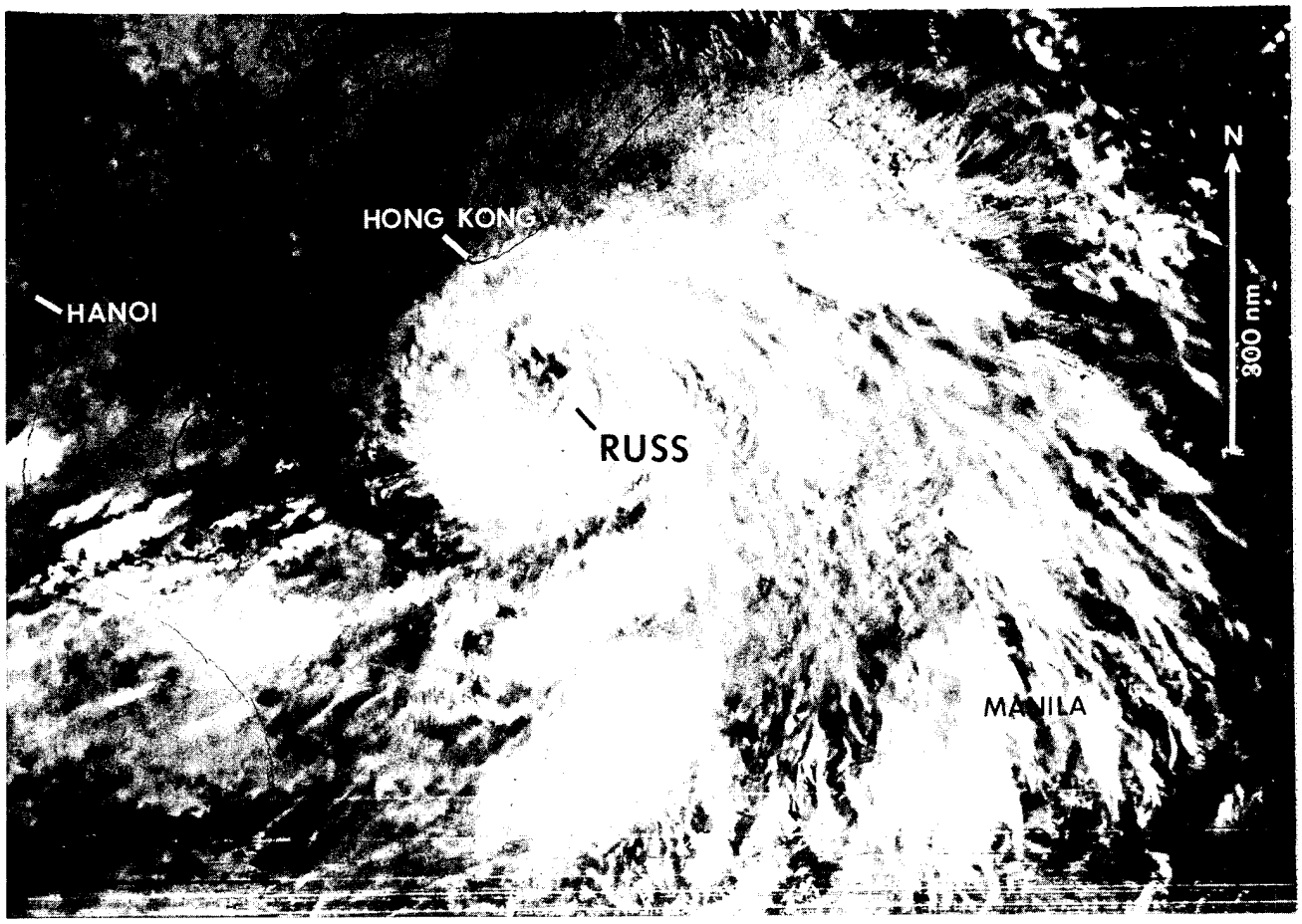

Figure 3-05-1 Russ with a ragged eye nears its peak intensity to the south of Hong Kong (060214Z June infrared DMSP imagery).

On 02 June, as the low-level southwest monsoonal flow over the South China Sea interacted with the well-anchored Mei-yu front (see Appendix A) that extended from south of Japan to near Hong Kong, surface pressures began to fall at the extreme southern end of the front. A tropical disturbance, about 75 nm (140 km) east of Hainan Island, was first mentioned on the Significant Tropical Weather Advisory at 020600Z May. By the evening of 03 June, with deep convection consolidated over the circulation center of this tropical disturbance, a Tropical Cyclone Formation Alert was issued at 031900Z. During the following day, the convection remained over the circulation center, and the JTWC issued the first warning on Tropical Depression 05W at 040600Z. The tropical depression slowly tracked in a northeastward direction for two days in association with deep southwesterly monsoonal steering flow. As the southwest monsoon weakened, Russ executed a clockwise loop back toward the west and slowly began to intensify. Russ reached its maximum intensity of 55 kt (28 m/sec) on 06 June as it developed a ragged banding-type eye (Figure 3-05-1). Russ went ashore at 080700Z on the northeastern Luichow Peninsula, and dissipated over southern China. Torrential rains caused severe flooding that killed hundreds of people and destroyed thousands of houses. The combined impacts of Russ and Sharon (06W) are discussed in the Tropical Storm Sharon narrative.

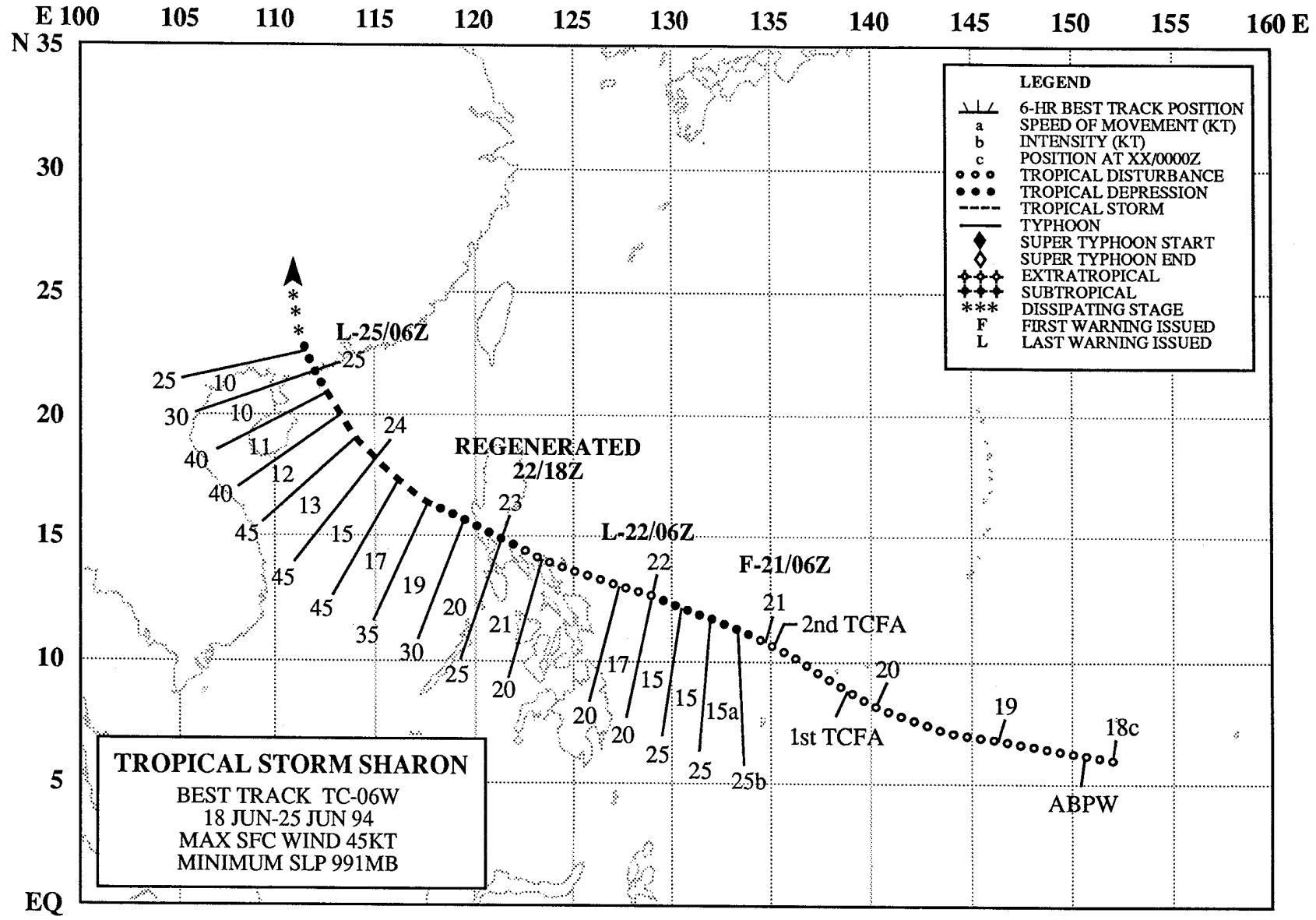
E 100
105
110
115
120
125
130
135
140
145
150
155
160 E
N 35
30
25
20
15
10
5
EQ
96
LEGEND
6-HR BEST TRACK POSITION
a SPEED OF MOVEMENT (KT)
b INTENSITY (KT)
c POSITION AT XX/0000Z
TROPICAL DISTURBANCE
TROPICAL DEPRESSION
TROPICAL STORM
TYPHOON
SUPER TYPHOON START
SUPER TYPHOON END
EXTRATROPICAL
SUBTROPICAL
*** DISSIPATING STAGE
F FIRST WARNING ISSUED
L LAST WARNING ISSUED
L-25/06Z
REGENERATED
22/18Z
L-22/06Z
F-21/06Z
2nd TCFA
1st TCFA
ABPW
TROPICAL STORM SHARON
BEST TRACK TC-06W
18 JUN-25 JUN 94
MAX SFC WIND 45KT
MINIMUM SLP 991MB

TROPICAL STORM SHARON (06W)

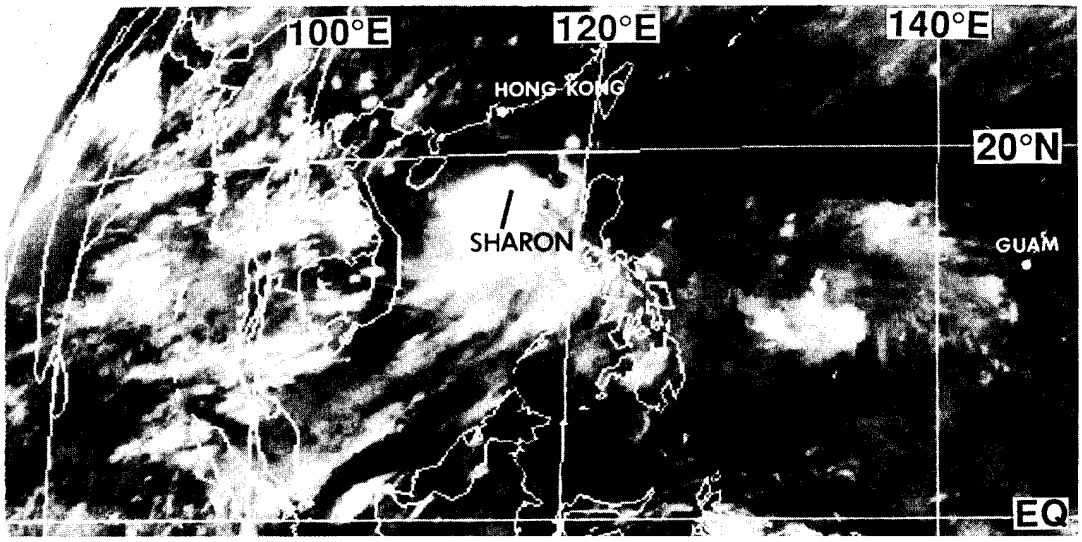

Figure 3-06-1 Just prior to its upgrade to Tropical Storm Sharon, TD 06W is located in the South China Sea to the south of Hong Kong. The lack of cirrus outflow northeast of the system center suggests that Sharon is being sheared by strong upper-level northeasterly winds (231230Z June infrared GMS imagery).

After Tropical Storm Russ (05W) went ashore in southern China on 08 June, the tropical western North Pacific quieted until mid-June when the convection in the near equatorial trough began to increase. An area of convection just south of Chuuk in the eastern Caroline Islands began to consolidate, and was first mentioned on the 180600Z June Significant Tropical Weather Advisory. The tropical disturbance moved west-northwestward at 15 kt (28 km/hr) and became more organized, prompting issuance of a Tropical Cyclone Formation Alert (TCFA) at 200730Z. When the tropical disturbance moved out of the predicted development area, a second TCFA (valid at 202300Z) was issued, followed by a 210600Z warning. Shortly thereafter, intensification arrested; most likely due to an increase in vertical wind shear. Twenty-four hours after the first warning, a final warning was issued. However, as the disturbance approached southeastern Luzon, it linked to the southwest monsoonal flow in the South China Sea that extended eastward. The convection flared again, which led to a regenerated warning valid at 221800Z. After crossing Luzon and entering the South China Sea, Sharon reached its peak intensity of 45 kt (23 m/sec) on the morning of 24 June. Vertical shearing due to strong upper-level northeasterly winds stymied further intensification (Figure 3-06-1). At 250600Z, the final warning was issued after the tropical storm went ashore in southern China, about 60 nm (110 km) east of the location where Tropical Storm Russ (05W) had gone ashore a week earlier. The combined flooding associated with Russ and Sharon left more that 1,400 people dead. The damage, which included the destruction of nearly one million houses in southern China, was estimated in excess of US$6 billion.

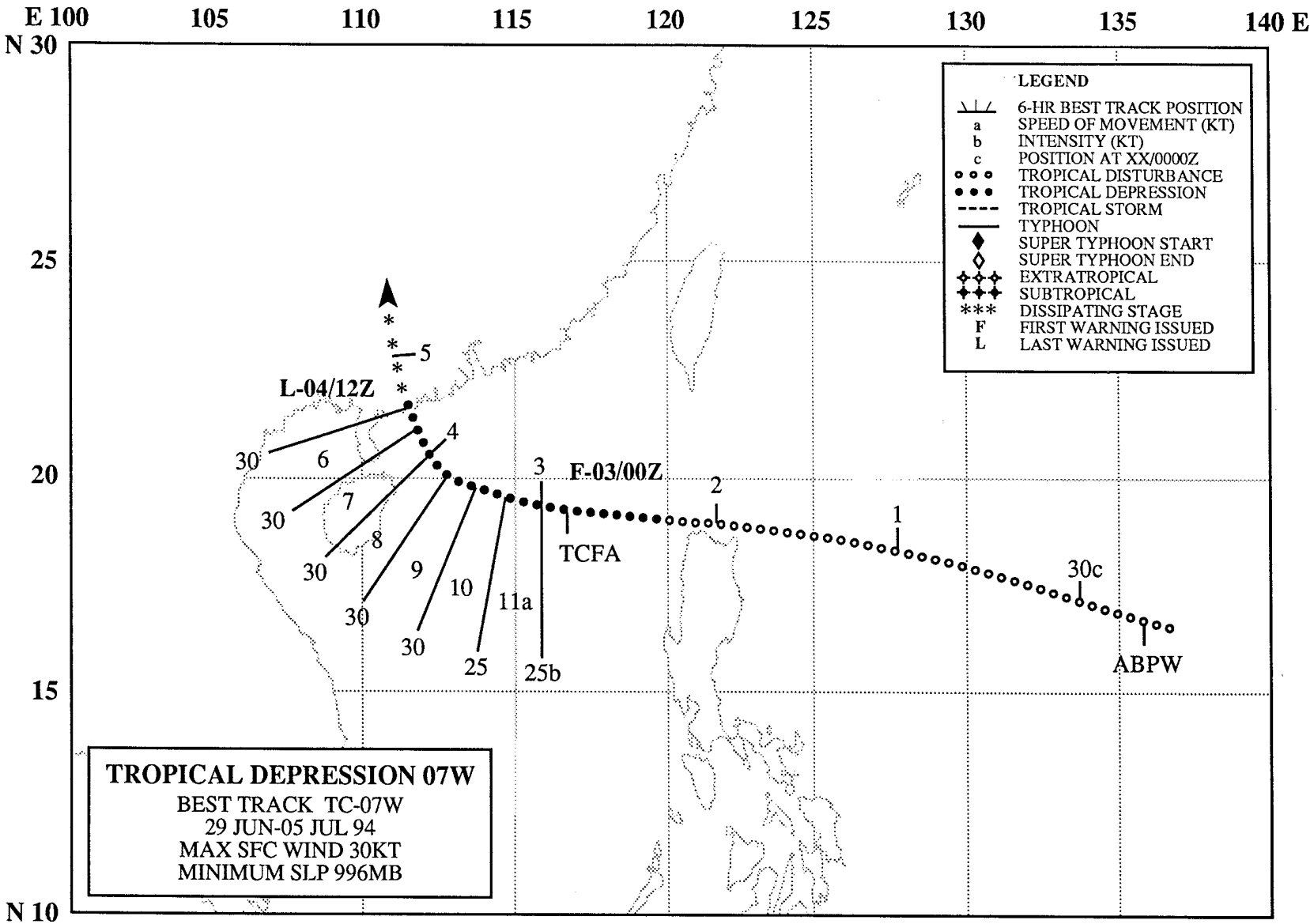
E 100
105
110
115
120
125
130
135
140 E
N 30
25
20
15
N 10
LEGEND
6-HR BEST TRACK POSITION
a SPEED OF MOVEMENT (KT)
b INTENSITY (KT)
c POSITION AT XX/0000Z
TROPICAL DISTURBANCE
TROPICAL DEPRESSION
TROPICAL STORM
TYPHOON
SUPER TYPHOON START
SUPER TYPHOON END
EXTRATROPICAL
SUBTROPICAL
*** DISSIPATING STAGE
F FIRST WARNING ISSUED
L LAST WARNING ISSUED
L-04/12Z
F-03/00Z
TCFA
ABPW
30
6
30
7
30
8
30
9
30
10
25
11a
25b
4
3
2
1
30c
5
TROPICAL DEPRESSION 07W
BEST TRACK TC-07W
29 JUN-05 JUL 94
MAX SFC WIND 30KT
MINIMUM SLP 996MB

TROPICAL DEPRESSION 07W

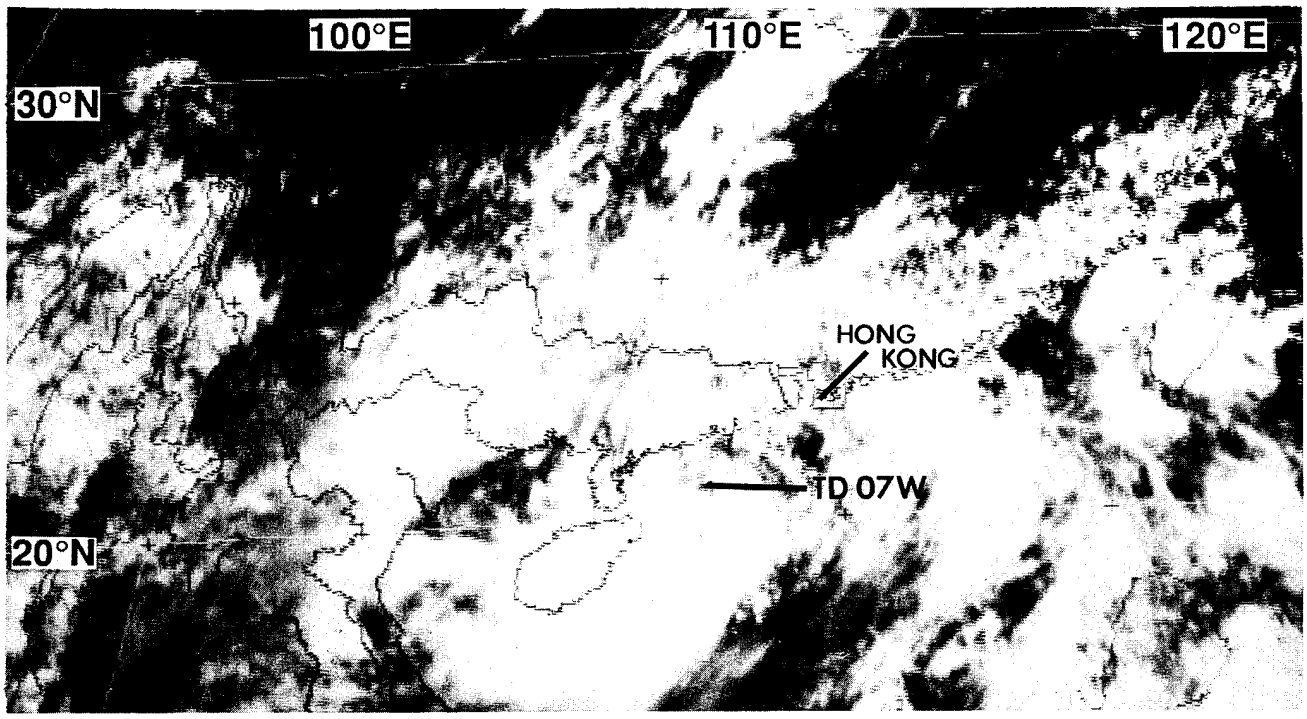

Figure 3-07-1 The result of strong northeasterly upper-level shear, Tropical Depression 07W exhibits a partially exposed low-level circulation center (LLCC) (040031Z July visible GMS imagery).

Tropical Depression (TD) 07W, the third tropical cyclone of June, developed in the monsoon trough around 17°N 135°E, late on 29 June. Under the influence of strong vertical shear, it never intensified above tropical depression intensity. The system moved across the Philippine Sea at 14-15 kt (26-28 km/hr). On 02 June, it passed north of Luzon into the South China Sea. Influenced by deep steering associated with the southwest monsoon, TD 07W slowed in forward speed, and turned toward the northwest. It reached its 30 kt (15 m/sec) maximum intensity just prior to making landfall in southern China (Figure 3-07-1), virtually in the same spot that Tropical Storm Sharon (06W) had gone ashore two weeks earlier. TD 07W dissipated over southern China. Heavy rains and flooding associated with TD 07W led to four people killed, two people missing, 6,700 houses destroyed, another 50,000 damaged, and 365 mines and factories forced to close. Total loses were estimated at $US 114 million.

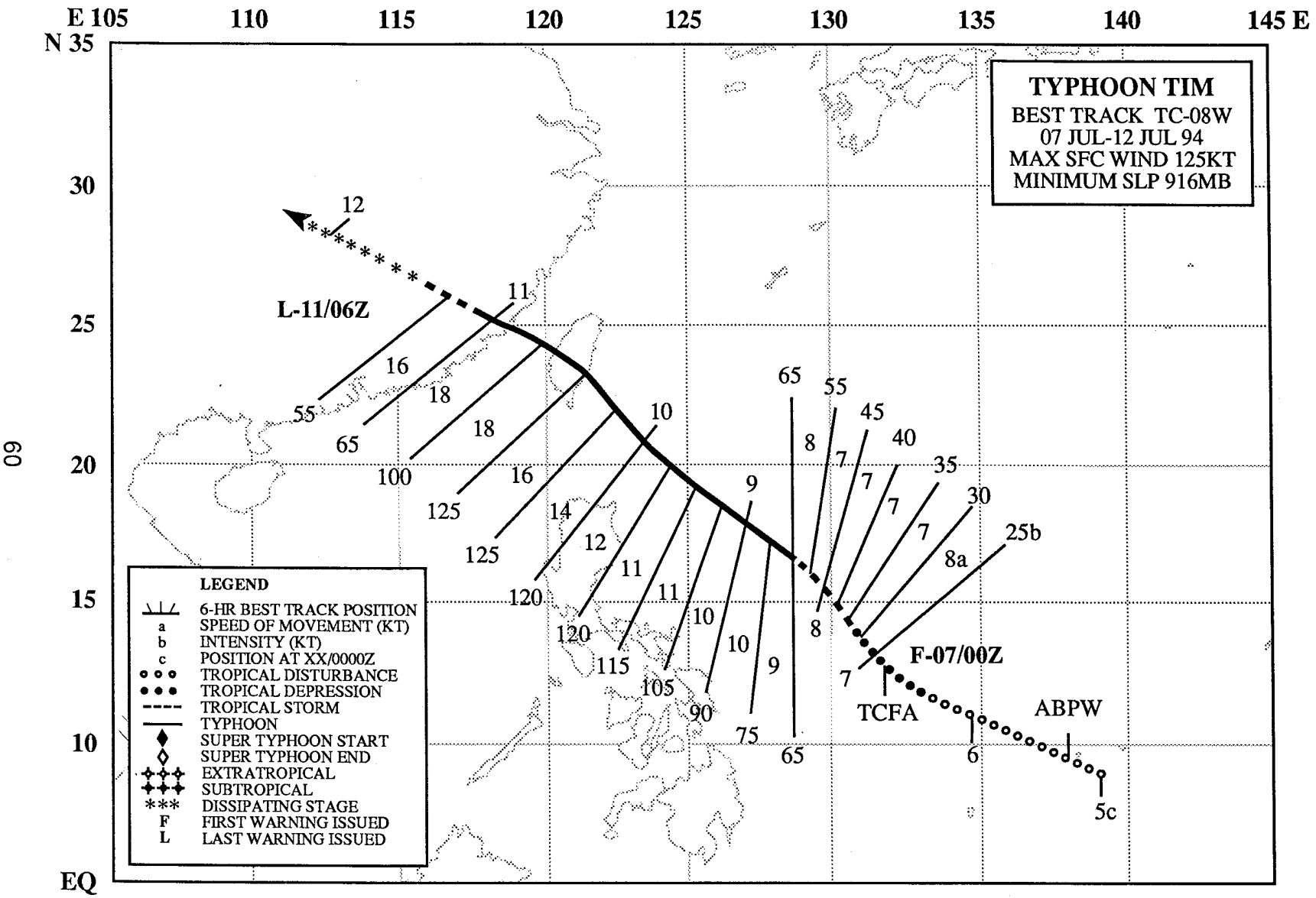
E 105
110
115
120
125
130
135
140
145 E
N 35
30
25
20
15
10
EQ
60
TYPHOON TIM
BEST TRACK TC-08W
07 JUL-12 JUL 94
MAX SFC WIND 125KT
MINIMUM SLP 916MB
L-11/06Z
F-07/00Z
TCFA
ABPW
LEGEND
6-HR BEST TRACK POSITION
a SPEED OF MOVEMENT (KT)
b INTENSITY (KT)
c POSITION AT XX/0000Z
TROPICAL DISTURBANCE
TROPICAL DEPRESSION
TROPICAL STORM
TYPHOON
SUPER TYPHOON START
SUPER TYPHOON END
EXTRATROPICAL
SUBTROPICAL
*** DISSIPATING STAGE
F FIRST WARNING ISSUED
L LAST WARNING ISSUED

TYPHOON TIM (08W)

I. HIGHLIGHTS

After a week of relative calm in the western North Pacific, a tropical disturbance developed in the Caroline Islands on 05 July. The disturbance moved northwestward and was upgraded to Tropical Storm Tim. On 08 July, it underwent an episode of rapid intensification. A peak intensity of 125 kt (64 m/sec) was reached at 100600Z. Tim and Vanessa (09W) underwent a binary interaction that resulted in the decay and absorption of the smaller Vanessa into Tim's outer circulation. Tim made landfall in central Taiwan at 101200Z. Gusts to 98 kt (51 m/sec) were reported at Chengkung (WMO 46761).

II. TRACK AND INTENSITY

In early July, the Tropical Upper Tropospheric Trough (TUTT) intensified across the western North Pacific. Trade winds beneath the TUTT dominated the low-level flow over most of the region, except south of 10°N where the axis of a weak monsoon trough extended across Micronesia to about 160°E. By 05 July, convection over the Philippine Sea had increased south of the TUTT, and the disturbance that would become Typhoon Tim was first mentioned on the Significant Tropical Weather Advisory at 050600Z July as an area of enhanced convection south of Chuuk. On the early morning of 06 July, a Tropical Cyclone Formation Alert was issued, followed two hours later by the first warning on Tropical Depression 08W. As this system approached 130°E, it was upgraded to Tropical Storm Tim. After Tim crossed 130°E, the southwest monsoon surged across the Philippines and into the storm.

Tim reached an intensity of 55 kt (28 m/sec) at about 080600Z, then started to rapidly intensify. It reached typhoon intensity at 081200Z enroute to its peak intensity of 125 kt (64 m/sec) on the morning of 10 July. From 09 to 11 July, Tim underwent a binary interaction with Tropical Storm Vanessa (09W) (See Vanessa's Summary). Tim, much larger than Vanessa, showed little track deviation as a result of the interaction.

Tim weakened rapidly after it made landfall at Hualien County in central Taiwan at 101200Z where maximum winds of 79 kt (41 m/sec) with gusts to 98 kt (51 m/sec) were reported at Chengkung (WMO 46761) and 64 kt with gusts to 81 kt (33 m/sec with gusts to 42 m/sec) at Hualien City (WMO 46763). Ten hours later, Tim moved into mainland China as a minimal typhoon where it dissipated a day-and-a-half later over the inland mountains. The final warning on Tim was issued at 110600Z.

III. DISCUSSION

There are two primary areas of interest concerning Typhoon Tim. The first is its rapid intensification, and the second is Tim's binary interaction with Tropical Storm Vanessa. The latter is covered in the Tropical Storm Vanessa (09W) summary.

Tim intensified normally from 070000Z to 080000Z July. During this interval the developing eye wall was suppressed on the west side, most probably by upper-level westerly wind flow south of the TUTT axis (Figure 3-8-1a,b). Twelve hours later (081200Z), the shear had relaxed. A complete eye wall formed, and peripheral bands of deep convection developed in all quadrants and an episode of rapid intensification began. From 081200Z until 091200Z, Tim intensified at a rate of 49 mb/day or 2.04 mb/hr. This meets the requirement for rapid intensification — 42 mb/day or 1.75 mb/hr — as designated by Holliday and Thompson (1979). After 091200Z, Tim's rate of intensification slowed, and it reached its peak intensity of 125 kt (64 m/sec) at 100600Z (Figure 3-08-2).

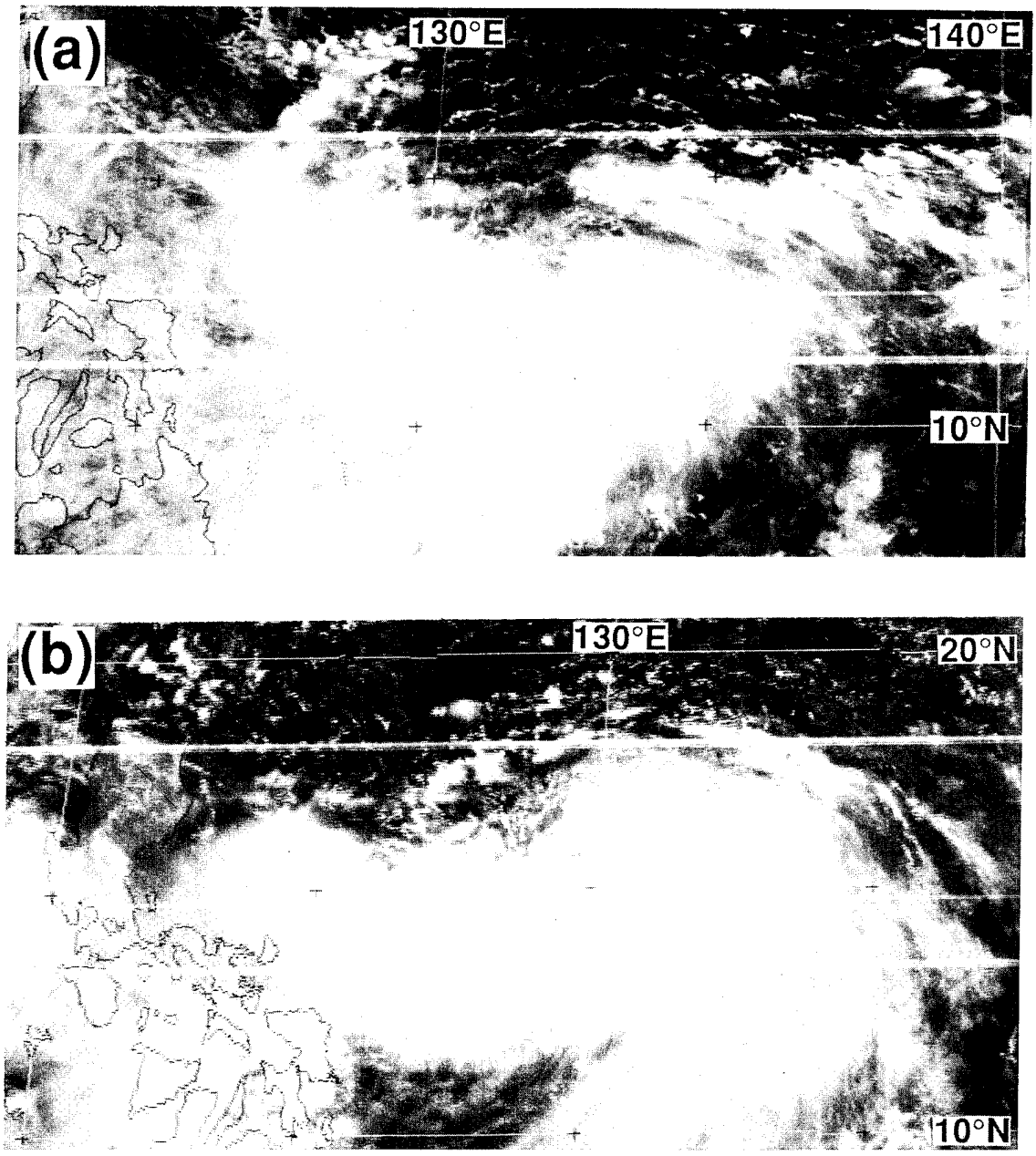

Figure 3-08-1 Tim intensifies despite apparent shearing from the west: (a) 070031Z July visible GMS imagery; (b) 080031Z July visible GMS imagery.

IV. IMPACT

In Taiwan, 39 fishermen were missing as a result of Tim when their fishing trawler ran aground near the eastern coastal city of Ilan. Elsewhere in Taiwan, four people were killed, and several highways were closed as a result of landslides from torrential rains.

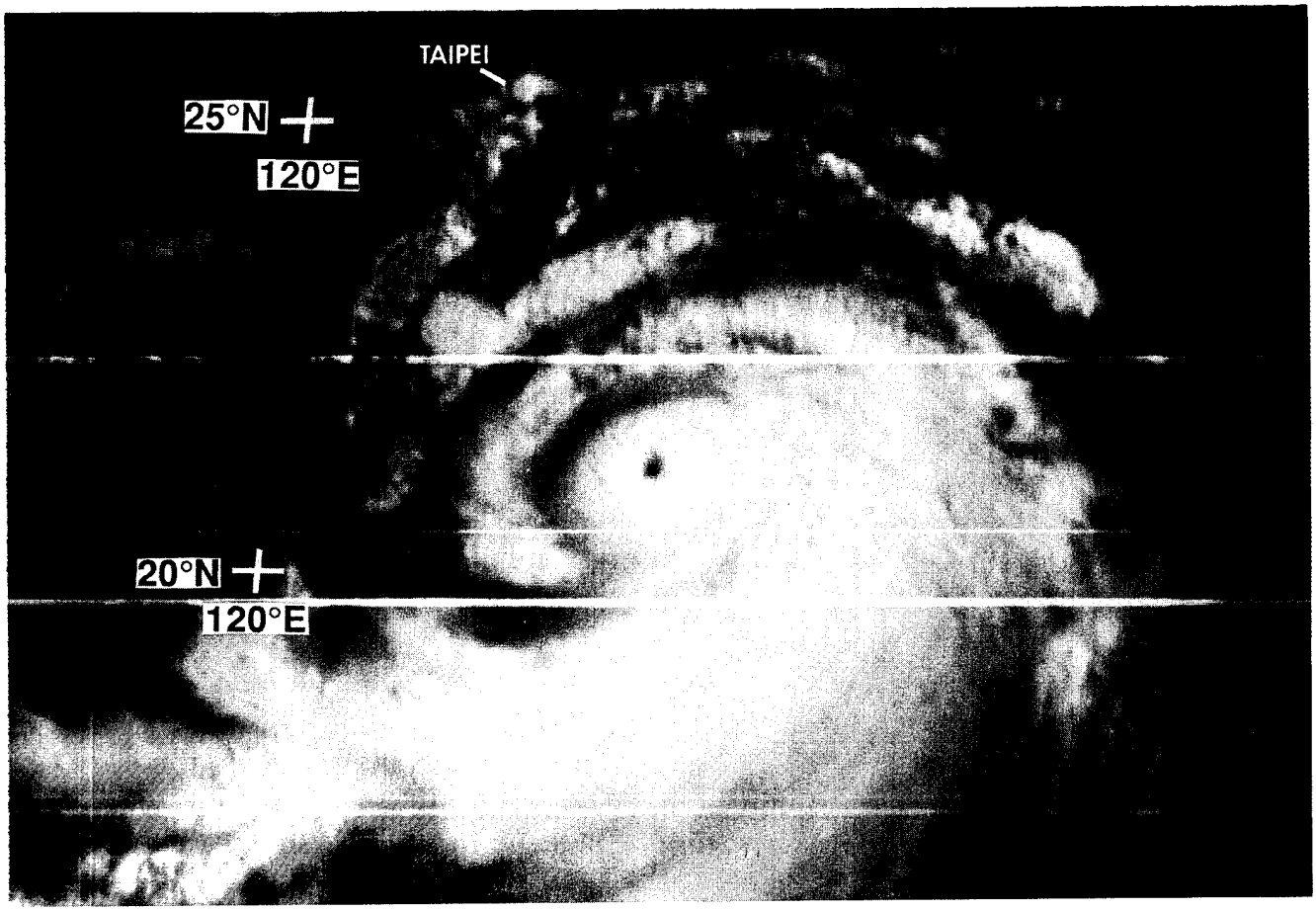

Figure 3-08-2 Tim at 120 kt (62 m/sec) six hours prior to reaching its peak intensity of 125 kt (64 m/sec) (100031Z July visible GMS imagery).

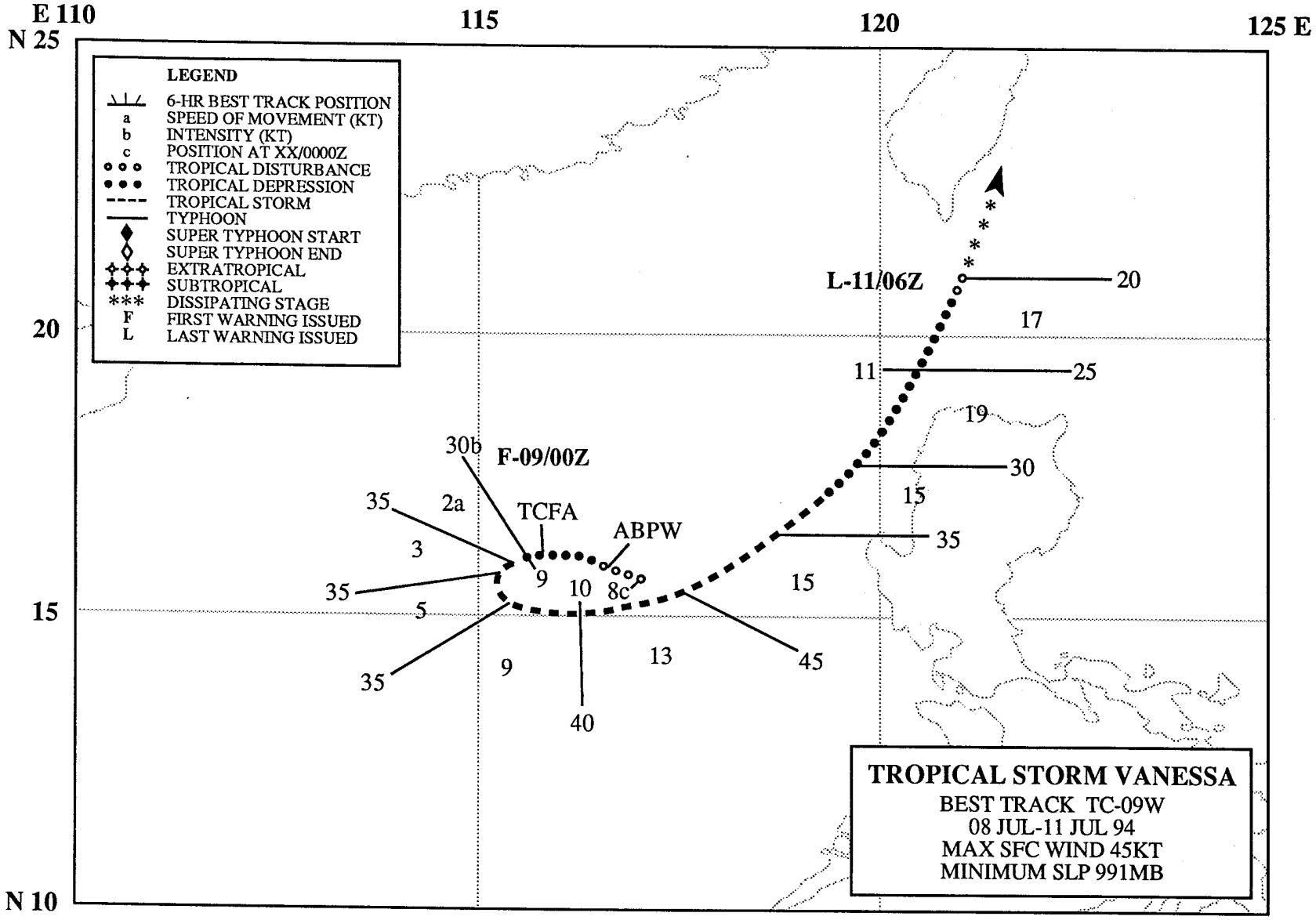
E 110
115
120
125 E
N 25
20
15
N 10
LEGEND
6-HR BEST TRACK POSITION
a SPEED OF MOVEMENT (KT)
b INTENSITY (KT)
c POSITION AT XX/0000Z
TROPICAL DISTURBANCE
TROPICAL DEPRESSION
TROPICAL STORM
TYPHOON
SUPER TYPHOON START
SUPER TYPHOON END
EXTRATROPICAL
SUBTROPICAL
*** DISSIPATING STAGE
F FIRST WARNING ISSUED
L LAST WARNING ISSUED
L-11/06Z
20
17
11
25
19
30b
F-09/00Z
30
15
35
2a
TCFA
ABPW
3
35
9
10
8c
15
35
5
9
13
45
35
40
TROPICAL STORM VANESSA
BEST TRACK TC-09W
08 JUL-11 JUL 94
MAX SFC WIND 45KT
MINIMUM SLP 991MB

TROPICAL STORM VANESSA (09W)

I. HIGHLIGHTS

The second of five tropical cyclones to form in the South China Sea during 1994, Vanessa was small. Interacting with the larger Typhoon Tim (08W), Vanessa moved northeastward, closing to within about 400 nm (740 km) of Tim. Vanessa's convection then was sheared away and its low-level circulation center was absorbed by Tim's outer circulation.

II. TRACK AND INTENSITY

During the first week of July, the monsoon trough extended across the South China Sea at about 15°N, and from there, east-southeastward into Micronesia. A few days prior to the formation of Vanessa in the South China Sea, larger-sized Typhoon Tim (08W) formed in the Philippine Sea and moved west-northwestward towards Taiwan. As Tim matured in the Philippine Sea, a tropical disturbance in the South China Sea, located just west of Luzon, began to show signs of development. Synoptic data and satellite imagery showed that a low-level circulation center had persisted for 24 hours, and this tropical disturbance was mentioned on the 080600Z July Significant Tropical Weather Advisory. Satellite imagery on the morning of 09 July showed that this system had become well organized (Figure 3-09-1). A Tropical Cyclone Formation Alert was issued at 082200Z followed by the first warning at 090000Z. After an initial period of slow westward motion, Vanessa executed a counterclockwise loop, and then tracked northeastward under the steering influence of Tim's larger circulation and deep southwesterly monsoon flow.

Vanessa reached a peak intensity of only 45 kt (23 m/sec), possibly due to vertical and horizontal shearing imposed on it by the larger Typhoon Tim (08W) (Figure 3-09-2), before it was destroyed in a merger with Tim. The final warning was issued at 110600Z when satellite imagery and synoptic data indicated that Vanessa's circulation had disappeared into Tim's southeastern quadrant.

III. DISCUSSION

Asymmetrical tropical cyclone merger — wherein one tropical cyclone loses its deep convection and its remnant low-level circulation is swept into the remaining intact tropical cyclone — is the norm for a binary interaction that ends in merger (Lander and Holland 1993). Vanessa's binary interaction with Typhoon Tim (Figure 3-09-3) was a typical case of the merger of two tropical cyclones. In contrast, the first-ever observed case of symmetrical dissolution of deep convection and merger of two tropical cyclones occurred later in the year when Pat (29W) and Ruth (30W) merged (see their summaries later in this chapter).

IV. IMPACT

Tropical Storm Vanessa battered the northern Philippines with strong winds and heavy rains. Torrential rains triggered landslides along major highways and explosions of superheated material on the slopes of Mount Pinatubo. One person was killed and three injured by flying debris from the Pinatubo explosions. In northern Luzon, a man was killed when the roof of his house collapsed.

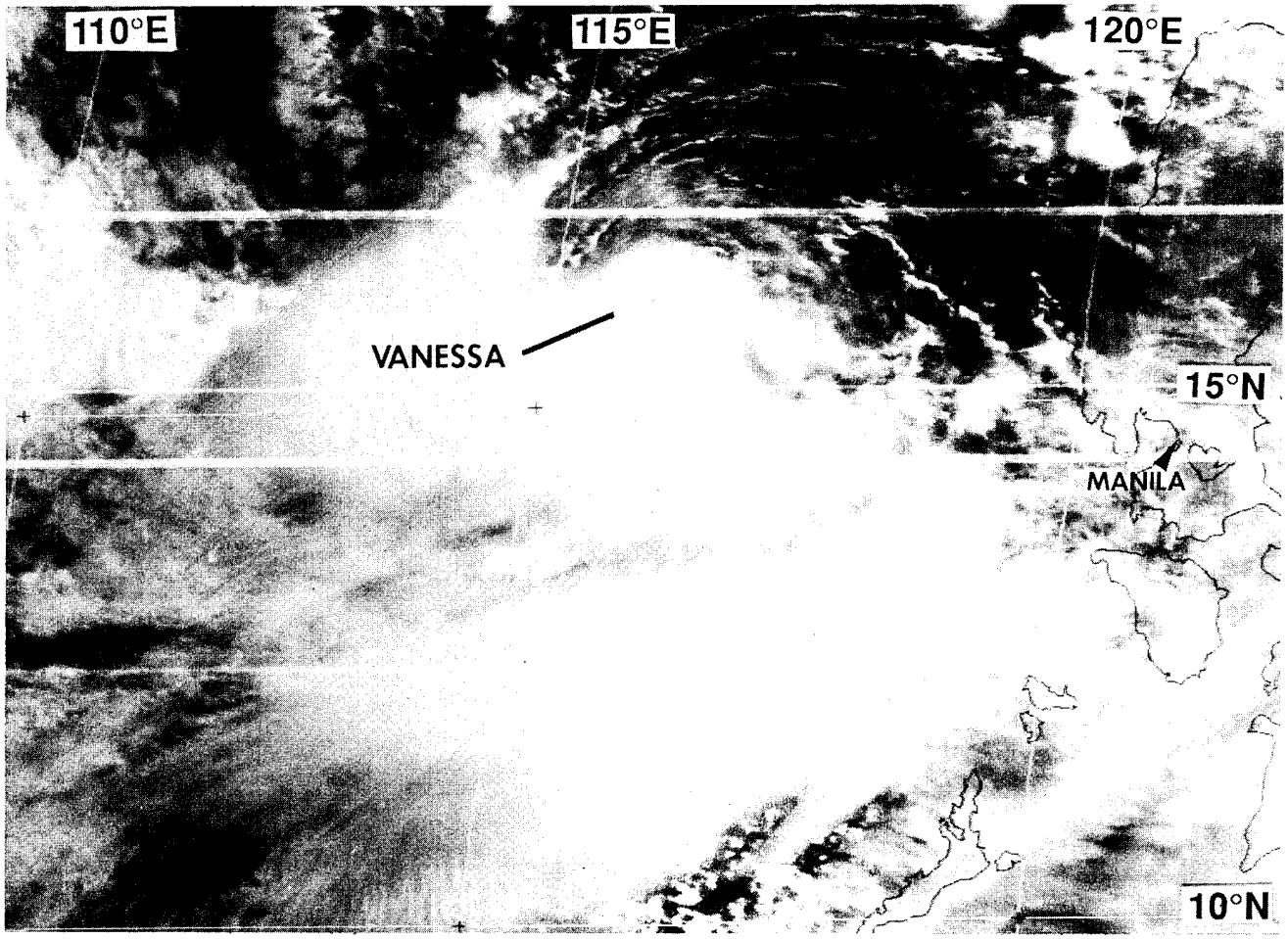

Figure 3-09-1 Well-organized low-level cloud lines and a central dense overcast prompted the first warning on Tropical Storm Vanessa (082331Z July visible GMS imagery).

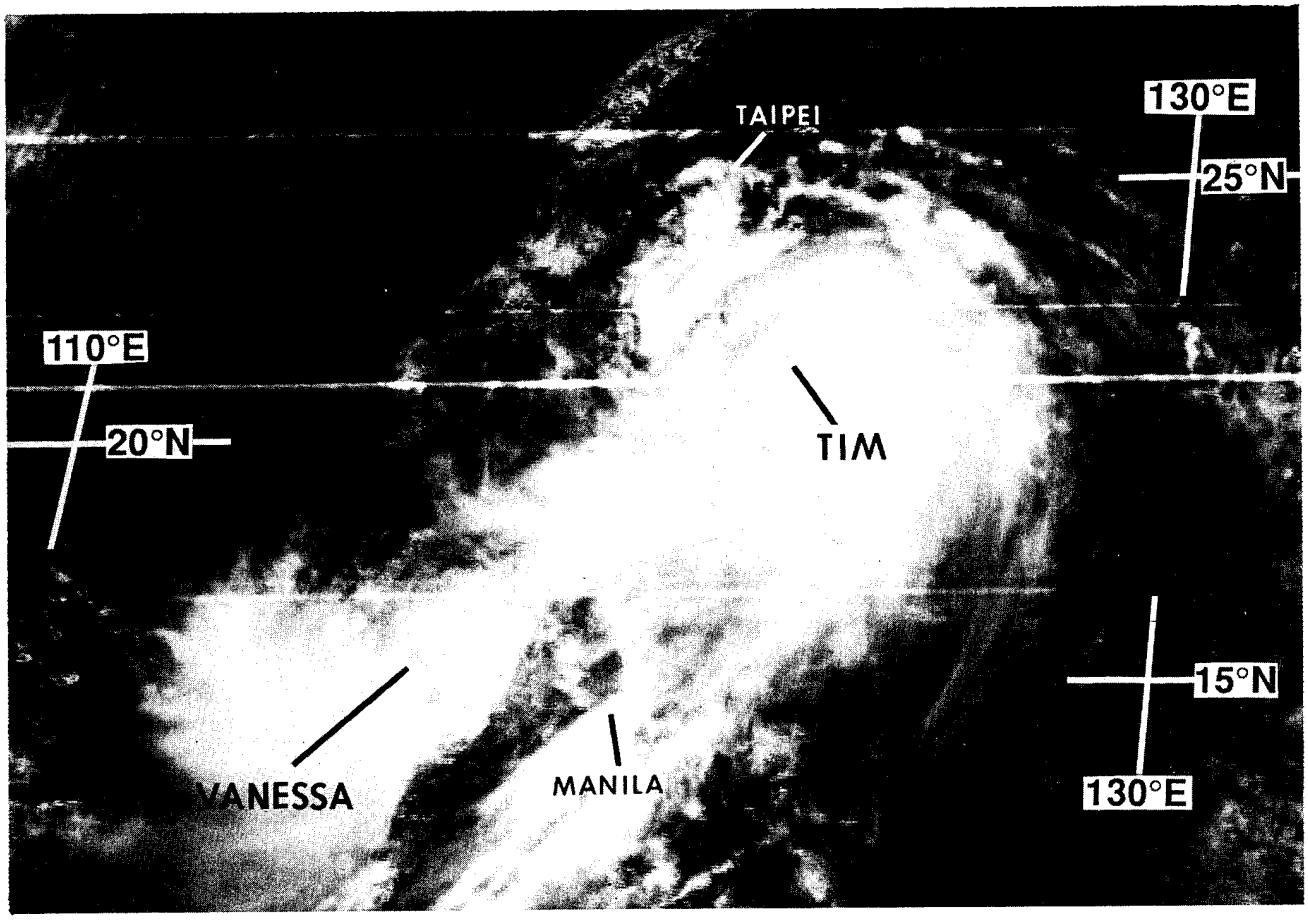

Figure 3-09-2 Vanessa is moving northeastward under the influence of the outer circulation of Typhoon Tim (08W) and strong southwesterly monsoonal flow (100131Z July visible GMS imagery).

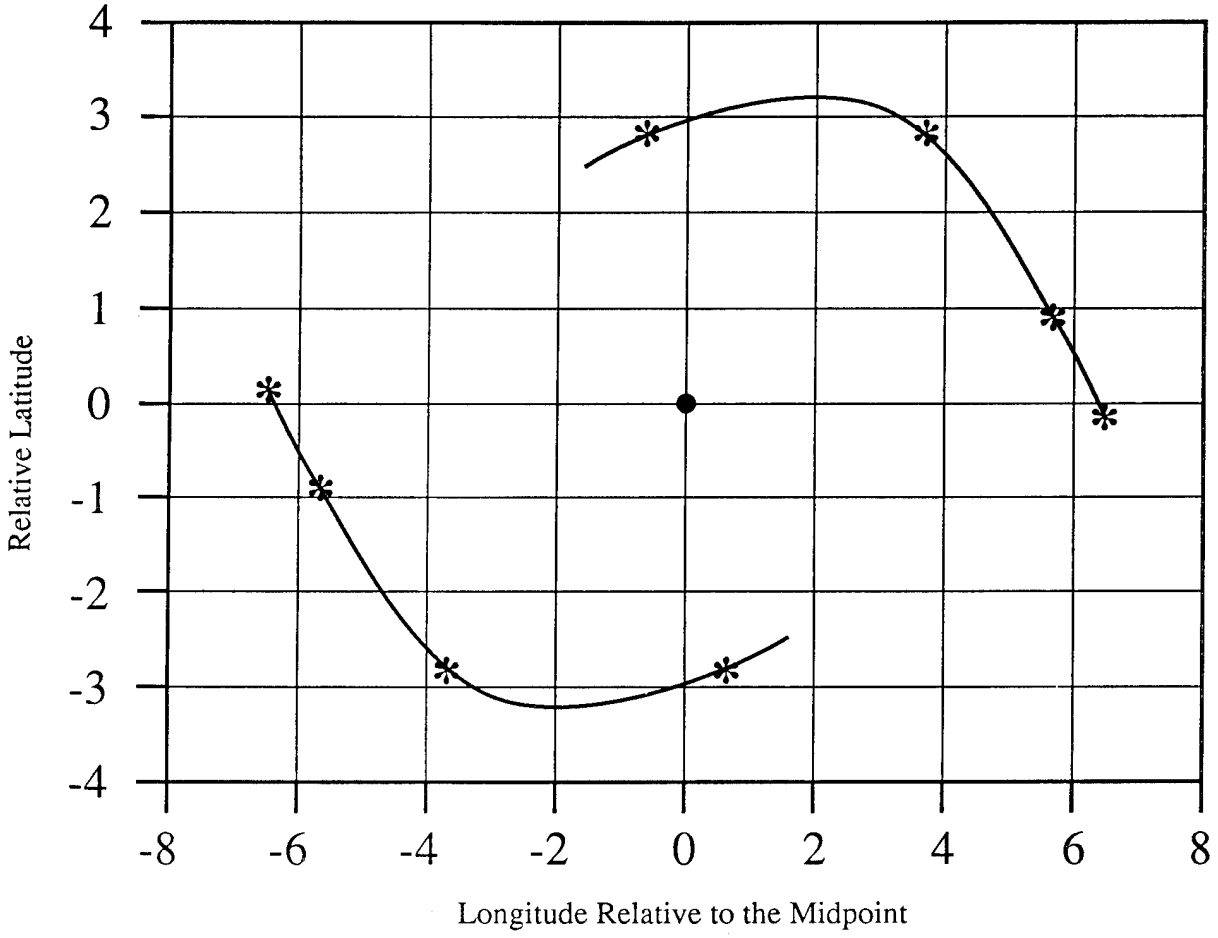

Figure 3-09-3 The binary interaction of Vanessa with Tim (08W) in a centroid-relative frame of reference.

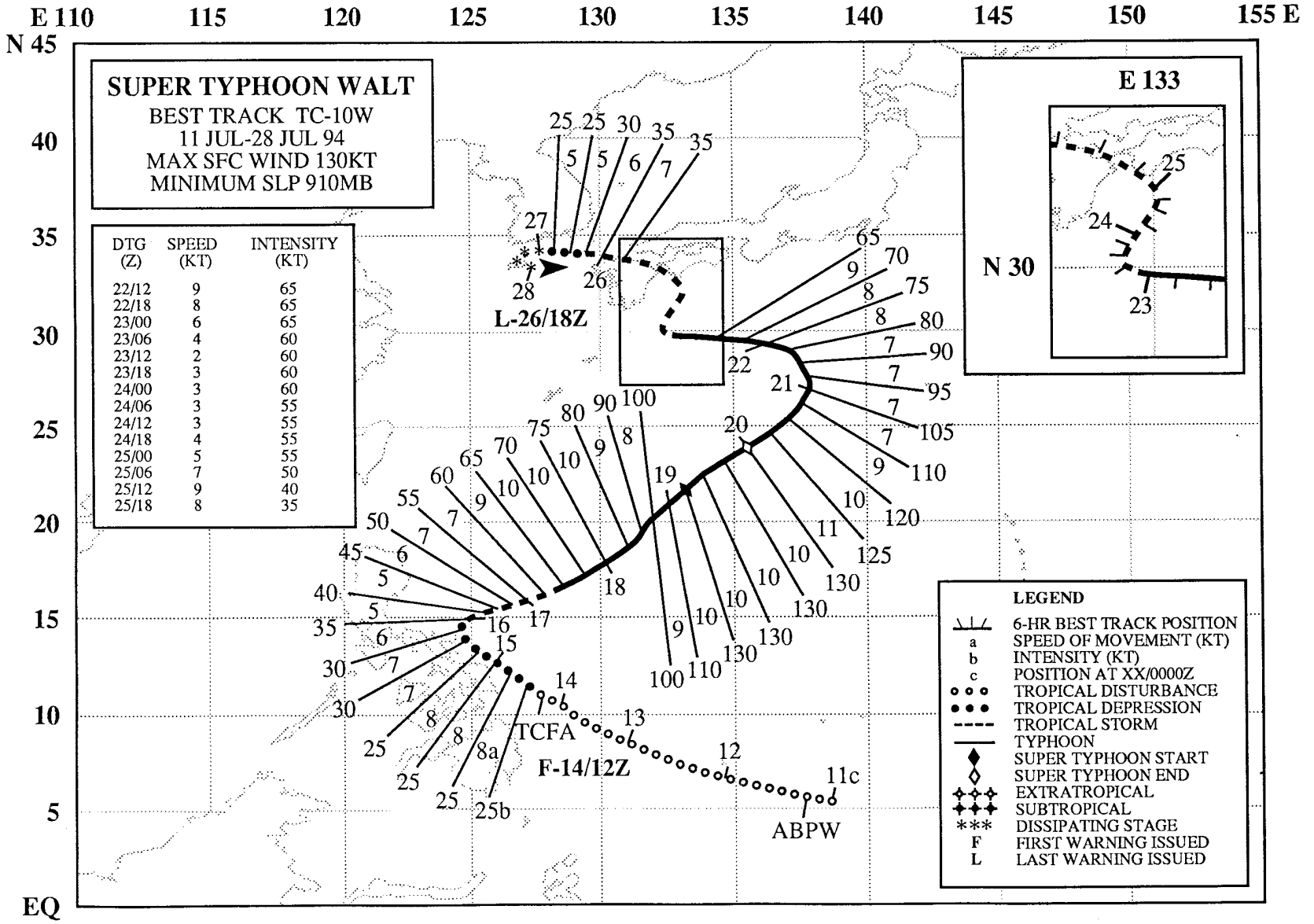
E 110
115
120
125
130
135
140
145
150
155 E
N 45
40
35
30
25
20
15
10
5
EQ
SUPER TYPHOON WALT
BEST TRACK TC-10W
11 JUL-28 JUL 94
MAX SFC WIND 130KT
MINIMUM SLP 910MB
DTG (Z) SPEED (KT) INTENSITY (KT)
22/12 9 65
22/18 8 65
23/00 6 65
23/06 4 60
23/12 2 60
23/18 3 60
24/00 3 60
24/06 3 55
24/12 3 55
24/18 4 55
25/00 5 55
25/06 7 50
25/12 9 40
25/18 8 35
L-26/18Z
TCFA
F-14/12Z
ABPW
E 133
N 30
LEGEND
6-HR BEST TRACK POSITION
a SPEED OF MOVEMENT (KT)
b INTENSITY (KT)
c POSITION AT XX/0000Z
TROPICAL DISTURBANCE
TROPICAL DEPRESSION
TROPICAL STORM
TYPHOON
SUPER TYPHOON START
SUPER TYPHOON END
EXTRATROPICAL
SUBTROPICAL
*** DISSIPATING STAGE
F FIRST WARNING ISSUED
L LAST WARNING ISSUED

69

SUPER TYPHOON WALT (10W)

I. HIGHLIGHTS

The first tropical cyclone of 1994 in the western North Pacific to become a super typhoon, Walt was the larger and more intense of three named tropical cyclones which, for several days, were located along the axis of a reverse-oriented monsoon trough (Figure 3-10-1 and Figure 3-10-2). Typical of tropical cyclones embedded in a reverse-oriented monsoon trough, Walt exhibited unusual motion: eastward motion at low latitudes followed by a turn to the north. After reaching its peak intensity of 130 kt (67 m/sec), Walt slowly decayed as it made a gradual turn from a northward to a westward track. Before dissipating in the Korea Strait, its remnant cloud system brought much needed rain to some drought-stricken portions of South Korea.

II. TRACK AND INTENSITY

During early July, the axis of the monsoon trough extended across much of Micronesia at rather low latitudes (5°-7°N). Most of the deep convection associated with this monsoon trough was located south of 10°N. By 11 July, a persistent cloud cluster had consolidated near Palau. The first mention of this

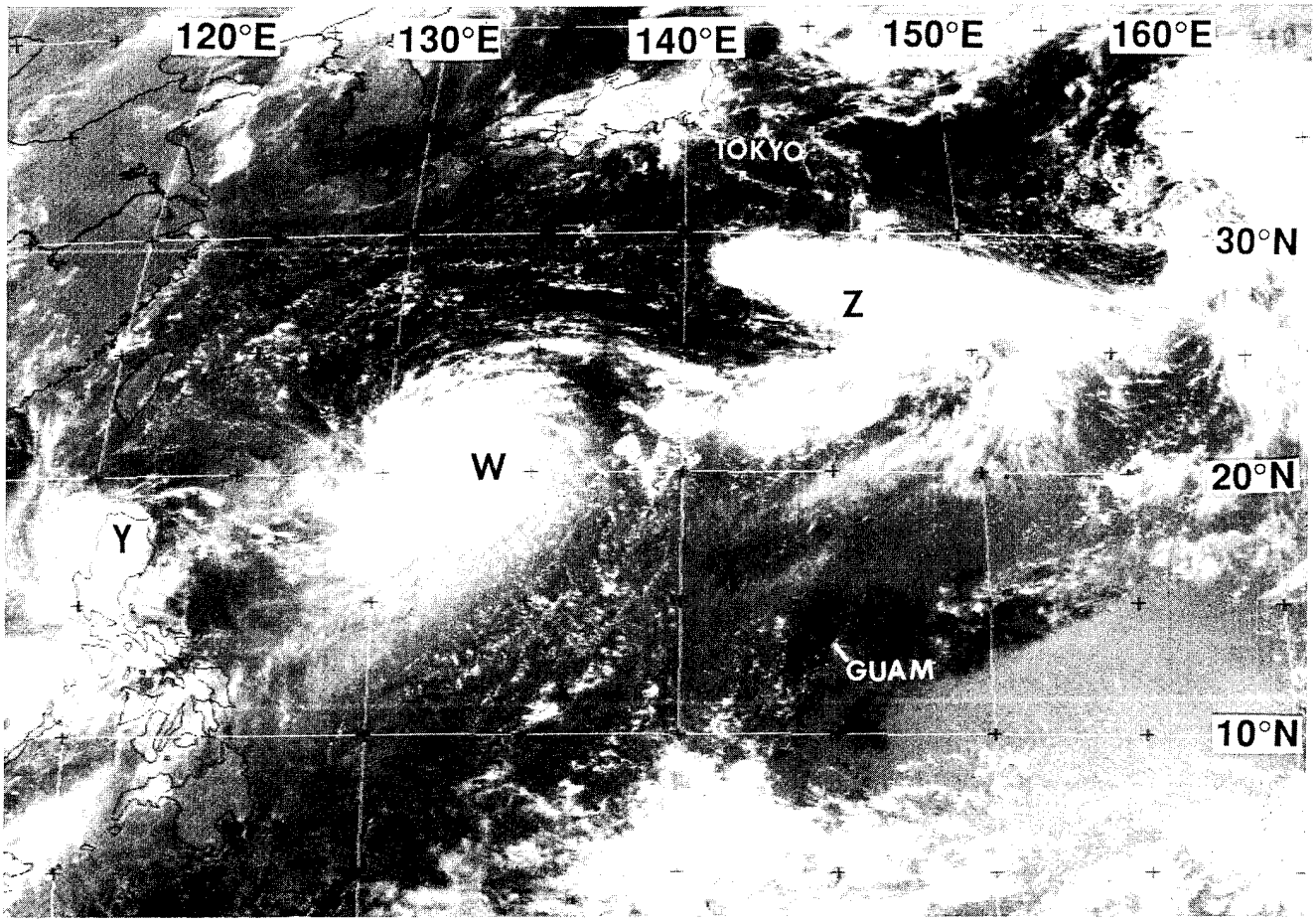

Figure 3-10-1 Yunya (11W), Walt , Zeke (12W), and a subtropical disturbance are aligned SW-NE along the axis of a reverse-oriented monsoon trough (190031Z July visible GMS imagery).

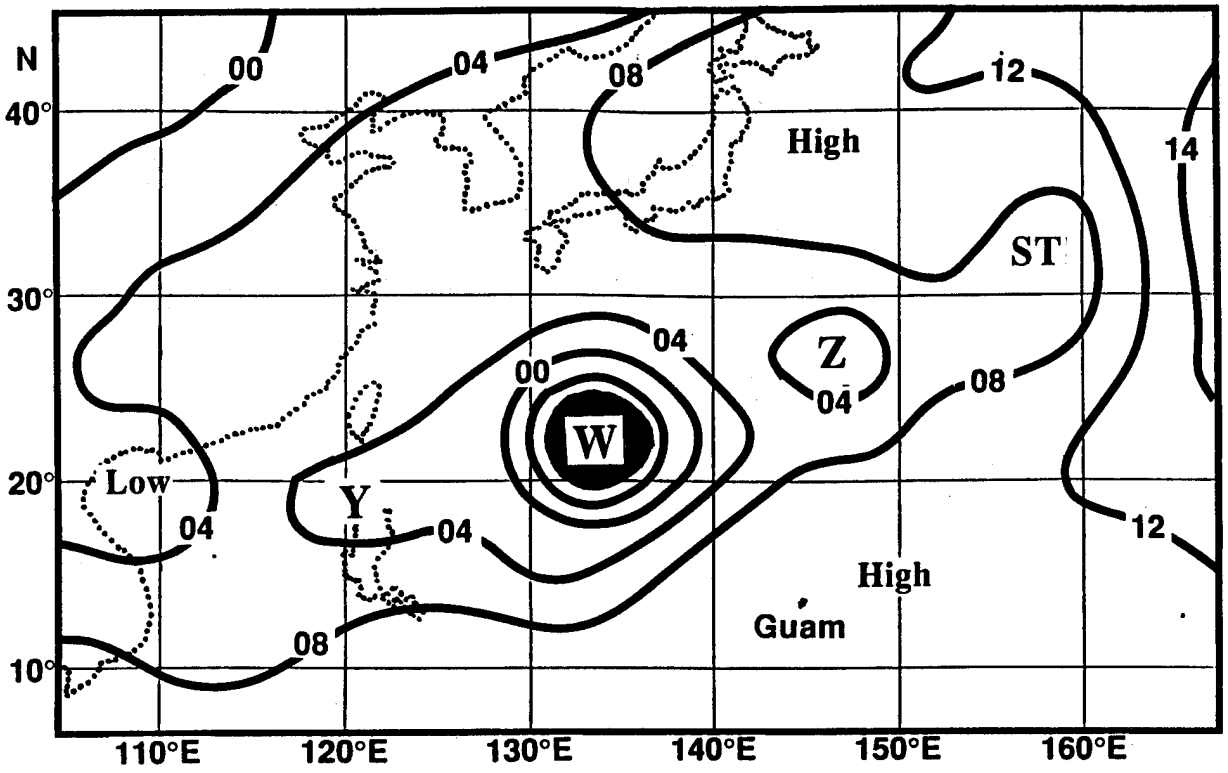

Figure 3-10-2 As in Figure 3-10-1, except sea-level pressure analysis at 190000Z July.

cloud cluster as a suspect tropical disturbance appeared on the 110600Z July Significant Tropical Weather Advisory. During the next few days, this tropical disturbance moved slowly northwestward. At 140800Z, the organization of the deep convection had further improved, and a Tropical Cyclone Formation Alert was issued. The first warning was issued soon thereafter at 141200Z.

Initially, Walt (as a tropical depression) moved northwestward towards Luzon. Then it slowed and turned towards the northeast at a relatively low latitude (15°N), and intensified. Concurrent with Walt's low-latitude turn toward the northeast, a long band of deep convective cloud clusters (which included Walt's cloud system) acquired a SW-NE (i.e., reverse) orientation, and extended from 15°N in the South China Sea to 30°N near the international date line. This cloud band signaled the onset of the year's first of three episodes of reverse orientation of the monsoon trough.

As Walt moved northeastward, it continued to intensify. By 190600Z its intensity peaked at the 130 kt (67 m/sec) super typhoon threshold (Figure 3-10-3). This peak intensity remained until 200000Z, when it began to slowly weaken. At 210000Z, Walt turned towards the west. Dropping below typhoon intensity shortly after 230000Z, Walt then tracked northward for two days. A westward turn at 250000Z led Walt to landfall at 250600Z on the southwestern end of the Japanese island of Shikoku. The estimated intensity at landfall was 50 kt (26 m/sec). Walt dissipated over water south of Korea after crossing southern Japan. The final warning was issued at 261800Z.

III. DISCUSSION

a. Unusual motion

The track of Super Typhoon Walt was north-oriented (JMA 1976). Tropical cyclones which move

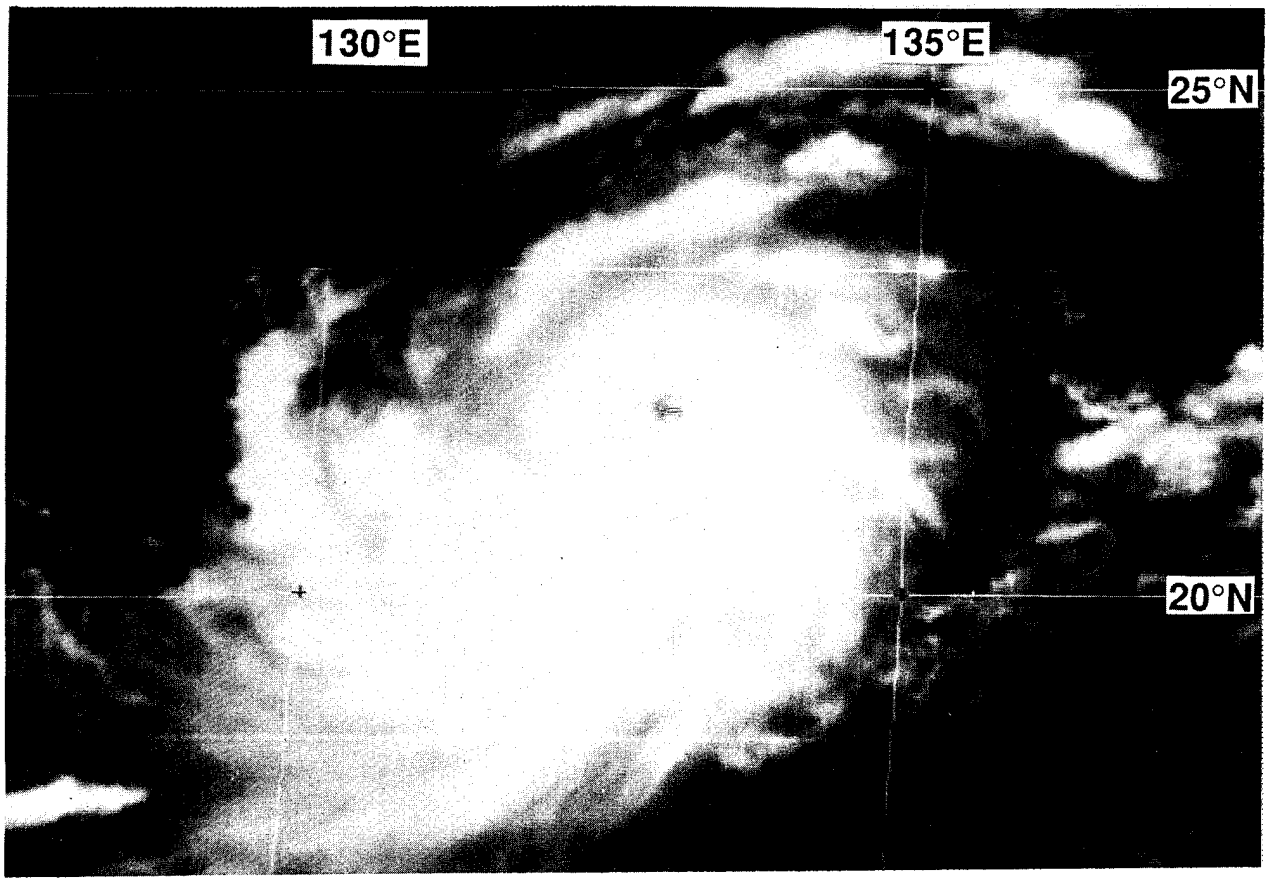

Figure 3-10-3 Walt at peak intensity (190600Z July visible GMS imagery).

on such tracks follow long generally northward paths from their genesis location into the mid-latitudes. A north-oriented track may feature large meanders and abrupt turns to the left or right. The speed of forward motion is often slower than average. Many north-oriented tracks feature eastward motion at low latitudes, and some even have an eastward component of motion for their entire track. Most north-oriented motion occurs during July through September (Lander 1995a).

The pattern of the large-scale low-level monsoon circulation of the western North Pacific has been shown to be a discriminator of tropical cyclone track type (Harr and Elsberry 1991; Lander 1995a). One pattern in particular, the reverse-oriented monsoon trough, has been shown by Lander (1995a) to be almost exclusively associated with north-oriented motion.

In its simplest description, the large-scale low-level circulation of summer over the western North Pacific can be described in terms of low-latitude southwesterlies, a monsoon trough and a subtropical ridge (Figure 3-10-4a). The axis of the summer monsoon trough of the western North Pacific usually emerges from East Asia at about 20° N to 25°N, and extends southeastward to a terminus southeast of Guam (13°N ; 145°E) (Sadler et al. 1987). Most of the tropical cyclones which develop in the western North Pacific form in the monsoon trough. When the axis of the monsoon trough is in its normal orientation (NW-SE), tropical cyclones tend to move northwestward on tracks close to those expected from climatology. As an episodic event, the axis of the monsoon trough becomes displaced to the north of its usual location and takes on a SW-NE (i.e., reverse) orientation (see Figure 3-10-4b). When the monsoon trough acquires a reverse orientation, tropical cyclones along it tend to move on north-oriented tracks, as was the case with Walt.

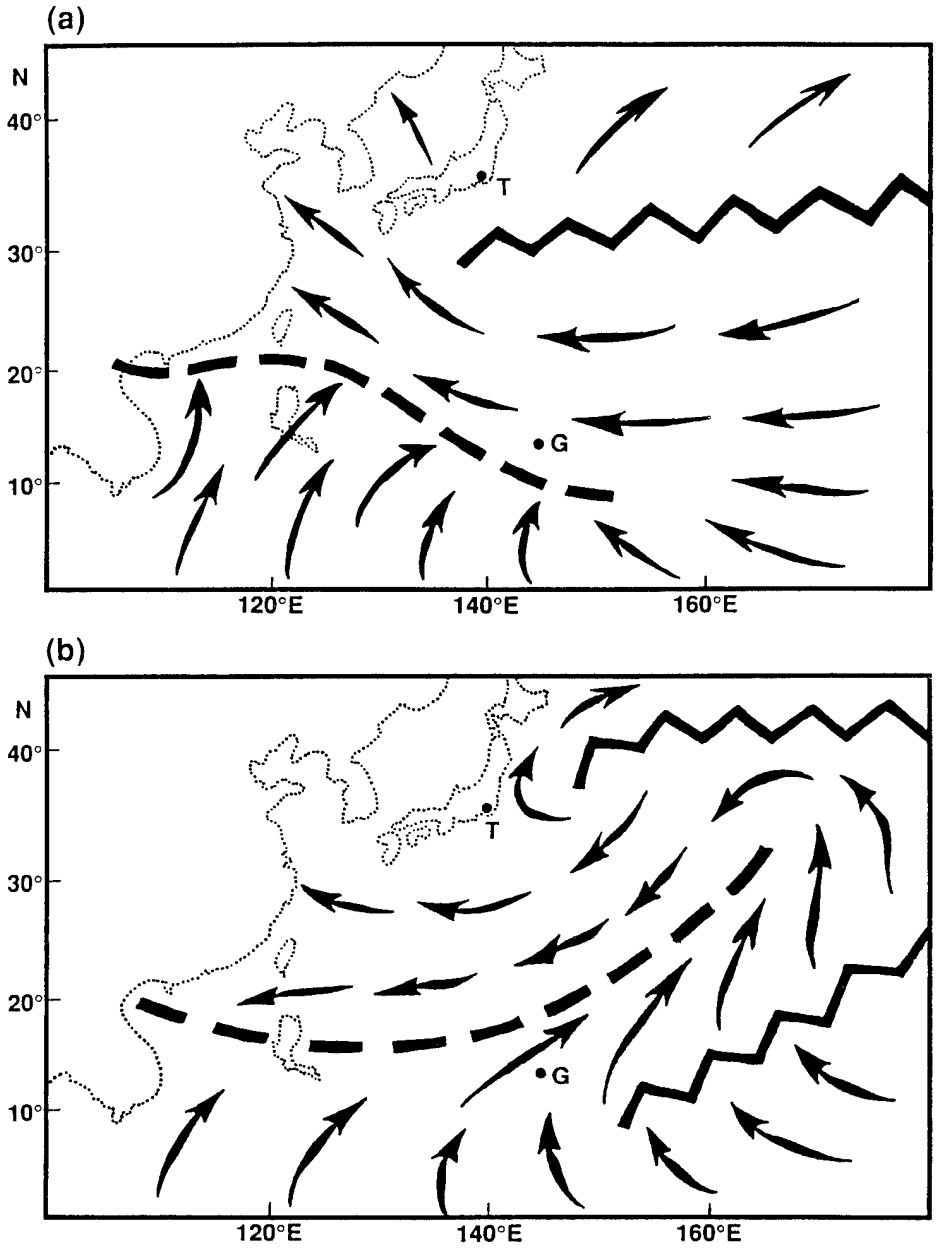

Figure 3-10-4 The low-level circulation of summer in the tropics of the western North Pacific: (a) the long-term average; and (b) a schematic illustration of the low-level circulation associated with a reverse-oriented monsoon trough. Bold zig-zag lines indicate ridge axes, and bold dashed line indicates the axis of the monsoon trough. Arrows indicate wind direction. The location of Guam (G) and Tokyo (T) are indicated.

b. Decay over warm water

After reaching super typhoon intensity over the warm waters of the Philippine Sea, Walt gradually weakened while moving slowly northward towards southern Japan. Although it was over warm sea surface temperatures, Walt weakened from 130 kt (67 m/sec) at 200000Z to 50 kt (26 m/sec) by 250600Z (the time of landfall in southern Japan) without any signs of appreciable vertical shear. By 280600Z Walt had completely dissipated.

c. Forecast performance

Overall, the official forecasts for Walt were good. The track forecast extracted from the NOGAPS model (the objective aid, "NGPS", received at the JTWC) and the forecast low-level wind fields made by the NOGAPS model had two periods of difficulty during the lifetime of Walt. The biggest problem with the numerical guidance provided by the Navy's NOGAPS model (e.g., wind and height fields, and the track aid "NGPS") was in the prediction of the size of Walt in relation to the prediction of the sizes of two other tropical cyclones, Yunya (11W) and Zeke (12W), that accompanied Walt along the axis of the monsoon trough. Early in Walt's life, the NOGAPS model was greatly over-forecasting the size and intensity of the pre-Zeke tropical disturbance that was located to the east of Walt. At the same time, the size and intensity of Walt were under-forecast by NOGAPS. As a result, the model output showed Walt dissipating and being swept eastward into the exaggerated circulation of Zeke (12W).

A few days later, the NOGAPS forecasts radically changed. They began to over-forecast the size of Walt, causing the model-predicted track of the smaller Zeke (12W) to be affected (i.e., to undergo a binary interaction with Walt that moved it too far to the north and west). Walt did eventually become a large and very intense typhoon, so the NOGAPS forecasts which called for Walt to grow extremely large verified reasonably well; however, this relatively minor error had significant consequences on the track forecasts of Zeke (12W) (see Zeke's summary).

IV. IMPACT

No reports of fatalities or significant damage were received. As a weak tropical storm passing over southern Japan, peak recorded wind gusts were near 35 kt (17 m/sec). Rainfall in southern portions of the Korean Peninsula caused by Walt helped to alleviate ongoing severe drought conditions.

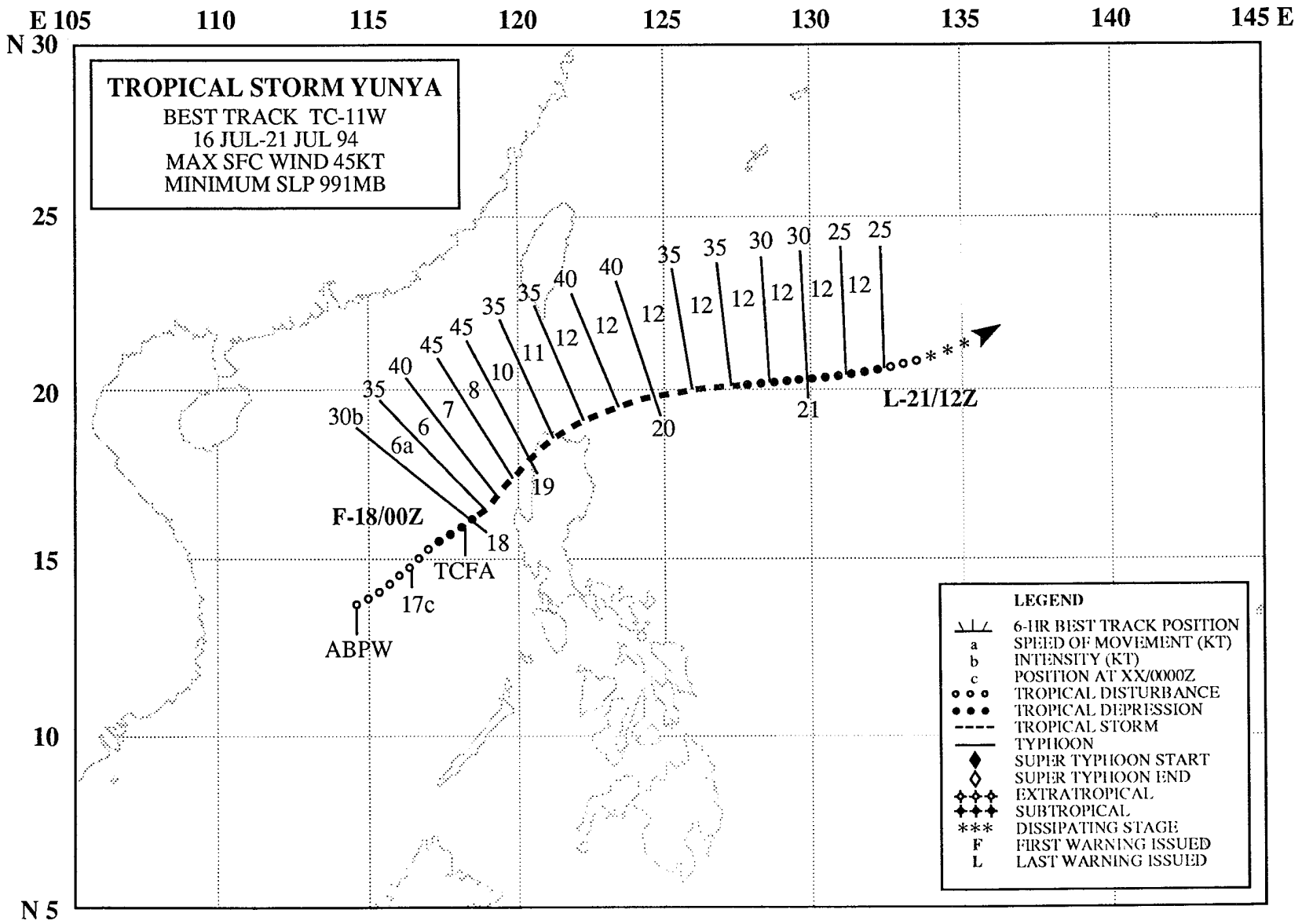
TROPICAL STORM YUNYA
BEST TRACK TC-11W
16 JUL-21 JUL 94
MAX SFC WIND 45KT
MINIMUM SLP 991MB
E 105
110
115
120
125
130
135
140
145 E
N 30
25
20
15
10
N 5
F-18/00Z
TCFA
ABPW
L-21/12Z
LEGEND
6-HR BEST TRACK POSITION
SPEED OF MOVEMENT (KT)
INTENSITY (KT)
POSITION AT XX/0000Z
TROPICAL DISTURBANCE
TROPICAL DEPRESSION
TROPICAL STORM
TYPHOON
SUPER TYPHOON START
SUPER TYPHOON END
EXTRATROPICAL
SUBTROPICAL
DISSIPATING STAGE
FIRST WARNING ISSUED
LAST WARNING ISSUED

TROPICAL STORM YUNYA(11W)

I. HIGHLIGHTS

Yunya was a very small tropical cyclone that formed along the axis of a reverse-oriented monsoon trough. It was the westernmost of three tropical cyclones along this trough. The other two were Walt (10W) and Zeke (12W). Yunya exhibited unusual eastward motion for its entire track which resulted in a rare west-to-east crossing of Luzon. Weakened by its passage over Luzon, it briefly re-intensified over water in the Philippine Sea before dissipating.

II. TRACK AND INTENSITY

During mid-July, an active reverse-oriented monsoon trough dominated the low-level circulation of the western North Pacific. The cloudiness associated with the southwesterly monsoon flow stretched eastward from Southeast Asia, across the South China Sea and the Philippine islands; then east-northeastward across the Philippine Sea toward sub-tropical latitudes near the international date line. On or about 16 July, the monsoon cloud band evolved into a sequence of several distinct cloud clusters, three of which became named tropical cyclones: Walt (10W), Yunya, and Zeke (12W). By 160000Z, animated satellite imagery and synoptic data indicated that a weak low-level circulation center was associated with a cloud cluster over the South China Sea. This tropical disturbance was first mentioned in the 160600Z July Significant Tropical Weather Advisory. As the low-level circulation center moved toward the east-northeast, the organization of the associated deep convection improved (Figure 3-11-1), and at 172300Z a Tropical Cyclone Formation Alert was issued. The first warning was issued an hour later at 180000Z. The system was upgraded to Tropical Storm Yunya at 181800Z. Post analysis indicated that tropical storm intensity had most probably occurred 12 hours earlier at 180600Z. As Yunya neared landfall on the northwest corner of Luzon, its satellite could signature improved (Figure 3-11-2). At the landfall, shortly after 190000Z, its intensity was estimated to be 45 kt (23 m/sec). During the six-hour passage over land, its cloud structure became disorganized, and the best-track intensity was lowered to 35 kt (17 m/sec) at 190600Z. Moving eastward, Yunya was soon over water in the Philippine Sea. A brief period of re-intensification to 40 kt (21 m/sec) took place and persisted for six hours (191800Z to 200000Z). Deep convection then decreased, and the final warning was issued at 211200Z as Yunya moved eastward over water and dissipated.

III. DISCUSSION

a. Unusual motion

Yunya's motion had an eastward component for its entire track. This type of unusual motion is commonly associated with tropical cyclones which are located within a reverse-oriented monsoon trough. For a more thorough discussion of the characteristics of a reverse-oriented monsoon, and of its impacts upon the motion of tropical cyclones, see Walt's (10W) summary.

b. Small Size

Developing from a cloud cluster in the South China Sea, Yunya consolidated into a small core of deep convection to the north of an area of extensive deep convection in the southwesterly monsoon flow. Yunya's small cloud system appeared to be undergoing rapid improvement in organization as it made landfall on northern Luzon (Figure 3-11-2). Brand (1972) noted a preference for very small tropical cyclones to be located in the extreme western Pacific Ocean within a corridor extending from Luzon to Tokyo.

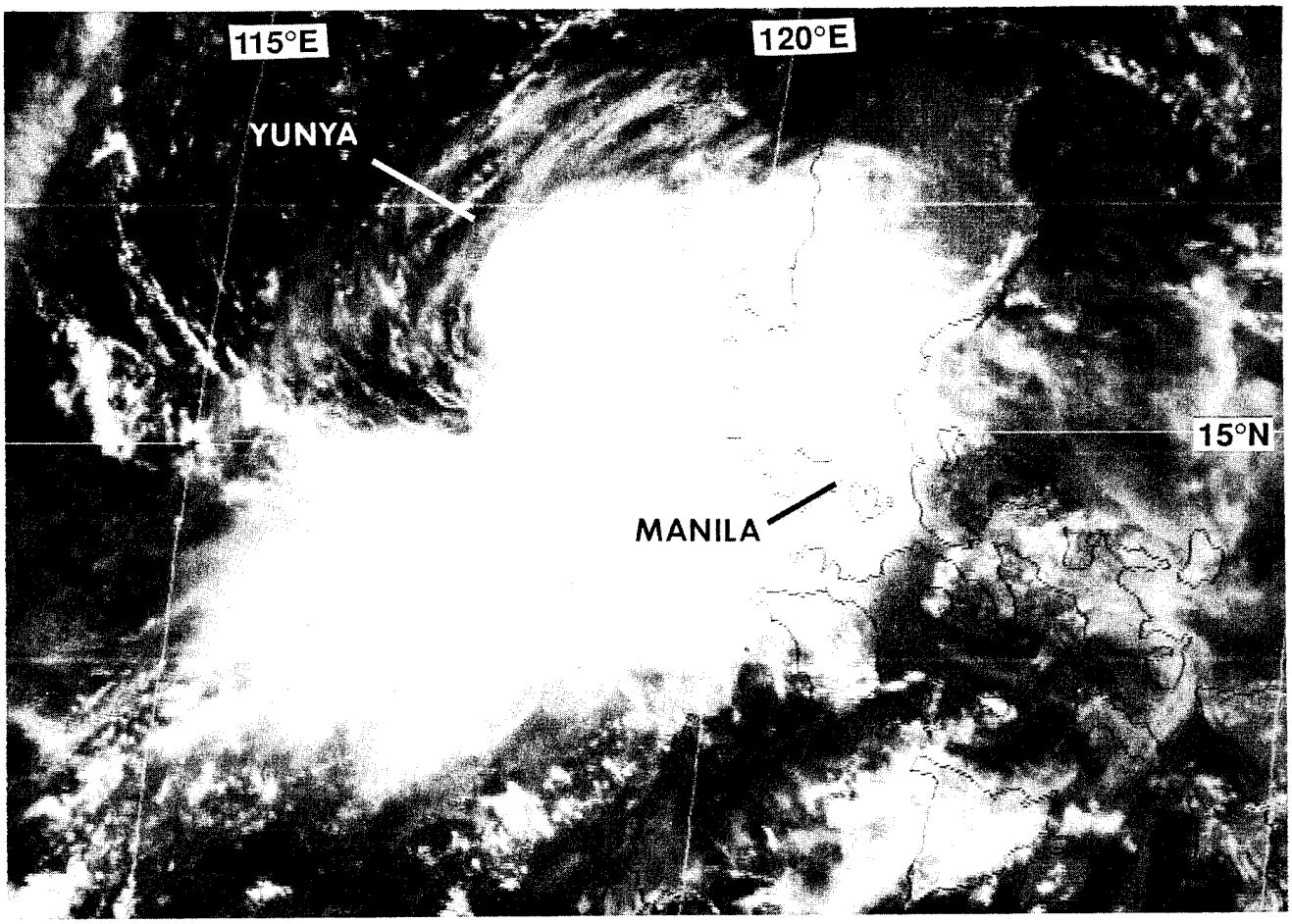

Figure 3-11-1 Curving low-level cloud lines, and organization of the deep convection into a curved band prompted the the first warning on Yunya. (180131Z July visible GMS imagery).

IV. IMPACT

Heavy rains from Yunya triggered landslides of volcanic debris from Mount Pinatubo. Monsoon flow to the south of Yunya had gusts in excess of 60 kt (31 m/sec) across the central plains of Luzon. No reports of serious damage were received. One man reportedly died of a heart attack in central Luzon after seeing his house swept away by floodwaters.

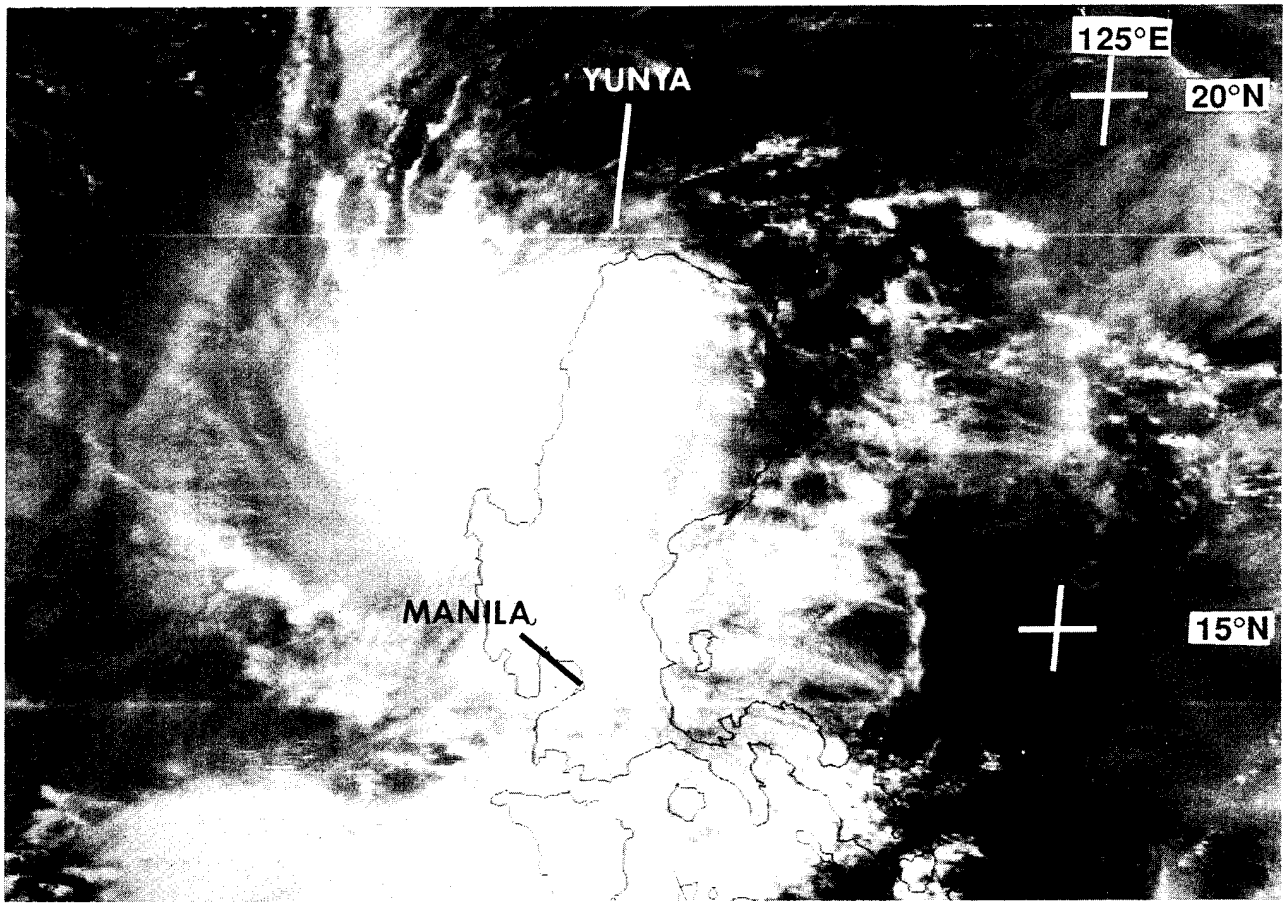

Figure 3-11-2 Yunya reaches its peak intensity of 45 kt (23 m/sec) as it makes landfall on the northwestern corner of Luzon. (182331Z July visible GMS imagery).

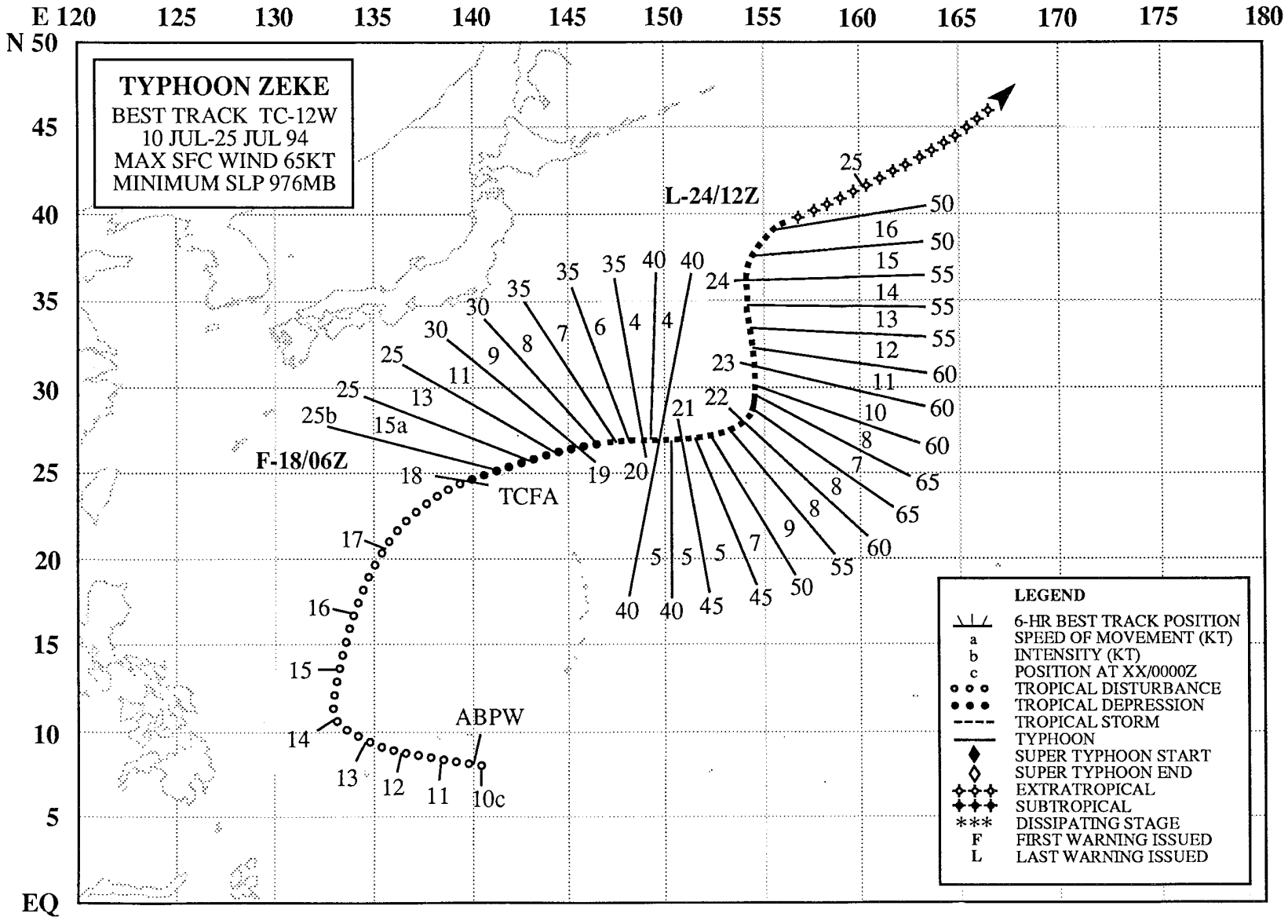
TYPHOON ZEKE
BEST TRACK TC-12W
10 JUL-25 JUL 94
MAX SFC WIND 65KT
MINIMUM SLP 976MB
E 120
125
130
135
140
145
150
155
160
165
170
175
180
N 50
45
40
35
30
25
20
15
10
5
EQ
L-24/12Z
F-18/06Z
TCFA
ABPW
LEGEND
6-HR BEST TRACK POSITION
SPEED OF MOVEMENT (KT)
INTENSITY (KT)
POSITION AT XX/0000Z
TROPICAL DISTURBANCE
TROPICAL DEPRESSION
TROPICAL STORM
TYPHOON
SUPER TYPHOON START
SUPER TYPHOON END
EXTRATROPICAL
SUBTROPICAL
DISSIPATING STAGE
FIRST WARNING ISSUED
LAST WARNING ISSUED

TYPHOON ZEKE (12W)

I. HIGHLIGHTS

Zeke was a small tropical cyclone that formed along the axis of a reverse-oriented monsoon trough. It was the easternmost of three tropical cyclones along this trough (see Figure 3-10-1 in Walt's (10W) summary). Zeke exhibited unusual "S" track motion which is almost exclusively associated with tropical cyclones embedded in a reverse-oriented monsoon trough (Lander 1995a). Zeke's brief attainment of typhoon intensity was verified by ship observation. Satellite imagery at the time of typhoon intensity winds was atypical: ragged, but tightly coiled spirals of relatively warm-topped convection, and alone did not support typhoon intensity.

II. TRACK AND INTENSITY

During early July, the axis of the monsoon trough extended across much of Micronesia at rather low latitudes (5° - 7°N). Most of the deep convection associated with this monsoon trough resided south of 10°N. On 14 July, two persistent cloud clusters had consolidated in the Philippine Sea to the east of Luzon. The westernmost cloud cluster became Walt (10W), while the easternmost later became Zeke. The first mention of the incipient tropical disturbance that would become Zeke appeared on the 140600Z July Significant Tropical Weather Advisory. This tropical disturbance was followed for several days as it moved first northward, then northeastward. During this time, Walt (10W) formed to the east of Luzon, southwest of the pre-Zeke tropical disturbance. Concurrent with Walt's (10W) low-latitude turn toward the northeast and the gradual turn to the northeast of the pre-Zeke disturbance, a long band of deep convective cloud clusters, that included the cloud systems of Walt (10W), Yunya (11W) and the pre-Zeke disturbance, had acquired a SW-NE (i.e., reverse) orientation. This reverse-oriented monsoon trough was the first of three reverse-oriented monsoon troughs during 1994, and stretched from 15°N in the South China Sea to 30°N near the international date line.

As the pre-Zeke tropical disturbance moved northeastward, it slowly intensified. At 180000Z, a Tropical Cyclone Formation Alert was issued. This alert stated, in part:

" . . . satellite and synoptic data indicate an active area of convection northeast of Tropical Storm Walt (10W) is showing signs of development. The disturbance is located beneath an area of light upper level winds with a TUTT cell located to the northwest of the system. . . ."

Based upon improved banding of the deep convection and the appearance of well-defined cyclonically curved low-level cloud lines, the first warning on Tropical Depression 12W was issued at 180600Z. Upper-level shear from the west seemed to be preventing intensification, and the system remained at tropical depression intensity until 191200Z. During the early morning of 20 July, tropical depression warning number 7 (191200Z) was amended to tropical cyclone warning number 7A. The amended warning stated, in part:

" . . . visual satellite imagery indicates Tropical Storm Zeke (12W) has a well defined low level circulation beneath an area of active convection . . . For this reason, TD 12W has been upgraded to tropical storm intensity and named 'Zeke'. . . ."

Moving eastward until 220000Z, Zeke then slowed and turned to the north. Shortly after turning northward, about 220600Z, synoptic data indicated that Zeke possessed winds of 65 kt (33m/sec), and at 220600Z, Zeke was upgraded to a typhoon. Zeke's life as a typhoon was short-lived, however, and at 221800Z it was downgraded to a 60 kt (31 m/sec) tropical storm. Moving on a track slightly west of north until 240000Z, Zeke gradually weakened. Turning gradually to the northeast after 240000Z, and

accelerating, Zeke began to acquire extratropical characteristics, and the final warning was issued at 241200Z.

III. DISCUSSION

a. Unusual motion

Zeke's track is a good example of the "S" motion, which is defined by Lander (1995a). This north-oriented motion features eastward movement at low latitude, a later bend to the north or northwest, and then eventually north-eastward motion as the system enters the mid-latitude westerlies. Of the 103 north-oriented tracks during the period 1978 to 1993, thirty five (34%) could be categorized as "S" motion. Of the 35 cases of "S" motion during the period 1978 to 1993, twenty eight cases (80%) occurred in association with a reverse-oriented monsoon trough, five cases occurred in association with a monsoon gyre, and two cases were associated with other environmental flow patterns. For a more thorough discussion of the characteristics of a reverse-oriented monsoon trough see Walt's (10W) summary.

b. Unusual satellite signature for a typhoon

During the morning of 22 July, the cloud signature of Zeke rapidly improved as a spiral band of cold-

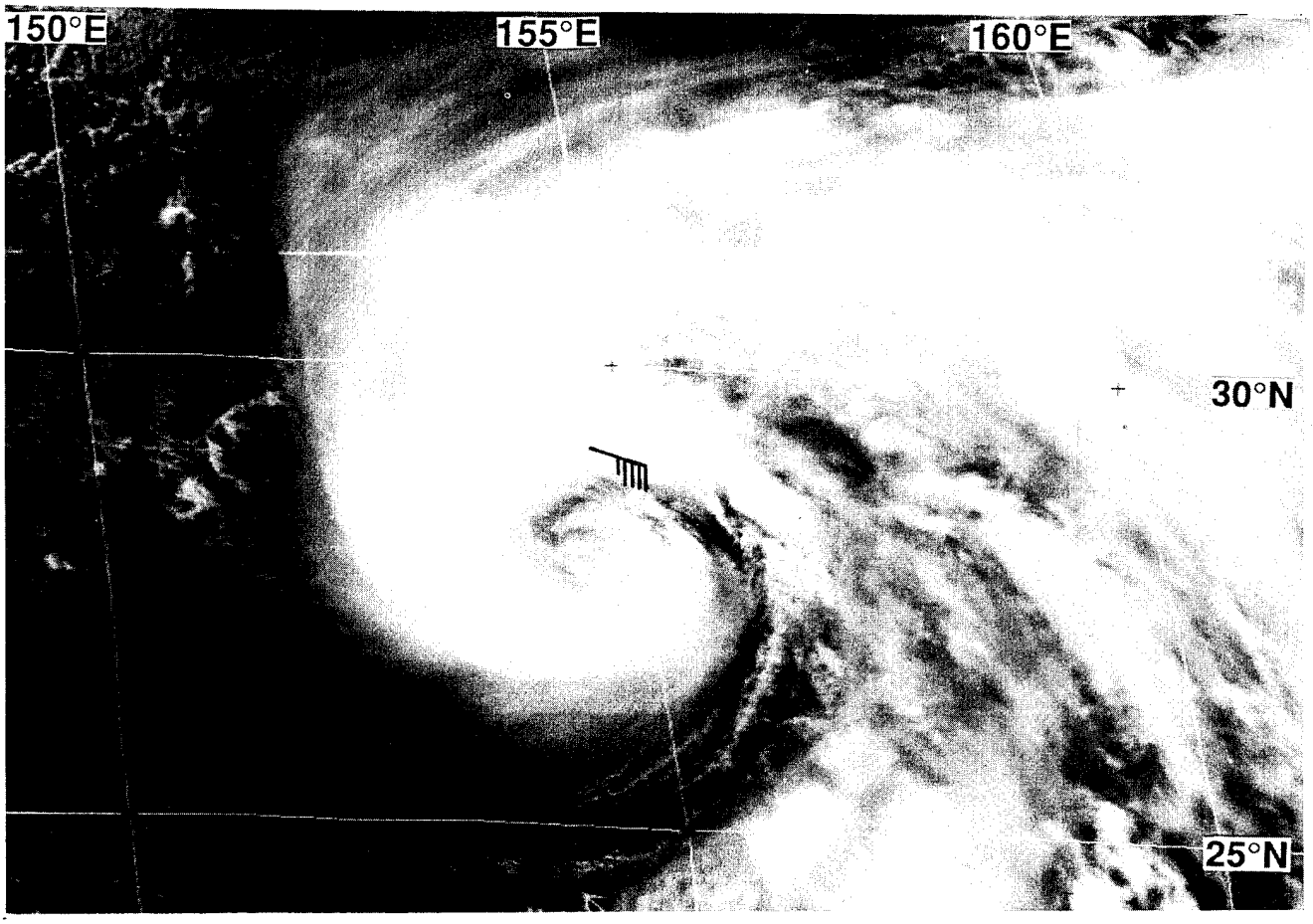

Figure 3-12-1 The deep convection begins to coil tightly around Zeke's low-level center (220031 July visible GMS imagery).

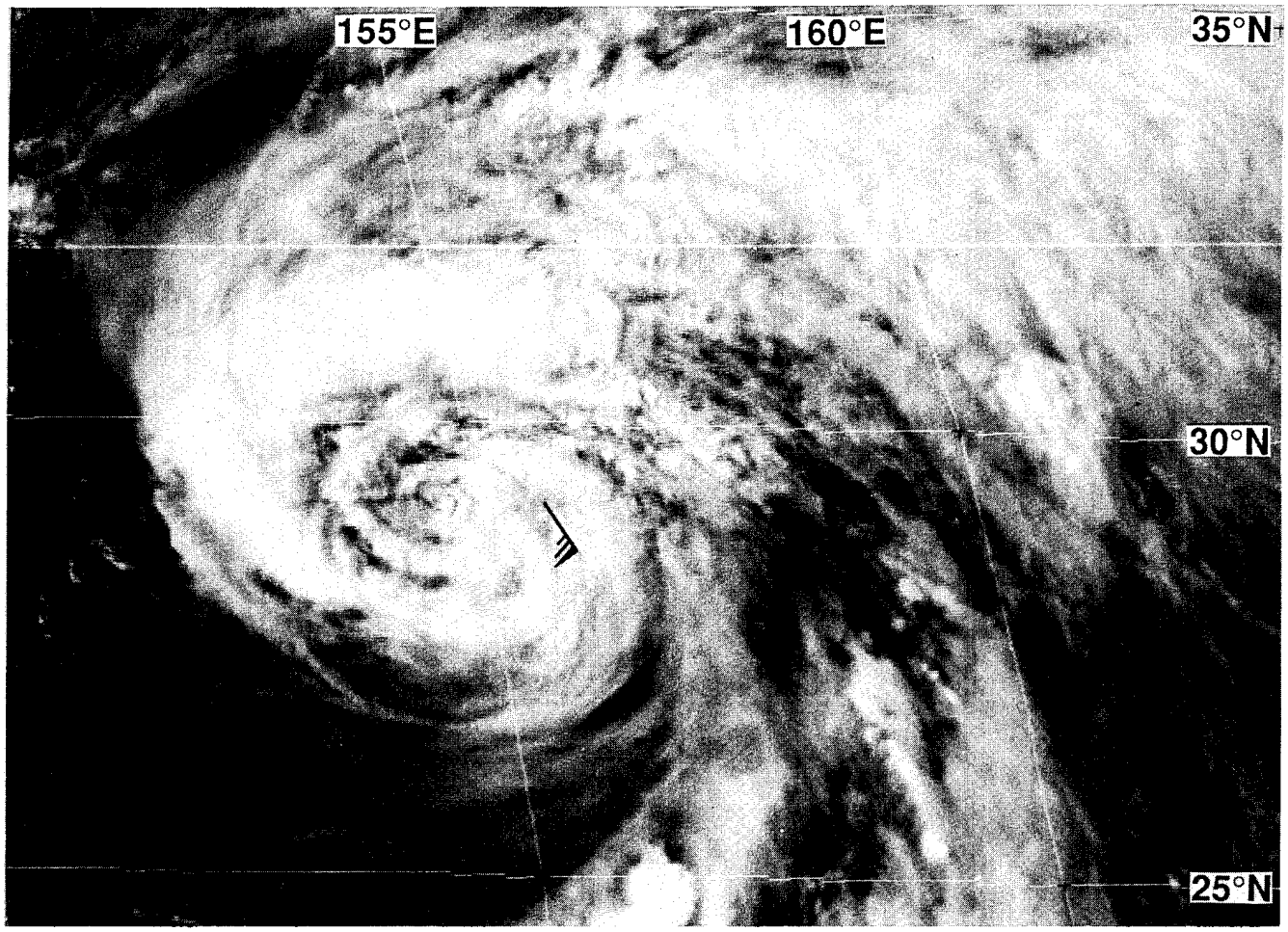

Figure 3-12-2 Bands of towering cumulus and relatively shallow convection are tightly wound and multi-coiled when a ship near Zeke's center reported typhoon intensity wind (220531Z July visible GMS imagery).

topped deep convection began to coil tightly around the exposed low-level center (Figure 3-12-1). At this time, a ship located north of the center of Zeke reported 45 kt (23 m/sec) sustained winds. Towards the evening of July 22, the single, cold-topped spiral of deep convection had evolved into a multi-coiled spiral of ragged warmer-topped convection (Figure 3-12-02). At the time of the imagery in Figure 3-12-2, the aforementioned ship had progressed into the eastern semi-circle of Zeke's circulation and reported typhoon-force winds. A satellite intensity estimate made at 220424Z July (an hour before the satellite imagery shown in Figure 3-12-2) indicated an intensity of T2.5 (minimal tropical storm intenisty), and remarks on this fix stated:

. . . "Zeke is becoming extratropical. Only a little deep convection remains near the center . . ."

If not for the 65 kt (33 m/sec) ship report, it is doubtful that the JTWC would have upgraded Zeke to a typhoon.

c. Forecast performance

Overall, the official forecasts for Typhoon Zeke were quite good. Similar to problems with the objective guidance described in the summary of Walt (10W), the track forecast extracted from the NOGAPS model (the objective aid, "NGPS", received at the JTWC) and the forecast low-level wind fields made

by the NOGAPS model had two periods of difficulty during the lifetime of Zeke. First, early in Zeke's life, the NOGAPS model over-developed its circulation into a very large tropical cyclone. Zeke, however, remained small for its entire life. Rather, it was Walt (10W) which became the largest and most intense of the three named tropical cyclones (Walt (10W), Yunya(11W), and Zeke) which were aligned SW-NE along the axis of a reverse-oriented monsoon trough. The erroneous initial over-development of Zeke caused the model to subsume Walt (10W) into Zeke's artificially large circulation by the 48-hour point of the forecast. The second problem occurred later in Zeke's life when the NOGAPS model over-developed the size of Walt's circulation. This, along with the model's loss of the eastern reaches of the reverse-oriented monsoon trough, contributed to NOGAPS forecasts of Zeke's motion too far to the north and west during the period 200000Z through 230000Z.

IV. IMPACT

Typhoon Zeke remained over open ocean its entire life, and no reports of fatalities or significant damage were received.

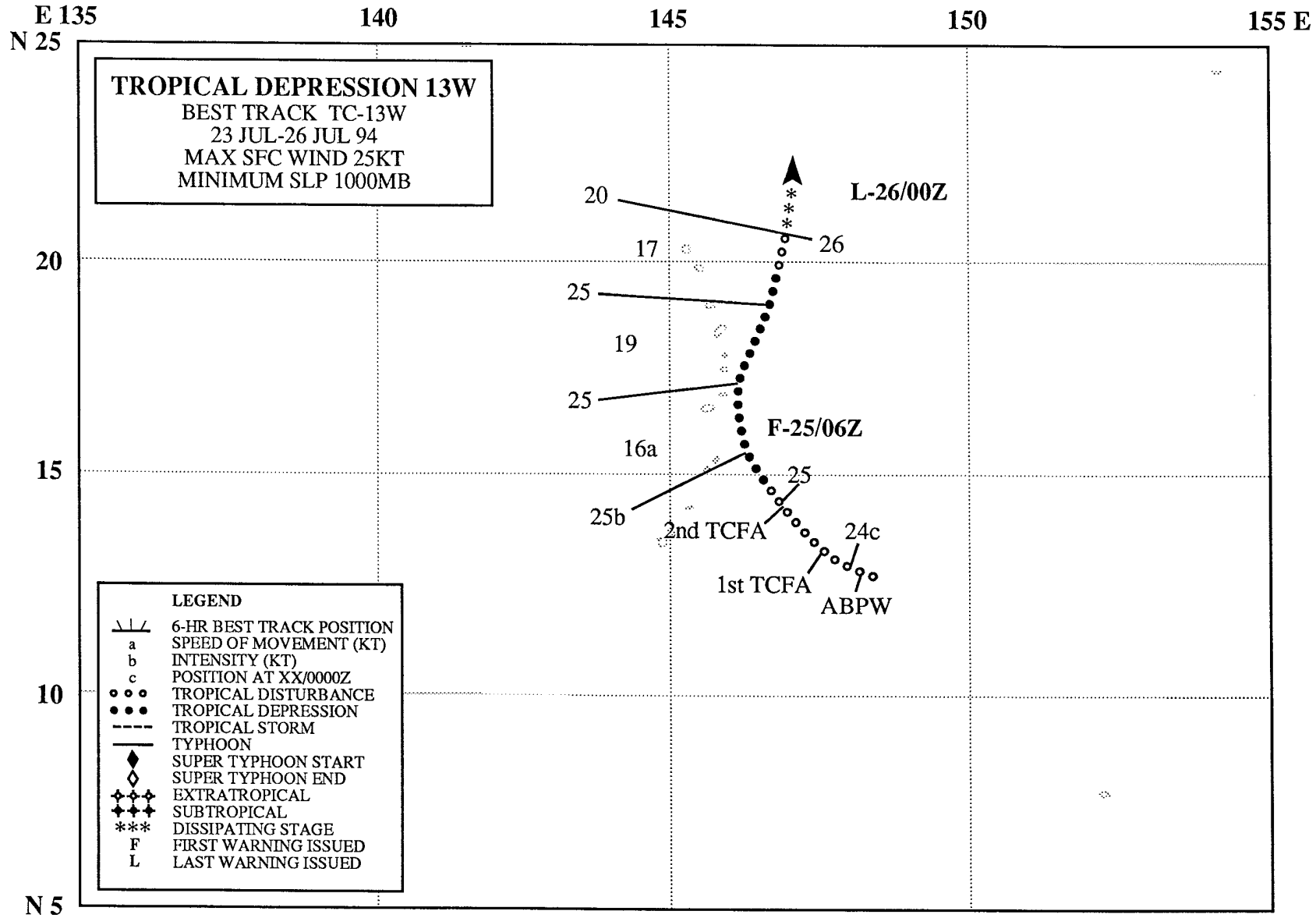
E 135
140
145
150
155 E
N 25
20
15
10
N 5
84
TROPICAL DEPRESSION 13W
BEST TRACK TC-13W
23 JUL-26 JUL 94
MAX SFC WIND 25KT
MINIMUM SLP 1000MB
20
26
L-26/00Z
17
25
19
25
F-25/06Z
16a
25
25b
2nd TCFA
24c
1st TCFA
ABPW
LEGEND
6-HR BEST TRACK POSITION
a SPEED OF MOVEMENT (KT)
b INTENSITY (KT)
c POSITION AT XX/0000Z
TROPICAL DISTURBANCE
TROPICAL DEPRESSION
TROPICAL STORM
TYPHOON
SUPER TYPHOON START
SUPER TYPHOON END
EXTRATROPICAL
SUBTROPICAL
*** DISSIPATING STAGE
F FIRST WARNING ISSUED
L LAST WARNING ISSUED

TROPICAL DEPRESSION 13W

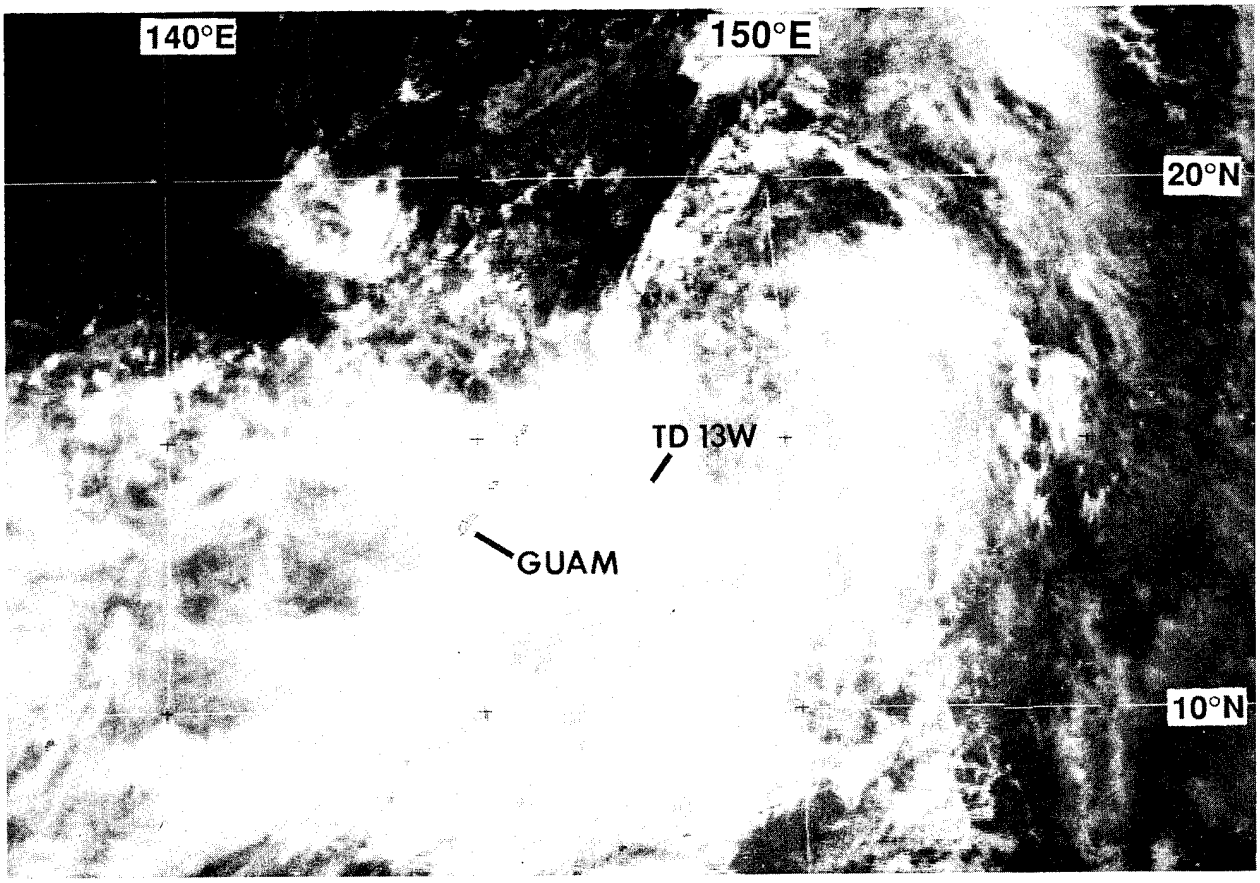

Figure 3-13-1 Tropical Depression 13W forms in the monsoon cloud band east of Guam (250424Z July visible GMS imagery).

Tropical Depression 13W, formed on 24 July, in association with a surge of the southwest monsoon across the Philippine Sea. Two Tropical Cyclone Formation Alerts were issued on the system: the first at 241051Z July, the second was at 242251Z after the disturbance center was relocated to the south. The first warning on Tropical Depression 13W was issued at 250600Z as the system passed about 40 nm (74 km) east of Saipan (WMO 91222) (Figure 3-13-1) while moving northward at 10-12 kt (19-22 km/hr) along the east side of a monsoon gyre. The depression was short-lived, however, as it dissipated less than a day later east of the northernmost of the Mariana Islands.

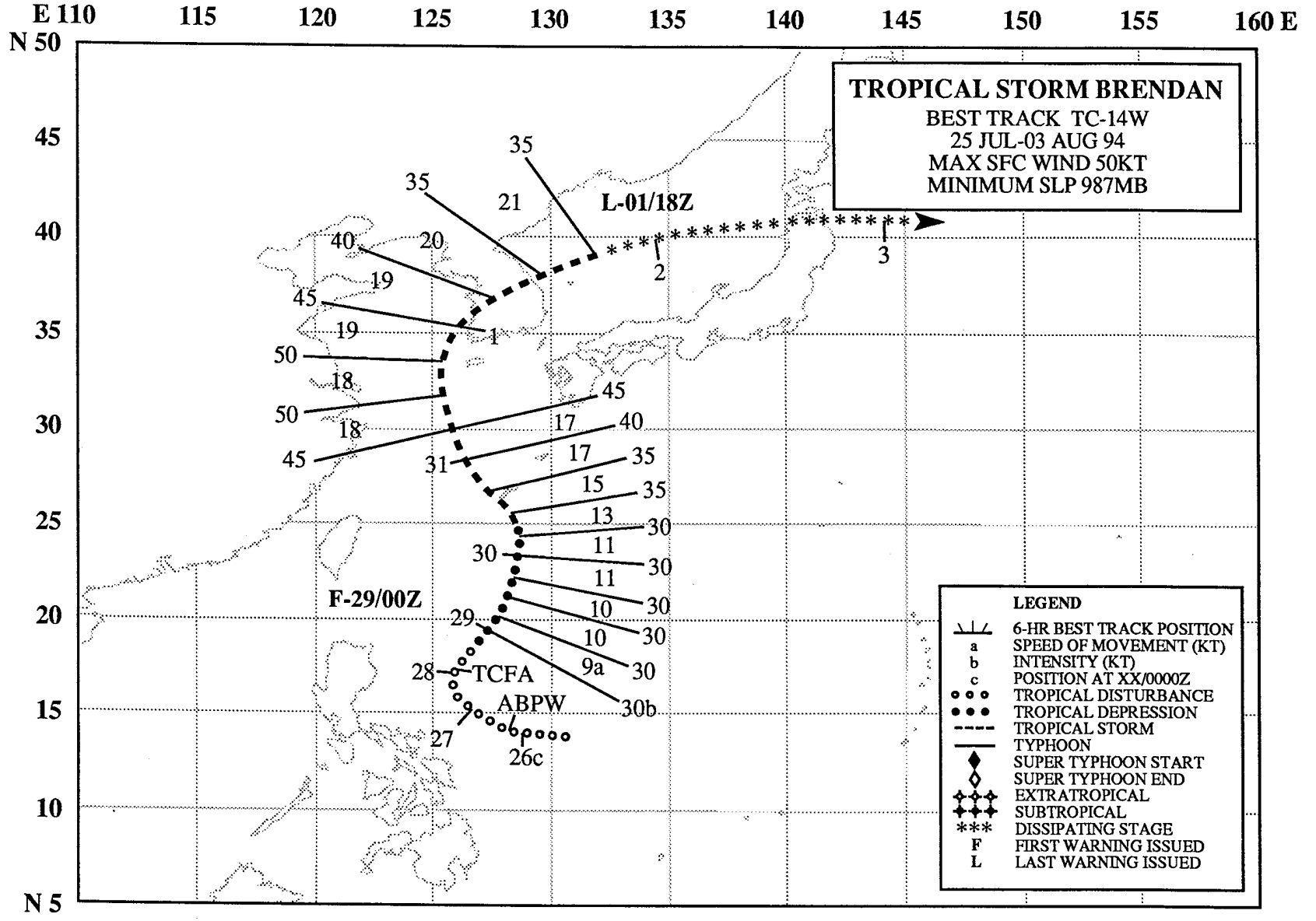
TROPICAL STORM BRENDAN
BEST TRACK TC-14W
25 JUL-03 AUG 94
MAX SFC WIND 50KT
MINIMUM SLP 987MB
L-01/18Z
F-29/00Z
TCFA
ABPW
LEGEND
6-HR BEST TRACK POSITION
SPEED OF MOVEMENT (KT)
INTENSITY (KT)
POSITION AT XX/0000Z
TROPICAL DISTURBANCE
TROPICAL DEPRESSION
TROPICAL STORM
TYPHOON
SUPER TYPHOON START
SUPER TYPHOON END
EXTRATROPICAL
SUBTROPICAL
DISSIPATING STAGE
FIRST WARNING ISSUED
LAST WARNING ISSUED
E 110
115
120
125
130
135
140
145
150
155
160 E
N 50
45
40
35
30
25
20
15
10
N 5

TROPICAL STORM BRENDAN (14W)

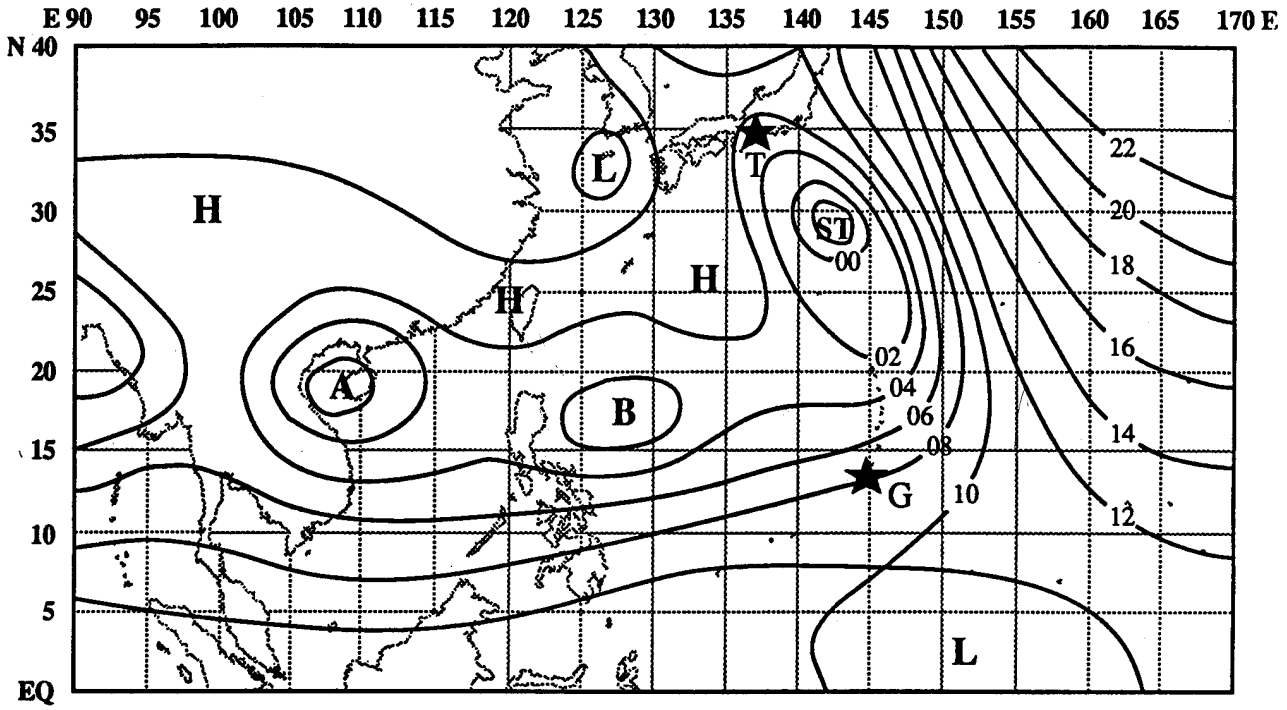

Figure 3-14-1 Sea-level pressure analysis at 280000Z July showing the location of the pre-Brendan (B) tropical disturbance in an active monsoon trough. A sub-tropical cyclone (ST) — possibly the continuation of Tropical Depression 13W — is seen southeast of Tokyo. A low pressure area in the Tonkin Gulf would later become Amy (15W) (A). Dotted lines outline major land masses, bold lines are isobars at 2 mb intervals, stars are labeled G for Guam and T for Tokyo.

I. HIGHLIGHTS

For six days, Brendan meandered northward in a sinusoidal pattern, passing over Okinawa, and eventually striking Korea on 01 August. Up to 8 inches (203 mm) of rain helped to alleviate drought conditions in some areas of the Korean peninsula.

II. TRACK AND INTENSITY

On 26 July, convection began to consolidate into a discrete tropical disturbance in the monsoonal cloud band over the Philippine Sea. This disturbance — the precursor to Brendan — was first mentioned on the 260600Z July Significant Tropical Weather Advisory. During the next two days, the disturbance moved at an average speed of 6 kt (11 km/hr), initially to the northwest, and then, in association with a surge in the southwest monsoon, it turned northward. Based upon improved organization of the deep convection, a Tropical Cyclone Formation Alert was issued at 280200Z. At this time the monsoon circulation was very active (Figure 3-14-1). The first warning on Tropical Depression 14W was issued at 290000Z based upon ship reports of 25 kt (13 m/sec) wind and sea-level pressure below 1000

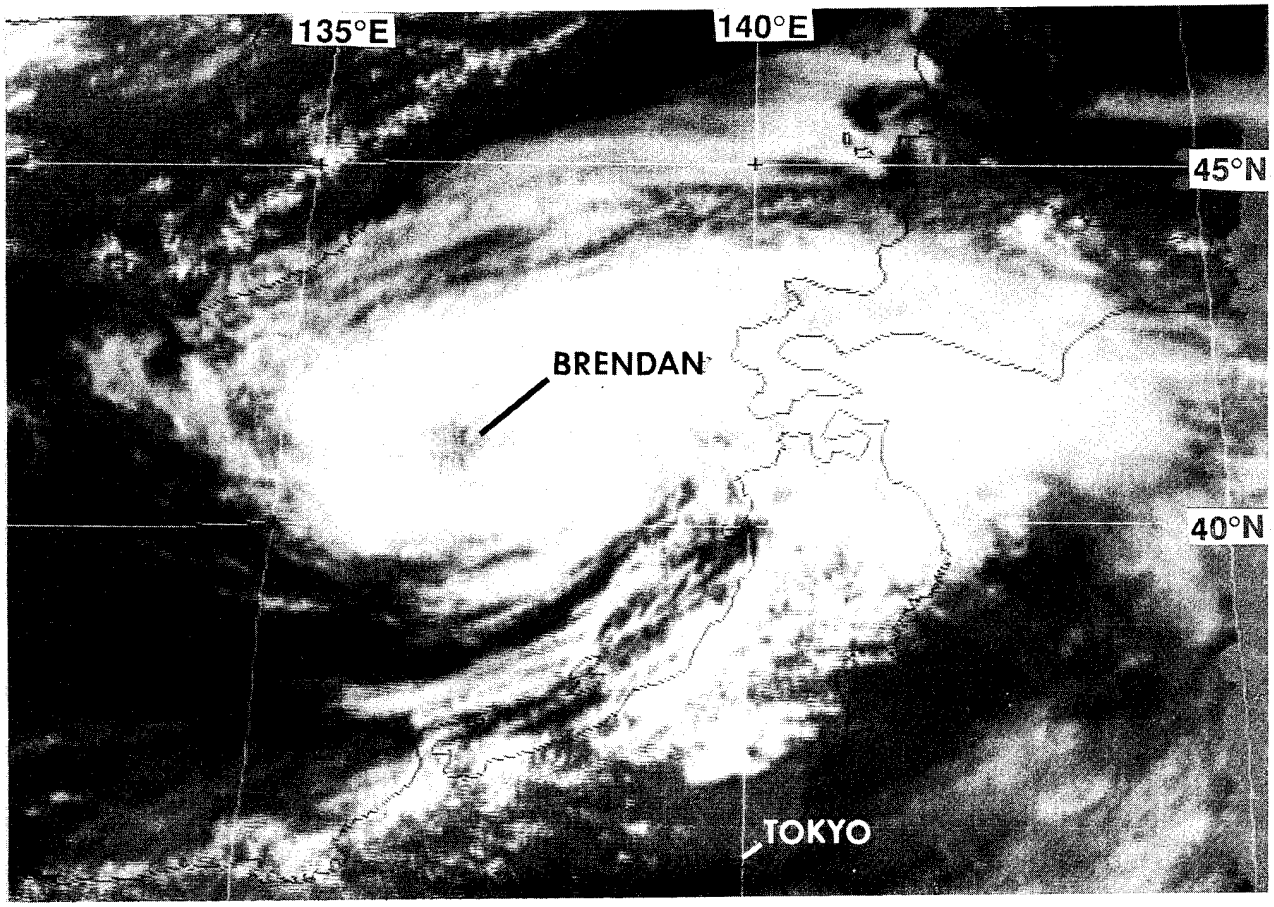

Figure 3-14-2 Brendan exhibits a well-defined exposed low-level circulation center as it approaches Okinawa (300631Z July visible GMS imagery).

mb. As Tropical Depression 14W accelerated northward, it reached tropical storm intensity on the evening of 30 July (Figure 3-14-2) just prior to crossing Okinawa.

Brendan was moving at 18 kt (33 km/hr) when it reached its maximum intensity of 50 kt (26 m/sec) about 120 nm (220 km) south of Cheju Island, Korea. The system reached its point of recurvature at 311800Z in the Yellow Sea, and then accelerated northeastward passing over the Korean peninsula. After weakening over Korea, Brendan continued to accelerate while crossing the Sea of Japan, became extra-tropical, and reintensified to 45 kt (23 m/sec). The system passed near Misawa, Japan at 021500Z August, and later merged with a frontal cloud band after crossing Japan.

III. DISCUSSION

As Brendan passed over Korea, it acquired characteristics of a hybrid tropical cyclone (i.e., possessing characteristics of both a tropical and extratropical cyclone) (Gray 1968, Hebert and Poteat 1975). As the system moved into the Sea of Japan, it elongated in an east-west direction, characteristic of an occlusion, but maintained organized convection near the central eye-like feature (Figure 3-14-3).

IV. IMPACT

Brendan's path over Korea left two dead and 28 missing as high waves overturned fishing boats. No other reports of significant damage were received.

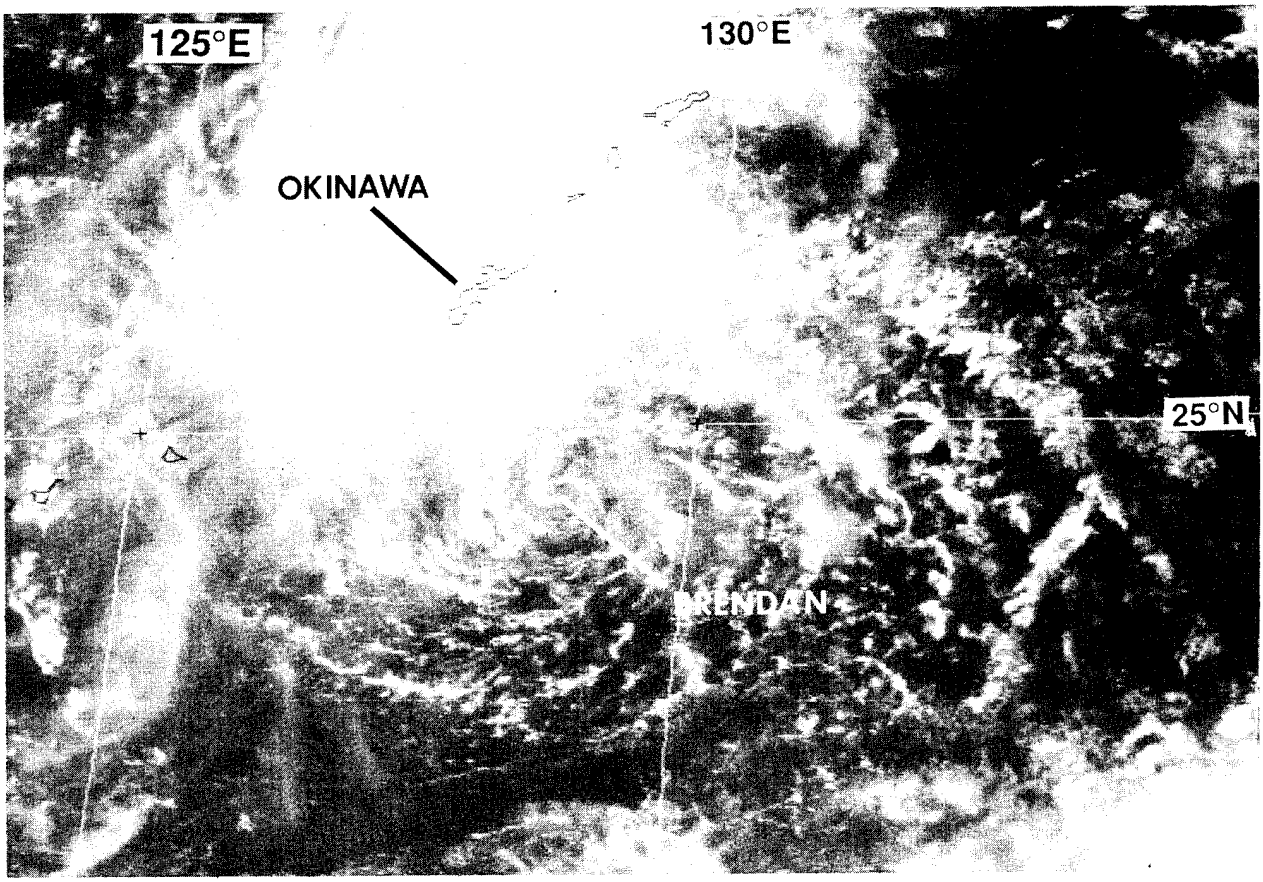

Figure 3-14-3 As a hybrid system, Brendan exhibits both tropical (e.g., organized central convection and an eye-like feature) and extratropical (e.g., the beginnings of a frontal cloud band in its eastern periphery) characteristics (020531Z August visible GMS imagery).

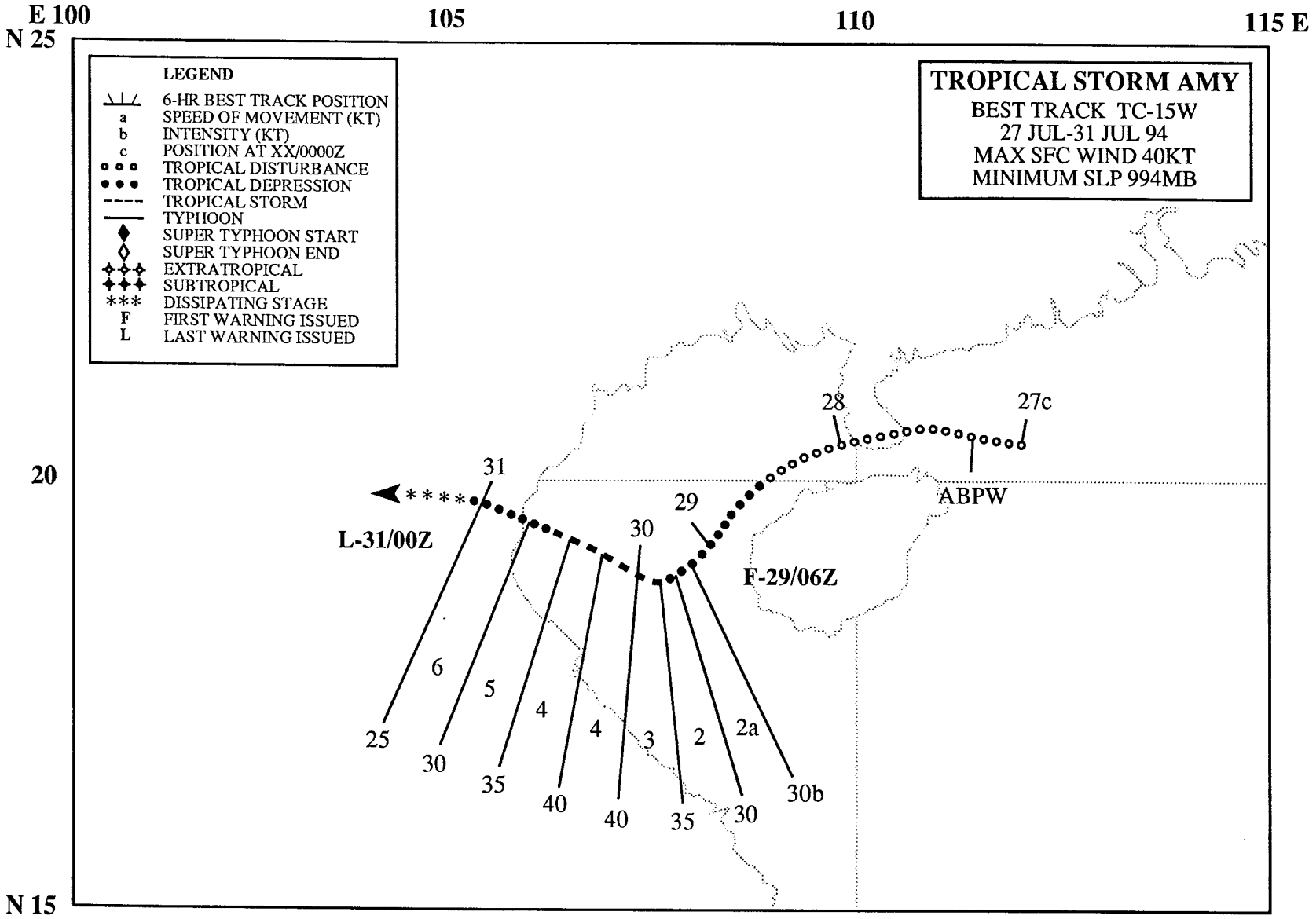
E 100
105
110
115 E
N 25
20
N 15
90
LEGEND
6-HR BEST TRACK POSITION
a SPEED OF MOVEMENT (KT)
b INTENSITY (KT)
c POSITION AT XX/0000Z
TROPICAL DISTURBANCE
TROPICAL DEPRESSION
TROPICAL STORM
TYPHOON
SUPER TYPHOON START
SUPER TYPHOON END
EXTRATROPICAL
SUBTROPICAL
*** DISSIPATING STAGE
F FIRST WARNING ISSUED
L LAST WARNING ISSUED
TROPICAL STORM AMY
BEST TRACK TC-15W
27 JUL-31 JUL 94
MAX SFC WIND 40KT
MINIMUM SLP 994MB
28
27c
31
29
30
ABPW
L-31/00Z
F-29/06Z
6
5
4
4
3
2
2a
25
30
35
40
40
35
30
30b

TROPICAL STORM AMY (15W)

Throughout most of July, an area of low sea-level pressure persisted in the region of the Gulf of Tonkin. This low-pressure area was a regional feature at the western end of the over-water portion of the monsoon trough [see Figure 3-14-1 in Brendan's (14W) summary]. For many days, thick layered cloudiness with embedded deep convection covered southern China, portions of Southeast Asia, and much of the South China Sea. On 29 July, an area of persistent convection associated with a low-level cyclonic circulation that had previously been located over Hainan Dao, moved over water. Based upon synoptic data and satellite imagery (Figure 3-15-1), the first warning on Tropical Storm Amy was issued at 290600Z. Amy reached an estimated peak intensity of 40 kt (20 m/sec) at 300000Z while over the Gulf of Tonkin. Moving slowly westward, it began to weaken while still over water, and later dissipated over land south of Hanoi.

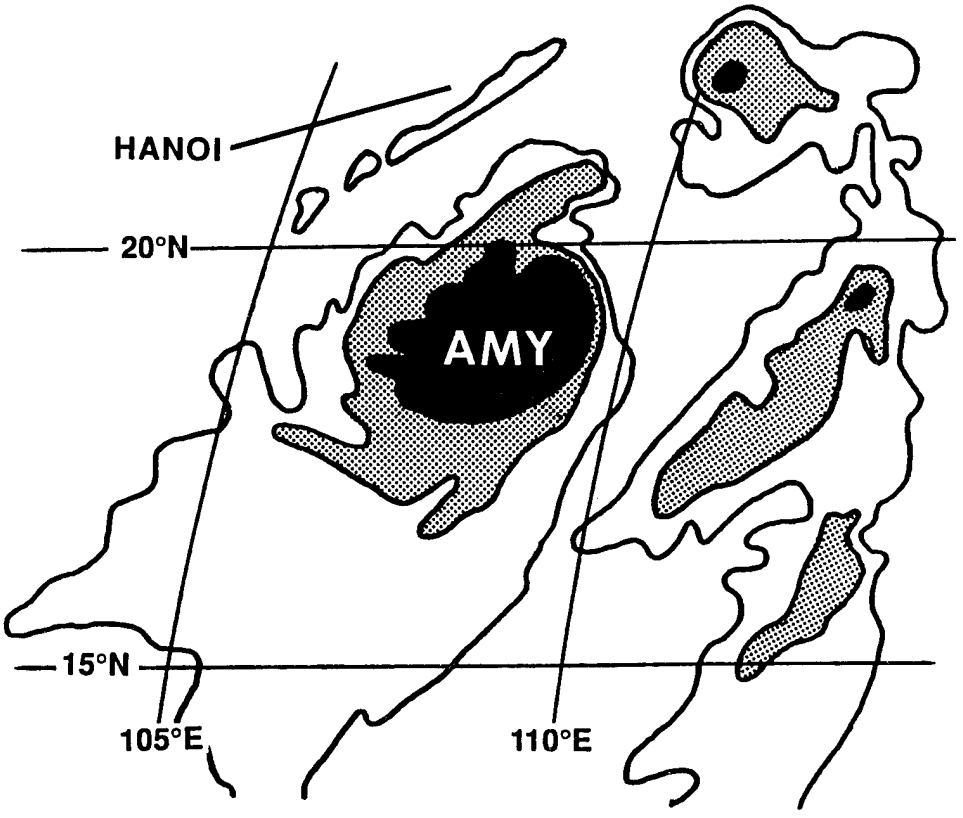

Figure 3-15-1 Schematic illustration of Amy's deep convection as it intensifies over water to the west of Hainan Dao. Cloud-top temperatures are indicated: outer contour = -31°C, shaded region ≤ -54°C, black region ≤ -70°C. (Adapted from 290424Z July enhanced infrared imagery.)

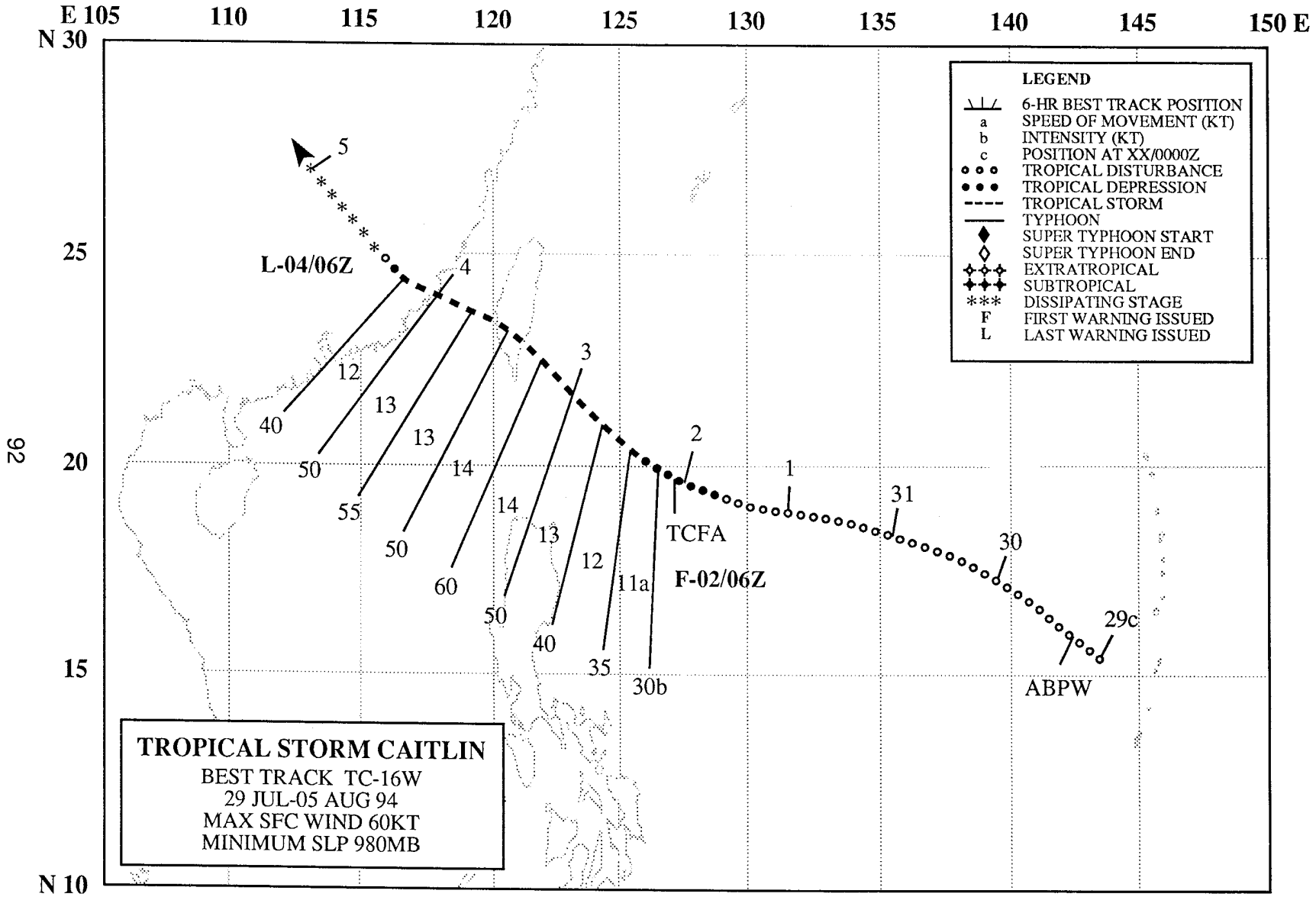
E 105
110
115
120
125
130
135
140
145
150 E
N 30
25
20
15
N 10
92
LEGEND
6-HR BEST TRACK POSITION
a SPEED OF MOVEMENT (KT)
b INTENSITY (KT)
c POSITION AT XX/0000Z
TROPICAL DISTURBANCE
TROPICAL DEPRESSION
TROPICAL STORM
TYPHOON
SUPER TYPHOON START
SUPER TYPHOON END
EXTRATROPICAL
SUBTROPICAL
*** DISSIPATING STAGE
F FIRST WARNING ISSUED
L LAST WARNING ISSUED
5
L-04/06Z
4
3
2
1
31
30
29c
ABPW
30b
35
40
50
60
50
55
50
40
12
13
13
14
14
13
12
11a
TCFA
F-02/06Z
TROPICAL STORM CAITLIN
BEST TRACK TC-16W
29 JUL-05 AUG 94
MAX SFC WIND 60KT
MINIMUM SLP 980MB

TROPICAL STORM CAITLAN (16W)

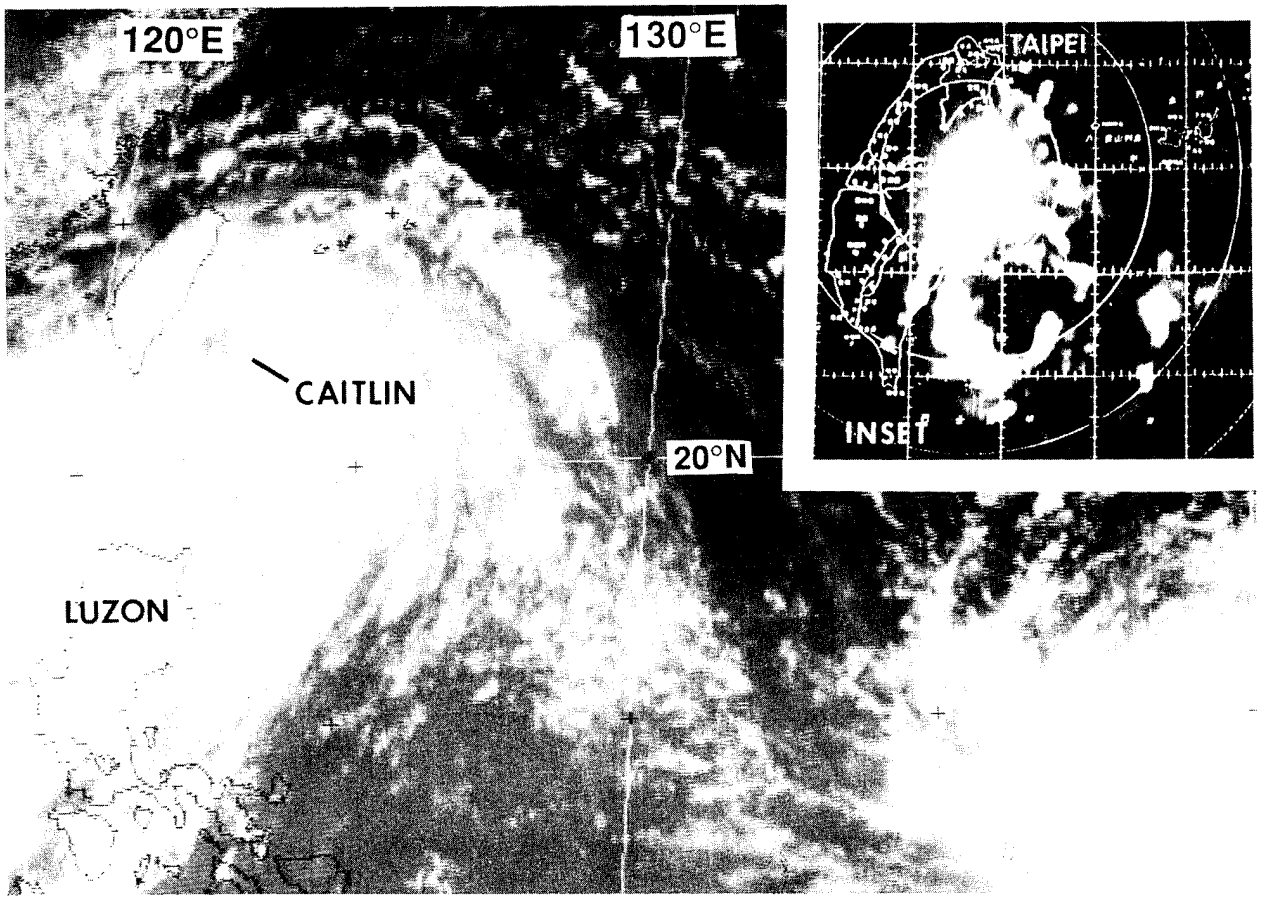

Figure 3-16-1 Tropical Storm Caitlin with a ragged banding type eye, some 60 nm (111 km) east of Taiwan (030424Z August visible GMS imagery). Inset shows Caitlin's radar reflectivity at 030700Z August. (Radar imagery courtesy of Taiwan Central Weather Bureau.)

On the morning of 29 July, a tropical disturbance developed in the monsoon trough northwest of Guam and west of Saipan. It was mentioned on the Significant Tropical Weather Advisory that afternoon (290600Z July). Development was very slow, but after four days, satellite imagery and synoptic data indicated that the disturbance was beginning to intensify, so a Tropical Cyclone Formation Alert was issued at 020000Z August. The first warning on Tropical Depression 16W was issued four hours later as the system continued to show signs of improving organization (e.g., convective curvature of the deep convection). In another six hours (at 021200Z), the system was upgraded to Tropical Storm Caitlin. It appeared to interact with a surge in the southwest monsoon, which resulted in a turn to the northwest, and an acceleration to 15 kt (28 km/hr) toward south central Taiwan. Caitlin reached its maximum intensity of 60 kt (31 m/s) at 030600Z (Figure 3-16-1a,b), three hours before going ashore in Hualien County, Taiwan, at 031015Z. Wind gusts in excess of typhoon force were experienced for a 21-hour period (030900Z to 040600Z) at Green Island, Taiwan (WMO 46760) as Caitlin passed a short distance to the north of the island. The system crossed Taiwan in six hours, and entered the Taiwan Straits at about 031500Z. Approximately ten hours later (040100Z), Caitlin went ashore on mainland China where it dissipated on 05 August. Caitlin caused heavy rains, as much as 3.3 inches (84 mm) in one hour, in China's Ningxia Hui Autonomous Region. The resulting mountain flooding killed eight people and left nine missing.

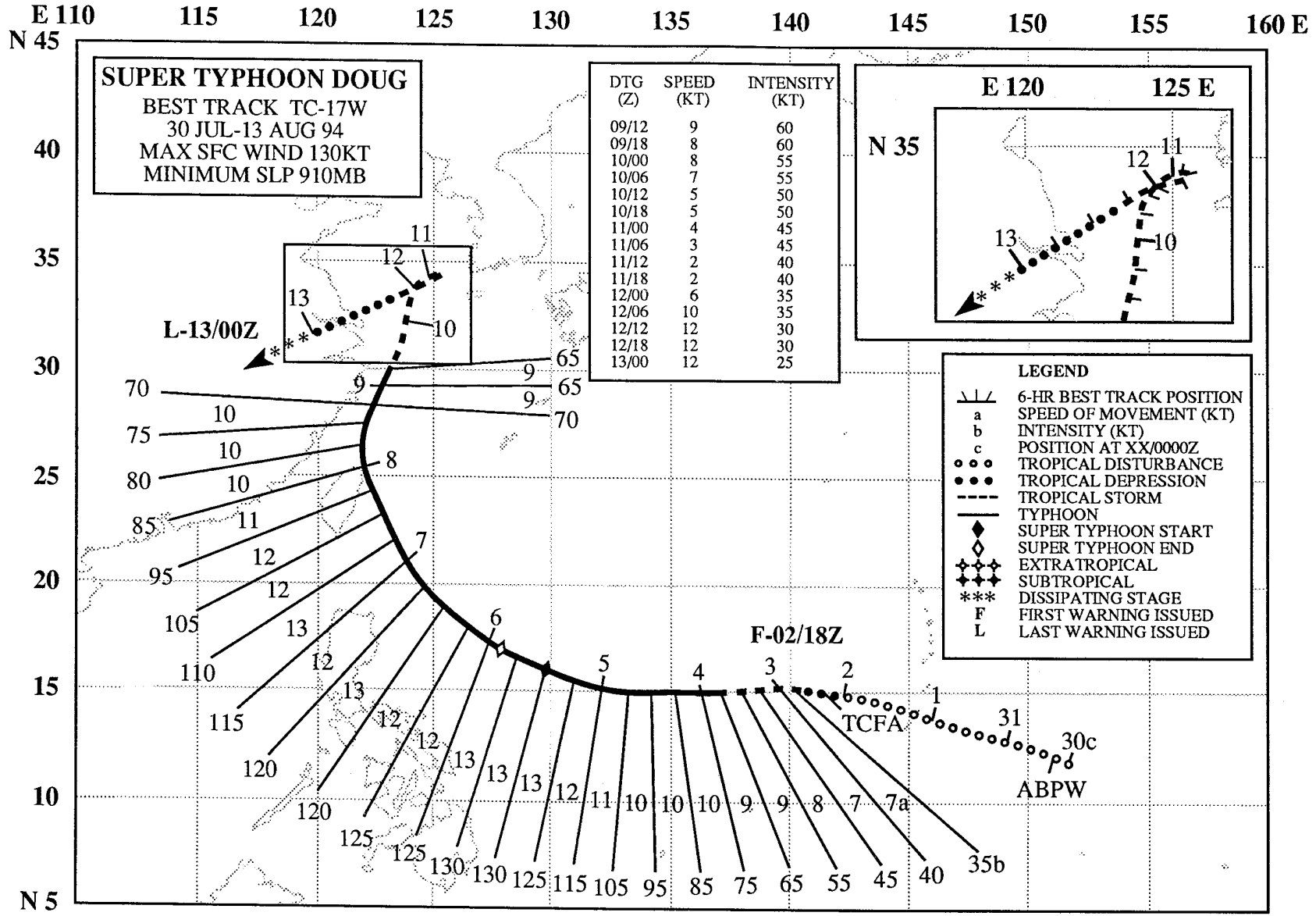
SUPER TYPHOON DOUG
BEST TRACK TC-17W
30 JUL-13 AUG 94
MAX SFC WIND 130KT
MINIMUM SLP 910MB
DTG (Z) SPEED (KT) INTENSITY (KT)
09/12 9 60
09/18 8 60
10/00 8 55
10/06 7 55
10/12 5 50
10/18 5 50
11/00 4 45
11/06 3 45
11/12 2 40
11/18 2 40
12/00 6 35
12/06 10 35
12/12 12 30
12/18 12 30
13/00 12 25
E 110 115 120 125 130 135 140 145 150 155 160 E
N 45 40 35 30 25 20 15 10 N 5
E 120 125 E
N 35
L-13/00Z
F-02/18Z
TCFA
ABPW
LEGEND
6-HR BEST TRACK POSITION
SPEED OF MOVEMENT (KT)
INTENSITY (KT)
POSITION AT XX/0000Z
TROPICAL DISTURBANCE
TROPICAL DEPRESSION
TROPICAL STORM
TYPHOON
SUPER TYPHOON START
SUPER TYPHOON END
EXTRATROPICAL
SUBTROPICAL
DISSIPATING STAGE
FIRST WARNING ISSUED
LAST WARNING ISSUED

94

SUPER TYPHOON DOUG (17W)

I. HIGHLIGHTS

Doug was the second of six tropical cyclones to attain super typhoon intensity in the western North Pacific basin during 1994. Doug exhibited some unusual structural characteristics: it had an abnormally large eye for a system of its intensity, which grew larger as the system intensified. Doug also went through an unusually long period of rapid intensification. Doug caused extensive damage and loss of life in Taiwan. After affecting Taiwan, Doug moved northward to Korea, creating the conditions which led to a Korean Air Lines A-300 crash landing at Cheju International Airport.

II. TRACK AND INTENSITY

The tropical disturbance that eventually became Super Typhoon Doug was first mentioned on the 300600Z July Significant Tropical Weather Advisory as an area of enhanced convection on the eastern end of a relatively weak monsoon trough that extended eastward across the southern Mariana Islands. After several episodes of normal diurnal fluctuations in deep convection (i.e., night maximum, day minimum), the disturbance began to maintain daytime convection. A Tropical Cyclone Formation Alert was issue at 020700Z August. The amount and organization of the convection increased during that night, and the first warning on Tropical Depression 17W was issued at 021800Z. At this time, the system was moving slowly westward at a speed of 7-8 kt (13-14 km/hr).

Doug began to increase its rate of intensification during the evening of 03 August, and reached typhoon intensity at 031800Z. For the following 48 hours, the system intensified at a steady rate of 10 kt (5 m/sec) / 6 hr or 40 kt (21 m/sec) per day. After reaching a peak intensity of 140 kt (72 m/sec) at 051800Z, Doug began to slowly weaken (Figure 3-17-1). Doug maintained an eye diameter of over 50 nm (95 km) from 051200Z to 060000Z. The Taiwanese radar at Hualien (46699) confirmed Doug's very large eye (Figure 3-17-2) when its intensity was estimated to be 125 kt (64 m/sec). A few hours later, Doug passed between the Taiwanese station of Suao (WMO 46706) and the Japanese station of Yonaguni-Shima (WMO 47912) (the southern-most of the Ryukyu islands). Table 3-17-1 shows the maximum wind speeds observed at these stations (based on the peak observed gust) as Doug passed between them over a 4-hour period. When the translation speed of 11 kt (20 km/hr) is factored into the winds at these stations to account for the asymmetry, the winds at the stations agree very well with each other and with the estimated sustained wind of 110 kt (57 m/sec) for Doug.

After passing very near the extreme northeastern tip of Taiwan (the western half of Doug's eye wall moved over land there), Doug turned to the north and then to the north-northeast. Doug weakened to tropical storm intensity after 090600Z when approximately 100 nm (185 km) southeast of Shanghai. At 091800Z, Doug produced sustained winds of 60 kt (31 m/sec) with a gust to 72 kt (37 m/sec) at Mosulpo, Cheju-Do (WMO 47187) when the storm was 180 nm (335 km) south-southwest of the island (Figure 3-17-3). The weakening system meandered toward the small islands at the southwestern tip of the Korean peninsula, and its convective organization and circulation weakened drastically. The remaining low-level circulation was redirected by low- to mid-level northeasterly flow on the southern periphery of a blocking high-pressure system over northern China. Doug, now downgraded to Tropical Depression 17W, then moved to the southwest across the Yellow Sea, and into mainland China. The final warning was issued at 120000Z as it dissipated northwest of Shanghai.

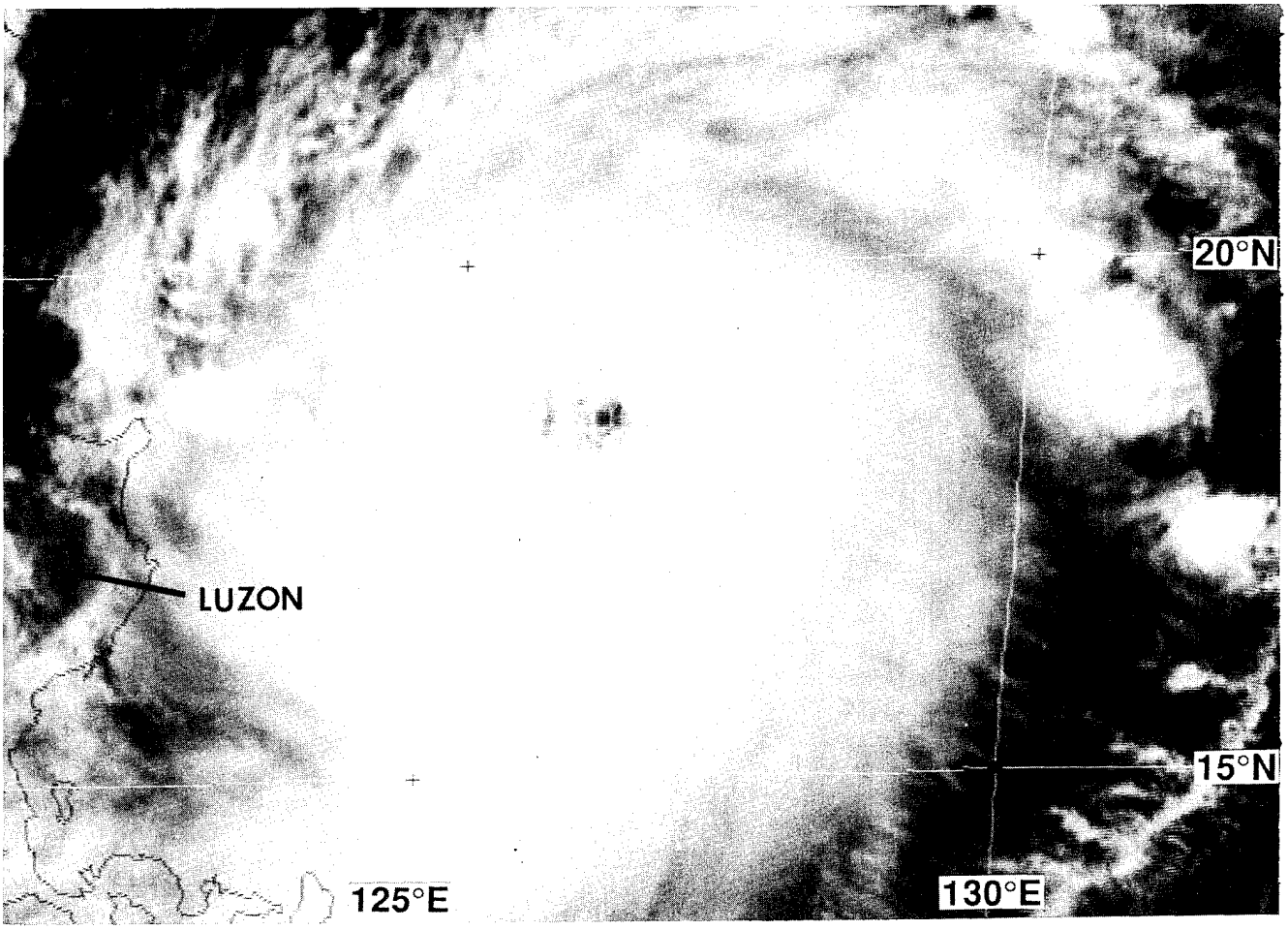

Figure 3-17-1 Super Typhoon Doug is located 240 nm (445 km) east of the northeast tip of Luzon just after reaching its 140 kt (72 m/sec) peak intensity (060530Z August visible GMS imagery).

III. DISCUSSION

There are two aspects of Doug's structure and evolution that were of special interest. The first was its long period of a high rate of intensification, and the second was the diameter of its eye that enlarged during intensification and shrunk during much of its weakening.

a. Unusual intensification rate of Doug.

Mundell (1990) indicates that most of the western North Pacific typhoons that reach super typhoon intensity undergo an episode of rapid intensification (central pressure falls > 42 mb/day (Holliday and Thompson 1979)), that usually lasts about 24 hours. From 030600Z to 051200Z, Doug increased in intensity at a rate of 10 kt (5 m/sec)/6 hr and peaked at 140 kt (72 m/sec) at 051800Z. The 24-hour falls of central pressure during much of Doug's intensifying phase gradually increased from the low 30s (mb per day) to values in the low 40s (mb per day) (Table 3-17-2). The periods 040600Z-050600Z and 041200Z-051200Z exhibited pressure falls of 42 mb and 43 mb respectively. The evolution of the intensities of Doug and Super Typhoon Yuri (1991), are representative of the minority of western North Pacific typhoons that intensify at rapid or near-rapid rates for unusually long periods (at least 48 hours). Characteristics common to both Doug and Super Typhoon Yuri (1991) include: very large size, an extended period of intensification rates near the lower threshold of the established criteria for rapid

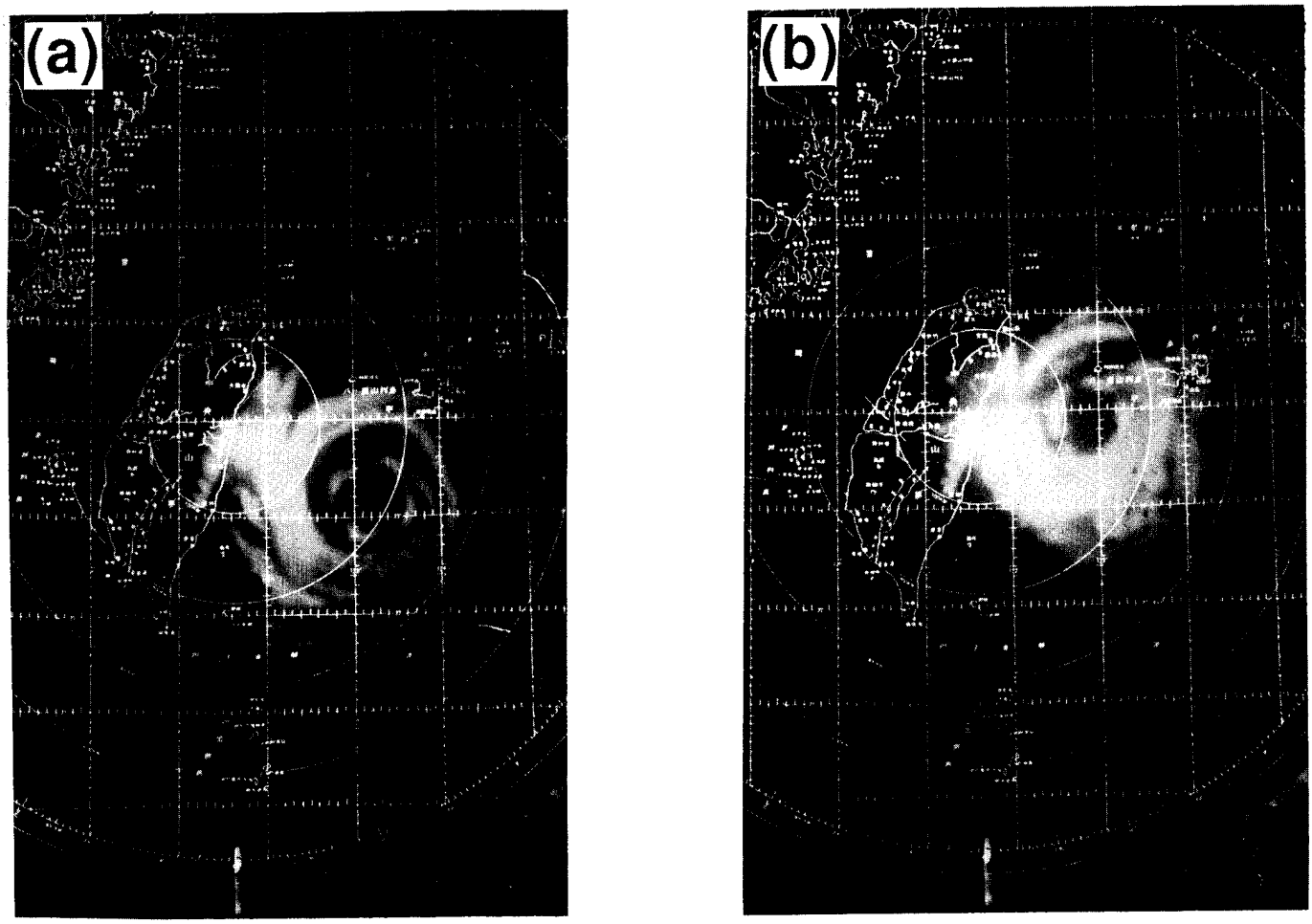

Figure 3-17-2 Two radar images of Typhoon Doug from the Hualien, Taiwan (WMO 46669) radar at: (a) 071000Z August , and (b) 071300Z August. In (a) the center of Doug's large eye was approximately 120 nm (220 km) southeast of the radar. In (b) the eye wall is nearing Yonaguni-Shima which recorded its peak gust of 136 kt (70.2 m/sec) at 131337Z. (Radar photos courtesy of the Central Weather Bureau, Taipei, Taiwan.)

intensification (> 42 mb per day), peak intensity in the 140-150 kt (75-77 m/sec) range, and relatively large eye diameters that bordered on the 45 nm (85 km) large-eye threshold set by Dvorak (1984) for purposes of capping intensity at 115 kt (59 m/sec).

b. Unusual eye behavior

Doug's eye diameter showed an unusual evolution. It increased in size from 11 to 47 nm (20 to 87 km) during Doug's intensification phase; expanded further to 57 nm (106 km) just after peaking; but then decreased in size as it weakened. Except for the six hours of expansion after reaching peak intensity, the trends were opposite to those normally observed, and lend further support to the premise that Doug did not undergo the typical process of rapid intensification, since the process normally involves shrinking of the eye.

The diameter of Doug's eye was abnormally large for a very intense typhoon, similar to the case of Super Typhoon Yuri (1991). The potential problem that occurs is with the rule in the technique that restricts the intensity of tropical cyclones for eye diameters of 45 nm (85 km) or greater: for large ragged eyes the intensity is capped at is 90 kt (46 m/sec); for large well-defined eyes the intensity is capped at 115 kt (59 m/sec). It is likely that both Doug and Yuri had large eyes with accompanying

intensities in excess of the Dvorak caps. During Doug's intensification phase, the large eye was embedded in the deep (eye wall area) convection by average distances over 120 nm (220 km). These are extraordinarily large embedded distances. Also, the percentage of cloud within three degrees latitude (180 nm) of the center that was colder than -70°C remained relatively high, even during the weakening phase. Super typhoons like Doug and Yuri may represent a special case of very large tropical cyclones with large eyes and very wide eye walls that can exceed the intensity bounds which Dvorak placed on tropical cyclones with large eyes.

IV. IMPACT

Doug spent much of its life over open ocean. However, during its passage near Taiwan, it produced torrential rains and strong winds, blowing vehicles off of highways. At least 19 people lost their lives, 45 were injured, and damage in Taiwan was estimated to be in excess of US $110 million. Destruction must also have been heavy in the southwestern Ryukyu islands, although no reports were received. The anemometer at Yonaguni-Shima (WMO 47912) failed when wind gusts reached 136 kt (70.2 m/sec). Doug also caused considerable flooding in China, but reports of damage were not received. As the system approached Korea, it created poor weather and gusty winds on Cheju-Do. A Korean Air Lines A-300 jet trying to land at Cheju International Airport (WMO 47182), buffeted by 40 kt (20 m/sec) winds, skidded on the wet runway into a barrier. Fortunately, all 160 passengers and crew got off the aircraft before it was engulfed in flames.

Table 3-17-1 Observed maximum winds at Suao, Taiwan (WMO 46706) and Yonaguni-Shima, Japan (WMO 47912), as Typhoon Doug passed between the two stations. Peak gusts are observed, but sustained winds are one-minute average based on 0.88 of peak gust (Atkinson 1974). "Distance" refers to the distance from the station to the typhoon center at the time of peak wind. "COR Vmax" shows what the expected peak gust would be when corrected for the 11 kt (20 km/hr) translation speed of Doug. "BT" is the best-track intensity at the time of the peak wind at each site.

Location	Date / Time (Z)	Peak Wind (kt)	Distance (nm)	COR Vmax (kt)	BT (kt)
Suao	071657	95G115	25	126	110
Yonaguni	071337	110G136	30	125	115

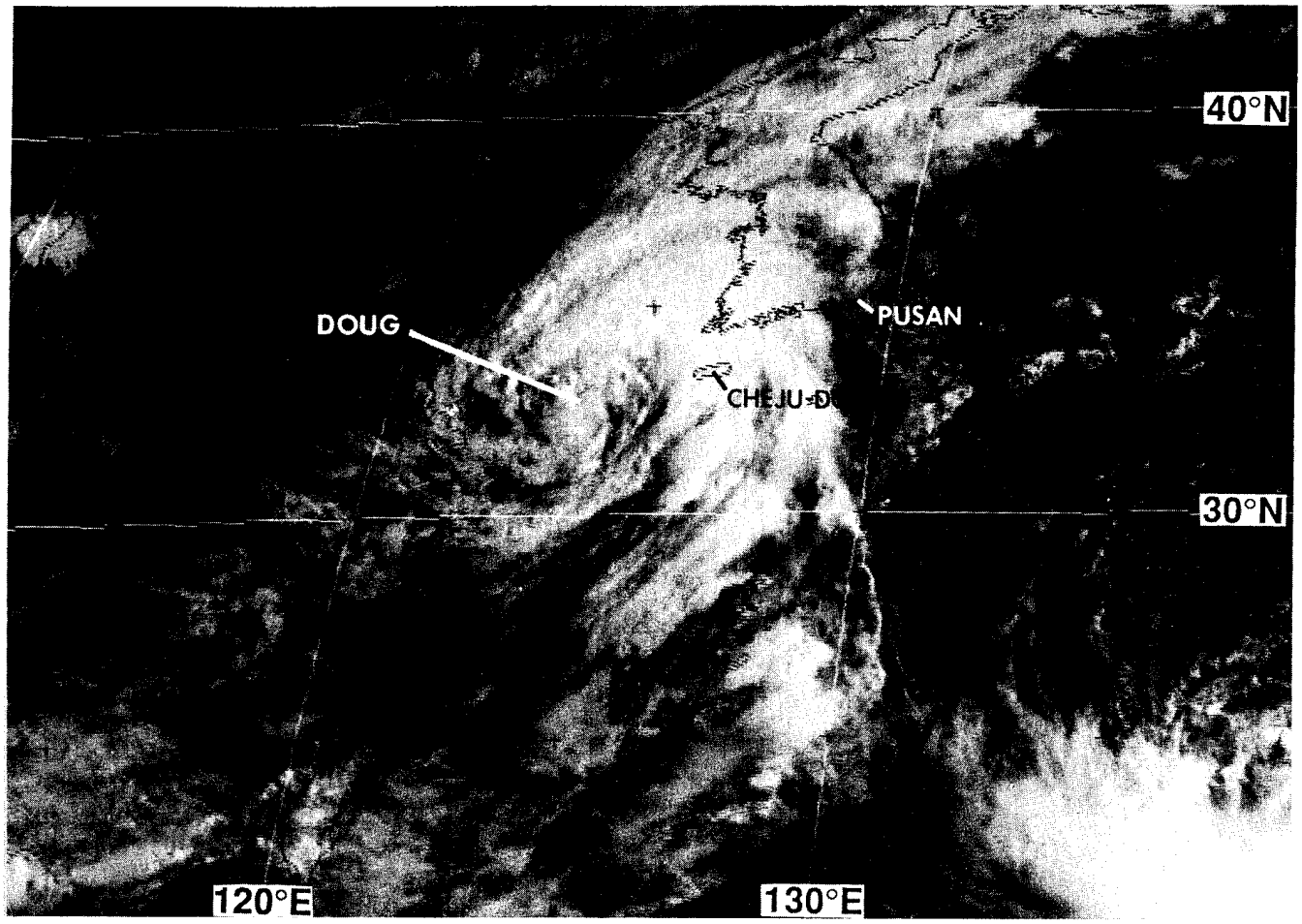

Figure 3-17-3 Tropical Storm Doug at 55 kt (28 m/sec) intensity as it moves toward Korea. Approximately six hours prior to picture time (091800Z), Cheju-Do (WMO 47187) received its peak wind gust of 72 kt (37 m/sec) (092331Z August visible GMS imagery).

Table 3-17-2 Twenty-four hour pressure changes for each six-hour warning period prior to Doug's maximum intensity, beginning at 030600Z and ending at 050600Z.

Date/Time Period	Wind Change (kt)	Pressure change (mb)
030600 - 040600	+40 (45 - 85)	-33 (991 - 958)
031200 - 041200	+40 (55 - 95)	-35 (984 - 949)
031800 - 041800	+40 (65 - 105)	-38 (976 - 938)
040000 - 050000	+40 (75 - 115)	-41 (968 - 927)
040600 - 050600	+40 (85 - 125)	-42 (958 - 916)
041200 - 051200	+40 (95 - 135)	-43 (949 - 906)
041800 - 051800	+35 (105 - 140)	-40 (938 - 898)
050000 - 060000	+25 (115 - 140)	-29 (927 - 898)
050600 - 060600	+15 (125 - 140)	-18 (916 - 898)

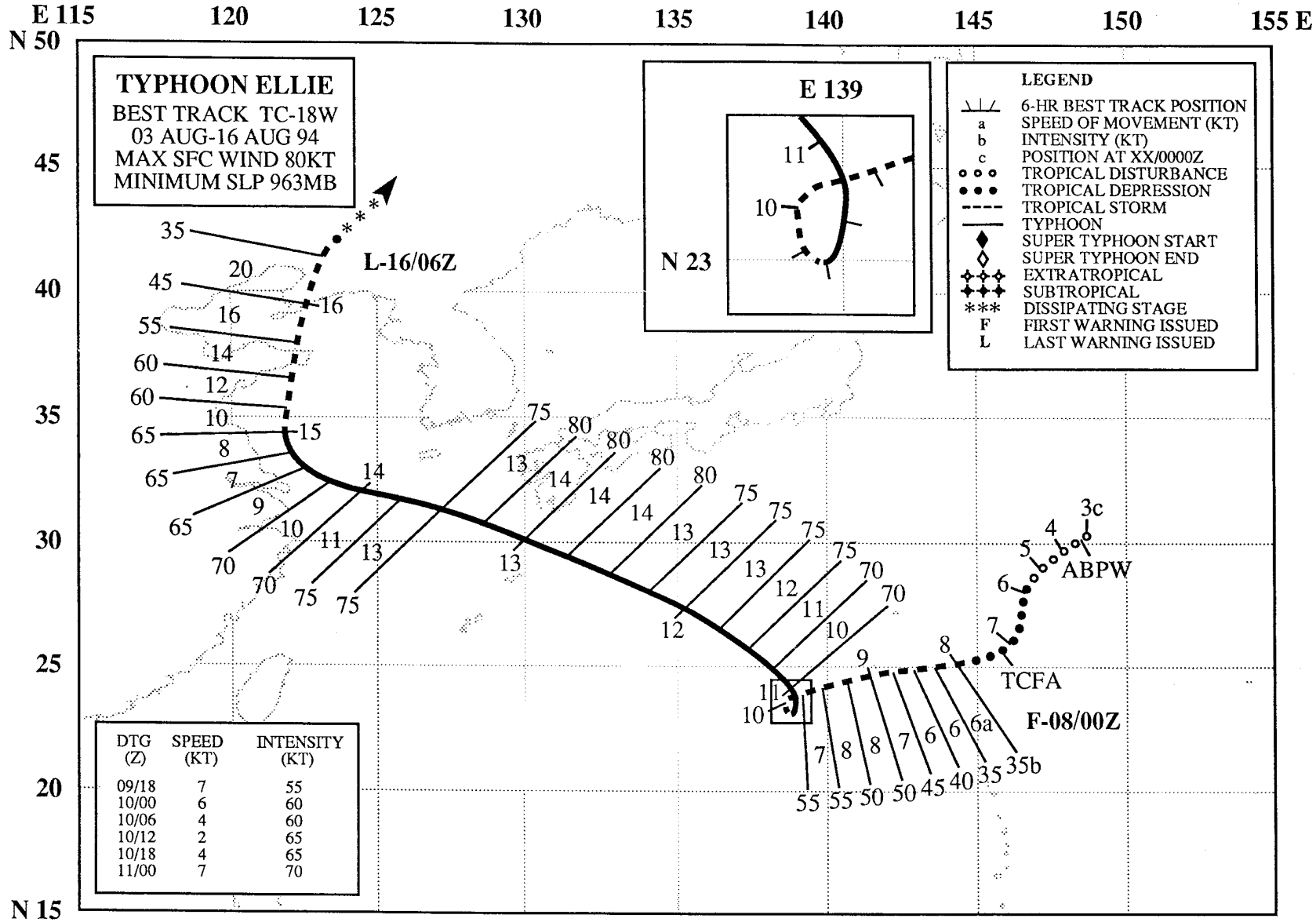
E 115
120
125
130
135
140
145
150
155 E
N 50
45
40
35
30
25
20
N 15
TYPHOON ELLIE
BEST TRACK TC-18W
03 AUG-16 AUG 94
MAX SFC WIND 80KT
MINIMUM SLP 963MB
E 139
N 23
LEGEND
6-HR BEST TRACK POSITION
SPEED OF MOVEMENT (KT)
INTENSITY (KT)
POSITION AT XX/0000Z
TROPICAL DISTURBANCE
TROPICAL DEPRESSION
TROPICAL STORM
TYPHOON
SUPER TYPHOON START
SUPER TYPHOON END
EXTRATROPICAL
SUBTROPICAL
DISSIPATING STAGE
FIRST WARNING ISSUED
LAST WARNING ISSUED
L-16/06Z
ABPW
TCFA
F-08/00Z
DTG (Z) SPEED (KT) INTENSITY (KT)
09/18 7 55
10/00 6 60
10/06 4 60
10/12 2 65
10/18 4 65
11/00 7 70

100

TYPHOON ELLIE (18W)

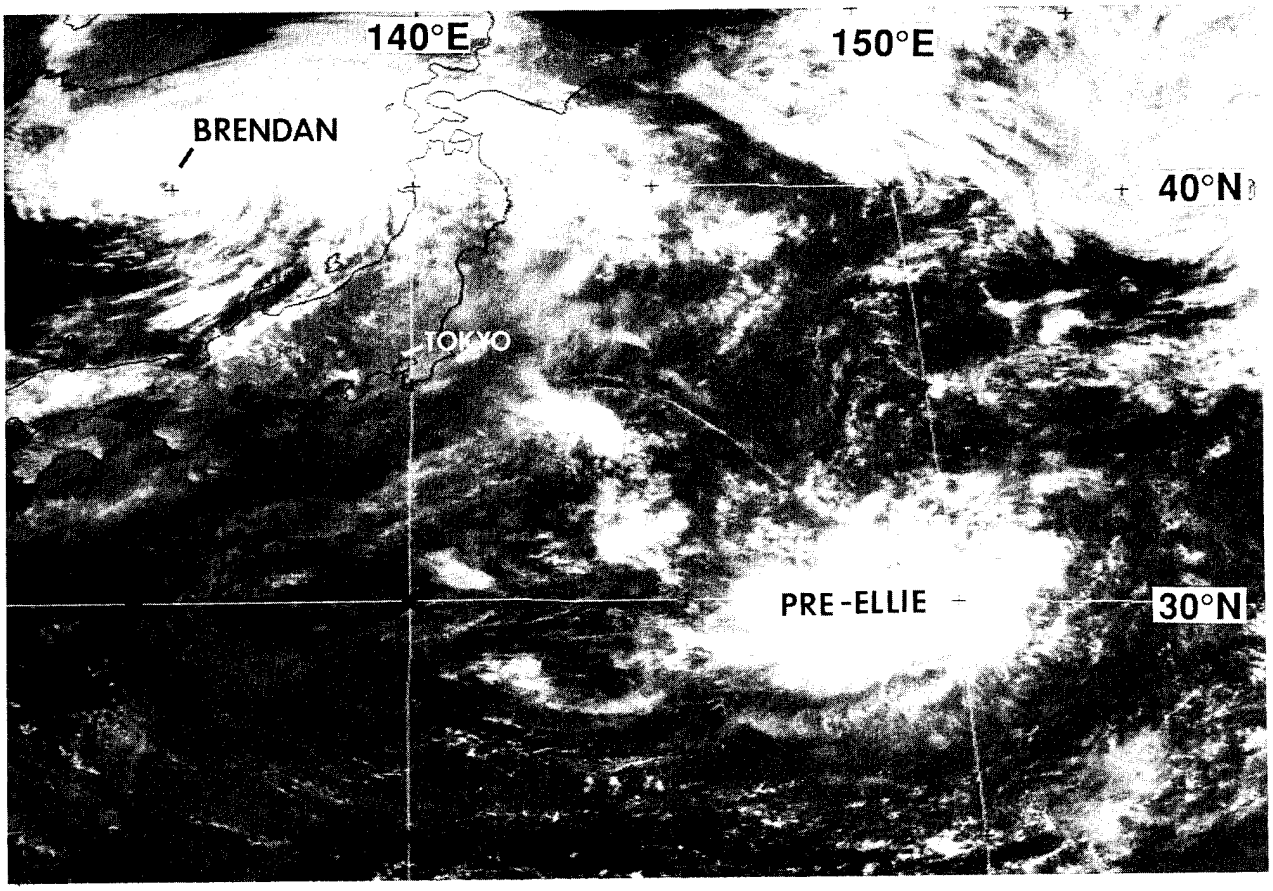

Figure 3-18-1 The small area of deep convection at the base of a weak mid-latitude trough drifted southward and became Ellie. The recurving Brendan is seen in the Sea of Japan (020031Z August visible GMS imagery).

I. HIGHLIGHTS

The tropical disturbance that became Ellie had an atypical origin in the sub-tropics about 500 nm (900 km) east-southeast of Tokyo. Ellie became a large typhoon with a large ragged eye. Prior to recurvature in the Yellow Sea, it moved on a westward track at high latitude (25°N). A peak wind gust of 87 kt (45 m/sec) was recorded by a station on the south coast of Kyushu, Japan, as Ellie passed 60 nm (110 km) to the south.

II. TRACK AND INTENSITY

On 02 August, an area of deep convection was observed at the base of a weak trough of low pressure which was moving eastward away from Japan (Figure 3-18-1). Drifting slowly southward, this area of deep convection persisted, prompting its first mention on the 030600Z August Significant Tropical Weather Advisory. For the next several days, this tropical disturbance continued to move slowly southward, and the areal extent of deep convection increased. An exposed low-level circulation center on the northern side of the deep convection became increasingly well defined. At 070630Z, a Tropical Cyclone Formation Alert was issued based upon increasing curvature of the main band of deep convection. At 080000Z, the first warning was issued on Tropical Depression 18W. By 081200Z, the

system was upgraded to Tropical Storm Ellie based upon synoptic data from the Volcano Islands [Chi Chi Jima (WMO 47971) recorded a peak gust of 48 kt (25 m/sec) and a minimum sea-level pressure of 1002.1 mb as the system passed nearby]. The system gradually turned to the west-southwest. On the morning of 09 August, a large ragged eye formed (Figure 3-18-2). On 10 August, the system stalled for approximately 24 hours, intensified, and grew in size. As it came out of its stall, Ellie moved on a west-northwestward track at a steady 13 kt (24 km/hr) for the next 72 hours (110600Z to 140600Z). At 110600Z, the system was upgraded to Typhoon Ellie, however post-analysis indicated that typhoon intensity was most probably reached at 101200Z. After becoming a typhoon, Ellie's intensity increased very slowly, reaching a peak of 80 kt (41 m/sec) at 121200Z. Throughout the entire period during which Ellie was at typhoon intensity (101200Z to 150000Z), the eye remained large (i.e., diameter in excess of 45 nm) and ragged, and the areal extent of the outer circulation was very large (Figure 3-18-3). At 130000Z, Ellie passed within 90 nm (170 km) of the southern coast of Kyushu. A comprehensive data set of peak wind and minimum sea-level pressure was obtained from stations in Japan (Figure 3-18-4). After 140600Z, Ellie turned northward and slowly weakened. It briefly touched land at Wendeng, China, then made final landfall midway between Dairen and the China-North Korea border with an intensity of 45 kt (23 m/sec). The final warning was issued at 160600Z as the remnants of Ellie moved northward over rugged terrain in northeastern China.

III. DISCUSSION

a. Unusual genesis

Most tropical cyclones of the western North Pacific form in the monsoon trough. Ellie was one of few that did not. Some of the few, like Tropical Depression 31W and Yunya (36W), form in the low-level tradewind easterly flow in association with cyclonic disturbances in the tropical upper tropospheric trough (TUTT). Others, like Ellie, form in the subtropics at the base of mid-latitude low-pressure troughs.

The disturbance that became Ellie evolved from an area of deep convection that first appeared at relatively high latitude (30°N) at the base of a weak mid-latitude trough. This area of convection drifted slowly southward and was associated with an intensifying low-level cyclonic circulation. After several days of slow improvement in the organization of deep convection, and a gradual increase in the intensity and size of the low-level circulation, this subtropical disturbance became a tropical cyclone.

b. Large eye and large size.

In its intensifying tropical storm stage, the deep convection near the center of Ellie gradually wrapped around a large (60 nm) relatively cloud-free center (Figure 3-18-2). Satellite analysts were reluctant to call this feature an eye, as significant breaks in the deep convection were evident. However, as the deep convection formed a more complete ring, it was diagnosed as a ragged eye wall at 120530Z, roughly six hours after the image in Figure 3-18-3. For most of its life, Ellie had a large ragged eye with a diameter of approximately 60 nm (110 km). The maximum intensity of Ellie as derived from application of Dvorak satellite imagery analysis was 80 kt (41 m/sec). The Dvorak technique caps intensity at 90 kt (46 m/sec) for typhoons with large ragged eyes; where large is defined as an eye diameter of 45 nm (85 km) or more.

Another of Ellie's structural characteristics was its large size. The size of a tropical cyclone is a fairly difficult parameter to objectively specify. The average radius to the outer-most closed isobar has been suggested as an objective measure of size (Merrill 1984). Another parameter suggested as a measure of size is the average radial distance to the point where the streamlines of the low-level flow become unidi-

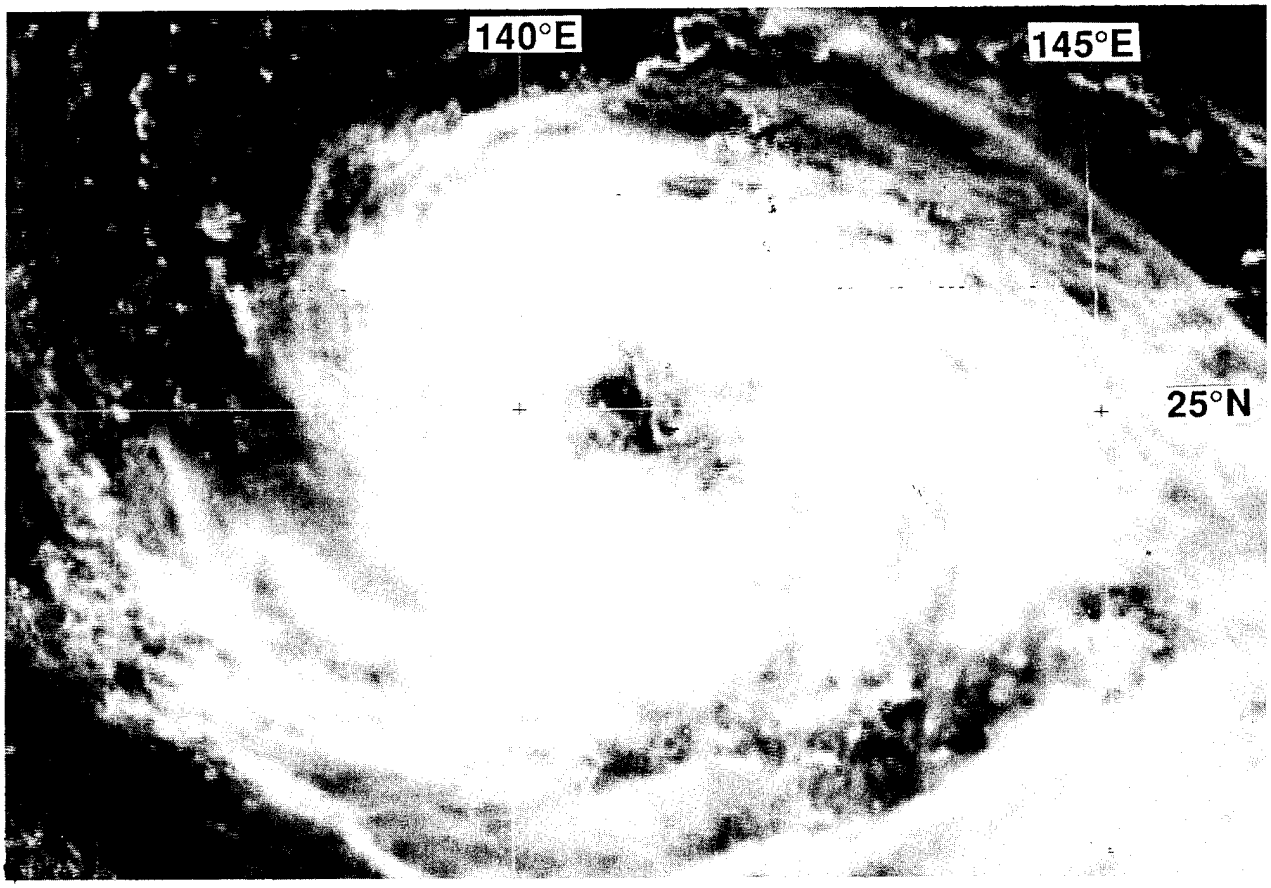

Figure 3-18-2 Ellie's deep convection begins to consolidate around a 60 nm (110 km) cloud-free center that would not be diagnosed as an eye for over another 72 hours (090231Z August visible GMS imagery).

rectional or anticyclonic. In the North Atlantic, where tropical cyclones are usually embedded in low-level easterly flow, the aforementioned size parameters may yield consistent results. However, in the western North Pacific, where tropical cyclones are usually embedded in the monsoon trough, the aforementioned parameters lead to an ambiguity: where does the tropical cyclone circulation end and the monsoon circulation begin? Disregarding the problems of objective determination of tropical cyclone size, it is certainly apparent on satellite imagery (Figure 3-18-3), that Ellie was large.

IV. IMPACT

No reports of injuries or of serious damage were received.

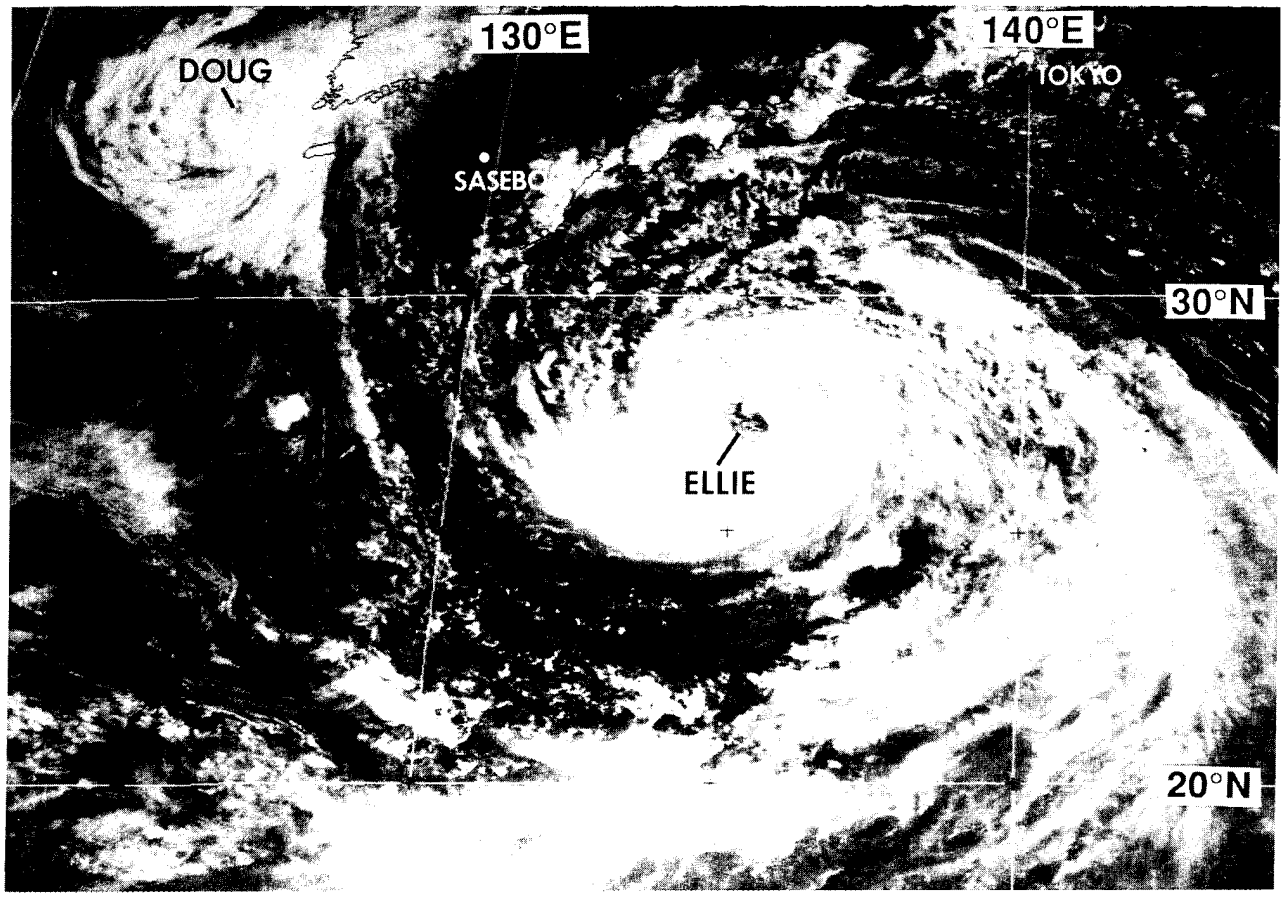

Figure 3-18-3 Ellie possesses a large ragged eye and a large outer circulation (112331Z August visible GMS imagery).

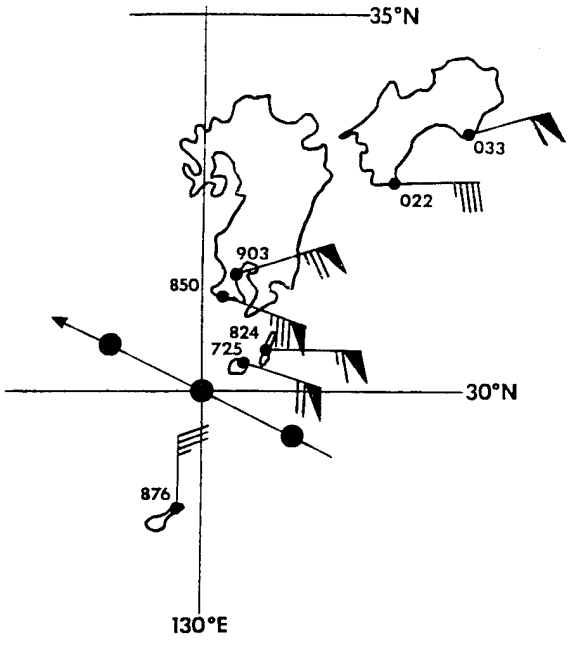

Figure 3-18-4 Maximum wind gusts and minimum sea-level pressure reported at several stations in southwestern Japan as Ellie passed through the region. Ellie's best-track is indicated by large dots. Wind is coded as follows: full barb = 10 kt, flag = 50 kt. Pressure is coded as follows: divide indicated value by 10 and add 900 (or add 1000 to values less than 100) to get pressure in units of millibars.

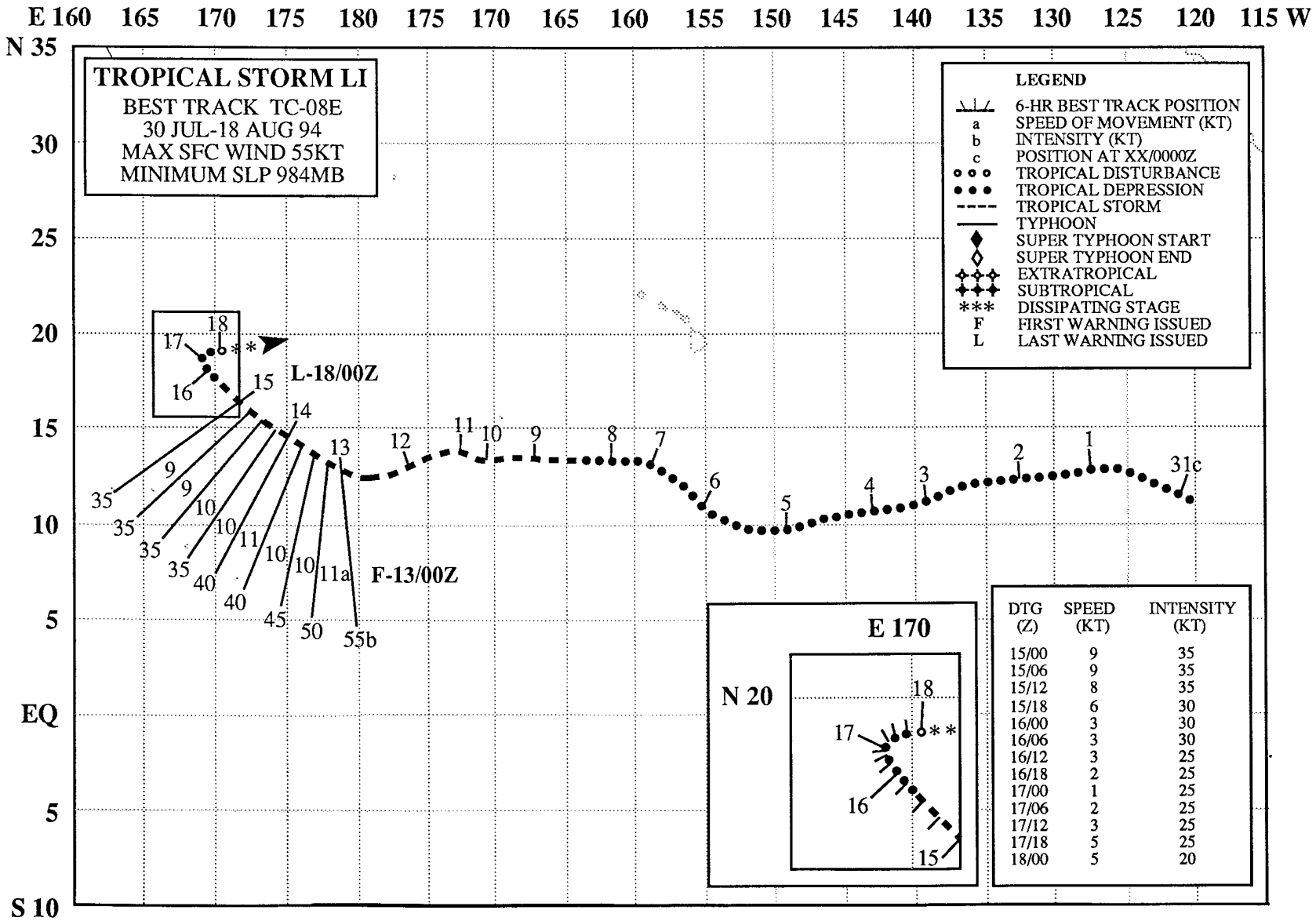
E 160 165 170 175 180 175 170 165 160 155 150 145 140 135 130 125 120 115 W
N 35
30
25
20
15
10
5
EQ
5
S 10
105
TROPICAL STORM LI
BEST TRACK TC-08E
30 JUL-18 AUG 94
MAX SFC WIND 55KT
MINIMUM SLP 984MB
LEGEND
6-HR BEST TRACK POSITION
a SPEED OF MOVEMENT (KT)
b INTENSITY (KT)
c POSITION AT XX/0000Z
TROPICAL DISTURBANCE
TROPICAL DEPRESSION
TROPICAL STORM
TYPHOON
SUPER TYPHOON START
SUPER TYPHOON END
EXTRATROPICAL
SUBTROPICAL
*** DISSIPATING STAGE
F FIRST WARNING ISSUED
L LAST WARNING ISSUED
L-18/00Z
F-13/00Z
E 170
N 20
DTG (Z) SPEED (KT) INTENSITY (KT)
15/00 9 35
15/06 9 35
15/12 8 35
15/18 6 30
16/00 3 30
16/06 3 30
16/12 3 25
16/18 2 25
17/00 1 25
17/06 2 25
17/12 3 25
17/18 5 25
18/00 5 20

TYPHOON LI (08E)

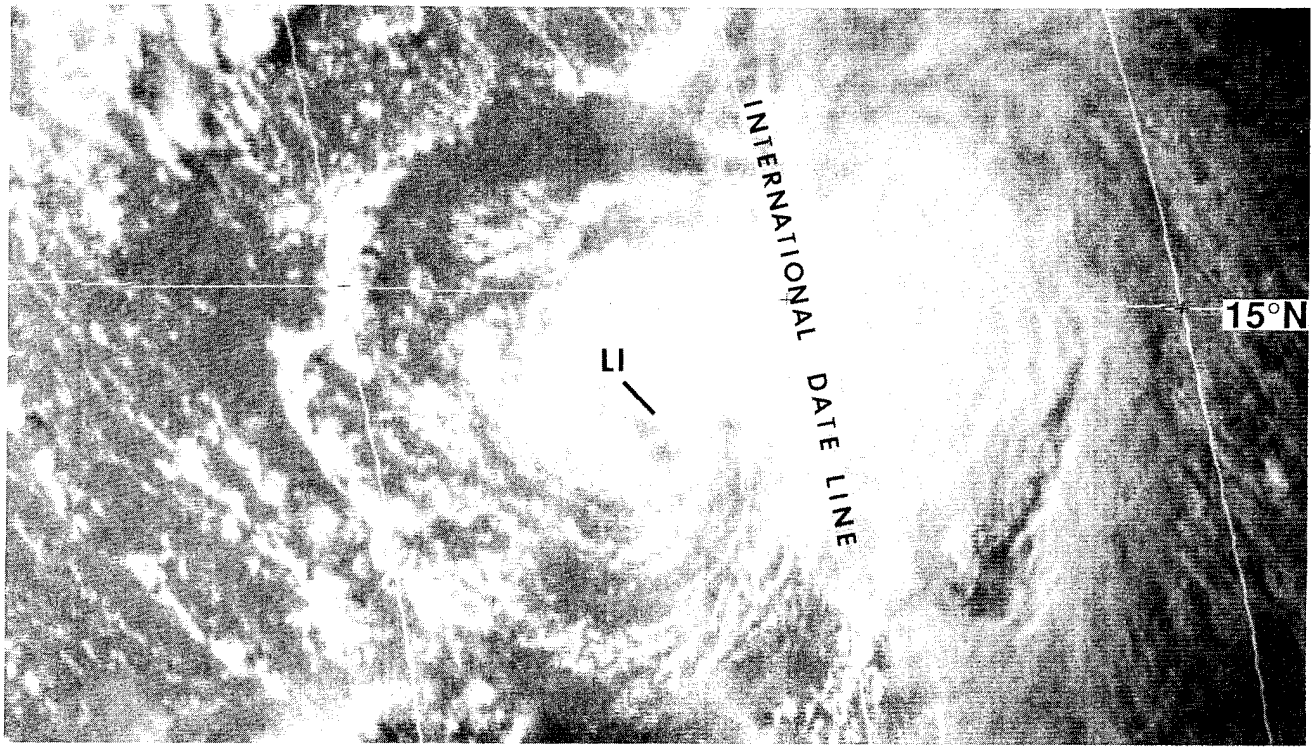

Figure 3-08E-1 Tropical Storm Li just after crossing the international date line with 50 kt (26 m/sec) (130531Z August visible GMS imagery). Li is about 250 nm (465 km) east of Wake Island.

Li, like John (08E), was unusual in that it traversed the areas of responsibility of all three US tropical cyclone warning centers — the National Hurricane Center (NHC), the Central Pacific Hurricane Center (CPHC), and the Joint Typhoon Warning Center (JTWC). During its 18-day life, it traveled over 3600 nm (6670 km), and 59 warnings were issued on the system.

Li was first observed as a disturbance in the monsoon trough of the eastern North Pacific, near 11°N; 120°W on 30 July. As it moved westward, it slowly intensified, and on 03 August, the disturbance crossed 140°W. At 030600Z, CPHC issued the first warning on Tropical Depression 08E. For the next two days, the depression tracked west-southwestward at 12-18 kt (22-33 km/hr) with 25 kt (13 m/sec) winds. On 05 August, the system turned toward the northwest; lost nearly all of its deep convection, and warnings were discontinued. A day later, warnings were reissued after convection again flared. On 06 and 07 August, the tropical depression passed about 600 nm (1111 km) south of the Hawaiian Island chain. Late on 07 August, TD 08E took a westward track, and at 081200Z, it was upgraded to Tropical Storm Li. A day later, it passed 180 nm (333 km) south of Johnston Island with 45 kt (23 m/sec) sustained winds. For the next 48 hours, Li slowly intensified, and at 121200Z, it was upgraded by the CPHC to Hurricane Li. Peak intensity was 65 kt (33 m/s). The CPHC issued its final warning on Hurricane Li at 121800Z as it crossed the international date line into the JTWC's area of responsibility. At 130000Z, JTWC issued its first warning on the system, downgrading Li to a 55-kt (28-m/sec) tropical storm, as strong upper level westerly winds south of a TUTT cell sheared the convection on Li's west side (Figure 3-08E-1). Li steadily weakened, and at 160600Z it was downgraded to a tropical depression. The depression continued to drift to the northwest, and the 59th and final warning was issued at 180000Z as TD 08E dissipated over water.

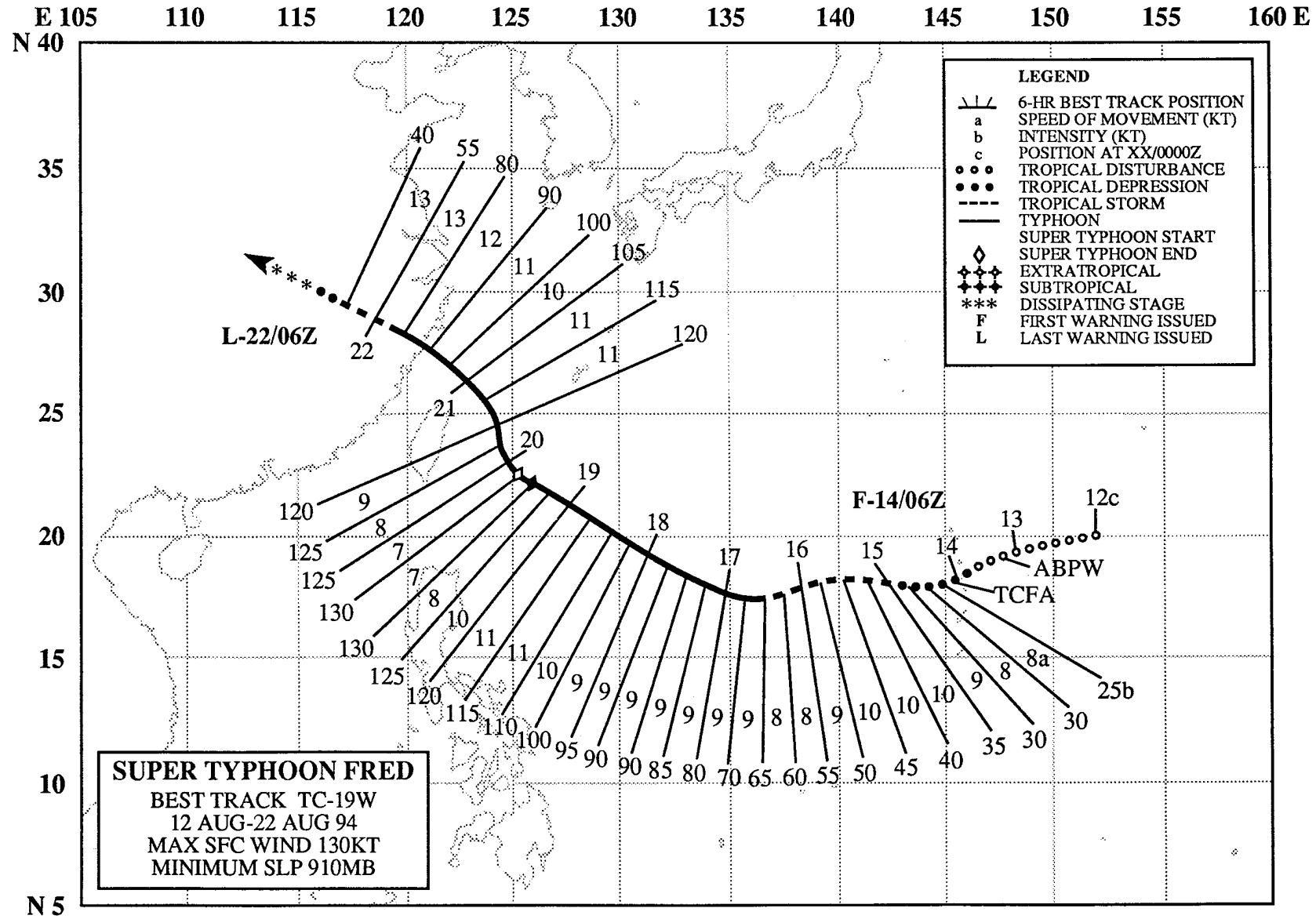
E 105
110
115
120
125
130
135
140
145
150
155
160 E
N 40
35
30
25
20
15
10
N 5
107
LEGEND
6-HR BEST TRACK POSITION
a SPEED OF MOVEMENT (KT)
b INTENSITY (KT)
c POSITION AT XX/0000Z
TROPICAL DISTURBANCE
TROPICAL DEPRESSION
TROPICAL STORM
TYPHOON
SUPER TYPHOON START
SUPER TYPHOON END
EXTRATROPICAL
SUBTROPICAL
*** DISSIPATING STAGE
F FIRST WARNING ISSUED
L LAST WARNING ISSUED
L-22/06Z
F-14/06Z
ABPW
TCFA
SUPER TYPHOON FRED
BEST TRACK TC-19W
12 AUG-22 AUG 94
MAX SFC WIND 130KT
MINIMUM SLP 910MB

SUPER TYPHOON FRED (19W)

I. HIGHLIGHTS

As Typhoon Ellie (18W) approached southwestern Japan, the embryo of Super Typhoon Fred was developing about 1200 nm (2200 km) to the southeast. The developing system moved west-southwestward for four days, reaching typhoon intensity on 16 August. Like Doug (17W), which occurred earlier in the month, Fred reached super typhoon intensity without going through an episode of rapid intensification. Near the southern Ryukyu Islands, Fred began to weaken from its 130 kt (67 m/sec) peak intensity and veered to the northwest. It passed about 120 nm (220 km) north of Taipei before the system resumed a west-northwestward track and continued to weaken. Fred's landfall on mainland China on 21 August near the city of Wenzhou coincided with an unusually high astronomical tide, generating some of the highest tides of the last two decades in that region. Resultant flooding and strong winds took an estimated 1,000 lives in Wenzhou alone.

II. TRACK AND INTENSITY

The tropical disturbance that would become Fred was first mentioned on the 130600Z August Significant Tropical Weather Advisory. It initially tracked toward the west-southwest, equatorward of the mid-level subtropical ridge. The disturbance continued to develop, a Tropical Cyclone Formation Alert was issued at 140400Z followed by the first warning at 140600Z. On the morning of 15 August, Tropical Depression 19W was upgraded to Tropical Storm Fred. For the next five days the storm intensified at a rate of 20 kt (10 m/sec) per day, reaching typhoon intensity on the night of 16 August (Figure 3-19-1) and super typhoon intensity on the night of 19 August (Figure 3-19-2).

When Fred became a super typhoon, it was heading to the west-northwest on a course toward Taiwan. About 250 nm (460 km) southwest of Okinawa, Fred began to rapidly weaken, and veered north-northwestward passing to the north of Taiwan. The period of north-northwestward motion was short-lived, leading to passage between Ishigaki-jima (WMO 47918) and Miyako-jima (WMO 47927) (Figure 3-19-3). After passing through the southern Ryukyu islands, Fred resumed its previous west-northwestward heading, and continued to weaken (but at a much slower rate) as it approached mainland China. At 211200Z, Nanji Shan (WMO 58765) (a small island about 120 nm southeast of Wenzhou) recorded ten-minute sustained winds of 80 kt (41 m/sec) (92 kt one-minute average sustained wind) and a sea-level pressure of 956.7 mb (Figure 3-19-5). The final warning was issued at 220600Z as Fred dissipated over the Yangtze River valley near Wuhan.

III. DISCUSSION

a. Rate of intensification

Most super typhoons undergo a period of rapid intensification (Mundell 1990); where rapid intensification is defined as a 24-hour period during which the central pressure falls by at least 42 mb. However, Fred did not go through a period of rapid intensification (Table 3-19-1). In addition, the eye did not shrink significantly as usually occurs with rapid intensification, nor did it expand and develop a very thick eye wall as did Doug (17W). In fact, the size of the eye vacillated considerably (Table 3-19-2). Beginning on 15 August at 1200Z, Fred moved westward in tandem with a TUTT cell to its northeast. The effects (if any) of TUTT cells upon tropical cyclone motion and intensity are not well-understood.

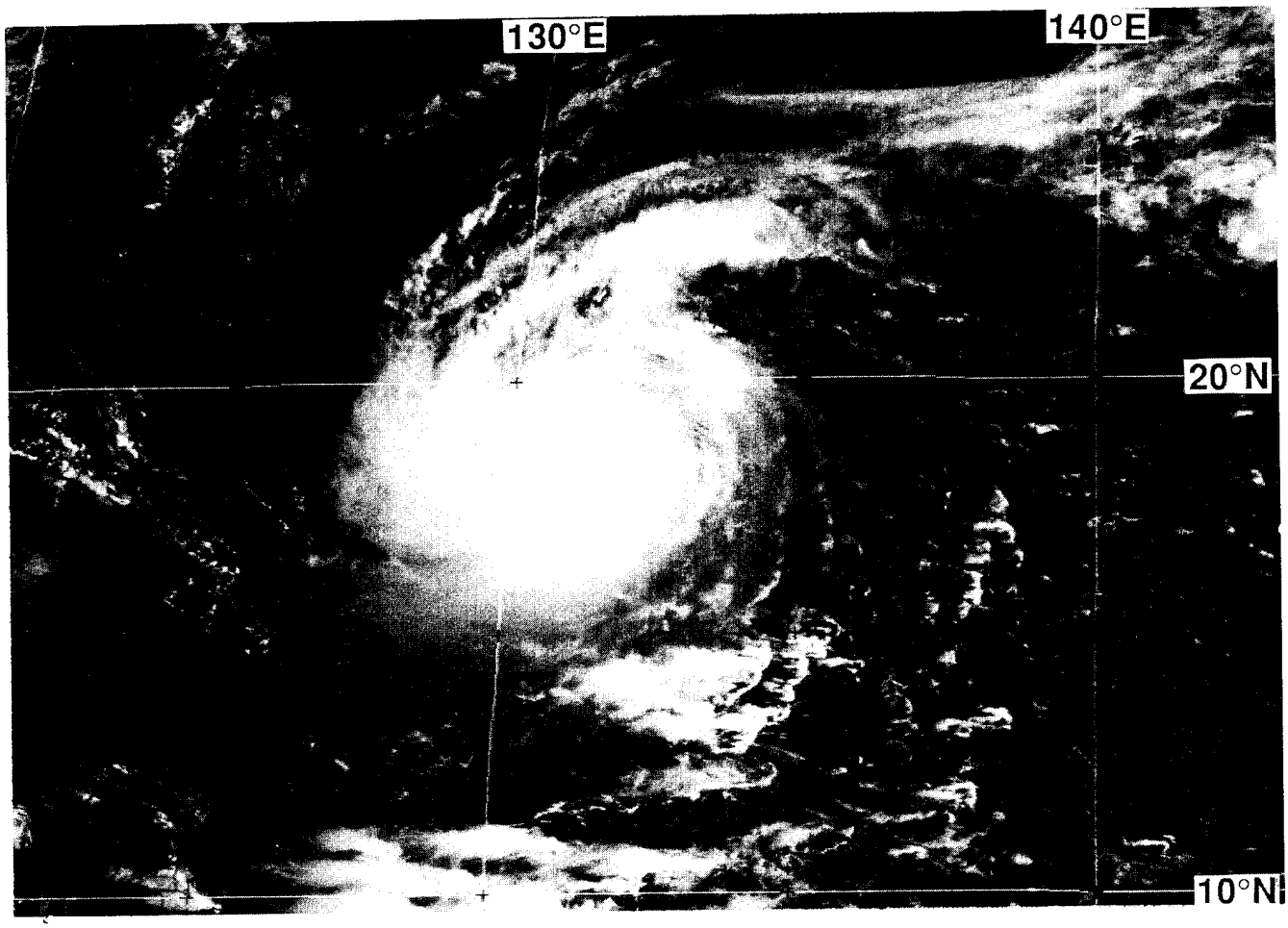

Figure 3-19-1 Fred attains typhoon intensity (172331Z August visible GMS satellite imagery).

b. Rate of weakening

Fred weakened rapidly following its peak of 130 kt (67 m/sec). This rapid weakening is substantiated by the observed minimum pressure and maximum wind during eye passage over Ishigaki-jima (WMO 47918), and by the maximum winds seen at Miyako-jima (see Figure 3-19-4). After leaving these stations, however, it appears that the rate of weakening slowed to less than 5 kt (2.6 m/sec) per 6-hour interval, since 92 kt (converted 1-min average) maximum sustained winds were observed at Nanji Shan (WMO 58765), China, as Fred struck the coast. Since this report was obtained at the synoptic hour of 211200Z it is likely that it represents neither the maximum wind nor the lowest pressure in Fred's core at landfall.

As with Doug (17W), Fred's eye did not expand after reaching peak intensity (Table 3-19-2). After 201800Z, the eye diameter began to shrink from 32 nm (59 km) to 11 nm (20 km) before it disappeared from the satellite imagery.

IV. IMPACT

No information was received concerning damage from Fred in the southern Ryukyu Islands. Damage in China was summarized in the August 31, 1994 Weekly Climate Bulletin of the U.S. National Climate Analysis Center of NOAA:

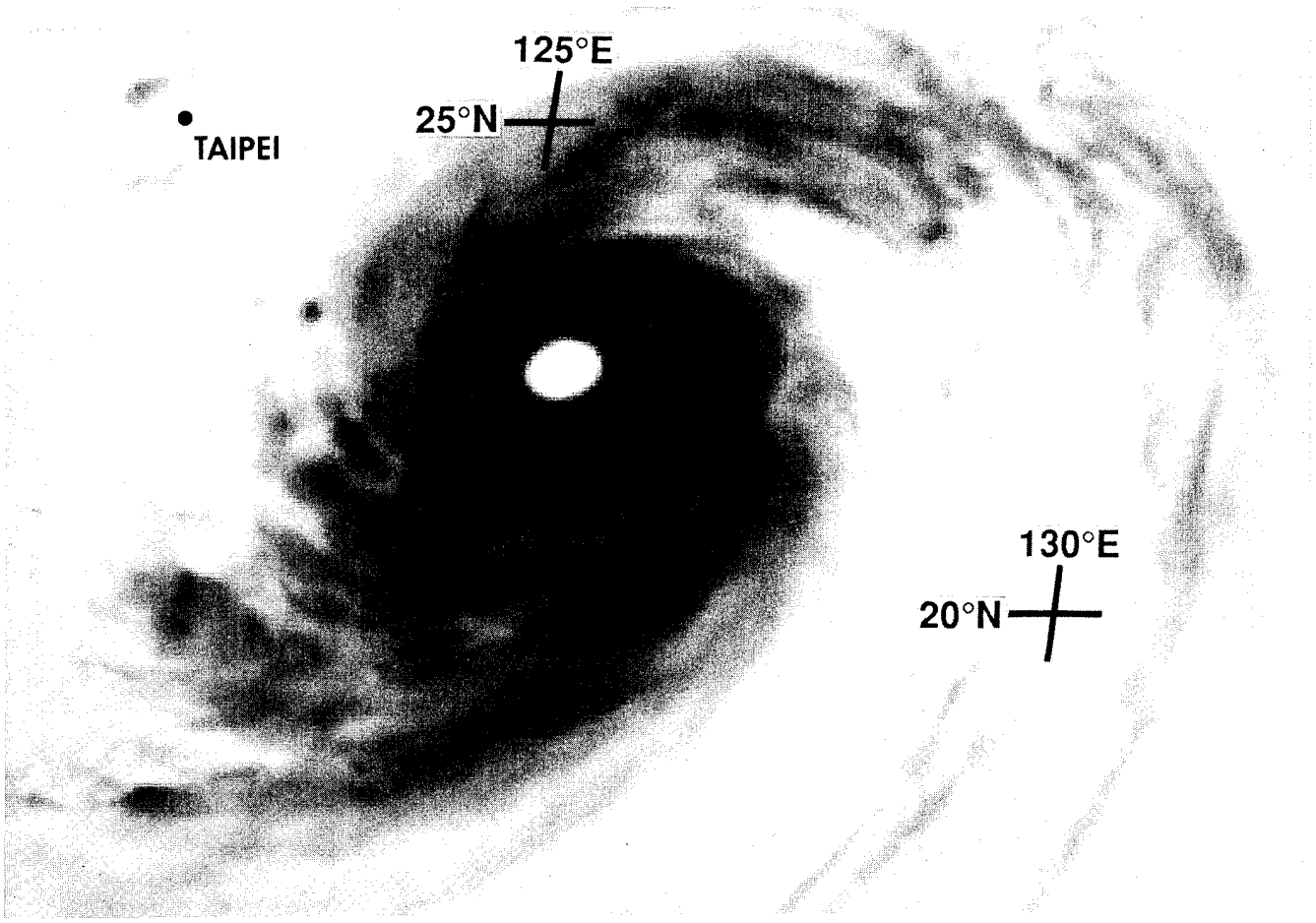

Figure 3-19-2 Fred at its peak intensity of 130 kt (67 m/sec) (191831Z August inverse infrared GMS imagery). Note: in an inverse infrared image, the cold clouds are dark and the warm sea surface is white.

"Typhoon Fred, packing wind gusts over 295 kph [160 kt] at one time, slowly weakened as it tracked north of Taiwan and into southern Zhejiang province in China. Generally, 100-225 mm (3.9-8.9 in) of rain fell along and near the path of the storm, flooding large sections of northern Taiwan and southern Zhejiang province. According to press reports, Fred's landfall near the city of Wenzhou coincided with an unusually high astronomical tide, thereby generating some of the highest tides of the last two decades in and near Wenzhou. Resultant flooding combined with strong winds to take an estimated 1,000 lives in Wenzhou alone, according to to city officials. In addition, local officials indicated that Fred, the region's worst storm in over a century, demolished 100,000 homes, damaged another 700,000 dwellings, isolated more than two million individuals, forced the closure of Wenzhou airport for at least two weeks, damaged over 3000 km^2 (875 mi^2) of farmland, caused flooding in more than 180 towns, and forced 90,000 enterprises to suspend production. Total economic losses may top $1.2 billion (U.S.)."

Table 3-19-1 Twenty-four hour pressure fall for each 6-hour interval during the intensification of Typhoon Fred. Winds are in knots and represent best-track winds; pressures are in millibars and are derived from winds using the Atkinson-Holliday wind-pressure relationship (Atkinson and Holliday 1977).

Time (Z)	24-hr Wind Range	24-hr Pressure Range	24-hr Pressure Fall
1600-1700	55-75 kt	984-968 mb	16 mb
1606-1706	60-80	980-963	17
1612-1712	65-85	976-959	17
1618-1718	70-90	971-954	17
1700-1800	75-95	968-949	19
1706-1806	80-100	963-943	20
1712-1812	85-110	961-932	29
1718-1818	90-115	954-927	27
1800-1900	95-120	949-922	27
1806-1906	100-125	939-916	23
1812-1912	110-130	932-910	22
1818-1918	115-125	927-916	11

Table 3-19-2 Comparison of Dvorak T-number, best track intensity and infrared eye diameter for Typhoon Fred from initial 55 kt (28 m/s) intensity to after landfall in China.

Date/Time (Z)	T-number	Intensity (kt)	Eye Diam (nm)
160000	3.5	55	NA
160600	3.5	60	NA
161200	4.0	65	27
161800	4.5	70	24
170000	5.0	75	25
170600	5.0	80	17
171200	5.0	85	29
171800	5.0	90	24
180000	5.0	95	22
180600	5.0	100	21
181200	6.0	110	16
181500	6.0	115	16
181800	6.0	115	25
182100	6.0	120	35
190000	6.0	120	24
190300	6.0	120	29
190600	6.5	125	30
190900	6.5	125	30
191200	7.0	130	33
191800	6.0	125	38
200000	6.0	120	32
200600	5.5	110	26
201200	6.0	105	34
201800	5.0	100	26
210000	4.5	95	18
210600	4.5	95	11
211200	4.0	90	NA
211800	4.0	80	NA

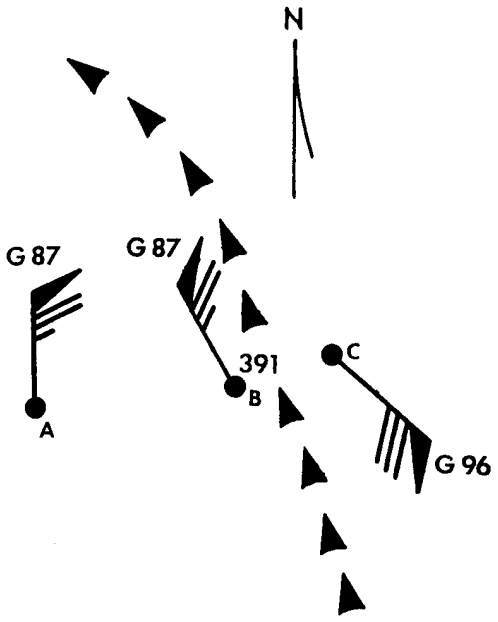

Figure 3-19-3 Wind and pressure data at Yonaguni-jima (WMO 47912) (labeled A), Ishigaki-jima (WMO 47918) (labeled B), and Miyako-jima (WMO 47927) (labeled C) at 201200Z. Peak 10-minute sustained winds are plotted and peak gusts are indicated. The pressure of 939.1 mb recorded at Ishigaki-jima is plotted as 391. The track of Fred is indicated by the trail of arrows.

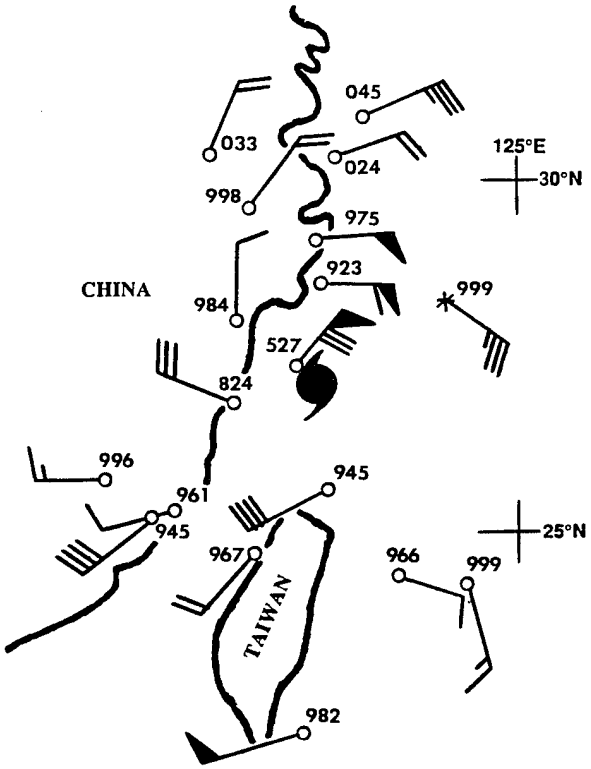

Figure 3-19-4 Synoptic reports at 211200Z August as Fred makes landfall on the east coast of China. Winds are 10-minute sustained averages.

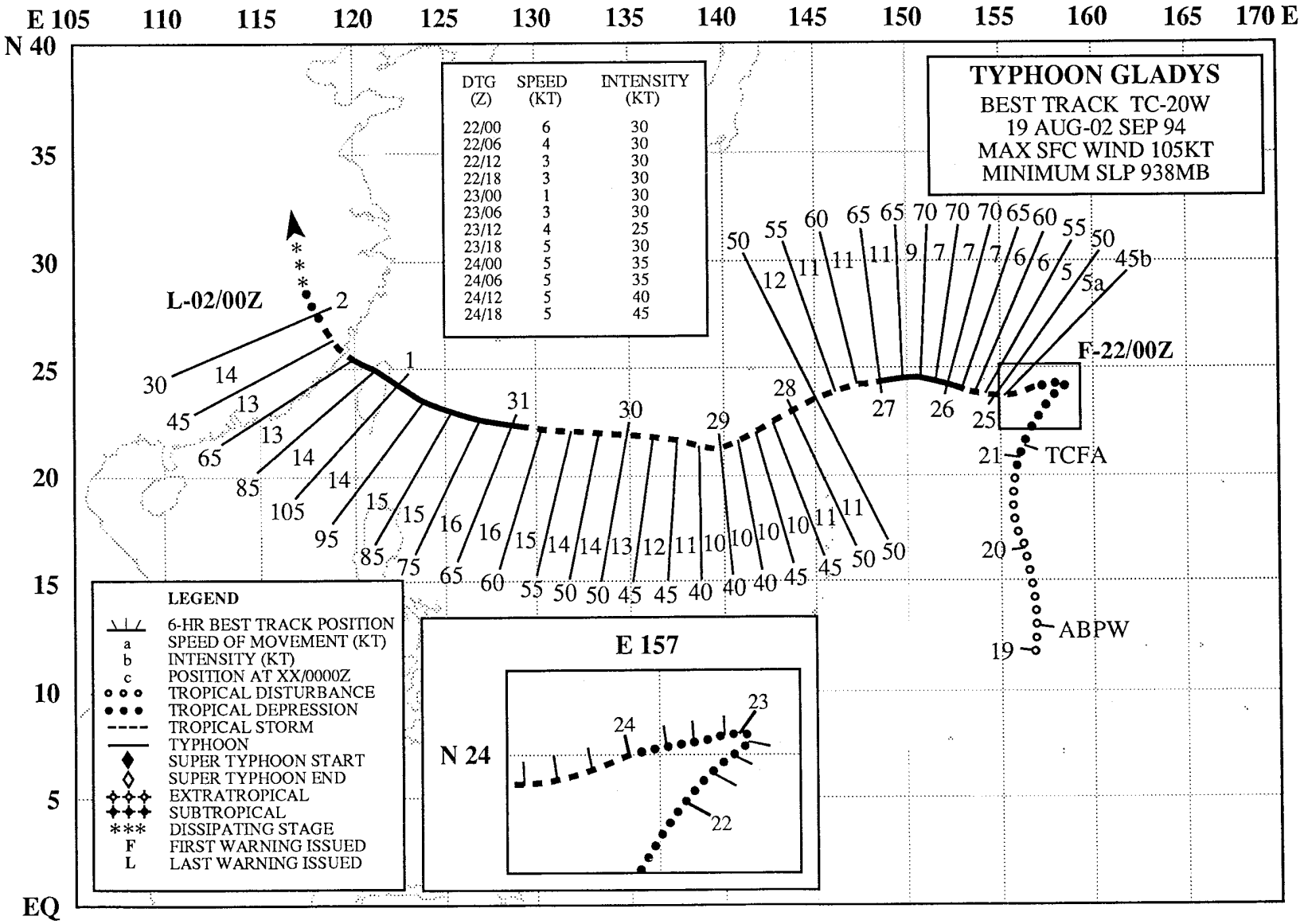
E 105 110 115 120 125 130 135 140 145 150 155 160 165 170 E
N 40 35 30 25 20 15 10 5 EQ
TYPHOON GLADYS
BEST TRACK TC-20W
19 AUG-02 SEP 94
MAX SFC WIND 105KT
MINIMUM SLP 938MB
DTG (Z) SPEED (KT) INTENSITY (KT)
22/00 6 30
22/06 4 30
22/12 3 30
22/18 3 30
23/00 1 30
23/06 3 30
23/12 4 25
23/18 5 30
24/00 5 35
24/06 5 35
24/12 5 40
24/18 5 45
L-02/00Z
F-22/00Z
TCFA
ABPW
LEGEND
6-HR BEST TRACK POSITION
a SPEED OF MOVEMENT (KT)
b INTENSITY (KT)
c POSITION AT XX/0000Z
TROPICAL DISTURBANCE
TROPICAL DEPRESSION
TROPICAL STORM
TYPHOON
SUPER TYPHOON START
SUPER TYPHOON END
EXTRATROPICAL
SUBTROPICAL
DISSIPATING STAGE
F FIRST WARNING ISSUED
L LAST WARNING ISSUED
E 157
N 24

TYPHOON GLADYS (20W)

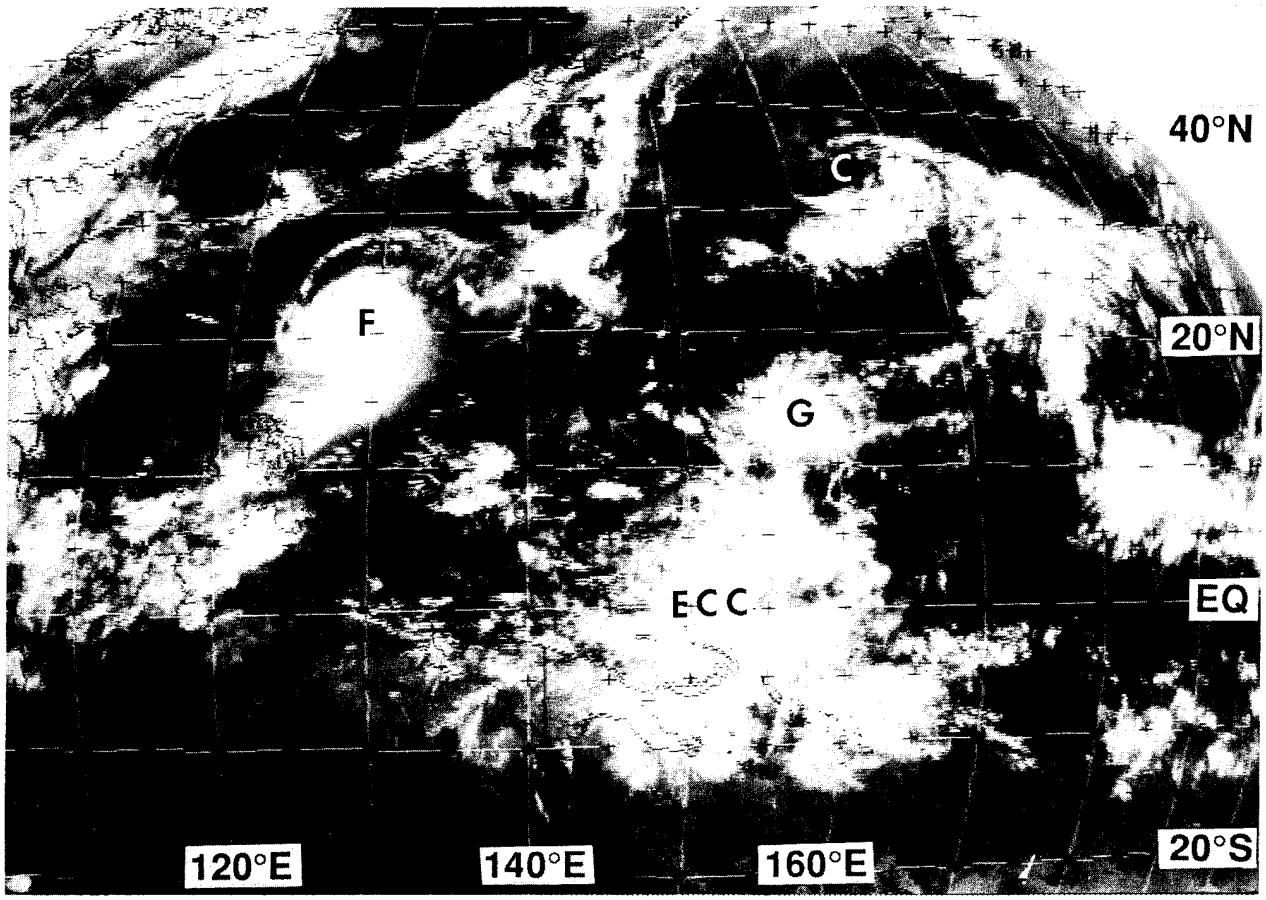

Figure 3-20-1 A complex cloud pattern over the western North Pacific basin preceded the formation of Gladys. An equatorial cloud cluster (ECC), an upper tropospheric cut-off low (C), and Typhoon Fred (F) figure prominently in the large-scale environment of the pre-Gladys tropical disturbance (G) (190031Z August infrared GMS imagery).

I. HIGHLIGHTS

For the first half of its life, Gladys was a very small tropical cyclone that exhibited large fluctuations of intensity. Ground-truth wind measurements from Minami-Torishima (WMO 47991) and from a station at its landfall site in Taiwan indicated that real-time estimates of Gladys' intensity (when near these sites) were too low. Images from Taiwan-based radar showed that as Gladys approached Taiwan it had well-developed concentric eye walls.

II. TRACK AND INTENSITY

As Gladys was forming, the large-scale distribution of cloudiness (Figure 3-20-1) and the large-scale structure of the troposphere over the western North Pacific had become quite complex. An upper-tropospheric cold-core low dominated the distribution of cloudiness in the subtropics of the western North Pacific,near the international date line, and had induced an inverted trough of low pressure in the sea-level pressure field there. A weak monsoon trough extended east-southeastward from near Taiwan to about 13°N 160°E. A large cluster of deep convection and associated cirrus debris accompanied monsoonal westerly winds along the equator from 150°E to 160°E.

During the daylight hours of 19 August, a small area of persistent deep convection embedded in anti-

cyclonically curved cirrus debris (Figure 3-20-2) was observed at the eastern end of the monsoon trough where synoptic data indicated the presence of a weak surface circulation. This tropical disturbance was first mentioned on the 190600Z August Significant Tropical Weather Advisory. After drifting northward for almost two days, satellite imagery showed low-level cloud lines wrapping underneath a convective cloud mass. A Tropical Cyclone Formation Alert was issued at 210430Z. The first warning was issued at 220000Z; it stated, in part:

". . . [Tropical Depression] 20W has an organized low level circulation which is partially exposed on the northwest side of the convective cloud mass. The deep convection is displaced less than 30 nm southeast of the cyclone center. This is a small tropical cyclone . . . SSM/I data does not indicate that gale-force winds exist near the center. . . . The NOGAPS model does not analyze Tropical Depression 20W as a distinct feature, nor does it develop the system in the prog series. . . . Climatology favors a peak intensity of less than 55 kt . . . we anticipate that Tropical Depression 20W will reach minimal tropical storm intensity in about 24 hours, and peak at about 50 knots in 60 hours. . . ."

After 221800Z, Tropical Depression 20W made an abrupt turn toward the west. This may have been in response to the sub-tropical ridge building to its north as two upper-tropospheric cold-core lows, one near the international date line, and another near Japan, weakened. After the system turned toward the west, it began to intensify. It was upgraded to Tropical Storm Gladys at 240000Z. By the morning of 25 August, it developed an eye (Figure 3-20-3). About nine hours after the imagery in Figure 3-20-3, Gladys passed about 30 nm (50 km) south of Minami-Torishima (WMO 47991), where a peak gust of 74 kt (38 m/sec) was recorded at 250956Z. Continuing on a westward track, Gladys appeared to come under the influence of westerly shear and weakened considerably (Figure 3-20-4). At 281800Z, its intensity dropped to 40 kt (21 m/sec). As Gladys moved westward toward Taiwan, it underwent a second period of intensification. At 010000Z September, shortly before Gladys' landfall on Taiwan, the intensity reached 105 kt (54 m/sec) (Figure 3-20-5). Gladys increased in size from very small to average during this second intensification phase. While crossing the northern half of Taiwan, Gladys weakened considerably. It then tracked inland over mainland China. The final warning was issued at 020000Z September as Gladys dissipated over land.

III. DISCUSSION

a. Ground-truth intensity verification

Ground-truth verification of Gladys' intensity was obtained at two points along its track: (1) Minami-Torishima (WMO 47991), and (2) northern Taiwan. At 250900Z, Gladys passed about 30 nm (50 km) south-southwest of Minami-Torishima (WMO 47991), (Figure 3-20-6). This island experienced a seven-hour period of sustained gale-force wind. The peak gust of 74 kt (38 m/sec) was recorded at 250956Z, and the minimum sea level pressure of 1001.4 mb was recorded at 250951Z. This peak wind and minimum pressure indicate that Gladys was a typhoon when it passed south of Minami-Torishima. Based on these measurements, the final best-track intensity of Gladys was increased to 65 kt (33 m/sec) from the real-time 55 kt (28 m/sec) satellite-derived estimate.

The second ground-truth verification was obtained when Gladys came ashore in northern Taiwan. Suao (WMO 46706), recorded a peak gust of 133 kt (68.6 m/sec) at 010232Z and a minimum sea level pressure reading of 960.3 mb at 010247Z. The over-water one-minute sustained wind speed associated with a 133 kt gust is 105 kt (54 m/sec). Thus, the peak gust measured at Suao was used to increase the final best-track intensity to 105 kt from the real-time satellite-derived intensity estimate of 85 kt (44 m/sec).

b. Concentric eye walls

As Gladys approached Taiwan's northeastern coast, weather radar located at Hualien (WMO 46699) was able to gather some detailed images of the structure of its core. From the time when the eye first appeared at the outer range of the radar, until approximately one hour before landfall, the core was comprised of concentric eye walls (Figure 3-20-7). At 311600Z, the inner eye wall was a complete ring about 10 nm (20 km) in thickness that surrounded a small central clearing about 6 nm (10 km) across (Figure 3-20-7c). A 10 nm (20 km) moat surrounded the inner eye wall and separated it from a 10 nm (20 km)-thick outer eye wall. For nearly ten hours, this structure prevailed. There was no evidence of contraction of the outer eye wall. Few tropical cyclones are observed to have well-defined concentric eye walls, although it has been suggested that most very intense tropical cyclones (i.e., those tropical cyclones with intensities in excess of 100 kt) have concentric eye walls at some point in their evolution (Willoughby 1982, 1990). Another observation made by Willoughby is that when concentric eye walls are present, the outer eye wall tends to contract and eventually replace the inner eye wall. In the case of Gladys, it appears that a steady-state structure of well-defined concentric eye walls was maintained for 10 hours. Landfall ultimately disrupted that structure.

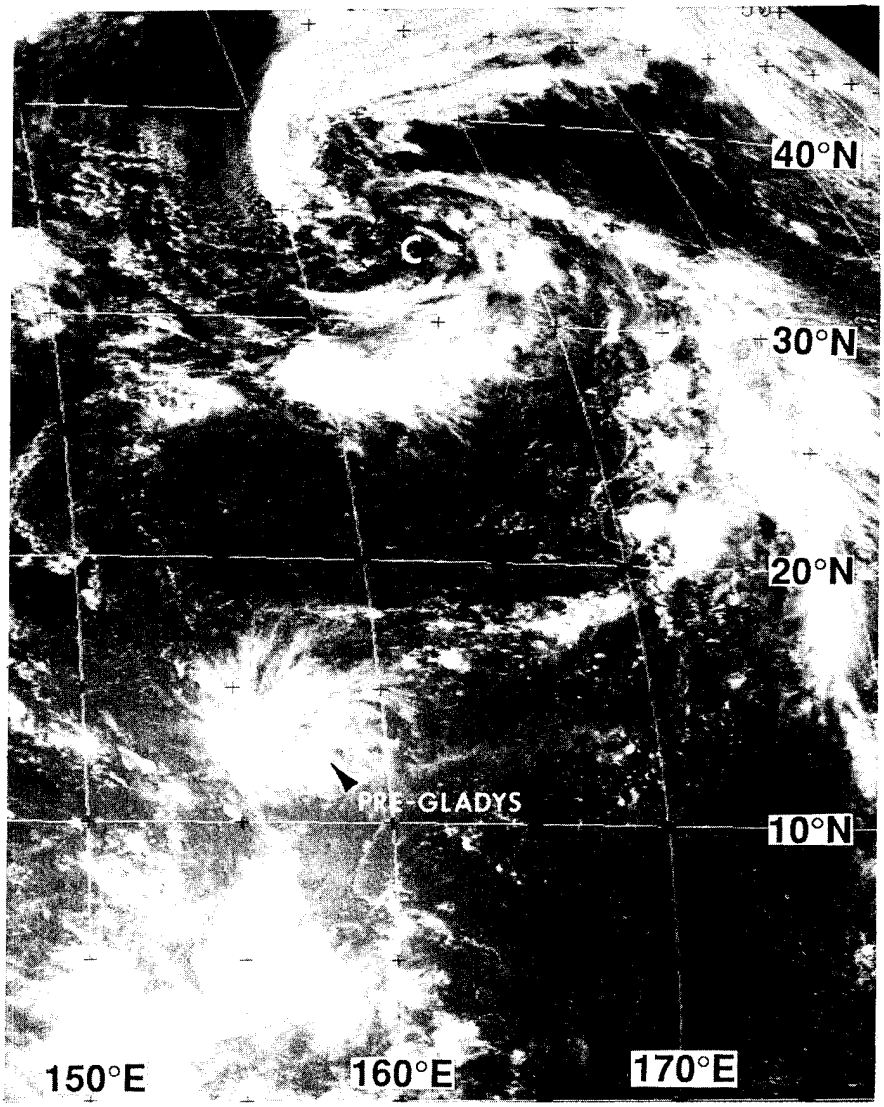

Figure 3-20-2 An area of persistent deep convection associated with anticyclonically curved cirrus outflow, defines the tropical disturbance that would later become Gladys (190031Z August visible GMS imagery). The "C" shows the location of a large upper-tropospheric cut-off low.

c. Forecast performance

The westward-moving Gladys presents an ideal case for illustrating the poleward bias reported by Carr (personal communication) to exist in the NOGAPS model for very small westward-moving tropical cyclones (Figure 3-20-8). According to Carr, NOGAPS effective grid spacing is too large to properly analyze a very small to small tropical cyclone. The bogus vortex inserted into the analysis starts out too large and usually expands if the model intensifies the system. Since the poleward propagation of a vortex is size-dependent (i.e., the larger the vortex, the greater the poleward prop-

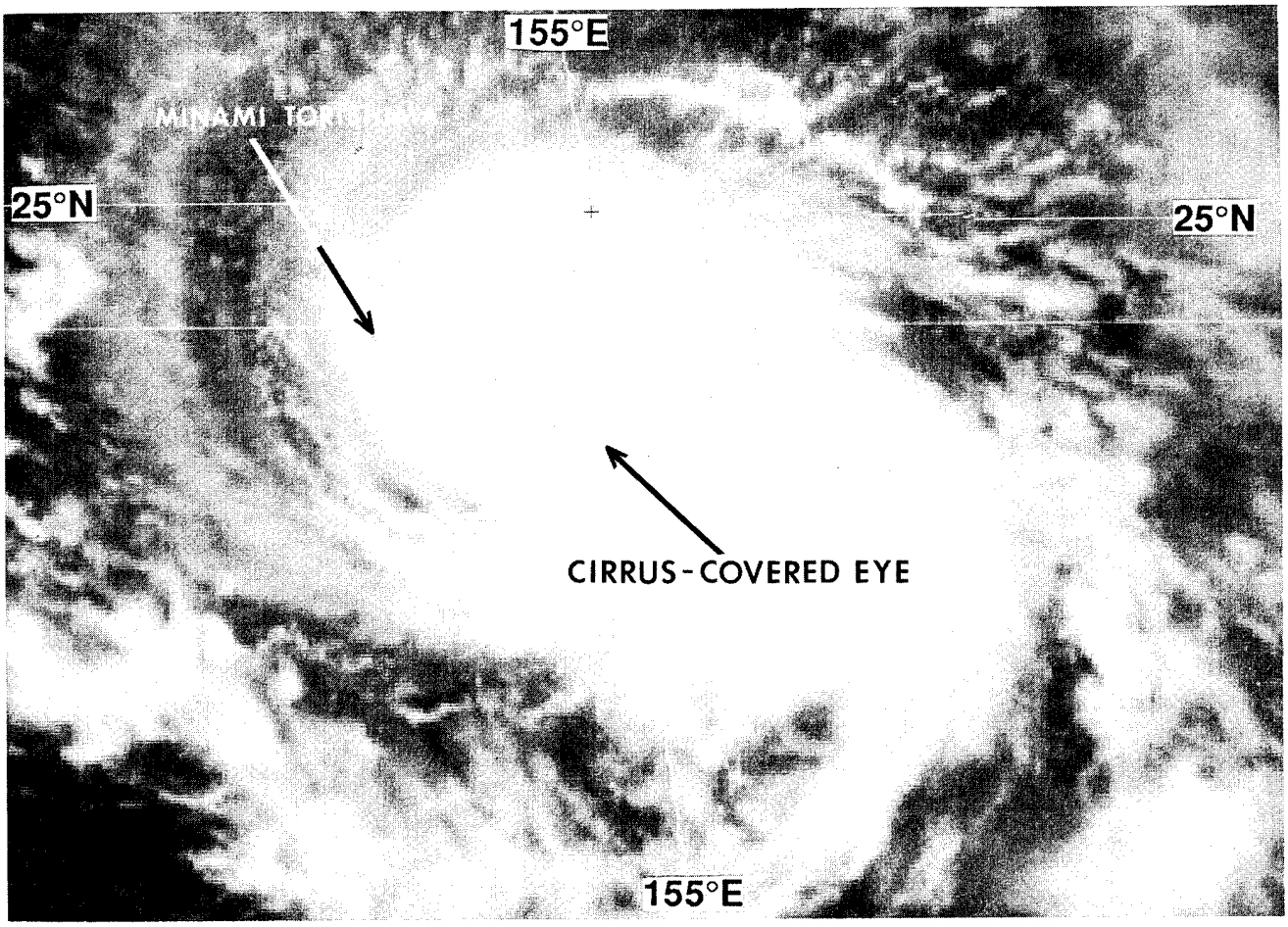

Figure 3-20-3 An eye appears in Gladys' central dense overcast (250131Z August visible GMS imagery).

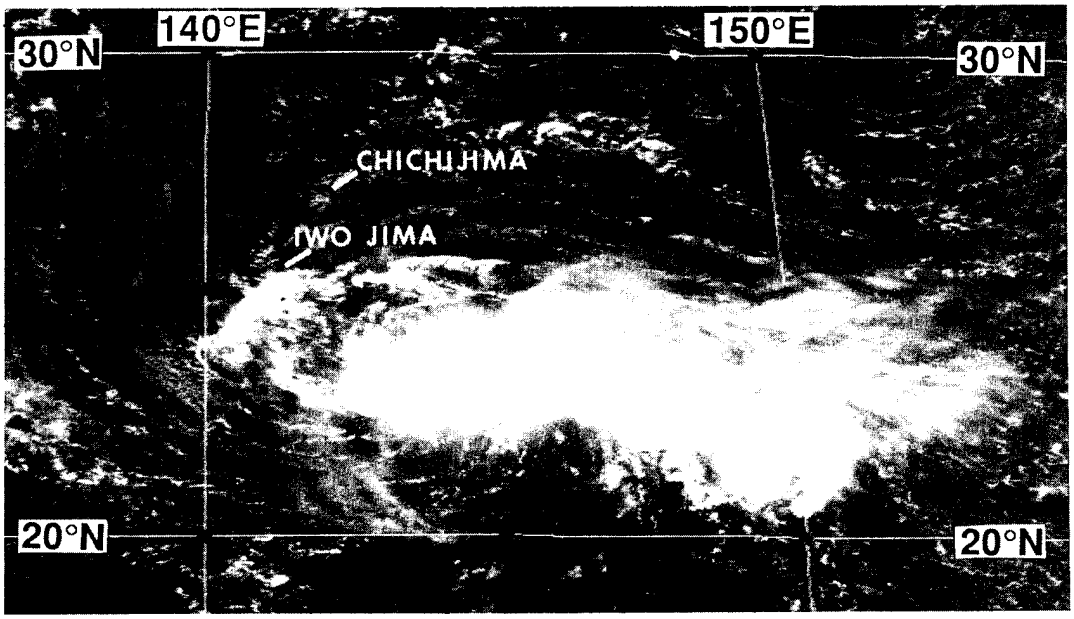

Figure 3-20-4 Gladys' low-level circulation center becomes partially exposed as the system experiences westerly shear (280031Z August visible GMS imagery).

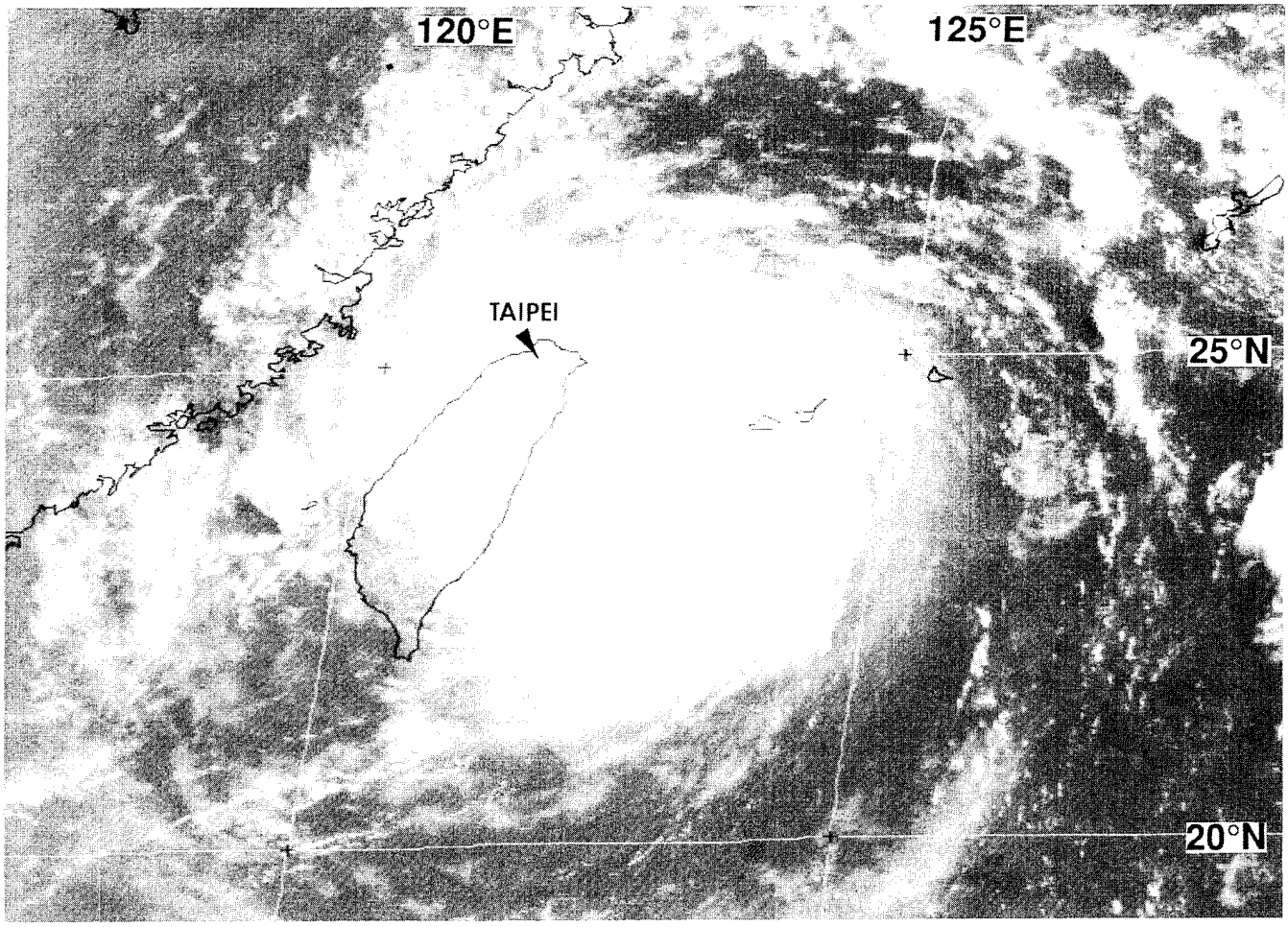

Figure 3-20-5 Gladys at peak intensity (312331Z August visible GMS imagery).

agation), it is almost a guarantee that the NOGAPS forecast will be to the right of track for a very small westward-moving tropical cyclone.

IV. IMPACT

Typhoon Gladys battered Taiwan with high wind and heavy rain. A peak wind gust of 133 kt (68.6 m/sec) was recorded at Suao (WMO 46706). Six deaths were recorded. A woman was killed when a utility pole fell on her car, a man drowned in a flooded river, and three other people were killed by falling objects. Another woman was killed when strong winds caused her house to collapse.

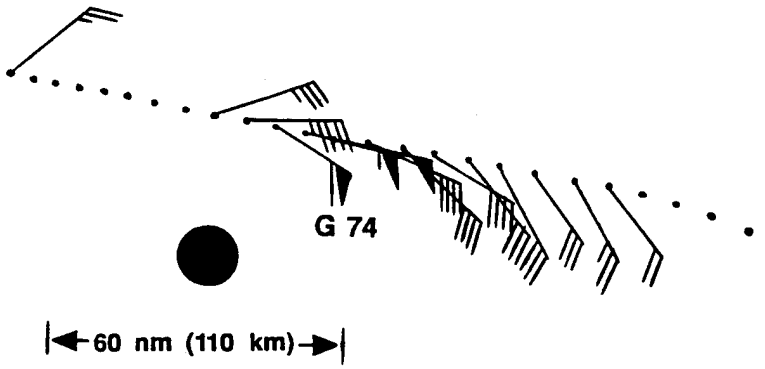

Figure 3-20-6 The wind recorded at Minami-Torishima (WMO 47991) as Gladys passed to the south (each small dot is a one-hour time step). The reference frame has been adjusted to the center of Gladys (large black dot).

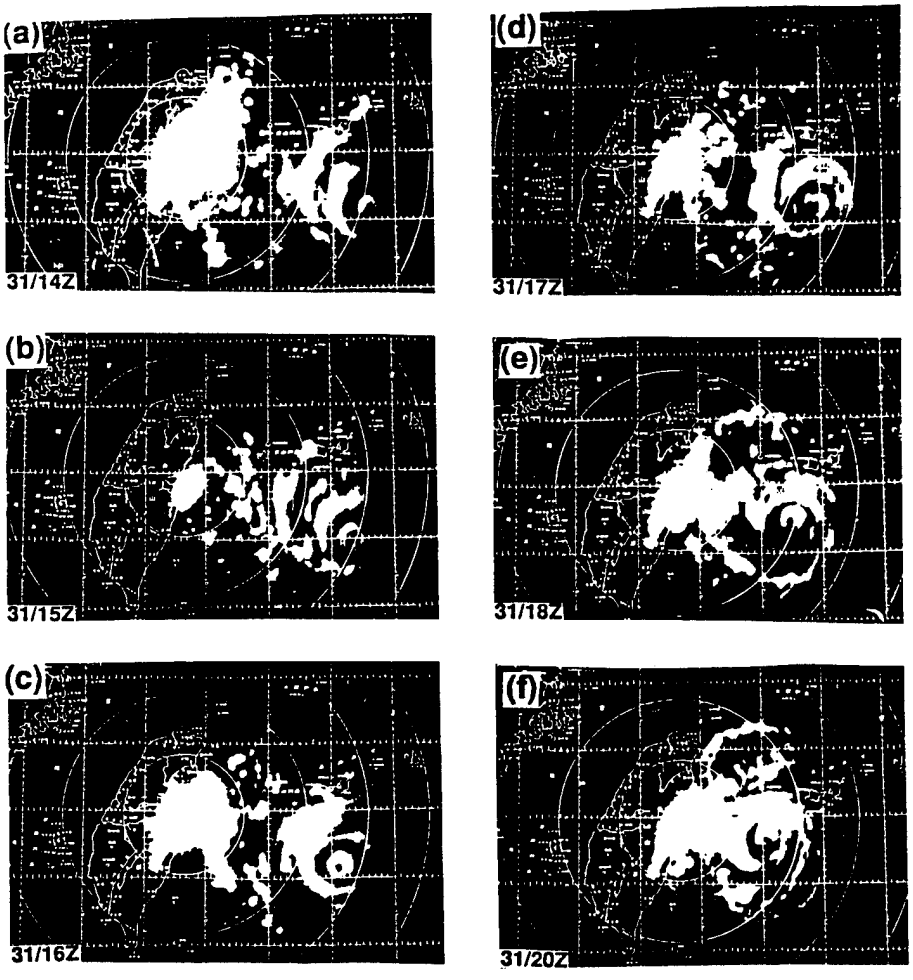

Figure 3-20-7 (a-f) Ground-based radar depictions of the concentric eye walls of Typhoon Gladys as it neared the coast of Taiwan. Time of radar image is indicated on each panel. (Radar images courtesy of the Taiwan Central Weather Bureau.)

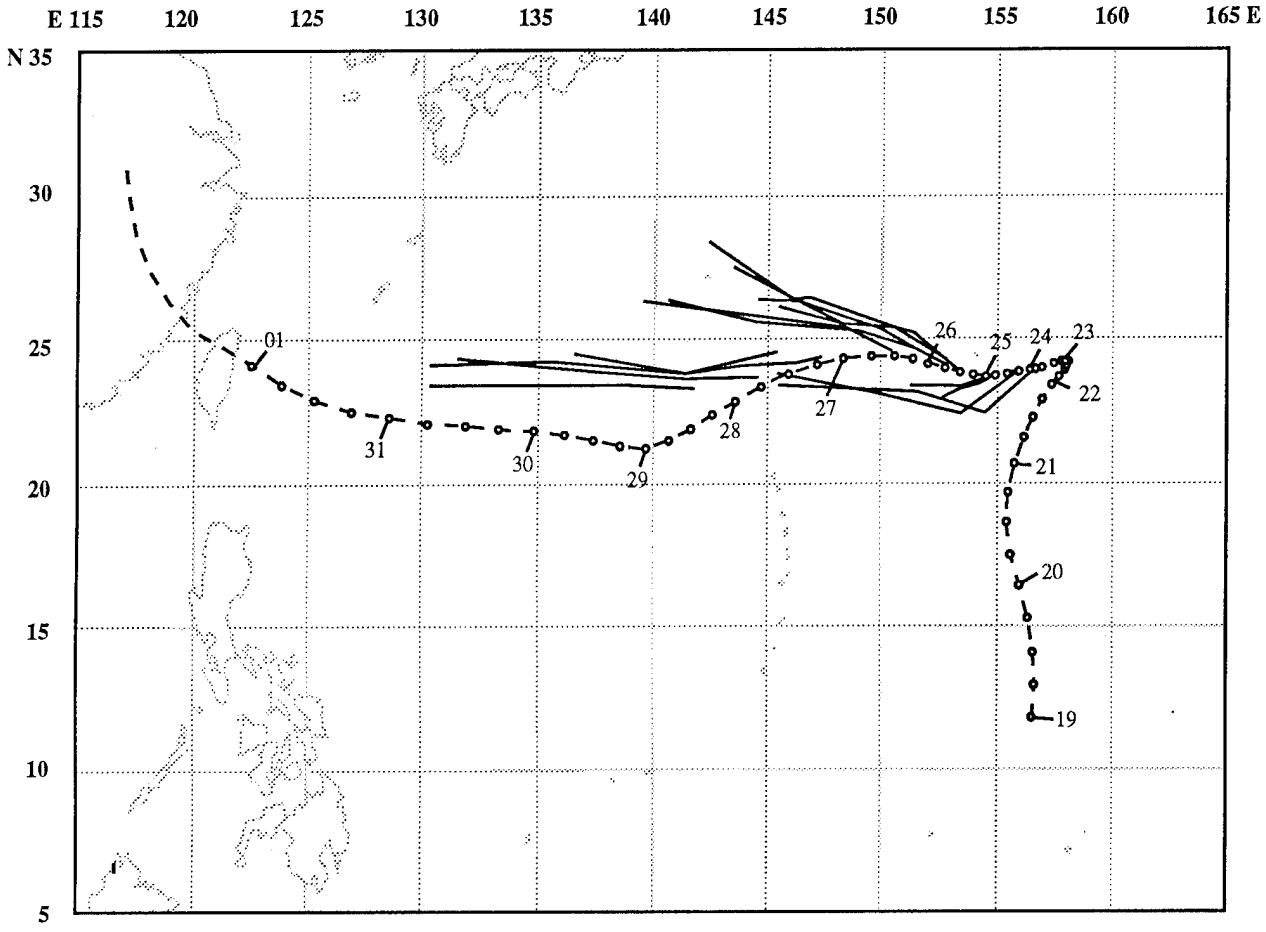

Figure 3-20-8 NOGAPS track forecasts show poleward bias.

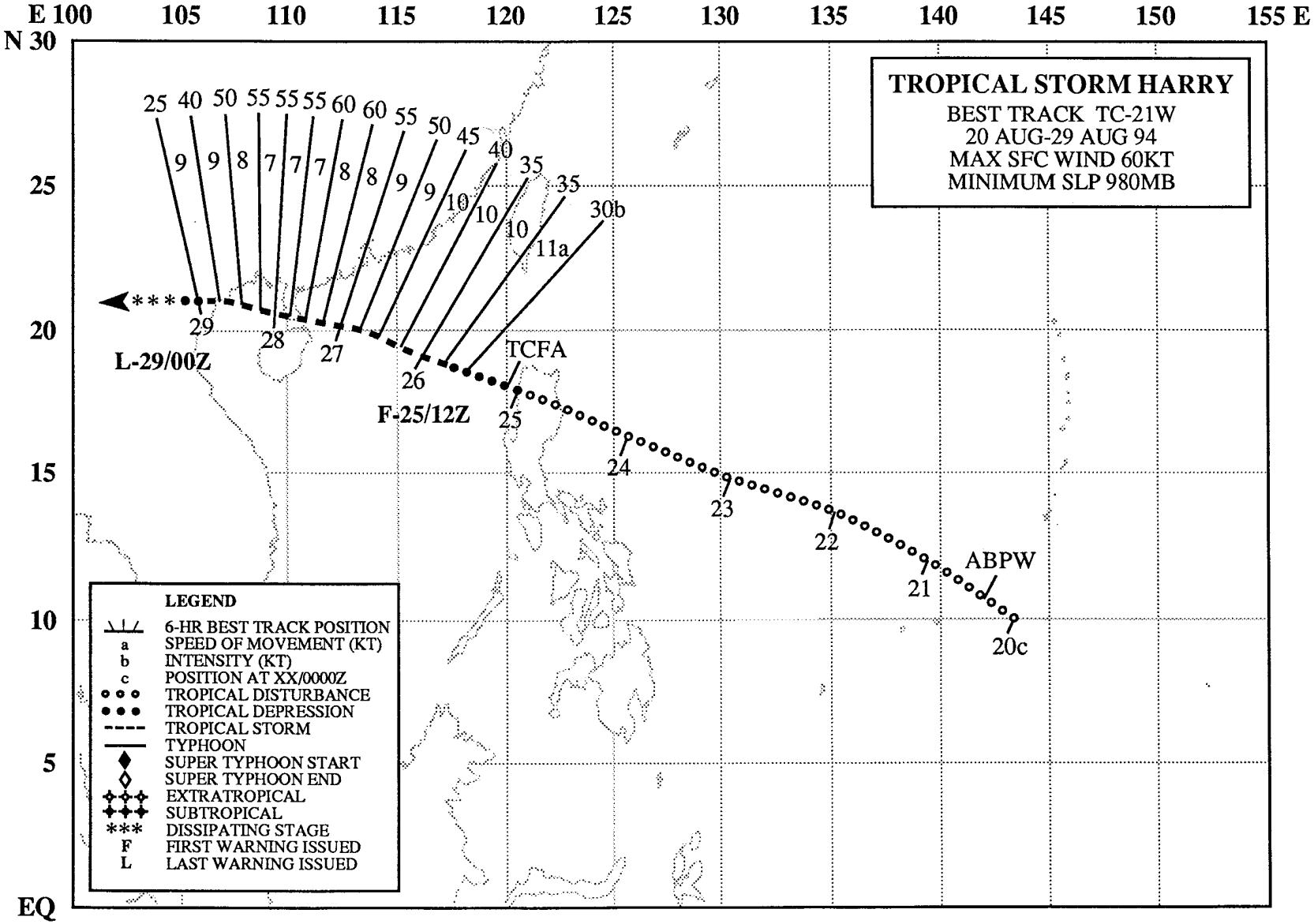
E 100
105
110
115
120
125
130
135
140
145
150
155 E
N 30
25
20
15
10
5
EQ
TROPICAL STORM HARRY
BEST TRACK TC-21W
20 AUG-29 AUG 94
MAX SFC WIND 60KT
MINIMUM SLP 980MB
25 40 50 55 55 55 60 60 55 50 45 40 35 35 30b
9 9 8 7 7 7 8 8 9 9 10 10 10 11a
29
28
27
26
25
24
23
22
21
20c
L-29/00Z
F-25/12Z
TCFA
ABPW
LEGEND
6-HR BEST TRACK POSITION
a SPEED OF MOVEMENT (KT)
b INTENSITY (KT)
c POSITION AT XX/0000Z
TROPICAL DISTURBANCE
TROPICAL DEPRESSION
TROPICAL STORM
TYPHOON
SUPER TYPHOON START
SUPER TYPHOON END
EXTRATROPICAL
SUBTROPICAL
*** DISSIPATING STAGE
F FIRST WARNING ISSUED
L LAST WARNING ISSUED

121

TROPICAL STORM HARRY (21W)

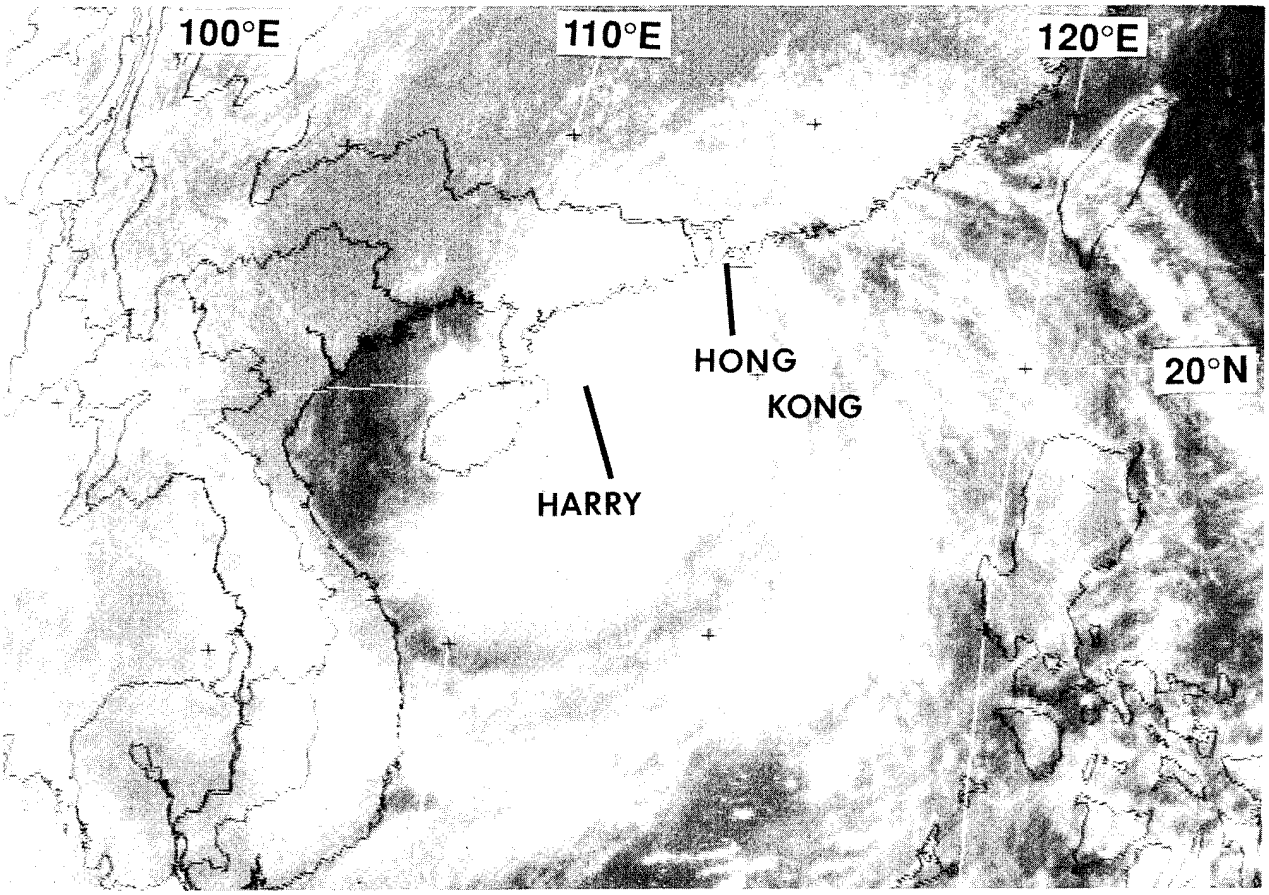

Figure 3-21-1 Harry near its peak intensity of 60 kt (31 m/sec) when located about 210 nm (390 km) southwest of Hong Kong (270231Z August visible GMS imagery).

As Typhoon Fred approached the southwestern Ryukyu Islands of Japan on 20 August, convection began to reappear in the monsoon trough about 250 nm (463 km) southwest of Guam. A disturbance was mentioned that afternoon on the 200600Z August Significant Tropical Weather Advisory. For five days, the disturbance moved to the west-northwest with very little intensification. After it crossed the northern part of Luzon, a Tropical Cyclone Formation Alert was issued at 250000Z followed by the first warning on Tropical Depression 21W at 251200Z. By 251800Z, the system had reached tropical storm intensity. During the next 36 hours, Harry intensified at a rate of 5 kt (2.6 m/sec) per 6 hours while moving west-northwestward at 8-10 kt (15-19 km/hr). On the morning of 27 August, Harry passed 150 nm (278 km) south of Hong Kong where 79 km/hr (43 kt) 10-minute averaged sustained winds were recorded at Waglan Island at 270145Z. A peak gust of 104 km/hr (56 kt) was recorded at 270310Z at the same site. Less than three hours later, Harry reached its peak intensity of 60 kt (31 m/sec) (Figure 3-21-1), six hours before crossing the southern portion of the Luichou Peninsula of China. Harry slowly weakened as it crossed the Gulf of Tonkin, and went ashore at 281500Z just east of Haiphong, Vietnam, with 50 kt (26 m/sec) winds. The final warning was issued at 290000Z after Harry's weakened circulation had moved inland near Hanoi.

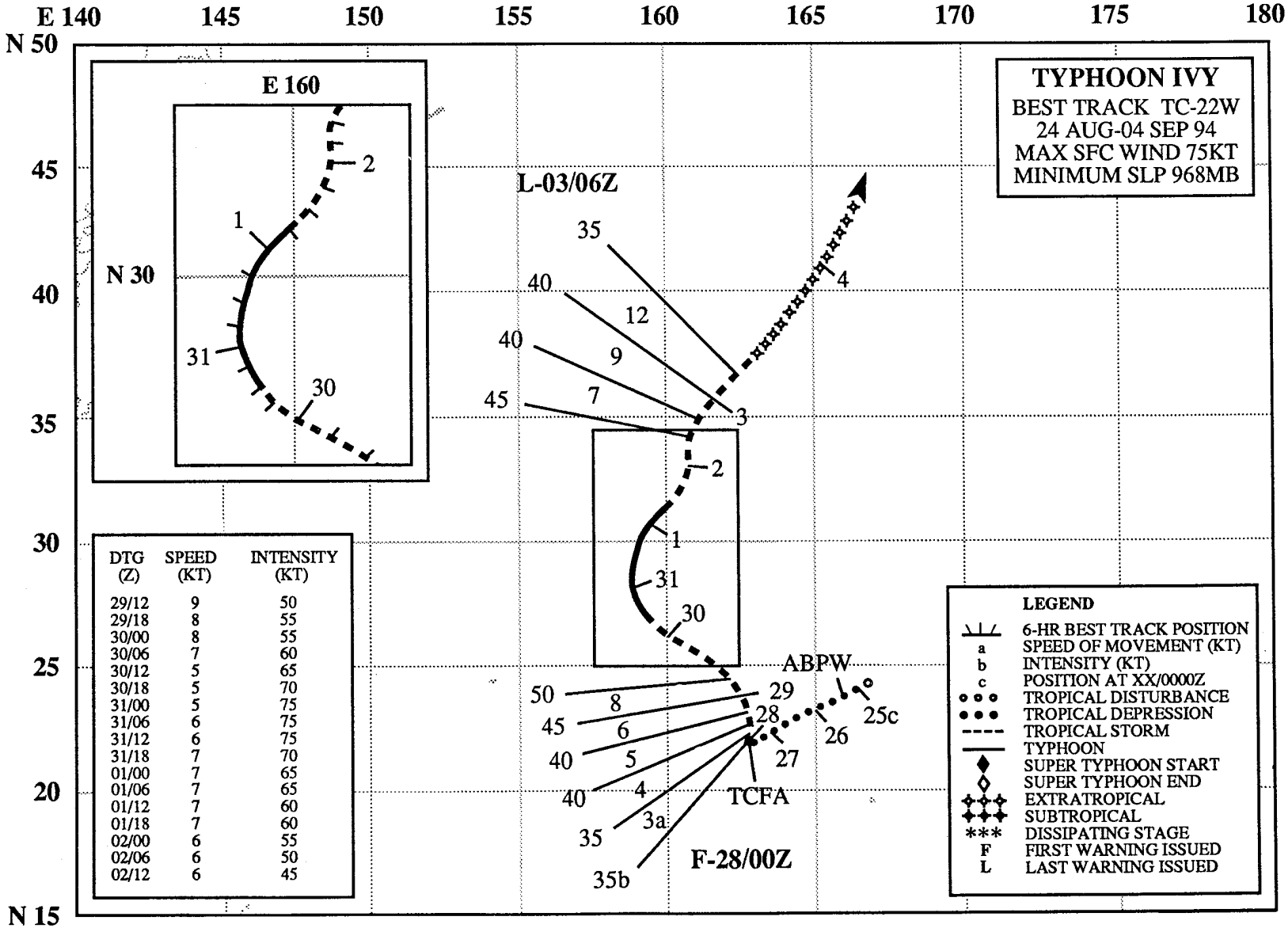
E 140
145
150
155
160
165
170
175
180
N 50
45
40
35
30
25
20
N 15
E 160
N 30
1
2
31
30
L-03/06Z
35
40
12
40
9
45
7
4
3
2
1
31
30
ABPW
50
8
29
45
6
28
25c
40
5
26
27
40
4
TCFA
35
3a
35b
F-28/00Z
TYPHOON IVY
BEST TRACK TC-22W
24 AUG-04 SEP 94
MAX SFC WIND 75KT
MINIMUM SLP 968MB
DTG (Z) SPEED (KT) INTENSITY (KT)
29/12 9 50
29/18 8 55
30/00 8 55
30/06 7 60
30/12 5 65
30/18 5 70
31/00 5 75
31/06 6 75
31/12 6 75
31/18 7 70
01/00 7 65
01/06 7 65
01/12 7 60
01/18 7 60
02/00 6 55
02/06 6 50
02/12 6 45
LEGEND
6-HR BEST TRACK POSITION
a SPEED OF MOVEMENT (KT)
b INTENSITY (KT)
c POSITION AT XX/0000Z
TROPICAL DISTURBANCE
TROPICAL DEPRESSION
TROPICAL STORM
TYPHOON
SUPER TYPHOON START
SUPER TYPHOON END
EXTRATROPICAL
SUBTROPICAL
*** DISSIPATING STAGE
F FIRST WARNING ISSUED
L LAST WARNING ISSUED

TYPHOON IVY (22W)

I. HIGHLIGHTS

Ivy developed within an area of disturbed weather located in the subtropics (i.e., north of 20°N) at a time when the low-level and upper-level wind patterns throughout the western North Pacific were unusual. Ivy was a small tropical cyclone that moved on a north-oriented track.

II. TRACK AND INTENSITY

The tropical disturbance that would eventually become Ivy formed in the same complex environment within which Gladys (20W) formed. As Ivy was forming, the large-scale distribution of cloudiness (Figure 3-22-1 and Figure 3-22-2) and the large-scale structure of the troposphere over the western North Pacific was quite complex. [For a more complete description of the structure of the atmosphere during this time see the Track and Intensity section of Gladys' (20W) summary.]

During the daylight hours of 25 August, satellite imagery and synoptic data indicated that a low-level circulation center was exposed to the north of an area of deep convection near 24°N 166°E. This disturbance was first mentioned on the 250600Z August Significant Tropical Weather Advisory. For the next 36 hours, this disturbance drifted southwestward and showed signs of gradual intensification. A Tropical Cyclone Formation Alert was issued at 271700Z when satellite imagery depicted an increase in the amount of deep convection near the still-exposed low-level circulation center. The sea-level pressure at Wake Island (WMO 91245), located 200 nm (370 km) east-southeast of the low-level center, fell 3.5 mb over 24 hours. At 280000Z, a tropical depression warning was issued on Tropical Depression 22W. The system intensified more rapidly than anticipated, and on warning number 02, issued at 280600Z, Tropical Depression 22W was upgraded to Tropical Storm Ivy. Ivy then began to track slowly northward while embedded in a complex environment that also featured Gladys (20W) and John (10E). Ivy gradually intensified, and at 310000Z was upgraded to a typhoon. Peak intensity of 75 kt (39 m/sec) was reached at 310000Z (Figure 3-22-3). During the next three days (310000Z August to 030000Z September), Ivy drifted slowly north-northeastward and slowly weakened. After 030000Z, the system accelerated toward the northeast and was absorbed into the frontal cloud band of a midlatitude low. The final warning was issued at 030600Z, as the accelerating Ivy acquired extratropical characteristics.

III. DISCUSSION

a. Formation north of 20°

Ivy was one of five tropical cyclones during 1994 that first attained 25 kt (13 m/sec) (best-track) intensity north of 20°N. Two of these tropical cyclones, Tropical Depression 31W and Yuri (36W), formed in direct association with TUTT cells. The other three, Ellie (18W), Gladys (20W), and Ivy, formed in complex environments that featured TUTT cells and midlatitude troughs which penetrated into subtropical latitudes. Ivy did not form in direct association with the TUTT or a TUTT cell, but rather began as an area of enhanced convection beneath diffluent upper-level northwesterly winds at the base of a midlatitude trough (Figure 3-22-4). As a result, the system was sheared, with the low-level center located northwest of the primary deep convection. As Ivy intensified, a cut-off low formed at the base of the aforementioned midlatitude trough and moved to the west of Ivy. This cut-off low weakened the vertical shear, and contributed to weak, deep, southerly flow over Ivy. Drifting in a general

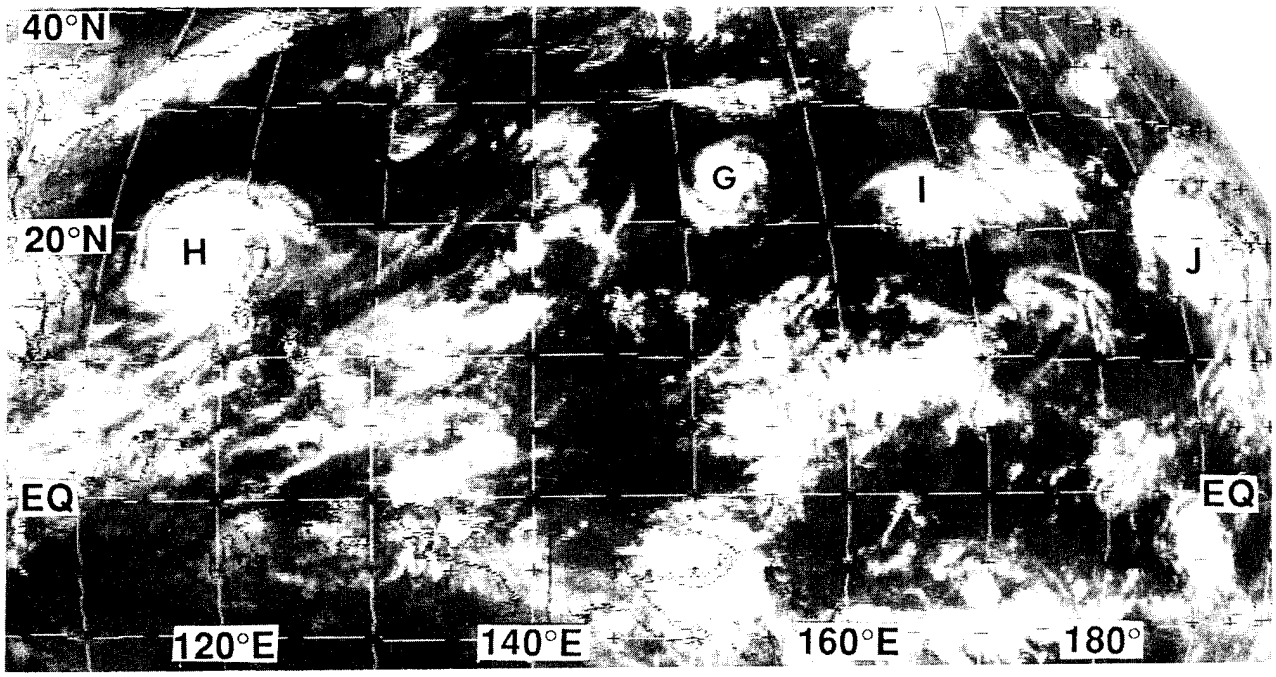

Figure 3-22-1 Ivy formed in a complex environment containing numerous clusters of deep convection and other tropical cyclones. G= Gladys (20W), H = Harry (21W), I = Ivy, and J = John (10E). (260031Z August infrared GMS imagery.)

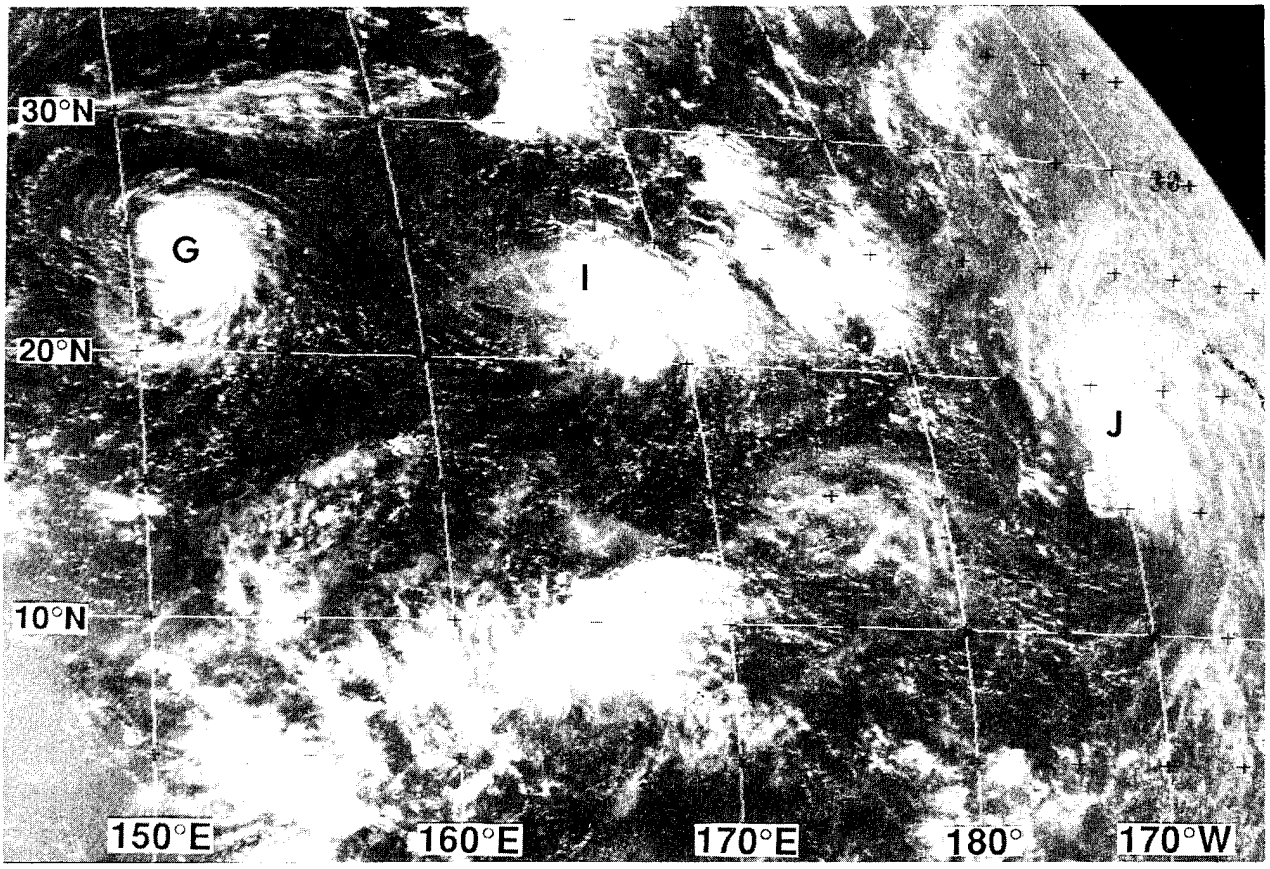

Figure 3-22-2 Ivy developed from a cluster of deep convection located about half way between Gladys (20W) and John (10E) (260231Z August visible GMS imagery). G = Gladys (20W), I = Ivy and J = John (10E)

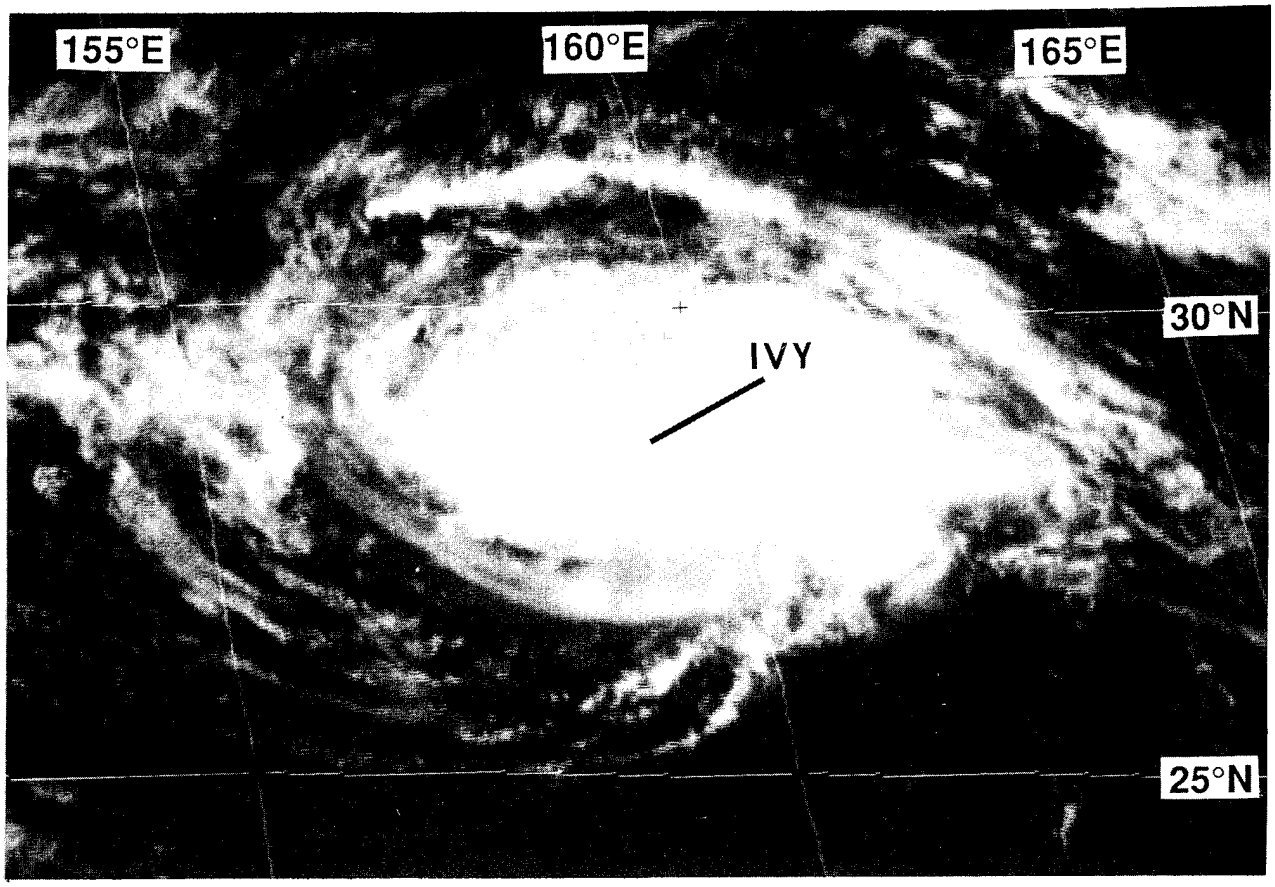

Figure 3-22-3 Ivy reaches its peak intensity of 75 kt (39 m/sec) (302331Z August visible GMS imagery)

northward direction, Ivy became a typhoon at 301200Z August. After moving poleward of 35°N shortly after 021800Z September, Ivy began to accelerate toward the north-northeast ahead of an advancing frontal system.

b. Unusual structure of the low-level wind field

As discussed above, Ivy formed within an area of deep convection associated with the extension into the subtropics of a mid-latitude trough (most tropical cyclones which develop in the western North Pacific form in the monsoon trough). This led to an unusual low-level wind field structure, in which an east-west chain of three tropical cyclones (with Ivy in the center) was positioned well north of a weak monsoon trough (Figure 3-22-5). A zone of light easterly winds separated the monsoon trough from the chain of cyclones.

IV. IMPACT

Ivy spent its entire life over open water. Its only impact was the diverting of shipping around its path.

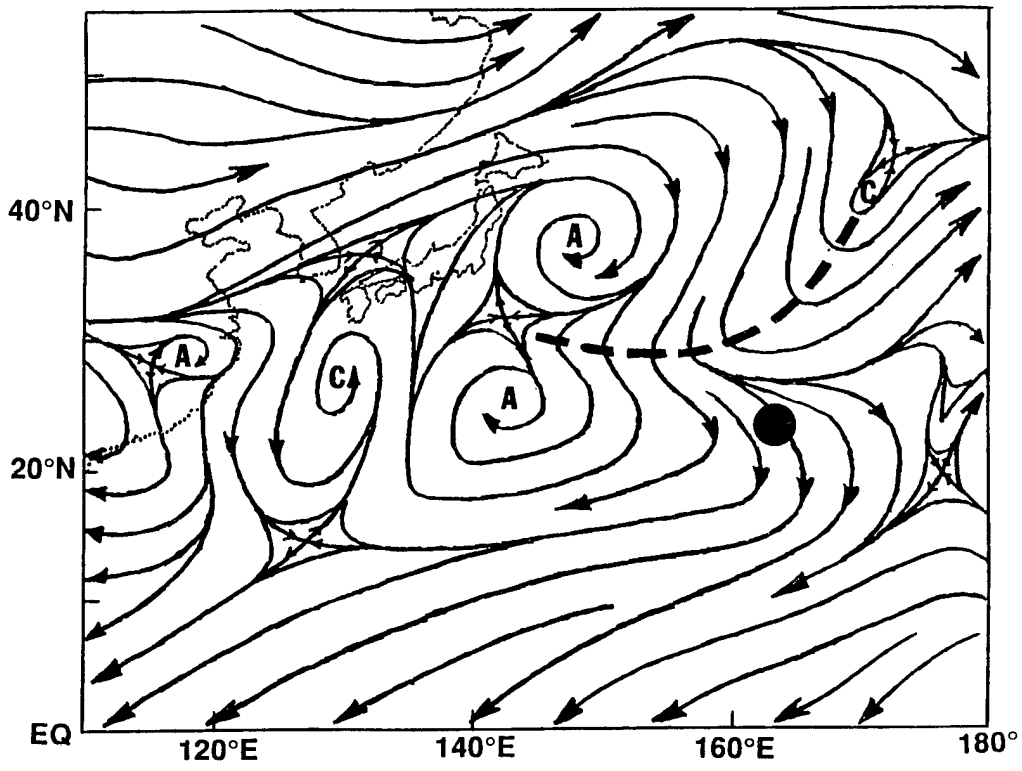

Figure 3-22-4 Streamlines of 200 mb wind (adapted from the 271200Z NOGAPS analysis. Dashed line indicates trough axis, c = cyclonic circulation centers, a = anticyclones, large dot indicates location of the developing Ivy.

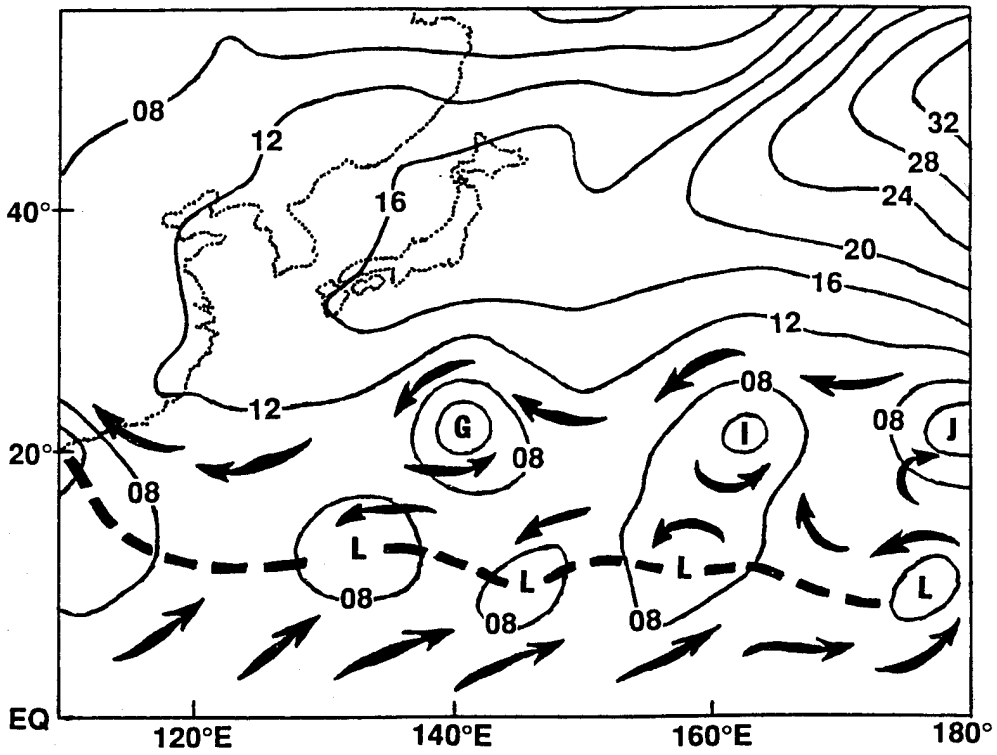

Figure 3-22-5 Contour analysis of the sea-level pressure (adapted from the 281200Z August NOGAPS surface pressure analysis). Dashed line = monsoon trough, C = cyclonic circulation center, G = Gladys (20W), I = Ivy, J = John (10E). Contours are at 4 mb intervals.

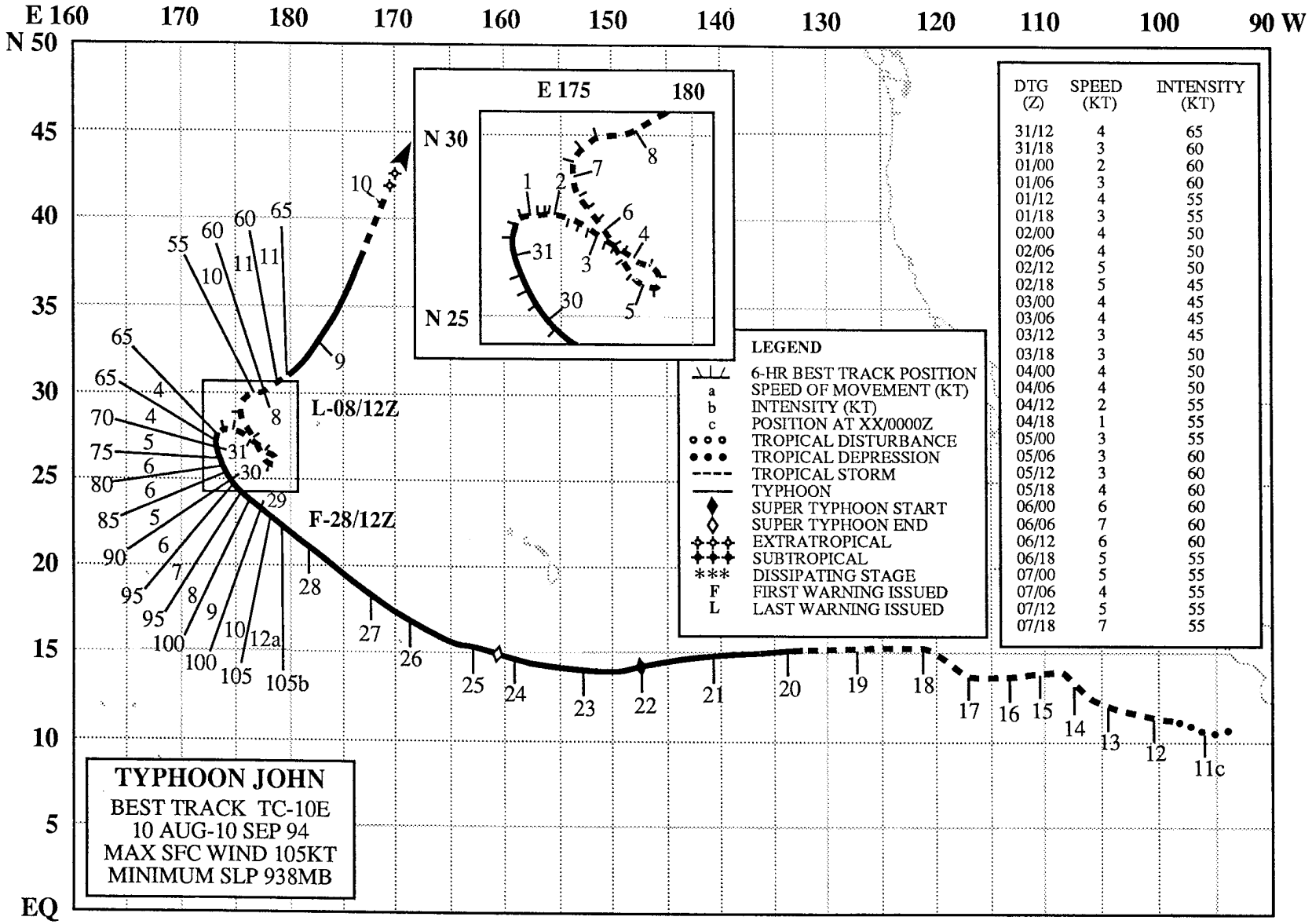

DTG (Z)	SPEED (KT)	INTENSITY (KT)
31/12	4	65
31/18	3	60
01/00	2	60
01/06	3	60
01/12	4	55
01/18	3	55
02/00	4	50
02/06	4	50
02/12	5	50
02/18	5	45
03/00	4	45
03/06	4	45
03/12	3	45
03/18	3	50
04/00	4	50
04/06	4	50
04/12	2	55
04/18	1	55
05/00	3	55
05/06	3	60
05/12	3	60
05/18	4	60
06/00	6	60
06/06	7	60
06/12	6	60
06/18	5	55
07/00	5	55
07/06	4	55
07/12	5	55
07/18	7	55

TYPHOON JOHN (10E)

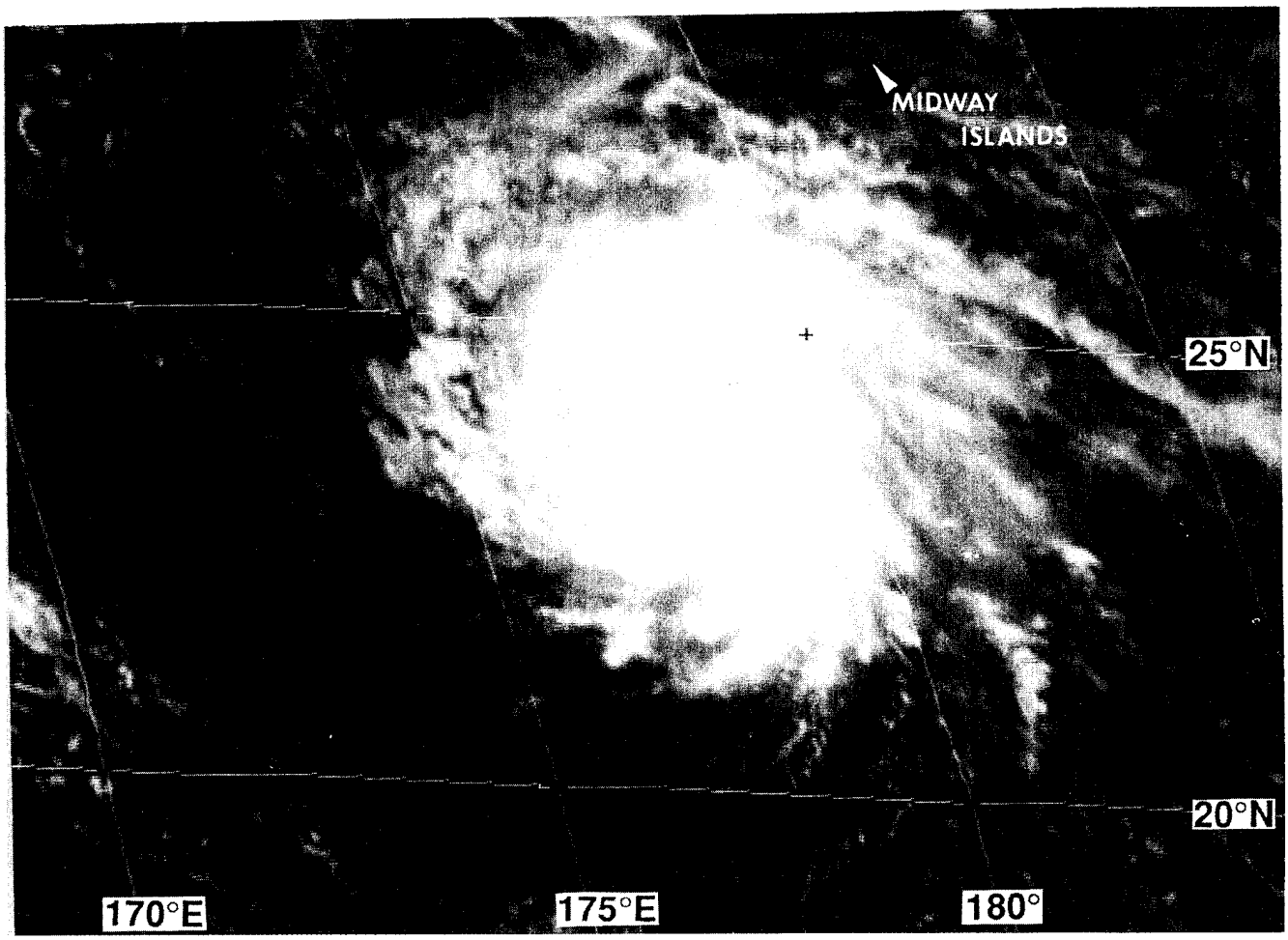

Figure 3-10E-1 A view of John shortly after it crossed the international date line (282331Z August visible GMS imagery).

I. HIGHLIGHTS

John was the longest-lived tropical cyclone on record. Between the National Hurricane Center (Miami), the Central Pacific Hurricane Center (Honolulu) and the JTWC (Guam), a cumulative total of 120 warnings were issued on this system over the course of 31 days. While in the western North Pacific (JTWC's area of responsibility), John weakened from typhoon intensity to tropical storm intensity. Just before it re-crossed the international date line, it reintensified to a typhoon. As John began to reintensify, diagnosed intensities from satellite imagery were much lower than indicated by ship reports near the system center.

II. TRACK AND INTENSITY

Beginning as a tropical depression off the southwest coast of Guatemala at 100600Z August, John traveled across the entire eastern North Pacific. It crossed the international date line and into the western North Pacific at 280900Z. When John was located 300 nm (555 km) south of the island of Hawaii at 230000Z, its intensity peaked at 150 kt (77 m/sec) — an unusually intense hurricane for that region. Moving steadily westward, it then weakened considerably (to 80 kt) and passed only 20 nm north of Johnston Atoll where some damage was reported (see Impact section). As it neared the international

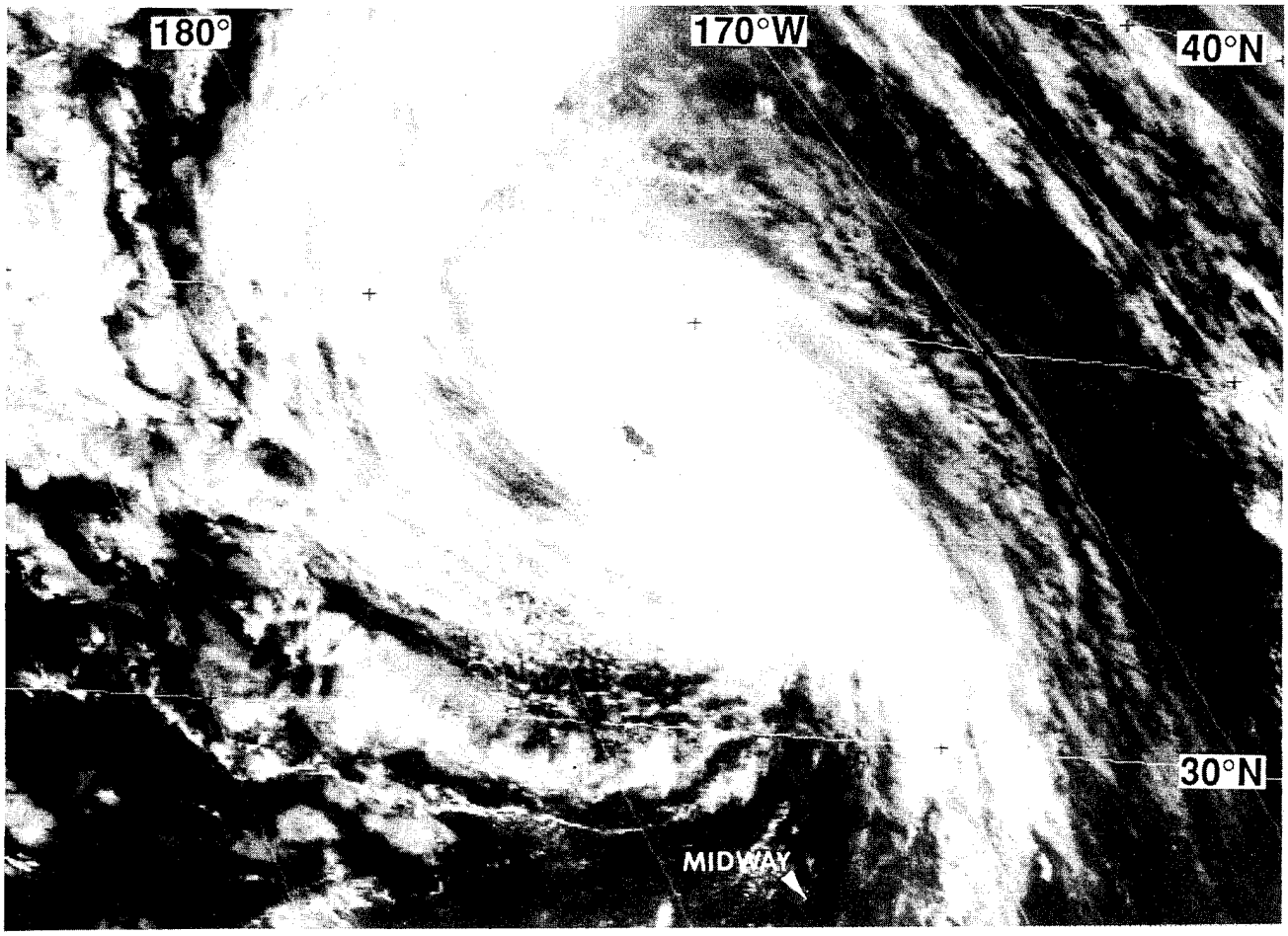

Figure 3-10E-2 Having moved back into the eastern North Pacific, John is once again at typhoon intensity (090031Z September visible GMS imagery).

date line from the east, John began to reintensify. It reached a secondary peak intensity of 105 kt (54 m/sec) at 281200Z as it entered the JTWC's area of responsibility (Figure 3-10E-1). The system weakened while meandering west of the international date line approximately 500 nm (925 km) west-southwest of Midway island. At 021800Z, real-time intensity estimates fell to 30 kt (15 m/sec) (these were later adjusted to 45 kt on the final best track), just prior to another period of intensification. A third and final peak intensity of 70 kt (36 m/sec) was attained at 081800Z after the system had recurved and moved back across the date line into the eastern North Pacific (Figure 3-10E-2 and Figure 3-10E-3). Rapid northeastward motion then ensued. The system became extratropical and gradually weakened, and the Central Pacific Hurricane Center, Honolulu, issued the final warning (warning number 120 — the most ever for a TC) at 100000Z September.

III. DISCUSSION

a. Long life

The average life span of a tropical cyclone in the western North Pacific is approximately 6.5 days. Of the 420 tropical cyclones during the period 1980-1993, 156 (37%) lasted seven days or more and only 11 (2.6%) persisted for 14 days or longer. Of the tropical cyclones that have spent their entire lives in the western North Pacific, the two longest-lived tropical were Wayne (1986) (with an 18-day life span) and Nat (1991) (with a 17-day life span). Some tropical cyclones which formed in the eastern or cen-

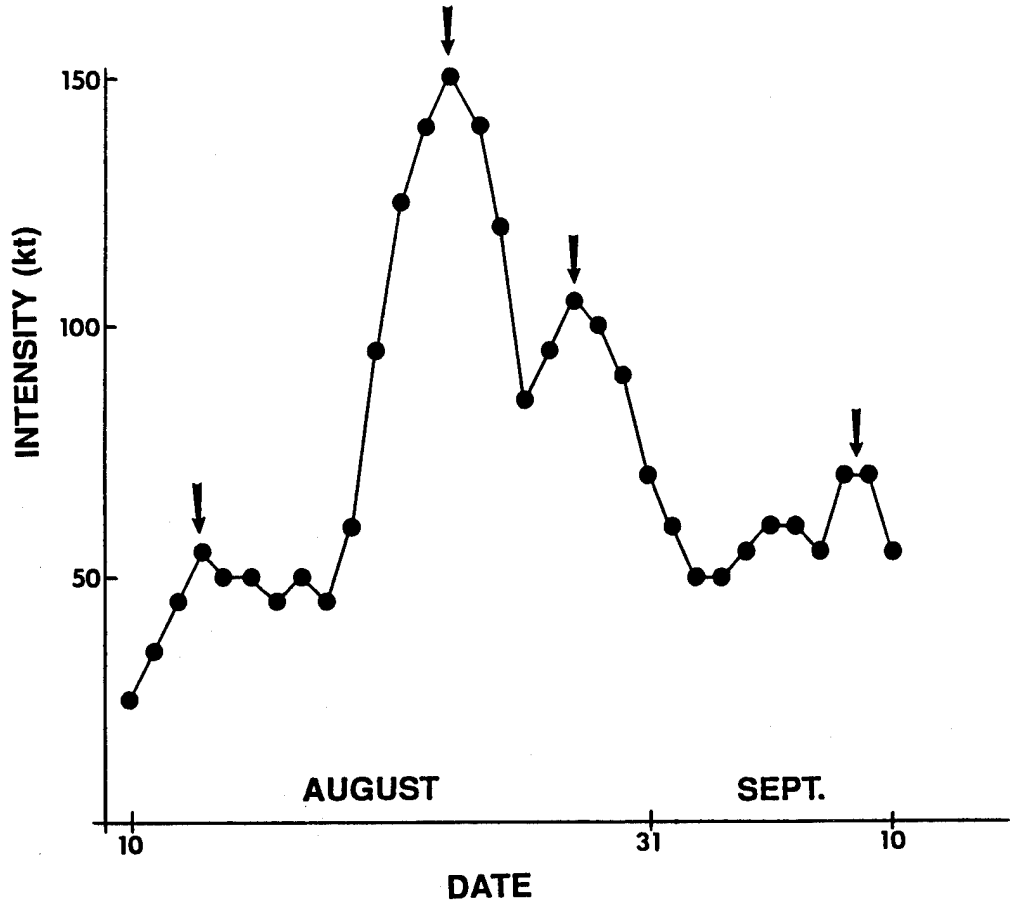

Figure 3-10E-3 A plot of John's intensity versus time. Each dot marks the highest intensity of each calendar day from August 10 to September 10.

tral Pacific and moved westward across the international date line into the western North Pacific have had longer life spans. For example, Enrique (1991), a tropical cyclone originating in the eastern North Pacific, lasted 20 days (including one day west of the date line). Keoni (1993), a tropical cyclone which originated in the central North Pacific, persisted for 24 days (including 9 days in the western North Pacific). John's total life span of 31 days (including 11 days in the western North Pacific) sets the record.

b. A problem with the intensity

After reaching a low-point of intensity at 021800Z September, John began to slowly reintensify. In real time, on or about 021800Z September, intensity estimates of John (based upon satellite imagery) fell below tropical storm intensity. Thus, John became a tropical depression on warning numbers 91 through 94 (the four warnings issued at six-hour intervals from 021800Z to 031200Z). On these warnings, the extended outlook beyond 48 hours called for dissipation as a significant tropical cyclone. However, on warning number 95 (031800Z September), John was upgraded to minimal tropical storm intensity with later weakening still indicated in the forecast. Twenty-four hours later, at 041800Z, the warning indicated that John was still at minimal tropical storm intensity, and the extended outlook continued to call for it to weaken. Two reports from a ship near John at this time, which were not received in real time at the JTWC, indicated that the intensity of John was under-estimated:

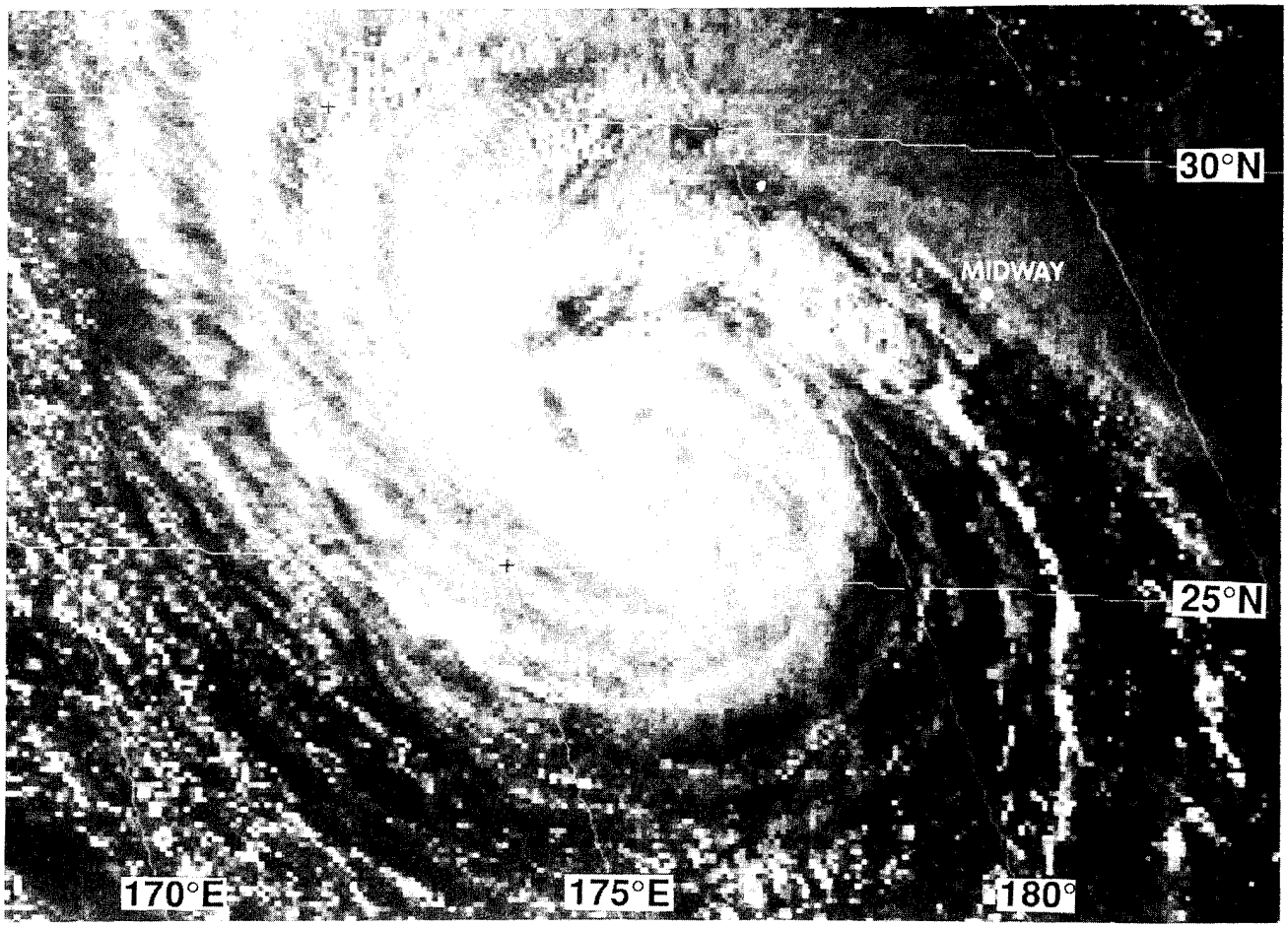

Figure 3-10E-4 John as seen in the low sun angle of evening. In real time, at the time of this picture, the warning intensity was 35 kt (18 m/sec). The final best-track intensity was upped to 60 kt (31 m/sec) based upon synoptic reports (050530Z September visible GMS imagery).

041500Z, 27.3°N 178.9°E, wind = 090 deg at 55 kt, SLP = 991.2 mb
041800Z, 27.6°N 177.7°E, wind = 050 deg at 55 kt, SLP = 993.5 mb.

Twelve hours after the valid time of these ship reports, the real-time intensity estimates were still probably too low. The 050530Z satellite imagery shown in Figure 3-10E-4 was diagnosed in real time to be of minimal tropical storm intensity. In post analysis, it was determined (based upon the aforementioned ship reports), that John was likely much more intense at this time — 60 kt vice 35 kt. With respect to the best-track intensity, each warning issued by the JTWC during the period 011200Z through JTWC's final warning at 081200Z, was anywhere from 5 to 25 kt too low.

IV. IMPACT

John spent all of its life over open water, and its greatest impact was felt when it skirted just north of Johnston Atoll. The Army's chemical weapons incinerator on Johnston Atoll had to be shut down, and all 1100 military and civilian personnel evacuated to Honolulu. The incinerator and ammunition storage areas weathered the storm well, but high winds caused minor to extensive damage to numerous support buildings and personnel billets. Electrical power and telephone communications were interrupted.

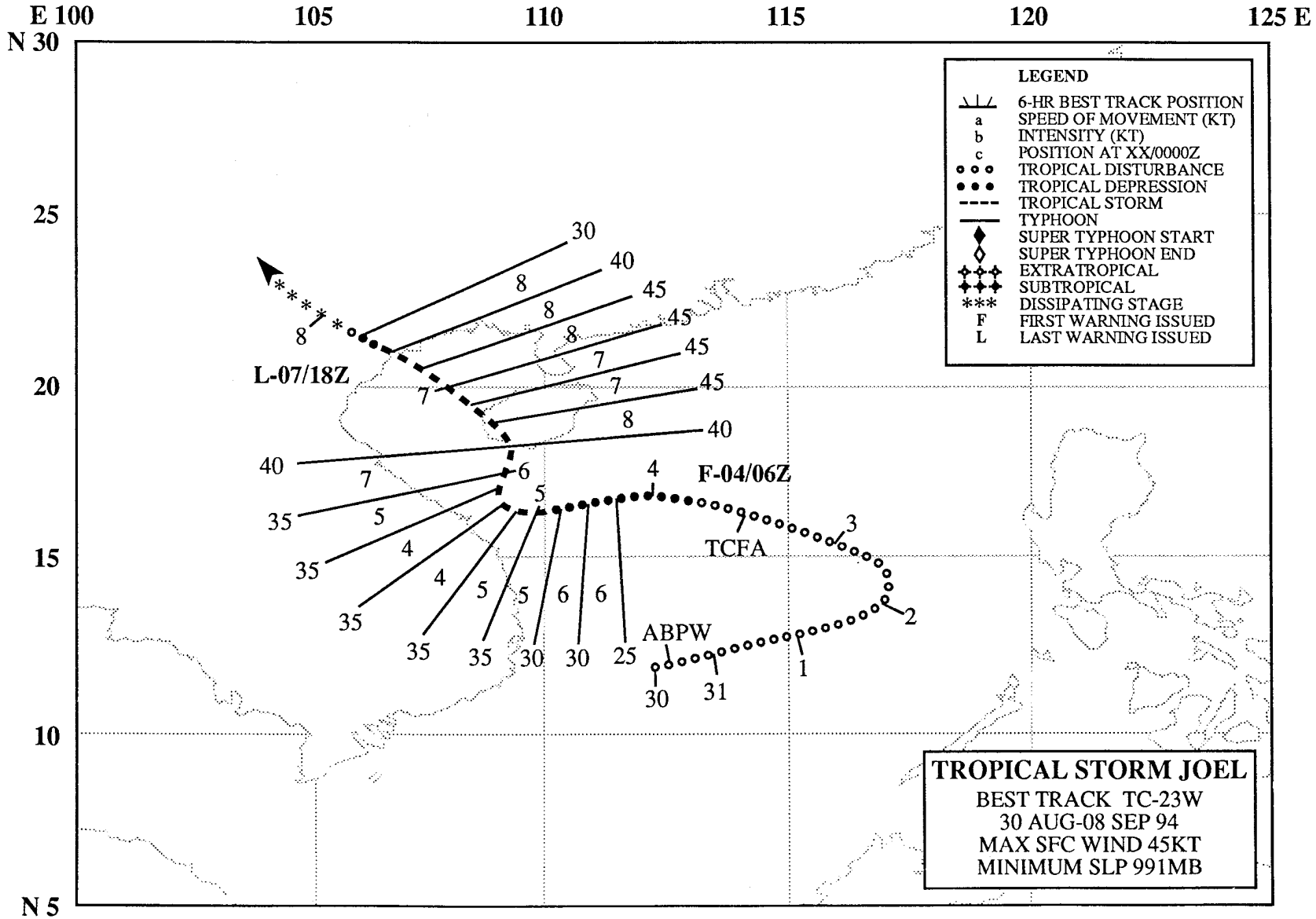
E 100
105
110
115
120
125 E
N 30
25
20
15
10
N 5
LEGEND
6-HR BEST TRACK POSITION
a SPEED OF MOVEMENT (KT)
b INTENSITY (KT)
c POSITION AT XX/0000Z
TROPICAL DISTURBANCE
TROPICAL DEPRESSION
TROPICAL STORM
TYPHOON
SUPER TYPHOON START
SUPER TYPHOON END
EXTRATROPICAL
SUBTROPICAL
*** DISSIPATING STAGE
F FIRST WARNING ISSUED
L LAST WARNING ISSUED
L-07/18Z
F-04/06Z
TCFA
ABPW
TROPICAL STORM JOEL
BEST TRACK TC-23W
30 AUG-08 SEP 94
MAX SFC WIND 45KT
MINIMUM SLP 991MB

TROPICAL STORM JOEL (23W)

As Typhoon Gladys (20W) approached Taiwan, the monsoon trough in the South China Sea became active near 12°N. An area of persistent convection within this trough was first mentioned on the 300600Z August Significant Tropical Weather Advisory. For three days, the disturbance moved east-northeastward, and upon reaching 117°E at 020000Z September, it turned toward the west-northwest. At 031130Z, the JTWC issued a Tropical Cyclone Formation Alert, which was followed 19 hours later by the first warning on Tropical Depression 23W. During most of its westward track, strong upper level winds from the north-northeast kept the deep convection south of the small low level circulation center. By the morning of 05 September, the upper level winds began to weaken. This allowed the convection to wrap around the north side of the system, and the depression was upgraded to Tropical Storm Joel. About 50 nm (93 km) east-northeast of Da Nang and 70 nm (130 km) east of Hue, Vietnam, Joel turned sharply toward the north. At 060600Z, the tropical storm passed over the extreme southwestern edge of Hainan Island where it reached its estimated maximum intensity of 45 kt (23 m/sec). Joel then turned to the northwest. After entering the Gulf of Tonkin, a ragged, cloud-filled banding-type eye appeared (Figure 3-23-1). At about 071000Z, Joel went ashore near Haiphong, and moved inland toward Hanoi. News reports (09 September USA Today) indicated that Joel knocked down large trees in Hanoi. The final warning was issued on Tropical Depression 23W at 071800Z as it dissipated over land west of Hanoi.

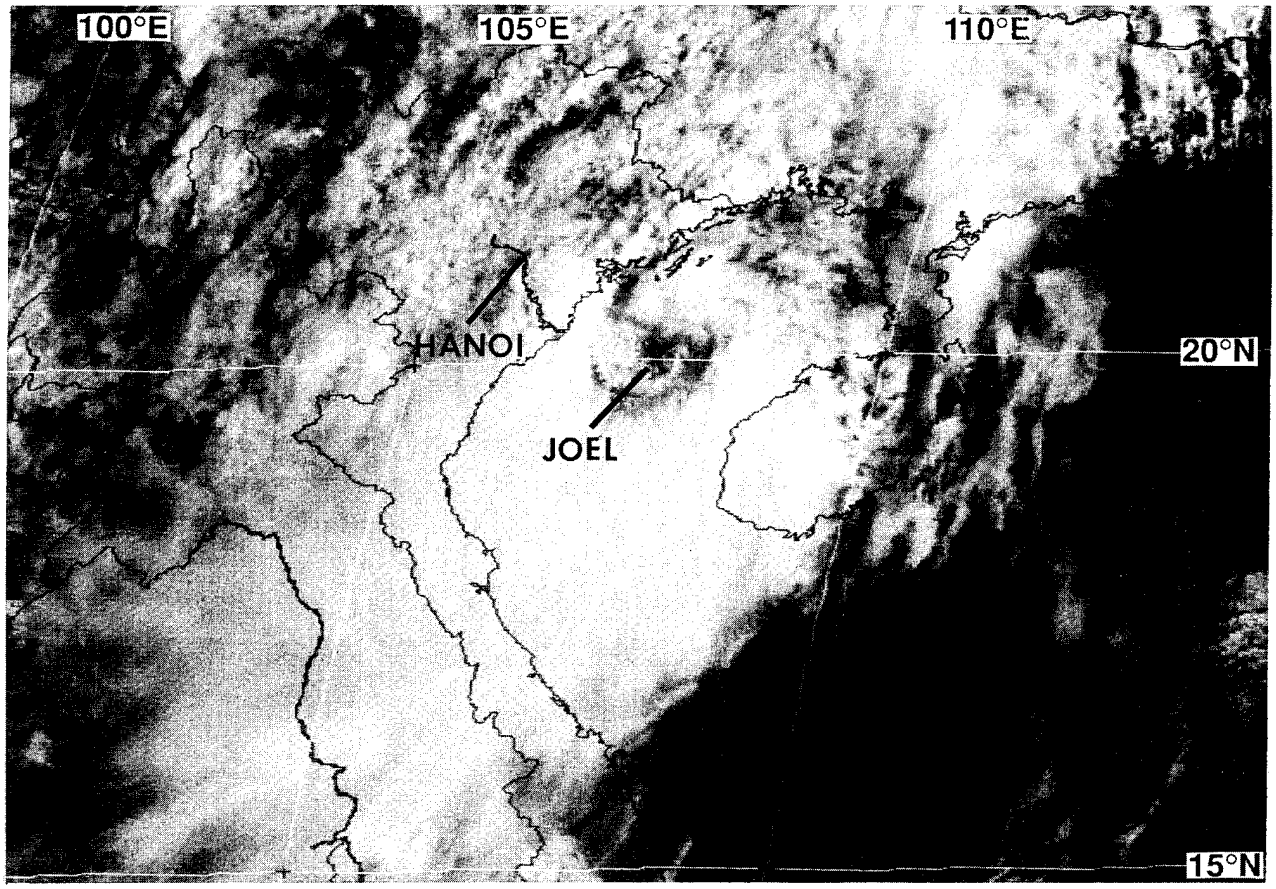

Figure 3-23-1 Tropical Storm Joel about 60 nm (111 km) southeast of the Vietnam coast, near Haiphong (070031Z September GMS visible imagery).

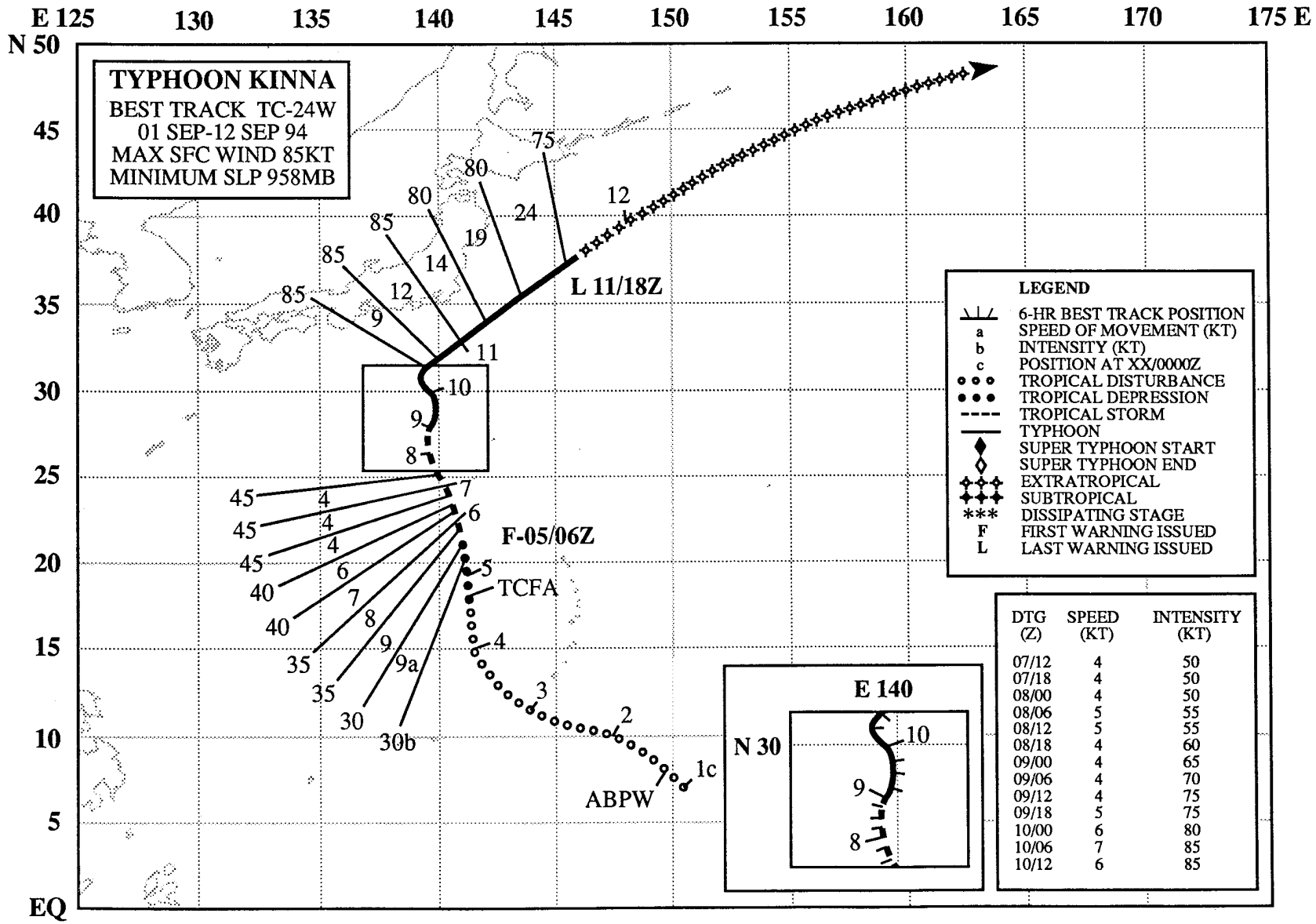

DTG (Z)	SPEED (KT)	INTENSITY (KT)
07/12	4	50
07/18	4	50
08/00	4	50
08/06	5	55
08/12	5	55
08/18	4	60
09/00	4	65
09/06	4	70
09/12	4	75
09/18	5	75
10/00	6	80
10/06	7	85
10/12	6	85

TYPHOON KINNA (24W)

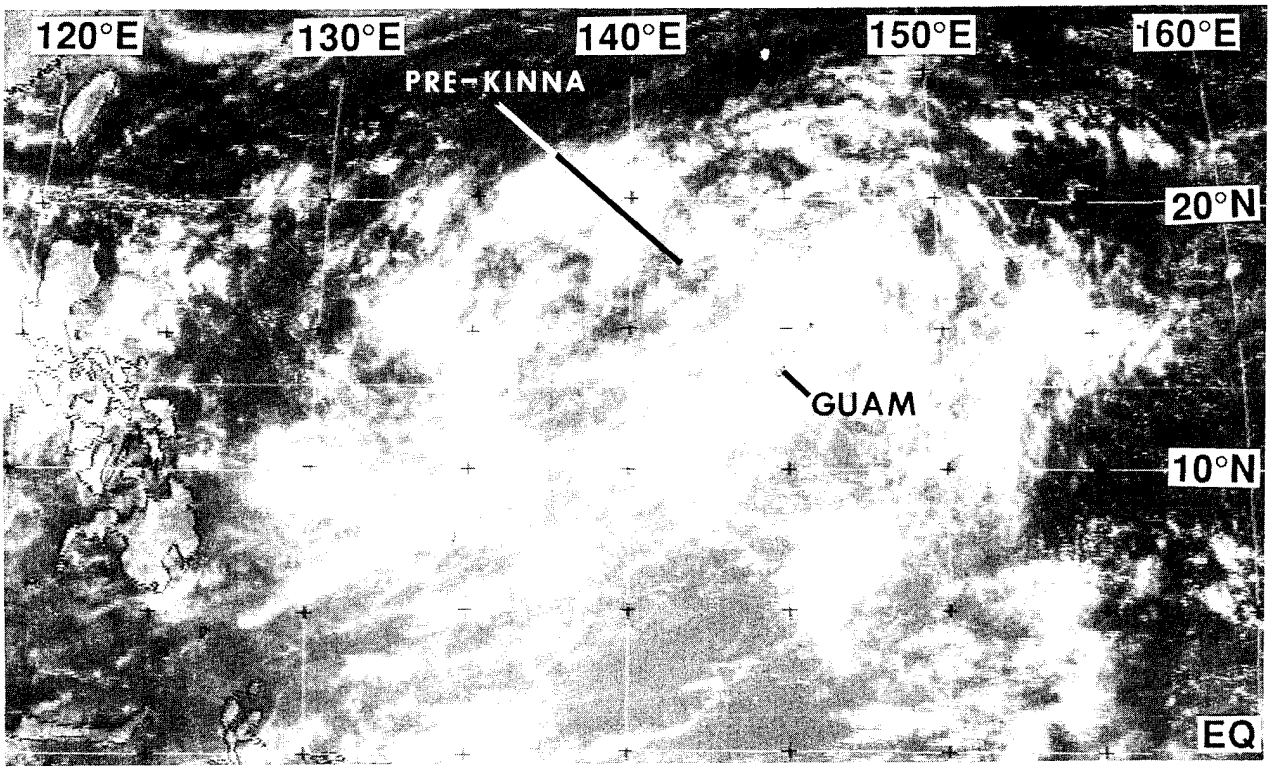

Figure 3-24-1 The pre-Kinna tropical disturbance is embedded within the cloudiness associated with a large monsoon depression (040231Z September visible GMS imagery).

I. HIGHLIGHTS

The tropical disturbance that became Kinna emerged from the northeastern quadrant of a monsoon depression. It moved on a north-oriented track. After peaking at 85 kt (44 m/sec), Kinna recurved and accelerated to more than 40 kt (74 km/hr). Kinna was a small tropical cyclone.

II. TRACK AND INTENSITY

At 010600Z September, the disturbance, that would eventually develop into Typhoon Kinna, was first mentioned on the Significant Tropical Weather Advisory when a small area of new convection appeared in the eastern Caroline Islands within the monsoon trough. For the next three-and-one-half days, the disturbance persisted as the monsoon trough moved northward, and a large monsoon depression formed near the Mariana Islands. The pre-Kinna disturbance became part of this monsoon depression on 04 September (Figure 3-24-1), and later moved north and detached from the monsoon depression (Figure 3-24-2). A Tropical Cyclone Formation alert was issued at 042000Z as an area of organized convection appeared to be emerging from the northeastern quadrant of the monsoon depression. When this convection became better organized, the JTWC issued the first warning on Tropical Depression 24W at 050600Z. Twelve hours later, the depression was upgraded to Tropical Storm Kinna. In addition to its intensification on 05 September, Kinna began to slow in forward speed as it entered a region of light southerly steering flow. Kinna remained under the influence of this weak northward steering until it moved poleward of the mid-level sub-tropical ridge on 10 September. At 070000Z, Tropical Storm Kinna passed 30 nm (56 km) west of Iwo Jima (WMO 47981) where a gust of 45 kt (23 m/sec) was

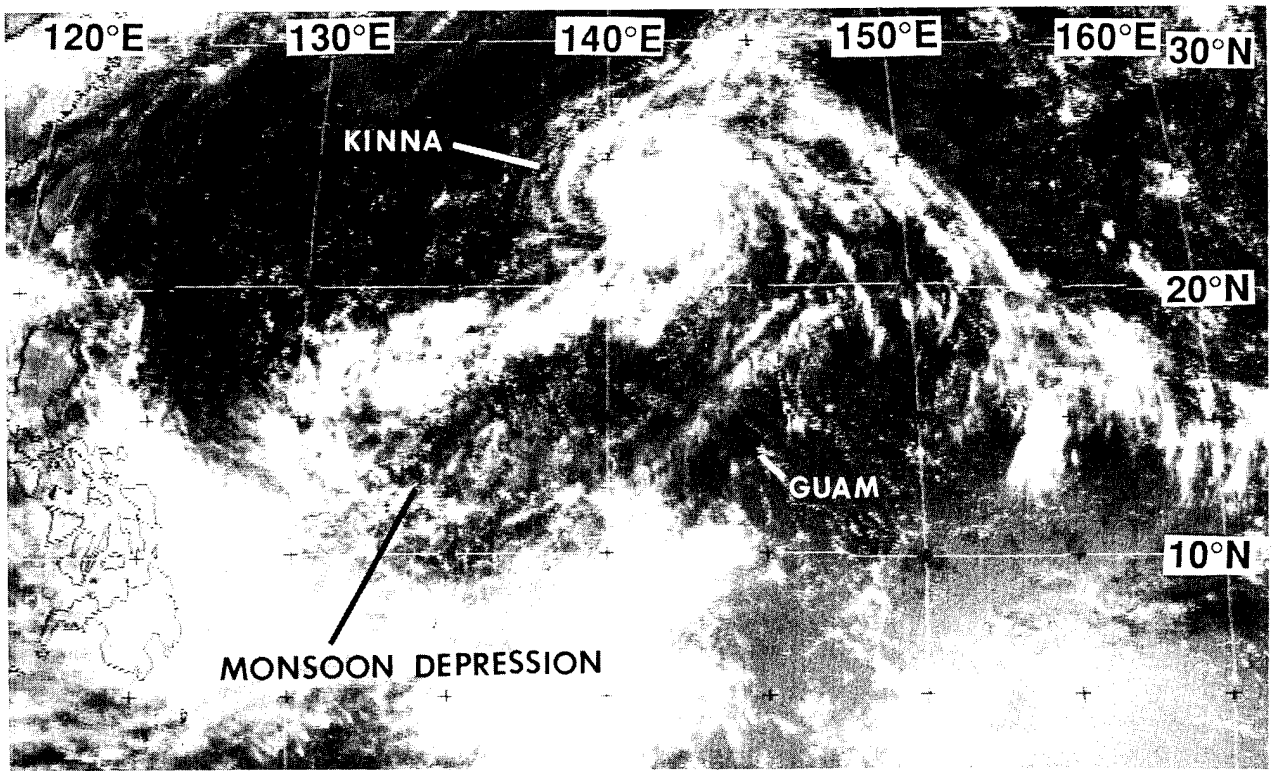

Figure 3-24-2 Kinna has moved north and become detached from the monsoon depression within which it had earlier been embedded (060031Z September visible GMS imagery).

recorded. Kinna was upgraded to typhoon intensity at 090000Z, and at 100600Z, just prior to recurvature, Typhoon Kinna reached its peak intensity of 85 kt (44 m/sec) (Fig. 3-24-3). Recurvature took the typhoon on a track that passed about 200 nm (370 km) east of Yokosuka, Japan. At 101700Z, Hachijojima (WMO 47678) recorded a peak gust of 30.8 m/sec (60 kt) as Typhoon Kinna was about 90 nm (167 km) to the south. Following recurvature, Kinna began to accelerate rapidly, eventually reaching speeds in excess of 40 kt (75 km/hr). The rapid acceleration kept Kinna's intensity high, despite its loss of symmetrical central deep convection. By the evening of 12 September, Kinna was absorbed into the cloud band of a rapidly moving front and acquired the appearance of a wave on the front.

III. DISCUSSION

The track forecasts for Kinna were challenging, as there were two plausible scenarios: one which favored northward motion, and another which favored west-northwestward motion. Both the statistical and the dynamic guidance oscillated between these scenarios during the period 06 to 10 September. Except for small, relatively short-lived meanders, the small-sized Kinna kept moving to the north, eventually passing through the mid-tropospheric sub-tropical ridge. Through-the-ridge motion (Sandgathe 1987) is typically expected of much larger tropical cyclones whose storm-induced changes to their environment allow them to modify and pass through a preexisting sub-tropical ridge (Elsberry and Abbey 1991). Overall, the track forecast errors for Typhoon Kinna were about 15 percent better than the long-term average at 24 and 48 hours, and close to average at 72 hours. Intensity forecast errors were less than 10 kt (5 m/s) at all forecast periods.

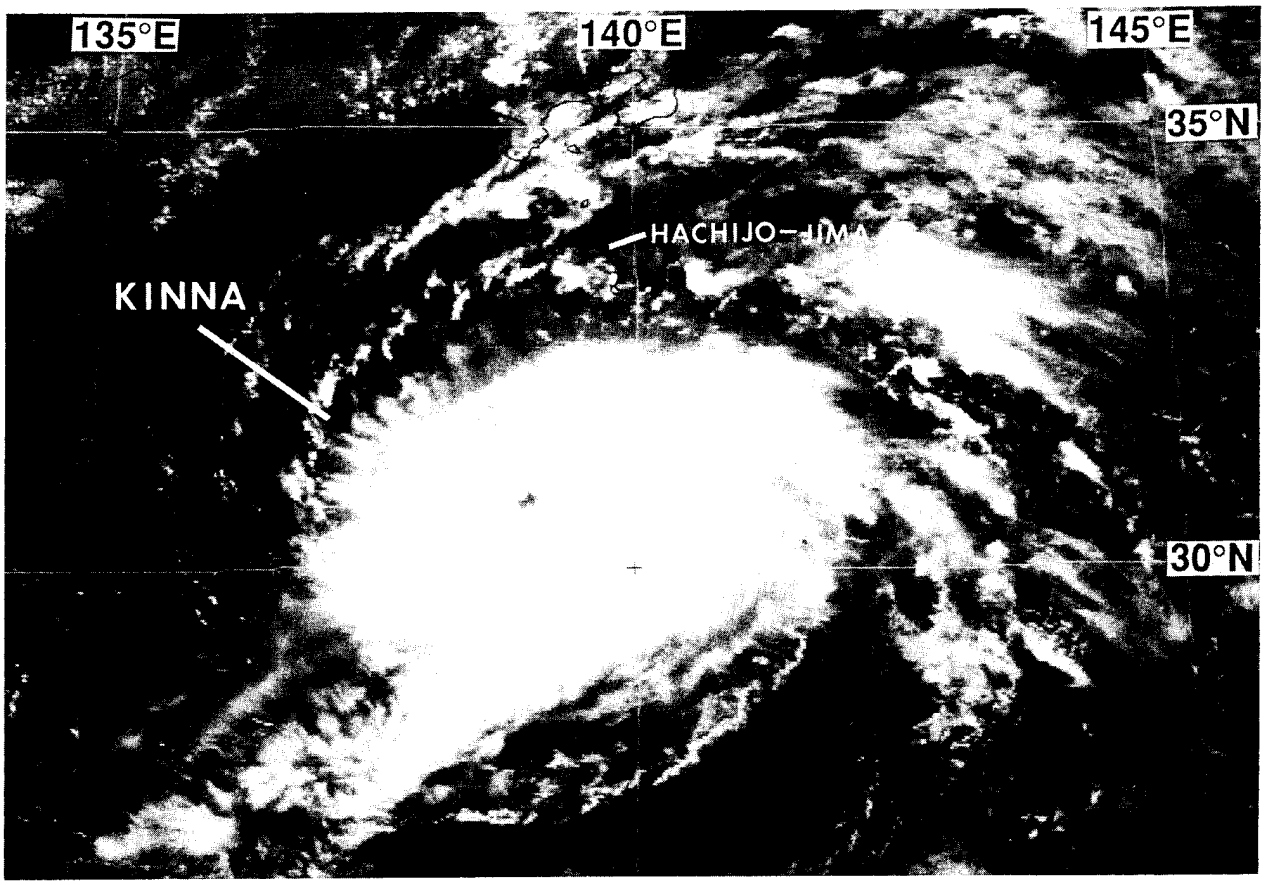

Figure 3-24-3 Kinna at its peak intensity of 85 kt (44 m/sec) (100531Z September visible GMS imagery).

IV. IMPACT

Kinna spent its entire life over open water. It turned away from the densely populated Kanto Plain area on the Japanese main island of Honshu, and produced potentially destructive winds only at Hachijo-jima, a small island about 150 nm (280 km) south of Tokyo.

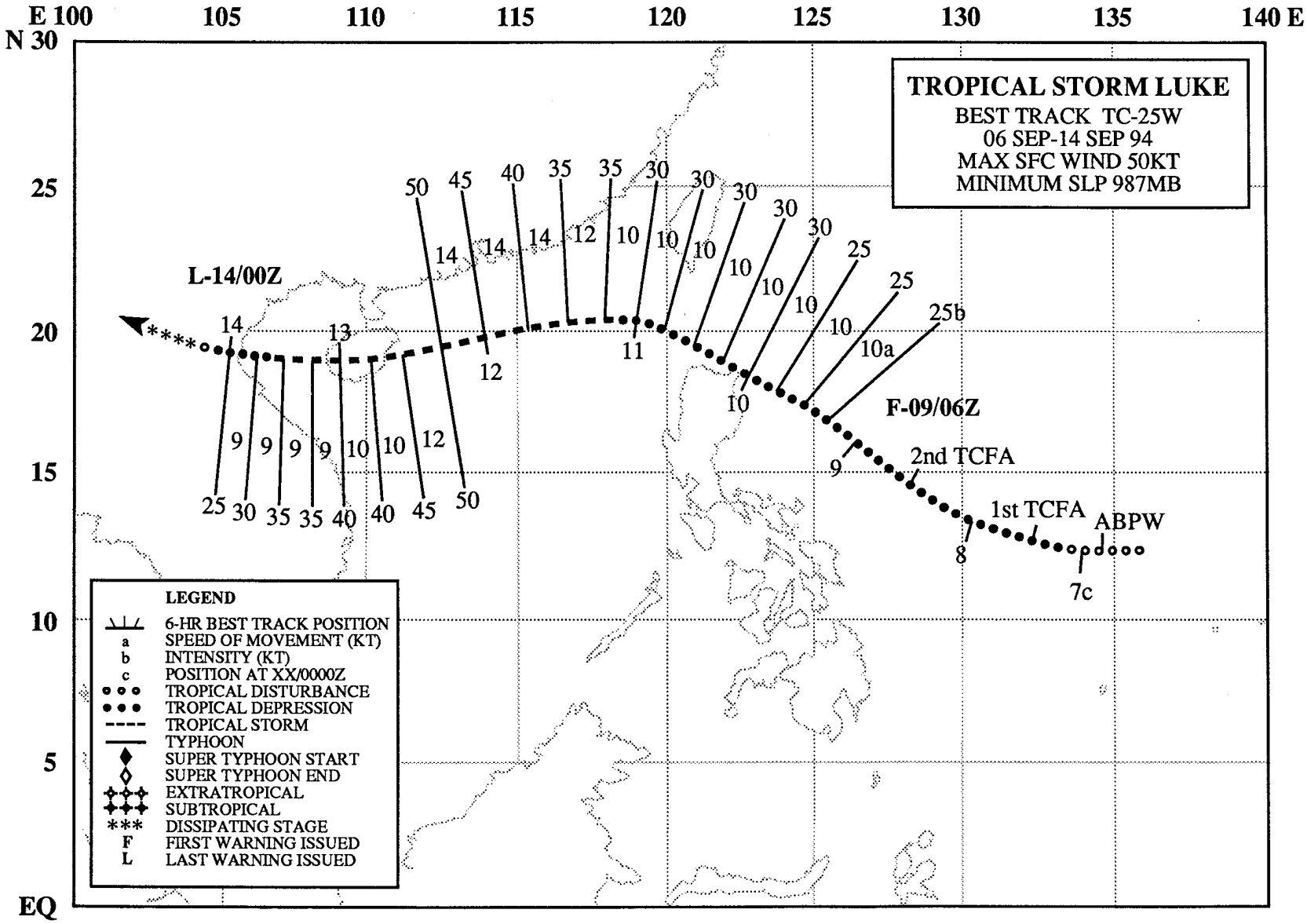
E 100
105
110
115
120
125
130
135
140 E
N 30
25
20
15
10
5
EQ
TROPICAL STORM LUKE
BEST TRACK TC-25W
06 SEP-14 SEP 94
MAX SFC WIND 50KT
MINIMUM SLP 987MB
L-14/00Z
F-09/06Z
2nd TCFA
1st TCFA
ABPW
7c
LEGEND
6-HR BEST TRACK POSITION
a SPEED OF MOVEMENT (KT)
b INTENSITY (KT)
c POSITION AT XX/0000Z
TROPICAL DISTURBANCE
TROPICAL DEPRESSION
TROPICAL STORM
TYPHOON
SUPER TYPHOON START
SUPER TYPHOON END
EXTRATROPICAL
SUBTROPICAL
*** DISSIPATING STAGE
F FIRST WARNING ISSUED
L LAST WARNING ISSUED

TROPICAL STORM LUKE (25W)

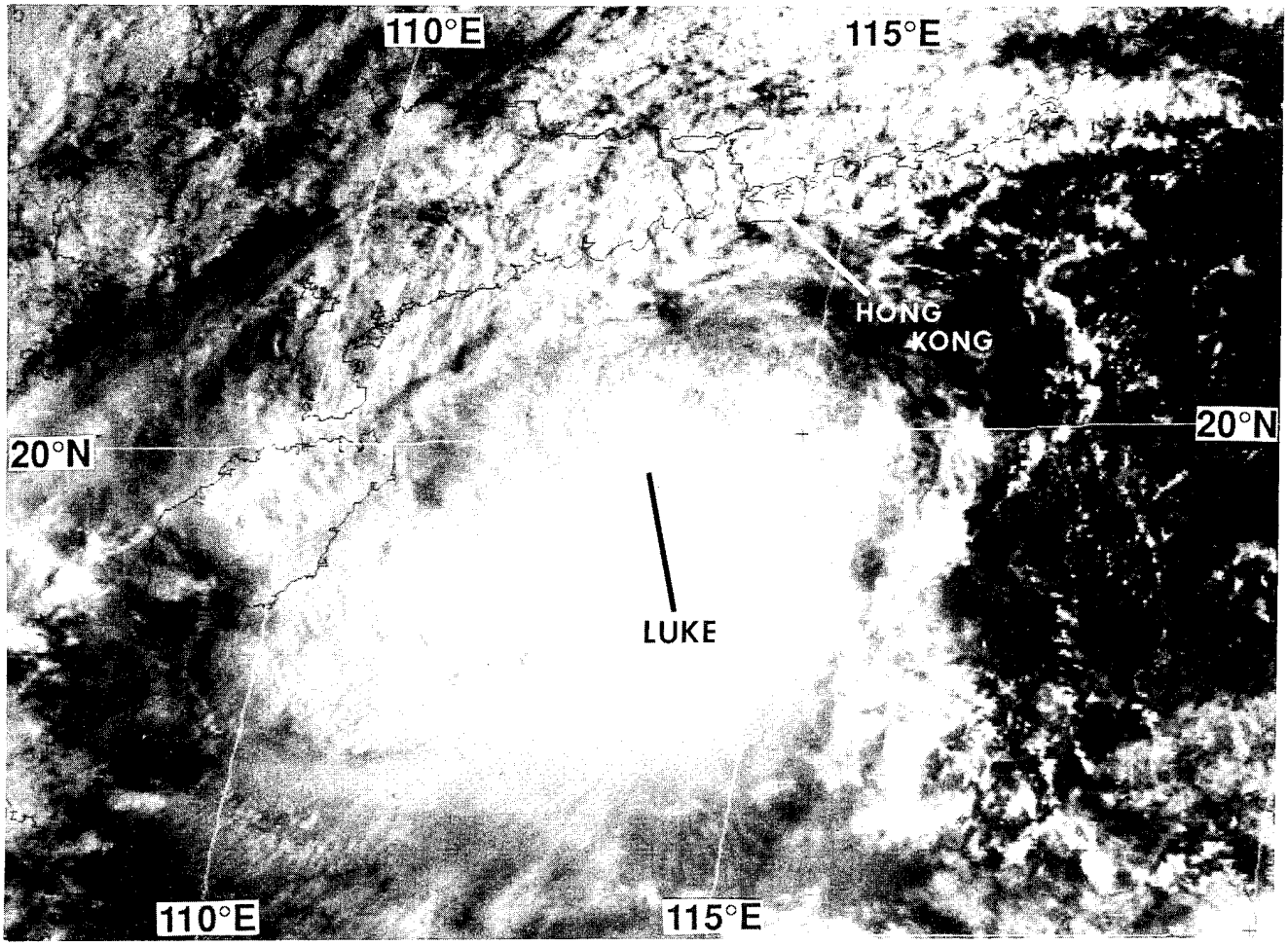

Figure 3-25-1 Tropical Storm Luke at 45 kt (23 m/sec) intensity and still intensifying while southwest of Hong Kong and east of Hainan Island (112331Z September visible GMS imagery).

While Tropical Storm Kinna (24W) was moving north along 140°E longitude, a monsoon depression covered an area from the Philippines to Yap [see Figure 3-24-2 in Kinna's (24W) summary]. This monsoon depression became Luke. When a large area of persistent deep convection to the west of the exposed low-level circulation center of this monsoon depression began to acquire cyclonic curvature, it was first mentioned on the 061800Z September Significant Tropical Weather Advisory. The disturbance moved slowly westward, and a Tropical Cyclone Formation Alert (TCFA) was issued at 071130Z. Intensification was slow. A second TCFA was issued 24 hours after the first. When the convection began to consolidate around a compact center, the first warning was issued on Tropical Depression 25W at 090600Z. For the next two days, the depression moved to the northwest at 10 kt (19 km/hr), passing just offshore of the northeastern tip of Luzon. On the afternoon of 11 September, the system was upgraded to Tropical Storm Luke, and turned to the west. On the morning of 12 September, Luke passed about 140 nm (260 km) south of Hong Kong. A peak gust of 94 km/hr (51 kt ; 26 m/sec) was recorded at Waglan Island (WMO 45009), Hong Kong, at 111422Z. Ten hours later, Luke reached

its 50 kt (26 m/sec) peak intensity 75 nm (140 km) east of Hainan Island (Figure 3-25-1). Hainan Island's rugged terrain, with mountains to 6,000 ft (1830 m), weakened the storm. Continuing westward, Luke went ashore in Vietnam as a tropical depression. The final warning was issued at 140000Z.

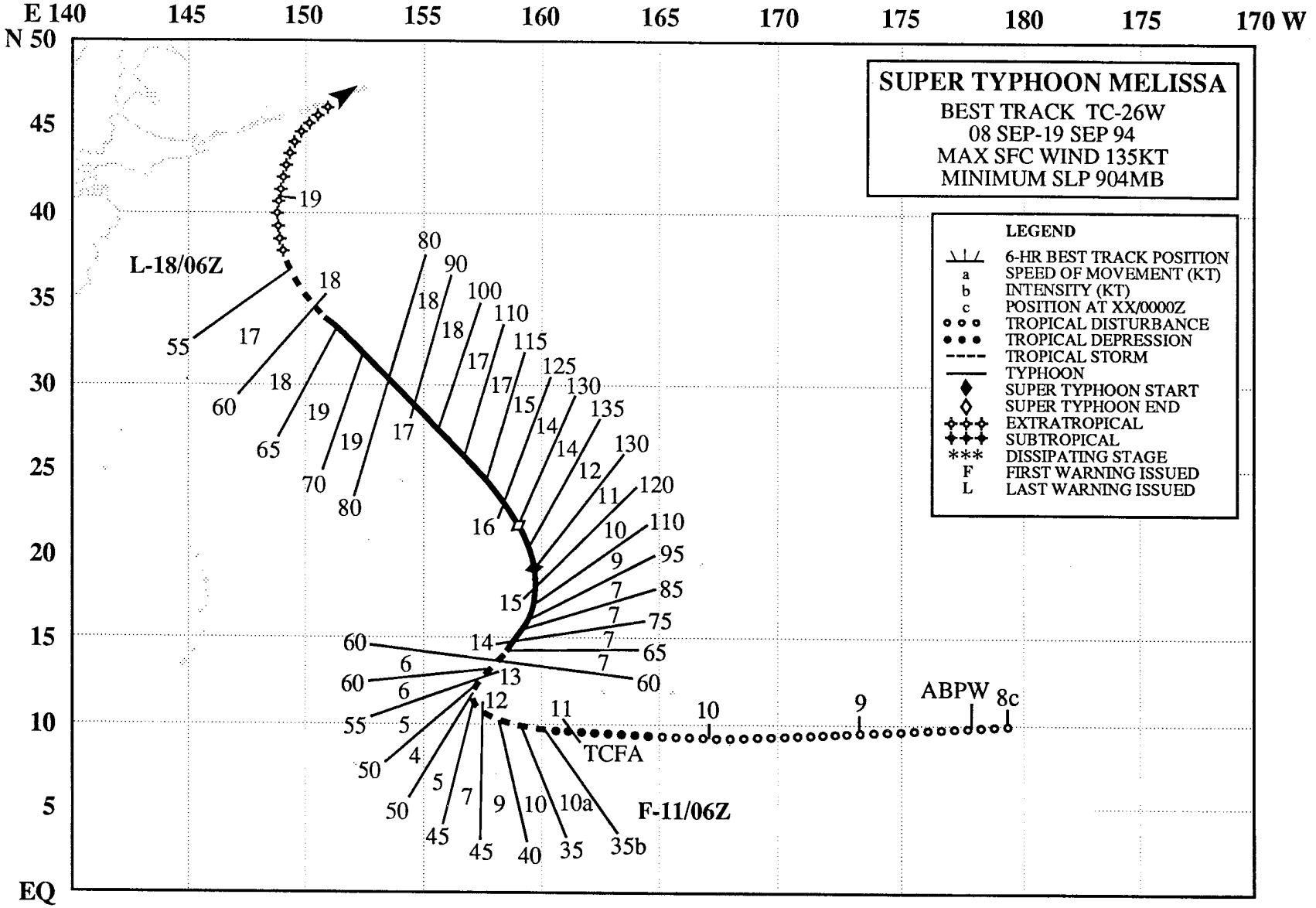
E 140
145
150
155
160
165
170
175
180
175
170 W
N 50
45
40
35
30
25
20
15
10
5
EQ
SUPER TYPHOON MELISSA
BEST TRACK TC-26W
08 SEP-19 SEP 94
MAX SFC WIND 135KT
MINIMUM SLP 904MB
LEGEND
6-HR BEST TRACK POSITION
a SPEED OF MOVEMENT (KT)
b INTENSITY (KT)
c POSITION AT XX/0000Z
TROPICAL DISTURBANCE
TROPICAL DEPRESSION
TROPICAL STORM
TYPHOON
SUPER TYPHOON START
SUPER TYPHOON END
EXTRATROPICAL
SUBTROPICAL
*** DISSIPATING STAGE
F FIRST WARNING ISSUED
L LAST WARNING ISSUED
L-18/06Z
F-11/06Z
TCFA
ABPW
8c

SUPER TYPHOON MELISSA (26W)

I. HIGHLIGHTS

Melissa was one of the largest and most intense September typhoons to develop east of Guam in recent history. The system first appeared on 08 September near the international date line in an El Niño / Southern Oscillation (ENSO)-induced region of abnormally warm sea surface temperatures. Melissa turned abrubtly to the north as it became associated with a strong surge in the monsoonal southwesterly winds, and its subsequent track was north-oriented. It rapidly intensified, peaking at 135 kt (69 m/sec). On 15 September, a cross section of the cloud-top topography (which included the eye) was obtained by a Lidar (Light imaging and detection radar) as part of a Space Shuttle experiment. As a point of interest, meteorologists at Bracknell, England, indicated that Melissa was the "most severe tropical [cyclone]" ever developed by their operational global spectral model.

II. TRACK AND INTENSITY

Since 1991, warm sea surface temperatures associated with a prolonged ENSO event have persisted near the international date line, creating favorable conditions for eastward displacement of large-scale deep convection. On 08 September, the weakened remnants of Hurricane Kristy (11E), which developed in the eastern Pacific on 27 August, tracked westward at about 15 kt (28 km/hr) across the date line along the 10°N latitude line. This disturbance was first listed as a suspect area in the Western North Pacific on the Significant Tropical Weather Advisory at 080600Z September. On the night of 10 September, the remnants of Kristy (11E) disappeared in the eastern end of the monsoon cloud band which extended into the Marshall Islands. A low-level cyclonic circulation (most probably not the remnants of Kristy) with characteristics of a monsoon depression then grew dramatically, prompting forecasters at the JTWC to issue a Tropical Cyclone Formation Alert at 110000Z. Organization increased during the daylight hours of 11 September, and the first warning on Tropical Depression 26W was issued at 110600Z. Post analysis indicated that the winds at that time were most probably already at tropical storm intensity. Shortly afterward, cross-equatorial flow from the Southern Hemisphere began to strengthen between 150°E and 160°E. As Melissa crossed 160°E, it began to interact with a surge of deep southwesterly monsoon flow, and perhaps in response to this, it slowed and turned toward the north.

By 13 September, Melissa was moving to the northeast. It rapidly developed a deep central dense overcast (CDO) (Figure 3-26-1) and a small eye (Figure 3-26-3) as it was beginning to rapidly intensify (Holliday and Thompson, 1979). It attained typhoon intensity at 131800Z, and in 42 hours, Melissa had reached its peak intensity of 135 kt (69 m/sec). Pressures over the same period are estimated to have fallen 72 mb to a low of 904 mb. Near its peak intensity (Figure 3-26-2), astronauts in the Space Shuttle Discovery probed Melissa's eye with Lidar as part of the Lidar In-Space Technology Experiment (LITE) (Figures 3-26-4 and 3-26-5). Melissa's rapid intensification and Lidar imaging are discussed in greater detail in Section III.

As the large typhoon moved farther northward, it became less influenced by the monsoon flow to the south and more influenced by the strong ridge to the northeast. Melissa began to move to the northwest around the western periphery of the ridge, and accelerated from 10 kt (19 km/hr) on 14 September to 18 kt (33 km/hr) on 18 September (when it weakened to tropical storm intensity). Late on the morning of 19 September, Melissa passed through the axis of the sub-tropical ridge and recurved. By 20

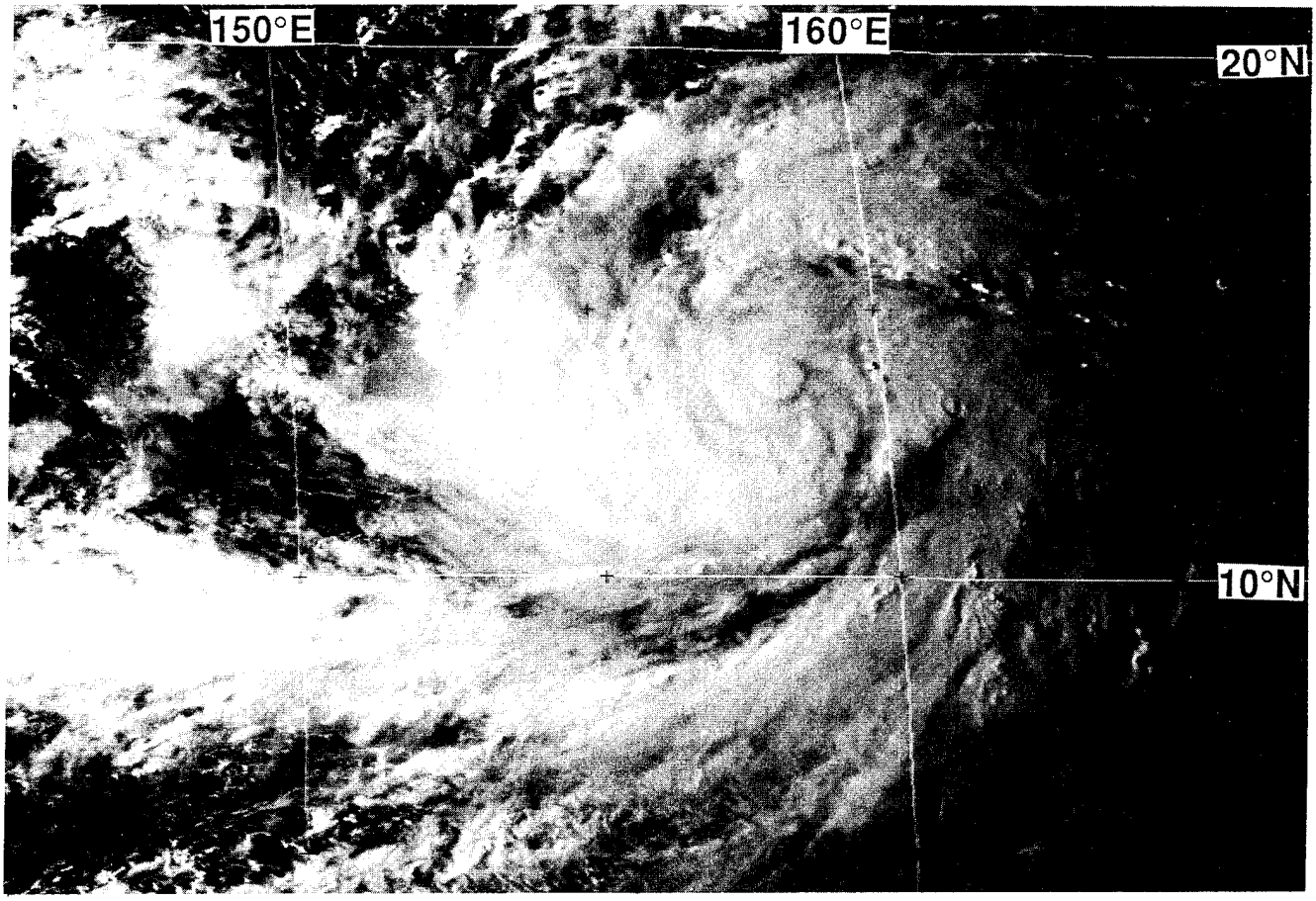

Figure 3-26-1 A very cold circular cirrus shield begins to grow near Melissa'a center (130631Z September visible GMS imagery).

September, Melissa had undergone a compound transformation (Brand and Guard, 1977) into a large extratropical low.

Both track and intensity forecast errors for Melissa were larger than normal. Climatological- and statistical-based aids did not anticipate the northward turn near 160°E. Although forecast fields and derived track aids from dynamic models indicated a northward turn, they lacked consistency in their forecasts. Track errors were 113 nm (209 km), 252 nm (467 km), and 421 nm (780 km) at 24-, 48-, and 72-hours respectively. The intensity errors were 15 kt (7.7 m/sec) at 24 hours, and 27 kt (14 m/sec) at 48 and 72 hours.

III. DISCUSSION

a. Rapid intensification of Melissa

From 140600Z until 150600Z, Typhoon Melissa underwent a period of rapid intensification during which its intensity increased from 85 kt (44 m/sec) to 130 kt (67 m/sec) while pressures fell an estimated 49 mb. The rapid intensification process is defined by Holliday and Thompson (1979) as an episode of intensification where pressure falls are > 1.75 mb/hr or > 42 mb/day. Table 3-26-1 shows the best-track winds, the estimated 6-hourly change in pressures, and the 6-hourly and 24-hourly rates of change of these parameters during the rapid intensification of Melissa. Unlike the increase of the eye diameters of Doug (17W) and Fred (19W) as they rapidly intensified, Melissa's eye diameter decreased during its rapid intensification.

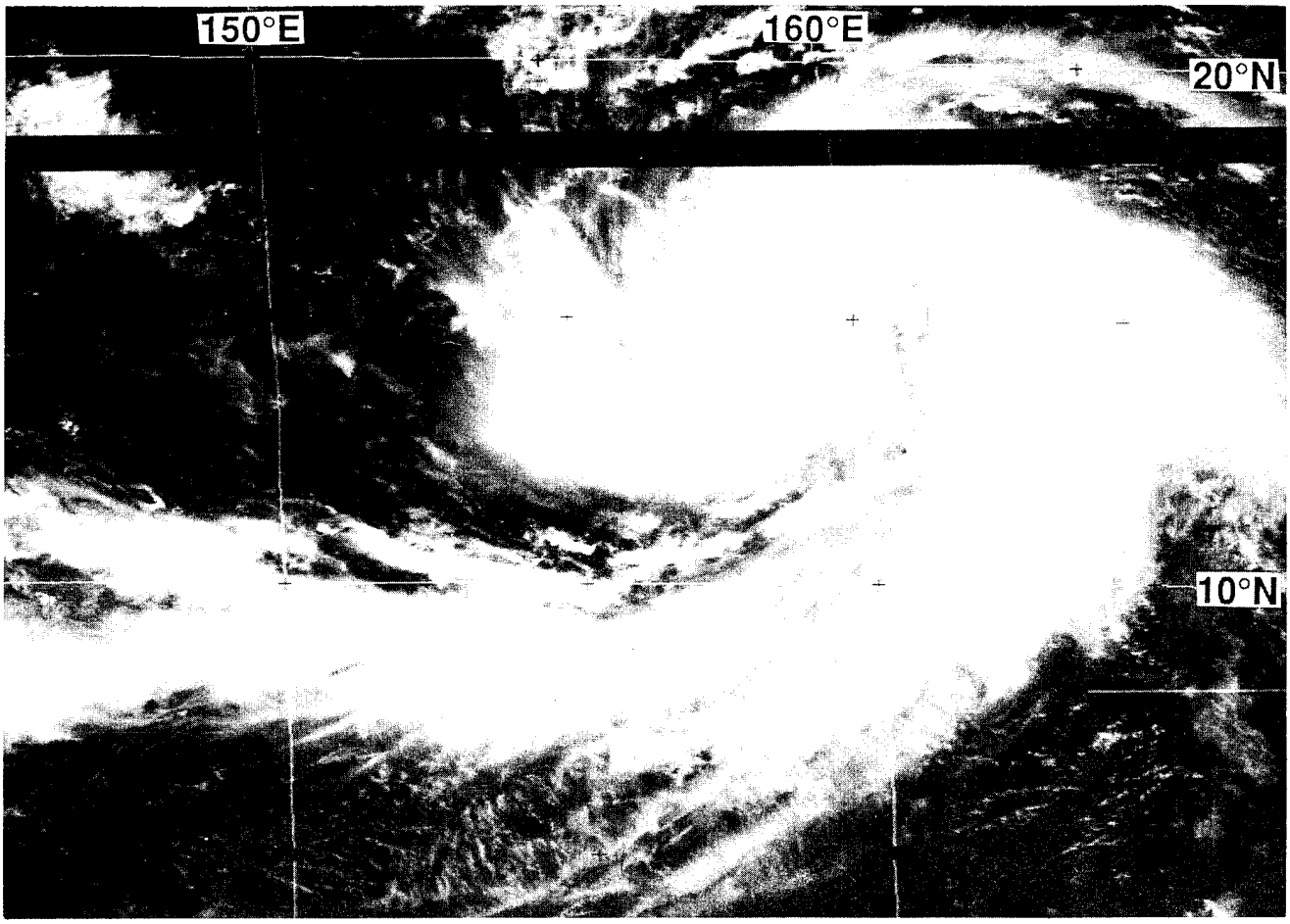

Figure 3-26-2 A small eye has formed (132331Z September visible GMS imagery).

b. Melissa imaged by Lidar

As Melissa was near maximum intensity, LITE on the Space Shuttle Discovery observed the typhoon with Lidar (Figures 3-26-4 and 3-26-5). Melissa's intensity at the time was 130 kt (67 m/sec) (Figure 3-26-3). The Lidar image shows the eye of the super typhoon, surrounded by a deck of cirrus near 15-17 km (8-9 nm) altitude. The inner edge of the wall cloud is visible, sloping inward from the top where the eye diameter is 45 km (25 nm) to the bottom where the eye diameter is 30 km (16 nm). Some scatterers (most probably thin cirrus) also appear over the eye itself. The data and its interpretation was provided by Mr. Charles Trepte, Aerosol Research Branch, NASA Langley Research Center.

IV. IMPACT

As large and intense as Super Typhoon Melissa was, it spent its life over open ocean, missing the many Mariana Islands and the Japanese island of Minami-Tori-Shima. The typhoon's large circulation covered nearly 1 million square miles of the Pacific.

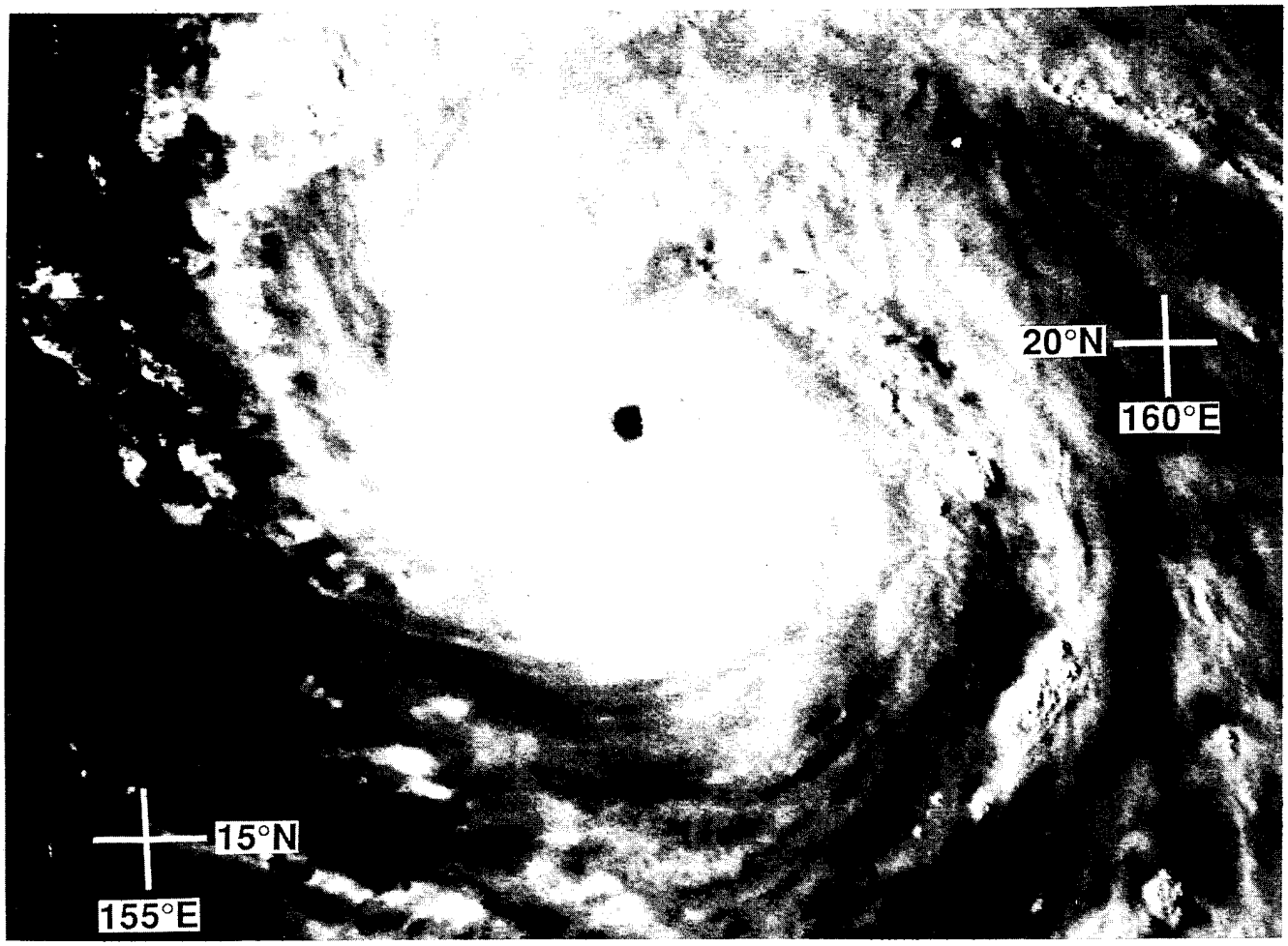

Figure 3-26-3 Melissa near peak intensity (150537Z September visible GMS imagery). Melissa was probed by a Lidar aboard the Space Shuttle Discovery at this time.

Date/Time (Z)	Wind Range (kt)	Pressure Rng (mb)	RateDP (mb)	
			1-hr	24-hr
13/12-13/18	60-65	980-976	-0.67	
13/18-14/00	65-75	976-968	-0.75	
14/00-14/06	75-85	968-959	-1.50	
14/06-14/12	85-95	959-949	-1.67	-31
14/12-14/18	95-110	949-933	-2.67	-43
14/18-15/00	110-120	933-922	-1.83	-46
15/00-15/06	120-130	922-910	-2.00	-49
15/06-15/12	130-135	910-904	-1.00	-45
15/12-15/18	135-130	904-910	1.00	23

Table 3-26-1 Pressure changes and rates of change for each six-hour warning period during the intensification of Super Typhoon Melissa, beginning at 131200Z and ending at 151800Z.

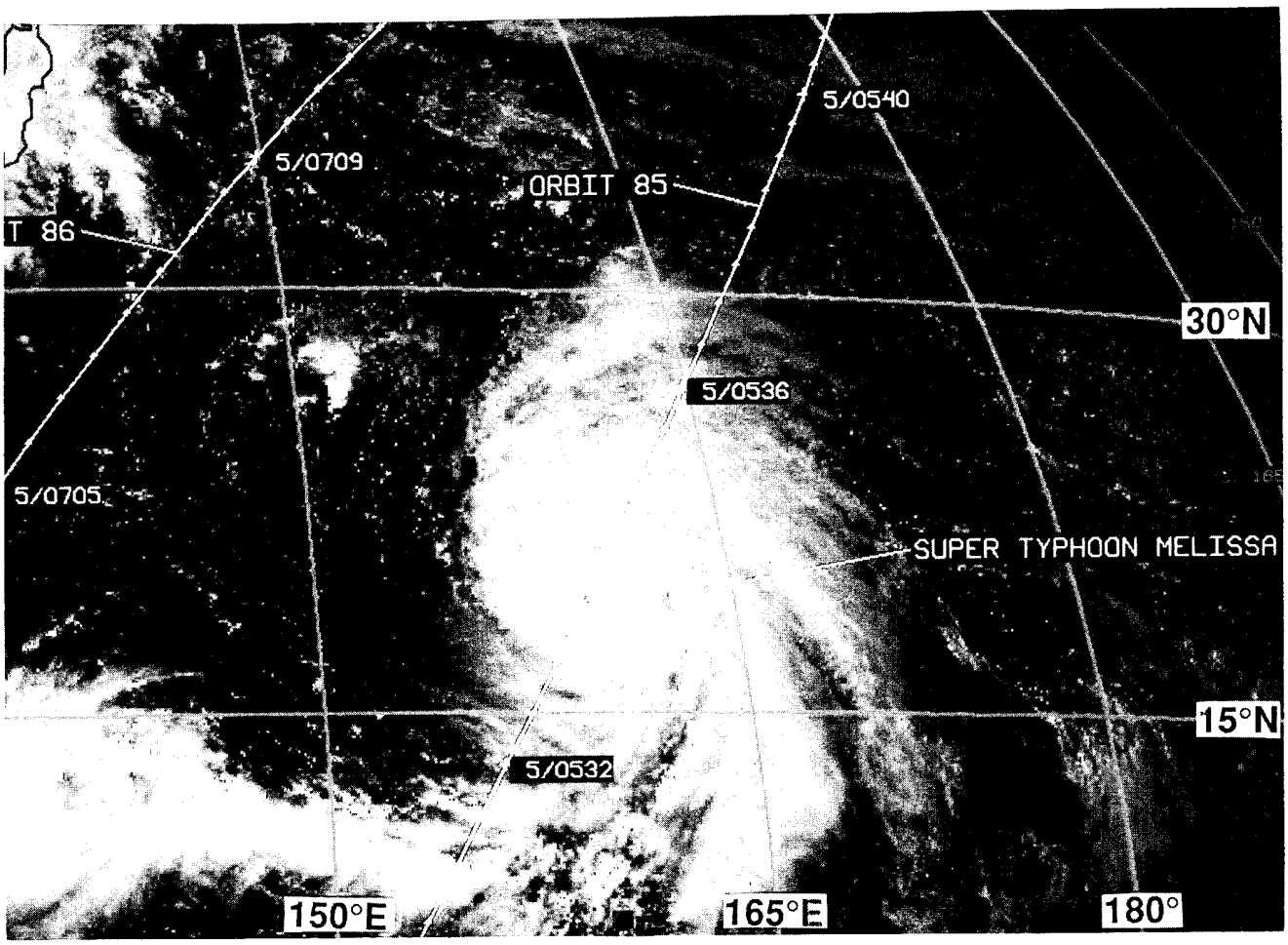

Figure 3-26-4 During orbit number 85, the Space Shuttle Discovery passes directly over Melissa.

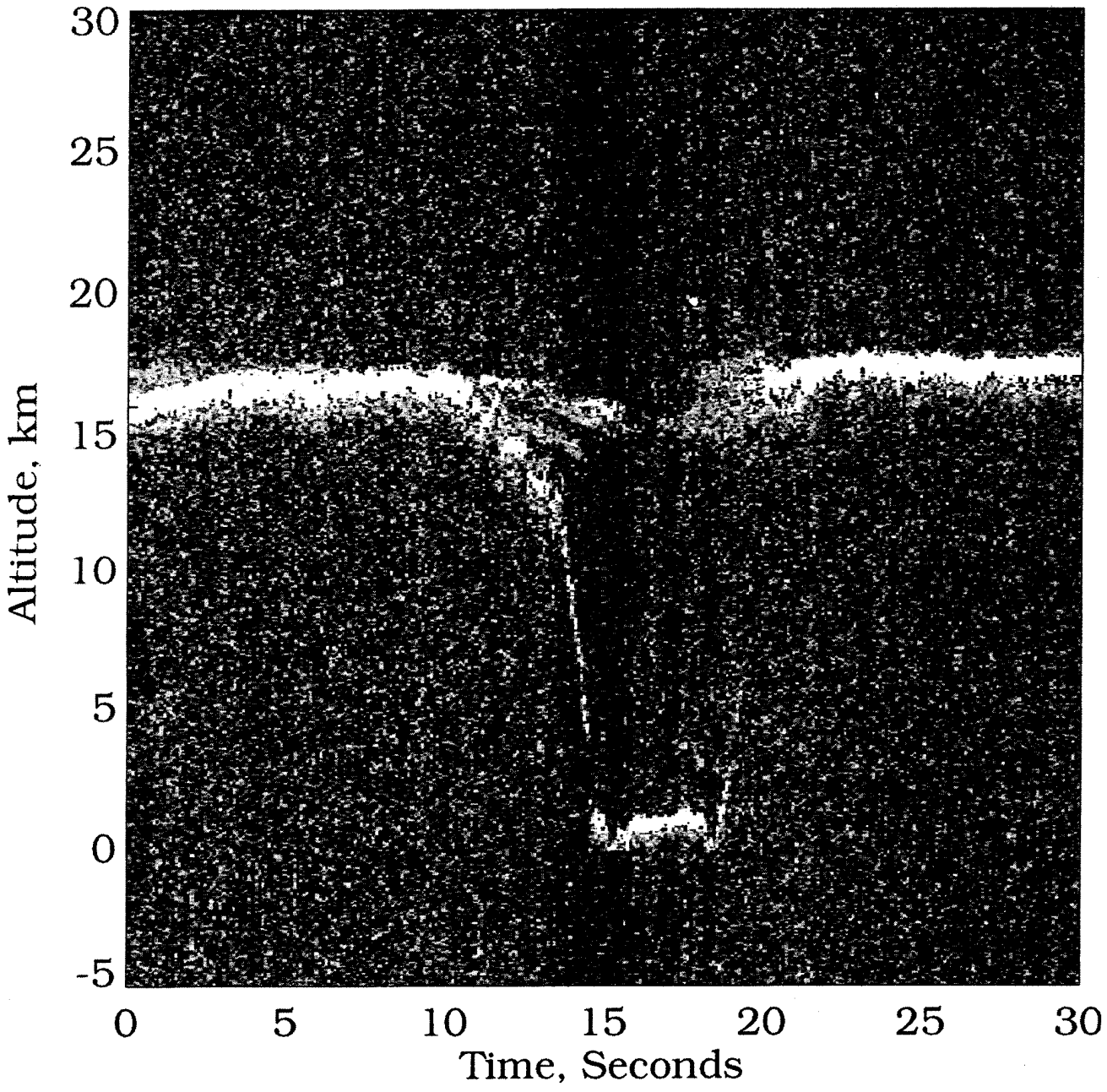

Figure 3-26-5 An altitude-time plot of the 532 nanometer LITE data raw signal distribution showing a cross-section of Melissa's eye at 150357Z September.

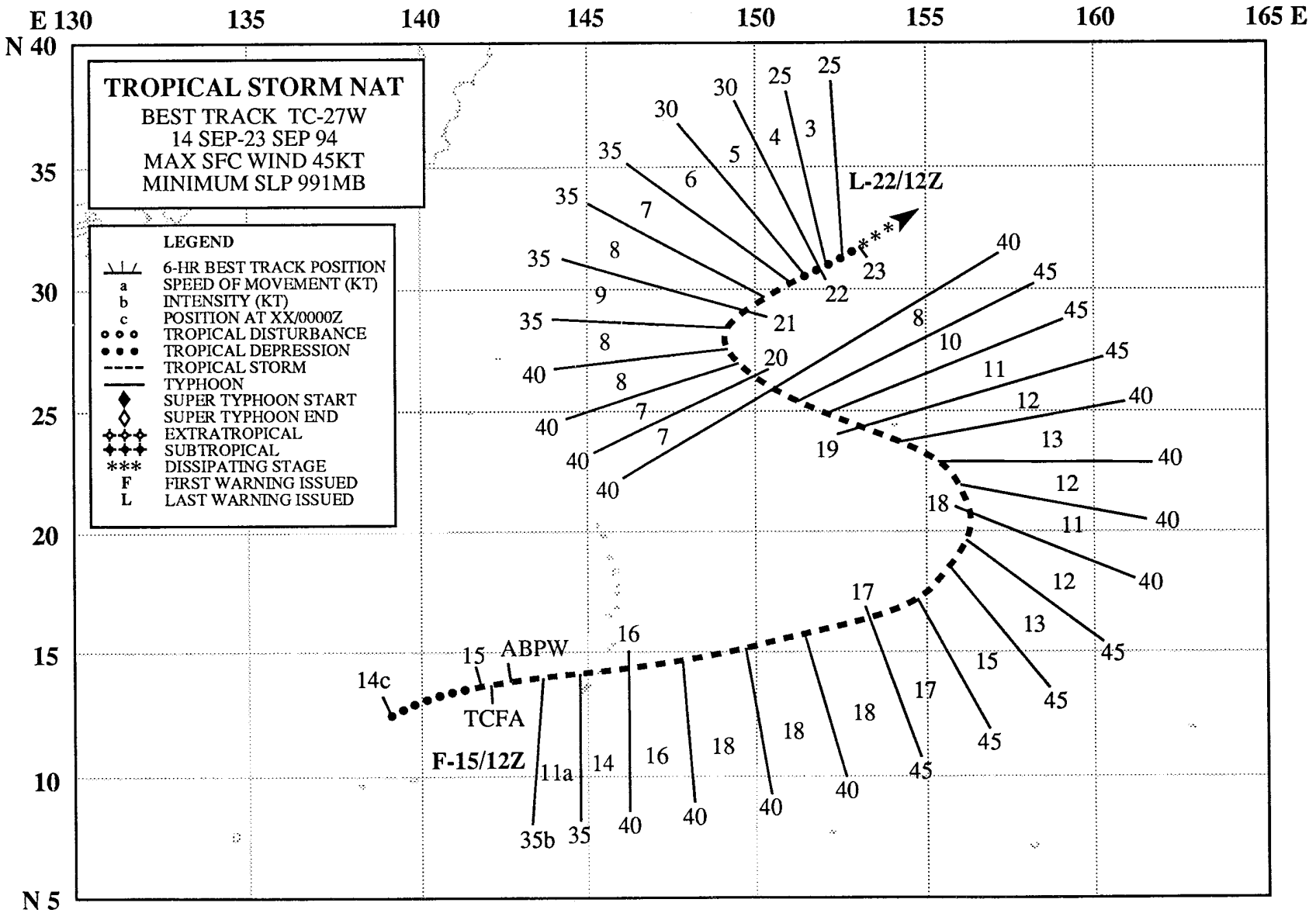
E 130
135
140
145
150
155
160
165 E
N 40
35
30
25
20
15
10
N 5
TROPICAL STORM NAT
BEST TRACK TC-27W
14 SEP-23 SEP 94
MAX SFC WIND 45KT
MINIMUM SLP 991MB
LEGEND
6-HR BEST TRACK POSITION
a SPEED OF MOVEMENT (KT)
b INTENSITY (KT)
c POSITION AT XX/0000Z
TROPICAL DISTURBANCE
TROPICAL DEPRESSION
TROPICAL STORM
TYPHOON
SUPER TYPHOON START
SUPER TYPHOON END
EXTRATROPICAL
SUBTROPICAL
*** DISSIPATING STAGE
F FIRST WARNING ISSUED
L LAST WARNING ISSUED
L-22/12Z
F-15/12Z
TCFA
ABPW
14c
35b
11a
***
149

TROPICAL STORM NAT (27W)

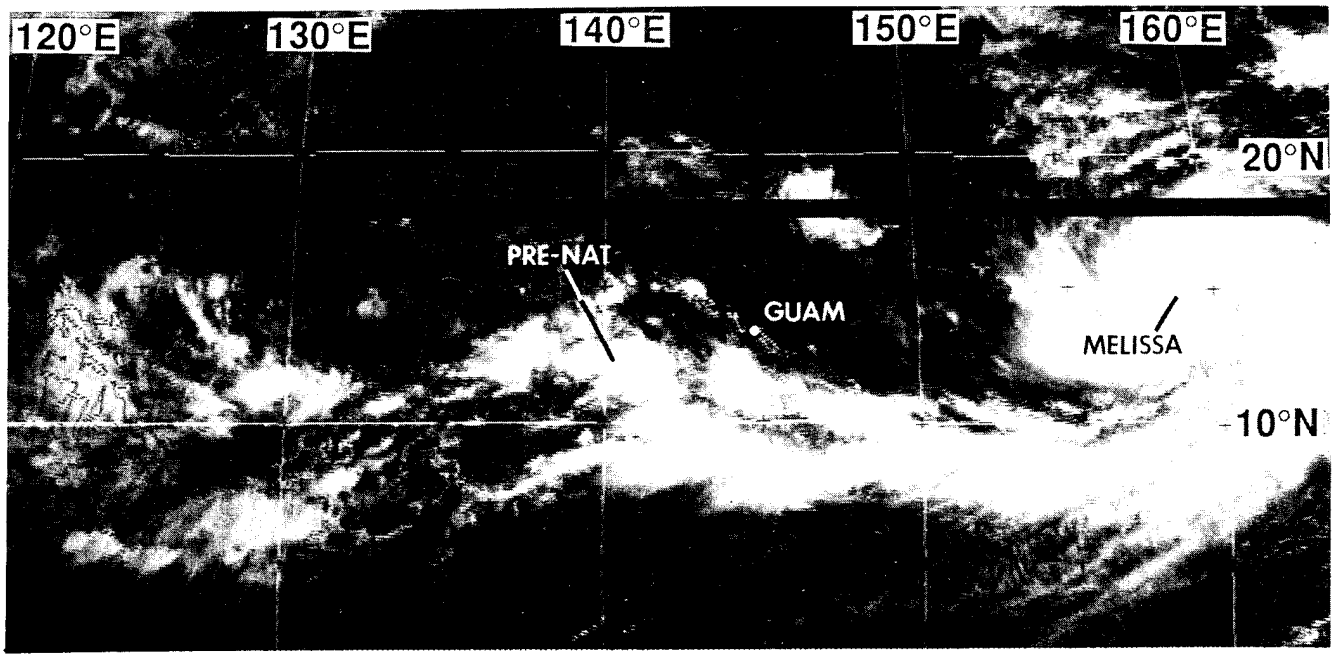

Figure 3-27-1 A monsoon cloud band stretches from the Philippines eastward toward Typhoon Melissa (26W). The first sign of organization of the tropical disturbance which became Nat is seen in the bulge of deep convection west of Guam (132331Z September visible GMS imagery).

I. HIGHLIGHTS

Nat was a small and relatively short-lived tropical cyclone that exhibited unusual "S" motion (Lander 1995a). Moving eastward at low latitude on the first leg of its "S" track, Nat passed to the north of Guam, and within range of Guam's NEXRAD.

II. TRACK AND INTENSITY

By 14 September, a monsoon cloud band stretched from the Philippines eastward to the large cloud system associated with Super Typhoon Melissa (26W) (Figure 3-27-1). In response to the formation of a tropical disturbance to the west of Guam (Figure 3-27-2), a Tropical Cyclone Formation Alert was issued at 150230Z September that stated, in part:

". . . surface pressures in the Marianas have fallen significantly over the past 24 hours, and winds on the south side of this 'monsoon depression' type of disturbance are approaching gale-force intensity. . . . This disturbance should continue to move east-northeastward with the prevailing southwest monsoon flow . . ."

The first warning on Tropical Depression 27W was issued at 151200Z when the system was located about 60 nm (110 km) west-northwest of Guam. It was upgraded to Tropical Storm Nat at 161200Z. In post-analysis, it was determined that Nat had most probably reached tropical storm intensity at 150000Z, and thus it was at minimal tropical storm intensity when it passed 40 nm (75 km) north of Guam at 151800Z. Wind and pressure measurements from conventional recording instruments located on Guam, and wind measurements obtained from Guam's NEXRAD, were the basis of the final best-track intensity estimates.

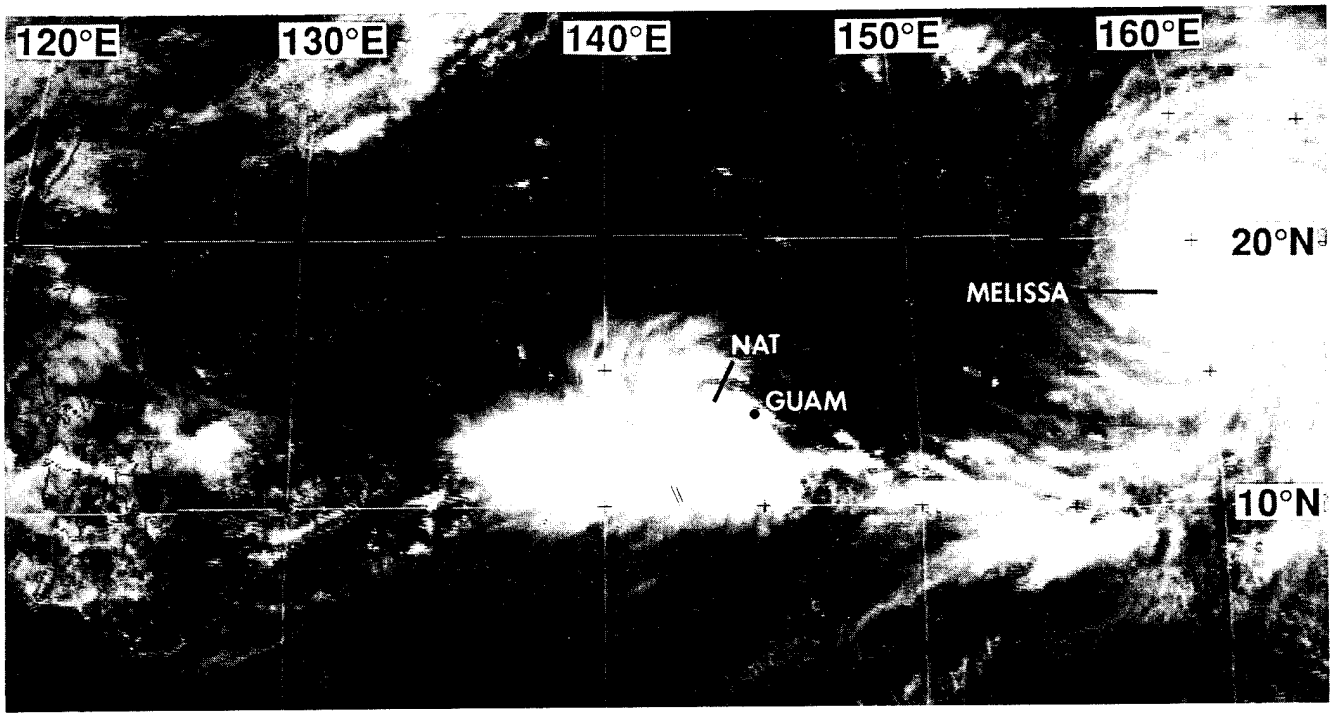

Figure 3-27-2 An area of deep convection has become organized west of Guam. Post analysis indicated that this system had already reached tropical storm intensity (150031Z September visible GMS imagery).

In the prognostic reasoning message (WDPN31 PGTW 151500) written to support the first warning, it was stated that:

"[the] track forecast philosophy is for this system to be a part of the overall monsoon surge that continues to move into Melissa (26W) . . . dynamic forecast aids indicate that the steering will be northeastwards where the system will be absorbed into [Melissa]. . . . We expect this system [Nat] to be weak throughout its existence."

As Nat continued on its northeastward track, it slowly intensified to a peak of 45 kt (23 m/sec). Considerable easterly shear appeared to be the major factor limiting Nat's intensification (Figure 3-27-3). Nat was not absorbed into Melissa's larger circulation as suggested earlier, but did remain weak throughout its life.

Between 170000Z and 190000Z, Nat's heading backed from northeastward to northwestward. Then, between 190000Z and 220000Z, Nat's heading veered from northwestward to northeastward to complete a nearly perfect "S" - shaped track. As Nat moved along the upper half of its "S" track, it separated from the major monsoon cloud band to the south, and decayed over open water near 30°N ; 150°E. The final warning was issued at 221200Z.

III. DISCUSSION

Nat was one of a very small percentage of tropical cyclones that move eastward at low latitude in the western North Pacific during the active months of July through September. Such cases of eastward motion most often occur when a tropical cyclone is embedded in the deep southwesterly flow of a very active monsoon. While on the lower east-bound leg of its "S"-shaped track, Nat passed 40 nm (74 km) to the north of Guam. Guam's NEXRAD provided a unique look at the structure of this unusual tropical cyclone.

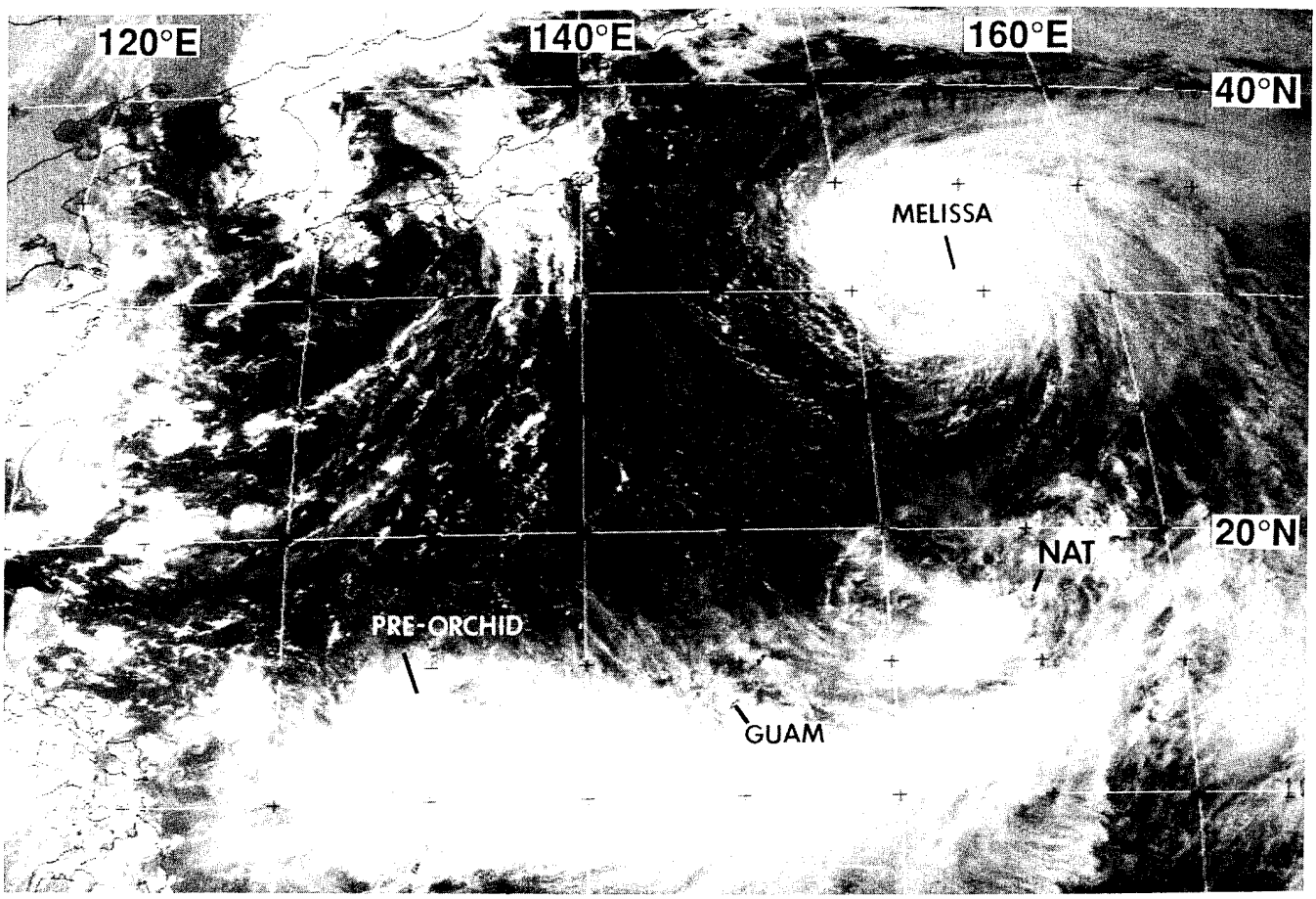

Figure 3-27-3 Nat's low-level circulation center is located to the east of its deep convection under the influence of easterly shear (170531Z September visible GMS imagery).

a. NEXRAD's view of a monsoon squall

On the morning of 15 September (at approximately 150000Z), a cloud band on the outer fringes of Nat's circulation (see Figure 3-27-2) passed over Guam from the southwest and was accompanied by a sudden wind squall. Peak gusts reached 48 Kt (24 m/sec) at the JTWC atop Nimitz Hill (see Figure 3-27-4). Using the "base velocity" product on the NEXRAD, the inbound squall was detected when it was about 40 nm (75 km) south of the island, or about one-half hour before its passage over Guam. A vertical cross section of the radial velocity, looking southwestward straight through the oncoming squall line, showed that the peak inbound winds with a velocity near 50 kt (25 m/sec) were confined within the lowest 10,000 feet of the troposphere. Shortly after the passage of the squall, the "velocity azimuth display" (VAD) product obtained from the NEXRAD showed another commonly observed property of high-wind events associated with the monsoon or with tropical cyclones affecting Guam: very deep unidirectional flow extending to at least 40,000 ft (200 mb).

b. Locating the center of Nat's poorly defined circulation

Nat's closest point of approach to Guam was 40 nm (75 km) to the north at 151800Z. This was well-within the 124 nm (230 km) range of the NEXRAD's capability to observe radial velocity. Nat was poorly organized while passing to the north of Guam, and locating the center with the radar was difficult. Several radar products were examined in order to increase the confidence of the fix; these includ-

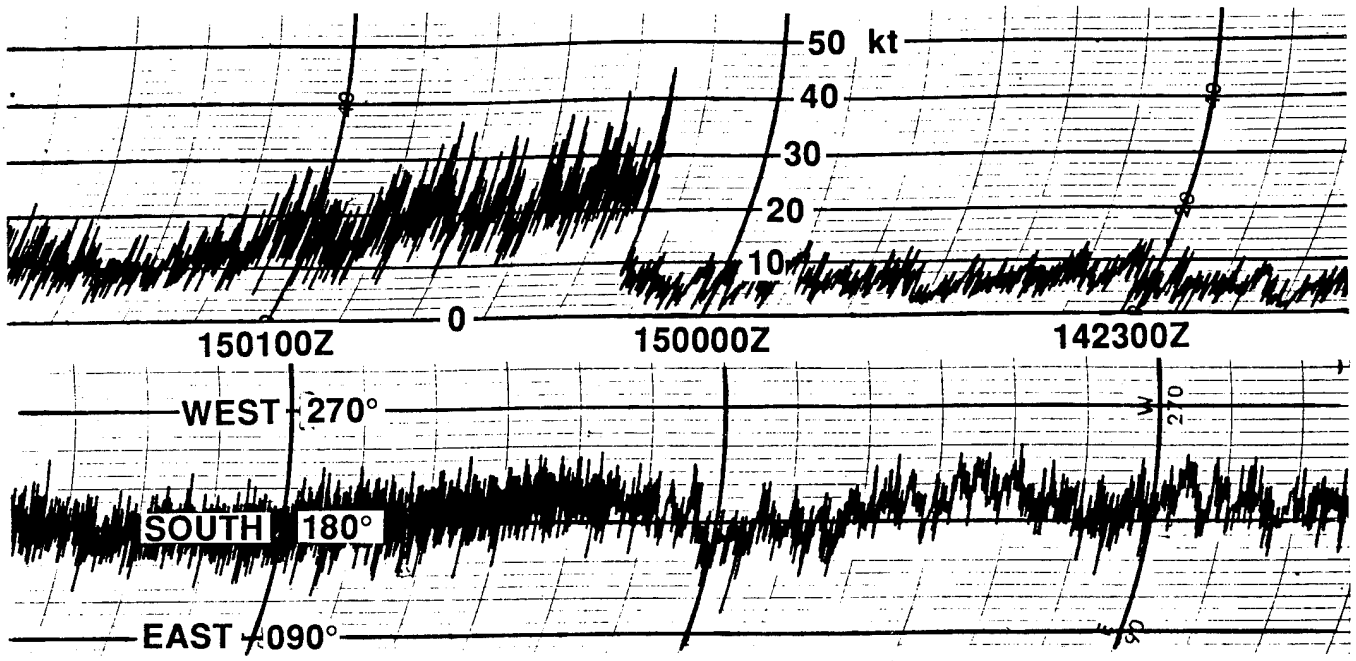

Figure 3-27-4 Recording anemometer trace at the JTWC showing the sudden onset of wind in the first squall associated with Nat.

ed: the base reflectivity, the base velocity, animation of the base reflectivity, convective cell tracking, and the one- and three-hour integrated rainfall products. In Nat's case, the distribution of deep convection as depicted by satellite (Figure 3-27-5a), and by the base reflectivity from the NEXRAD (Figure 3-27-5b), was poorly organized . The isodop (line of zero radial velocity) was useful for estimating the bearing of the center to the site (Figure 3-27-5c). The most striking depiction of the wind pattern in Nat was obtained from the three-hour precipitation product (Figure 3-27-5d). Despite the disorganized appearance of the cloud elements in satellite imagery and on the NEXRAD'S base reflectivity product, the short-term (i.e., one-hour and three-hour) integrated rainfall products showed a high degree of organization and helped increase the confidence of the estimated low-level center postition.

IV. IMPACT

Throughout its entire life, Nat remained at sea and reached a peak intensity of only 45 kt (23 m/sec). However, for such a weak system, it had a disproportionate impact on the island of Guam, mostly in the form of freak accidents. As Nat approached the island of Guam on September 15, a squall line in the outer circulation of Nat passed across the island. Winds gusted to 48 kt (25 m/sec) at the JTWC as this squall passed. Two tourists who were parasailing were seriously injured when winds in this squall snapped the tow rope which attached their parasail to the boat. A second squall later in the evening damaged power lines, causing a half-hour loss of power to several villages. Strong winds on the morning of 16 September, when Nat was located about 100 nm (185 km) to the northeast of Guam, knocked a security guard off a gangplank and into the water at the commercial port. The man, who could not

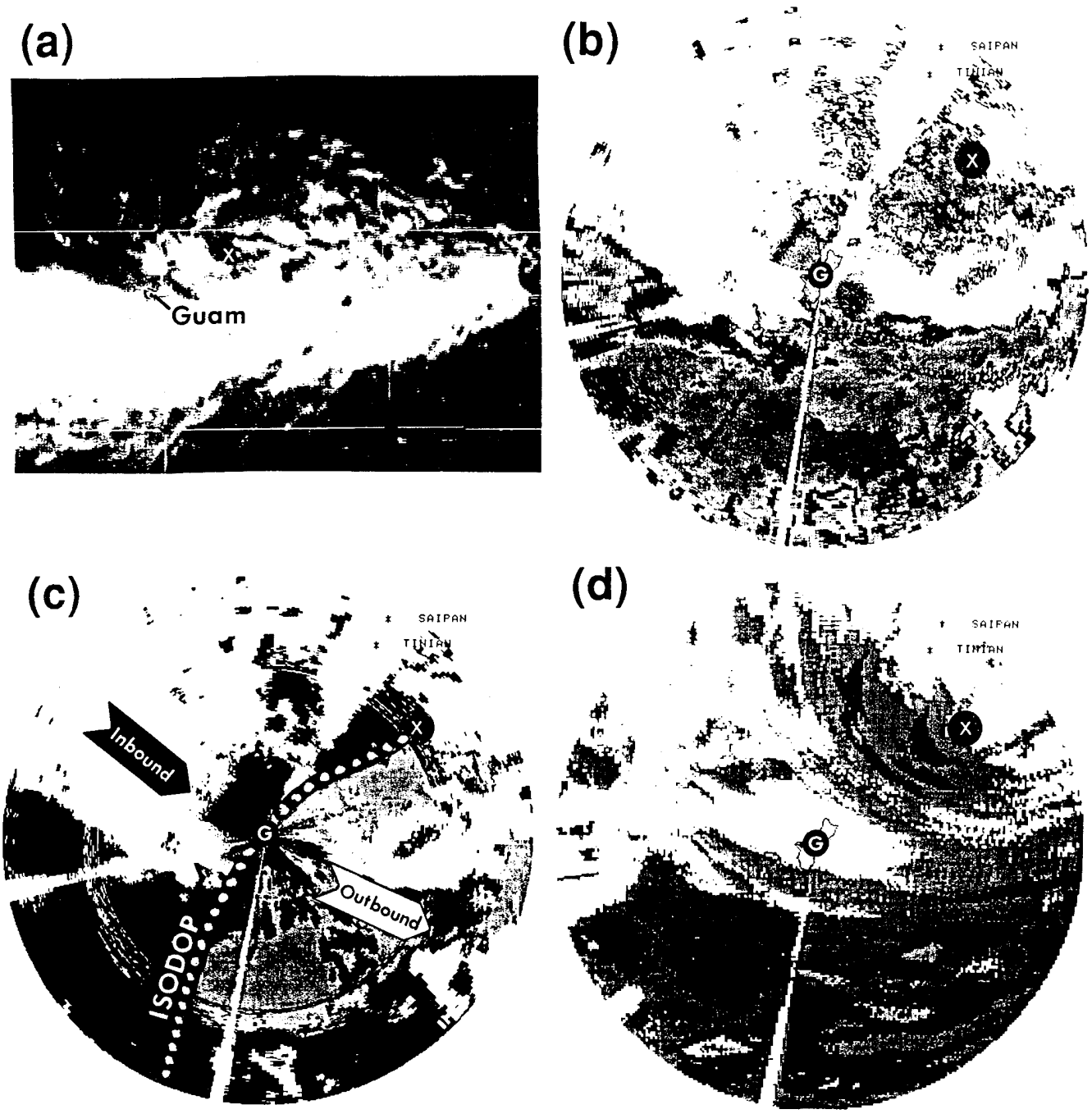

Figure 3-27-5 A combination of products from satellite and weather radar were used to locate the center of the poorly organized Nat as it passed north of Guam. (a) Nat's poorly organized central convection as seen by satellite (160031Z September visible GMS imagery), and (b) by Guam's NEXRAD (160058Z September NEXRAD base reflectivity). (c) The isodop (line of zero radial velocity) extends towards Nat's estimated center location (160058Z September NEXRAD base velocity). (d) Note the higher degree of organization apparent on the three-hour precipitation product (160058Z September NEXRAD three-hour precipitation). Nat's estimated center location is indicated by the small white "x" within the black dot.

swim, drowned. Two of his co-workers also were knocked into the water and nearly drowned. Later, on the morning of 17 September, when Nat was located about 500 nm (925 km) northeast of Guam, a thunderstorm developed over Guam in weak northwesterly wind flow. Lightning in this thunderstorm struck at a track meet and injured about 20 people. Most were treated for light electric shock and dizziness. Another lightning bolt from this same thunderstorm struck the commercial power line feeding Guam's NEXRAD, knocking the system out for over one month and causing $90,000 worth of damage.

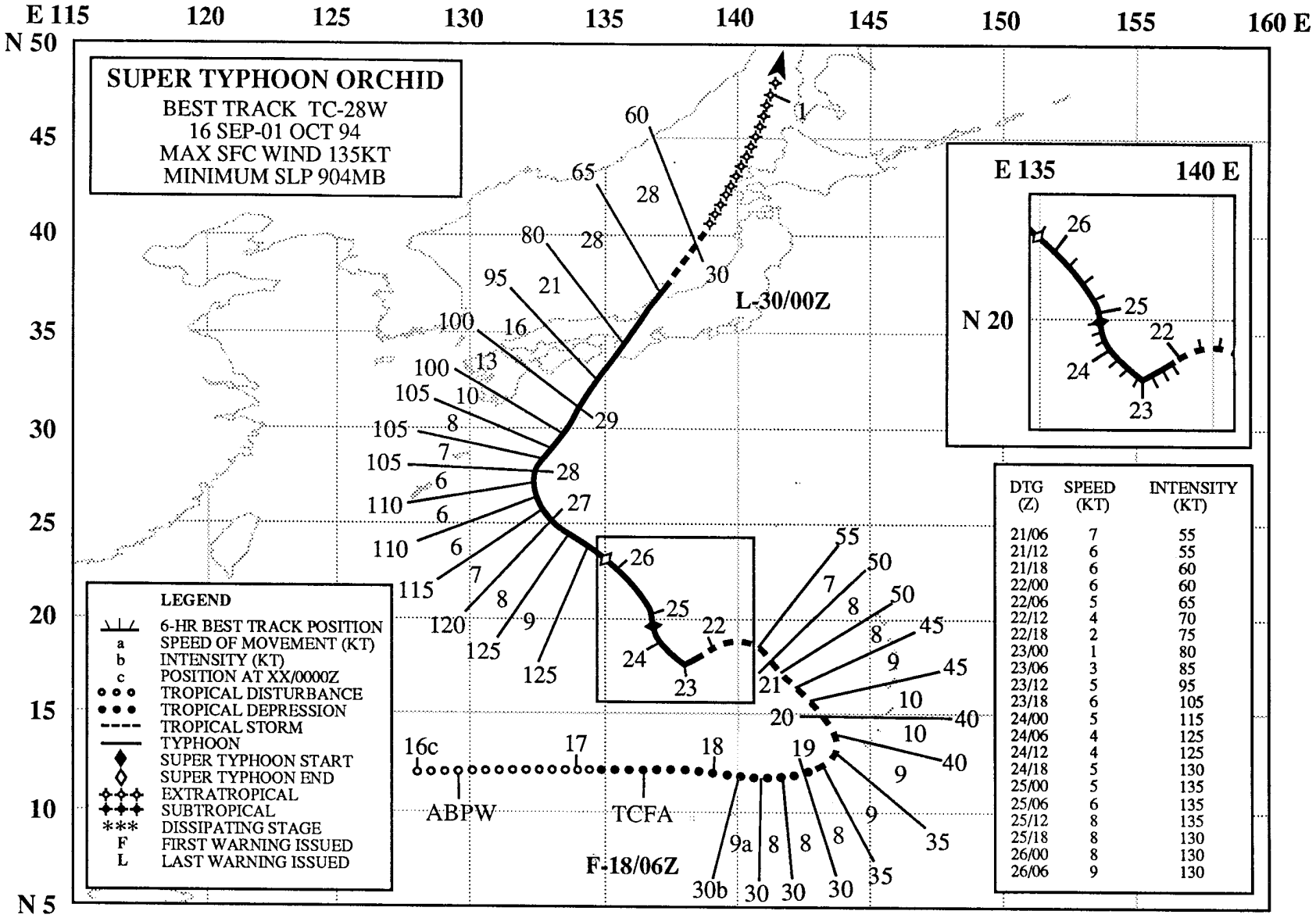

DTG (Z)	SPEED (KT)	INTENSITY (KT)
21/06	7	55
21/12	6	55
21/18	6	60
22/00	6	60
22/06	5	65
22/12	4	70
22/18	2	75
23/00	1	80
23/06	3	85
23/12	5	95
23/18	6	105
24/00	5	115
24/06	4	125
24/12	4	125
24/18	5	130
25/00	5	135
25/06	6	135
25/12	8	135
25/18	8	130
26/00	8	130
26/06	9	130

TYPHOON ORCHID (28W)

I. HIGHLIGHTS

The fifth super typhoon of 1994, Orchid was one of eight tropical cyclones to form during the very active month of September. Orchid underwent unusual motion (e.g., eastward motion at low latitude) that can be attributed to the influence of the large-scale monsoon circulation. Unlike most very intense tropical cyclones, Orchid did not appear to go through a period of rapid intensification. Orchid affected the island of Guam and later, after recurvature, it crossed the Japanese island of Honshu.

II. TRACK AND INTENSITY

The tropical disturbance that became Orchid was first detected about 100 nm (185 km) east of the Philippine island of Samar, and was mentioned on the 160600Z September Significant Tropical Weather Advisory. The disturbance moved slowly eastward under the influence of deep-layer westerly flow associated with an active monsoon. At 171130Z September, when the disturbance was located about 250 nm (460 km) north-northwest of Yap, a Tropical Cyclone Formation Alert was issued based upon improved organization of deep convection. The first warning was issued on Tropical Depression 28W at 180600Z as the organization of the satellite-observed deep convection continued to improve. The system continued eastward along about 12°N, towards the island of Guam. At 190000Z, Tropical Depression 28W began a turn toward the north. It was upgraded to Tropical Storm Orchid at 191200Z as the system (moving northward) passed 60 nm (110 km) to the west of Guam. During the next 48 hours (191200Z to 211200Z), Orchid moved northwestward at about 6 kt (11 km/hr) and slowly intensified. On the morning of 22 September, the system turned toward the southwest, then 24 hours later it turned back toward the northwest forming a V-shaped notch in its track. Typhoon intensity was first attained at 211800Z based upon its cloud structure as observed by satellite (Figure 3-28-1). During the next three days, Orchid's intensity increased at a normal rate of one "T" number per day, and by 250000Z it reached peak intensity of 135 kt (69 m/sec). After reaching peak intensity, the system accelerated toward the northwest, and slowly weakened (Figure 3-28-2). On 27 September, Orchid slowed its speed of forward motion as it approached its recurvature point. After 271800Z, Orchid turned toward the north-northeast and began to accelerate. At approximately 291000Z, Orchid made landfall on the Pii peninsula of the Japanese main island of Honshu. The eye passed just to the west of the coastal city of Tanabe (WMO 47778), where a minimum pressure of 960.9 mb and a peak gust of 92 kt (47 m/sec) were recorded. A central pressure of 961 mb supports an intensity of 85 kt (44 m/sec) sustained one-minute average wind with gusts to 105 kt (54 m/sec) using the Atkinson and Holliday (1977) wind-pressure relationship. Orchid crossed the mountainous island of Honshu at a forward speed of nearly 25 kt (46 km/hr) and entered the Sea of Japan as a minimal typhoon. On the afternoon of 30 September, Orchid passed over western Hokkaido with sustained winds of 55-60 kt (28-31 m/sec). On the evening of 01 October, the system dissipated over Sakhalin Island, at a latitude poleward of 50°N.

III. DISCUSSION

a. Monsoonal influences on Orchid's motion

From 160000Z (when Orchid was first detected) until 190600Z (when Orchid reached minimal tropical storm intensity), the system moved eastward more than 800 nm (1480 km). This unusual motion was the result of relatively deep westerly monsoon flow along the band of deep convection associated with a reverse-oriented monsoon trough that was connected to the major rain band on the south side of

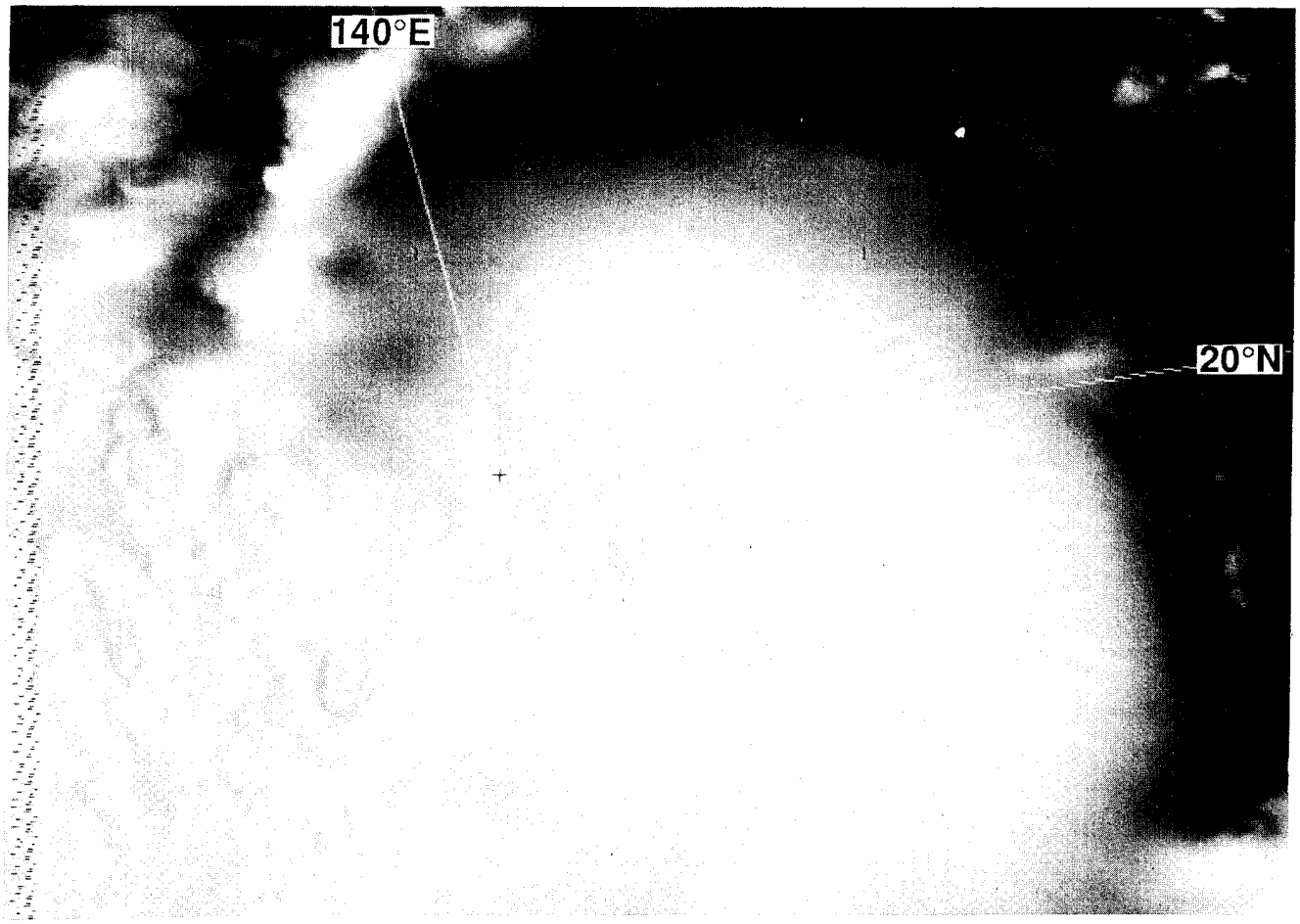

Figure 3-28-1 Orchid at 60 kt (31 m/sec) intensity at a location about 400 nm (750 km) northwest of Guam (212331Z September visible GMS imagery).

Melissa (26W). When Orchid reached about 142°E, it turned sharply to the north, passing 60 nm (110 km) west of Guam. After passing Guam, Orchid turned to the northwest. On 22 September, it turned abruptly to the southwest for 18 hours, then stalled and headed to the northwest, tracing a "V" shape.

The character and evolution of the mid-tropospheric subtropical ridge and the midlatitude disturbances passing poleward of this ridge have long been cited as the causative agents of the behavior of storms in most post analyses (e.g., Matsumoto 1984; Sandgathe 1987; and past ATCRs issued by the JTWC). Other factors deemed to be of importance to TC motion in the WNP include: binary interaction (Brand 1970, Dong and Neumann 1983, and Lander and Holland 1993), and the effects of the large-scale monsoon circulation (Harr and Elsberry 1991, Lander 1994a, and Carr and Elsberry 1994). The effects of the monsoon circulation on tropical cyclone motion have recently been receiving more attention.

A plausible explanation for the erratic "V" motion of Orchid is a monsoonal effect described by Carr and Elsberry (1995). They studied the properties of the motion of a tropical cyclone that resulted from the interaction between the tropical cyclone and a larger-sized "monsoon gyre" located to its north or west. The tropical cyclone undergoes about 180° of a counter-clockwise orbit around the gyre, and the two systems approach. Eventually the tropical cyclone merges with the gyre. Upon merger, the track abruptly changes to a steady northwestward drift (Figure 3-28-3). This theoretical motion and the actual

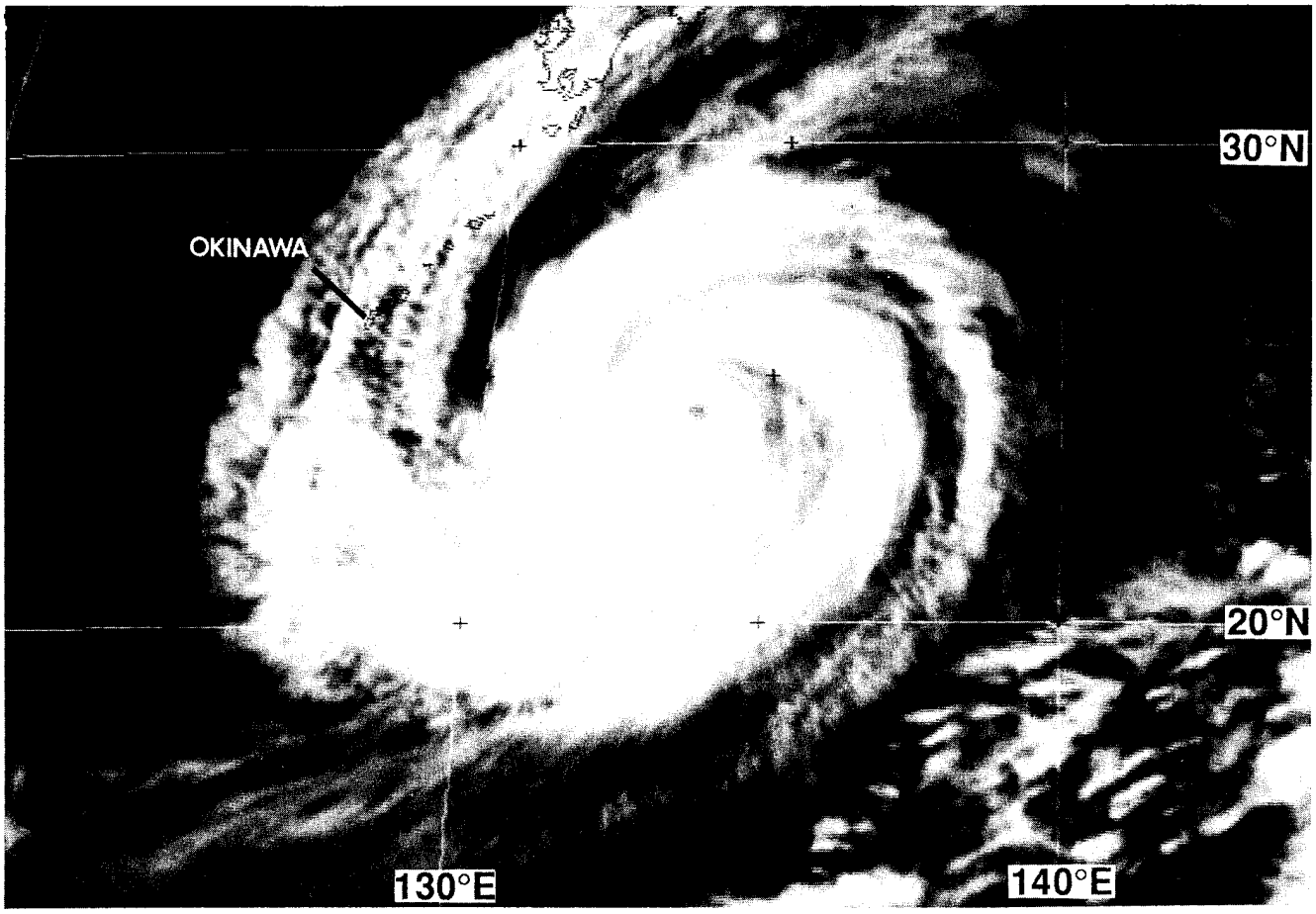

Figure 3-28-2 Orchid's intensity is 115 kt (59 m/sec) as it nears its point of recurvature (261538Z September infrared GMS imagery).

motion of Orchid are similar. Although Orchid was embedded in a reverse-oriented monsoon trough, there was, at the time of its "V" motion, a separate low-pressure area to its west (Figure 3-28-4a) with which Orchid could conceivably have orbited and merged (Figure 3-28-4b).

b. Changes in eye size during intensification

Orchid was the third super typhoon — the two others were Fred (17W) and Doug (19W) — that exhibited changes in the size of the eye that were contrary to those normally expected during the intensifying and weakening phases of a typhoon's life cycle. Orchid's eye expanded during the intensification period and it shrank during the weakening phase (see Figure 3-28-1). The changes in the size of Orchid's eye were not as dramatic as those that occurred with Doug (17W) or Fred (19W), but in each case, the changes were contrary to those expected.

IV. IMPACT

Orchid spent most of its life at sea. During its brush past Guam as a tropical storm, Orchid caused some local flooding. A peak gust of 46 kt (24 m/sec) was recorded at the JTWC. Orchid's passage over central Japan helped to alleviate a two-month drought which in some areas had left reservoirs dry. No reports of casualties or damage were received, however Orchid forced the cancellation of 400 international and domestic flights across Japan, and stopped the operation of over 100 ferry routes.

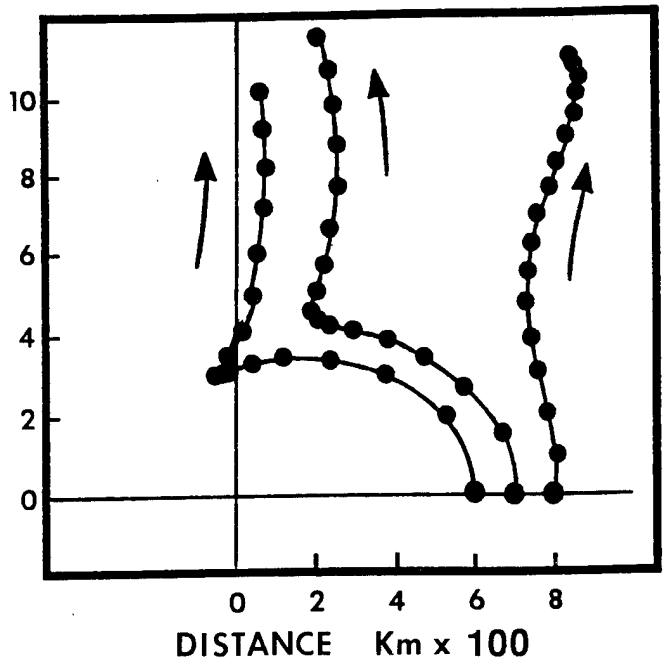

Figure 3-28-3 Typical track changes associated with the interaction of a tropical cyclone with a monsoon gyre. Dots show positions at six-hour intervals for 96 hours of the simulated tracks of three tropical cyclones placed at 600, 700, and 800 km respectively east of the center of a monsoon gyre. (Figure adapted from Carr and Elsberry, 1995.)

Table 3-28-1 Changes in the size of Orchid's eye diameter during the period when a well-defined eye was visible.

DATE/TIME (Z)	BEST-TRACK INTENSITY (kt)	EYE DIAMETER (nm)
23/00	80	26
23/06	85	17
23/12	95	18
23/18	105	17
24/00	115	16
24/06	125	14
24/12	125	18
24/18	130	14
25/00	135	21
25/06	135	18
25/12	135	11
25/18	130	19
26/00	130	23
26/06	130	30
26/12	125	26
26/18	125	22
27/00	120	22
27/06	115	13
27/12	110	11
27/18	110	14
28/00	105	12
28/06	105	17
28/12	105	14
28/18	100	14
29/00	100	9

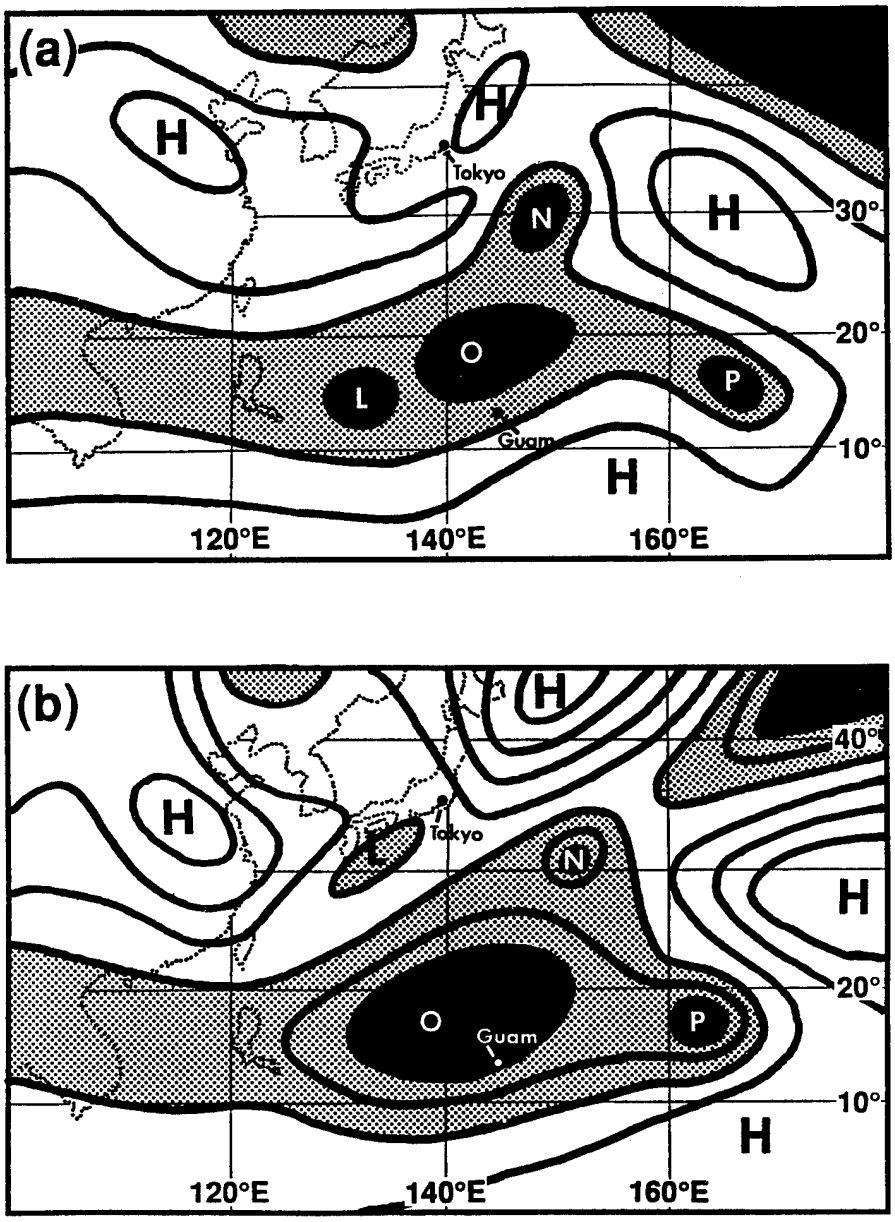

Figure 3-28-4 (a) Sea-level pressure (SLP) analysis at 210000Z October showing the location of Orchid in the monsoon trough. A low-pressure area to the west of orchid, labeled, L, may possibly have interacted with Orchid to cause Orchid's unusual southwestward motion which began at about this time. Key: Shaded regions are lower than 1010 mb, black regions are lower than 1008 mb. O = Orchid, N = Nat (27W), P = Pat (29), L = low-pressure area, and H = high pressure area. Contours are at 2 mb intervals. (b) SLP analysis at 231200Z October showing that Orchid has merged with the low-pressure area previously to its west. At this time, Orchid turned towards the northwest. Key: same as in (a) except that the black regions are lower than 1006 mb.

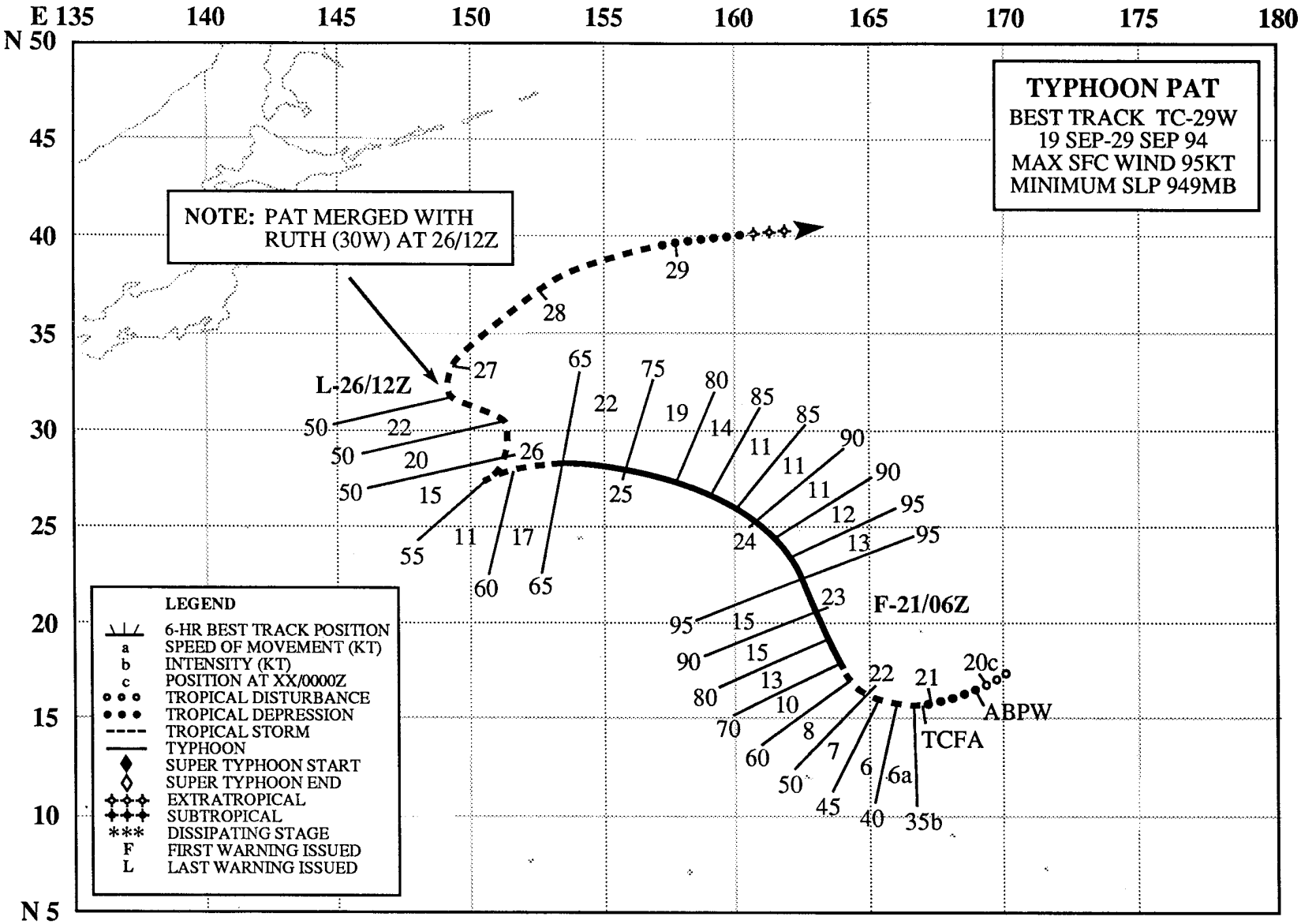
E 135
140
145
150
155
160
165
170
175
180
N 50
45
40
35
30
25
20
15
10
N 5
TYPHOON PAT
BEST TRACK TC-29W
19 SEP-29 SEP 94
MAX SFC WIND 95KT
MINIMUM SLP 949MB
NOTE: PAT MERGED WITH
RUTH (30W) AT 26/12Z
L-26/12Z
F-21/06Z
TCFA
ABPW
LEGEND
6-HR BEST TRACK POSITION
SPEED OF MOVEMENT (KT)
INTENSITY (KT)
POSITION AT XX/0000Z
TROPICAL DISTURBANCE
TROPICAL DEPRESSION
TROPICAL STORM
TYPHOON
SUPER TYPHOON START
SUPER TYPHOON END
EXTRATROPICAL
SUBTROPICAL
DISSIPATING STAGE
FIRST WARNING ISSUED
LAST WARNING ISSUED

TYPHOON PAT (29W)

I. HIGHLIGHTS

The symmetrical collapse of deep convection during the merger of Pat with Tropical Storm Ruth (30W) is the first documented case of such an event. Pat developed at the extreme eastern terminus of a reverse-oriented monsoon trough. Pat's overall track pattern was an unusual north-oriented "S" shape that included a period of rapid counter-clockwise mutual orbit with Ruth (30W). Pat was a small typhoon.

II. TRACK AND INTENSITY

During the latter half of September, the circulation of the western North Pacific was dominated by an active monsoon trough. The low-level southwesterly winds associated with this trough had extended far to the north and east of normal, and the axis of this monsoon trough had a SW-NE (i.e., reverse) orientation. All of the tropical cyclones which formed in association with it — Melissa (26W), Nat (27W), Orchid (28W), Pat and Ruth (30W) — moved on north-oriented, "S"-shaped, tracks.

The tropical disturbance which became Typhoon Pat, was first observed at the far eastern reaches of the monsoon trough. It was listed as a suspect area on the 200600Z September Significant Tropical Weather Advisory when synoptic data and satellite imagery indicated that a low-level circulation center (with deep convection sheared to its southeast) had formed near Wake Island. An increase in the amount and organization of deep convection associated with this system prompted the JTWC to issue a Tropical Cyclone Formation Alert at 210400Z. The first warning followed at 210600Z.

Initially moving slowly west-southwestward, Pat turned toward the north-northwest and intensified. At 230000Z, when located about 270 nm (500 km) northwest of Wake Island, Pat reached 90 kt (46 m/sec) (Figure 3-29-1). It reached its peak intensity of 95 kt (48 m/sec) at 230600Z and began to weaken after 231200Z. At 240000Z, the system began to take a more westward course as it entered a easterly steering regime between a strong ridge to its north and another tropical cyclone — Tropical Storm Ruth (30W) — to its southwest. At 241200Z, Pat and Ruth (30W) abruptly increased their rate of centroid-relative cyclonic orbit. At 261200Z, the two tropical cyclones merged into a single vortex. The merged Pat and Ruth then recurved, and the final warning was issued at 281200Z. Post-analysis of synoptic data and satellite imagery indicated that the system most probably was a minimal tropical storm until 281800Z and a tropical depression until 291200Z.

III. DISCUSSION

The interaction of two adjacent tropical cyclones is often referred to as the Fujiwhara effect after the pioneering laboratory and observational studies of Fujiwhara (1921, 1923, and 1931). Fujiwhara demonstrated that the relative motion of two adjacent cyclonic vortices was composed of cyclonic orbit around their centroid, coupled with a mutual attraction. The rate of orbit steadily increases as the vortices spiral inward toward one another and eventually the two vortices coalesce into one vortex located at the centroid.

Usually the behavior of two adjacent tropical cyclones differs from the classical Fujiwhara effect in several aspects; prominent among these is the usual failure of tropical cyclones to merge. Because of these differences, the interaction between two tropical cyclones is usually called binary interaction. Dong and Neumann (1983) studied the behavior of interacting tropical cyclones and defined binary interaction as the occurrence of two named tropical cyclones which co-exist for at least 48 hours during

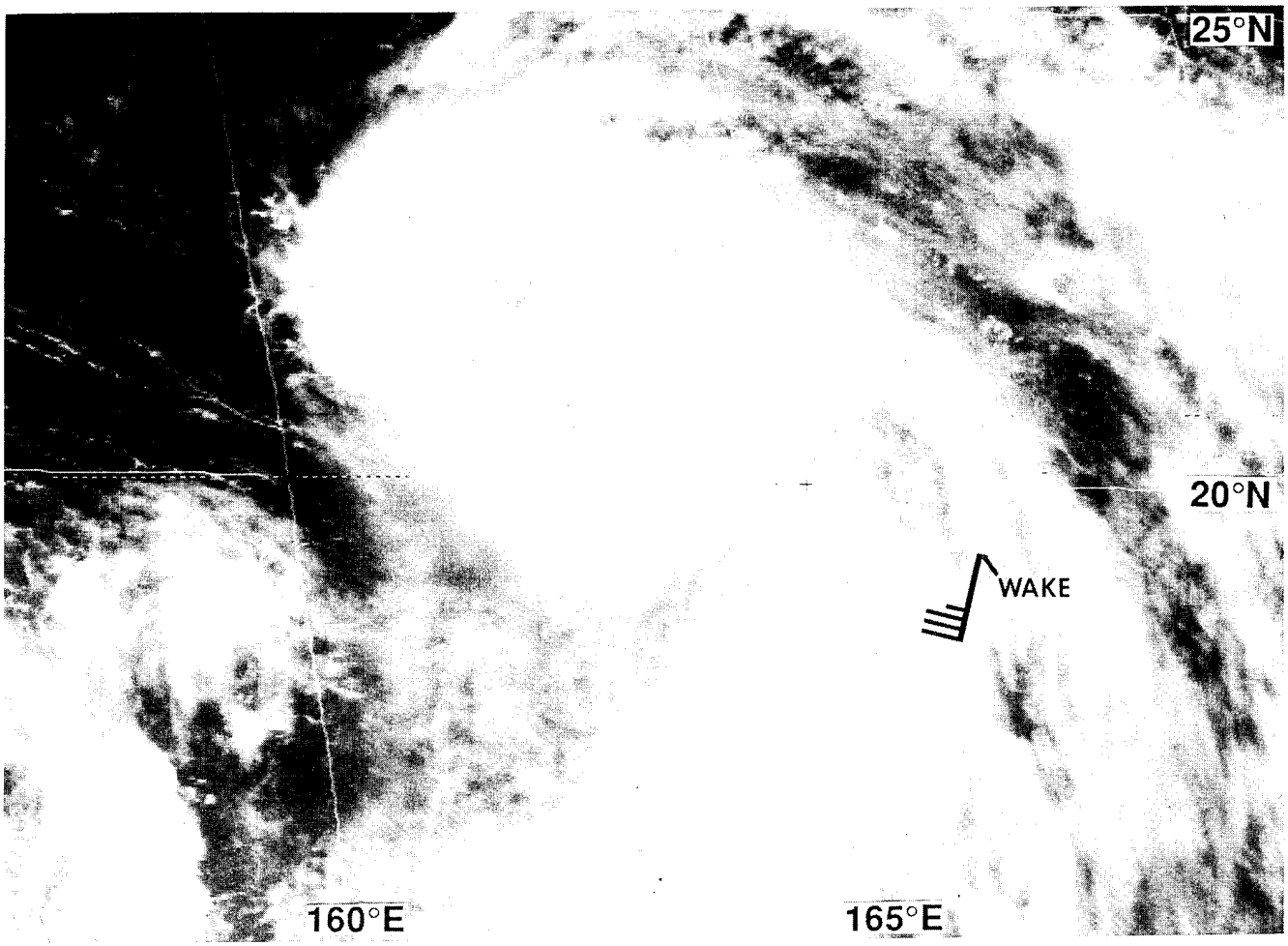

Figure 3-29-1 Pat at 90 kt (46 m/sec) six hours before its peak intensity of 95 kt (48 m/sec). The 230000Z gradient-level wind at Wake Island (WMO 91245) is plotted (230031Z September GMS visible imagery).

which time they approach within at least 780 nm (1450 km) and reach at least tropical storm intensity. The separation criterion was based on other studies by Brand (1970), which showed that mutual cyclonic orbit tends to dominate when storms approach within this distance. Brand further noted that mutual orbit tends to commence suddenly. Lander and Holland (1993) developed a generalized model of binary interaction (Figure 3-29-2), and showed that the classical Fujiwhara model of converging cyclonic rotation about a centroid followed by merger is rarely observed.

In all previously known cases of tropical cyclone merger, only one of the tropical cyclones experiences a loss of deep convection, followed by strong horizontal shearing and incorporation into the circulation of the surviving tropical cyclone. Prior to the interaction between Pat and Ruth, the symmetrical collapse of the deep convection of both tropical cyclones as they merge into a single vortex had not been documented (Lander 1995b).

During the last week of September, the tropical atmosphere over the western North Pacific Ocean was dominated by a very active monsoon trough. At the time of the satellite imagery in figure 3-29-3, two named tropical cyclones had formed in the monsoon cloud band — Orchid (28W) and Pat. A tropical depression (30W) (that later became Tropical Storm Ruth) was located between these two named storms. Over the next two days, Pat moved rapidly northwestward, and the tropical depression (30W) between Pat and Orchid (28W) was upgraded to Tropical Storm Ruth. Ruth (30W) initially moved northeastward and rapidly approached Pat. Over a 22-hour period, 250230Z to 260030Z, Pat and Ruth

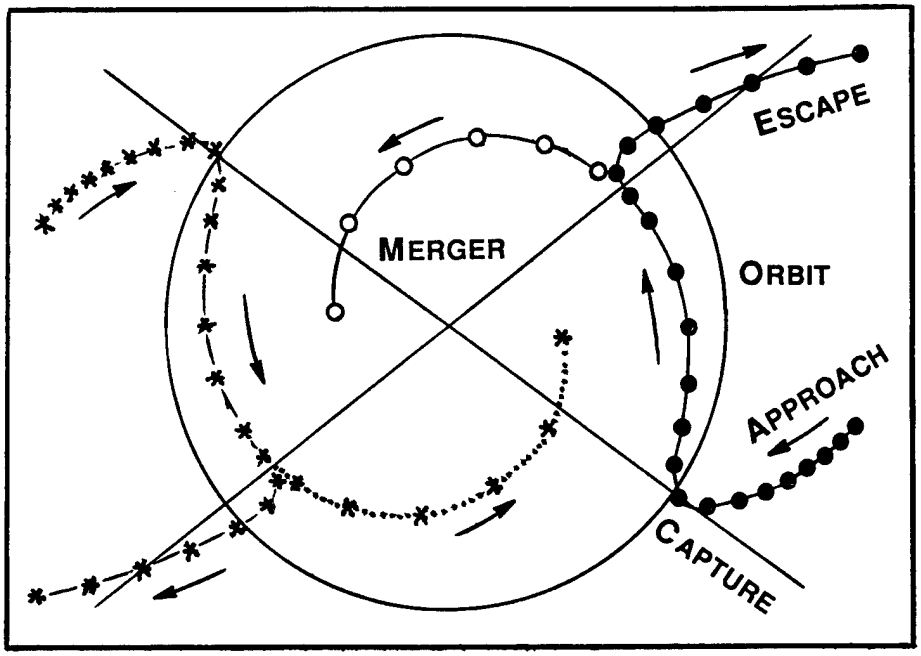

Figure 3-29-2 Model of binary interaction of two tropical cyclones containing the major elements of approach and capture, followed by mutual orbit, then escape or merger (from Lander and Holland 1993).

(30W) approached to within 200 nm (370 km) (Figure 3-29-4) and underwent about 180° of cyclonic orbit relative to their centroid (Figure 3-29-5a,b). The orbit continued during the night (260600Z to 261800Z), and during this period both systems lost their central convection and merged to become one vortex by the next morning (262330Z) (Figure 3-29-6).

At first, the merged vortex lacked significant central convection, but it still possessed tropical-storm intensity wind. The merged vortex (designated by the JTWC as Ruth) regained central convection within 24 hours following the merger (Figure 3-29-7). Later, Ruth (i.e., the merged Pat and Ruth) recurved into midlatitudes and decayed.

IV. IMPACT

No reports of significant damage or fatalities were received.

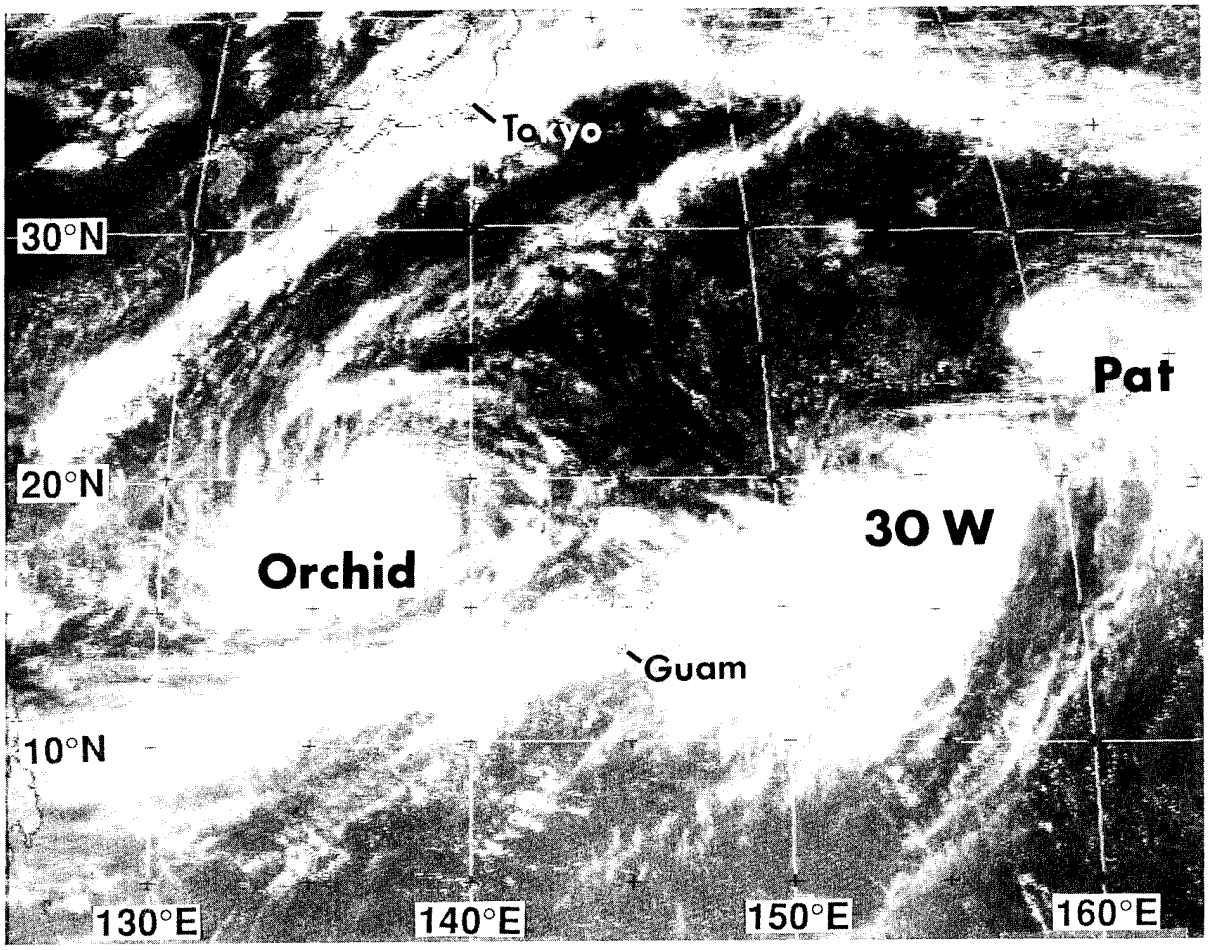

Figure 3-29-3 An active reverse-oriented monsoon trough. Typhoon Orchid, Tropical Depression 30W (later becoming Ruth), and Typhoon Pat are indicated (240031Z September GMS visible imagery).

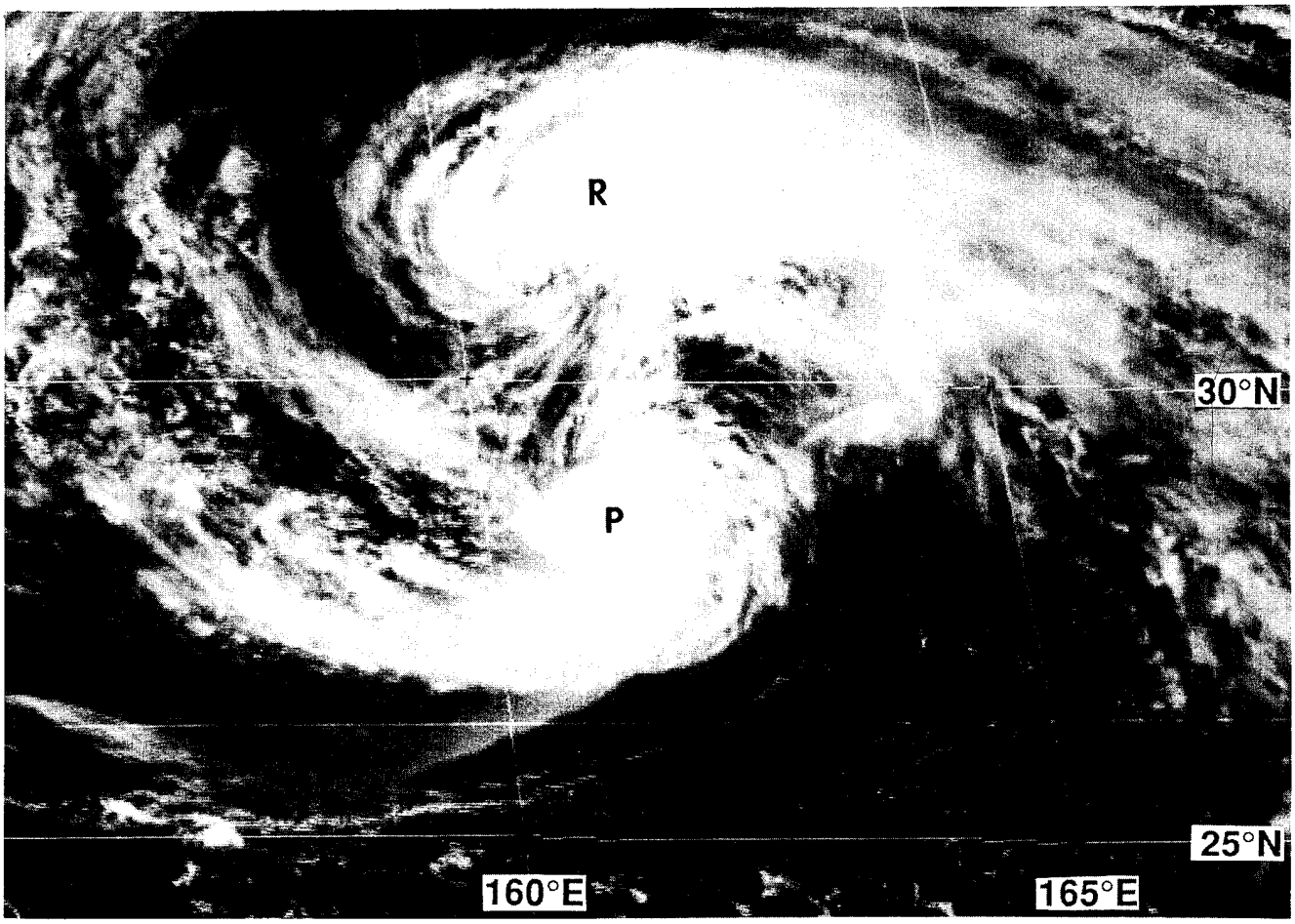

Figure 3-29-4 Pat and Ruth (30W) have moved to within 200 nm (370 km) of one another (260131Z September GMS visible imagery).

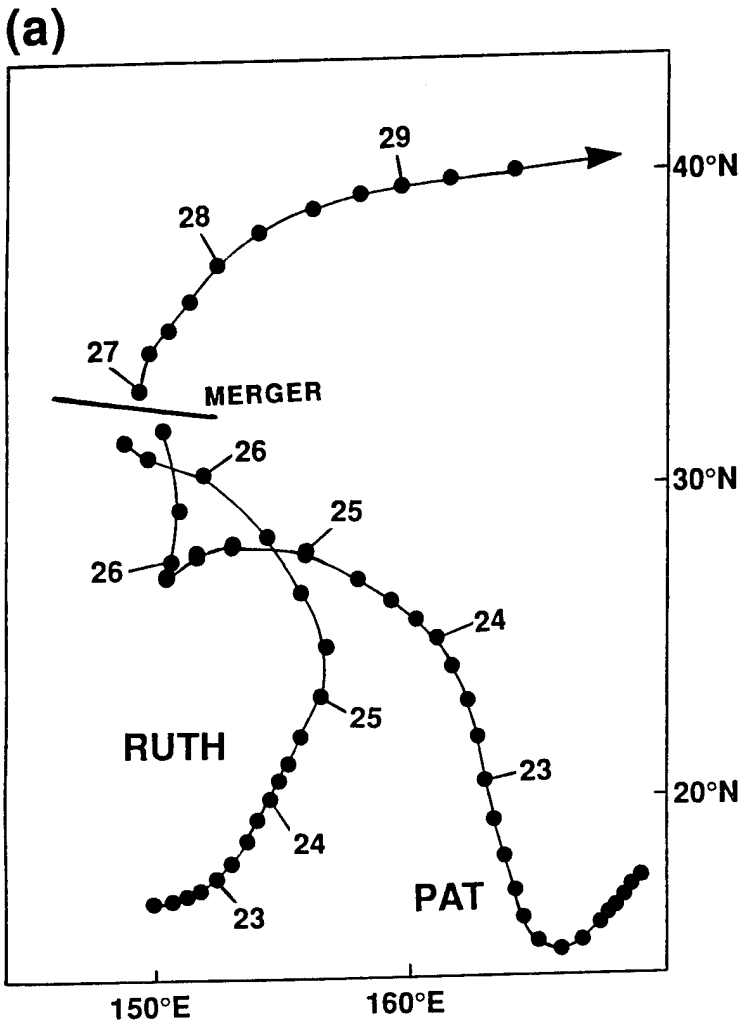

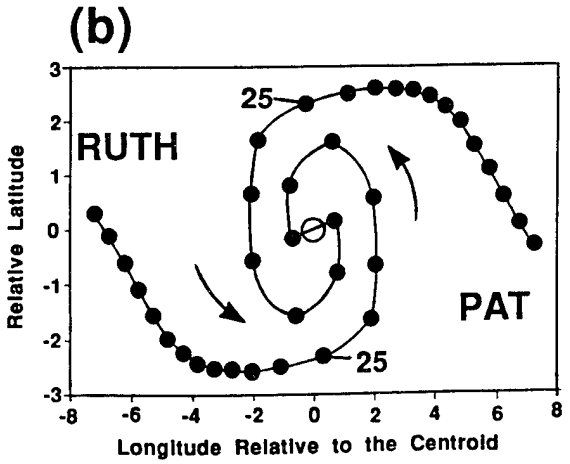

Figure 3-29-5 The tracks of Pat and Ruth (30W) in two reference frames: (a) Earth-relative [Black dots are at six-hour intervals. The positions at 0000Z are indicated. The merger location is shown as a solid bar, after which the two tracks become one], and (b) Centroid-relative [Black dots are at six-hour intervals. Positions at 250000Z September are indicated. The open circle is the centroid, where merger takes place shortly after 261200Z September]. (Adapted from Lander, 1995b).

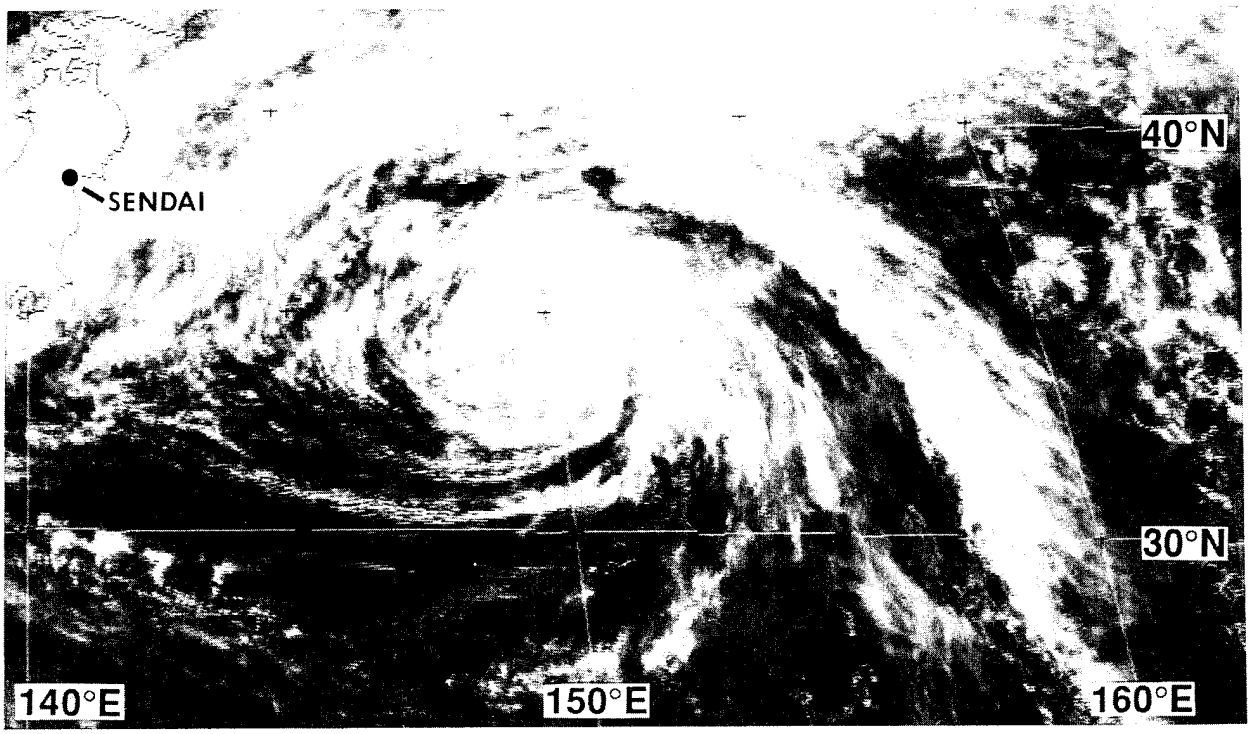

Figure 3-29-6 The single vortex that is the merged Pat and Ruth (30W). Deep central convection is absent, but ship reports and tightly wound low-level cloud lines support surface winds of tropical storm intensity (270031Z September visible GMS imagery).

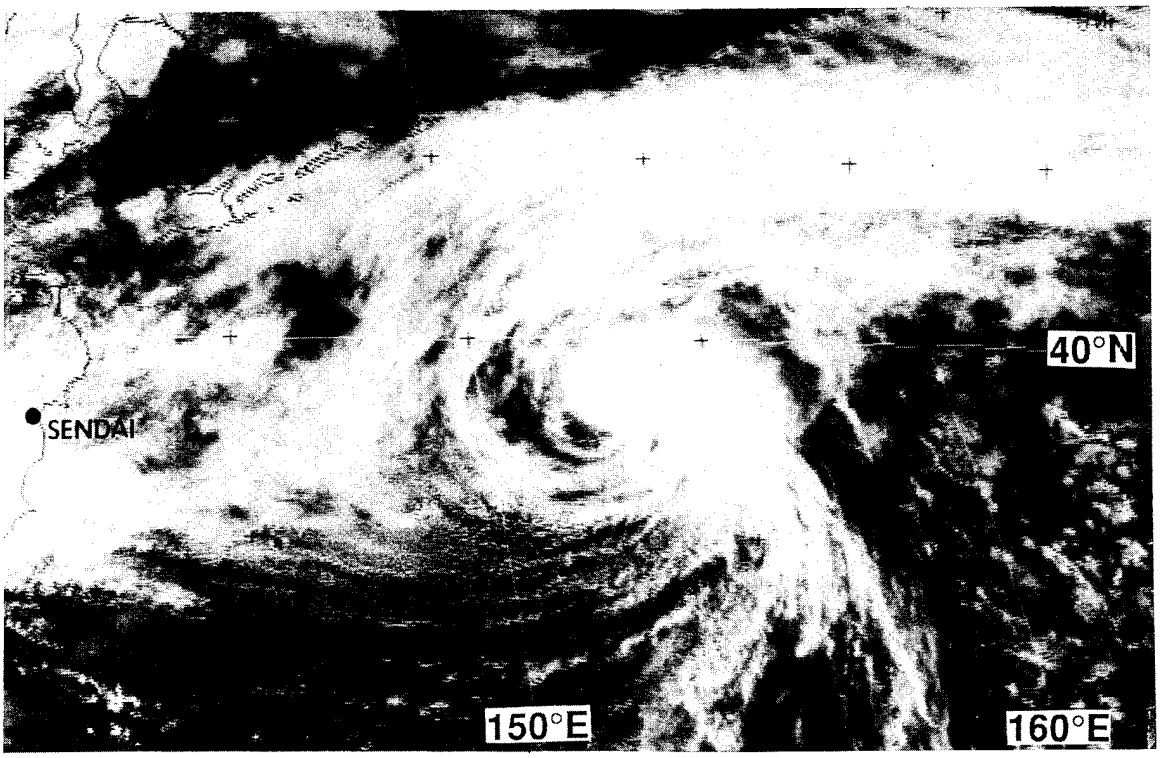

Figure 3-29-7 Central deep convection has been re-established as the merged Pat and Ruth begins its recurvature into midlatitudes (280031Z September visible GMS imagery).

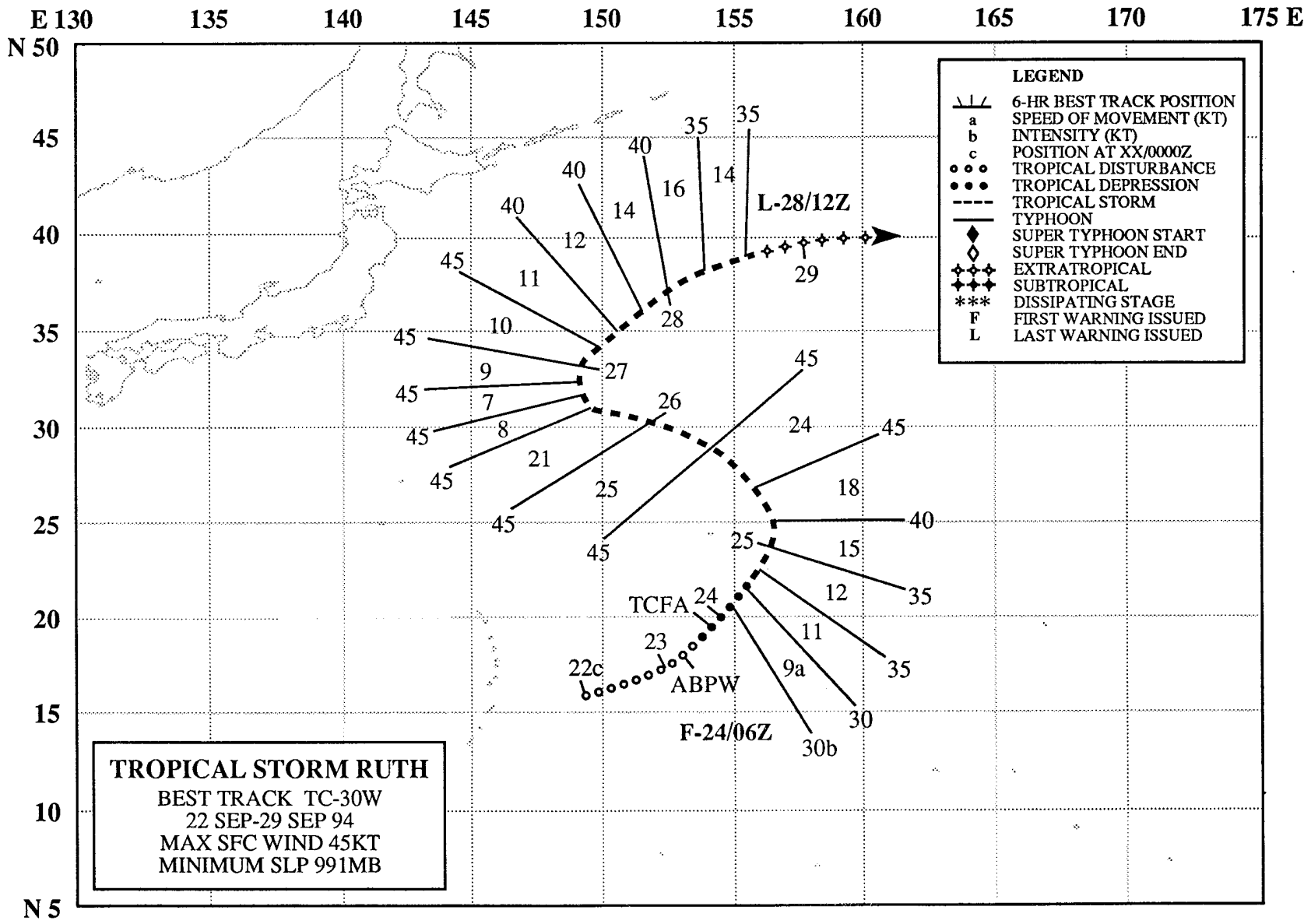
E 130
135
140
145
150
155
160
165
170
175 E
N 50
45
40
35
30
25
20
15
10
N 5
LEGEND
6-HR BEST TRACK POSITION
a SPEED OF MOVEMENT (KT)
b INTENSITY (KT)
c POSITION AT XX/0000Z
TROPICAL DISTURBANCE
TROPICAL DEPRESSION
TROPICAL STORM
TYPHOON
SUPER TYPHOON START
SUPER TYPHOON END
EXTRATROPICAL
SUBTROPICAL
*** DISSIPATING STAGE
F FIRST WARNING ISSUED
L LAST WARNING ISSUED
L-28/12Z
F-24/06Z
TCFA
ABPW
TROPICAL STORM RUTH
BEST TRACK TC-30W
22 SEP-29 SEP 94
MAX SFC WIND 45KT
MINIMUM SLP 991MB

TROPICAL STORM RUTH (30W)

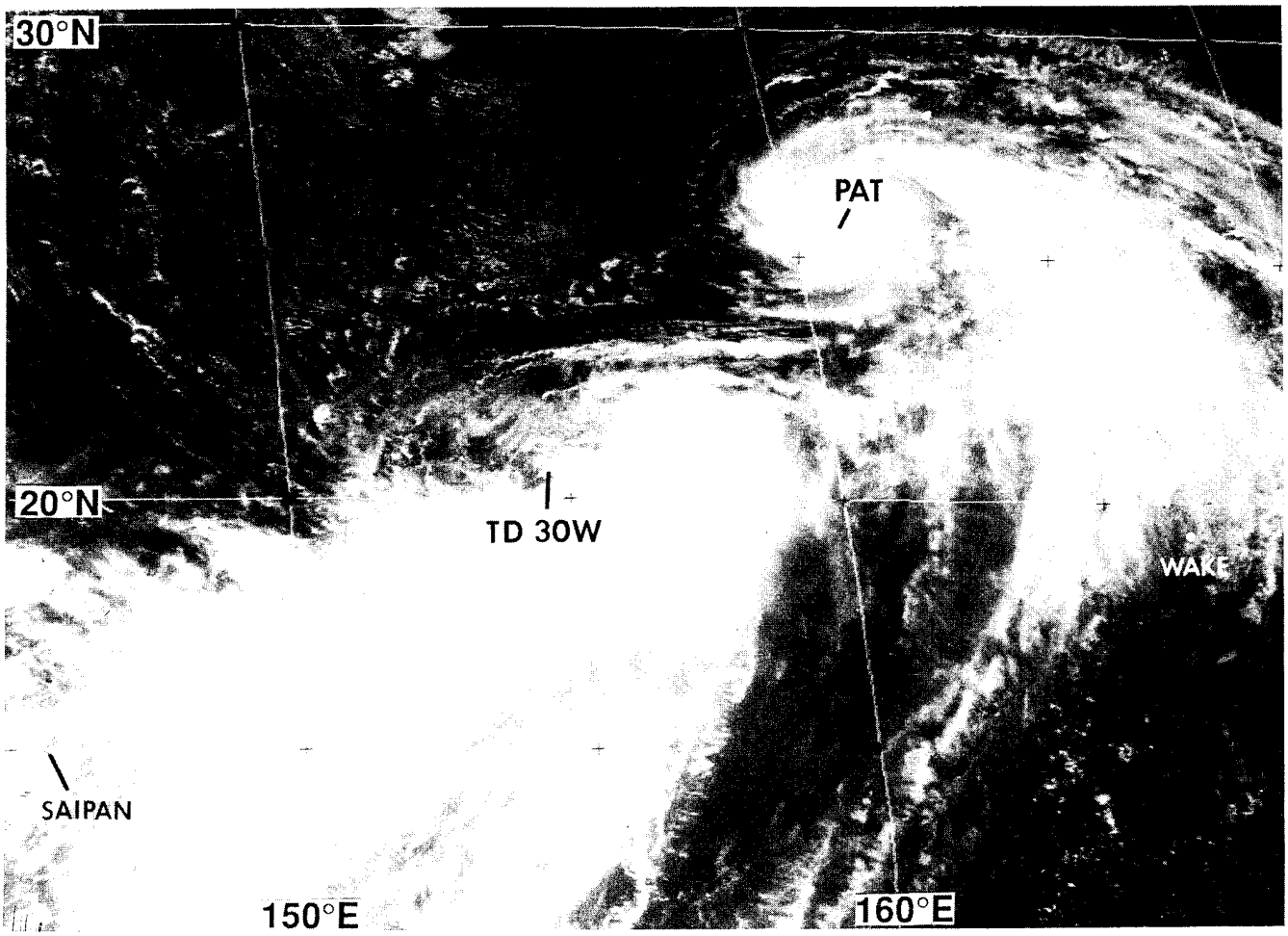

Figure 3-30-1 Cyclonically curved lines of deep convection and low-level cloud lines indicate that the tropical disturbance, which later became Tropical Storm Ruth, was intensifying (240131Z September visible GMS imagery).

I. HIGHLIGHTS

The symmetrical collapse of deep convection during the merger of Ruth with Pat (29W) is the first documented case of such an event (Lander 1995b). Ruth exhibited unusual motion: a north-oriented "S"-shaped track.

II. TRACK AND INTENSITY

Based on 24 hours of persistence, an area of deep convection (located along the axis of a reverse-oriented monsoon trough) was first identified as a tropical disturbance on the 230600Z September Significant Tropical Weather Advisory. Increased cyclonic curvature of the convective cloud bands in this tropical disturbance prompted the JTWC to issue a Tropical Cyclone Formation Alert at

231800Z. Continued improvement in the organization of the deep convection and the presence of well-defined, cyclonically curved, low-level cloud lines during the daylight hours of 24 September (Figure 3-30-1) led to the first warning on Tropical Depression 30W at 240600Z. The system was upgraded to Tropical Storm Ruth at 250600Z. Ruth initially moved northeastward under the steering influence of deep southwesterly monsoonal flow. As it moved northeastward, the separation distance between Ruth and Pat (29W) steadily decreased and a binary interaction ensued. The binary interaction culminated in merger, and at 261200Z, Ruth and Pat (29W) became one vortex. The merged Ruth and Pat (29W) then recurved and the final warning was issued at 281200Z.

III. DISCUSSION

For a complete discussion of the first documented case of the symmetrical collapse of the deep convection of both tropical cyclones during merger, see the discussion section in the summary of Typhoon Pat (29W).

IV. IMPACT

No reports of significant damage or fatalities were received.

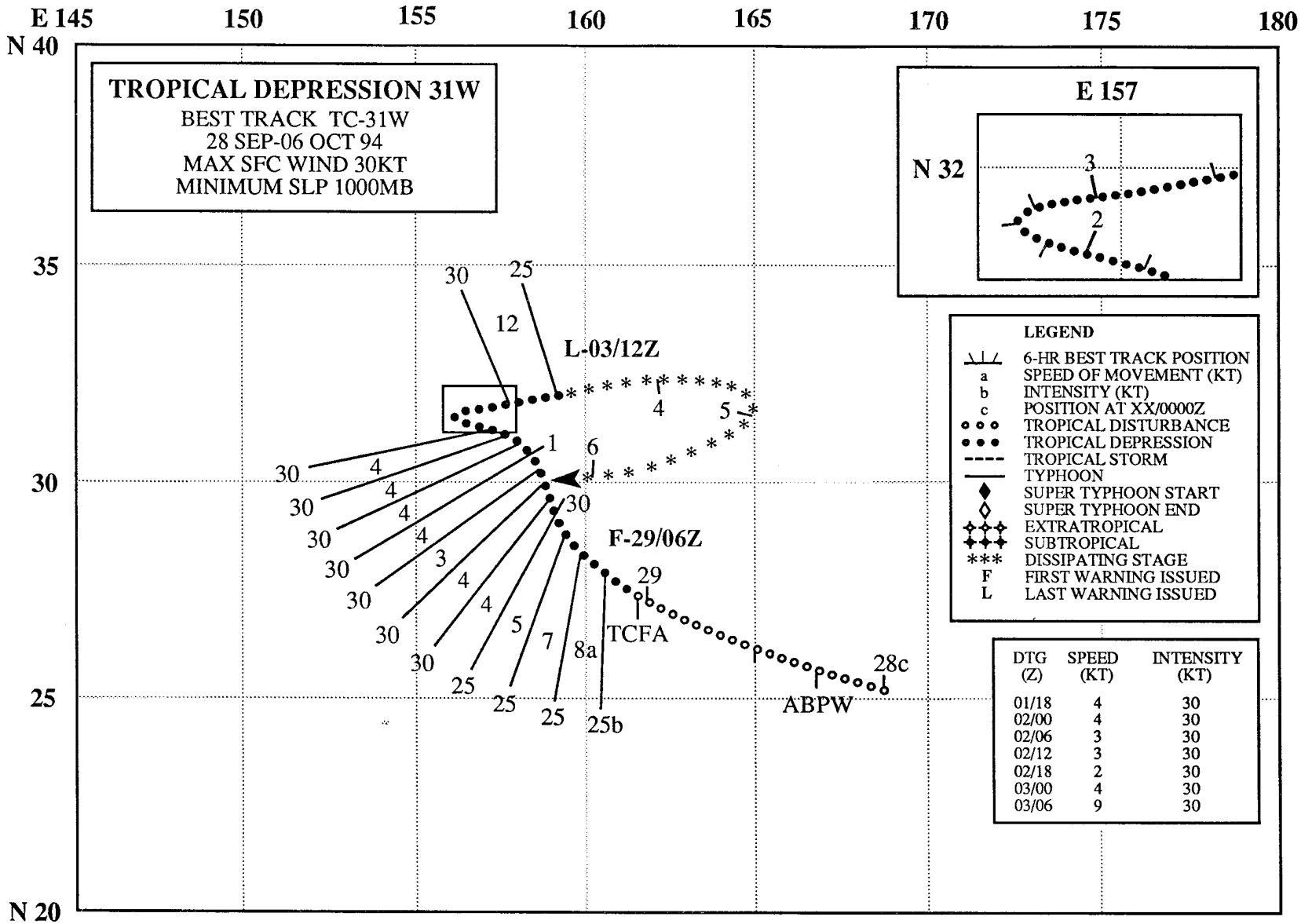

DTG (Z)	SPEED (KT)	INTENSITY (KT)
01/18	4	30
02/00	4	30
02/06	3	30
02/12	3	30
02/18	2	30
03/00	4	30
03/06	9	30

TROPICAL DEPRESSION 31W

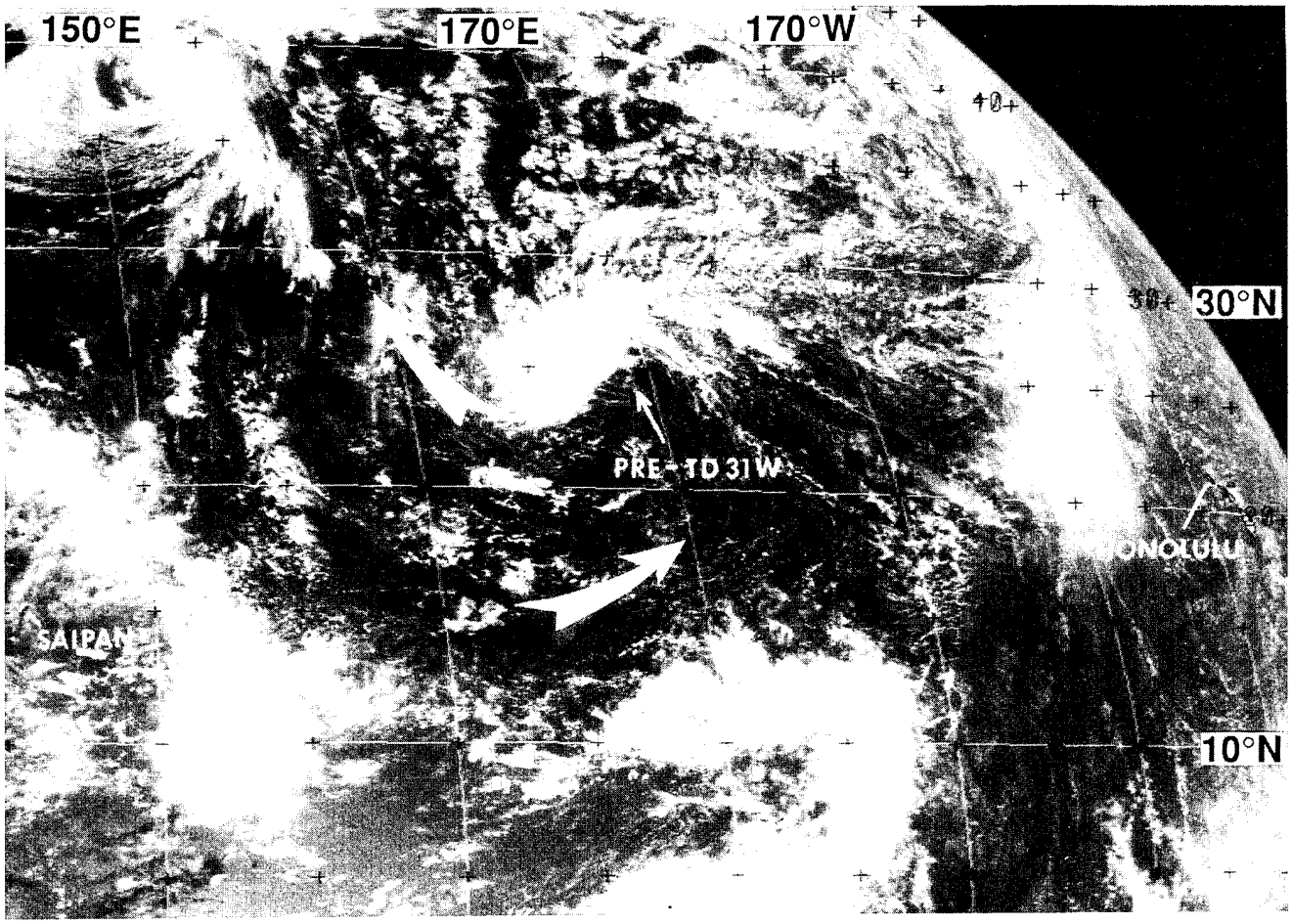

Figure 3-31-1 An area of deep convection located on the north side of an upper-level cold-core cyclonic vortex (i.e., a TUTT cell) precedes the formation of Tropical Depression 31W. Arrows indicate upper-tropospheric wind flow. (280031Z September GMS visible imagery.)

I. HIGHLIGHTS

Tropical Depression 31W was one of two tropical cyclones during 1994 — the other was Tropical Storm Yuri (36W) — that developed in direct association with a cyclonic vortex in the tropical upper tropospheric trough (TUTT) (i.e., a TUTT cell). TD 31W was a small tropical cyclone that developed at high latitude (25°N).

II. TRACK AND INTENSITY

During the last week of September, an area of persistent cloudiness associated with an upper-level trough was quasi-stationary northwest of the Hawaiian Islands. On 26 September, an upper-tropospheric cyclonic vortex detached from this trough and began to drift westward toward the international date line (i.e., it became a westward moving TUTT cell). Accompanying this TUTT cell was a small area of deep convection which was associated with some low-level cloud lines indicating the possibility of a low-level circulation. The TUTT cell moved rapidly westward, and crossed the international date line on 27 September. The small area of deep convection persisted on its north side (Figure 3-31-1), and it

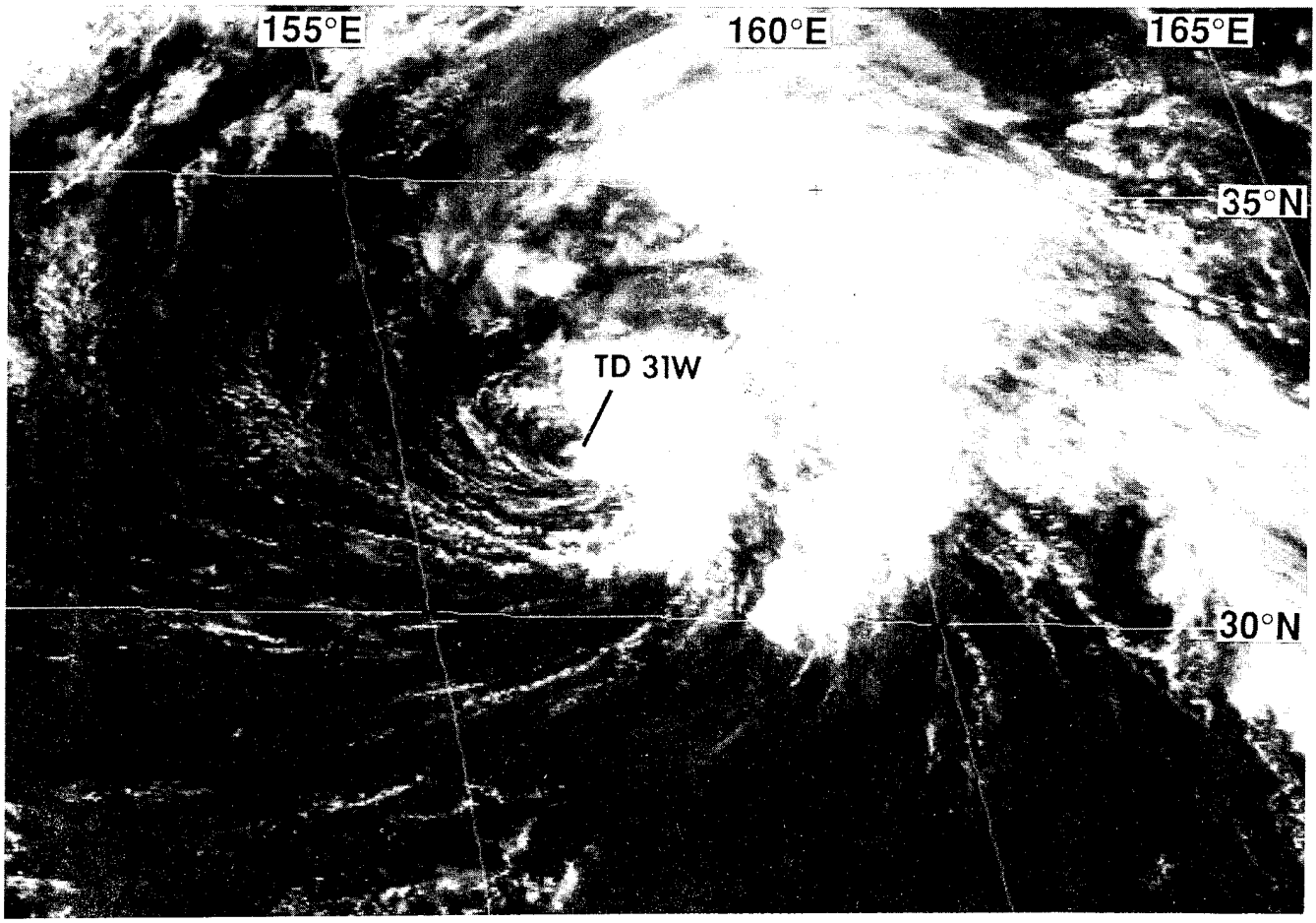

Figure 3-31-2 Well-organized low-level cloud lines accompany an area of deep convection as Tropical Depression 31W moves eastward and begins to dissipate (030031Z October visible GMS imagery).

was included on the 280600Z September Significant Tropical Weather Advisory. At 290600Z, the first warning was issued on Tropical Depression 31W. Remarks on this first warning included:

" . . . The tropical disturbance east of Marcus island [WMO 47991] has intensified into Tropical Depression 31W, This system is well organized but lacks any significant deep convection. Some moderate convection has developed around the system center and numerous low-level cloud lines were noted spiraling into the tight circulation. . . ."

Tropical Depression 31W failed to become a tropical storm. For most of its life it lacked significant deep convection. Often, it was merely composed of tightly wound low-level cloud lines. After the system recurved at 021200Z October, it acquired significant deep convection and exhibited its most impressive satellite signature (Figure 3-31-2). The final warning was issued at 031200Z, as the system moved eastward and weakened.

III. DISCUSSION

The formation of Tropical Depression 31W in direct association with a cold low in the tropical upper tropospheric trough (i.e., a TUTT cell) is hypothesized to be a distinct mechanism of tropical cyclogenesis that has not been previously addressed (see also the discussion section in Yuri's (36W) summary). The closest description of this process is Sadler (1976). However, in Sadler's model, the

tropical cyclone forms about 1000 km to the southeast of a TUTT cell where diffluent upper-level southwesterly wind enhances deep convection (Figure 3-31-3a). The TUTT cell also acts to enhance upper-level outflow from the incipient tropical cyclone. In Sadler's model, the tropical cyclone may originate in the low-level monsoon trough, and as such, it is indirectly affected by the TUTT cell. Tropical cyclones like Tropical Depression 31W and Yuri (36W), form near the core of the TUTT cell, embedded in low-level tradewind flow at sub-tropical latitudes (i.e., north of 20°N) (Figure 3-31-3b). The cloud systems of such tropical cyclones tend to be isolated in the cloud-free zone between the cloudiness associated with the monsoon trough and the extensive cloudiness associated with the polar front.

IV. IMPACT

No reports of damage or injuries were received.

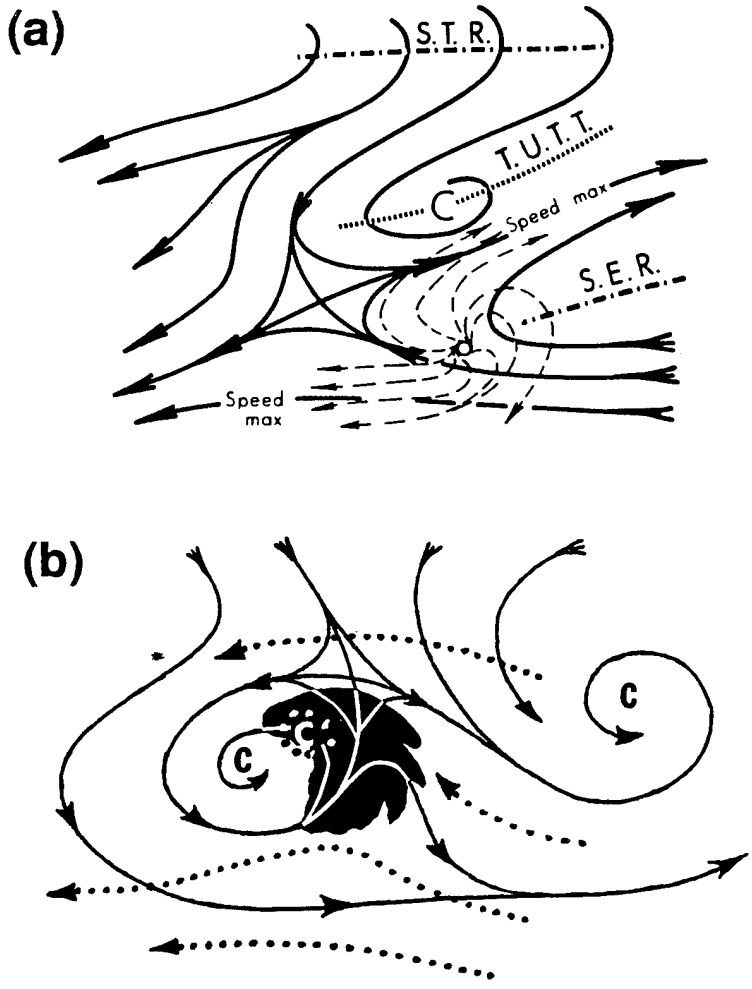

Figure 3-31-3 (a) Sadler's (1976) model of the indirect role of a TUTT cell in tropical cyclogenesis. S.T.R. = subtropical ridge, T.U.T.T. = tropical upper tropospheric trough, and S.E.R. = sub-equatorial ridge. (b) Schematic illustration of the direct role of a TUTT cell in the genesis of Tropical Depression 31W and of Tropical Storm Yuri (36W). Solid lines are 200 mb streamlines, dotted lines are low-level flow. Black-shaded area shows deep convection.

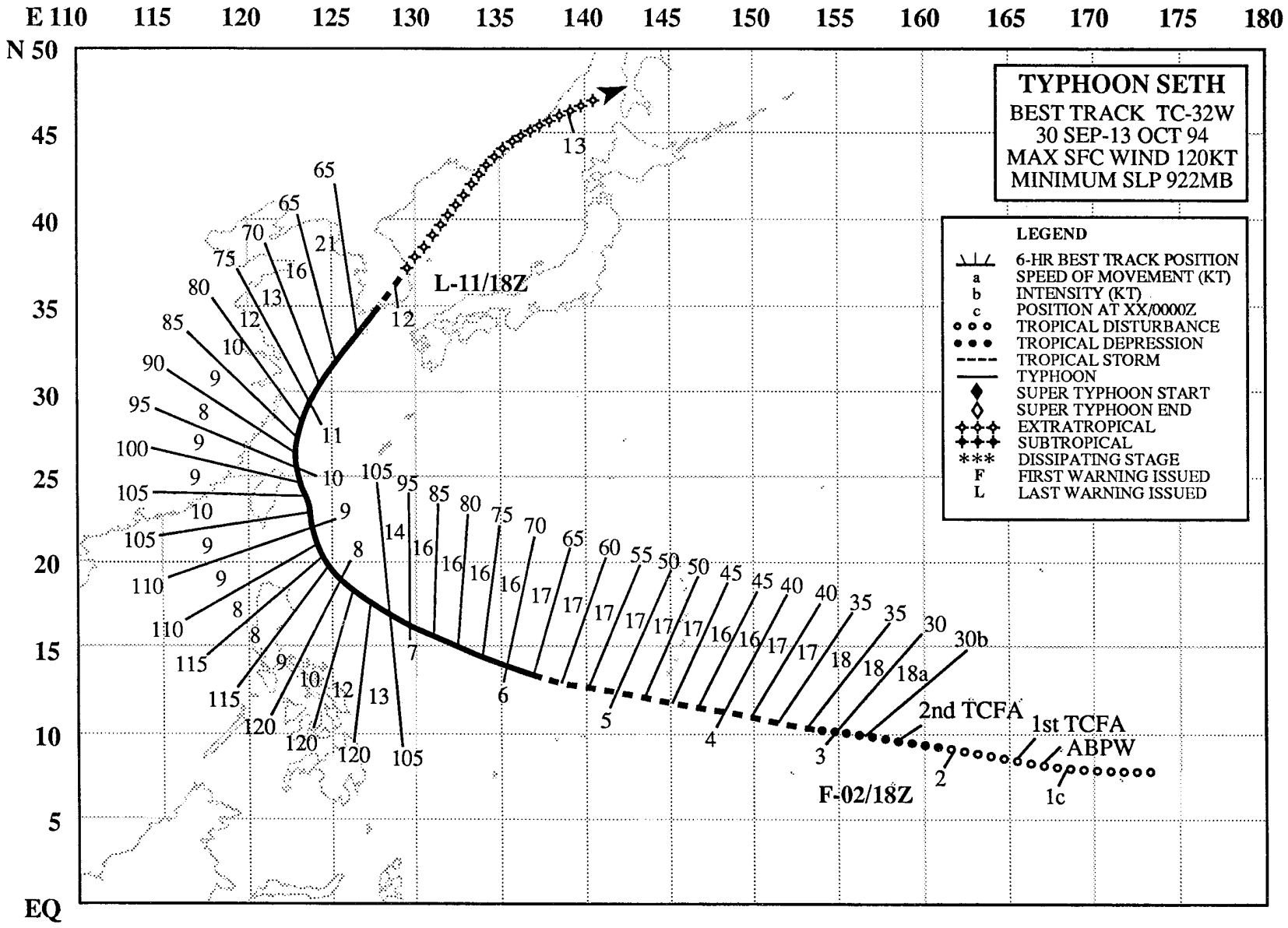
E 110 115 120 125 130 135 140 145 150 155 160 165 170 175 180
N 50 45 40 35 30 25 20 15 10 5 EQ
TYPHOON SETH
BEST TRACK TC-32W
30 SEP-13 OCT 94
MAX SFC WIND 120KT
MINIMUM SLP 922MB
LEGEND
6-HR BEST TRACK POSITION
a SPEED OF MOVEMENT (KT)
b INTENSITY (KT)
c POSITION AT XX/0000Z
TROPICAL DISTURBANCE
TROPICAL DEPRESSION
TROPICAL STORM
TYPHOON
SUPER TYPHOON START
SUPER TYPHOON END
EXTRATROPICAL
SUBTROPICAL
*** DISSIPATING STAGE
F FIRST WARNING ISSUED
L LAST WARNING ISSUED
L-11/18Z
F-02/18Z
2nd TCFA
1st TCFA
ABPW
1c
2
3
4
5
6
7
12
13
30b
18a

178

TYPHOON SETH (32W)

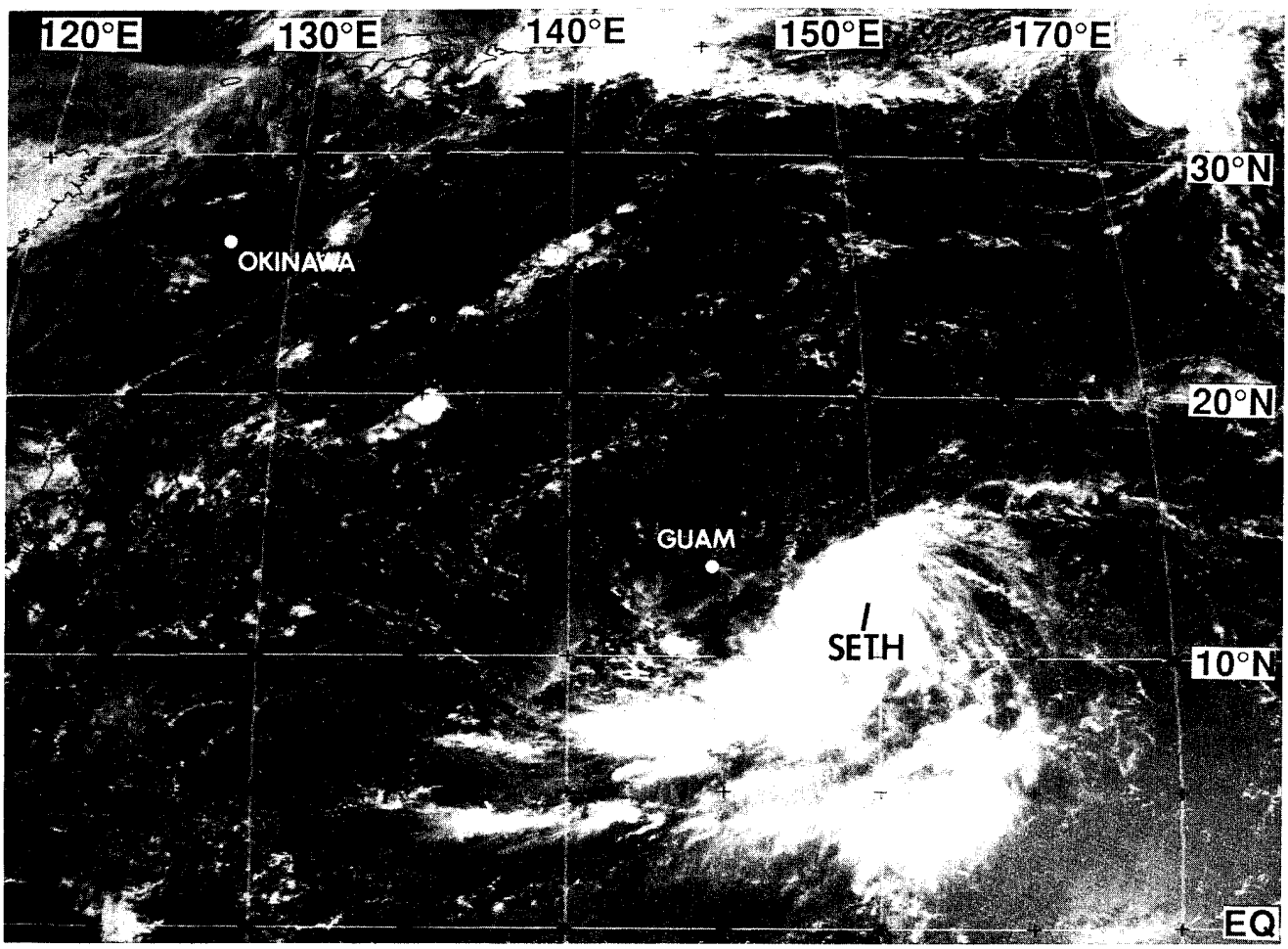

Figure 3-32-1 Seth and accompanying rain bands are seen isolated in an unusually cloud-free tropics (032331Z October visible GMS imagery).

I. HIGHLIGHTS

Seth originated from a tropical disturbance at low latitude in the Marshall Islands and moved on a typical recurving track. After recurving east of Taiwan, Seth moved northeastward and impacted the Korean peninsula. During the period of Seth's extra-tropical transition, as it moved through the Yellow Sea toward Korea, intensity estimates made from satellite imagery were low and illustrate the need for the development of new diagnostic techniques to address extra-tropical transition.

II. TRACK AND INTENSITY

Seth developed from an isolated area of deep convection in the Marshall Islands and tracked across the western North Pacific during a period when the basin was relatively cloud-free, and the monsoon circulation (which had earlier been extremely active) had become very weak (Figure 3-32-1). Synoptic data at 010000Z October indicated that a low-level cyclonic circulation center developed in the Marshall Islands in association with this area of deep convection. This tropical disturbance was first mentioned on the 010600Z October Significant Tropical Weather Advisory. At 011100Z, a Tropical Cyclone Formation Alert (TCFA) was issued by JTWC. Remarks in this TCFA included:

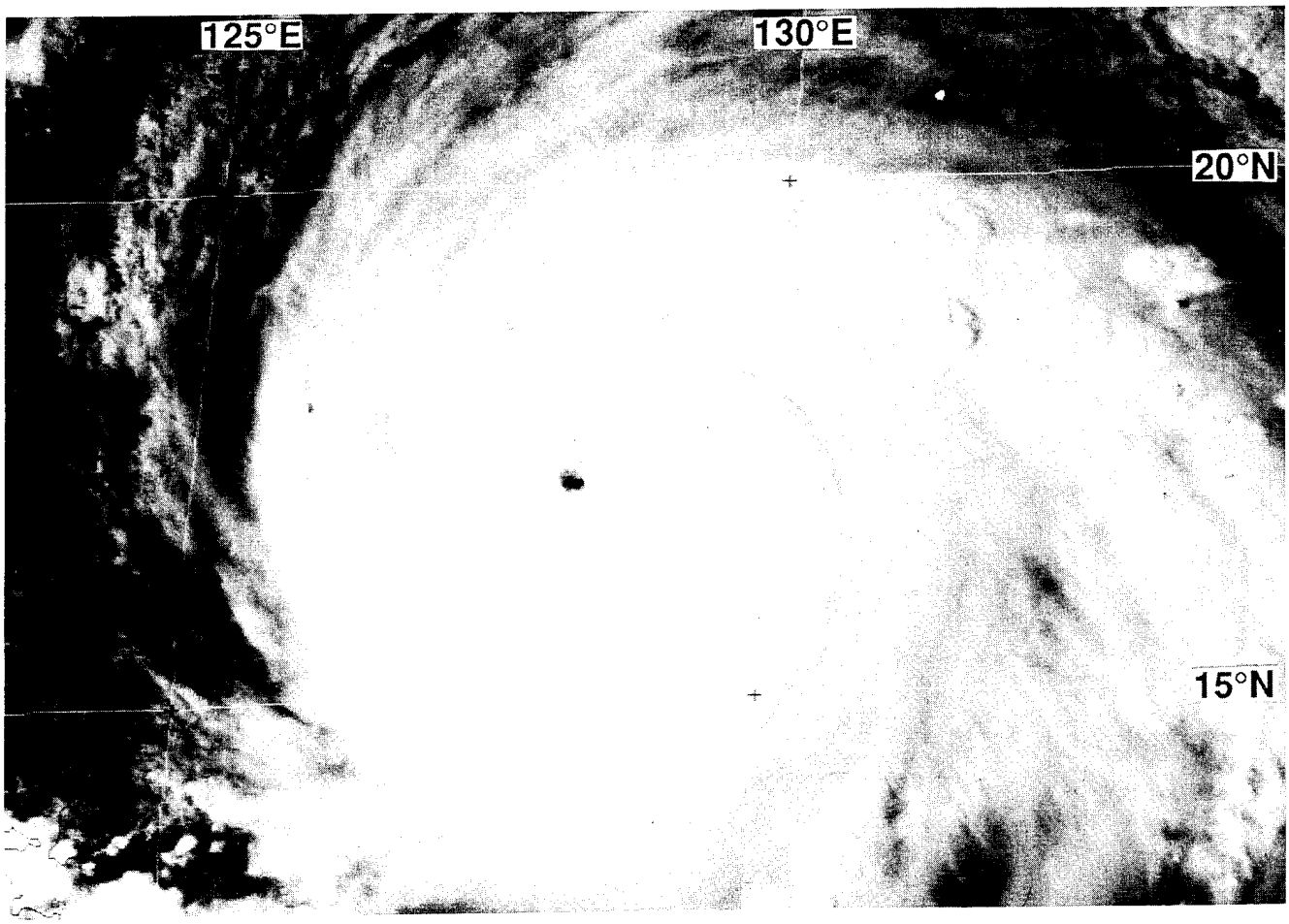

Figure 3-32-2 Nearing its peak intensity, Seth's eye becomes well-defined (070631Z October visible GMS imagery).

". . . [The] tropical disturbance passing through the Marshall Islands has exhibited signs of development over the past 12 hours. Satellite imagery and synoptic data indicate a persistent low-level circulation center . . . 24 hour pressure falls at Kwajalein were close to three millibars as the system passed by. . . . If the system continues moving at its present rapid forward speed, the potential for further development will be reduced. . . ."

Failing to intensify, a second TCFA was issued 24 hours later (at 021100Z). The first warning on Tropical Depression 32W was issued at 021800Z when satellite imagery indicated that deep convection associated with the system had increased and become more centralized. A normal rate of intensification of one "T" number per day ensued as Seth moved on a west-northwestward track. Typhoon intensity was attained at 051800Z. Turning gradually to the northwest, Seth steadily intensified (Figure 3-32-2) and reached peak intensity of 120 kt (62 m/sec) at 071200Z. Seth then moved on a broad recurving track, passing to the east of Taiwan and later over the Korean Peninsula. The point of recurvature occurred at 100600Z when Seth was 90 nm (170 km) north-northeast of Taipei. By this time Seth's intensity dropped to 90 kt (46 m/sec). Seth accelerated as it approached the Korean Peninsula. At 111800Z, it passed directly over the island of Cheju Do (located in the Yellow Sea about 100 km south of the Korean Peninsula). Moving at a forward speed in excess of 30 kt (55 km/hr), the system crossed the Korean Peninsula, entering the Sea of Japan shortly after 120000Z. Based upon the acquisition of extratropical characteristics, the final JTWC warning was issued at 111800Z. After entering the Sea of

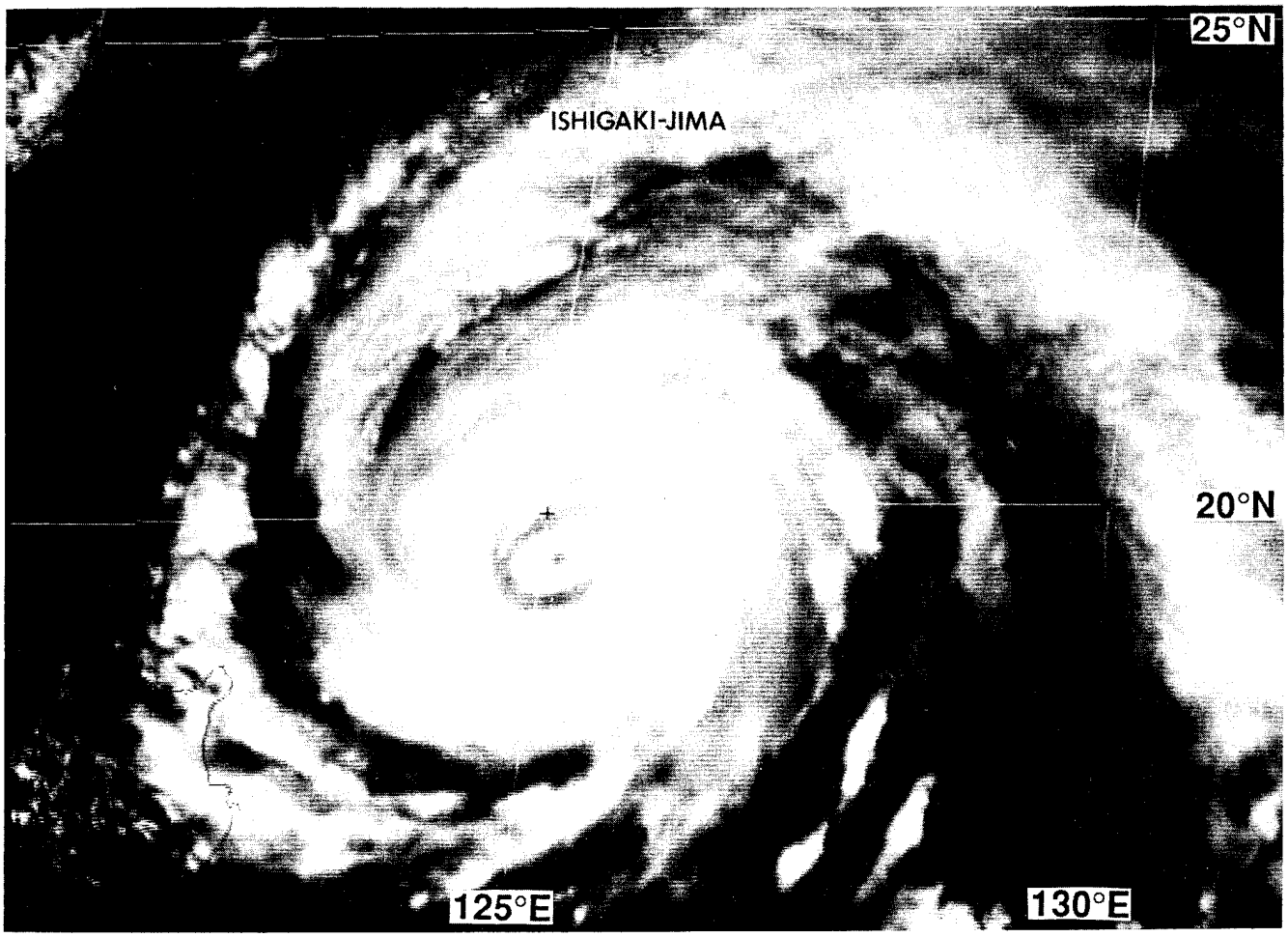

Figure 3-32-3 An eye within an eye. Concentric wall clouds appear as Seth begins to weaken (080331Z October visible GMS imagery).

Japan, the system continued to move rapidly northeastward toward the Kamchatka Peninsula with winds in excess of 50 kt (26 m/sec) until 130000Z.

III. DISCUSSION

a. Concentric eye walls

Approximately 30 hours after attaining peak intensity, Seth acquired well-defined concentric eye walls (Figure 3-32-3). After another 24 hours, and with continued weakening, vestiges of the inner eye wall — seen clearly in Figure 3-32-3 — were still present in satellite imagery. At this time (approximately 090000Z), Seth came within range of the Hualien radar. At first, poorly defined concentric eye walls appeared on the radar image (not shown). Then, while moving northward through the southwestern end of the Ryukyu Islands , Seth's eye became quite ragged.

Well-defined concentric eye-walls (Figure 3-32-3) are rarely seen in conventional satellite imagery. The JTWC suspects that they are more common than indicated by their rate of appearance in satellite imagery. For example, even though they were obscured by cirrus in satellite imagery, well-defined concentric eye walls appeared on radar as Gladys (20W) approached Hualien (see the discussion of concentric eye walls in the Gladys summary).

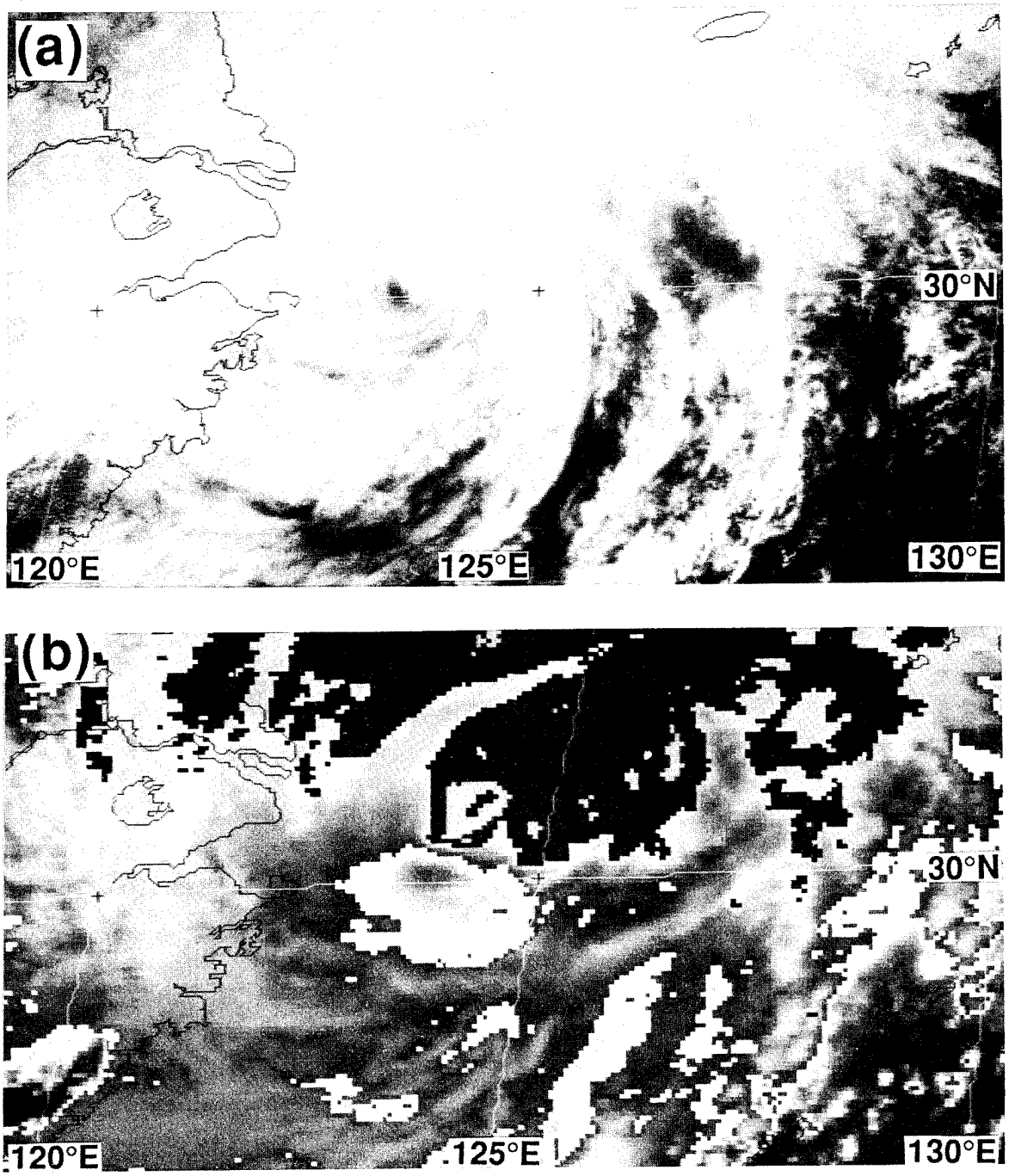

Figure 3-32-4 Satellite intensity estimates begin to decrease as Seth's central dense overcast is sheared away to the north side of the low-level circulation center by southwesterly winds aloft as the process of extra-tropical transition begins: (a) 110131Z October visible GMS imagery, and (b) 110131Z October enhanced infrared GMS imagery. The enhancement is the Basic Dvorak (BD) curve.

b. Extratropical transition

One of the more difficult forecast and warning challenges faced by the JTWC for Seth occurred as the typhoon approached the Korean peninsula. Eighteen hours prior to landfall on the peninsula, Seth began to lose its central deep convection while in the process of transitioning into an extratropical low (Figure 3-32-4a,b). Applying Dvorak's satellite intensity analysis to the transitioning system, the diag-

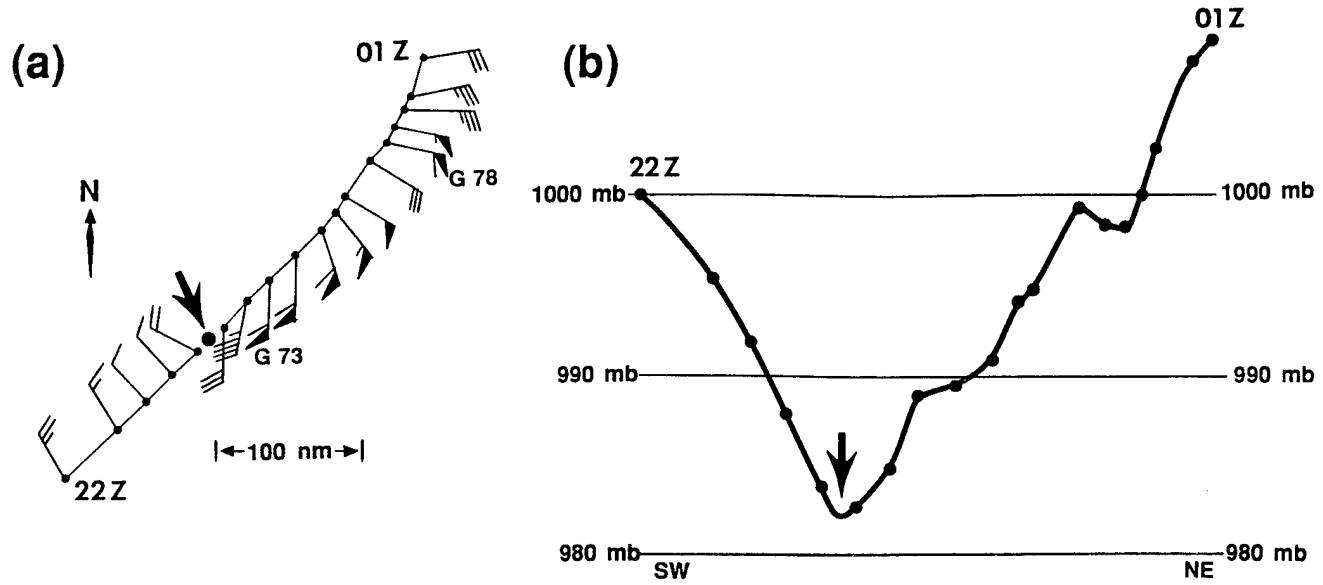

Figure 3-32-5 Schematic depictions of (a) winds and (b) sea-level pressure recorded at Cheju Do (WMO 47187) during Seth's passage. The data are plotted with respect to Seth's center (indicated by an arrow).

nosed intensity began to fall to unrealistically low values (Table 3-32-1). Wind and pressure reports from Cheju Do (WMO 47187) (Figure 3-32-5a,b), and from other stations, indicated that Seth retained typhoon intensity up to its landfall on the southern coast of South Korea.

Application of Dvorak's satellite intensity estimates to Seth as it began to acquire extratropical characteristics yielded values which were as much as three "T" numbers below the real-time intensity (Table 3-32-1). In an attempt to produce more accurate intensity estimates (from satellite imagery) on recurving tropical cyclones that are undergoing extra-tropical transition, the subtropical classification scheme of Hebert and Poteat (1975) has been used. For Seth, this scheme yielded "ST" numbers which corresponded to intensities far lower than those observed. This is not surprising since the scheme developed by Hebert and Poteat was intended to be applied to intensifying midlatitude lows that have acquired organized deep convection. The attempt to use Hebert and Poteat's system in reverse (i.e. on tropical cyclones that are becoming extratropical following recurvature) is most probably a misapplication. Analysts at the JTWC also tried to apply to the recurving Seth, a technique for estimating the intensity of mid-latitude cyclones from satellite imagery (Smigielski and Mogil 1992). Again, it was difficult to derive intensities high enough.

IV. IMPACT

At 041800Z, Seth , with a best-track at an intensity of 50 kt (26 m/sec), passed 102 nm (190 km) south of Guam, where a peak wind gust of 41 kt (21 m/sec) was recorded. No reports of damage or injuries were received. The next region affected by Seth was Taiwan and the southern Ryukyu Islands. A peak gust of 110 kt (57 m/sec) and a minimum pressure of 952 mb was recorded at Yonaguni Jima (WMO 47912) as the western inner edge of Seth's eye-wall cloud passed over. No reports of damage or injuries were received from this region. At Cheju Do (WMO 47187), a peak wind gust of 78 kt (40 m/sec) was recorded as Seth approached from the southwest. Wind gusts to near 70 kt (36 m/sec) and rainfall in excess of 300 mm (11.8 inches) affected portions of South Korea. Torrential rains near the

eastern port city of Samchok resulted in flooding that killed one person, forced the evacuation of 550 people, inundated 178 houses and interrupted rail traffic. However, the rain from Seth brought relief to many drought-parched areas of South Korea.

Table 3-32-1 Intensity estimates derived from satellite imagery during Seth's extratropical transition. In the code, T = Dvorak tropical numbers, ST = Hebert and Poteat subtropical numbers, and the number that follows the "/" is the current intensity, which is always held higher in cases when the cyclone is weakening.

Time (Z)	Code	Best Track Intensity (kt)	Intensity (kt)
102330Z	T 3.0/4.0	65	75
110144Z	T 3.0/4.0	65	70
110232Z	T 3.5/4.0	65	70
110530Z	T 2.5/3.5	55	70
111115Z	T 1.5/2.5	35	65
111130Z	ST 1.5/2.5	35	65
111151Z	T 1.5/2.5	35	65
111300Z	ST 1.0/2.0	30	65
111730Z	ST 1.0/2.0	30	65
112330Z	ST 1.0/2.0	30	60
120125Z	ST 1.0/1.0	25	60
120530Z	ST 1.0/2.0	30	60

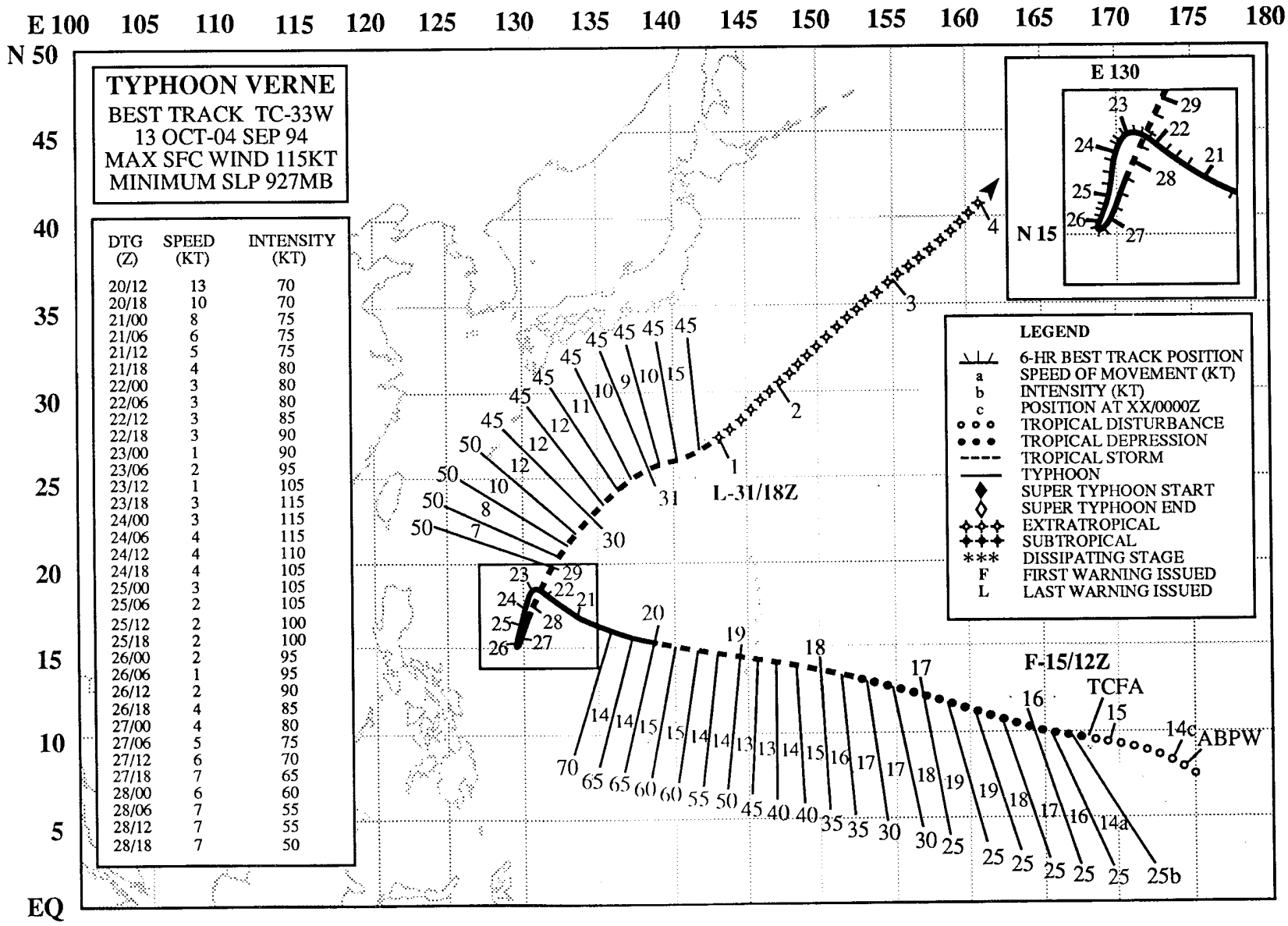
E 100 105 110 115 120 125 130 135 140 145 150 155 160 165 170 175 180
N 50 45 40 35 30 25 20 15 10 5 EQ
TYPHOON VERNE
BEST TRACK TC-33W
13 OCT-04 SEP 94
MAX SFC WIND 115KT
MINIMUM SLP 927MB
DTG (Z) SPEED (KT) INTENSITY (KT)
20/12 13 70
20/18 10 70
21/00 8 75
21/06 6 75
21/12 5 75
21/18 4 80
22/00 3 80
22/06 3 80
22/12 3 85
22/18 3 90
23/00 1 90
23/06 2 95
23/12 1 105
23/18 3 115
24/00 3 115
24/06 4 115
24/12 4 110
24/18 4 105
25/00 3 105
25/06 2 105
25/12 2 100
25/18 2 100
26/00 2 95
26/06 1 95
26/12 2 90
26/18 4 85
27/00 4 80
27/06 5 75
27/12 6 70
27/18 7 65
28/00 6 60
28/06 7 55
28/12 7 55
28/18 7 50
E 130
N 15
LEGEND
6-HR BEST TRACK POSITION
a SPEED OF MOVEMENT (KT)
b INTENSITY (KT)
c POSITION AT XX/0000Z
TROPICAL DISTURBANCE
TROPICAL DEPRESSION
TROPICAL STORM
TYPHOON
SUPER TYPHOON START
SUPER TYPHOON END
EXTRATROPICAL
SUBTROPICAL
*** DISSIPATING STAGE
F FIRST WARNING ISSUED
L LAST WARNING ISSUED
L-31/18Z
F-15/12Z
TCFA
ABPW

TYPHOON VERNE (33W)

I. HIGHLIGHTS

Typhoon Verne was a relatively long-lived tropical cyclone that passed within range of Guam's NEXRAD. Several special cross-sections of reflectivity and radial velocity were obtained through Verne's center and peripheral cloud bands. Verne underwent unusual motion in the Philippine Sea: for over seven days it meandered within 150 nm (280 km) of 17°N ; 130°E.

II. TRACK AND INTENSITY

During the first week of October, the deep tropics of the western North Pacific became inactive (Figure 3-33-1a). Higher-than-normal pressure accompanied a reduction in deep convection. By mid-October, deep convection began to increase in low latitudes, especially east of 140°E, and an active monsoon trough formed along about 10°N (Figure 3-33-1b). By the third week of October, this monsoon trough evolved into a chain of four tropical cyclones: Teresa (34W), Verne, Wilda (35W), and Yuri (36W) (Figure 3-33-1c).

The tropical disturbance that became Verne was first mentioned on the 131800Z October Significant Tropical Weather Advisory when an area of deep convection associated with a broad low-level cyclonic circulation formed in the Marshall Islands. At 150800Z, a Tropical Cyclone Formation Alert was issued when this disturbance showed signs of increased organization. Continued improvement in the convective banding features prompted the first warning at 151200Z. Tropical Depression 33W moved west-northwestward along the axis of the monsoon trough, and its intensification rate remained slow. At 171800Z Tropical Depression 33W was upgraded to Tropical Storm Verne. Continuing on a steady west-northwestward track, Verne passed 50 nm north of Guam during the early morning hours of October 19. Verne acquired a CDO and its estimated intensity was 50 kt (26 m/sec). At 200000Z Verne was upgraded to a typhoon based upon intensity estimates from satellite imagery. Verne continued on a steady west-northwestward track until 210600Z when it abruptly slowed. It then meandered within 150 nm of 17°N ; 130°E for seven days. Verne reached a peak intensity of 115 kt (59 m/sec) at 231800Z while moving slowly southward in the Philippine Sea (Figure 3-33-2). After Verne turned northward at 260600Z, it steadily weakened, and by 280600Z it had dropped below typhoon intensity. The final warning was issued at 010000Z November as Verne recurved east of Japan and became extratropical.

III. DISCUSSION

a. NEXRAD's view of Verne

Verne's closest point of approach to Guam was 50 nm (90 km) to the north at 180000Z. In addition to Verne's CDO, peripheral cloud bands tracked well-within the 124 nm (230 km) range of the NEXRAD's Doppler velocity sensor. Many radar products were examined, including: the base reflectivity, the base velocity, animation of the base reflectivity, convective cell tracking, and the one- and three-hour integrated precipitation products.

1. STORM-TOTAL PRECIPITATION

For almost two days (180420Z to 200030Z), Guam's NEXRAD provided a continuous integration of the precipitation associated with Verne (Figure 3-33-3). NEXRAD-estimated rainfall of over one inch fell in a 120 nm (220 km)-wide swath along Verne's track. Maximum estimated storm-total rainfall values of four to six inches occurred in a narrower swath. The NEXRAD underestimated storm-total pre-

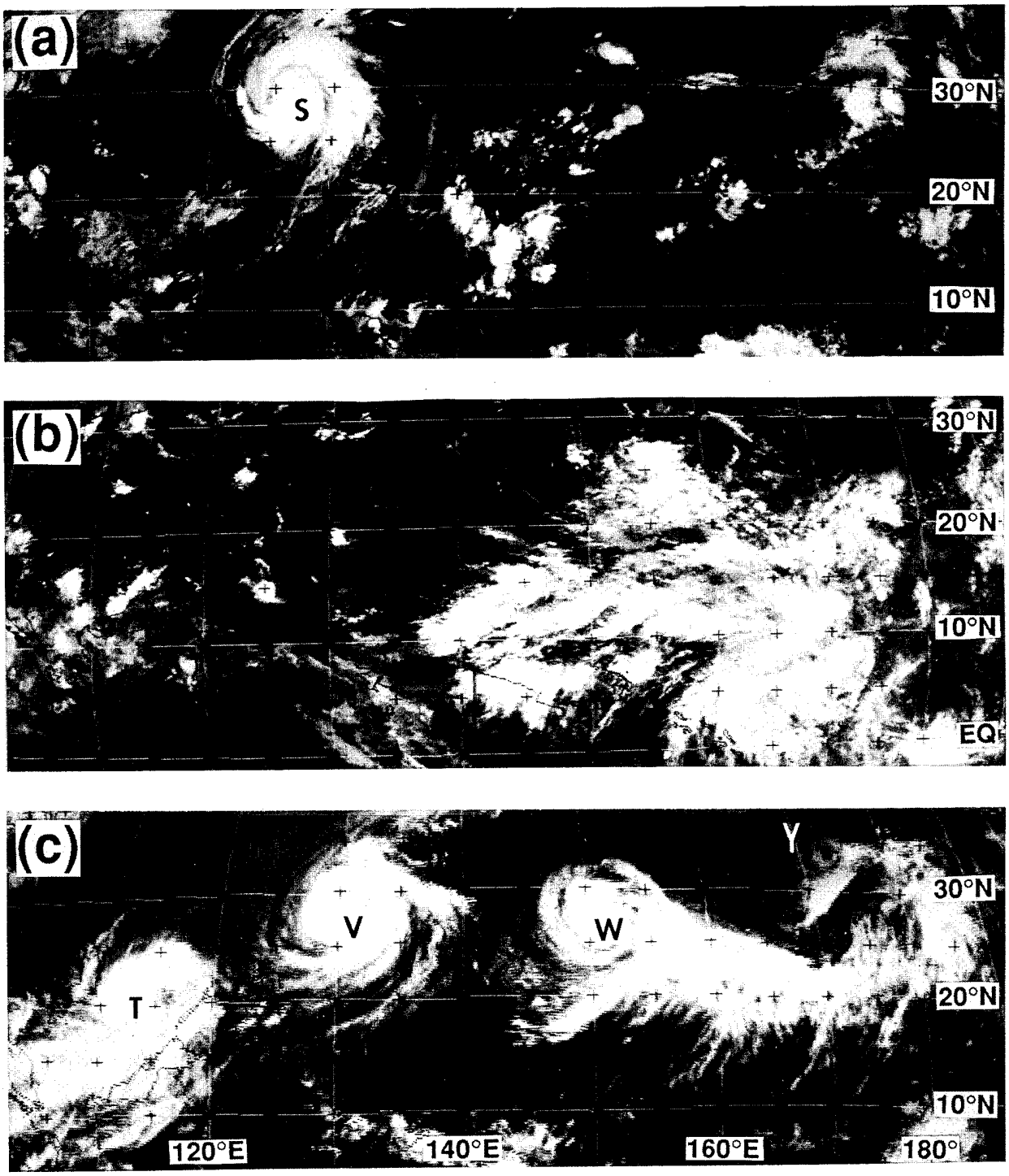

Figure 3-33-1 Evolution of the large-scale distribution of deep convection in the western North Pacific during October. (a Things are very quiet in the tropics as Seth (S) moves out of the region (080031Z October infrared GMS imagery). (b) An increase in the amount of deep convection accompanies near-equatorial westerlies east of 140°E (140031Z October infrared GMS imagery). (c) Four named tropical cyclones — T = Teresa (34W), V = Verne, W = Wilda (35W) and Y = Yuri (36W) — are lined up WSW-ENE across the western North Pacific basin (230531Z October infrared GMS imagery).

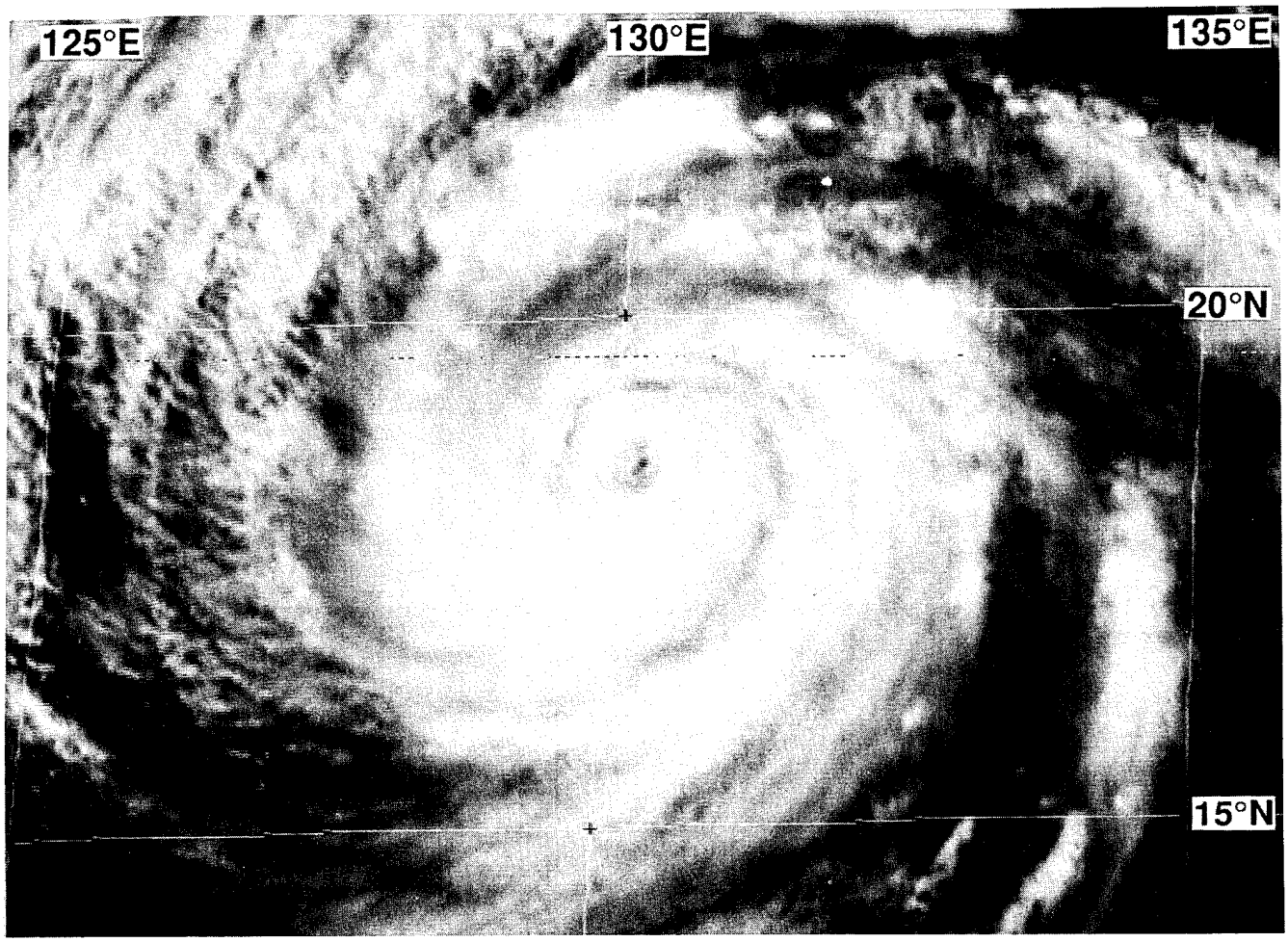

Figure 3-33-2 Verne's eye is becoming better defined as it nears its peak intensity (230424Z October visible GMS imagery).

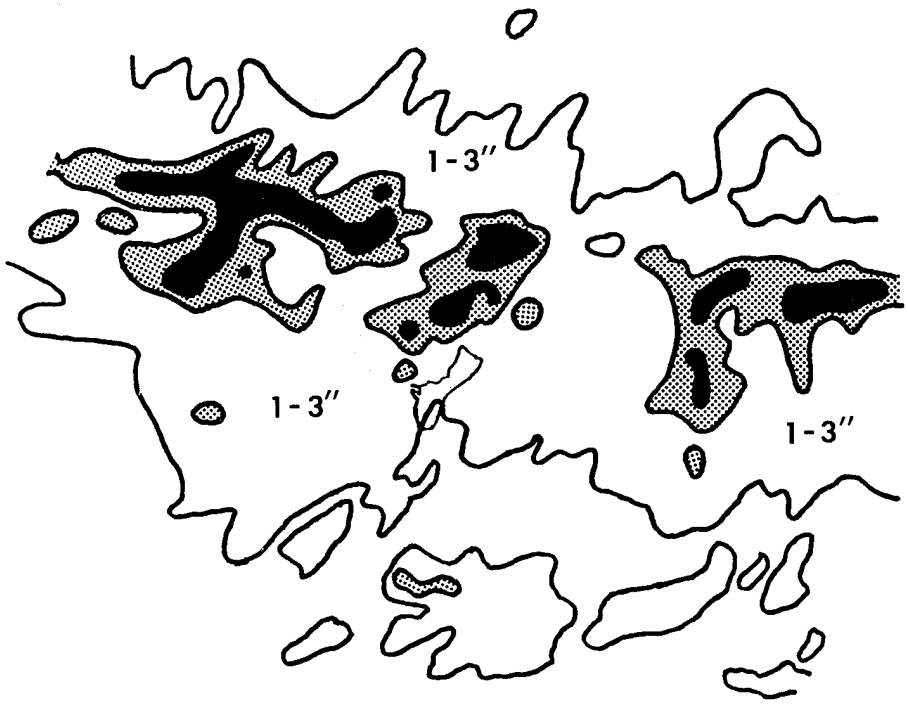

Figure 3-33-3 Estimated precipitation deposited by Verne as it tracked north of Guam (NEXRAD storm-total precipitation algorithm for the period 180420Z to 200030Z October). Outer contour = 1", shaded region received between 3" and 4", black regions received 4" or more.

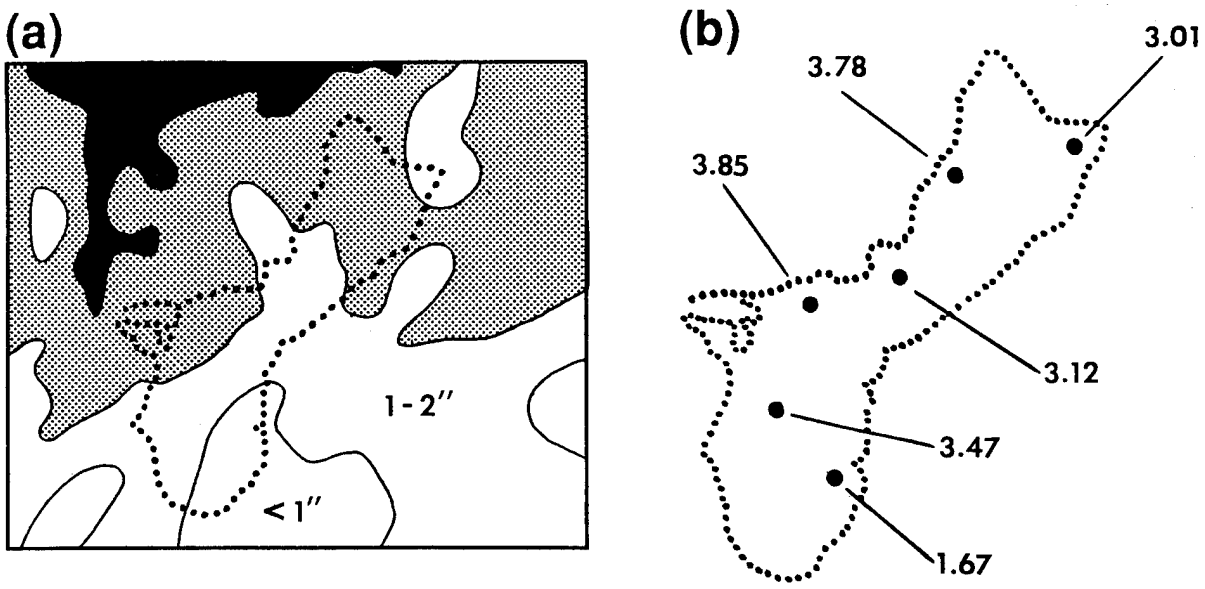

Figure 3-33-4 (a) Enlargement of the Guam region showing NEXRAD storm-total precipitation during Verne. Outer contour = 1", shaded region received between 2" and 3", black region received 3" or more. (b) Storm-total precipitation during Verne measured on Guam.

cipitation by 33% to 50% when compared to rainfall measured on Guam (Figure 3-33-4a,b). In almost all heavy rain events on Guam for which NEXRAD storm-total precipitation estimates were available for comparison to actual observations from around the island, the NEXRAD estimates are short by 25%-50% of the measured values. Despite these under-estimations, the rainfall distribution shown by NEXRAD has agreed quite well with the observed distribution.

2. PATTERN AND EVOLUTION OF THE WIND AND DEEP CONVECTION

When Verne passed to the north of Guam, it was a tropical storm with a satellite intensity estimate of 50 kt (26 m/sec). Its satellite-observed structure was a CDO pattern with a banding feature (Figure 3-33-5). The thick cirrus canopy of Verne's CDO in early morning, low-sun-angle, visible satellite imagery (not shown) was seen to have an overshooting convective tower embedded in rather featureless dense cirrus. The dense cirrus obscured highly organized lower-level cloud structures as observed by the NEXRAD. The base reflectivity, vertical cross-sections through Verne's core, and the echo-top product obtained from Guam's NEXRAD showed that Verne was composed of a central arc of deep convection wrapping roughly half-way around the southeastern semi-circle of Verne's cloud-free center. This deep convection rose to at least 60,000 ft (18 km) in one convective cell (i.e., hot tower) on the eastern side of Verne's inner core (Figure 3-33-6). This convective hot tower was not steady-state, but was observed to go through three episodes of intense build-up followed by a period of weakening. With each pulse of the central hot tower, the inner-core convection became more organized and nearly formed an eye wall. As the hot tower weakened, the curvature of the inner-core convection lessened. In synchrony with the pulses of the inner-core hot tower, the reflectivity in the nearest rainband to the south of the inner core intensified, then subsided.

Even the wind structure of Verne's inner core was affected by the pulsing of Verne's central hot tower. Prior to a major pulse of the hot tower when Verne was near its closest point of approach to

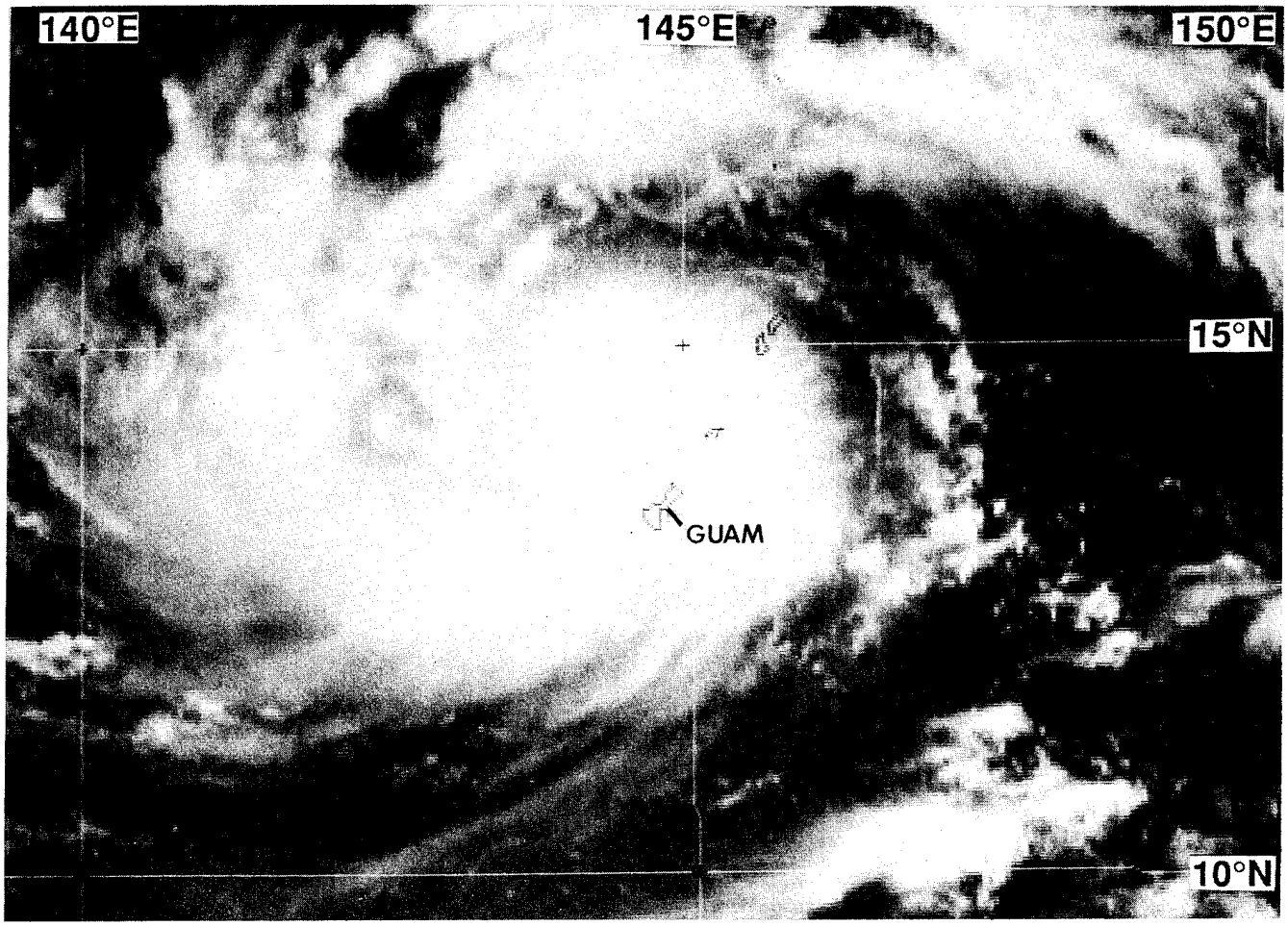

Figure 3-33-5 Verne near its closest point of approach to Guam. Verne's CDO obscures its low-level center (182331Z October visible GMS imagery).

Guam, the NEXRAD-observed wind speed on a vertical slice cut east-west through Verne's center showed the text-book signature of a low-level cyclone overlain by an upper-level anticyclone. When the hot tower became very active, the wind on the same slice cut through Verne's core showed that in the hot tower, the outbound southerlies were carried upward throughout the column (Figure 3-33-7). Another feature of the vertical structure of the wind in Figure 3-33-7, is that the maximum low-level winds (both inbound and outbound) were at 4,000 ft (1.2 km), which was the lowest elevation observable by the radar at this range.

b. Unusual motion

Verne continued on a steady west-northwestward track until 210600Z when it abruptly slowed and then meandered within 150 nm (275 km) of 17°N ; 130°E for seven days. In finer detail, Verne's motion during this period consisted of a slow westward drift between 210600Z to 230000Z, a slow southward drift between 230000Z to 260600Z, and a turn to the north-northeast after 260600Z. Later, shortly before 281200Z, Verne began a modest acceleration toward the north-northeast. Verne's period of unusual motion began when the monsoon trough axis acquired a reverse orientation (see Figure 3-33-1c). At this time, 500 mb heights became higher in the ridge axis southeast of the trough than in the ridge axis to the north of the trough. Additionally, strong low-level northeasterly winds persisted over

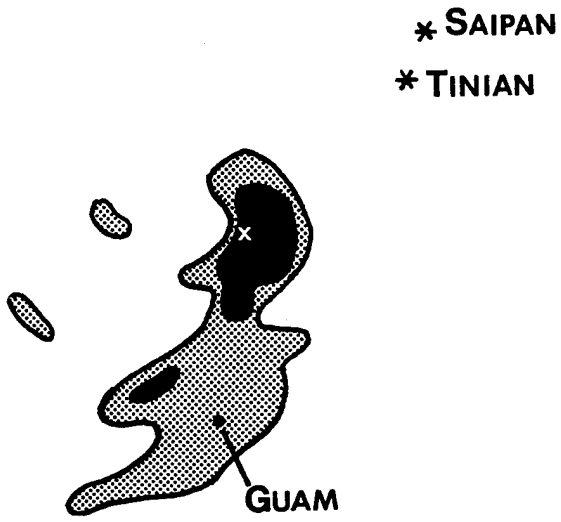

Figure 3-33-6 Echo tops as seen by Guam's NEXRAD at 182318Z showing Verne's lone "hot tower" on the southeastern side of its inner core. Outer contour = 35,000 ft, black shaded region shows tops over 40,000 ft. Maximum top at this time was 56,000 ft. Small "x" denotes estimated location of Verne's low-level circulation center.

the western half of the Philippine Sea and the South China Sea. It is likely that these two environmental factors combined to cause Verne to stall.

c. Air-sea interactions

It has long been known that tropical cyclones leave a trail of reduced sea surface temperature (SST) across the ocean surface. This cooling, which can reach 6°C and may persist for several weeks, is predominantly caused by turbulent mixing which deepens the oceanic mixed layer (Kepert 1993). Modeling and observational studies show the bulk of the cooling occurs to the right of the track in the northern hemisphere (Price 1981, Holland 1987). One might expect that the cooling of the SST by a tropical cyclone might alter the horizontal and vertical structure of the atmospheric boundary layer in such a way so as to affect the intensity, structure and behavior of the tropical cyclone itself. In coupled air-sea models (e.g., Kurihara 1992), the maximum surface wind in a tropical cyclone is reduced by upwards of 5-10% by the induced cooling of the SST.

Given that a tropical cyclone causes cooling of the sea surface, it might be of particular interest to observe the intensity changes of tropical cyclones which stall over water for extended periods of time. A testable hypothesis is that tropical cyclones which remain quasi-stationary over water for extended periods of time weaken (or at best, do not increase in intensity) as the underlying SST falls. Such reasoning has been used operationally in the past by the JTWC to forecast rapid weakening of a tropical cyclone (e.g., Jack 1989). While Verne remained quasi-stationary for seven days within 150 nm (280 km) of 17°N ; 130°E, it intensified from 75 kt to 115 kt (its peak intensity) during the first two days of its stall, it weakened from 115 kt to 105 kt during the next two-day period of its seven-day stall, and then began to lose intensity more rapidly (a 60 kt decrease from 105 kt to 55 kt) during the latter three days. Although Verne weakened significantly during the latter portion of its stall, it is inappropriate to claim that the storm-induced cooling of the SST was the major factor contributing to this weakening. More research is necessary to confirm the role of tropical cyclone induced SST changes upon the tropical cyclone itself.

IV. IMPACT

Verne brought gusty winds and heavy rain to Guam, Rota, Tinian and Saipan. Some minor damage to vegetation was reported on Guam. Reports from Saipan indicated more extensive fallen or uprooted trees. No reports of storm-related injuries or damage to houses or buildings were received. The maximum wind gust measured on Guam was 60 kt (31 m/sec).

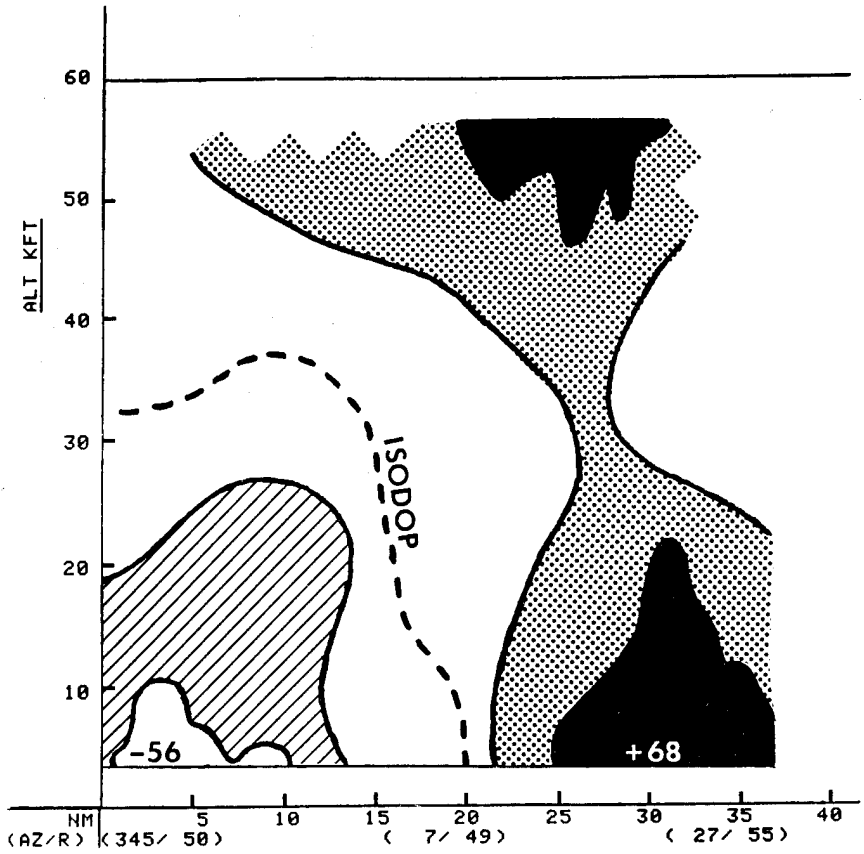

Figure 3-33-7 East-west cross-section (looking north) cut through the center of Verne shows inbound or outbound velocity with respect to Guam's NEXRAD. The hot tower on the eastern side of Verne's low-level center appears to have carried southerly (outbound) winds aloft resulting in a deepening of Verne's cyclonic circulation (182324Z October NEXRAD velocity cross section).

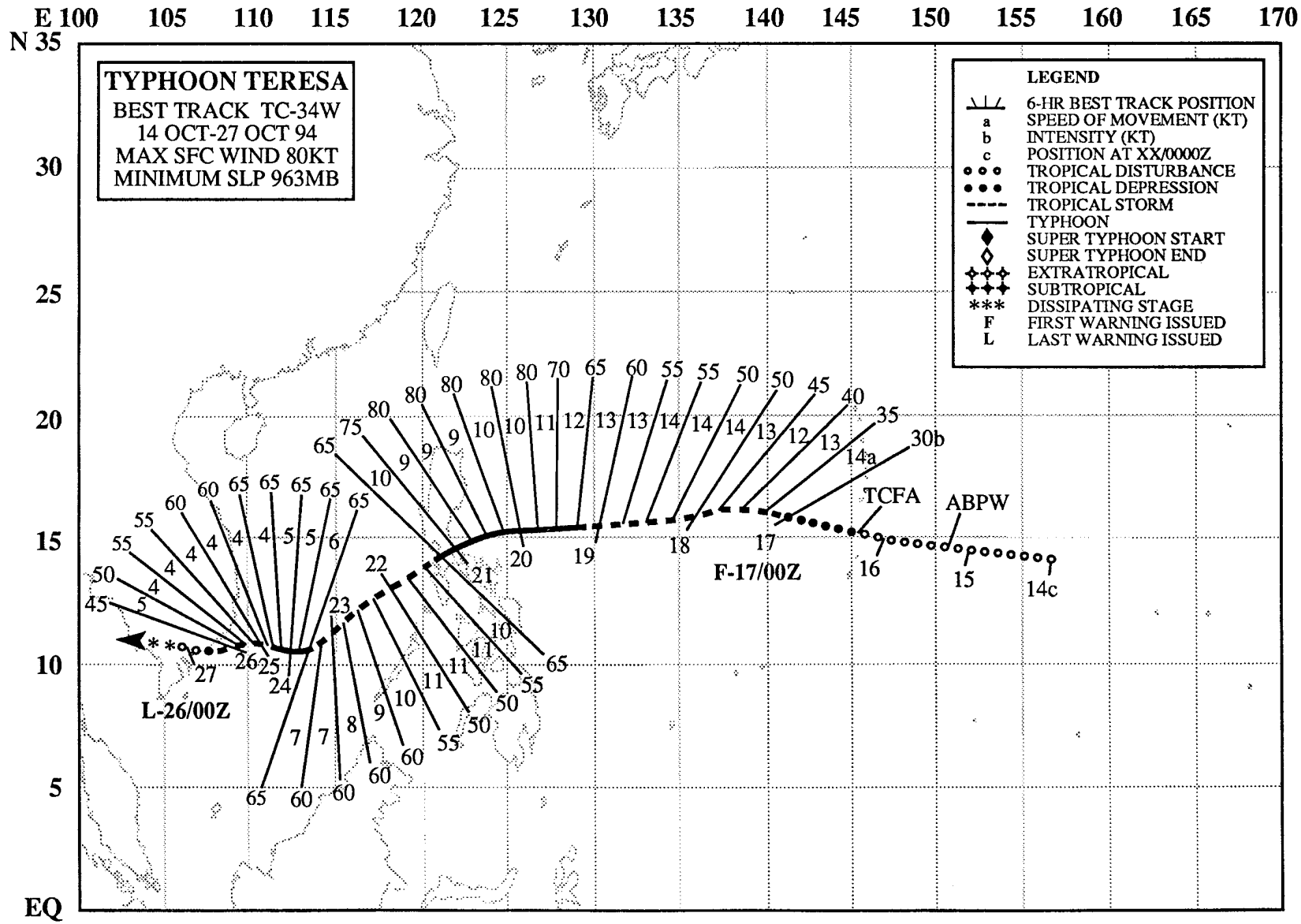
TYPHOON TERESA
BEST TRACK TC-34W
14 OCT-27 OCT 94
MAX SFC WIND 80KT
MINIMUM SLP 963MB
LEGEND
6-HR BEST TRACK POSITION
a SPEED OF MOVEMENT (KT)
b INTENSITY (KT)
c POSITION AT XX/0000Z
TROPICAL DISTURBANCE
TROPICAL DEPRESSION
TROPICAL STORM
TYPHOON
SUPER TYPHOON START
SUPER TYPHOON END
EXTRATROPICAL
SUBTROPICAL
*** DISSIPATING STAGE
F FIRST WARNING ISSUED
L LAST WARNING ISSUED
E 100 105 110 115 120 125 130 135 140 145 150 155 160 165 170 E
N 35 30 25 20 15 10 5 EQ
L-26/00Z
F-17/00Z
TCFA
ABPW

TYPHOON TERESA (34W)

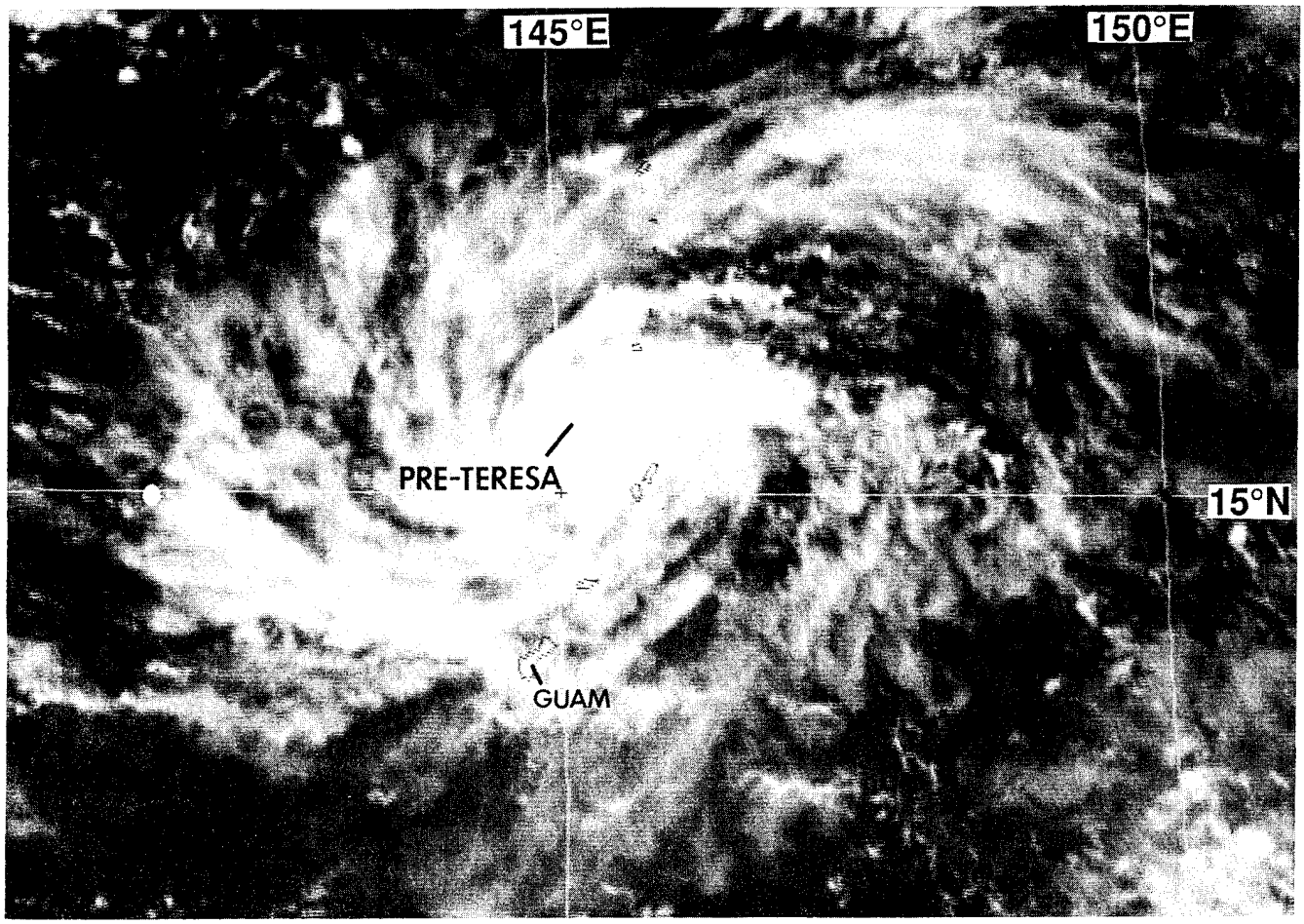

Figure 3-34-1 Well-organized low-level cloud lines and a symmetrical pattern of cirrus outflow prompted the JTWC to issue a Tropical Cyclone Formation Alert shortly after the time of this picture (160531Z October visible GMS imagery).

I. HIGHLIGHTS

Unusual southwestward motion brought Typhoon Teresa on a path across the central Philippine islands where it caused loss of life and much damage. The forecast performance of the objective guidance was especially poor as Teresa impacted the Philippines. Teresa was the westernmost tropical cyclone of a multiple outbreak that, at one point, featured four tropical cyclones in the western North Pacific.

II. TRACK AND INTENSITY

By mid-October, deep convection began to increase in the low latitudes of the western North Pacific, especially east of 140°E where westerly winds south of the monsoon trough increased. The atmospheric conditions leading to the formation of Teresa are included in Verne's (33W) summary.

The tropical disturbance that became Teresa was first mentioned on the 150600Z October Significant Tropical Weather Advisory. At this time, an area of deep convection had consolidated about 300 nm (550 km) east of the southern Mariana Islands. This disturbance moved westward and passed near Saipan at approximately 160600Z (Figure 3-34-1). A Tropical Cyclone Formation Alert was issued at

160730Z, followed by the first warning on Tropical Depression 34W at 170000Z. The system was upgraded to Tropical Storm Teresa at 170600Z. Moving westward at a steady 14 kt (25 km/hr), Teresa intensified at a normal rate and became a typhoon at 190600Z. The peak intensity of 80 kt (41 m/sec) was reached at 191800Z (Figure 3-34-2). Teresa was then only 300 nm (550 km) east of the Philippine island of Luzon and heading west-southwestward. Between the hours of 200600Z and 210600Z, the system crossed southern Luzon, passing just south of Manila (Figure 3-34-3). Emerging into the South China Sea after crossing southern Luzon, Teresa had weakened to 50 kt (26 m/sec). In response to steering influences of a strong northeast monsoon over the northern half of the South China Sea, Teresa continued to move southwestward, losing about 4 degrees of latitude (14.5°N to 10.5°N) between 210600Z and 231200Z. During this time period, the system slowly reintensified and by 231200Z it became a typhoon. Upon reaching typhoon intensity for a second time, Teresa turned toward the west and its speed of forward motion slowed to 5 kt (10 km/hr). Moving westward toward the coast of southern Vietnam, Teresa began to weaken. The final warning was issued at 260000Z as the system continued to weaken over water. The remnants of Teresa made landfall on the coast of southern Vietnam shortly after 261200Z, and passed over Ho Chi Minh City at approximately 270000Z.

III. DISCUSSION

a. A NEXRAD view of Teresa

When the tropical disturbance that became Teresa passed near Saipan, it came just within the 124 nm (230 km) Doppler range of Guam's NEXRAD. A velocity cross section was obtained through its center at 160736Z (two hours after the visible satellite imagery in Figure 3-34-1). The NEXRAD velocity cross section revealed a cyclonic circulation extending from 15,000 ft (the lowest beam elevation) upward to 30,000 ft (the highest elevation of precipitation targets). The peak inbound velocity of 18 kt (9 m/sec) was located about 40 nm (75 km) to the west of the peak outbound velocity of 14 kt (7 m/sec).

b. Forecast performance

The overall official track forecasts for Teresa were exceptionally good. At two periods, the objective track guidance became unreliable: shortly before landfall in the Philippines, and later, as the system neared the coast of Viet Vietnam. While it was east of the Philippines, the objective guidance called for Teresa to stall east of the Philippines. This bias in the objective guidance was detected quickly, and the official forecast brought Teresa across the Philippines and into the South China Sea. As Teresa neared the coast of Vietnam, the NOGAPS numerical guidance exhibited a bias to the north of track. This bias was also quickly detected, and the official forecast did not err as drastically.

IV. IMPACT

Teresa swept across Manila and nearby provinces on the Philippine island of Luzon. Its typhoon intensity winds uprooted trees, toppled utility poles, and destroyed homes and crops. Six people were reported killed by falling trees and flying debris. In a separate incident, 17 people were reported to be dead or missing when a Maltese oil tanker, the *Thanassis A*, sank in the South China Sea in heavy seas associated with Teresa and the Northeast Monsoon. Nineteen other crew members were rescued.

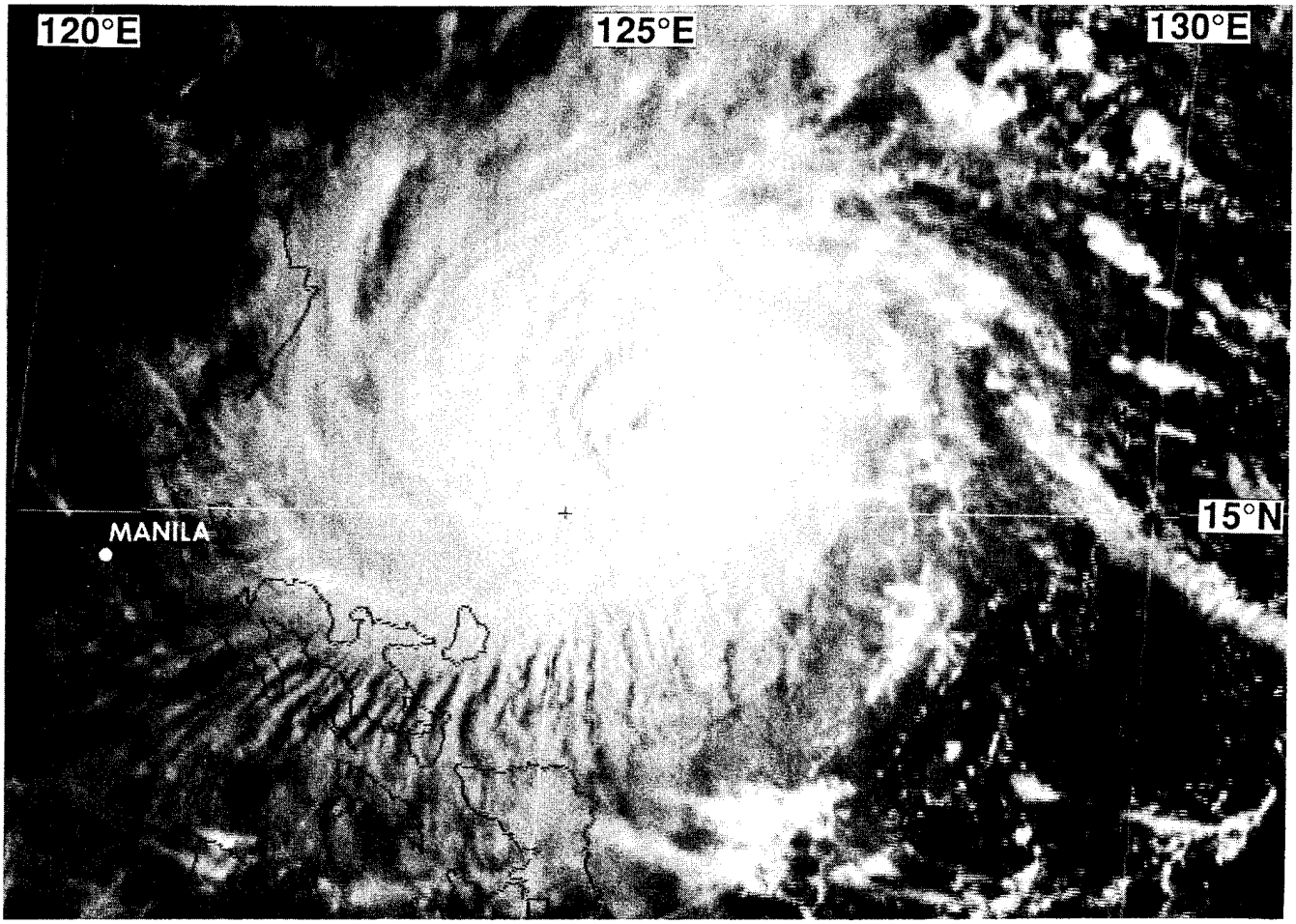

Figure 3-34-2 The low sun angle of morning helps to bring out the structure of Teresa's cloud system about eight hours prior to reaching its peak intensity (192224Z October visible GMS imagery).

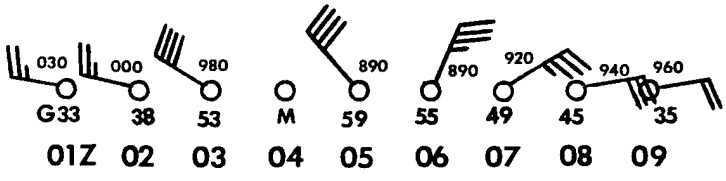

Figure 3-34-3 Hourly synoptic data recorded at Manila (WMO 98429) during Teresa's passage a short distance to the south of the city. Wind flags show sustained wind. The time of observation, gusts, and sea-level pressure are indicated.

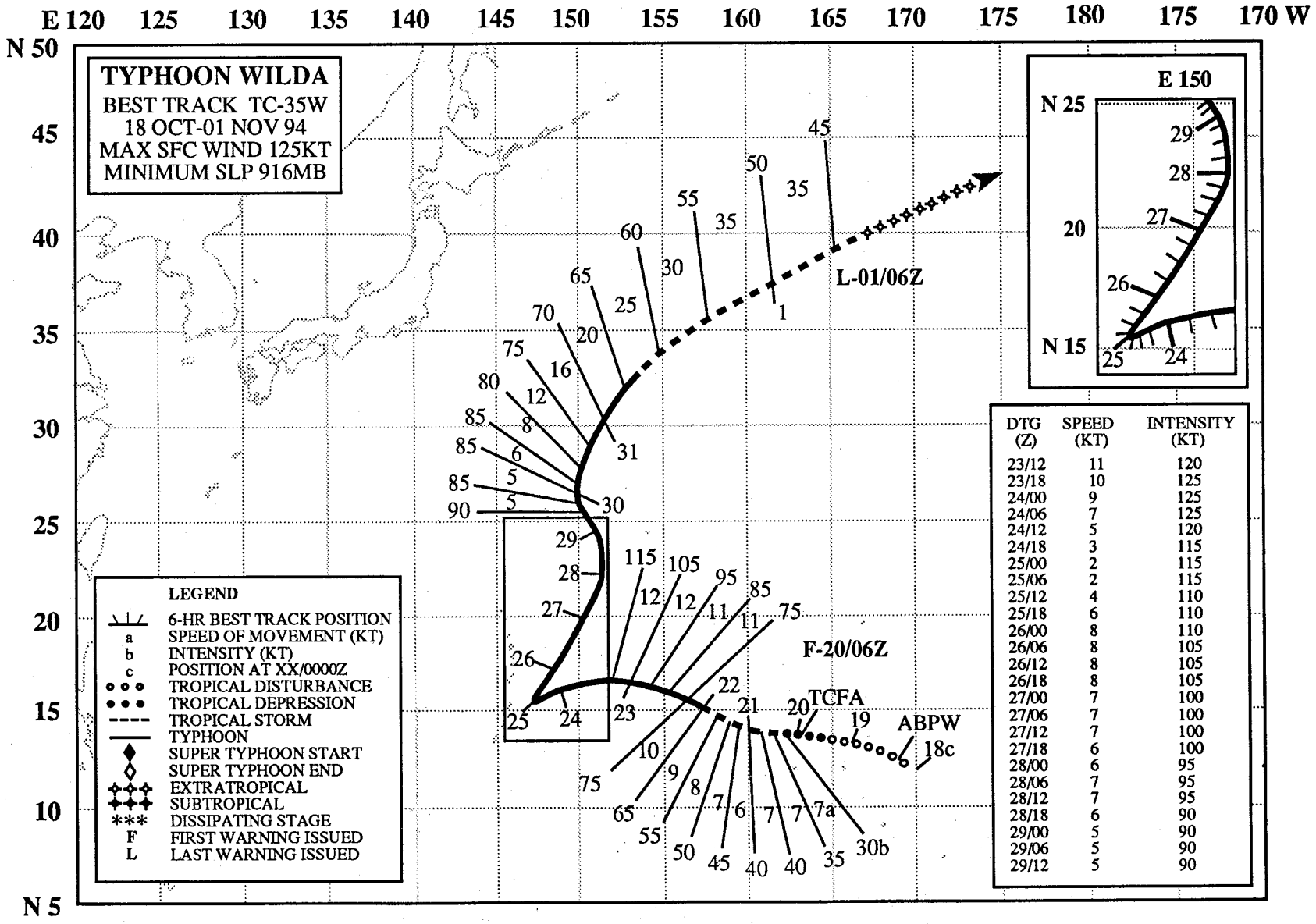

DTG (Z)	SPEED (KT)	INTENSITY (KT)
23/12	11	120
23/18	10	125
24/00	9	125
24/06	7	125
24/12	5	120
24/18	3	115
25/00	2	115
25/06	2	115
25/12	4	110
25/18	6	110
26/00	8	110
26/06	8	105
26/12	8	105
26/18	8	105
27/00	7	100
27/06	7	100
27/12	7	100
27/18	6	100
28/00	6	95
28/06	7	95
28/12	7	95
28/18	6	90
29/00	5	90
29/06	5	90
29/12	5	90

TYPHOON WILDA (35W)

I. HIGHLIGHTS

The third tropical cyclone of a mid-October four-storm outbreak, Wilda exhibited unusual motion. Wilda intensified to a peak of 125 kt (64 m/sec) during a quasi-stationary period near 15.6N ; 147.2E. During the stall, the monsoon trough within which Wilda was embedded acquired a reverse orientation. Coming out of the stall, Wilda moved on a slow north-oriented "S"-track.

II. TRACK AND INTENSITY

By mid-October, an active monsoon trough extended across the Philippine Sea (at 15°N), and from there, east-southeastward to a terminus in the Marshall Islands. At 180600Z, there were two named tropical cyclones — Teresa (34W) and Verne (33W) — and a tropical disturbance located along this trough axis. This tropical disturbance, which later became Wilda, was was first mentioned on the 180600Z October Significant Tropical Weather Advisory when it was located near 10°N; 170°E at the eastern terminus of the monsoon trough. At 192230Z a Tropical Cyclone Formation Alert was issued based on increased central deep convection and a well-organized cirrus outflow pattern. At 200600Z the first warning was issued based upon persistence of the central deep convection and a rapid improvement in the organization of the central and peripheral deep convection. At 201800Z, Tropical Depression 35W was upgraded to Tropical Storm Wilda, and at 220000Z, Wilda was upgraded to a typhoon. Post-analysis of satellite and synoptic data indicated that Wilda most probably became a 25 kt (12 m/sec) tropical depression at 191200Z, and a tropical storm at 201200Z.

After becoming a typhoon, Wilda first moved west-northwestward, then westward along about 16.7°N, and then west-southwestward, threatening Saipan. At approximately 241200Z, Wilda abruptly slowed and remained quasi-stationary for 24 hours at a position about 90 nm (170 km) ENE of Saipan and 180 nm (330 km) NE of Guam (Figure 3-35-1). Wilda's intensity peaked at 125 kt (64 m/sec) at 231800Z, just as it began to turn west-southwestward towards Saipan. Later, during its one-day stall, it began to weaken slightly. At 251200Z, Wilda began to move toward the northeast on what would prove to be the first leg of a typical "S" track (Lander 1995a). While moving northeastward, Wilda weakened from 115 kt to 95 kt. After 280600Z, Wilda turned toward the north-northwest and weakened further. After 291800Z, Wilda turned northeastward (on the last leg of its "S" track) and accelerated. At 010600Z November, the final warning was issued as Wilda tracked northeastward at 35 kt (65 km/hr), and its cloud signature indicated that a transition to an extra-tropical cyclone had occurred.

III. DISCUSSION

a. NEXRAD's view of Wilda

When Wilda stalled northeast of Guam, it was at its closest point of approach of 180 nm (330 km). Although poorly defined, Wilda's eye was discernible on the NEXRAD reflectivity product for a short time. The poor eye definition was likely due to signal attenuation by heavy rainbands and a beam height of 20,000 ft at Wilda's 180 nm range. In contrast, Wilda's extensive peripheral cloud bands remained well-within radar range for several days.

For almost two days (240220Z to 260005Z), Guam's NEXRAD provided a continuous integration of the precipitation associated with Wilda. Estimated rainfall magnitudes and gradients were extreme (Figure 3-35-2). Over five inches fell in a narrow swath between Guam and Saipan. Within two small regions, covering an area of approximately 1400 square miles (roughly the land area of the state of

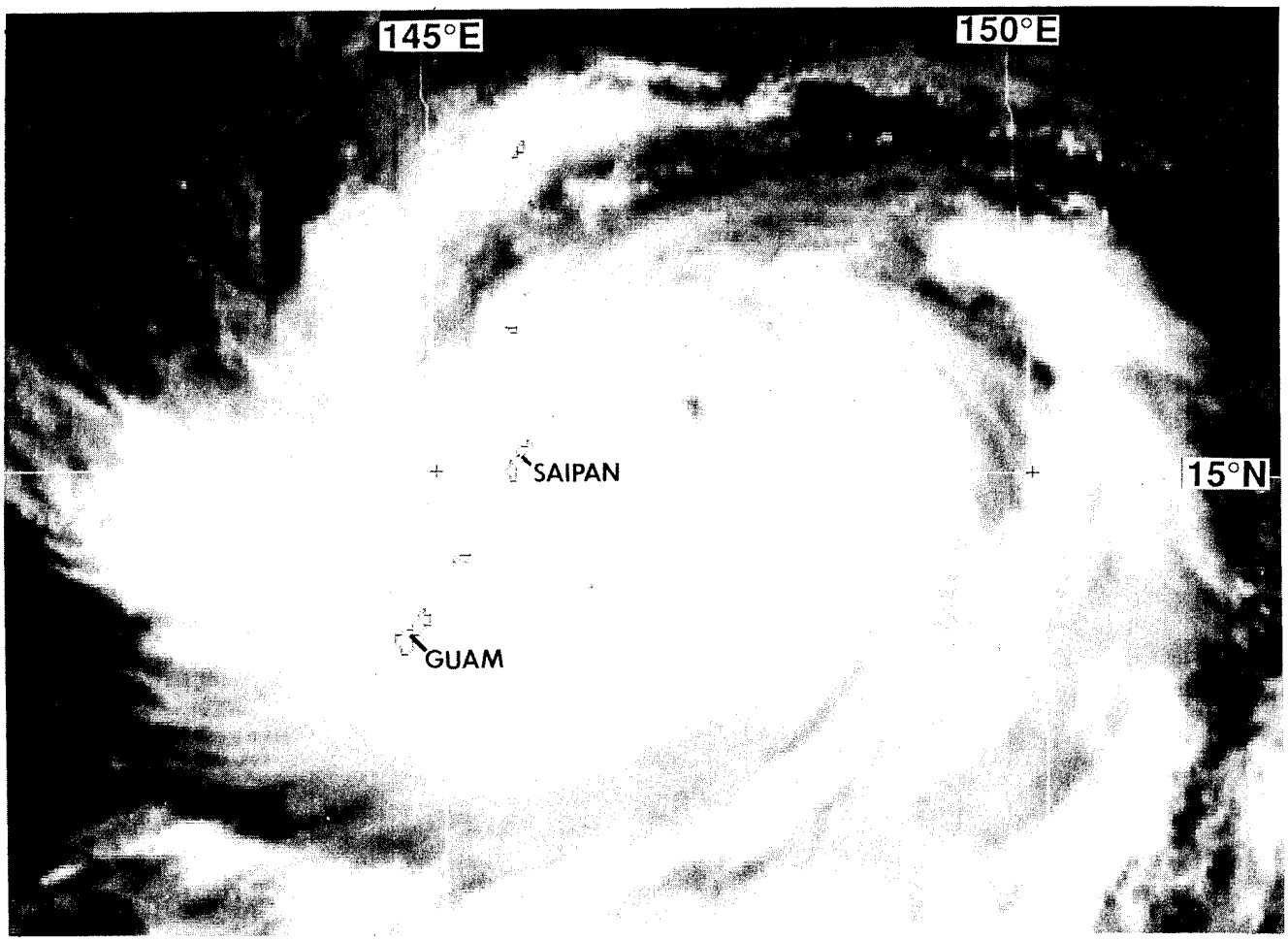

Figure 3-35-1 Wilda at an intensity of 115 kt (59 m/sec) has stalled about 90 nm (170 km) east-northeast of Saipan (242331Z October visible GMS imagery).

Rhode Island), over ten inches of rain was estimated to have fallen. On the island of Guam, the storm-total precipitation estimated by NEXRAD (Figure 3-35-3a) is about 20% short of the rainfall actually measured during Wilda's passage (Figure 3-35-3b). This was the most accurate storm-total precipitation estimated by NEXRAD on Guam to date. NEXRAD estimates are historically 25%-50% less than the measured values (for example, see Verne's (33W) summary). Its representation of the spatial distribution of rainfall (in this case, a narrow band of 3-4" inches of rain across the middle of the island with lighter amounts on the northern and southern ends of the island) was good.

b. Unusual motion

The monsoon trough which became active during mid-October was initially oriented WNW-ESE, and the tropical cyclones along its axis moved on west-northwesterly tracks consistent with climatology. Then, by virtue of the differential motions of Teresa (34W), Verne (33W), Wilda (35W), and Yuri (36W), the axis of the trough became oriented WSW-ENE (i.e., reverse oriented) at approximately 230000Z (see Figure 3-33-1c in Verne's summary). Concurrent with the monsoon trough's reverse orientation, Verne (33W) and Wilda stalled, and then moved on north-oriented tracks. After emerging from its one day stall, Wilda moved on an "S" shaped track (a track type which is almost exclusively associated with reverse orientation of the monsoon trough (Lander 1995a)).

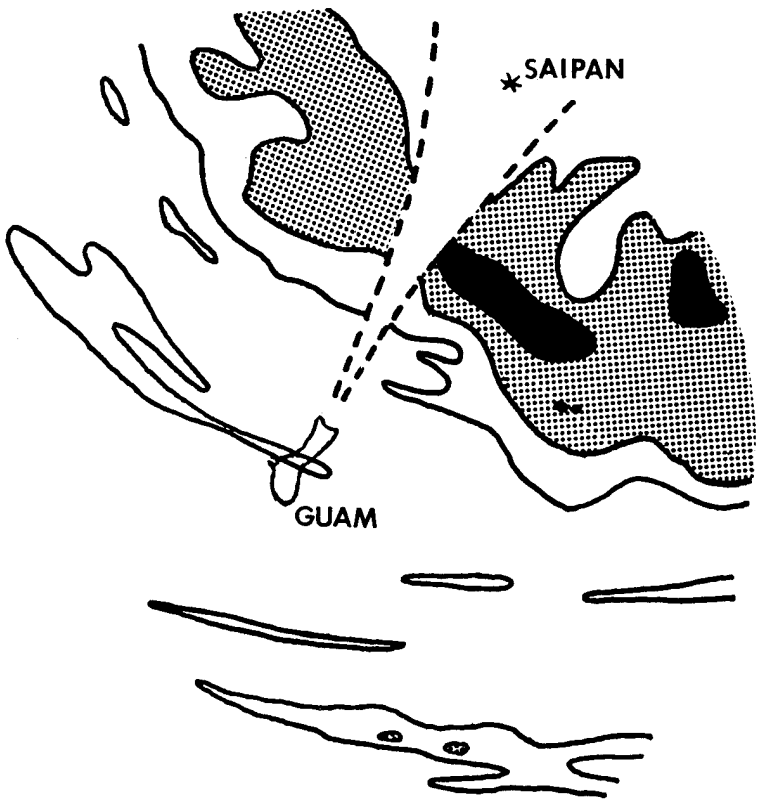

Figure 3-35-2 Estimated rainfall deposited by Wilda within 124 nm of Guam (NEXRAD storm-total precipitation for the period 240220Z to 252147Z October). Outer contour is three inches, half-tone indicates 5 to 10 inches, black-shaded area indicates 10 inches or more. The dashed lines enclose the area of radar beam blockage.

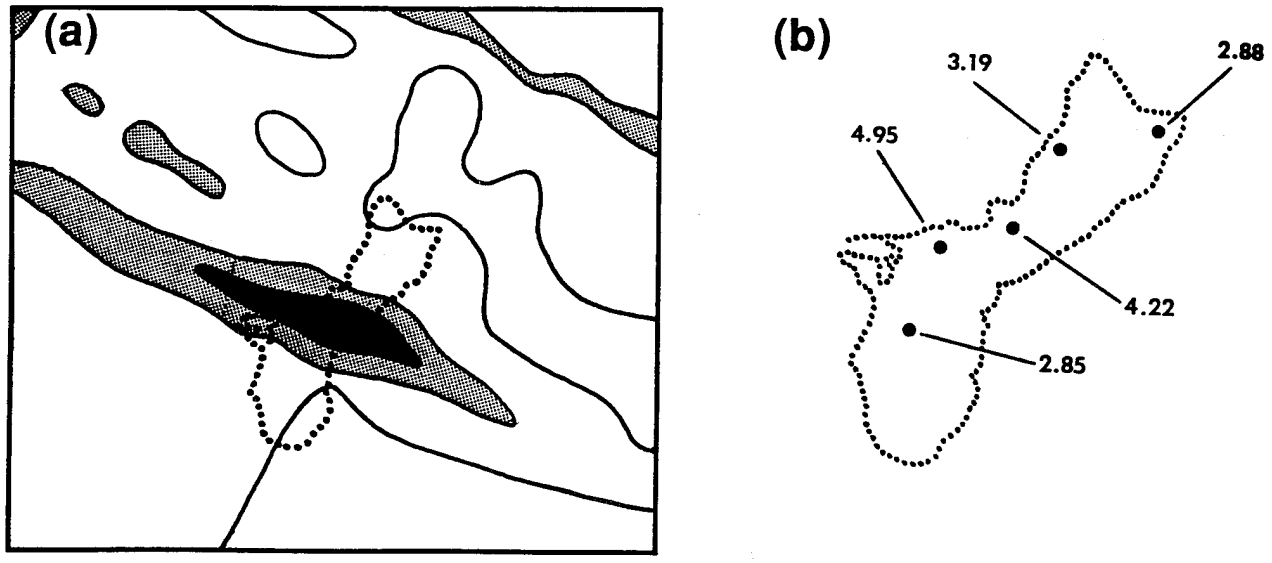

Figure 3-35-3 (a) Rainfall deposited on Guam by Wilda as estimated by NEXRAD during the period 240220Z to 252147Z October. Outer contour is 2 inches, half-tone indicates three to four inches, black-shaded area indicates four inches or more. (b) Rainfall measured on Guam during Wilda's passage.

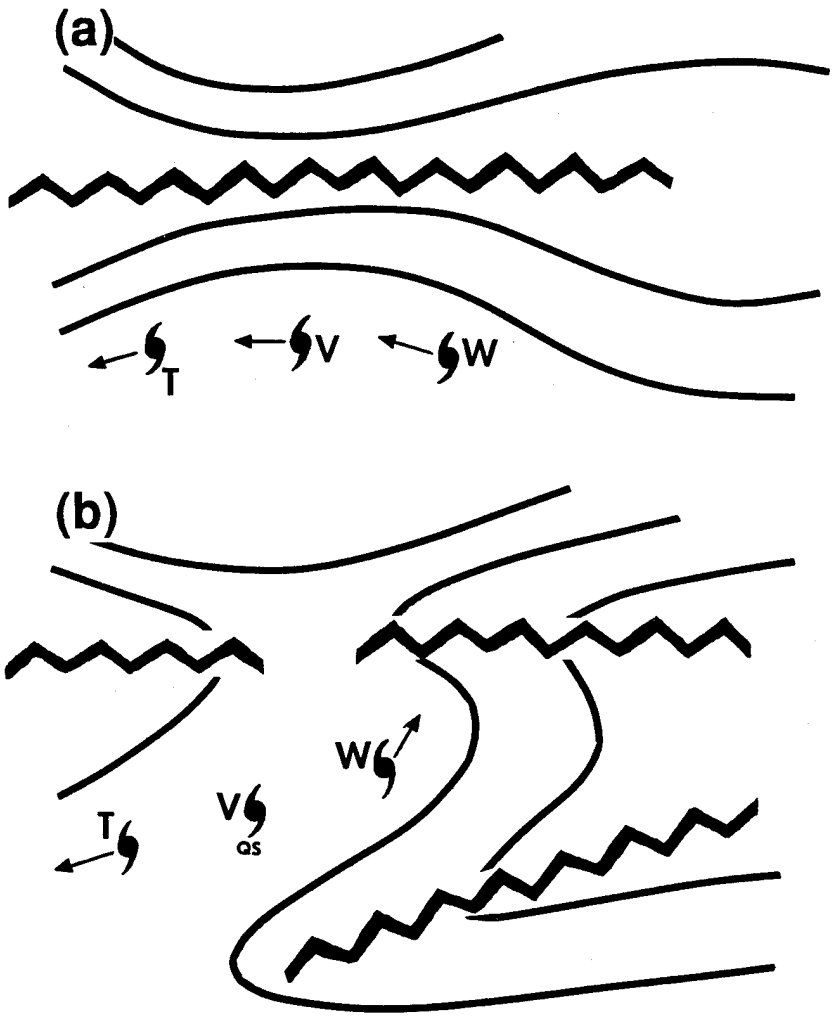

Figure 3-35-4 (a) Schematic illustration of the pattern of the 500 mb heights (adapted from NOGAPS analyses) in the western North Pacific while Teresa (T), Verne (V) and Wilda (W) moved westward. (b) Pattern of the 500 mb heights as the monsoon trough acquired a reverse orientation, and Wilda began to move northeastwards. Contours values are arbitrary. Zig-zag lines indicate ridge axes. Arrows depict motion of the tropical cyclones. QS = quasi-stationary.

The stall and the "S" track of Wilda were associated with an interesting evolution of the 500 mb pattern. At first, while Teresa (34W), Verne (33W), and Wilda were moving west-northwestward, the 500 mb height field featured a zonally oriented subtropical ridge (Figure 3-35-4a). As the monsoon trough acquired a reverse orientation, two ridge axes began to influence the motion of the tropical cyclones: one ridge axis was the preexisting subtropical ridge, and the other ridge axis developed to the southeast of the monsoon trough (Figure 3-35-4b). While Wilda was moving west-northwestward, the highest 500 mb heights were along the axis of the subtropical ridge. As Wilda stalled, pressure heights increased in the new ridge to the southeast. When pressure heights in the southeastern ridge exceeded the pressure heights along the subtropical ridge axis, Wilda began to move northeastward. The two-ridge structure at 500 mb (Figure 3-35-4b) remained in place as Wilda moved northward. The top half of Wilda's "S" motion occurred as Wilda moved through the subtropical ridge axis and entered the mid-latitude westerlies.

c. Air-sea interactions

As discussed in Verne's (33W) summary, tropical cyclones are known to cause cooling of the sea surface. This leads to the testable hypothesis that tropical cyclones which remain quasi-stationary over water for extended periods may weaken as the underlying sea surface temperature (SST) falls. Like

Verne (33W), Wilda provides a good test case.

While Wilda remained quasi-stationary for about 24 hours near 15.7°N ; 147.2°E, it weakened slightly from 125 kt (its peak intensity) to 115 kt. Later, coming out of its stall, it weakened slightly, but remained near 100 kt (51 m/sec) for the next three days. As was the case with Verne (33W), one can draw few conclusions from the case of Wilda about feedback of tropical cyclone induced SST changes upon the tropical cyclone itself (without rigorous study). At best, it can be shown that both Verne (33W) and Wilda induced some cooling of the SST (Figure 3-35-5).

d. Forecast performance

Despite unusual motion, the track forecasts errors for Wilda were lower than average, with mean errors at 24, 48, and 72 hours of 115, 193, and 223 nm respectively. Long-range (48 and 72-hour) track errors showed increases at three places along Wilda's track: (1) as it turned west-southwestward toward its stall position (forecasts then were for continued westward motion); (2) as it moved northeastward after the stall (forecasts then did not anticipate the magnitude of the bend back toward the north-northwest as Wilda executed the middle portion of its "S" track); and, (3) at the point of recurvature into the mid-latitude westerlies (the timing of the acceleration to the northeast was a problem).

Intensity forecasts were quite poor at two times: (1) in the early stages, the intensity was significantly under-forecast by as much as 35 kt at 24 hours, 45 kt at 48 hours and 50 kt at 72 hours ; and, (2) upon coming out of its stall and moving northeastward, the rate of weakening was over-forecast. Real-time diagnosis of intensity was 25 kt low (with respect to the final best-track intensity estimates) as Wilda reached its peak intensity; up to 20 kt too high during Wilda's stall; and then within 5 kt of the final best-track intensity as Wilda executed the "S" portion of its track.

IV. IMPACT

Wilda brought gusty winds, hazardous surf, and heavy rain to Guam, Rota, Tinian and Saipan. The highest recorded wind gust recorded on Guam was 74 kt (38 m/sec) at the JTWC. On Saipan, high winds downed trees and power lines, and pulled tin roofs from houses. Eleven people were injured in typhoon-related accidents. At the Saipan port, two tugboats sank, a flat barge was lost, and 50 welding machine units were destroyed. Offshore, the Philippine-registered ship, *M/V Ronda*, nearly sank in 30 to 40 foot high seas. On Guam, three surfers were missing and presumed drowned in rough seas off the northern end of the island. A surfboard and two boogie boards washed ashore, but the surfers were never found.

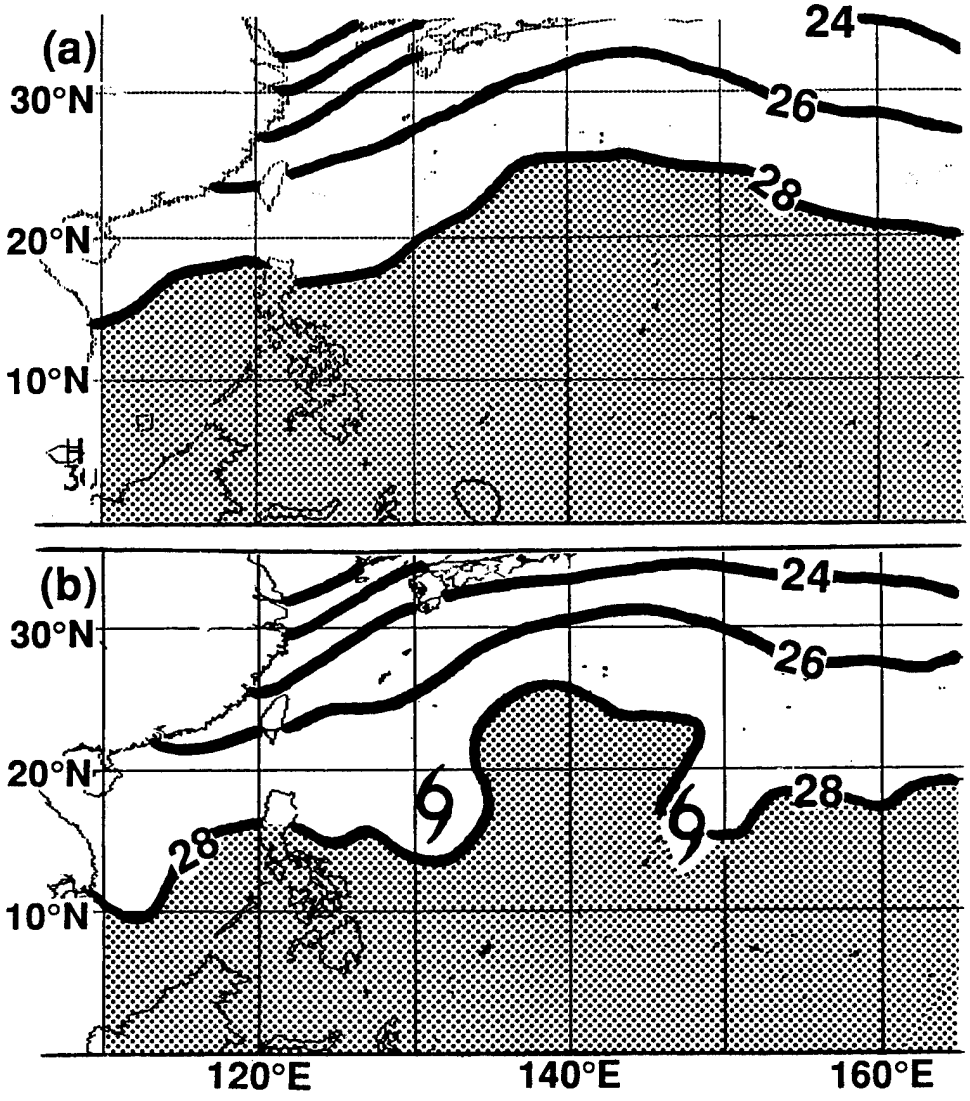

Figure 3-35-5 (a) SST analysis at 211200Z October. (b) SST analysis at 271200Z October. Notice the cooling of the SST at the stall locations of Verne (33W) and Wilda.

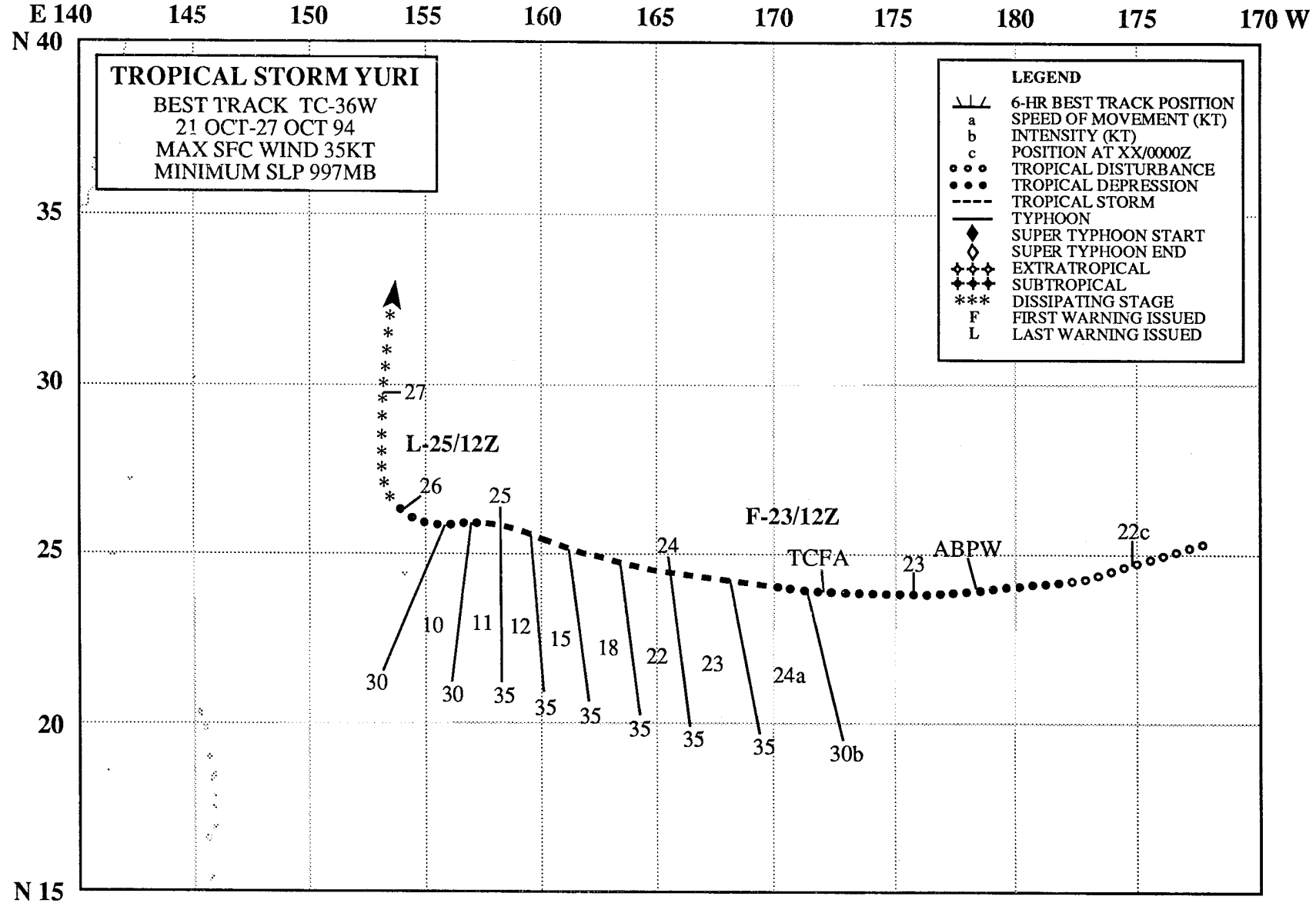
E 140
145
150
155
160
165
170
175
180
175
170 W
N 40
35
30
25
20
N 15
TROPICAL STORM YURI
BEST TRACK TC-36W
21 OCT-27 OCT 94
MAX SFC WIND 35KT
MINIMUM SLP 997MB
LEGEND
6-HR BEST TRACK POSITION
a SPEED OF MOVEMENT (KT)
b INTENSITY (KT)
c POSITION AT XX/0000Z
TROPICAL DISTURBANCE
TROPICAL DEPRESSION
TROPICAL STORM
TYPHOON
SUPER TYPHOON START
SUPER TYPHOON END
EXTRATROPICAL
SUBTROPICAL
*** DISSIPATING STAGE
F FIRST WARNING ISSUED
L LAST WARNING ISSUED
L-25/12Z
F-23/12Z
TCFA
ABPW
27
26
25
24
23
22c
10
11
12
15
18
22
23
24a
30
30
35
35
35
35
35
35
30b

TROPICAL STORM YURI (36W)

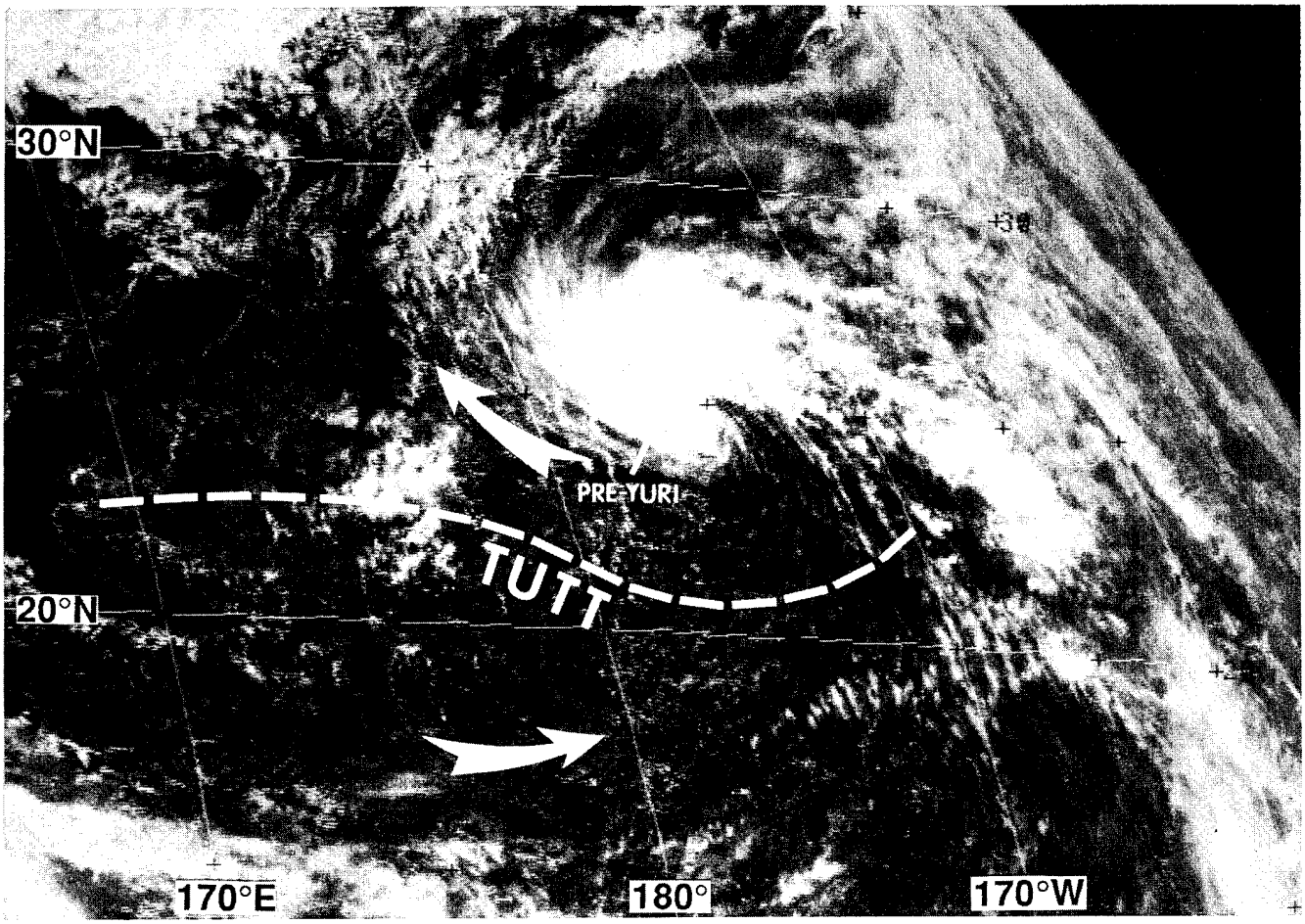

Figure 3-36-1 The tropical disturbance which later became Tropical Storm Yuri is seen northwest of Hawaii along the axis of the TUTT (212331 visible GMS imagery).

I. HIGHLIGHTS

Yuri was a small, short-lived tropical cyclone which formed at relatively high latitude (25°N) in direct association with a TUTT cell. Forming east of the international date line in a relatively cloud-free area (Figure 3-36-1), the disturbance that became Yuri, moved rapidly westward at 21 kt (40 km/hr). For a couple of days, the low-level southwest monsoon stretched from the Philippines all the way out to the south of Yuri. This temporarily placed Yuri at the eastern reaches of the reverse-oriented monsoon trough that also included Teresa (34W), Verne (33W), and Wilda (35W).

II. TRACK AND INTENSITY

The low-level circulation of the western North Pacific during late October was dominated by an active monsoon trough. In the upper troposphere, the axis of the tropical upper tropospheric trough (TUTT) stretched along 25°N from about 150°E to a position (30°N ; 160°W) northwest of Hawaii. This TUTT overlaid a relatively cloud-free region between the monsoon cloudiness to the south and the cloudiness associated with the polar front to north. A distinct area of persistent convective clouds formed in association with a TUTT cell that was northwest of Hawaii on 22 October. This area of con-

Figure 3-36-2 The remnant low-level circulation of Yuri (252331Z visible GMS imagery).

vection was clearly associated with a low-level circulation center. Moving rapidly westward at nearly 21 kt (40 km/hr), this circulation crossed the international date line shortly after 221200Z. The 221800Z October Significant Tropical Weather Advisory noted that a weak low-level circulation center which appeared to be developing beneath a TUTT cell had crossed the international date line. Based upon well-organized low-level cloud lines in satellite imagery, a Tropical Cyclone Formation Alert was issued at 230000Z. The first warning on Tropical Depression 36W was issued at 231200Z. The rationale for issuing the first warning is stated in the prognostic reasoning message (WDPN34 PGTW 231500):

"... [at 231200Z] animated infrared satellite imagery shows that Tropical Depression 36W is moving rapidly westward near Wake island. Well-defined lower level cumulus lines are evident on infrared metsat data as well as DMSP nighttime visible imagery. There is a lack of deep convection near the center, but animation shows the cloud elements spinning around the cyclone center at a velocity estimated at 30 to 40 knots. It is possible that this system is most intense at the 850-700 mb level above the surface. We have no [conventional] synoptic data to support our current intensity estimate. The Dvorak satellite analysis model for intensity estimates does not handle these types of hybrid systems very well, so it is likely the satellite intensity estimates on Tropical Depression 36W [may] be significantly lower than the actual winds at the surface."

During the night of 23 October, a small area of deep convection formed on the southeastern side of the well-defined low-level circulation center of Tropical Depression 36W. In addition, low-level cloud motion (obtained from the satellite-derived cloud-motion bulletin issued by the JMA) of 40 kt (20 m/sec) was observed on the north side of the circulation. These data prompted an upgrade of the system to Tropical Storm Yuri at 231800Z. Yuri remained at minimal tropical storm intensity until 250000Z. The loss of all deep convection and a degradation in the appearance of the low-level cloud lines, indicated that the system had weakened to tropical depression intensity at 250600Z. The final warning was issued at 251200Z. The remnant low-level circulation of Yuri (Figure 3-36-2) was captured nicely by the scatterometer aboard the ERS-1 satellite at 260000Z (Figure 3-36-3).

III. DISCUSSION

a. Unusual genesis

Most of the tropical cyclones of the western North Pacific form along the axis of the monsoon trough. On rare occasions, a tropical cyclone forms from a small convective cloud cluster in direct association with a TUTT cell. The cloud system of such tropical cyclones is often isolated in the relatively cloud-

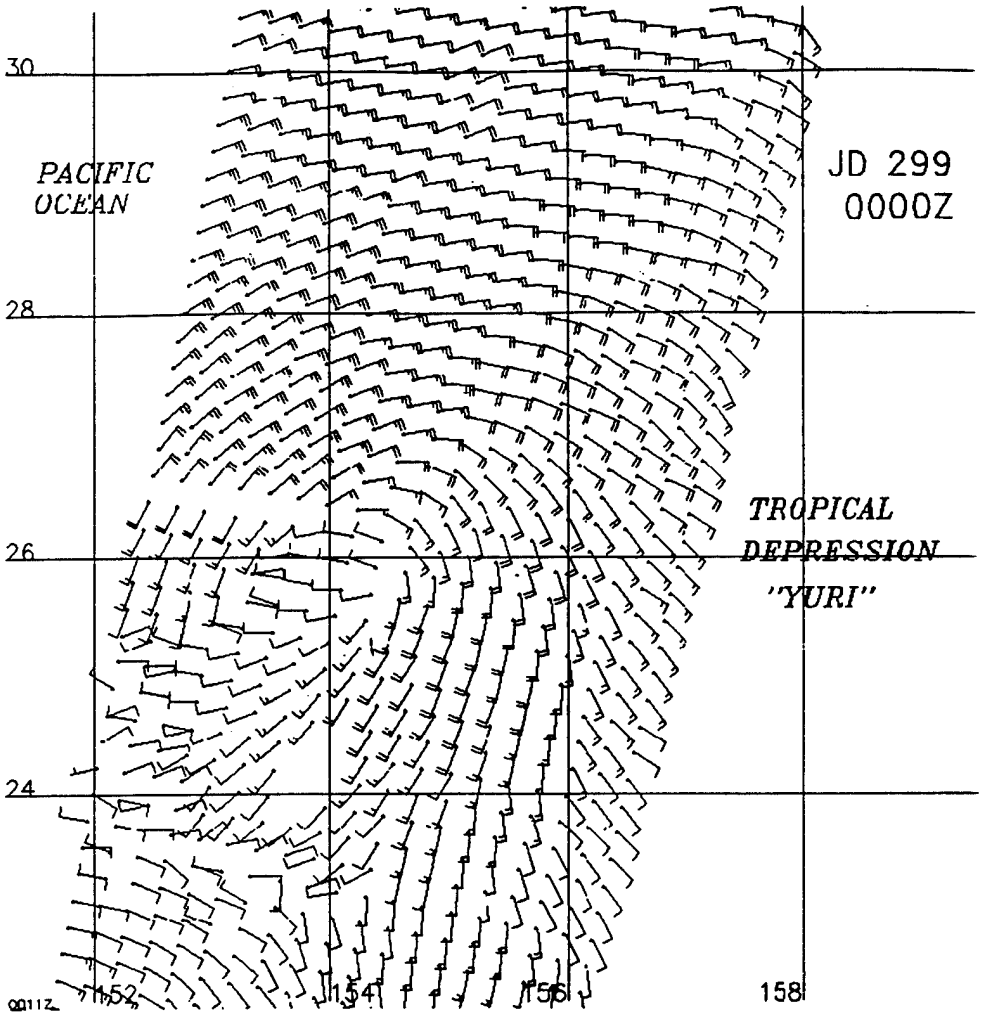

Figure 3-36-3 Low-level wind flow derived from the scatterometer aboard the ERS-1 satellite showing the remnant circulation of Yuri (260000Z October ERS-1 scatterometer-derived wind).

free region between the cloudiness associated with the monsoon trough and the cloudiness associated with the polar front. These TUTT-cell induced tropical cyclones are usually small-sized and isolated in easterly low-level winds (i.e., the low-level wind returns to easterly a few hundred kilometers equatorward of the system). (see also the summary of Tropical Depression 31W, which — like Yuri — formed in direct association with a TUTT cell.)

In recent years, we have observed that tropical cyclones which form along the TUTT axis, in association with TUTT cells, tend to form to the northeast of the center of the TUTT cell where the upper-level winds are from the south or southeast, and are highly diffluent (Figure 3-36-4a,b). This mode of formation is quite different from the influence of TUTT cells on tropical cyclone development suggested by Sadler (1976). In this paper, Sadler hypothesizes that TUTT cells aid tropical cyclone development by providing a diffluent upper-level outflow region in the southeast quadrant of a TUTT cell which is located to the northwest of a developing tropical cyclone (Figure 3-36-4c). In an earlier paper by Sadler (1967), he hypothesizes that TUTT cells may penetrate to the surface and create an inverted trough or a vortex in the tradewind flow. In fact, he claims that TUTT-cell penetration to the surface is the primary source for disturbances in the trade winds during summer. This process, though providing a better description of the formation of Yuri and TD 31W (and of other recent tropical cyclones (e.g., Gordon, 1989) observed to have formed in direct association with TUTT cells), lacks a description of the role of

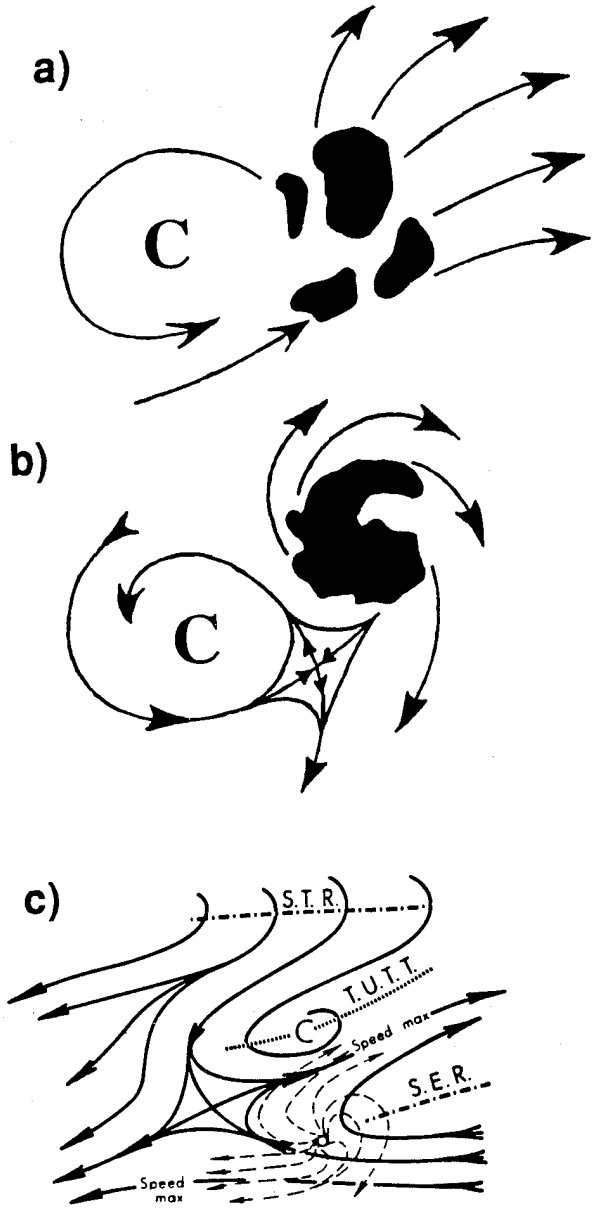

Figure 3-36-4 (a) Cloud clusters to the east of a TUTT cell prior to development of a low-level circulation center. (b) A tropical cyclone which has evolved from a cloud cluster near a TUTT cell. Black silhouettes represent deep convection, arrows depict 200 mb flow, large "C" represents the center of the TUTT cell. (c) A TUTT cell provides an upper-level outflow channel to a developing tropical cyclone (After Sadler, 1976). STR is the subtropical ridge; SER the sub-equatorial ridge; TUTT, the tropical upper tropospheric trough.

deep convection in the formation of the surface low, and is vague about whether the tropical cyclones that form in such cases are initiated by the reflection of the TUTT cell at the surface or whether they are independently produced by convective processes associated with the TUTT cell.

IV. IMPACT

No reports of serious damage or injuries were received.

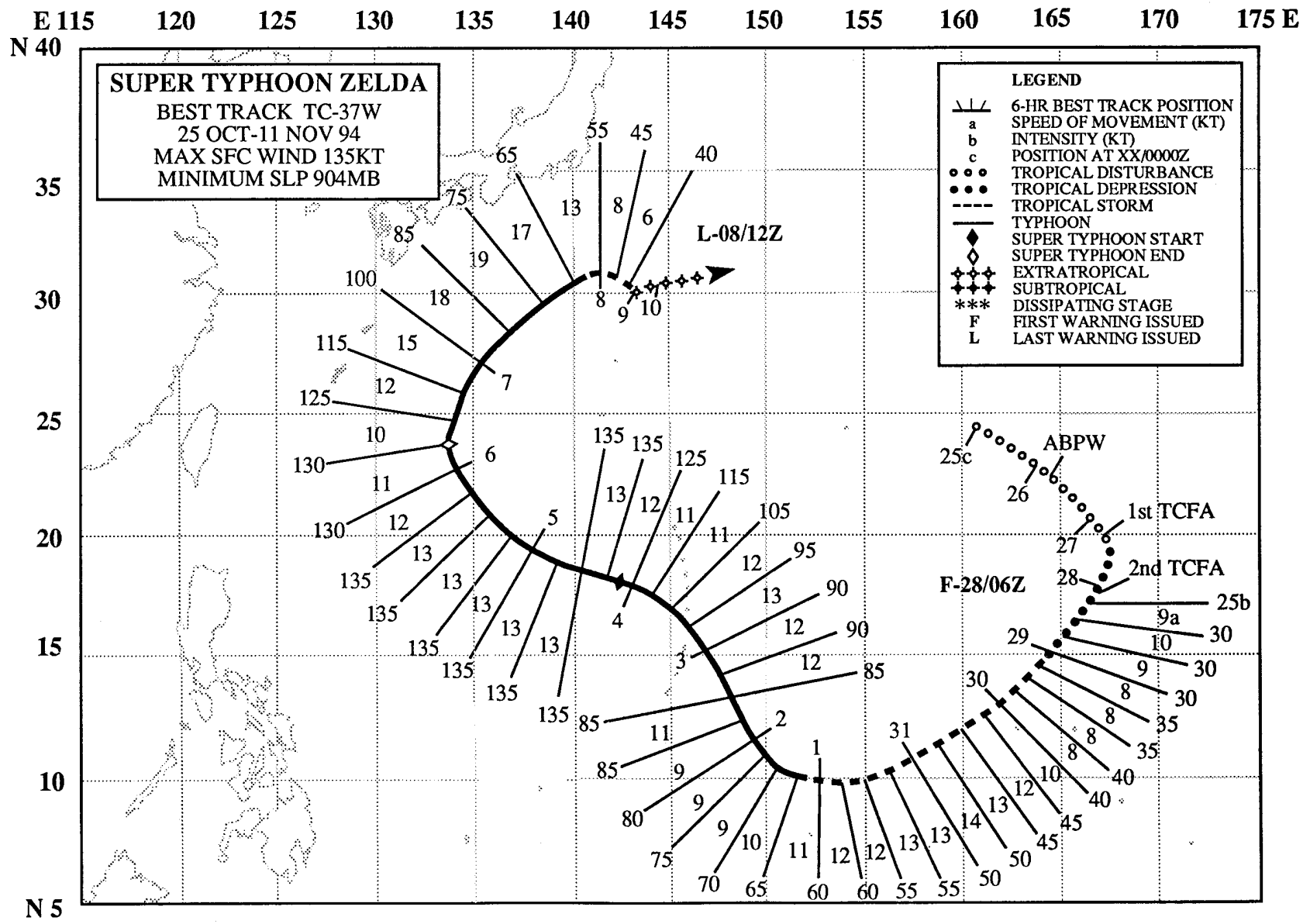
SUPER TYPHOON ZELDA
BEST TRACK TC-37W
25 OCT-11 NOV 94
MAX SFC WIND 135KT
MINIMUM SLP 904MB
LEGEND
6-HR BEST TRACK POSITION
SPEED OF MOVEMENT (KT)
INTENSITY (KT)
POSITION AT XX/0000Z
TROPICAL DISTURBANCE
TROPICAL DEPRESSION
TROPICAL STORM
TYPHOON
SUPER TYPHOON START
SUPER TYPHOON END
EXTRATROPICAL
SUBTROPICAL
DISSIPATING STAGE
FIRST WARNING ISSUED
LAST WARNING ISSUED
L-08/12Z
F-28/06Z
ABPW
1st TCFA
2nd TCFA
E 115
120
125
130
135
140
145
150
155
160
165
170
175 E
N 40
35
30
25
20
15
10
N 5

SUPER TYPHOON ZELDA (37W)

I. HIGHLIGHTS

Zelda was the sixth, and final, super typhoon of 1994. During the first half of Zelda's life, it exhibited unusual motion: it moved from a subtropical latitude (25°N) southward into the deep tropics (10°N). Zelda passed to the north of Guam, and within range of Guam's NEXRAD.

II. TRACK AND INTENSITY

The tropical disturbance that became Zelda developed at the eastern reaches of a reverse-oriented monsoon trough that was defined by a line drawn SW-NE through the centers of Teresa's (34W) remnants, Typhoon Verne (34W), and Typhoon Wilda (35W) (Figure 3-37-1a). The first mention of this disturbance on the 260600Z October Significant Tropical Weather Advisory stated, in part:

" . . . the low level circulation that is part of the reverse oriented monsoon trough . . . has had persistent convection for over 12 hours. . . . the potential for significant tropical cyclone development is fair. . . ."

Based on satellite imagery that showed tightly wound low-level cloud lines to the northwest of a an area of deep convection, and on synoptic reports that verified the presence of a low-level cyclonic circulation, a Tropical Cyclone Formation Alert (TCFA) was issued at 270500Z. Over the next 18 hours, the system did not show any signs of intensifying. Based on satellite imagery (e.g., see Figure 3-37-2) and on synoptic reports from Wake Island (WMO 91245), a second TCFA was issued at 280230Z. Quoting from this second TCFA:

"The tropical disturbance [pre-Zelda] is now located south-southeast of Wake Island. Wake reported sea-level pressures as low as 1006.1 mb as the system [which was moving southward] passed to the east. Satellite imagery shows an exposed low level circulation center with weak convection sheared 50 nm to the south-southwest. Minimum sea level pressure is estimated at 1004 mb."

At 280600Z, the first warning on Tropical Depression 37W was issued as the satellite signature of the system improved. At this time, it was thought that Tropical Depression 37W was unlikely to become a tropical storm. Its history of slow development and evidence on satellite imagery of northeasterly shear on the system led JTWC forecasters to expect little further intensification. However, at 290600Z, Tropical Depression 37W was upgraded to tropical storm intensity based upon an improved satellite signature. Thereafter, Zelda continued to intensify at a slow pace, and, at 011200Z November, it was upgraded to typhoon intensity.

From the disturbance stage to the attainment of typhoon intensity, Zelda dropped equatorward from 25°N to 10°N along a very unusual "backwards C" -shaped track. This unusual motion is discussed in the next section. After becoming a typhoon (at 010600Z November), Zelda turned toward the northnorthwest and continued to slowly intensify. At 030000Z November, Zelda turned toward a more westward heading, and six hours later, at 030600Z, its eye passed over the island of Anatahan (Figure 3-37-3). After passing over Anatahan with an intensity of 95 kt (50 m/sec), Zelda's rate of intensification increased. During the 120-hour period 290000Z October to 030000Z November, the intensity increased at a fairly steady rate of 10 kt per day. Then, over the 24-hour period 030600Z to 040600Z November, there was a 40 kt increase of intensity from 95 kt (49 m/sec) to 135 kt (69 m/sec). For 36 hours (040600Z to 051800Z), Zelda's intensity held steady at its peak value of 135 kt (69 m/sec) (Figure 3-37-4). Zelda reached the point of recurvature at 060600Z November, 48 hours after reaching peak intensity. (Reaching peak intensity prior to recurvature is typical for most very intense tropical cyclones that

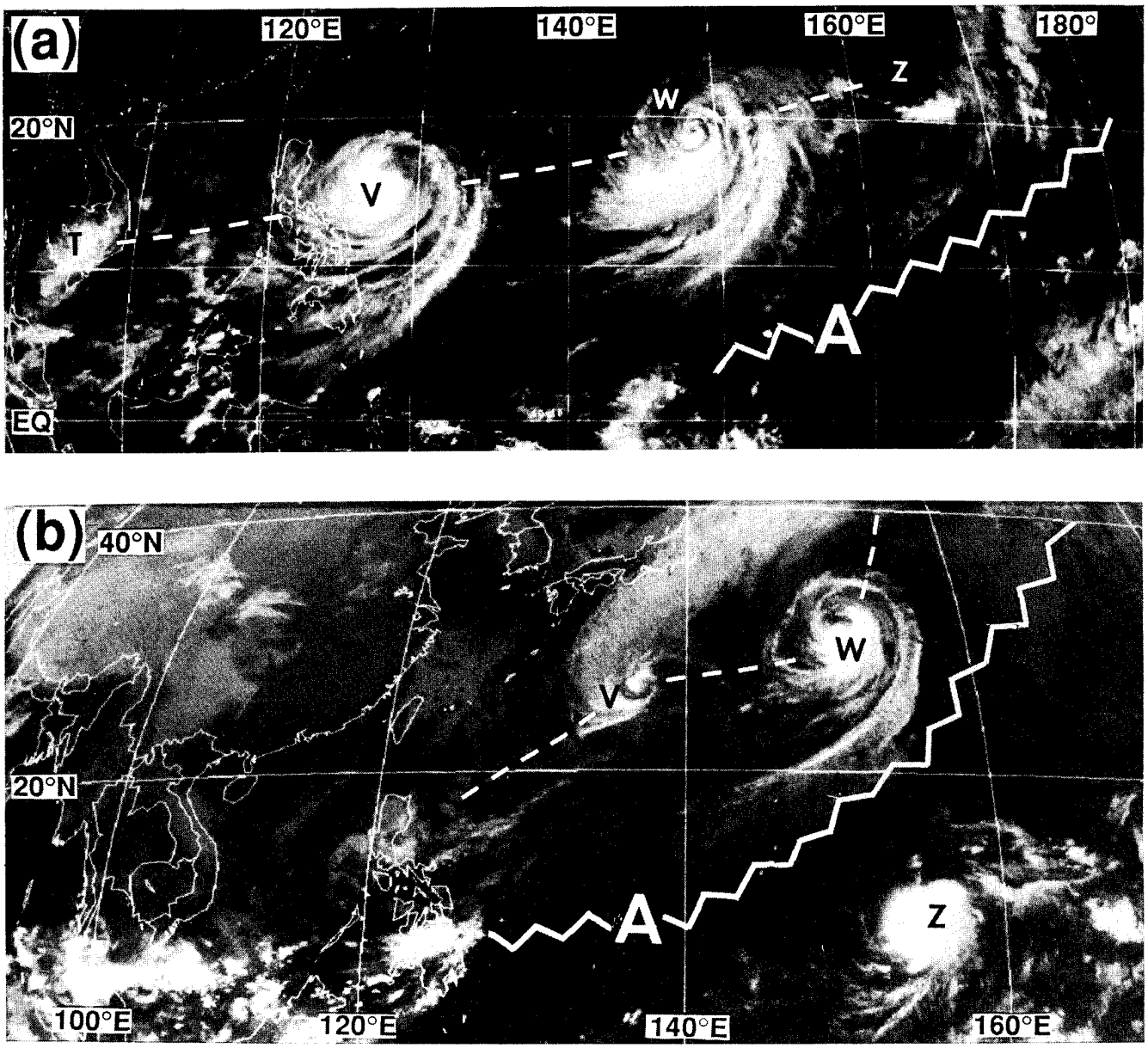

Figure 3-37-1 (a) The disturbance that would become Zelda (labeled, Z) lies at the eastern reaches of a reverse-oriented monsoon trough (dashed white line) that stretches from the remnants of Typhoon Teresa (34W) (T) — located over southeast Asia — northeastward through Verne (33W) (V) and Wilda (35W) (W). Zig-zag line indicates induced ridging southeast of the monsoon trough (260633Z October infrared GMS imagery). (b) Typhoons Verne (33W) (labeled, V) and Wilda (35W) (W) have gained latitude while Zelda (Z) has dropped southward (302332 October GMS IR imagery).

recurve — see the discussion of peak intensity versus timing of recurvature in the Typhoon Page (03W) summary.) After passing through the point of recurvature, Zelda began to weaken rapidly. In the 48-hour period 060600Z to 080600Z there was an 85 kt decrease in intensity from 130 kt (69 m/sec) to 45 kt (23 m/sec). The final warning was issued at 081200Z as Zelda acquired extratropical characteristics. The extratropical remnant of Zelda drifted eastward and dissipated over water near 30°N 145°E, almost back to where Zelda had begun.

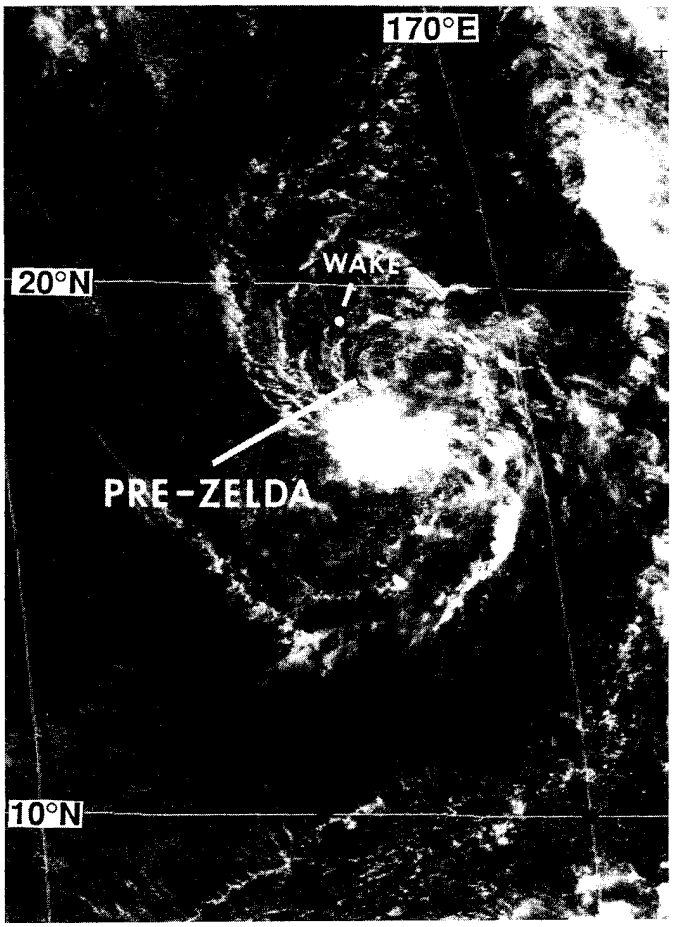

Figure 3-37-2 The exposed low-level circulation center of the tropical disturbance that would become Zelda can be seen to the north of a small area of deep convection, and is about 90 nm (165 km) south-southeast of Wake island (272331Z October visible GMS imagery).

III. DISCUSSION

a. Unusual motion

The full trace of Zelda's motion — from its early stages as a tropical disturbance near 25°N 160°E, to its dissipation near 30°N 145°E — forms one of the oddest shaped tracks of 1994. Particularly unusual was the early portion of Zelda's track wherein the system moved southward on a "backwards C" - shaped track. One hypothesis for this unusual motion is that Zelda was carried southward in the flow around an anticyclone which had formed to the southeast of typhoons Wilda (35W) and Verne (33W) (Figure 3-37-1a,b and Figure 3-37-5).

b. NEXRAD's view of Zelda

Beginning at 020740Z November and continuing through 031432Z, forecasters at Andersen Air Force Base, Guam, were able to provide to the JTWC hourly fixes on the center of Zelda's large eye (Figures 3-37-6 and 3-37-7). The high frequency (approximately hourly) of accurate fixes obtained from the NEXRAD for Zelda were very useful overall, but illustrated that the short-term track changes that are resolvable with the NEXRAD must be interpreted with caution. For several forecasts prior to 020000Z, numerical guidance and the official forecast indicated that Zelda, which was then moving westward, would turn to the northwest and pass near or over Guam. As the northwestward turn ensued after 010000Z, the motion became even more northward than forecast. By the 020000Z forecast, a new scenario was anticipated: numerical guidance and the official forecast now indicated that Zelda would move northwestward for 24 hours and then turn toward the west-northwest and pass near or over Saipan. However, from 021334Z to 021734Z the radar fixes indicated a north-northwestward movement. Incorporating this information, the warning at 021800Z indicated that Zelda would pass about 50 nm northeast of Saipan and then over Anatahan (a small island about 70 nm north of Saipan). At a critical time period — shortly after 021800Z — when JTWC forecasters were closely watching for evidence of Zelda's anticipated west-northwestward turn, the NEXRAD fixes (at 021832Z, 021936Z, and 022035Z) jogged to the west (see Figure 3-37-6). If interpreted as indicative of the onset of a major track change, these fixes could have been extrapolated to indicate that Zelda would pass very near or over Saipan. However, the next five radar fixes beginning at 022133Z showed northwestward motion that when extrapolated, indicated once again that Zelda would pass to the north of Saipan. Zelda passed 30 nm (55 km) to the northeast of Saipan and then directly over Anatahan.

The six-hour time step of the best track (Figure 3-37-6) and its subjective smoothing can not accommodate the short-term track changes indicated by the radar.

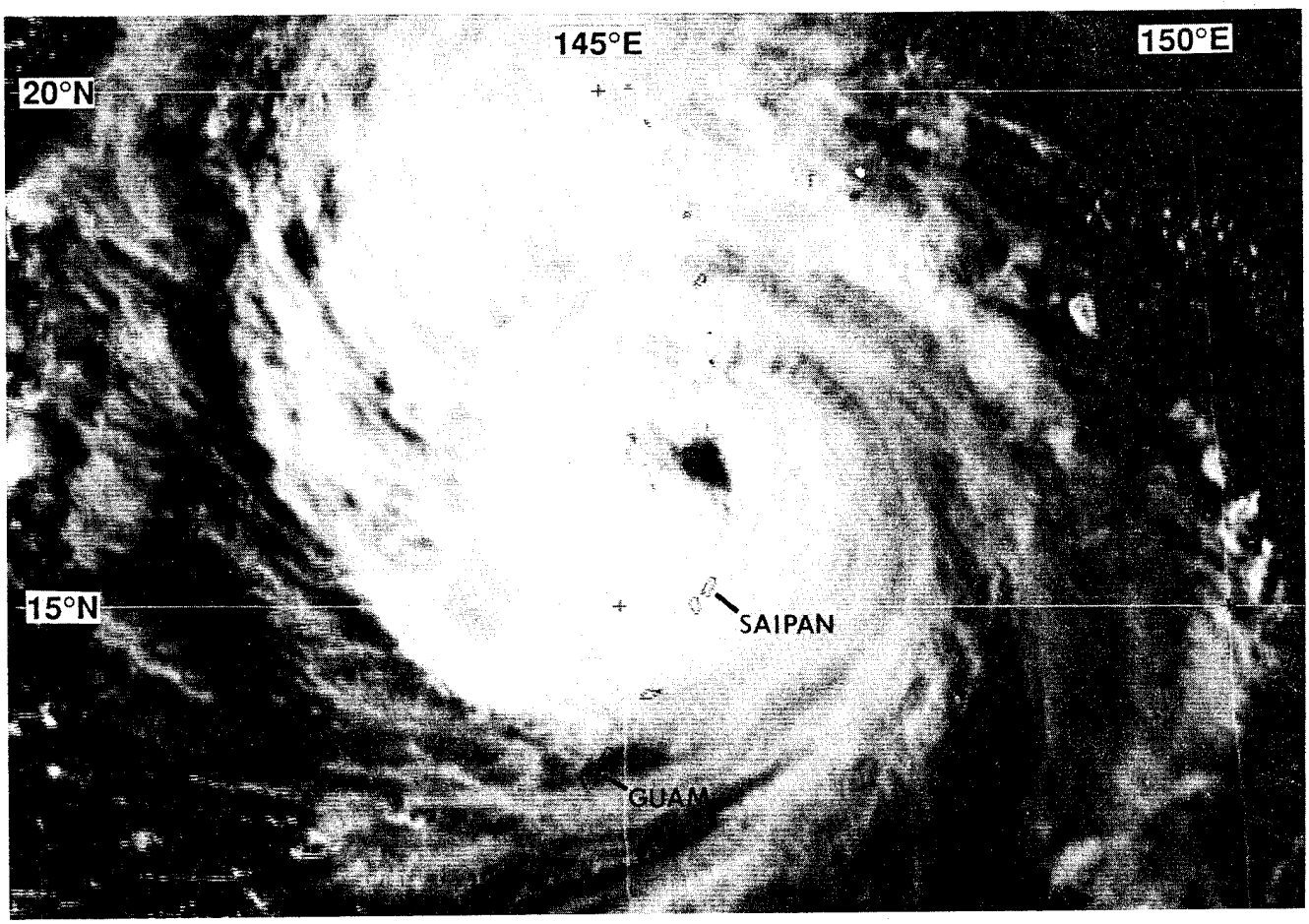

Figure 3-37-3 The island of Anatahan lies within Zelda's eye at the time of this satellite image (030631Z November visible GMS imagery).

IV. IMPACT

Of all the tropical cyclones that affected the Mariana island chain during 1994, Zelda had the most impact. High wind damaged homes in Saipan and Tinian. Hardest hit was the island of Anatahan — the northernmost inhabited island of the Commonwealth of the Northern Mariana Islands. The large eye of Zelda passed over Anatahan where the homes and crops of the 39 residents were devastated. All 39 residents were evacuated by the U.S. Navy and transferred to Saipan. Fortunately, no reports of serious injuries or deaths were received.

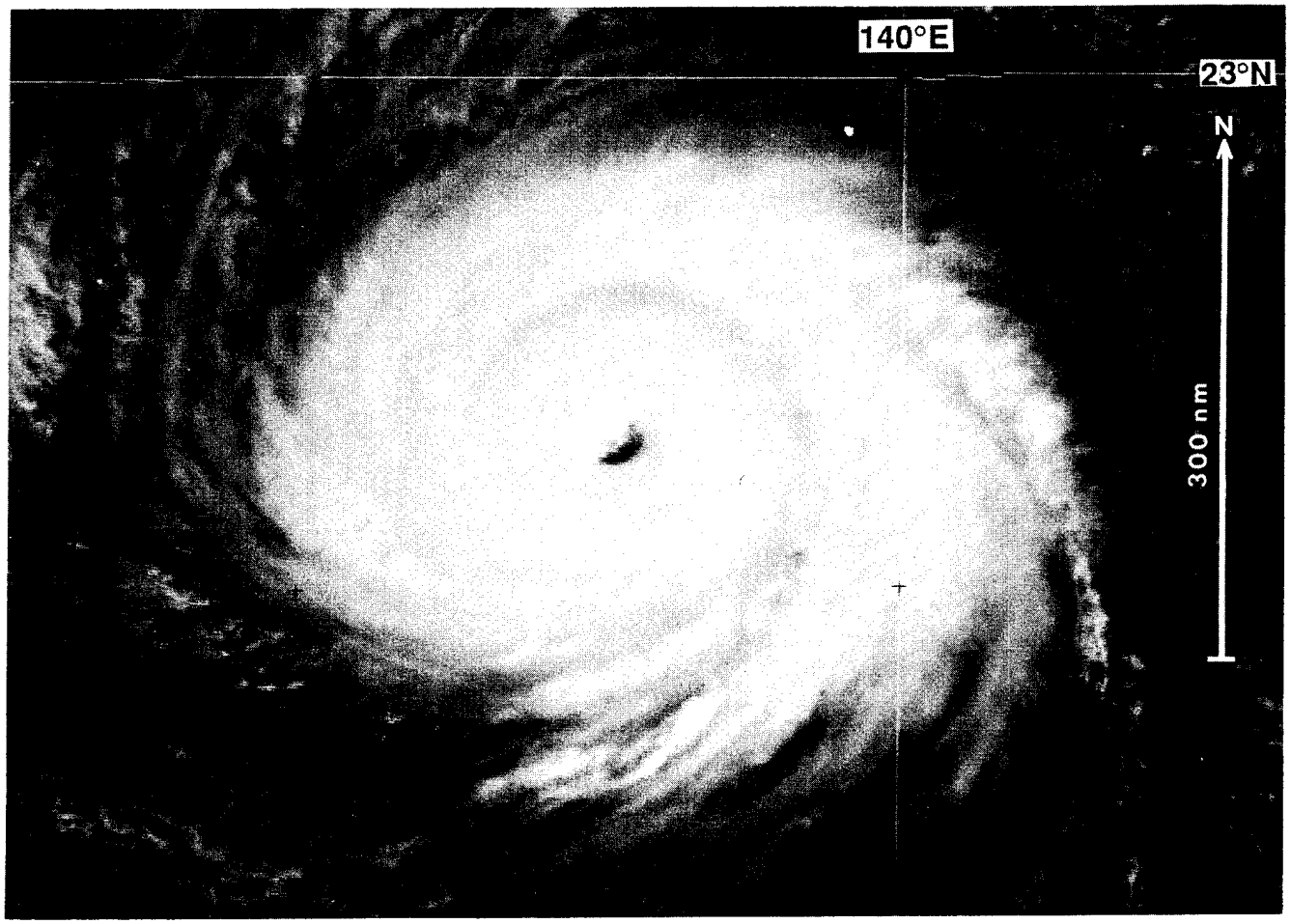

Figure 3-37-4 Super Typhoon Zelda at its peak intensity of 135 kt (69 m/sec) (042331Z November visible GMS imagery).

Figure 3-37-5 Schematic illustration of environmental factors possibly contributing to Zelda's unusual southward motion. Typhoons Verne (33W) (labeled, V) and Wilda (35W) (W) lie along the axis of a reverse oriented monsoon trough, whose axis is moving northward along with these two typhoons. A ridge (zig-zag line) has been induced in the lower and middle troposphere to the southeast of the monsoon trough, and Zelda (Z) has been steered southward around the anticyclonic circulation (labeled, A) along this ridge. The tracks of the tropical cyclones are indicated. Open circle = tropical storm intensity, filled circle = typhoon intensity. Black shaded regions are silhouettes of the deep convection.

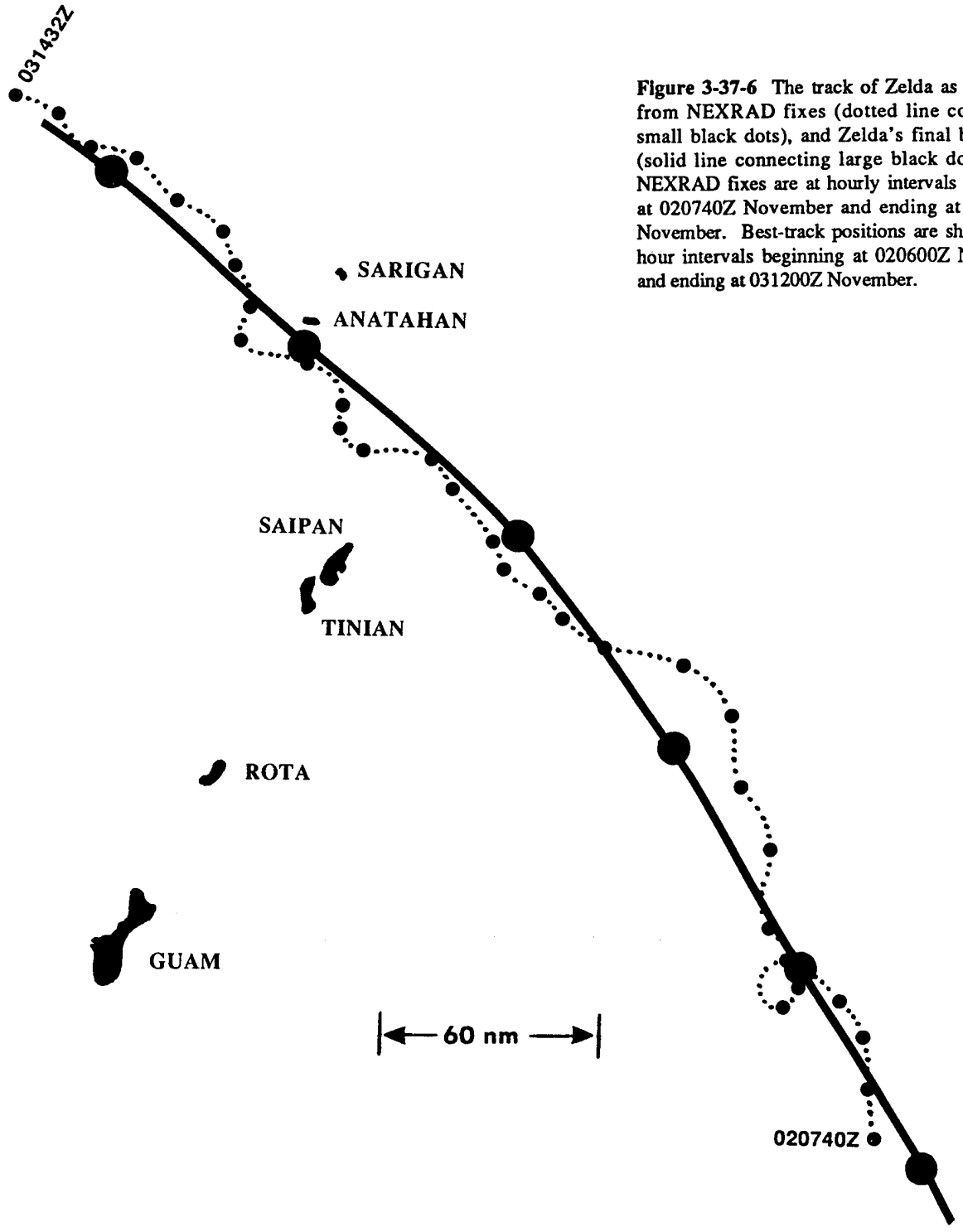

Figure 3-37-6 The track of Zelda as estimated from NEXRAD fixes (dotted line connecting small black dots), and Zelda's final best track (solid line connecting large black dots). The NEXRAD fixes are at hourly intervals beginning at 020740Z November and ending at 031432Z November. Best-track positions are shown at 6-hour intervals beginning at 020600Z November and ending at 031200Z November.

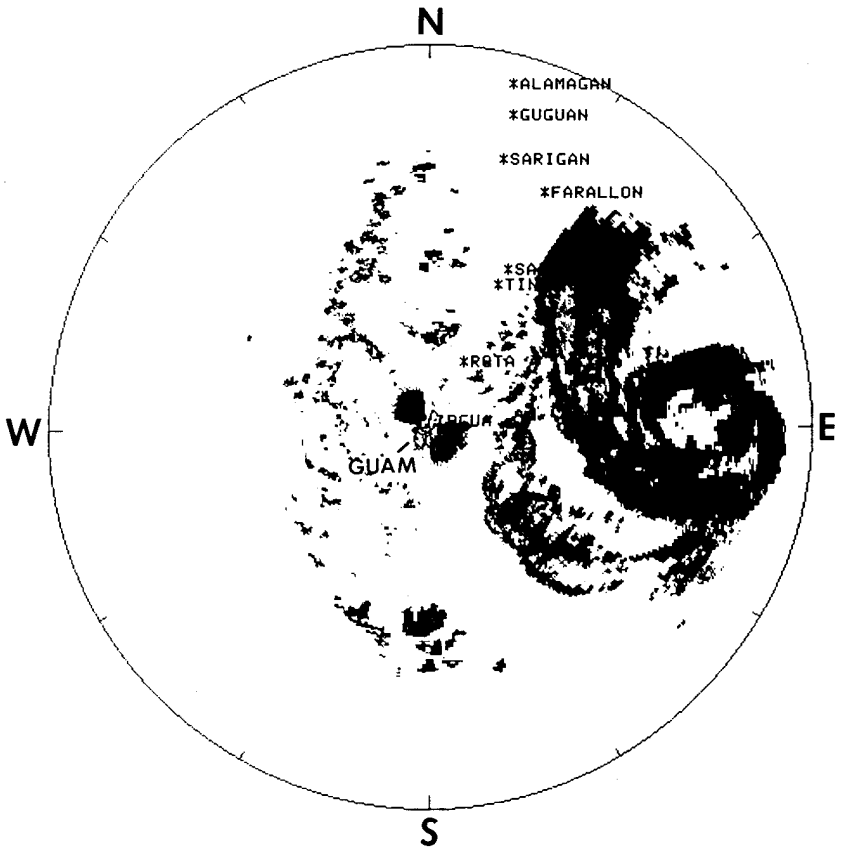

Figure 3-37-7 Zelda's relatively large eye is centered about 170 nm (315 km) to the east of Guam (021415Z November NEXRAD base reflectivity product).

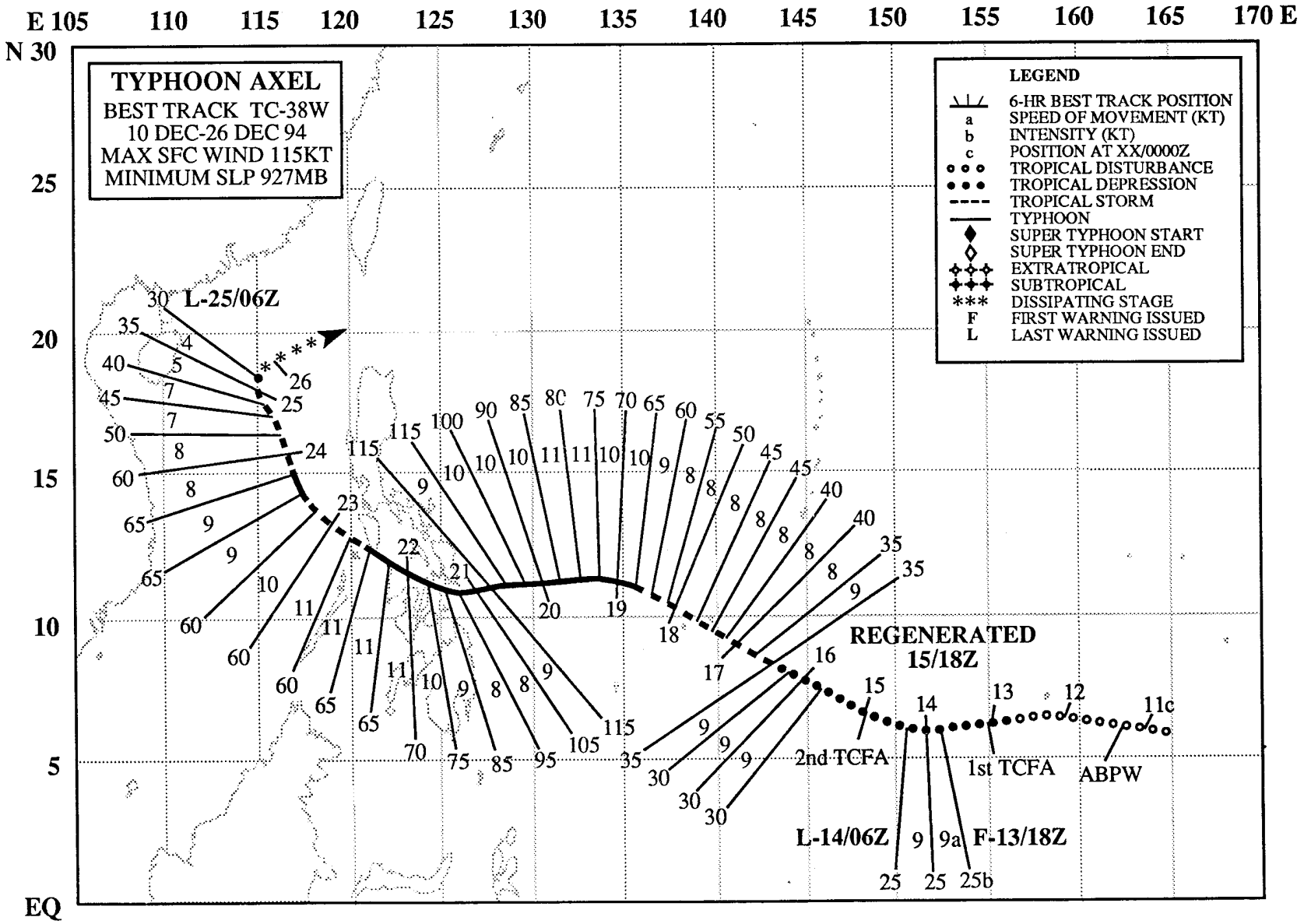
TYPHOON AXEL
BEST TRACK TC-38W
10 DEC-26 DEC 94
MAX SFC WIND 115KT
MINIMUM SLP 927MB
LEGEND
6-HR BEST TRACK POSITION
SPEED OF MOVEMENT (KT)
INTENSITY (KT)
POSITION AT XX/0000Z
TROPICAL DISTURBANCE
TROPICAL DEPRESSION
TROPICAL STORM
TYPHOON
SUPER TYPHOON START
SUPER TYPHOON END
EXTRATROPICAL
SUBTROPICAL
DISSIPATING STAGE
FIRST WARNING ISSUED
LAST WARNING ISSUED
L-25/06Z
REGENERATED
15/18Z
2nd TCFA
1st TCFA
ABPW
L-14/06Z
F-13/18Z
E 105
110
115
120
125
130
135
140
145
150
155
160
165
170 E
N 30
25
20
15
10
5
EQ

TYPHOON AXEL (38W)

I. HIGHLIGHTS

Axel formed in an active near-equatorial trough during the second week of December after a month of no tropical cyclone activity in the western North Pacific basin. At first, the tropical depression that became Axel failed to mature. The JTWC issued its first warning on the system when it was near Chuuk, then issued a final warning 12 hours later. Thirty-six hours after this final warning, regeneration occurred, and the JTWC resumed warning on the system. Axel crossed the central Philippines and caused extensive damage and loss of life. Approximately 24 hours prior to impacting the Philippines, satellite imagery indicated a very rapid, but brief intensification followed by rapid weakening.

II. TRACK AND INTENSITY

After Zelda (37W) dissipated east of Japan in early November, the tropics of the the western North Pacific became very quiet (i.e., the amount of deep convection was greatly reduced), and for more than a month thereafter, no significant tropical cyclones occurred. Axel ended this long period of inactivity as it formed in an active near-equatorial trough (Figure 3-38-1) during the second week of December. For several days prior to Axel's formation, the equitorial region near the international date line was the site of a large cluster of mesoscale convective complexes loosely organized in the twin-trough pattern of Figure 3-38-1a. By 13 December, a distinct low-level circulation center broke away from the cloud cluster and move toward the west. This circulation (pre-Axel) was accompanied by a twin circulation in the Southern Hemisphere (pre-TC 04P) (Figure 3-38-1b).

The tropical disturbance that became Axel was first mentioned on the 110600Z December Significant Tropical Weather Advisory based upon indications from surface reports in the eastern Caroline Islands that a broad surface circulation with an estimated minimum sea-level ppressure of 1006 mb lay beneath an upper-level anticyclone. A Tropical Cyclone Formation Alert was issued at 130100Z based upon 20-30 kt winds measured at an automated weather station on Oroluk Atoll, and also upon improvements in the satellite-observed organization of deep convection in the system. When synoptic observations at Chuuk (WMO 91334) included a gradient-level wind of 35 kt (18 m/sec) and a sea-level pressure below 1004 mb, the first warning was issued on Tropical Depression 38W at 131800Z. Twelve hours later, at 140600Z, a final warning (warning number 3) was issued on Tropical Depression 38W. Quoting from the remarks on this final warning:

". . . Tropical Depression 38W has lost its organization, and has weakened over the past 12 hours. The system is ill defined, and has multiple, weak circulations associated with it. . . . [it] will be closely monitored for signs of regeneration. . . ."

At 142330Z, a second formation alert was issued as the remnants of Tropical Depression 38W began to show signs of regeneration (i.e., an increase in the amount and organization of deep convection near the center of the broad low-level circulation). At 151200Z, warning number 4 was issued on the regenerated Tropical Depression 38W. At 161200Z, the system was upgraged to Tropical Storm Axel. Then, based on satellite imagery that revealed an 11 nm banding eye, Axel was upgraded to typhoon intensity at 190000Z.

Upon reaching 11°N at 181800Z, Axel turned from a west-northwestward heading to a westward heading. The prognostic reasoning for the track forecast at 190000Z included the following comments:

". . . our track forecast is still for Axel to lift slightly [i.e., gain latitude] over the next 24-36 hours

then track westward under the subtropical ridge. In the latter part of the forecast period, Axel should begin to dip back [i.e., move west-southwestward] over the southern Philippine islands. . . ."

After moving straight westward until 201200Z, Axel dipped slightly in latitude and passed south of the Philippine island of Samar between 210600Z and 211200Z, and then made landfall on the island of Leyte shortly after 211200Z. The estimated peak intensity of 115 kt (59 m/sec) occurred at 201200Z while Axel was east of the Philippines. As Axel neared the Philippine archipelago, the intensity fell to 85 kt (44 m/sec). The intensity dropped below the typhoon threshold after Axel crossed the Philippines and entered the South China Sea. Later, while in the South China Sea west of Luzon, Axel re-intensified to a minimal typhoon for two warning periods (231200Z and 231800Z). Thereafter, Axel weakened, and the final warning was issued at 250600Z when the deep convection and upper-level cloud cover was sheared away to the east of the exposed low-level circulation center. The system dissipated over water about 200 nm (370 km) southeast of Hong Kong.

III. DISCUSSION

a. Genesis in a near equatorial trough

According to climatology (e.g., Sadler et al. 1987), during November and December, the low-level monsoon westerly winds of the western Pacific collapse into a narrow band straddling the equator between 5°N and 5°S. At these latitudes, near-equatorial troughs are found which separate the monsoonal westerlies from the tradewinds to their north and south. Tropical cyclones may develop in the trough of either hemisphere, and sometimes they do so symmetrically, resulting in tropical cyclone twins.

The eastward penetration of monsoonal westerlies can be correlated to the values of the indices of the El Niño/Southern Oscillation (ENSO) (Lander 1994b); it is greatest when the Southern Oscillation Index (SOI) is strongly negative. During some years when the SOI is very low, the equatorial westerlies extend beyond the international date line. During the summer and autumn of 1994, the SOI was very low. By November 1994, equatorial westerlies pushed eastward into the Marshall Islands. Associated with these equatorial monsoonal westerlies was a region of large-scale deep convection resembling the depiction in Figure 3-38-1a.

The disturbance which became Typhoon Axel developed in the near-equatorial trough of the northern hemisphere (Figure 3-38-1b) in a large-scale monsoonal cloud system such as the one shown in Figure 3-38-1a. Typical of many tropical cyclones that form in the latter part of the year at low latitude in the eastern reaches of a near-equatorial trough, Axel intensified very slowly. After Axel moved a significant distance to the west along the trough axis, gained latitude, and broke from the extensive cloudiness associated with the equatorial westerlies it intensified more rapidly (Figure 3-38-1c). Axel was associated with a twin — TC 04P. Twin tropical cyclones develop simultaneously in each hemisphere and are symmetrical with respect to the equator (Lander 1990) (e.g., see Figure 3-38-1b).

b. Very short-lived high-intensity cloud signature

During the 24-hour period spanning 200000Z through 210000Z, Axel's satellite- observed cloud pattern underwent a remarkable evolution from a pattern indicative of a moderately intense typhoon, to a cloud pattern indicative of an extemely intense typhoon, and then back to a cloud pattern indicative of a moderately intense typhoon. The intensity of a tropical cyclone may be estimated from certain characteristics of its satellite cloud signature using techniques developed by Dvorak (1975, 1984). Most of the time, these characteristics evolve gradually, and the estimated intensity of a deepening tropical cyclone

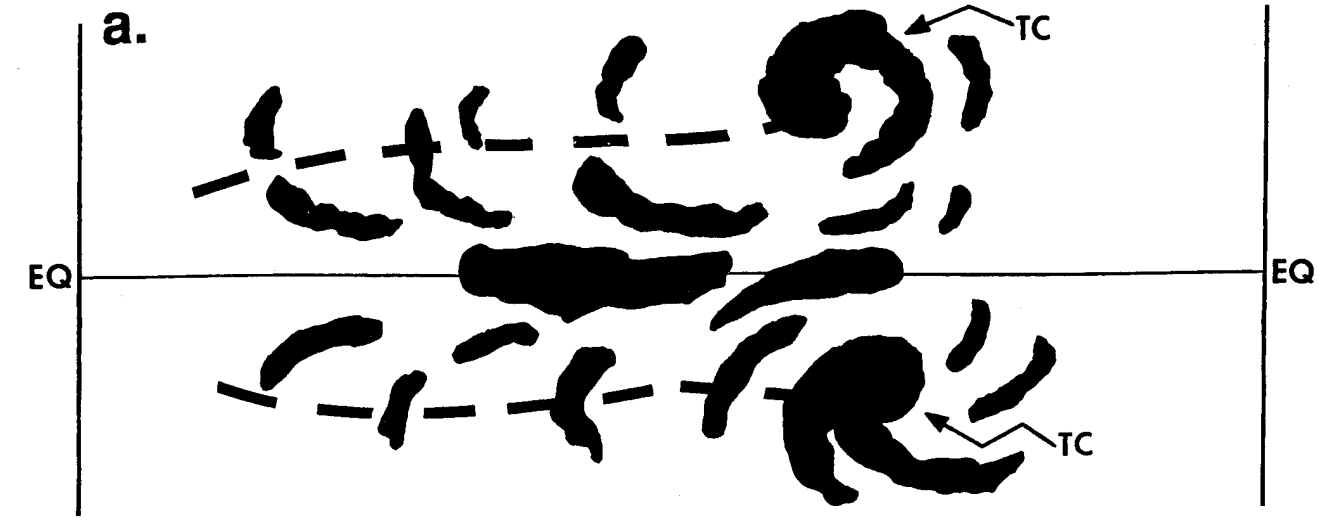
a.
TC
EQ
EQ
TC

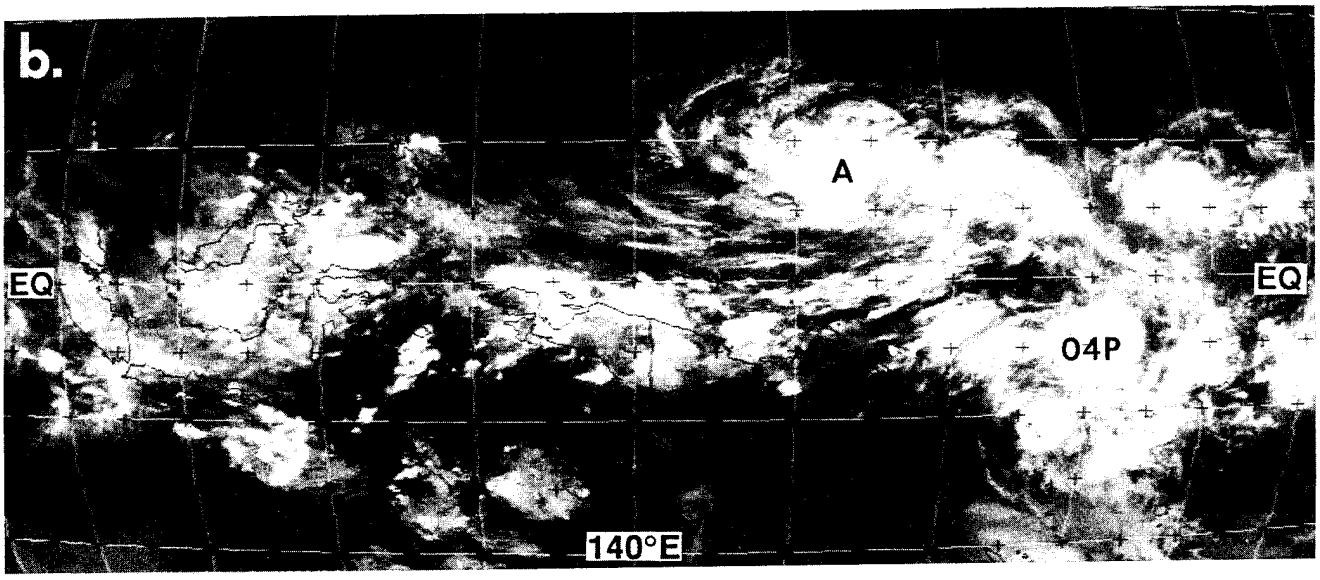
b.
A
EQ
EQ
04P
140°E

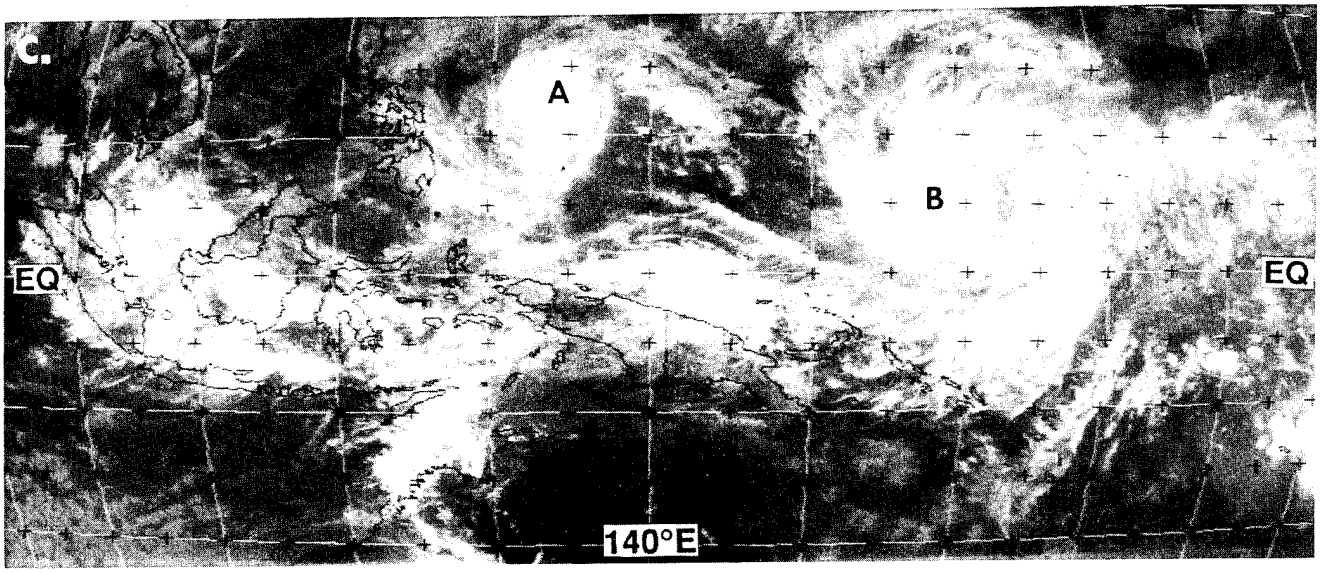
c.
A
B
EQ
EQ
140°E

Figure 3-38-1 (Preceeding page)(a) Schematic illustration of the twin-trough pattern that is common in the western Pacific during November and December. Black silhouettes indicated deep convection. Dashed line shows axes of the near-equatorial troughs. Tropical cyclones (labeled TC) are forming in each hemisphere. (b) Axel (labeled A) and Tropical Cyclone 04P are seen developing in near symmetry within a cloud pattern associated with twin near-equatorial troughs (122131Z December infrared GMS imagery). (c) Axel (labeled A) has moved west-northwestward along the axis of the monsoon trough and has become separated from the monsoonal cloudiness along the equator. A large monsoon depression (labeled B) that bacame Bobbie (39W) is seen forming at the eastern reaches of the monsoon trough in approximately the same area that Axel had formed a week earlier (190031Z December infrared GMS imagery).

typically rises by one "T" number per day until the peak intensity is reached. Few tropical cyclones reach a peak intensity above a T 6.0 (i.e., greater than 115 kt).

At 200532Z, the estimated intensity of Axel, based upon satellite imagery, was 77 kt (40 m/sec) (i.e., a "T" number of 4.5). A dramatic sharpening of Axel's eye, accompanied by thickening and cooling of the tops of the eye wall cloud, took place over the next six hours. An intensity estimate of T 7.0 may be derived from the 201231Z cloud signature (Figure 3-38-2). Zehr (personal communication), who developed an automated Dvorak routine, registered a T 7.3 for Axel at this time. However, soon after this peak, the eye (and the eye wall cloud) became poorly defined: the eye wall cloud tops warmed, and breaks appeared. At 202331, the estimated T number had dropped to 5.0 (see Table 3-38-1). For deepening tropical cyclones, the intensity of the tropical cyclone parallels the T number (i.e., there is no lead or lag between the satellite-observed T number and the corresponding intensity of the tropical cyclone). Axel is a rare case where the satellite intensity estimates exhibited extraordinarily large and extremely rapid changes. Without ground truth or in situ measurements, it is not possible to determine if the changes in the satellite-observed cloud signature of Axel corresponded to similar extraordinarily large and extremely rapid changes in the maximum sustained wind.

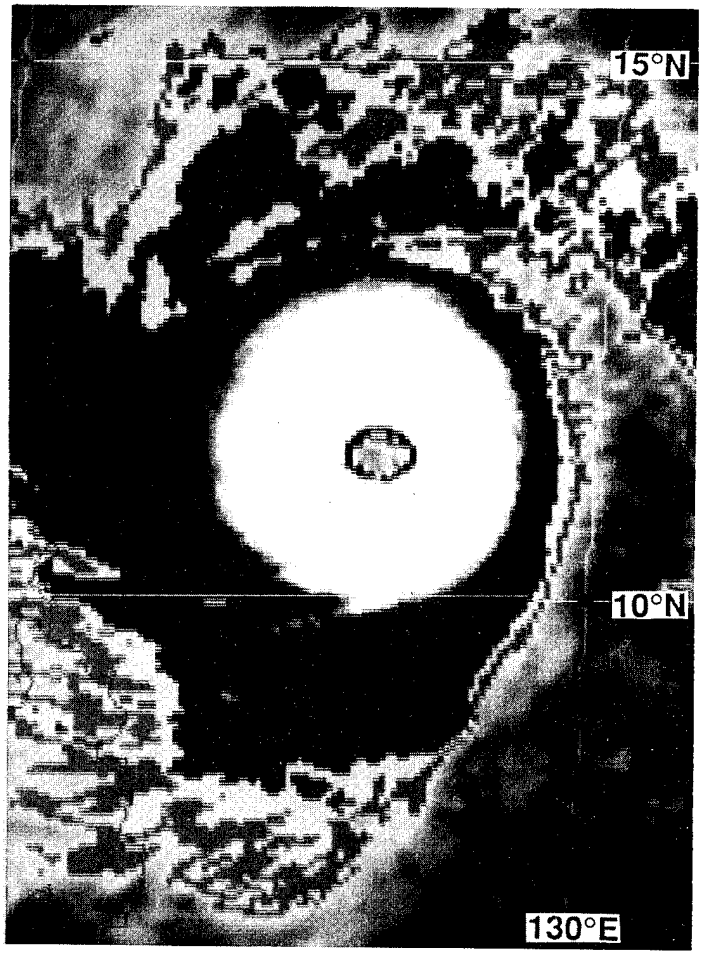

Figure 3-38-2 Axel shown at a time when its satellite cloud signature acquired characteristics of an extremely intense typhoon. The enhancement curve know as MB highlights the well-defined eye and the azimuthally symmetric wide and cold-topped eye wall. (201231Z December infrared GMS imagery).

IV. IMPACT

Axel's greatest impact was to the central Philippines. At 180000Z, with an intensity of 50 kt (26 m/sec), Axel passed 30 nm (55 km) to the north of Yap where only minor damage to vegetation was reported. In the Philippines, however, Axel's impact was far more serious. At least 12 people died in the central Philippines. Flood waters breached a dam, drowning five people and injuring 25 in Bacolod City, 260 nm (480 km) southeast of Manila. In Talcoban City, capital of Leyte province, seven people died and 17 were reported missing. On the southern

island of Mindanao, huge waves whipped up by the approaching typhoon destroyed 163 houses, leaving 897 people homeless. In total 1,443 houses were destroyed, leaving at least 7,930 people homeless. A 12-hour power blackout affected Manila when strong winds knocked down a major transmission line on Luzon.

TABLE 3-38-1 Estimated intensity of Axel from Enhanced Infrared Imagery (EIR) during the period 200031Z December to 202331Z December.

Time	T number	Corresponding wind speed
200031Z	4.5	77 kt (40 m/sec)
200532Z	4.5	77 kt (40 m/sec)
200831Z	5.5	102 kt (53 m/sec)
200931Z	5.5	102 kt (53 m/sec)
201024Z	6.0	115 kt (59 m/sec)
201131Z	7.0	140 kt (72 m/sec)
201231Z	7.0	140 kt (72 m/sec)
201331Z	7.0	140 kt (72 m/sec)
201531Z	6.5	127 kt (65 m/sec)
201624Z	6.5	127 kt (65 m/sec)
201831Z	5.5	102 kt (53 m/sec)
202031Z	5.5	102 kt (53 m/sec)
202331Z	5.0	90 kt (46 m/sec)

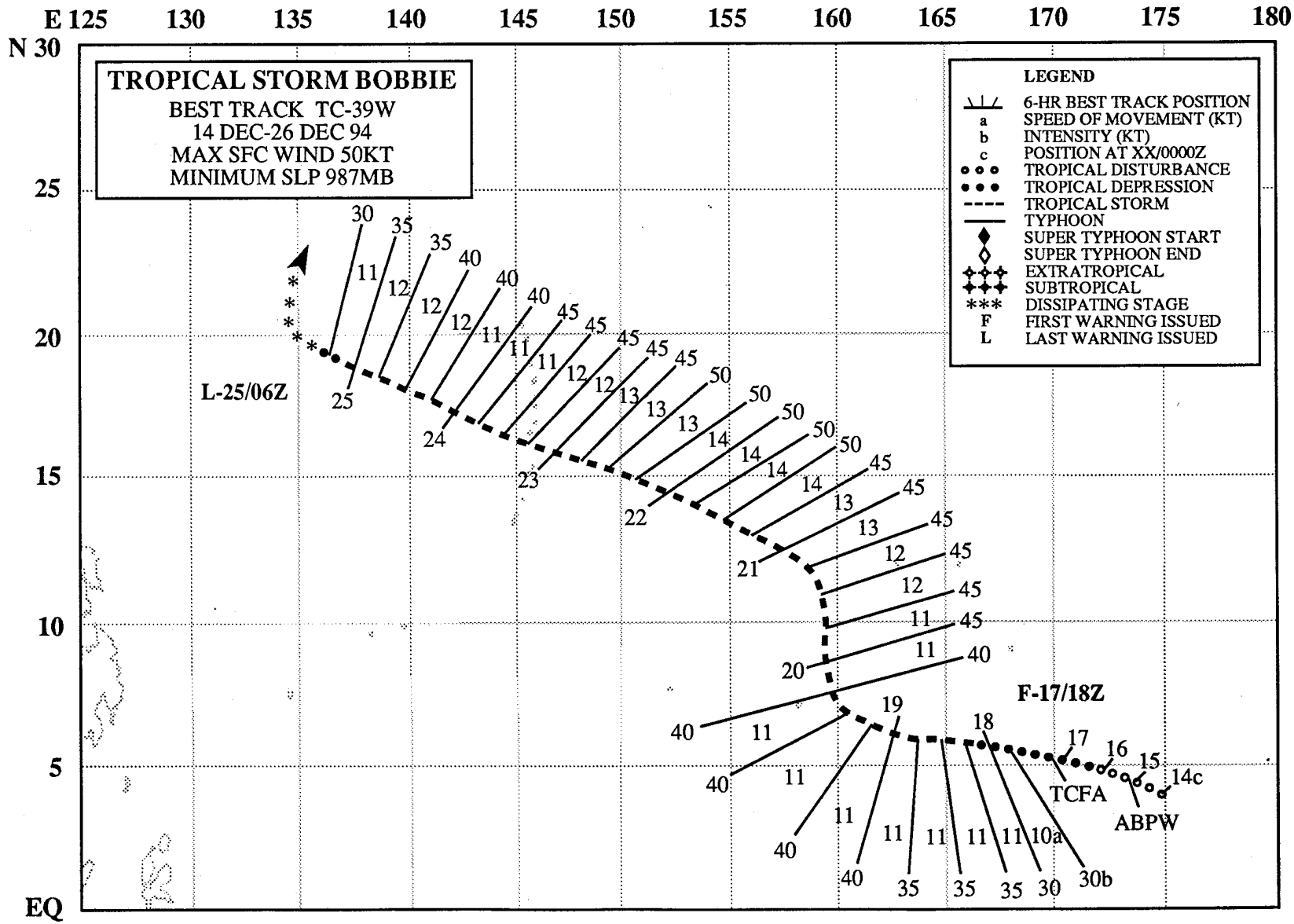
TROPICAL STORM BOBBIE
BEST TRACK TC-39W
14 DEC-26 DEC 94
MAX SFC WIND 50KT
MINIMUM SLP 987MB
LEGEND
6-HR BEST TRACK POSITION
a SPEED OF MOVEMENT (KT)
b INTENSITY (KT)
c POSITION AT XX/0000Z
TROPICAL DISTURBANCE
TROPICAL DEPRESSION
TROPICAL STORM
TYPHOON
SUPER TYPHOON START
SUPER TYPHOON END
EXTRATROPICAL
SUBTROPICAL
*** DISSIPATING STAGE
F FIRST WARNING ISSUED
L LAST WARNING ISSUED
E 125 130 135 140 145 150 155 160 165 170 175 180
N 30 25 20 15 10 5 EQ
L-25/06Z
F-17/18Z
TCFA
ABPW

TROPICAL STORM BOBBIE (39W)

I. HIGHLIGHTS

Bobbie was the last significant tropical cyclone of 1994 in the western North Pacific. For its entire life, it was a sheared system with the low-level circulation center displaced from the deep convection. Its low-level circulation center was often obscured beneath cirrus debris. The cirrus shield over its deep convection lacked the typical characteristics produced by shear. SSM/I imagery from the DMSP satellites, and scatterometer-derived winds from the ERS-1 satellite (in conjunction with conventional IR and visible imagery) were instrumental in determining the location and structure of Bobbie.

II. TRACK AND INTENSITY

During mid-December 1994, the large-scale low-level wind pattern of the deep tropics of the western North Pacific featured equatorial westerlies bounded by near-equatorial troughs at roughly 5°N and 5°S. The equatorial westerlies and associated large-scale deep convection extended eastward beyond the international date line. This flow pattern occurs frequently during the Spring and late Fall, and has been defined as the "twin trough" pattern (see Figure 3-39-1). Most episodes of twin tropical cyclones occur in association with this large-scale low-level wind pattern. On 15 December, an area of persistent convection associated with a broad, weak surface circulation in the Marshall Islands was mentioned in the 150600Z December Significant Tropical Weather Advisory. At 170430, a Tropical Cyclone Formation Alert was issued. It stated, in part:

" . . . a pre-existing [low-level] circulation with persistent convection [is intensifying]. . . . surface pressures [have dropped] in the vicinity of Majuro. Their synoptic observation from 170300Z showed [the] surface pressure at 1002.7 mb . . . this system is elongated east-west and may have several circulation centers."

Based on further synoptic data from the Marshall Islands, a tropical depression warning was issued at 171800Z. Remarks contained on this warning included:

" . . . this system is poorly organized at the present time, but is showing signs of steady development. The minimum central pressure in the broad low pressure region is estimated to be 1002 mb. If the [JTWC] anticipates that this tropical depression will reach tropical storm intensity, then a standard 72-hour tropical cyclone warning will be issued . . ."

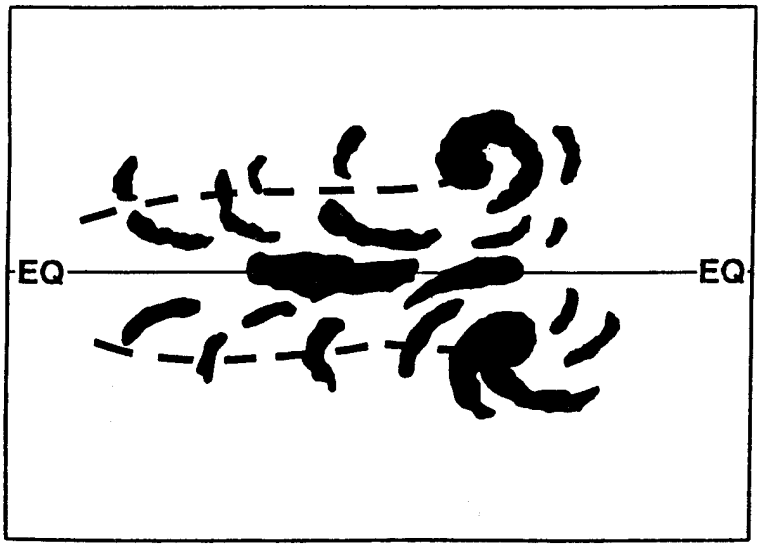

Figure 3-39-1 Schematic illustration of the distribution of deep convection associated with the "twin-trough" pattern. The axes of the near-equatorial troughs are represented by dashed lines.

At 181800, JTWC forecasters predicted that the the tropical depression would become a tropical storm in 24 hours, so a standard 72-hour tropical cyclone warning was issued. Remarks on this warning stated:

" . . . synoptic data from Micronesia

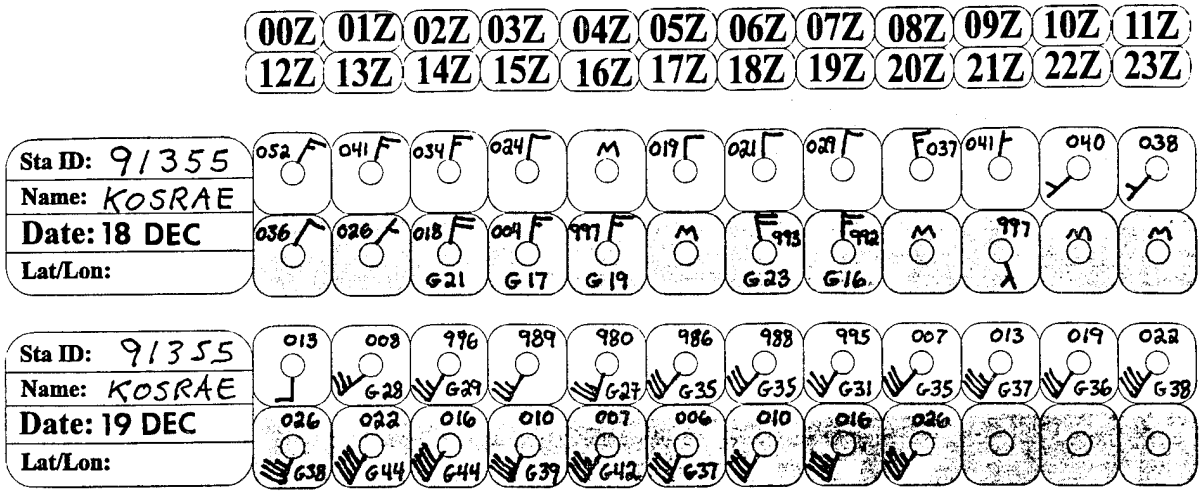

Figure 3-39-2 Time series of hourly synoptic observations at Kosrae (WMO 91355) as Bobbie passed near the island from east to west.

indicate that Tropical Depression 39W is steadily deepening over a large area. Near-gale force winds are present north of the broad low pressure center. . . . [the] warning position is based on the estimated position of the low pressure center from synoptic data; satellite imagery does not reveal a single, well-defined cyclone center and is considered to be unreliable at the present time. . . . "

This disturbance had the characteristics of a monsoon depression (JTWC 1993): a large (1500 km diameter) region of cyclonic wind flow, a relatively large (200 km diameter) light wind core, and a lack of persistent central convection. At 190000Z, the system was upgraded to Tropical Storm Bobbie based upon visible satellite imagery and synoptic reports from Kosrae (WMO 91355) and Pingelap (91352). Synoptic data from Kosrae (Figure 3-39-2) indicated that a band of 40 kt (21 m/sec) southwesterly wind existed in the southeastern quadrant of Bobbie.

At 191200Z, Bobbie turned toward the north for 24 hours and then, at 201200Z, resumed a west-northwesward track. Bobbie intensified very slowly and reached its peak intensity of 50 kt (26 m/sec) at 220000Z. Between 230000Z and 230600Z, the broad low-level center of Bobbie passed 60 nm (110 km) to the north of Saipan. Bobbie continued on a west-northwestward track until 251800Z when its remnant low-level circulation turned north and recurved.

III. DISCUSSION

In its simplest form, the deep convection associated with a "shear"-type tropical cyclone is displaced down-shear of the low-level circulation center (LLCC). The cirrus emanating from the top of this deep convection is carried farther down-shear leaving the LLCC exposed (i.e., not obscured by deep convection or by cirrus debris) (Figure 3-39-3). In such cases, the diagnosis of the position and intensity is relatively easy, especially during the daylight hours when the LLCC is easily detected in visible satellite imagery. The intensity is estimated based upon the tightness of curvature of the low-level cloud lines (Dvorak 1975) and by the separation distance of the LLCC from the edge of the cirrus canopy over the deep convection. On IR imagery, the intensity is estimated from the separation distance of the LLCC

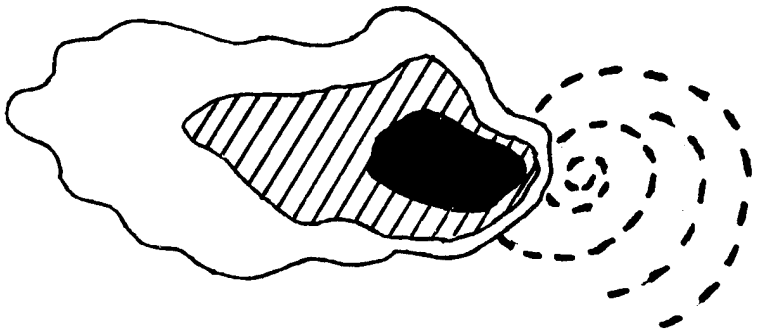

Figure 3-39-3 Schematic illustration of the structure of a typical sheared tropical cyclone. Black-shaded region shows coldest cloud top temperature. Dashed lines show low-level cloud lines. Vertical shear from the east has sharpened the temperature gradient on the eastern side of the deep convection, and has caused the low-level circulation center to become exposed on the eastern side of the deep convection.

from the edge of dense cirrus with a threshold equivalent black-body temperature of -42°C (Dvorak 1984). The highest intensity that can be diagnosed for a developing TC with a "shear" type cloud pattern is 55 kt (28 m/sec).

At intensities greater than 55 kt (28 m/sec), the LLCC tends to be under the dense cirrus canopy, or surrounded by spiral bands of deep convection. As soon as the LLCC is deemed to have moved under the cirrus canopy, the pattern type changes to "central dense overcast" (CDO). On visible satellite imagery, the intensity of a tropical cyclone with a CDO cloud pattern is determined primarily by the diameter of the CDO. On IR imagery, it is determined by the estimated embedded distance of the LLCC under the cold cirrus cloud canopy.

On some occasions, the LLCC of a tropical cyclone that possesses a "shear" type cloud pattern is often difficult to locate with conventional visible and IR imagery. Cirrus debris may obscure the low-level cloud lines. This is especially true at night when only IR imagery is available, and thin cirrus, which may not obstruct the view of the low-level cloud lines in visible imagery, is completely obstuctive to the view of low-level features. The nighttime difficulty of tracking an exposed LLCC has led to the common diagnostic error that has come to be known as the "sunrise surprise". This occurs when the analyst estimates the postion of the LLCC too close to the deep convection at night, only to find it displaced a larger distance from it on the first visible image of morning.

Even in the abscence of distinct low-level cloud lines marking the LLCC of a "shear" type tropical cyclone, the postion of the LLCC may be estimated (with less confidence) by other manifestations of shear in the deep convection. Under shearing conditions, the up-shear side of the cold-cloud canopy usually has a sharp edge (Figure 3-39-3), and the down-shear side the cirrus thins more gradually. On enhanced IR (EIR) imagery, sharp temperature gradients are found on the up-shear side of the cirrus cloud shield and much less steep gradients of temperature are found down-shear (Figure 3-39-3). For diagnostic purposes, it is best to position the LLCC on the up-shear edge of the cloud at a separation distance consistent with earlier visible imagery, and consistent with the past motion and expected changes of intensity.

For much of its life, Bobbie's cirrus outflow exhibited no appearent manifistation of shear. Its cirrus canopy and cirrus outflow were symmetrical with respect to the cloud system center (CSC). The persistent convection on the western side of the LLCC — at first showing conventional manifestations of shear (i.e., an easily detected LLCC east of the deep convection and cirrus outflow streaming westward from this deep convection) — became symmetrical in appearance (Figure 3-39-4). In addition to the

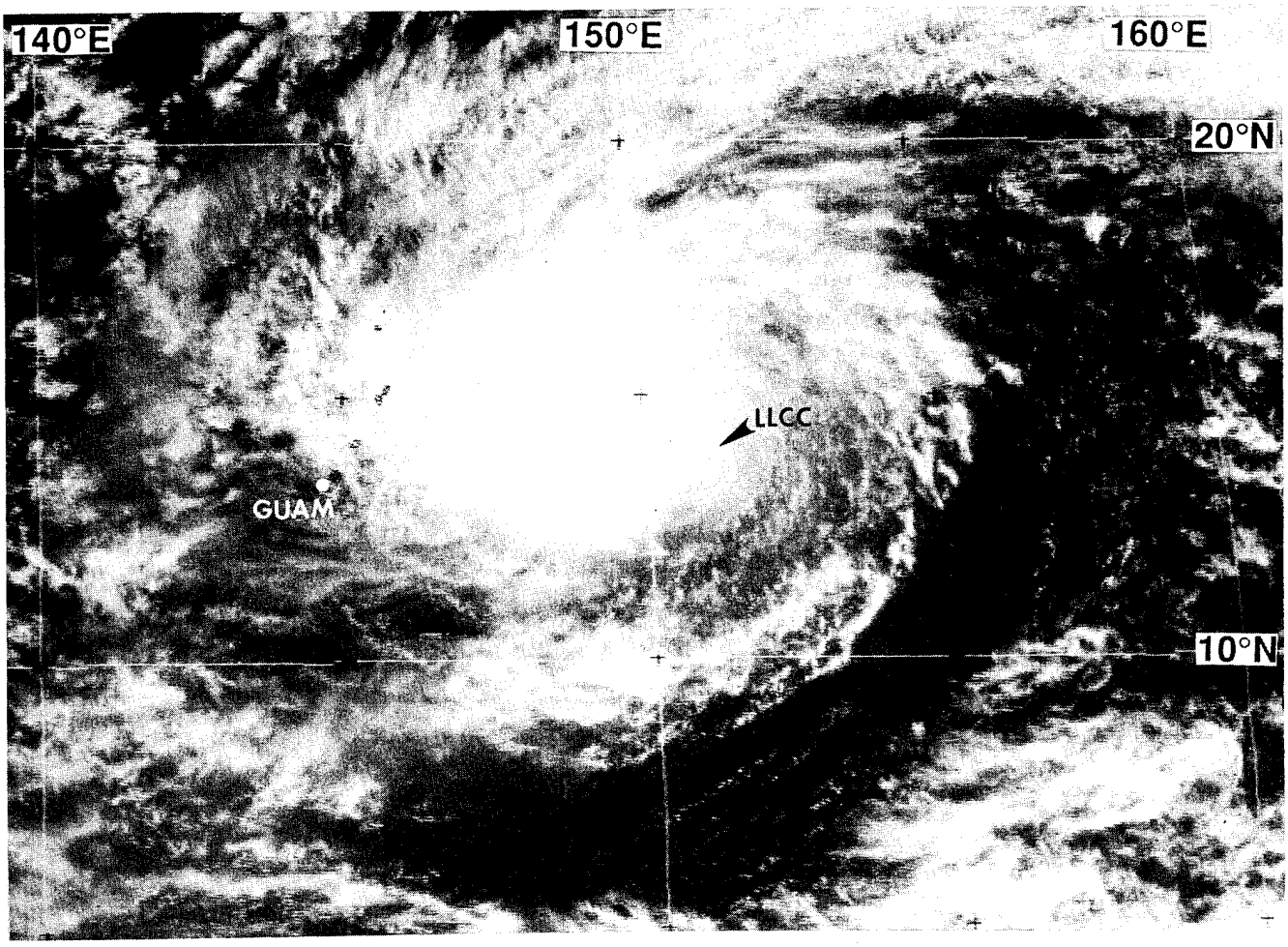

Figure 3-39-4 Bobbie at its peak intensity of 50 kt (26 m/sec). The low-level circulation center (labeled "LLCC") is displaced about 120 nm to the southeast of the center of the deep convection (220031Z December visible GMS imagery).

symmetry of the cloud shield, the LLCC was obscured by cirrus debris. At the time of the imagery in Figure 3-39-4, the LLCC was difficult to locate. Satellite analysts at the JTWC considered the option of locating the LLCC closer to the CSC, thereby increasing the intensity estimate of Bobbie to the typhoon threshold. However, the rapid motion resulting from such a placement, and the constraint of prior knowledge of the sheared structure of the system were factored into the decision to position the LLCC east of the CSC and thereby hold the intensity estimate below the typhoon threshold. Wind vectors obtained from the scatterometer aboard the ERS-1 satellite (Figure 3-31-5) later confirmed the large displacement of the LLCC from the CSC at the time of the satellite image in Figure 3-39-4.

A day later, the large displacement of the LLCC of Bobbie to the east-southeast of the CSC was confirmed by visible satellite imagery (Figure 3-39-6a) and by microwave imagery (Figure 3-39-b) obtained from a DMSP satellite. Conventional unenhanced IR imagery (Figure 3-39-6d) and enhanced IR imagery (Figure 3-39-6e) gave little indication of the large displacement of the LLCC from the CSC. Microwave images of Bobbie (Figures 3-39-6b,c) clearly depict the structure of the system: the roots of the deep convection responsible for the large oval-shaped cirrus cloud canopy seen in the visible and IR imagery (Figure 3-39-6a,d,e) are to the west of the LLCC along a major spiral band leading into a well-defined LLCC. Additional confirmation of the large (120 nm ; 220 km) displacement of the LLCC of

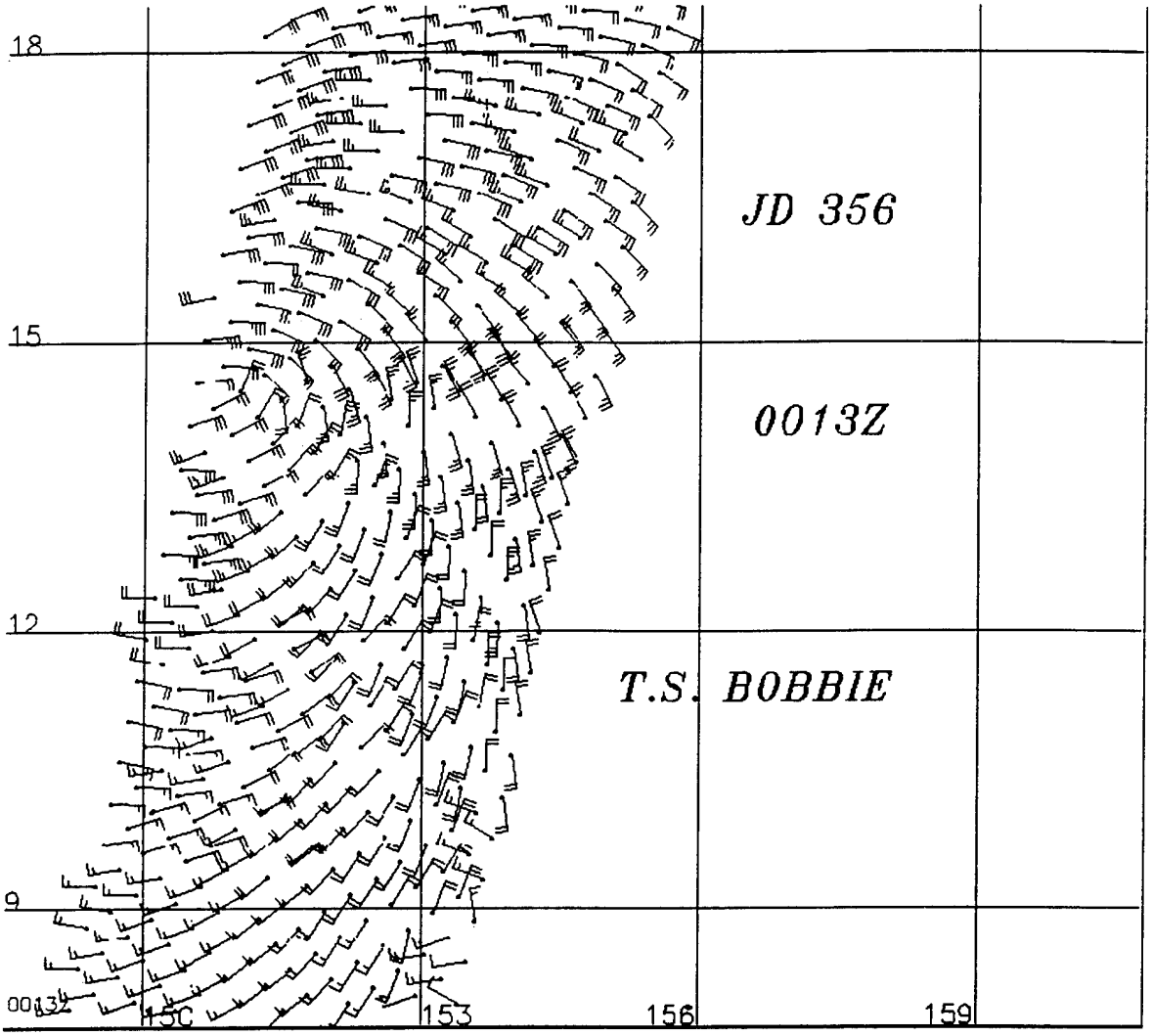

Figure 3-39-5 Wind vectors derived from the scatterometer aboard the ERS-1 satellite clearly indicate the location of Bobbie's low-level circulation center. Maximum wind vector is 35 kt (17 m/sec) on the north side of the circulation center. The timing of this pass (220013Z December) is nearly coincident with the visible image in Figure 3-39-4.

Bobbie from its CSC was obtained from synoptic reports in the Mariana Islands during Bobbie's passage through that region.

To summarize, the structure of Bobbie was difficult to diagnose for a large portion of its track, especially as it neared and passed through the Mariana island chain. Despite the presence of a persistent, large, oval-shaped dense cirrus canopy (which could have been diagnosed as the CDO of the system), a very careful study of visible satellite imagery, coupled with valuable additional information from microwave imagery and scatterometer winds indicated that the LLCC of Bobbie was well-displaced from the CSC (Figures 3-39-7). The total suite of multi-spectral information (visible, IR, active and passive microwave, and radar reflectivity) from numerous remote sensing platforms (i.e., the GMS, NOAA, DMSP, and ERS-1satellites; and, Guam's NEXRAD), was absolutely essential to accurately locating the LLCC of Bobbie, and reasonably diagnosing its intensity.

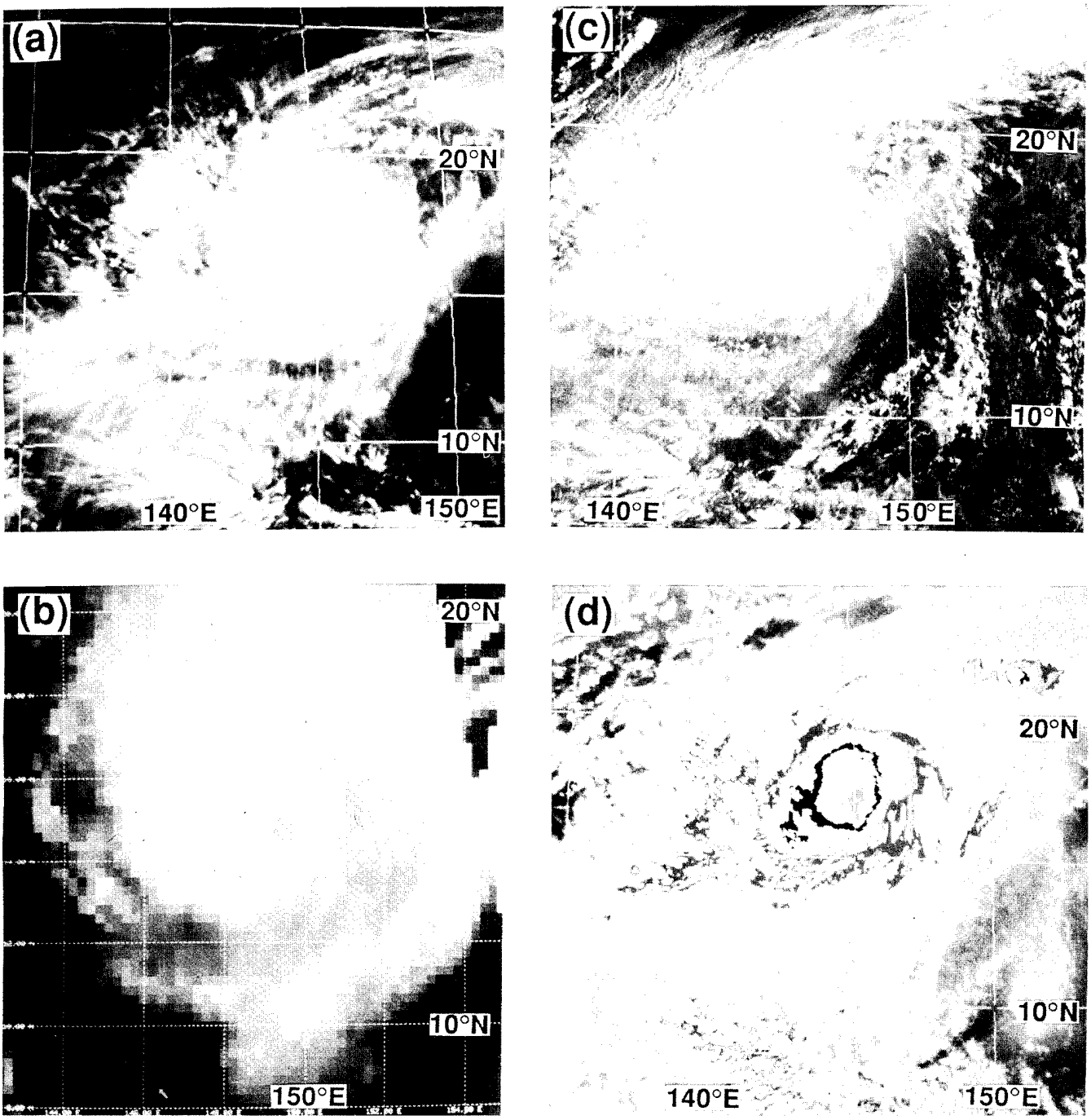

Figure 3-39-6 (a) Cirrus outflow from Bobbie's deep convection appears to be nearly symmetrical (230031Z December infrared GMS imagery). (b) Bobbie's deep convection is seen to be located on a major spiral band which wraps into a well-defined low-level circulation center (230014Z December DMSP 85H microwave imagery). (c)The low-level circulation center of Bobbie is relatively easy to locate beneath thin cirrus to the east-southeast of the deep convection (230031Z December GMS visible imagery). (d) Enhancing the IR imagery in (a) fails to reveal any of the traditional manifestations of vertical shear (230031Z December enhanced infrared GMS imagery).

IV. IMPACT

Bobbie brought heavy rain and gales to some islands and atolls in Micronesia. No reports of injuries or significant damage were received.

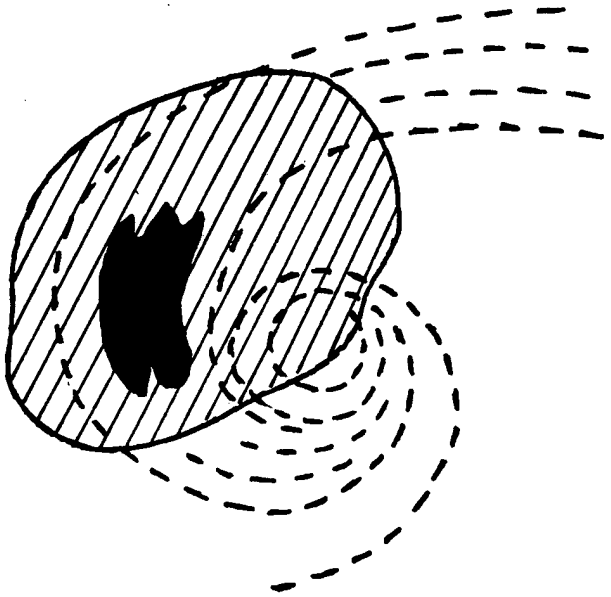

Figure 3-39-7 Schematic illustration of the structure of Bobbie as it passed through the Mariana island chain. Deep convection (black-shaded region) is located well to the west-northwest of the low-level circulation center, and is producing a large nearly symmetrical cirrus canopy (hatched region). The symmetry of the cirrus canopy, and its blocking of the view of the low-level circulation center, made diagnosis of the position and intensity of Bobbie relatively difficult. Microwave imagery and scatterometer-derived winds were valuable in defining the structure of Bobbie.

3.2 NORTH INDIAN OCEAN TROPICAL CYCLONES

1994 was an average year for North Indian Ocean tropical cyclone activity. Spring and fall in the North Indian Ocean are periods of transition between major climatic controls, and are the most favorable seasons for tropical cyclone activity. Of the five significant tropical cyclones that occured this year; three were in the spring (TC 01B, TC02B, and TC 03A), and two were in the fall (TC 04B and TC05A) (Table 3-5). The climatological average for tropical cyclone occurance in this basin is five, with peaks in the spring and fall (Table 3-6).

The best track composites for the 1994 North Indian Ocean tropical cyclones are shown in Figure 3-14. The most notable of these storms is Tropical Cyclone 02B. Its track and intensity characteristics are nearly identical to Tropical Cyclone 02B of 1991, which was responsible for 138,000 deaths in Bangladesh. Fortunately, the death toll from this year's TC 02B was far lower. The two tropical cyclones which occured in the North Arabian Sea (TC 03A in June and TC 05A in November) are interesting in that they both moved along non-climatological westward tracks.

Table 3-5 NORTH INDIAN OCEAN SIGNIFICANT TROPICAL CYCLONES FOR 1994

TROPICAL CYCLONE	PERIOD OF WARNING	NUMBER OF WARNINGS ISSUED	MAXIMUM SURFACE WINDS-KT	(M/SEC)	ESTIMATED MSLP (MB)
TC 01B	22 MAR - 25 MAR	11	40	(21)	994
TC 02B	29 APR - 03 MAY	18	125	(64)	916
TC 03A	07 JUN - 09 JUN	8	45	(23)	991
TC 04B	30 OCT - 31 OCT	4	45	(23)	991
TC 05A	15 NOV - 20 NOV	19	55	(28)	984
	TOTAL	60			

The criteria used in Table 3-6 are as follows:

1. If a tropical cyclone was first warned on during the last two days of a particular month and continued into the next month for longer than two days, then that system was attributed to the second month.
2. If a tropical cyclone was warned on prior to the last two days of a month, it was attributed to the first month, regardless of how long the system lasted.
3. If a tropical cyclone began on the last day of the month and ended on the first day of the next month, that system was attributed to the first month. However, if a tropical cyclone began on the last day of the month and continued into the next month for only two days, then it was attributed to the second month.

TABLE 3-6 LEGEND

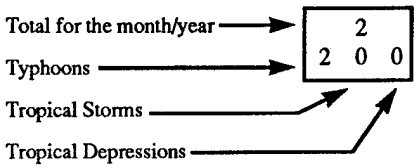

Table 3-6 DISTRIBUTION OF NORTH INDIAN OCEAN TROPICAL CYCLONES FOR 1975-1994

YEAR	JAN	FEB	MAR	APR	MAY	JUN	JUL	AUG	SEP	OCT	NOV	DEC	TOTALS
1975	1	0	0	0	2	0	0	0	0	1	2	0	6
	010	000	000	000	200	000	000	000	000	100	020	000	3 3 0
1976	0	0	0	1	0	1	0	0	1	1	0	1	5
	000	000	000	010	000	010	000	000	010	010	000	010	0 5 0
1977	0	0	0	0	1	1	0	0	0	1	0	2	5
	000	000	000	000	010	010	000	000	000	010	000	110	1 4 0
1978	0	0	0	0	1	0	0	0	0	1	2	0	4
	000	000	000	000	000	000	000	000	000	010	200	000	2 2 0
1979	0	0	0	0	1	1	0	0	2	1	2	0	7
	000	000	000	000	100	010	000	000	011	010	011	000	1 4 2
1980	0	0	0	0	0	0	0	0	0	0	1	1	2
	000	000	000	000	000	000	000	000	000	000	010	010	0 2 0
1981	0	0	0	0	0	0	0	0	1	0	1	1	3
	000	000	000	000	000	000	000	000	010	000	100	100	2 1 0
1982	0	0	0	0	1	1	0	0	0	2	1	0	5
	000	000	000	000	100	010	000	000	000	020	100	000	2 3 0
1983	0	0	0	0	0	0	0	1	0	1	1	0	3
	000	000	000	000	000	000	000	010	000	010	010	000	0 3 0
1984	0	0	0	0	1	0	0	0	0	1	2	0	4
	000	000	000	000	010	000	000	000	000	010	200	000	2 2 0
1985	0	0	0	0	2	0	0	0	0	2	1	1	6
	000	000	000	000	020	000	000	000	000	020	010	010	0 6 0
1986	1	0	0	0	0	0	0	0	0	0	2	0	3
	010	000	000	000	000	000	000	000	000	000	020	000	0 3 0
1987	0	1	0	0	0	2	0	0	0	2	1	2	8
	000	010	000	000	000	020	000	000	000	020	010	020	0 8 0
1988	0	0	0	0	0	1	0	0	0	1	2	1	5
	000	000	000	000	000	010	000	000	000	010	110	010	1 4 0
1989	0	0	0	0	1	1	0	0	0	0	1	0	3
	000	000	000	000	010	010	000	000	000	000	100	000	1 2 0
1990	0	0	0	1	1	0	0	0	0	0	1	1	4
	000	000	000	001	100	000	000	000	000	000	001	010	1 1 2
1991	1	0	0	1	0	1	0	0	0	0	1	0	4
	010	000	000	100	000	010	000	000	000	000	010	000	1 3 0
1992	0	0	0	0	1	2	1	0	1	3	3	2	13
	000	000	000	000	100	020	010	000	001	021	210	020	3 8 2
1993	0	0	0	0	0	0	0	0	0	0	2	0	2
	000	000	000	000	000	000	000	000	000	000	200	000	2 0 0
1994	0	0	1	1	0	1	0	0	0	1	1	0	5
	000	000	010	100	000	010	000	000	000	010	010	000	1 4 0
(1975-1994)													
AVERAGE	0.2	0.1	0.1	0.2	0.6	0.6	0.1	0.1	0.3	0.9	1.5	0.5	4.9
CASES	3	1	1	4	12	12	1	1	5	18	29	10	97

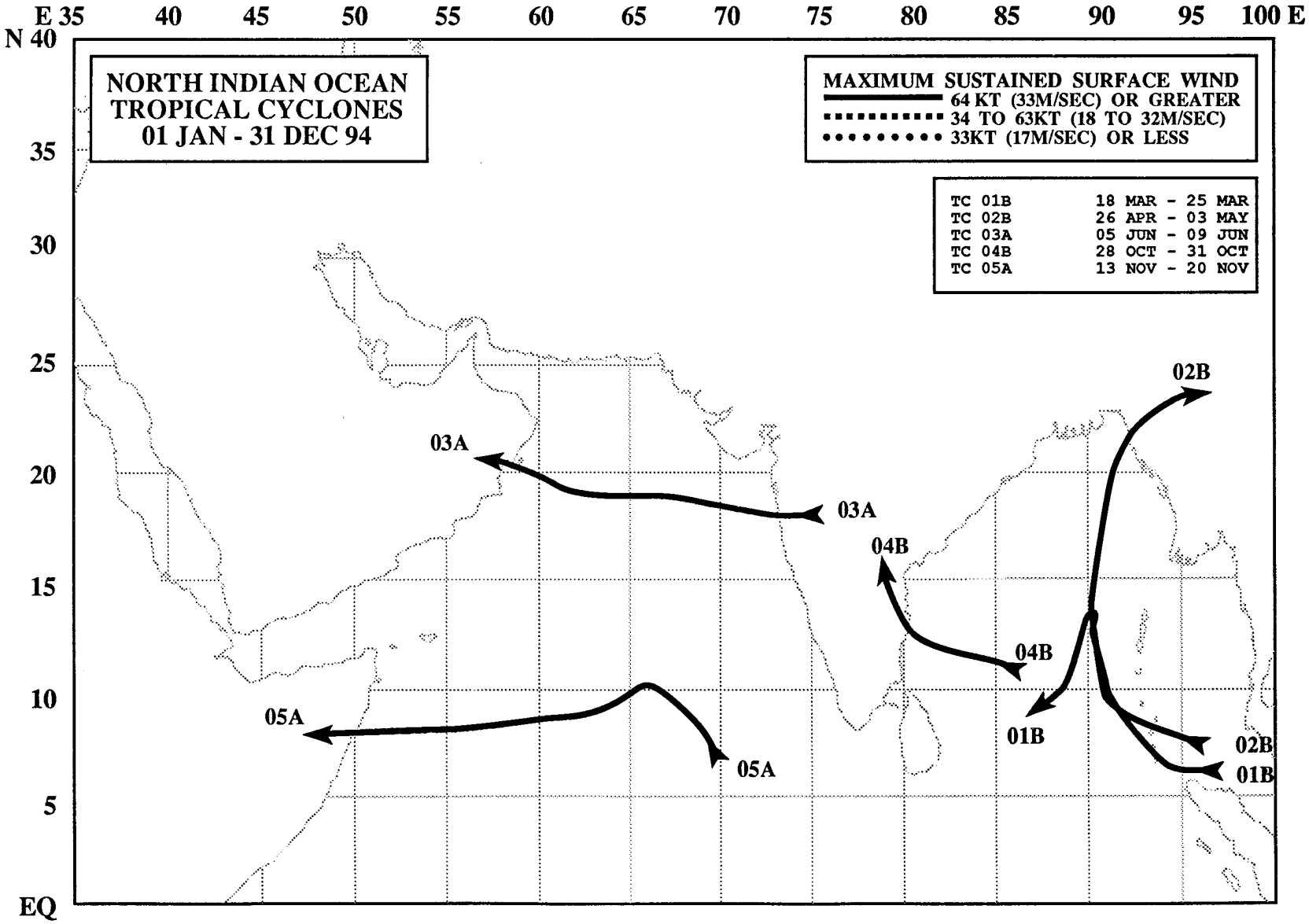

Figure 3-14 Composite best track for the North Indian Ocean tropical cyclones for 1994.

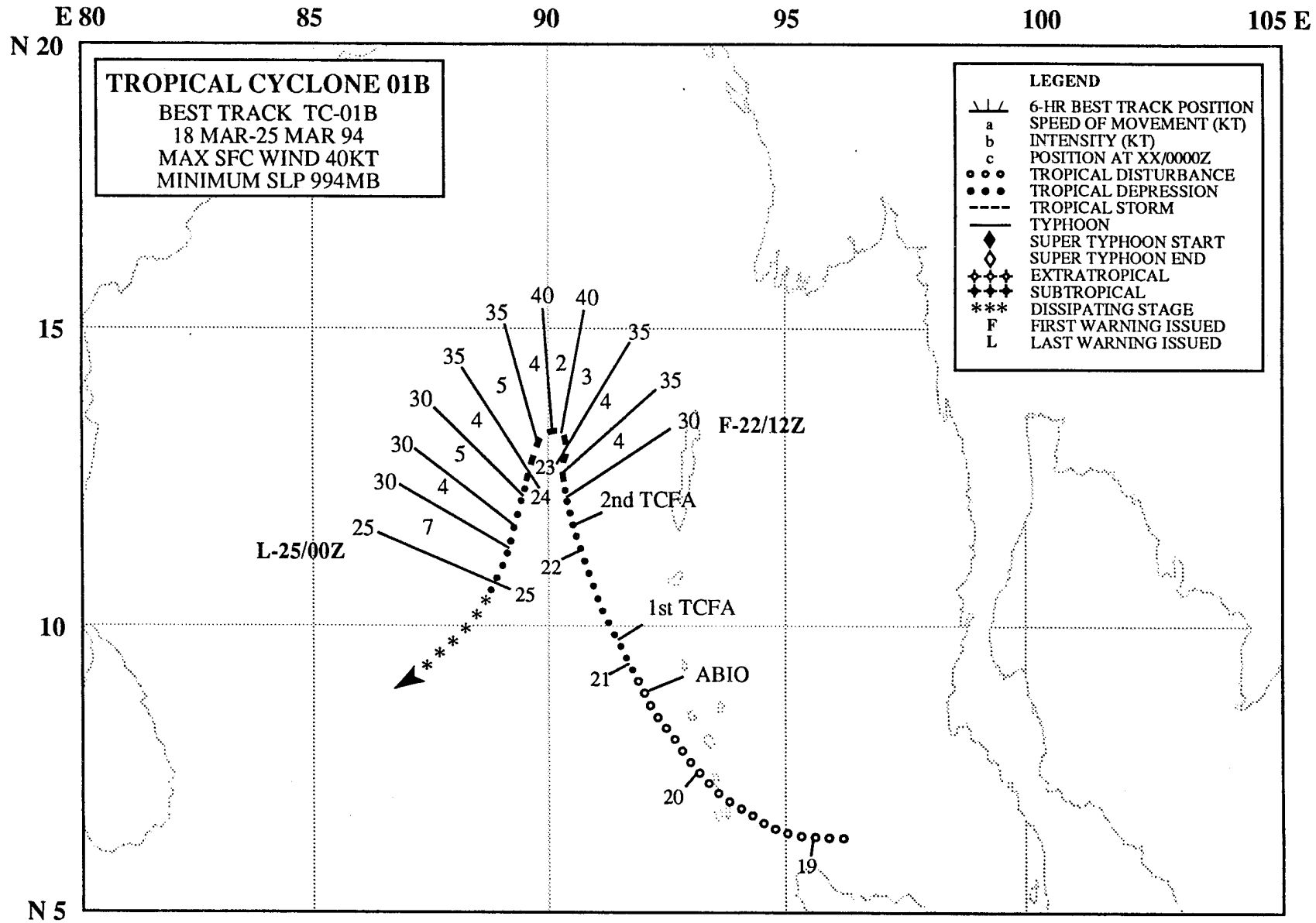
E 80
85
90
95
100
105 E
N 20
15
10
N 5
TROPICAL CYCLONE 01B
BEST TRACK TC-01B
18 MAR-25 MAR 94
MAX SFC WIND 40KT
MINIMUM SLP 994MB
LEGEND
6-HR BEST TRACK POSITION
a SPEED OF MOVEMENT (KT)
b INTENSITY (KT)
c POSITION AT XX/0000Z
TROPICAL DISTURBANCE
TROPICAL DEPRESSION
TROPICAL STORM
TYPHOON
SUPER TYPHOON START
SUPER TYPHOON END
EXTRATROPICAL
SUBTROPICAL
*** DISSIPATING STAGE
F FIRST WARNING ISSUED
L LAST WARNING ISSUED
F-22/12Z
2nd TCFA
1st TCFA
ABIO
L-25/00Z
19
20
21
22
23
24
25

TROPICAL CYCLONE 01B

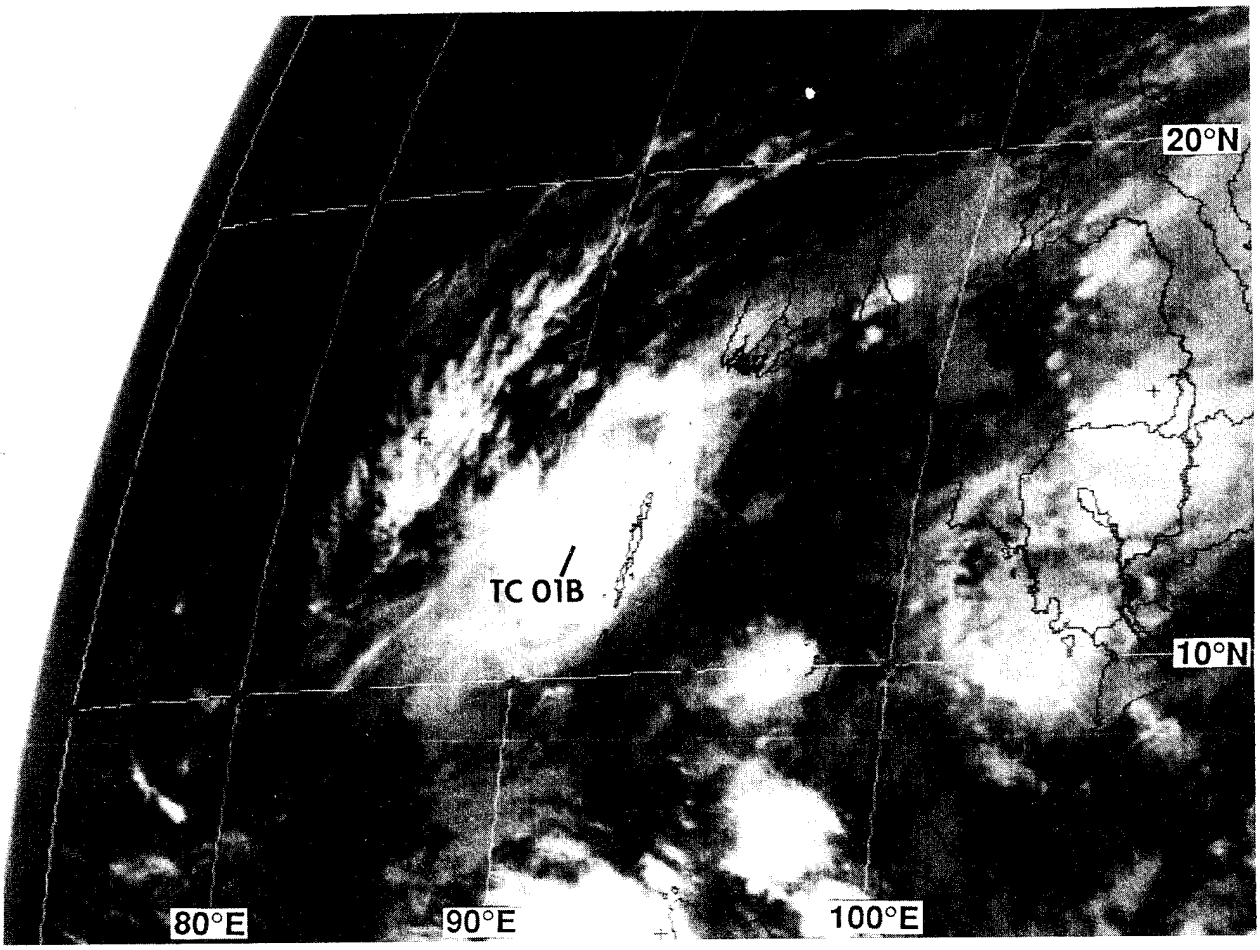

Figure 3-01B-1 Tropical Cyclone 01B near peak intensity in the central Bay of Bengal (222331Z March infrared GMS imagery).

Tropical Cyclone 01B was the first significant tropical cyclone to occur in the Northern Indian Ocean during 1994. It was first mentioned on the 201800Z March Significant Tropical Weather Advisory as area of persistent deep convection in the Bay of Bengal southwest of the Andaman Islands. Continued development led to a Tropical Cyclone Formation Alert, issued by JTWC at 210400Z. A second Tropical Cyclone Formation Alert at 220400Z was followed by the first warning at 221200Z. The tropical cyclone moved slowly and north-northwestward, reaching a peak intensity of 40 kt (21 m/sec) at 230600Z. The final warning was issued at 250000Z, as the weakening low-level vortex drifted south-southwestward.

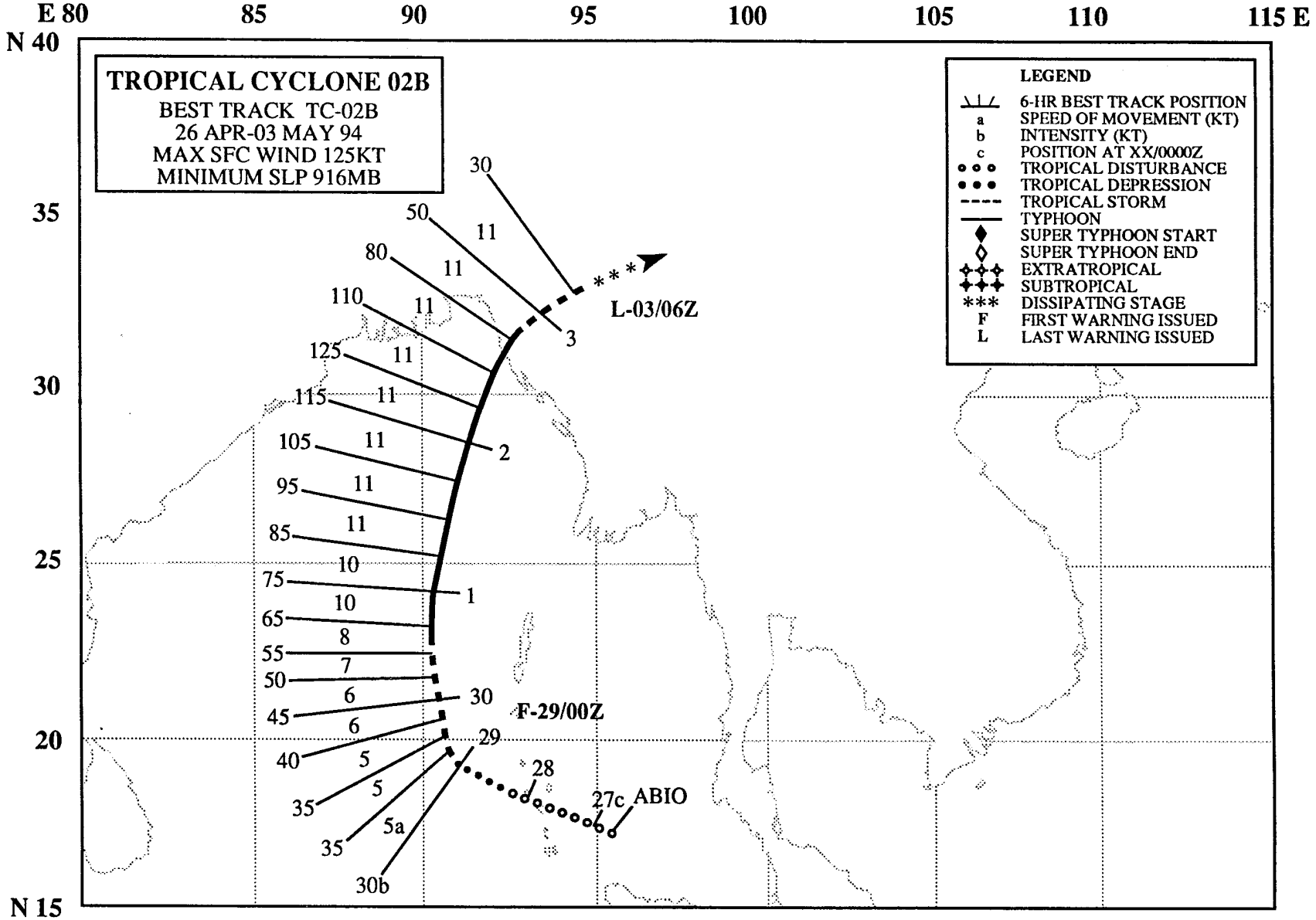
E 80
85
90
95
100
105
110
115 E
N 40
35
30
25
20
N 15
TROPICAL CYCLONE 02B
BEST TRACK TC-02B
26 APR-03 MAY 94
MAX SFC WIND 125KT
MINIMUM SLP 916MB
LEGEND
6-HR BEST TRACK POSITION
a SPEED OF MOVEMENT (KT)
b INTENSITY (KT)
c POSITION AT XX/0000Z
TROPICAL DISTURBANCE
TROPICAL DEPRESSION
TROPICAL STORM
TYPHOON
SUPER TYPHOON START
SUPER TYPHOON END
EXTRATROPICAL
SUBTROPICAL
*** DISSIPATING STAGE
F FIRST WARNING ISSUED
L LAST WARNING ISSUED
30
50 11
80 11
110 11
125 11
115 11
105 11
95 11
85 11
75 10
65 10
55 8
50 7
45 6
40 6
35 5
35 5
30b 5a
29
28
27c
3
2
1
30
***
L-03/06Z
F-29/00Z
ABIO

TROPICAL CYCLONE 02B

I. HIGHLIGHTS

Tropical Cyclone 02B was by far the most intense tropical cyclone in the North Indian Ocean during 1994. Its track and intensity evolution was very similar to that of the devastating TC 02B of 1991, which was responsible for extremely heavy loss of life in the densely populated Chittagong region of Bangladesh. The combination of a lower than expected storm tide, and a massive evacuation effort by disaster preparedness officials in Bangladesh helped to keep this year's casualties to a relative minimum.

II. TRACK AND INTENSITY

The tropical disturbance which became Tropical Cyclone 02B was first mentioned on the 261800Z April Significant Tropical Weather Advisory as an area of persistent convection in the southeastern Bay of Bengal. At 290000Z the first warning was issued based on consolidation of deep convection near the system center. TC 02B tracked generally north-northeastward and intensified at a normal rate (i.e. one "T" number per day). It reached a peak intensity of 125 kt (64 m/sec) — nearly supertyphoon intensity — on 02 May (Figure 3-02B-1). The system weakened slightly prior to making landfall in the vicinity of Cox's Bazar near the Bangladesh-Burma border. The system weakened rapidly over land and the final warning was issued at 030600Z May.

III. IMPACT

In virtually every respect (i.e. track, intensity, location and time of year) TC 02B of 1994 and TC 02B of 1991 were similar. However, the impact of the 1991 storm was far more devastating (138,000 dead in 1991 as opposed to less than 300 dead in 1994). A key difference associated with the impact of the two storms was the astronomical tides: TC 02B (1991) struck close to high tide (12.5 ft (3.8 m) above mean lower low water (MLLW)) and TC 02B (1994) made landfall almost exactly at low tide (3.5 ft (1.0 m) above MLLW). This large astronomical tidal range may have made a substantial difference in the amount of storm surge related flooding. A massive evacuation in which officials moved approximately 350,000 people to safety prior to the landfall of 1994's TC 02B, also played a role in the relatively low number of fatalities. Even so, wire reports indicated relatively heavy losses from TC 02B (1994). In addition to the official death toll of 285, over one half million people were left homeless, with total losses estimated at $125 million.

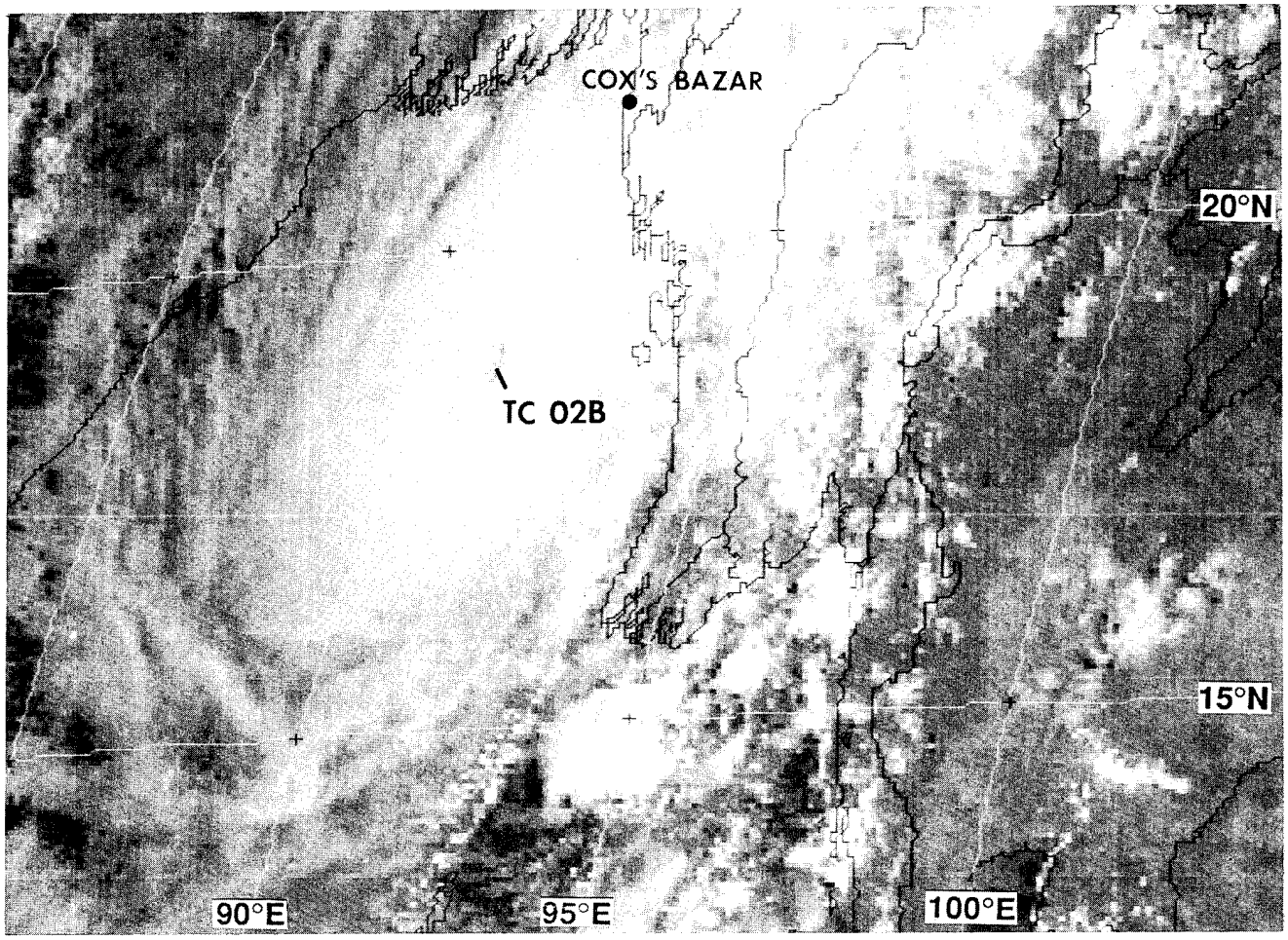

Figure 3-02B-1 Tropical Cyclone 02B moving north-northeastward in the Bay of Bengal. Maximum sustained winds at this time were estimated at 115 kt. (020031Z May visible GMS imagery).

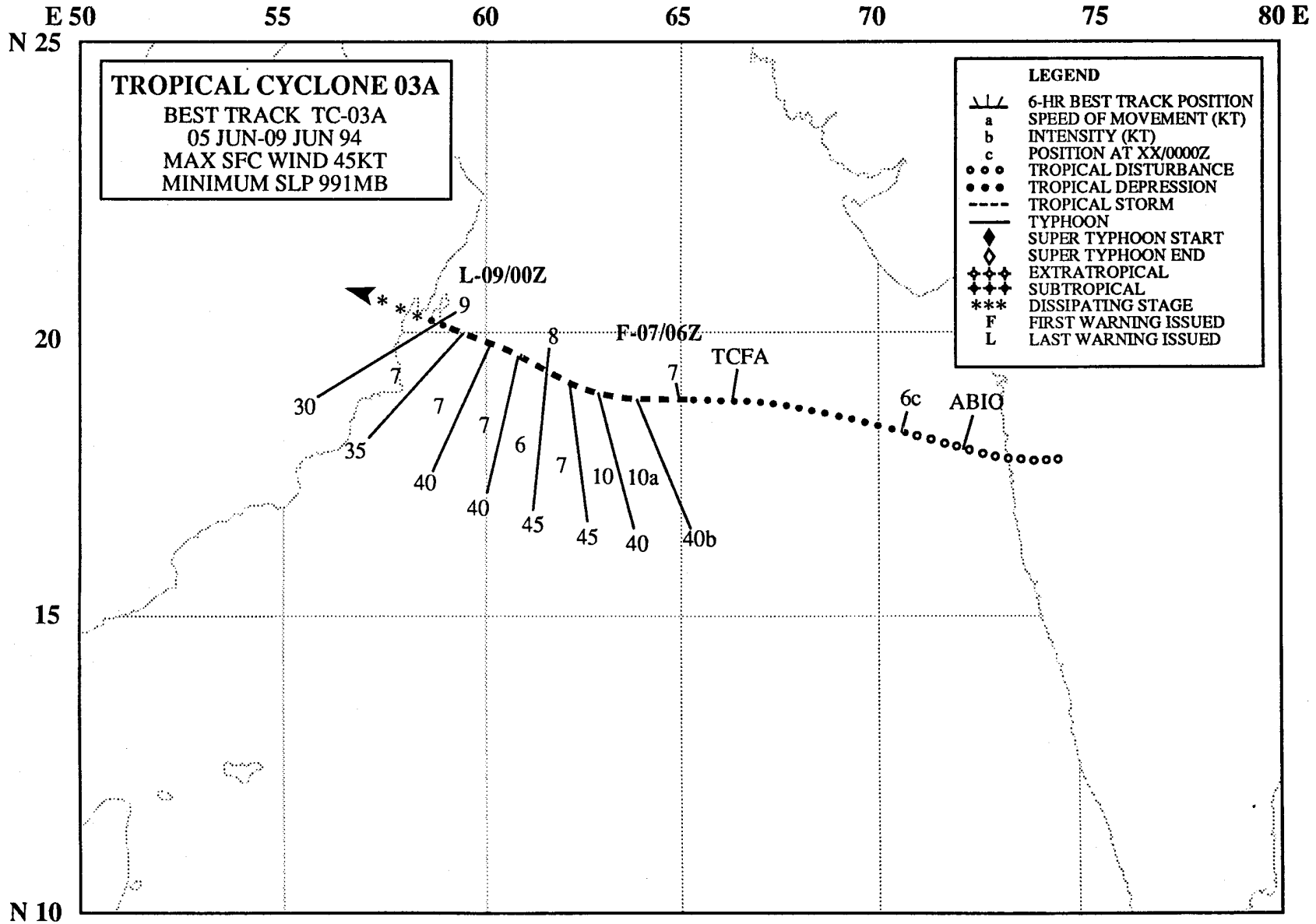
E 50
55
60
65
70
75
80 E
N 25
20
15
N 10
TROPICAL CYCLONE 03A
BEST TRACK TC-03A
05 JUN-09 JUN 94
MAX SFC WIND 45KT
MINIMUM SLP 991MB
LEGEND
6-HR BEST TRACK POSITION
a SPEED OF MOVEMENT (KT)
b INTENSITY (KT)
c POSITION AT XX/0000Z
TROPICAL DISTURBANCE
TROPICAL DEPRESSION
TROPICAL STORM
TYPHOON
SUPER TYPHOON START
SUPER TYPHOON END
EXTRATROPICAL
SUBTROPICAL
*** DISSIPATING STAGE
F FIRST WARNING ISSUED
L LAST WARNING ISSUED
L-09/00Z
F-07/06Z
TCFA
ABIO
6c
9
8
7
7
30
35
7
40
7
40
6
45
7
45
10
40
10a
40b

TROPICAL CYCLONE 03A

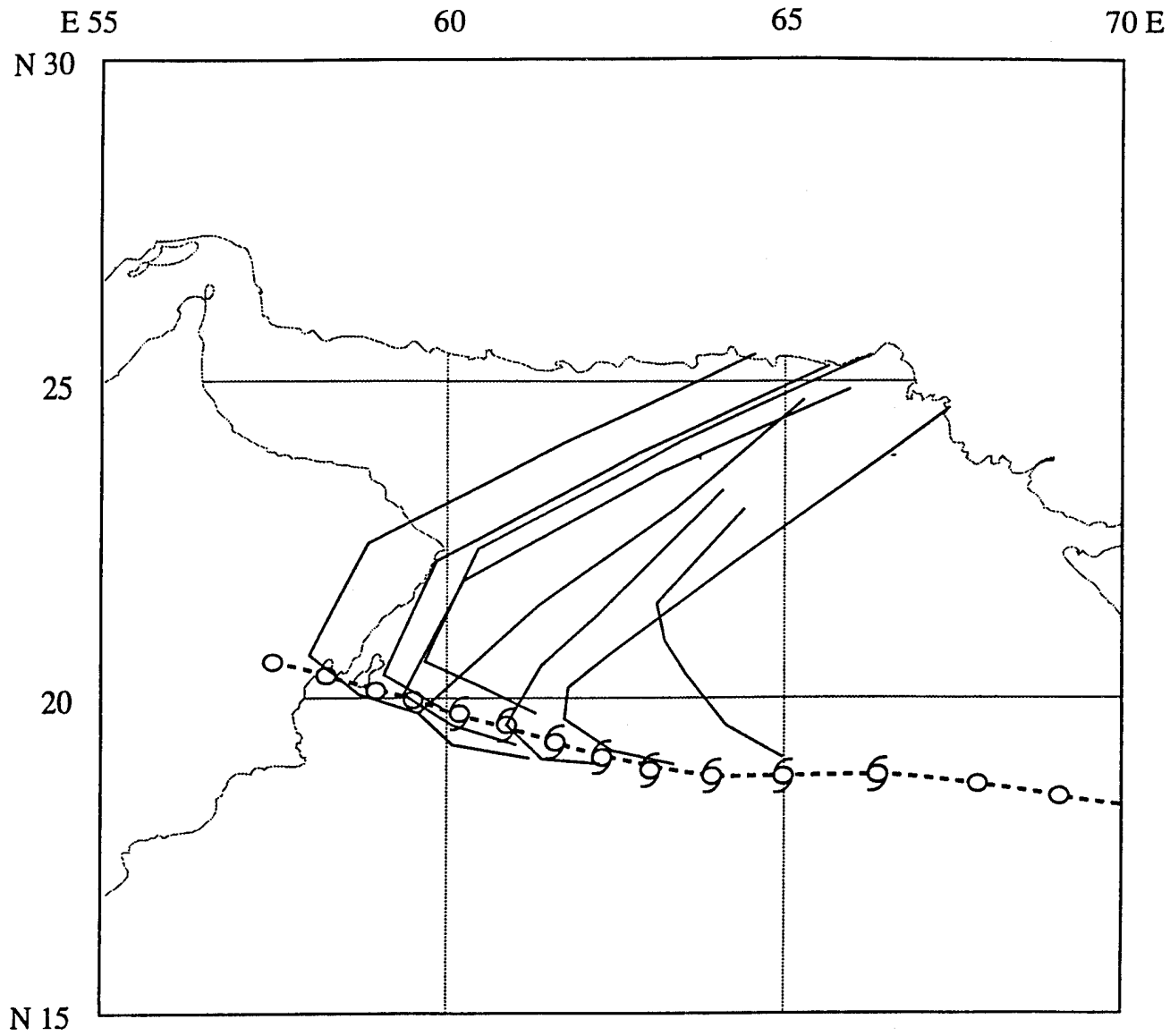

Figure 3-03A-1 The nonclimatological nature of TC 03A's track is shown by the forecast aid "CLIM", which is derived from the climatological data base for the area.

Tropical Cyclone 03A originated as a surface heat low over central India. It was first mentioned on the 051800Z June Significant Tropical Weather Advisory when the heat low moved westward into the North Arabian Sea, merged with the southwesterly monsoonal flow, and convection increased. Convective organization improved, and a Tropical Cyclone Formation alert was issued at 061800Z. The first warning followed at 070600Z. The system moved on a nonclimatological west-northwestward track (Figure 3-03A-1) and reached a maximum intensity of 45 kt (23 m/sec) at 071800Z. TC 03A began to weaken as it approached the coast of Oman, and the final warning was issued at 090000Z.

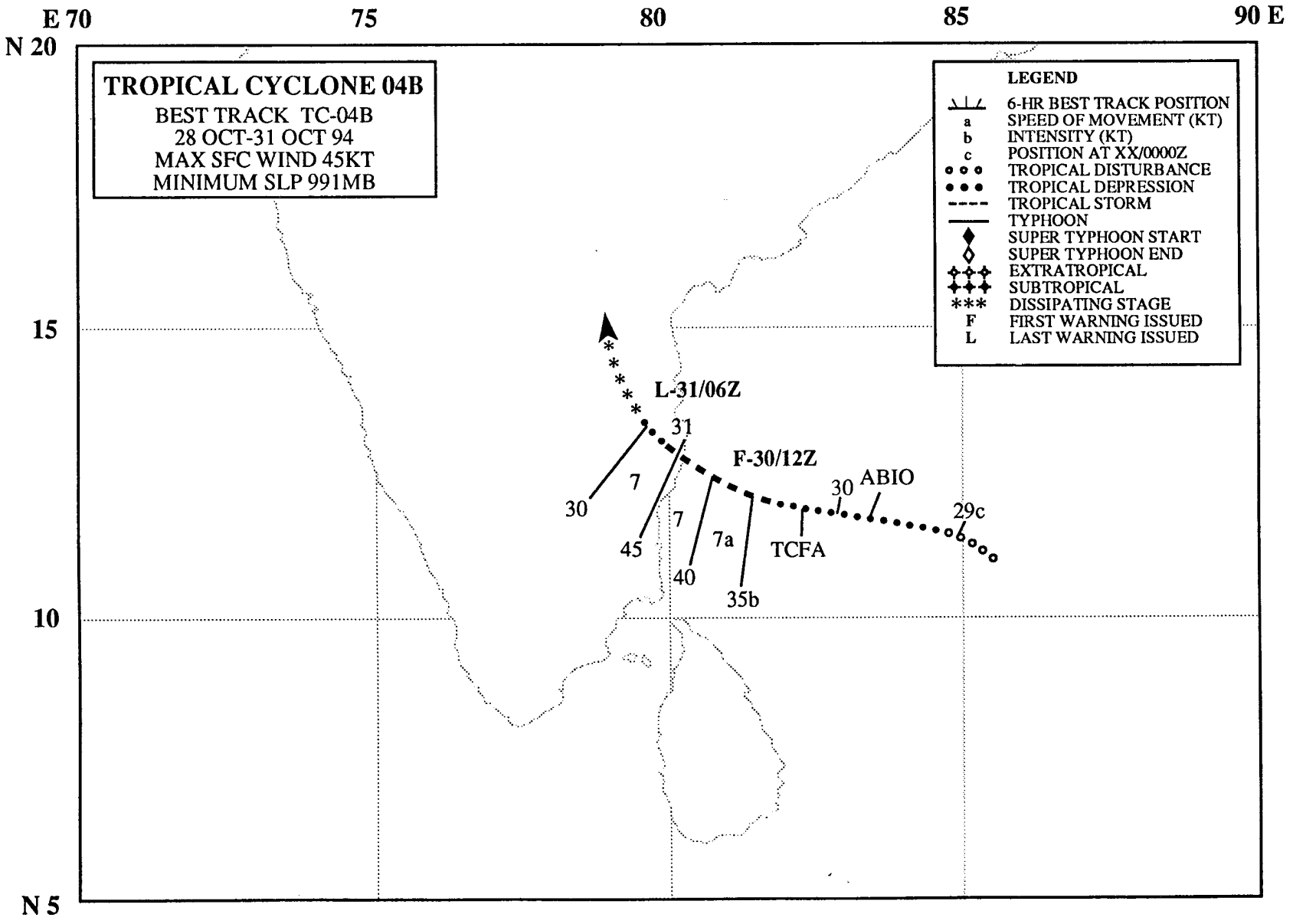
E 70
75
80
85
90 E
N 20
15
10
N 5
TROPICAL CYCLONE 04B
BEST TRACK TC-04B
28 OCT-31 OCT 94
MAX SFC WIND 45KT
MINIMUM SLP 991MB
LEGEND
6-HR BEST TRACK POSITION
a SPEED OF MOVEMENT (KT)
b INTENSITY (KT)
c POSITION AT XX/0000Z
TROPICAL DISTURBANCE
TROPICAL DEPRESSION
TROPICAL STORM
TYPHOON
SUPER TYPHOON START
SUPER TYPHOON END
EXTRATROPICAL
SUBTROPICAL
*** DISSIPATING STAGE
F FIRST WARNING ISSUED
L LAST WARNING ISSUED
L-31/06Z
31
F-30/12Z
30
7
45
7
40
7a
35b
TCFA
30
ABIO
29c

241

TROPICAL CYCLONE 04B

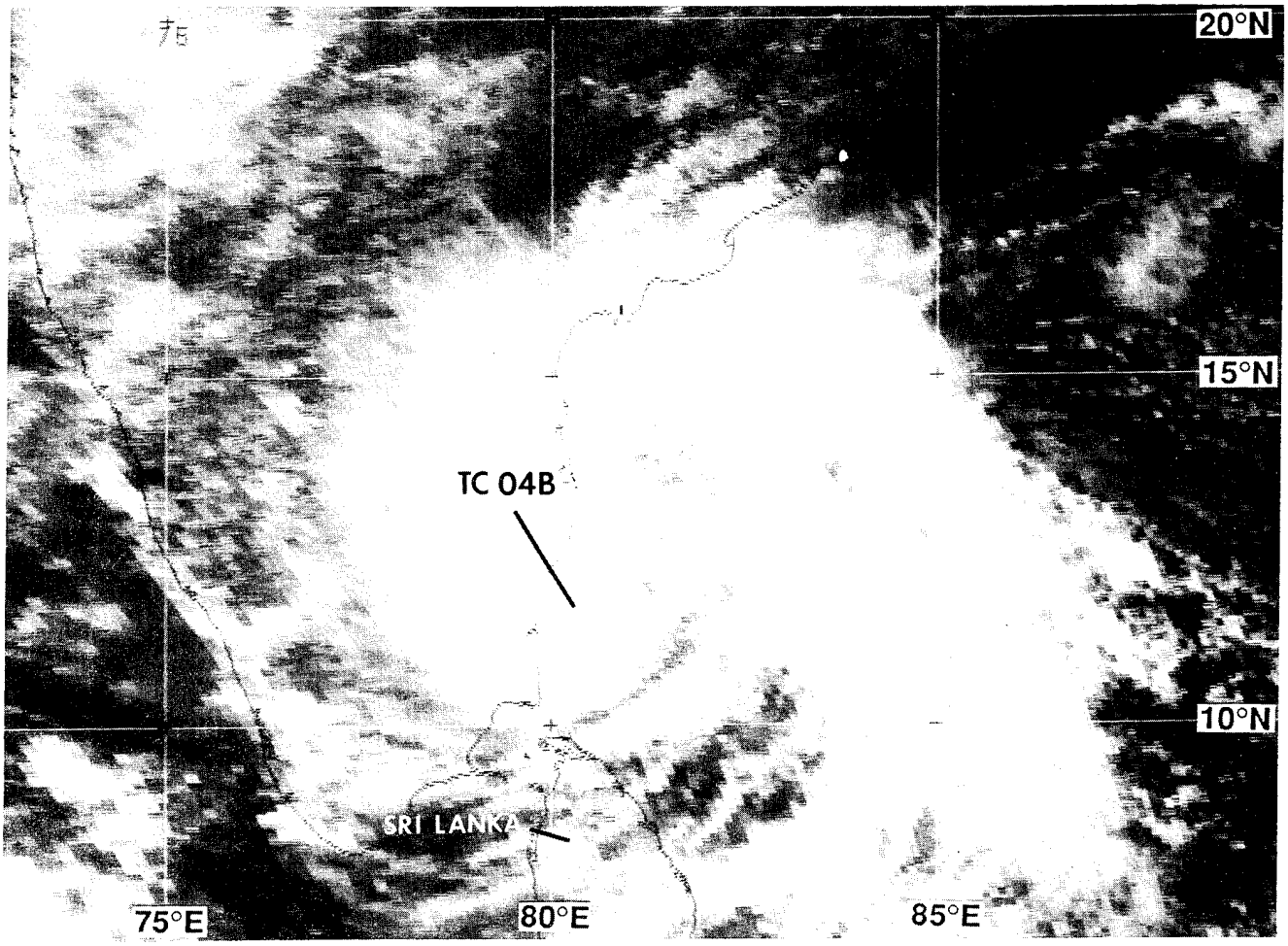

Figure 3-04B-1 Tropical Cyclone 04B approaches the southeast coast of India. The system reached peak intensity as it made landfall (300831Z October visible GMS imagery).

The disturbance that became Tropical Cyclone 04B was first mentioned on the 291800Z October Significant Tropical Weather Advisory, as an area of persistent convection began to consolidate northeast of Sri Lanka. Based on continued convective development, a Tropical Cyclone Formation Alert was issued at 300430Z, followed at 301200Z by the first warning. The tropical cyclone tracked westward towards India, and reached its peak intensity of 45 kt (23 m/sec) immediately prior to landfall, at 310000Z. A land synoptic station near TC 04B at landfall reported 40 kt (21 m/sec) winds and a 994.3 mb SLP. The final warning was issued at 310600Z as TC 04B weakened inland.

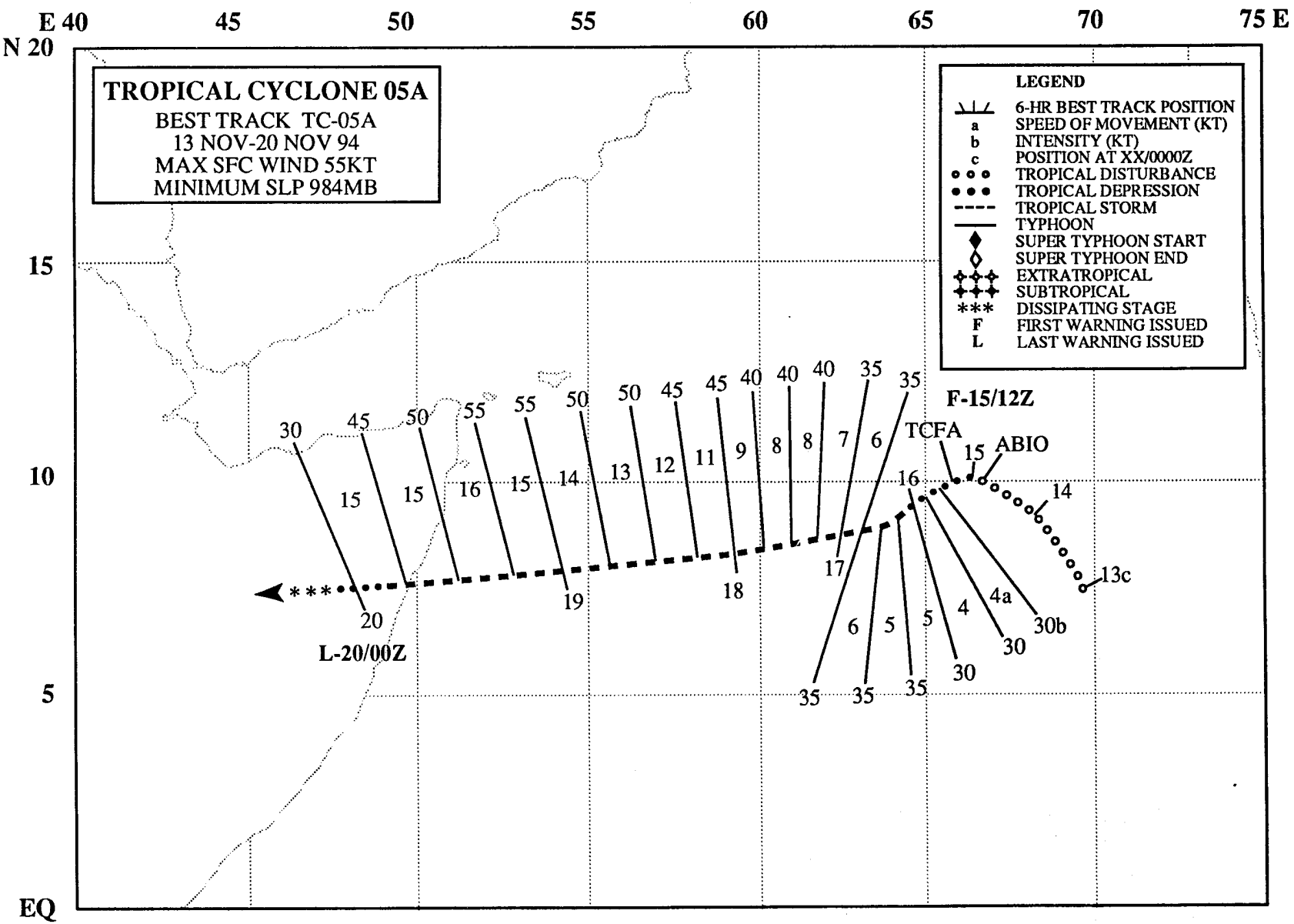
E 40
45
50
55
60
65
70
75 E
N 20
15
10
5
EQ
TROPICAL CYCLONE 05A
BEST TRACK TC-05A
13 NOV-20 NOV 94
MAX SFC WIND 55KT
MINIMUM SLP 984MB
LEGEND
6-HR BEST TRACK POSITION
a SPEED OF MOVEMENT (KT)
b INTENSITY (KT)
c POSITION AT XX/0000Z
TROPICAL DISTURBANCE
TROPICAL DEPRESSION
TROPICAL STORM
TYPHOON
SUPER TYPHOON START
SUPER TYPHOON END
EXTRATROPICAL
SUBTROPICAL
*** DISSIPATING STAGE
F FIRST WARNING ISSUED
L LAST WARNING ISSUED
F-15/12Z
TCFA
ABIO
L-20/00Z
13c
30b
4a

TROPICAL CYCLONE 05A

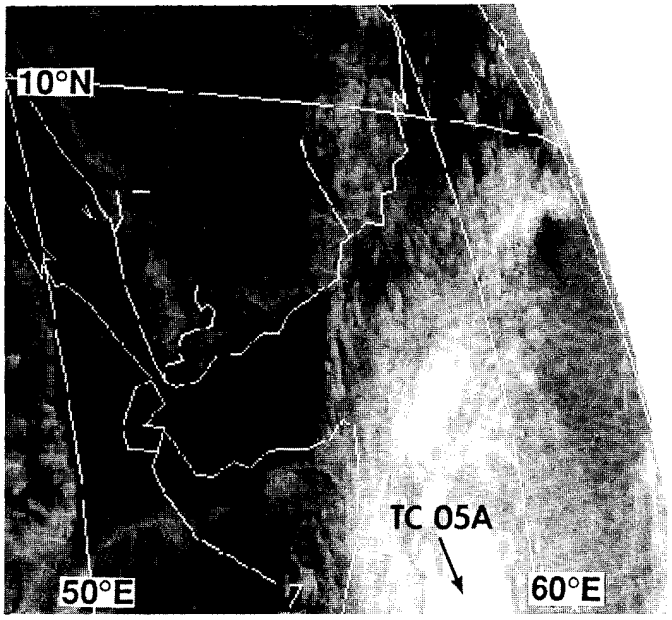

Figure 3-05A-1 Tropical Cyclone 05A approaching peak intensity (181714Z November infrared Meteosat imagery).

Tropical Cyclone 05A was first mentioned on the 041800Z November Significant Tropical Weather Advisory, as an area of convection in the eastern North Arabian Sea began to organize. Convection associated with this system increased and a Tropical Cyclone Formation Alert was issued at 150700Z, followed by the first warning at 151200Z. The system tracked toward the west-southwest and steadily intensified, reaching a peak intensity of 55 kt (28 m/sec) at 190000Z. The system made landfall over Somalia at 191800Z, and the final warning was issued at 200000Z, as the system dissipated rapidly over northeastern Africa.

4. SUMMARY OF SOUTH PACIFIC AND SOUTH INDIAN OCEAN TROPICAL CYCLONES

4.1 GENERAL

On 1 October 1980, JTWC's area of responsibility (AOR) was expanded to include the Southern Hemisphere from 180° east longitude, westward to the coast of Africa. Details on Southern Hemisphere tropical cyclones and JTWC warnings from July 1980 through June 1982 are contained in Diercks et al. (1982) and from July 1982 through June 1984, in Wirfel and Sandgathe (1986). Information on Southern Hemisphere tropical cyclones after June 1984 can be found in the applicable Annual Tropical Cyclone Report.

The NAVPACMETOCCEN, Pearl Harbor, Hawaii issues warnings on tropical cyclones in the South Pacific, east of 180° east longitude. In accordance with CINCPACINST 3140.1V, Southern Hemisphere tropical cyclones are numbered sequentially from 1 July through 30 June. This convention is established to encompass the Southern Hemisphere tropical cyclone season, which primarily occurs from January through April. There are two Southern Hemisphere ocean basins for warning purposes - the South Indian (west of 135° east longitude) and the South Pacific (east of 135° east longitude) - which are identified by appending the suffixes "S" and "P," respectively, to the tropical cyclone number.

Intensity estimates for Southern Hemisphere tropical cyclones are derived from the interpretation of satellite imagery using the Dvorak (1984) technique and, in rare instances, from surface observations. The Dvorak technique relates specific cloud signatures to maximum sustained one-minute average surface wind speeds. The conversion from maximum sustained winds to minimum sea-level pressure is obtained from Atkinson and Holliday (1977) (Table 4-1).

4.2 SOUTH PACIFIC AND SOUTH INDIAN OCEAN TROPICAL CYCLONES

The total number of significant tropical cyclones during the 1994 season (1 July 1993 - 30 June 1994) (Table 4-2) was 30 which was two more than the overall climatological mean for the past 13 years as shown in Table 4-3. However, looking at the annual variation of Southern Hemisphere Tropical Cyclones by ocean basins (Table 4-4), it becomes apparent that this mean value of 30 occurred with near normal activity in the South Pacific Ocean and

Table 4-1 MAXIMUM SUSTAINED 1-MINUTE MEAN SURFACE WINDS AND EQUIVALENT MINIMUM SEA-LEVEL PRESSURE (ATKINSON AND HOLLIDAY, 1977) RELATIONSHIP

WIND-KT	(M/SEC)	PRESSURE (MB)
30	(15)	1000
35	(18)	997
40	(21)	994
45	(23)	991
50	(26)	987
55	(28)	984
60	(31)	980
65	(33)	976
70	(36)	972
75	(39)	967
80	(41)	963
85	(44)	958
90	(46)	954
95	(49)	948
100	(51)	943
105	(54)	938
110	(57)	933
115	(59)	927
120	(62)	922
125	(64)	916
130	(67)	910
135	(69)	906
140	(72)	898
145	(75)	892
150	(77)	885
155	(80)	879
160	(82)	872
165	(85)	865
170	(87)	858
175	(90)	851
180	(93)	844

Australian basins and slightly higher than normal activity in the South Indain Ocean basin.

The JTWC was in warning status a total of 109 days, which included 44 days when warnings were issued on two or more Southern Hemisphere tropical cyclone. A chronology of the tropical cyclone activity is provided in Figure 4-1. All tropical cyclone warnings with the exception of those for Tropical Cyclone were preceded by Tropical Cyclone Formation Alerts. Composites of the best tracks appear in Figures 4-2 and 4-3.

Table 4-2 SOUTH PACIFIC AND SOUTH INDIAN OCEAN SIGNIFICANT TROPICAL CYCLONES
(1 JULY 1993 - 30 JUNE 1994)

TROPICAL CYCLONE	PERIOD OF WARNING	WARNINGS ISSUED	MAX SURFACE WINDS-KT (M/SEC)	ESTIMATED MSLP (MB)
01S Alexina	09 Nov - 13 Nov	13	60(31)	980
02S Bettina	26 Nov - 29 Nov	7	55(28)	984
03S Cecilia	13 Dec - 21 Dec	17	85(44)	958
04S Naomi	16 Dec - 17 Dec	3	55(28)	984
05P Rewa	28 Dec - 13 Jan	37	125(64)	915
06S Oscar	31 Dec - 04 Jan	12	40(21)	994
07P	06 Jan - 07 Jan	3	30(15)	1000
08S Daisy	10 Jan - 14 Jan	10	95(49)	949
09S Pearl	12 Jan - 19 Jan	16	90(46)	954
10S Edema	14 Jan - 18 Jan	10	50(26)	987
11P Sarah	22 Jan - 28 Jan	14	100(51)	944
12S Quenton	25 Jan - 28 Jan	7	75(39)	968
13S Geralda	27 Jan - 04 Feb	19	145(75)	892
14P Sadie	30 Jan - 31 Jan	3	35(18)	997
15S Hollanda	07 Feb - 14 Feb	17	105(54)	938
16S Ivy	10 Feb - 19 Feb	26	100(51)	944
17S	18 Feb - 20 Feb	6	35(18)	997
18P Theodore	23 Feb - 27 Feb	9	115(59)	927
19S Kelvina	07 Mar - 10 Mar	6	50(26)	987
20S Litanne	08 Mar - 17 Mar	19	130(67)	910
21S Mariola	11 Mar - 17 Mar	14	90(46)	954
22S Sharon	14 Mar - 18 Mar	19	110(57)	933
23S*Nadia	20-25 Mar/28-01 Apr	31	120(62)	922
24P Tomas	22 Mar - 25 Mar	8	105(54)	938
25P Usha	25 Mar - 28 Mar	7	55(28)	984
26S Odille	30 Mar - 14 Apr	36	105(54)	938
27S Tim	31 Mar - 01 Apr	4	40(21)	994
28S Vivienne	07 Apr - 12 Apr	10	70(36)	972
29P	24 Apr - 25 Apr	3	30(15)	1000
30S Willy	29 Apr - 30 Apr	3	40(21)	994
	JTWC Total	389		
		4*		
	Grand Total	393		

* Regenerated
** Warnings issued by NAVPACMETOCCEN

Table 4-3 MONTHLY DISTRIBUTION OF SOUTH PACIFIC AND SOUTH INDIAN OCEAN TROPICAL CYCLONES

YEAR	JUL	AUG	SEP	OCT	NOV	DEC	JAN	FEB	MAR	APR	MAY	JUN	TOTAL
(1959-1978) AVERAGE*	-	-	-	0.4	1.5	3.6	6.1	5.8	4.7	2.1	0.5	-	24.7
1981	0	0	0	1	3	2	6	5	3	3	1	0	24
1982	1	0	0	1	1	3	9	4	2	3	1	0	25
1983	1	0	0	1	1	3	5	6	3	5	0	0	25
1984	1	0	0	1	2	5	5	10	4	2	0	0	30
1985	0	0	0	0	1	7	9	9	6	3	0	0	35
1986	0	0	1	0	1	1	9	9	6	4	2	0	33
1987	0	1	0	0	1	3	6	8	3	4	1	1	28
1988	0	0	0	0	2	3	5	5	3	1	2	0	21
1989	0	0	0	0	2	1	5	8	6	4	2	0	28
1990	2	0	1	1	2	2	4	4	10	2	1	0	29
1991	0	0	1	1	1	3	2	5	5	2	1	1	22
1992	0	0	1	1	2	5	4	11	3	2	1	0	30
1993	0	0	1	1	0	5	7	7	2	2	2	0	27
1994	0	0	0	0	2	4	8	4	9	3	0	0	30
TOTAL	5	1	5	8	21	47	84	95	65	40	14	2	387
(1981-1994) AVERAGE	0.4	0.1	0.4	0.6	1.5	3.4	6.0	6.8	4.6	2.9	1.0	0.1	27.6

* (Gray, 1979)

Table 4-4 ANNUAL VARIATION OF SOUTHERN HEMISPHERE TROPICAL CYCLONES BY OCEAN BASIN

YEAR	SOUTH INDIAN (WEST OF 105°E)	AUSTRALIAN (105°E - 165°E)	SOUTH PACIFIC (EAST OF 165°E)	TOTAL
(1959-1978) AVERAGE*	8.4	10.3	5.9	24.7
1981	13	8	3	24
1982	12	11	2	25
1983	7	6	12	25
1984	14	14	2	30
1985	14	15	6	35
1986	14	16	3	33
1987	9	8	11	28
1988	14	2	5	21
1989	12	9	7	28
1990	18	8	3	29
1991	11	10	1	22
1992	11	6	13	30
1993	10	16	1	27
1994	16	10	4	30
TOTAL	175	139	73	387
(1981-1994) AVERAGE	12.5	9.9	5.2	27.6

* (Gray, 1979)

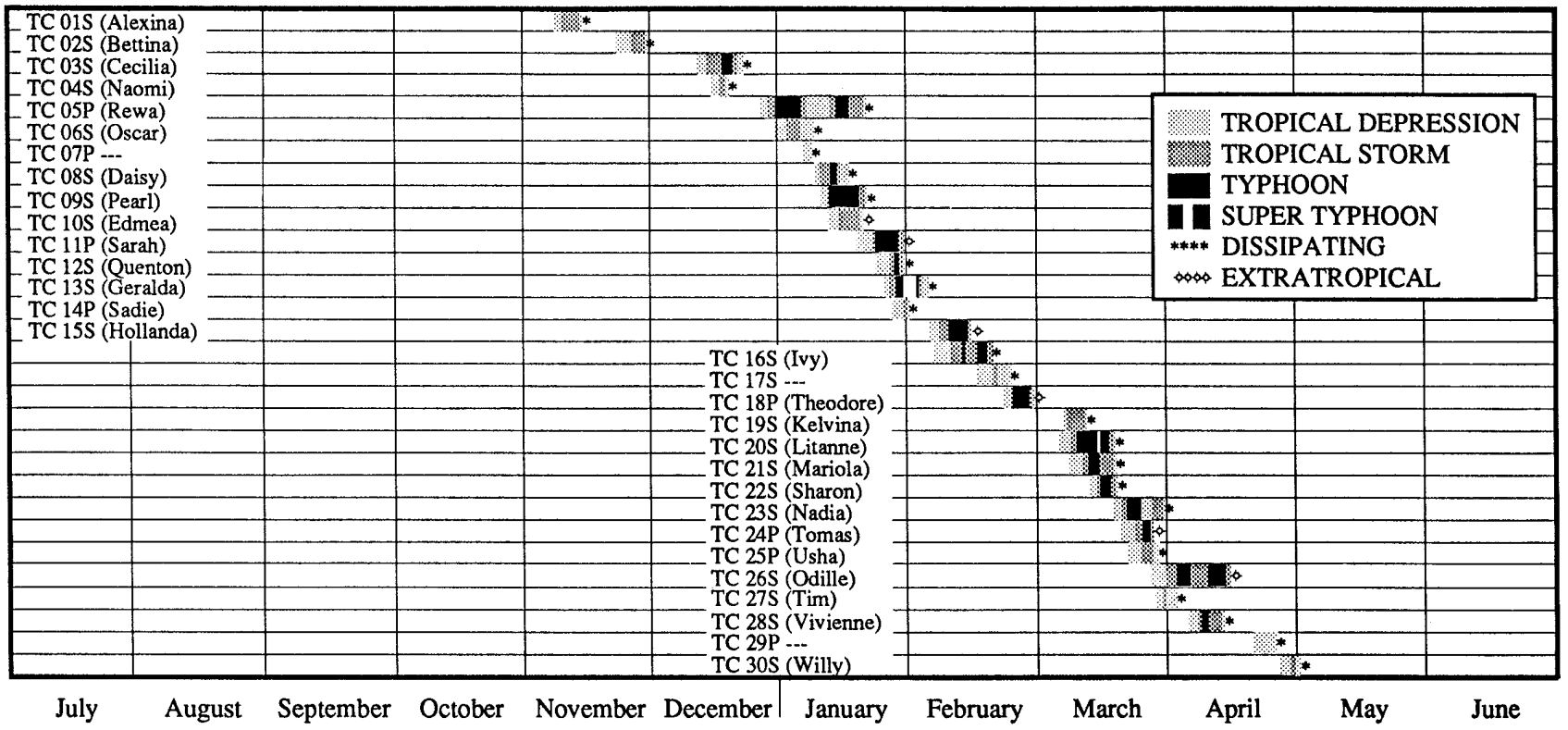

Figure 4-1 Chronology of South Pacific and South Indian Ocean tropical cyclones for 1994 (1 July 1993 - 30 June 1994).

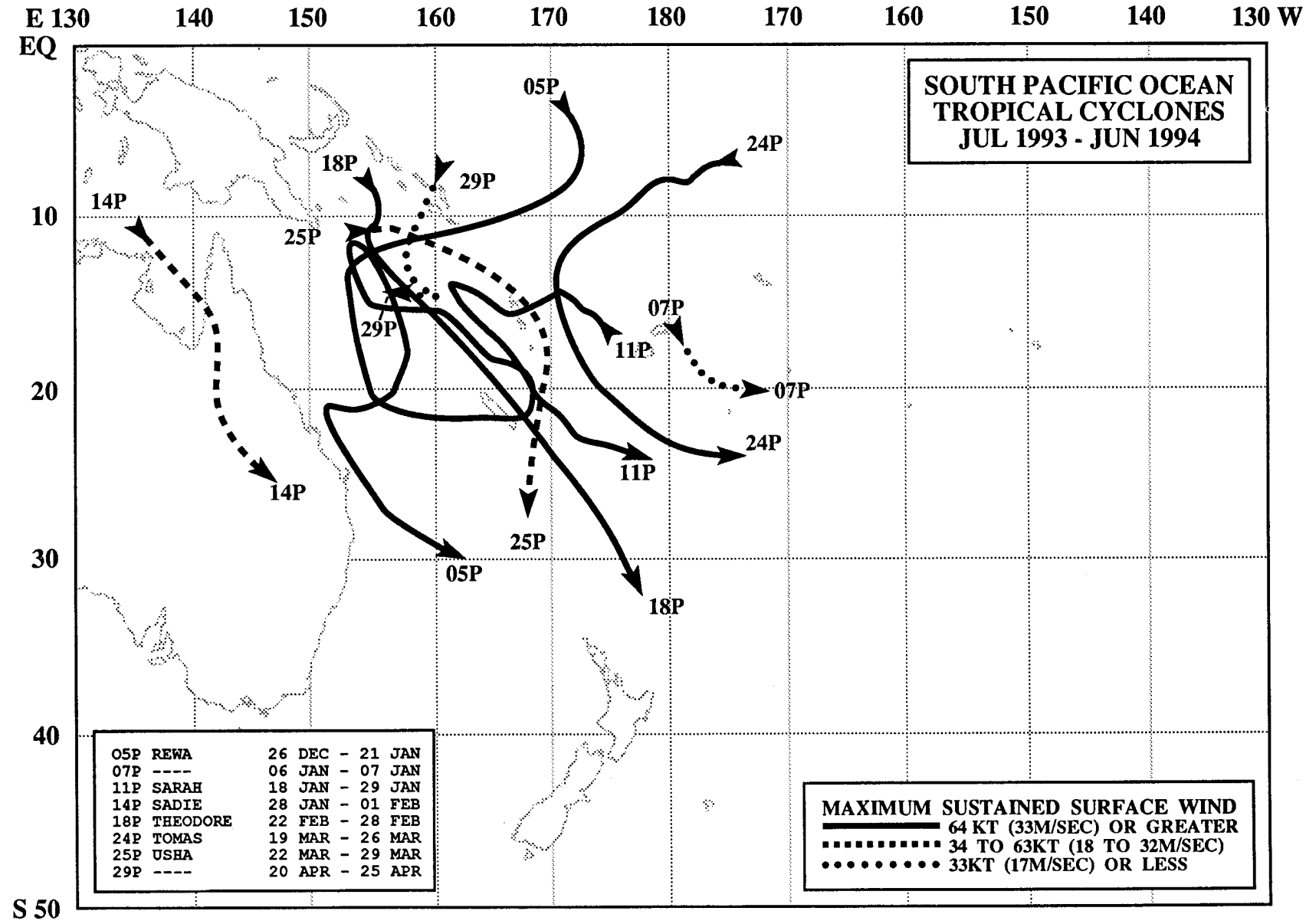

Figure 4-2 Tropical cyclone best tracks east of 130° east longitude .

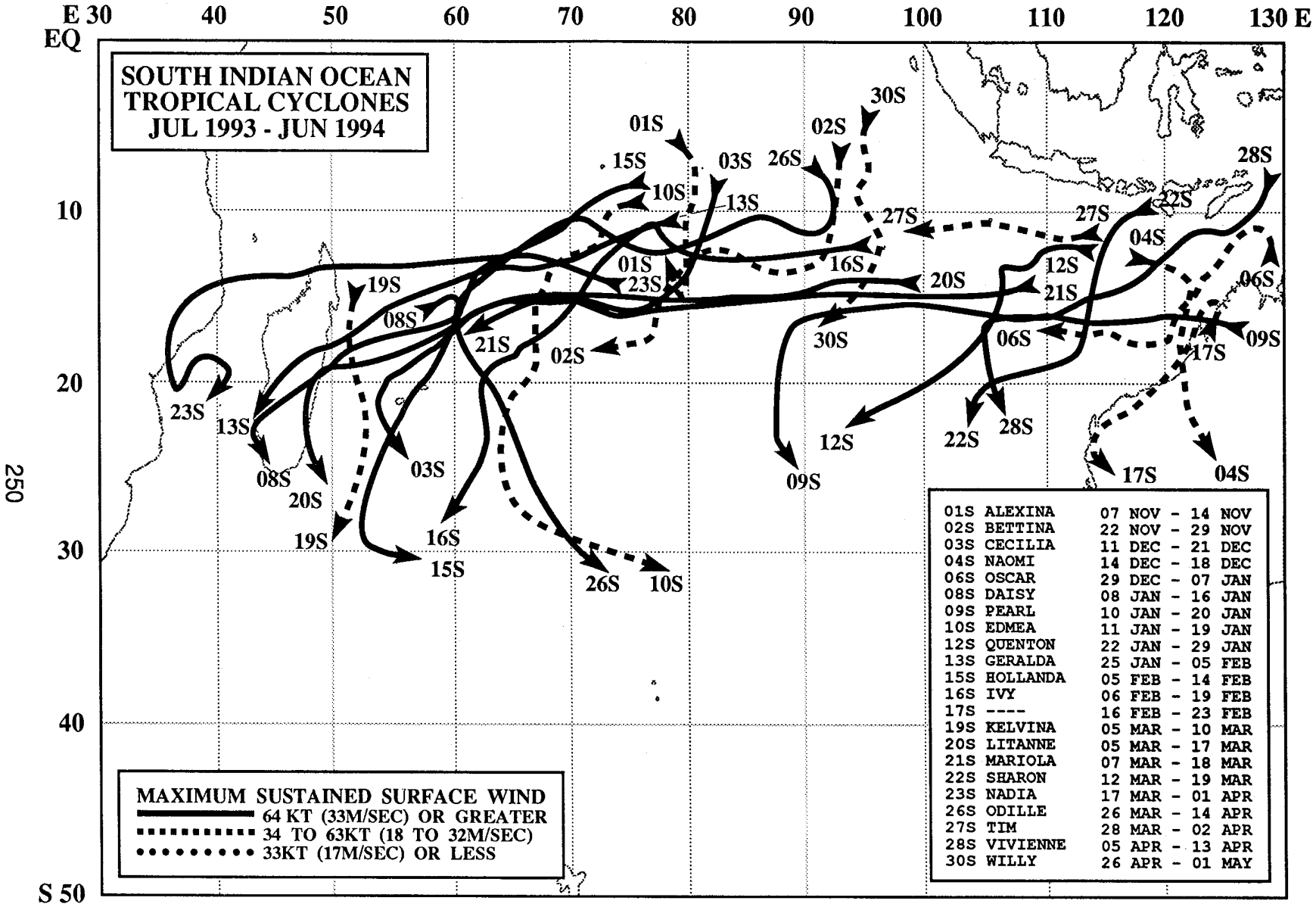

Figure 4-3 Tropical cyclone best tracks west of 130° east longitude.

5. SUMMARY OF FORECAST VERIFICATION

5.1 ANNUAL FORECAST VERIFICATION

Verification of warning positions and intensities at initial, 24-, 48- and 72-hour forecast periods was made against the final best track. The (scalar) track forecast, along-track and cross-track errors (illustrated in Figure 5-1) were calculated for each verifying JTWC forecast. These data, in addition to a detailed summary for each tropical cyclone, are included as Chapter 6. This section summarizes verification data for 1994 and contrasts it with annual verification statistics from previous years.

5.1.1 NORTHWEST PACIFIC OCEAN — The frequency distributions of errors for initial warning positions and 12-, 24-, 36-, 48- and 72-hour forecasts are presented in Figures 5-2a through 5-2f, respectively. Table 5-1 includes mean track, along-track and cross-track errors for 1978-1994. Figure 5-3 shows mean track errors and a 5-year running mean of track errors at 24-, 48- and 72-hours for the past 20 years. Table 5-2 lists annual mean track errors from 1959, when the JTWC was founded, until the present. Figure 5-4 illustrates JTWC intensity forecast errors at 24-, 48- and 72-hours for the past 20 years.

5.1.2 NORTH INDIAN OCEAN — The frequency distributions of errors for warning positions and 12-, 24-, 36-, 48- and 72-hour forecasts are presented in Figures 5-5a through 5-5f, respectively. Table 5-3 includes mean track, along-track and cross-track errors for 1978-1994. Figure 5-6 shows mean track errors and a 5-year running mean of track errors at 24-, 48- and 72-hours for the 20 years that the JTWC has issued warnings in the region.

5.1.3 SOUTH PACIFIC AND SOUTH INDIAN OCEANS — The frequency distributions of errors for warning positions and 12-, 24-, 36-, and 48-hour forecasts are presented in Figures 5-7a through 5-7e, respectively. Table 5-4 includes mean track, along-track and cross-track errors for 1981-1994. Figure 5-8 shows mean track errors and a 5-year running mean of track errors at 24- and 48-hours for the 13 years that the JTWC has issued warnings in the region.

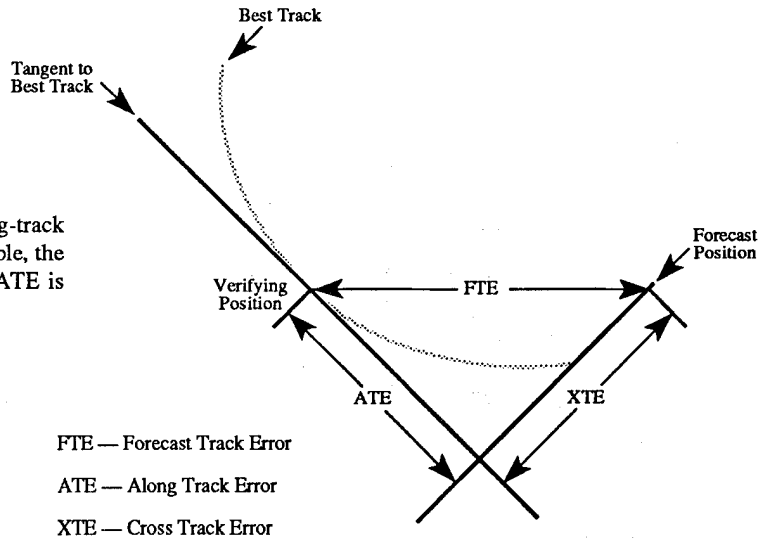

Figure 5-1 Definition of cross-track error (XTE), along-track error (ATE) and forecast track error (FTE). In this example, the XTE is positive (to the right of the best track) and the ATE is negative (behind or slower than the best track).

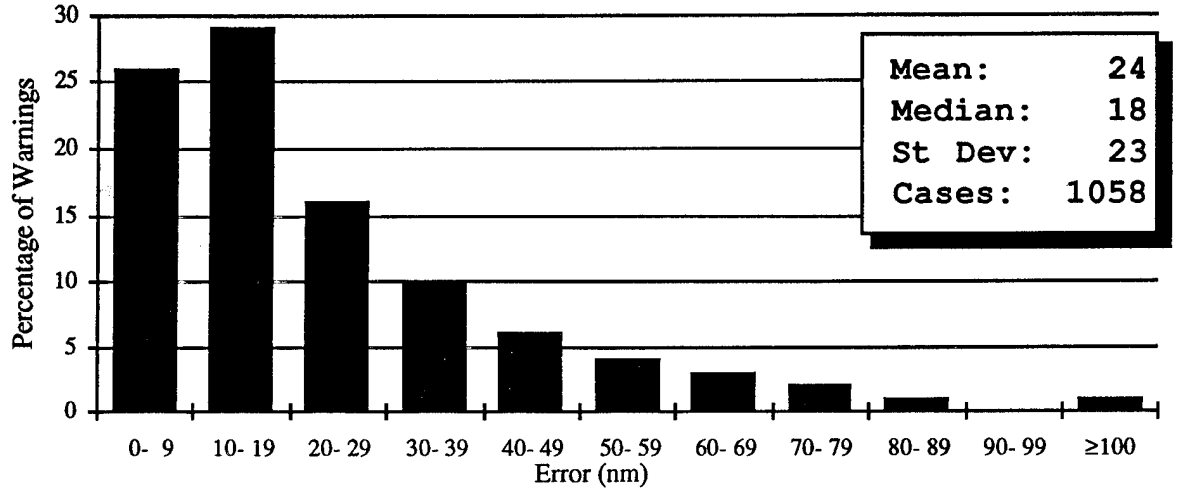

Figure 5-2a Frequency distribution of initial warning position errors (10-nm increments) for western North Pacific Ocean tropical cyclones in 1994. The largest error, 215 nm, occurred on Tropical Depression 01W.

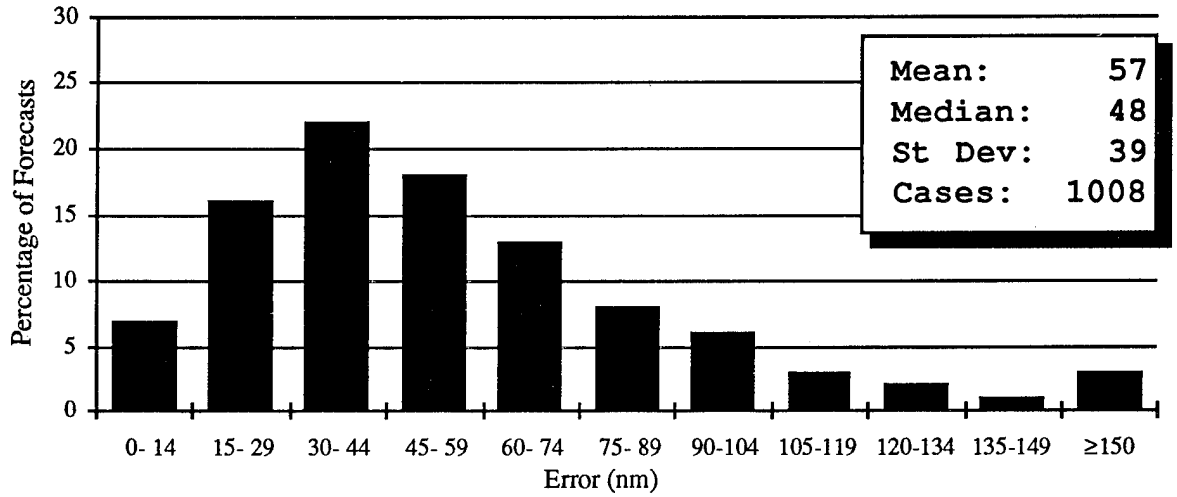

Figure 5-2b Frequency distribution of 12-hour track forecast errors (15-nm increments) for western North Pacific Ocean tropical cyclones in 1994. The largest error, 259 nm, occurred on Typhoon Wilda (35W).

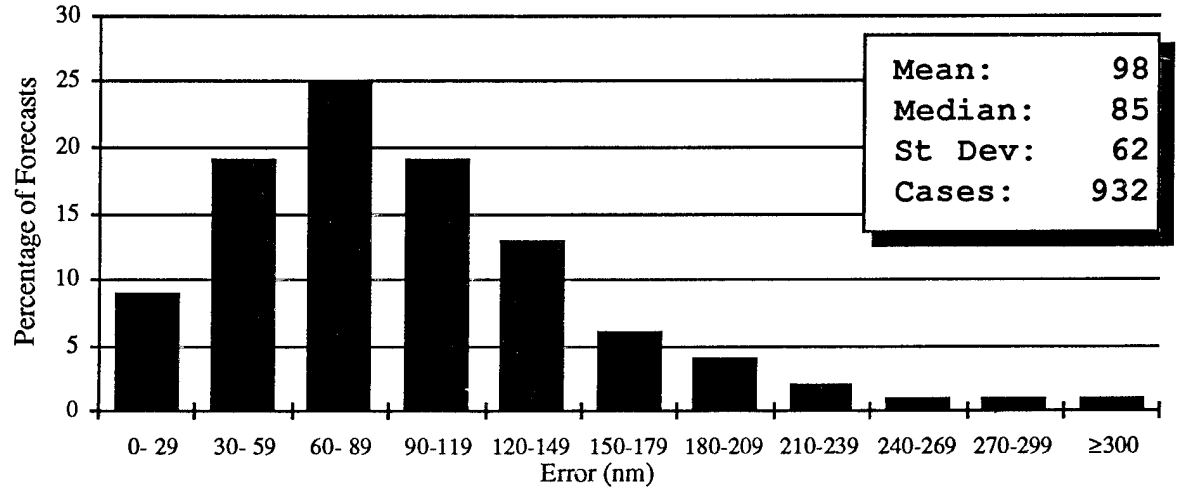

Figure 5-2c Frequency distribution of 24-hour track forecast errors (30-nm increments) for western North Pacific Ocean tropical cyclones in 1994. The largest error, 436 nm, occurred on Tropical Storm Ruth (30W).

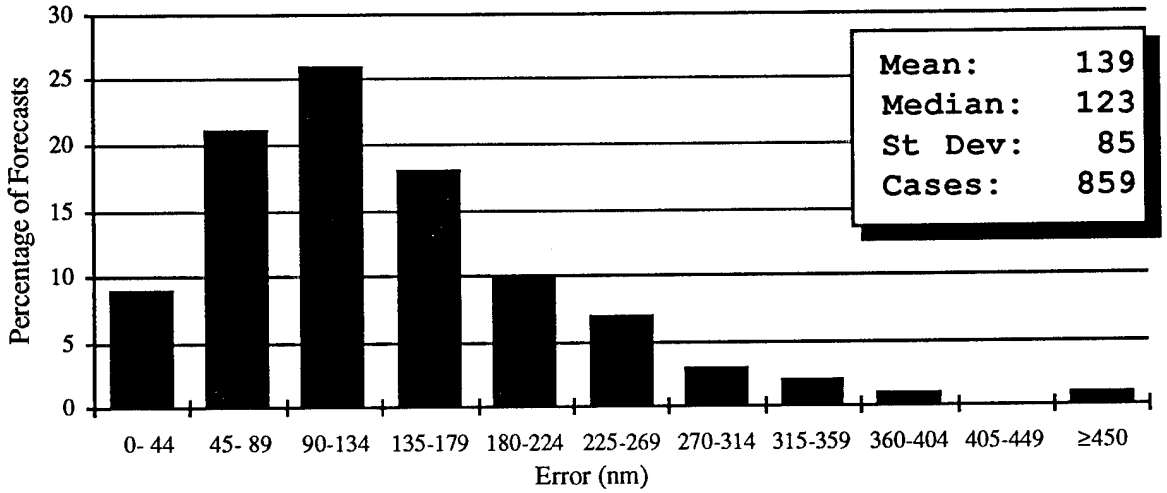

Figure 5-2d Frequency distribution of 36-hour track forecast errors (45-nm increments) for western North Pacific Ocean tropical cyclones in 1994. The largest error, 588 nm, occurred on Tropical Storm Vanessa (09W).

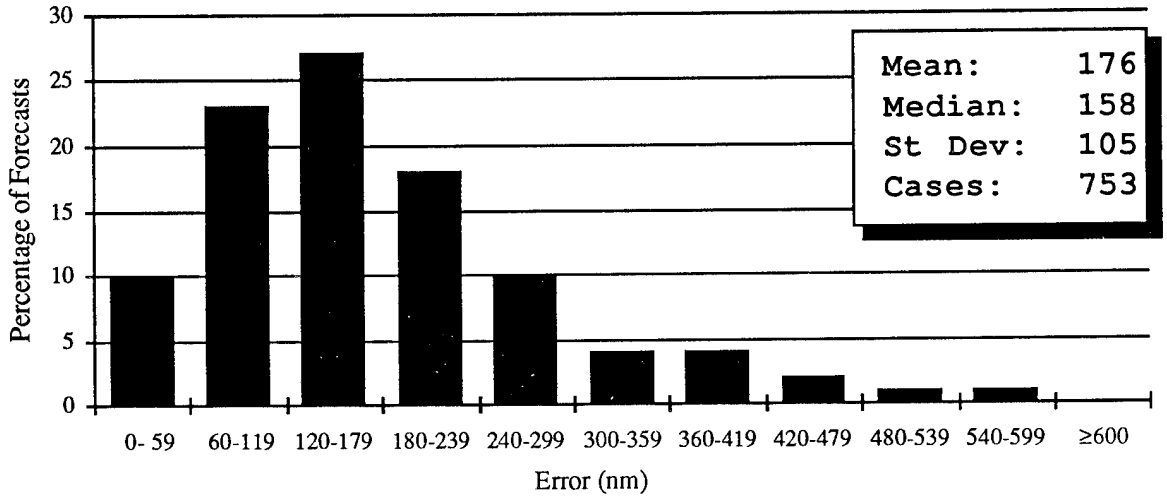

Figure 5-2e Frequency distribution of 48- hour track forecast errors (60-nm increments) for western North Pacific Ocean tropical cyclones in 1994. The largest error, 634 nm, occurred on Typhoon Pat (29W).

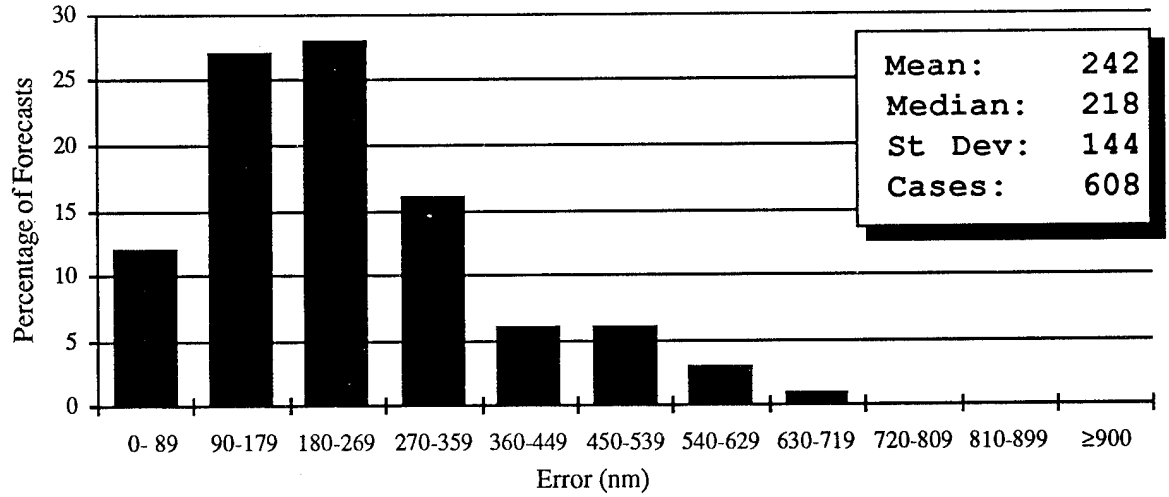

Figure 5-2f Frequency distribution of 72-hour track forecast errors (90-nm increments) for western North Pacific Ocean tropical cyclones in 1994. The largest error, 837 nm, occurred on Super Typhoon Melissa (26W).

Table 5-1 INITIAL WARNING POSITION AND FORECAST ERRORS (NM) FOR THE WESTERN NORTH PACIFIC 1978-1994.

YEAR	NUMBER OF WARNINGS	INITIAL POSITION	NUMBER OF FORECASTS	24-HOUR TRACK	24-HOUR ALONG	24-HOUR CROSS	NUMBER OF FORECASTS	48-HOUR TRACK	48-HOUR ALONG	48-HOUR CROSS	NUMBER OF FORECASTS	72-HOUR TRACK	72-HOUR ALONG	72-HOUR CROSS
1978	696	21	556	126	87	71	420	274	194	151	295	411	296	218
1979	695	25	589	125	81	76	469	227	146	138	366	316	214	182
1980	590	28	491	127	86	76	369	244	165	147	267	391	266	230
1981	584	25	466	124	80	77	348	221	146	131	246	334	206	219
1982	786	19	666	113	74	70	532	238	162	142	425	342	223	211
1983	445	16	342	117	76	73	253	260	169	164	184	407	259	263
1984	611	22	492	117	84	64	378	232	163	131	286	363	238	216
1985	592	18	477	117	80	68	336	231	153	138	241	367	230	227
1986	743	21	645	126	85	70	535	261	183	151	412	394	276	227
1987	657	18	563	107	71	64	465	204	134	127	389	303	198	186
1988	465	23	373	114	85	58	262	216	170	103	183	315	244	159
1989	710	20	625	120	83	69	481	231	162	127	363	350	265	177
1990	794	21	658	103	72	60	525	203	148	110	432	310	225	168
1991	835	22	733	96	69	53	599	185	137	97	484	287	229	146
1992	941	25	841	107	77	59	687	205	143	116	568	305	210	172
1993	853	26	725	112	79	63	570	212	151	117	437	321	226	173
1994	1058	24	932	98	85	62	753	176	158	105	608	242	218	144
AVERAGE 1978-1993	687	22	578	116	79	67	452	227	157	131	348	345	238	198

Note: Cross-track and along-track errors were adopted by the JTWC in 1986. Right-angle errors (used prior to 1986) were recomputed as cross-track and along-track errors after-the-fact to extend the data base. See Figure 5-1 for the definitions of cross-track and along-track errors.

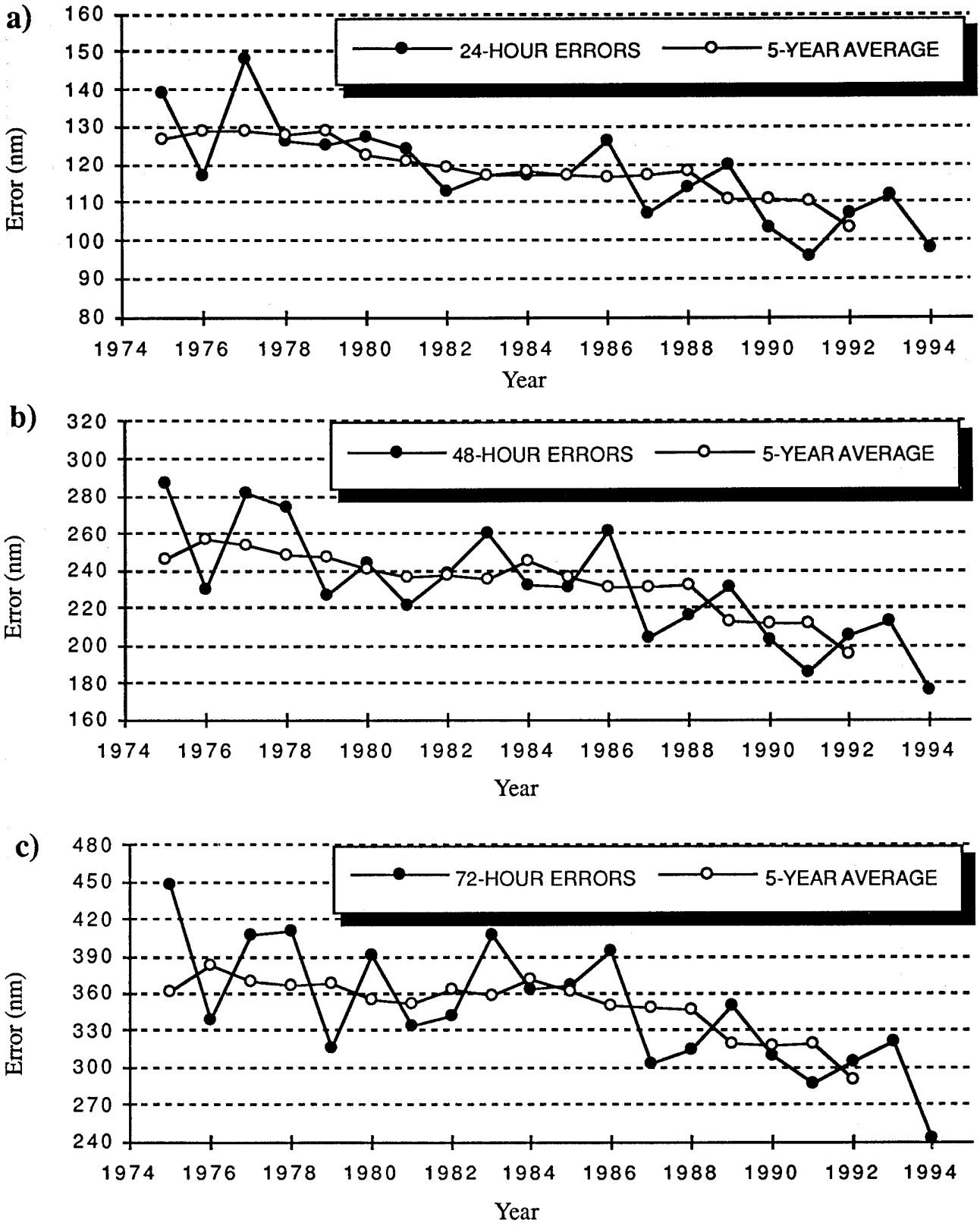

Figure 5-3 Mean track forecast error (nm) and 5-year running mean for a) 24 hours, b) 48 hours and c) 72 hours for western North Pacific Ocean tropical cyclones for the period 1975 to 1994.

Table 5-2 MEAN FORECAST TRACK ERRORS (NM) FOR WESTERN NORTH PACIFIC TROPICAL CYCLONES 1959-1994

	24-HOUR				48-HOUR				72-HOUR			
			Cross	Along			Cross	Along			Cross	Along
YEAR	TY[1]	TC	Track[2]	Track[2]	TY[1]	TC	Track[2]	Track[2]	TY[1]	TC	Track[2]	Track[2]
1959	117*				267*							
1960	177*				354*							
1961	136				274							
1962	144				287				476			
1963	127				246				374			
1964	133				284				429			
1965	151				303				418			
1966	136				280				432			
1967	125				276				414			
1968	105				229				337			
1969	111				237				349			
1970	98	104			181	190			272	279		
1971	99	111	64		203	212	118		308	317	177	
1972	116	117	72		245	245	146		382	381	210	
1973	102	108	74		193	197	134		245	253	162	
1974	114	120	78		218	226	157		357	348	245	
1975	129	138	84		279	288	181		442	450	290	
1976	117	117	71		232	230	132		336	338	202	
1977	140	148	83		266	283	157		390	407	228	
1978	120	127	71	87	241	271	151	194	459	410	218	296
1979	113	124	76	81	219	226	138	146	319	316	182	214
1980	116	126	76	86	221	243	147	165	362	389	230	266
1981	117	123	77	80	215	220	131	146	342	334	219	206
1982	114	113	70	74	229	237	142	162	337	341	211	223
1983	110	117	73	76	247	259	164	169	384	405	263	259
1984	110	117	64	84	228	233	131	163	361	363	216	238
1985	112	117	68	80	228	231	138	153	355	367	227	230
1986	117	121	70	85	261	261	151	183	403	394	227	276
1987	101	107	64	71	211	204	127	134	318	303	186	198
1988	107	114	58	85	222	216	103	170	327	315	159	244
1989	107	120	69	83	214	231	127	162	325	350	177	265
1990	98	103	70	81	191	203	138	162	299	310	211	242
1991	93	96	53	69	187	185	97	137	298	286	146	229
1992	97	107	59	77	194	205	116	143	295	305	172	210
1993	102	112	63	79	205	212	117	151	320	321	173	226
1994	96	98	53	71	172	176	101	123	244	242	146	163

1. Forecasts were verified when tropical cyclone intensities were at least 35 kt (18 m/sec).

2. Cross-track and along-track errors were adopted by the JTWC in 1986. Right-angle errors (used prior to 1986) were recomputed as cross-track errors after-the-fact to extend the data base. See Figure 5-1 for the definitions of cross-track and along-track.

* Forecast positions north of 35° north latitude were not verified.

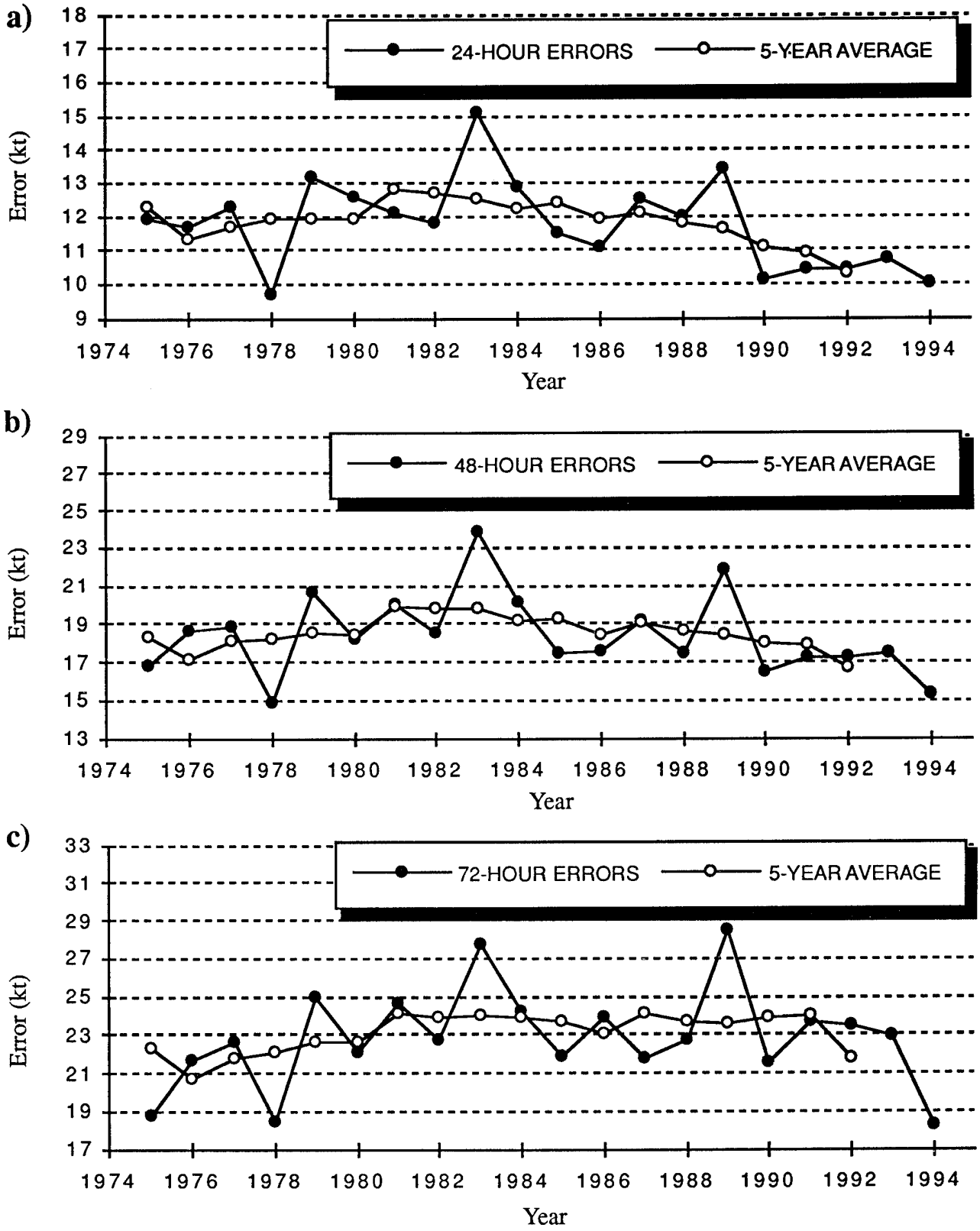

Figure 5-4 Mean intensity forecast errors (kt) and 5-year running mean for a) 24 hours, b) 48 hours and c) 72 hours for western North Pacific Ocean tropical cyclones for the period 1975 to 1994.

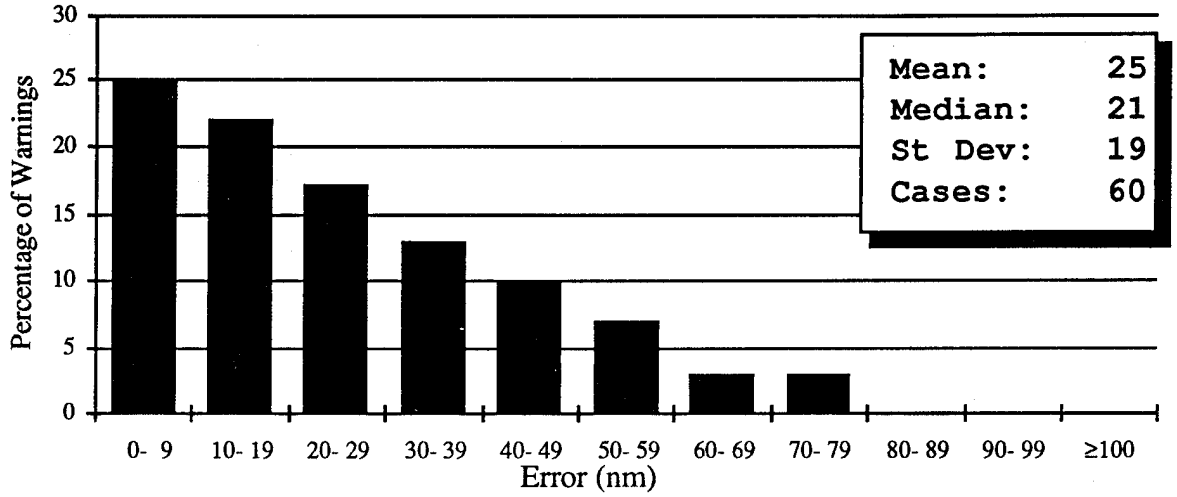

Figure 5-5a Frequency distribution of initial warning position errors (10-nm increments) for North Indian Ocean tropical cyclones in 1994. The largest error, 78 nm, was on TC01B.

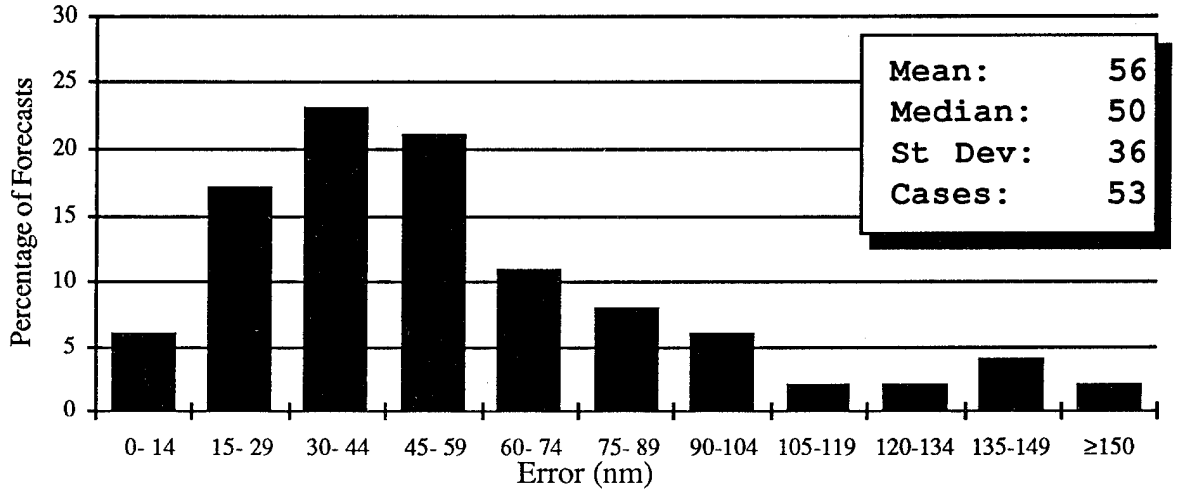

Figure 5-5b Frequency distribution of 12-hour track forecast errors (15-nm increments) for North Indian Ocean tropical cyclones in 1994. The largest error, 183 nm, was on TC01B.

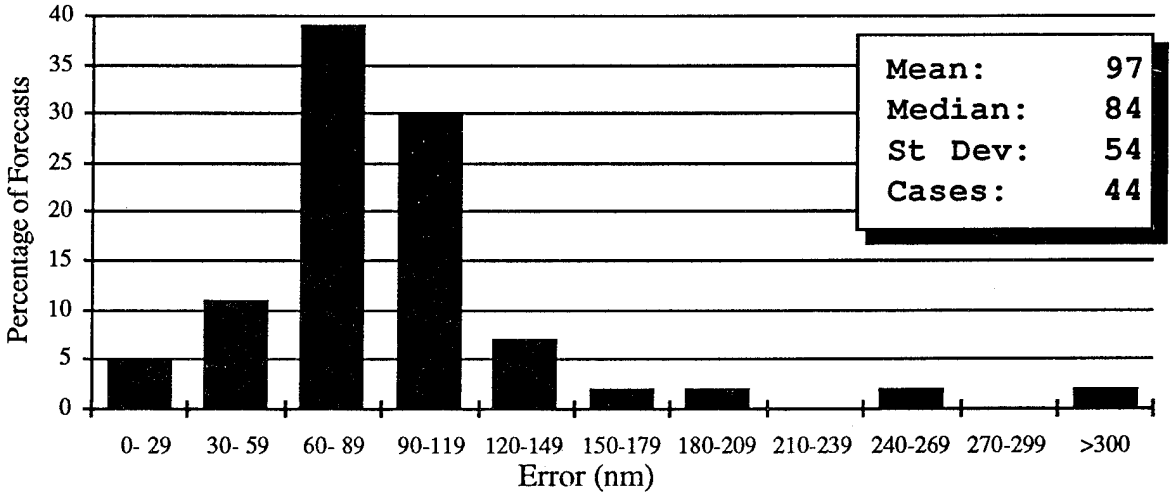

Figure 5-5c Frequency distribution of 24-hour track forecast errors (30-nm increments) for North Indian Ocean tropical cyclones in 1994. The largest error, 318 nm, was on TC01B.

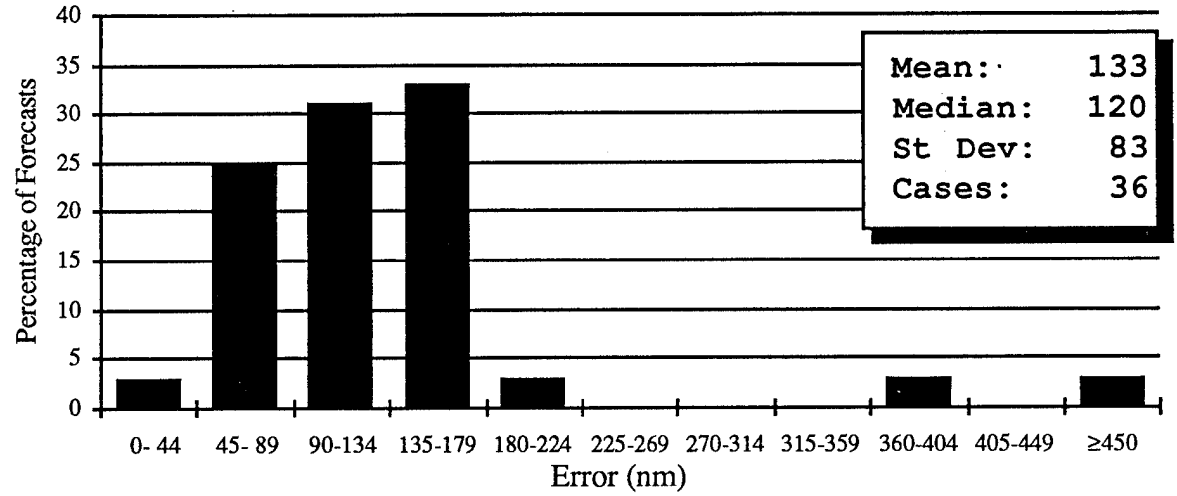

Figure 5-5d Frequency distribution of 36-hour track forecast errors (45-nm increments) for North Indian Ocean tropical cyclones in 1994. The largest error, 484 nm, was on TC01B.

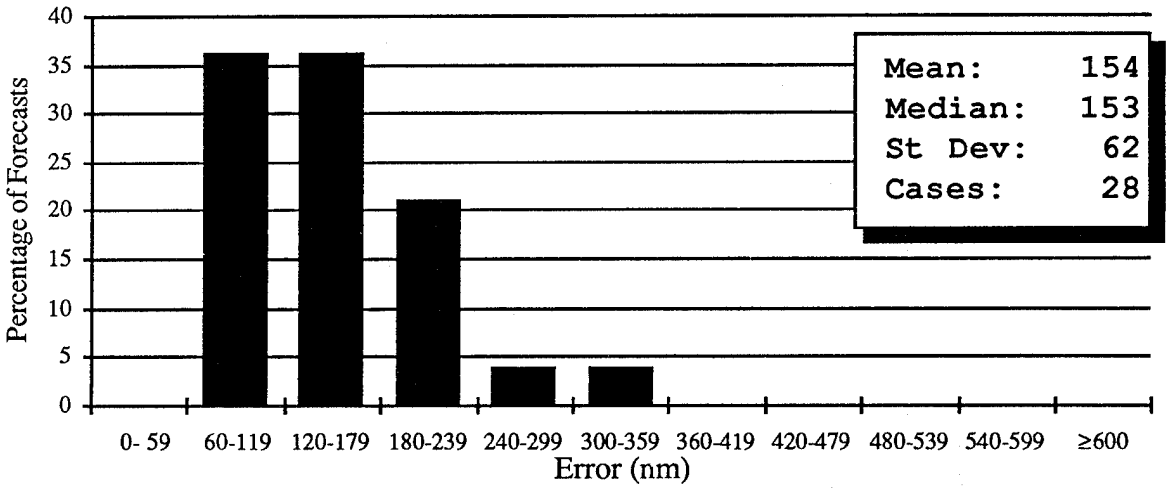

Figure 5-5e Frequency distribution of 48-hour track forecast errors (60-nm increments) for North Indian Ocean tropical cyclones in 1994. The largest error, 303 nm, was on TC01B.

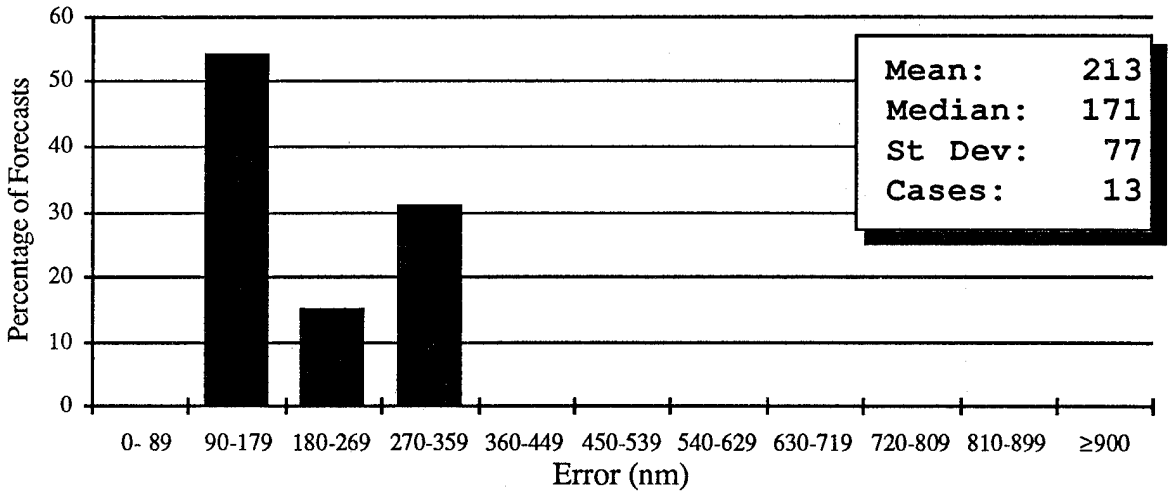

Figure 5-5f Frequency distribution of 72-hour track forecast errors (90-nm increments) for North Indian Ocean tropical cyclones in 1994. The largest error, 354 nm, was on TC02B.

Table 5-3 INITIAL POSITION AND FORECAST POSITION ERRORS (NM) FOR THE NORTH INDIAN OCEAN 1978-1994

YEAR	NUMBER OF WARNINGS	**INITIAL POSITION**	NUMBER OF FORECASTS	**24-HOUR** TRACK	ALONG	CROSS	NUMBER OF FORECASTS	**48-HOUR** TRACK	ALONG	CROSS	NUMBER OF FORECASTS	**72-HOUR** TRACK	ALONG	CROSS
1978	32	43	28	133	90	82	19	202	147	109	N/A			
1979	93	46	63	151	96	95	17	278	193	161	17	437	251	320
1980	14	41	7	115	81	71	38	93	25	88	1	167	97	137
1981	41	28	29	109	76	63	2	176	120	109	5	197	150	111
1982	55	35	37	138	110	68	17	368	292	209	7	762	653	332
1983	18	38	7	117	90	50	18	153	137	53	0			
1984	67	33	42	154	124	67	20	274	217	139	16	388	339	121
1985	53	31	30	122	102	53	8	242	119	194	0			
1986	28	52	16	134	118	53	7	168	131	80	5	269	189	180
1987	83	42	54	144	91	100	25	205	125	140	21	305	219	188
1988	44	34	30	120	89	63	18	219	112	176	12	409	227	303
1989	44	19	33	88	62	50	17	146	94	86	12	216	164	111
1990	46	31	36	101	85	43	24	146	117	67	17	185	130	104
1991	56	38	43	129	107	54	27	235	200	89	14	450	356	178
1992	191	35	149	128	73	86	100	244	141	166	62	398	276	218
1993	36	27	28	125	87	79	20	198	171	74	12	231	176	116
1994	60	25	44	97	80	44	28	153	124	63	13	213	177	92
AVERAGE 1978-1993	56	36	40	129	90	74	24	212	142	127	13	360	258	196

Cross-track and along-track errors were adopted by the JTWC in 1986. Right-angle errors (used prior to 1986) were recomputed as cross-track and along-track errors after-the-fact to extend the data base. See Figure 5-1 for the definitions of cross-track and along-track errors.

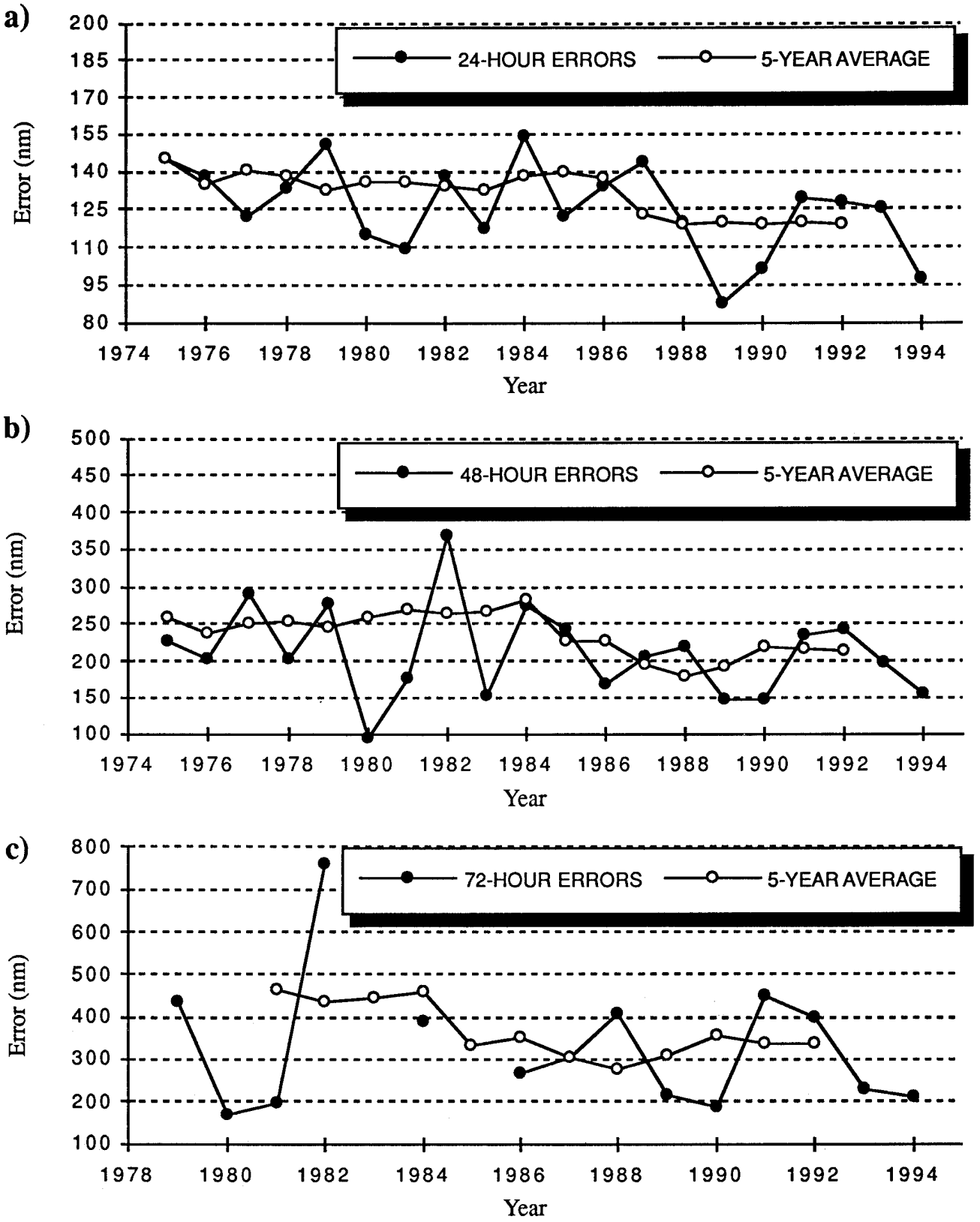

Figure 5-6 Mean track forecast errors (nm) and 5-year running mean for a) 24 hours, b) 48 hours and c) 72 hours for North Indian Ocean tropical cyclones for the period 1975 to 1994. Note: no 72-hour forecasts verified prior to 1979, and in 1983 and 1985.

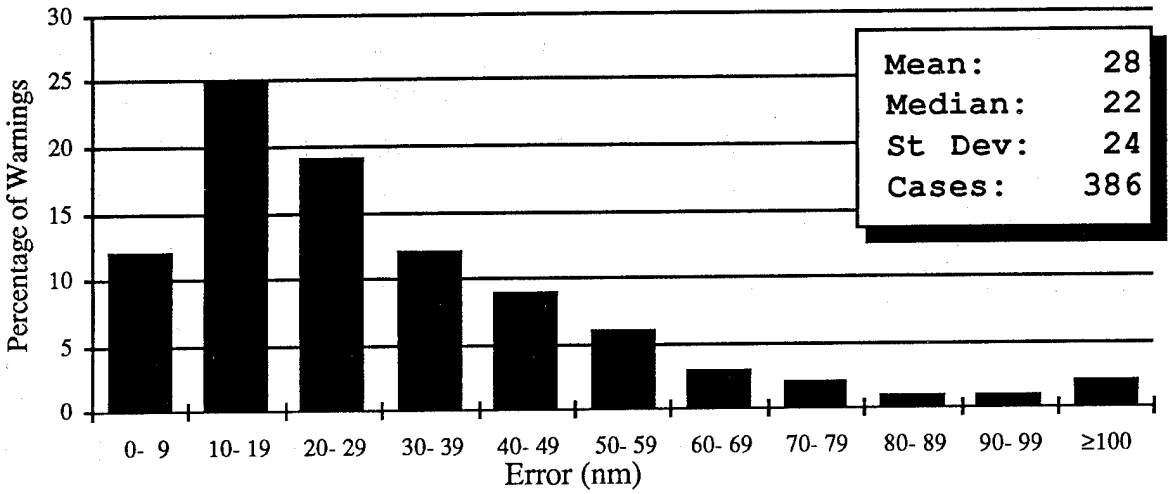

Figure 5-7a Frequency distribution of initial warning position errors (10-nm increments) for South Pacific and South Indian Ocean tropical cyclones in 1994. The largest error, 157 nm, occurred on Tropical Cyclone 01S (Alexina).

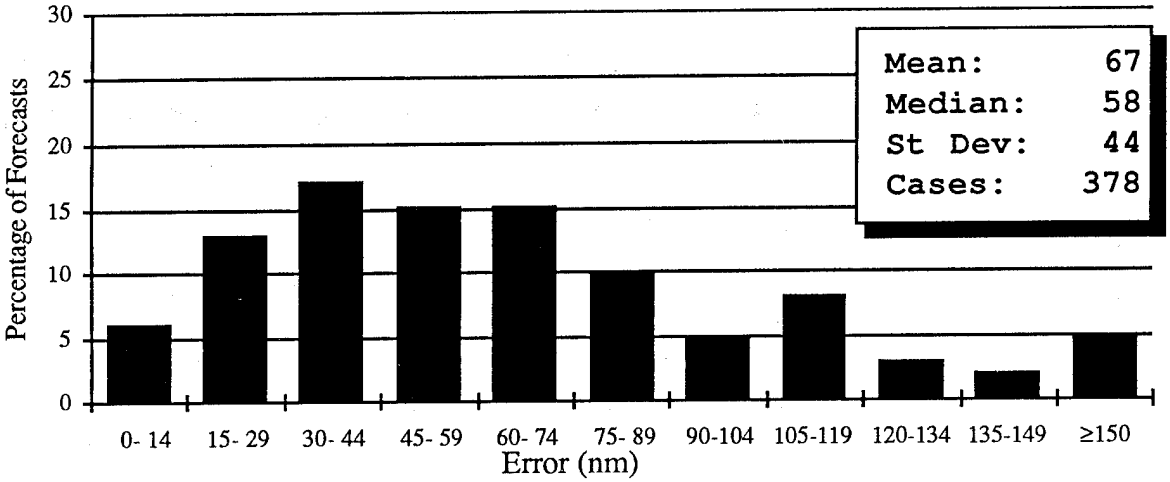

Figure 5-7b Frequency distribution of 12-hour track forecast errors (15-nm increments) for South Pacific and South Indian Ocean tropical cyclones in 1994. The largest error, 345 nm, occurred on Tropical Cyclone 29P.

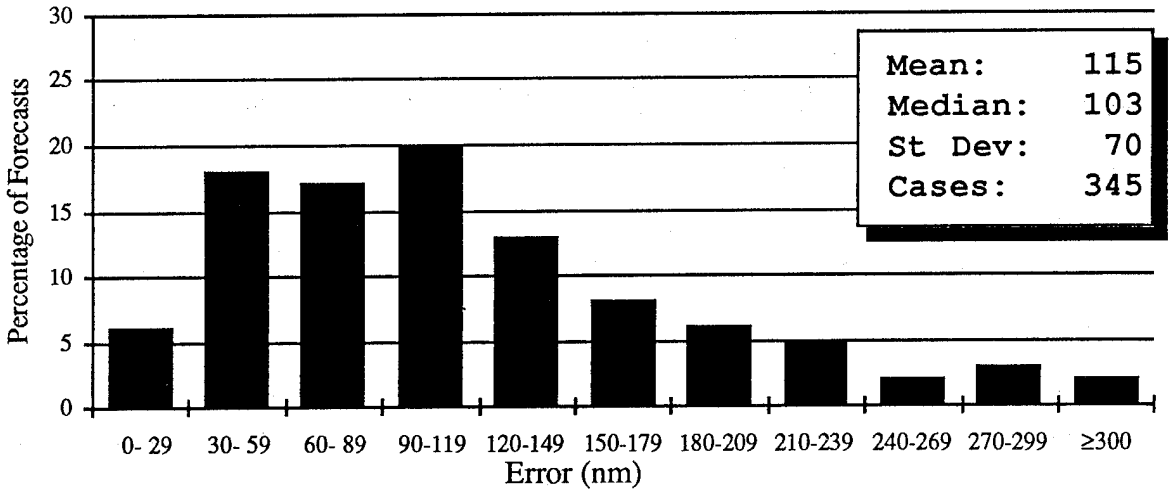

Figure 5-7c Frequency distribution of 24-hour track forecast errors (30-nm increments) for in the South Pacific and South Indian Ocean tropical cyclones in 1994. The largest error, 347 nm, occurred on Tropical Cyclone 05P (Rewa).

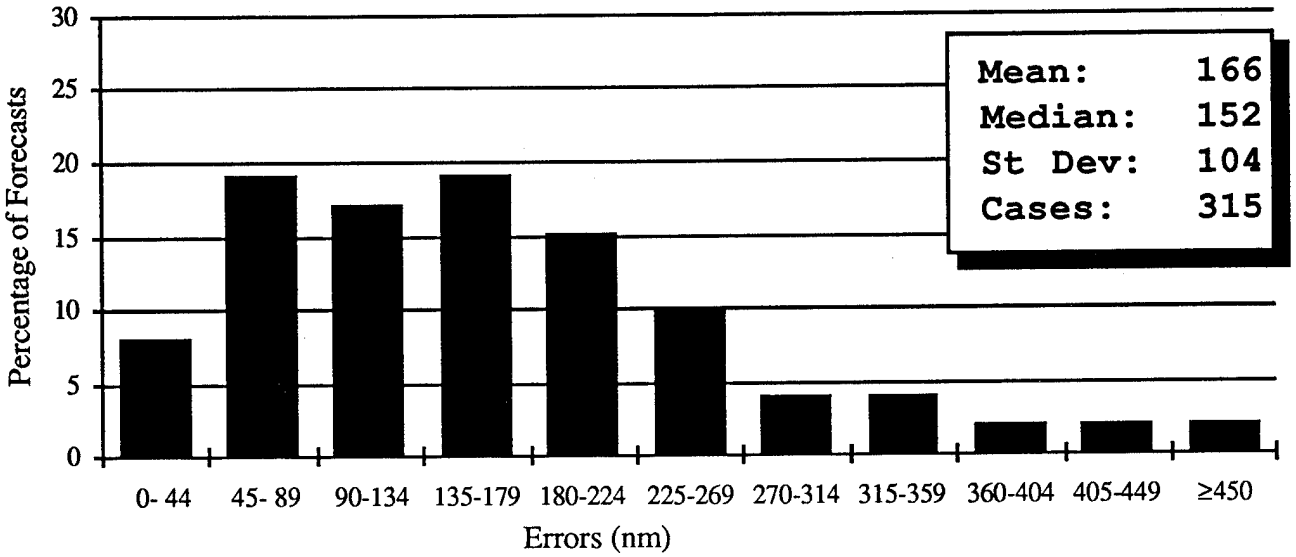

Figure 5-7d Frequency distribution of 36-hr track forecast errors (45-nm increments) for in the South Pacific and South Indian Ocean tropical cyclones in 1994. The largest error, 568 nm, occurred on Tropical Cyclone 05P (Rewa).

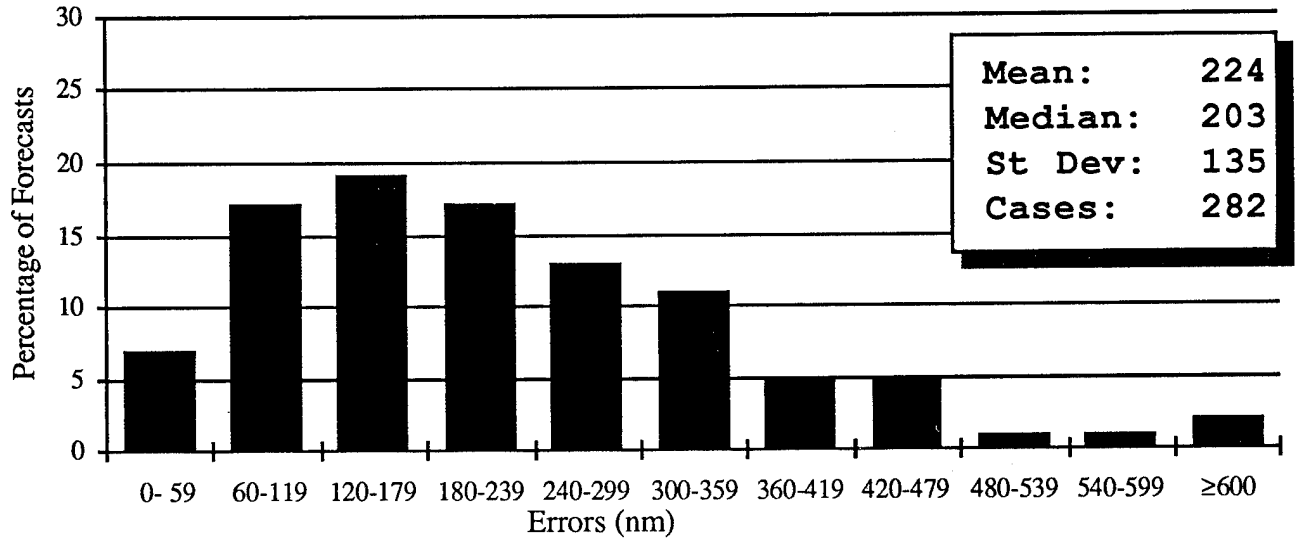

Figure 5-7e Frequency distribution of 48-hour track forecast errors (60-nm increments) for in the South Pacific and South Indian Ocean tropical cyclones in 1994. The largest error, 701 nm, occurred on Tropical Cyclone 05P (Rewa).

Table 5-4 INITIAL POSITION AND FORECAST POSITION ERRORS (NM) FOR THE SOUTHERN HEMISPHERE 1981-1994

YEAR	NUMBER OF WARNINGS	INITIAL POSITION	NUMBER OF FORECASTS	24-HOUR TRACK	24-HOUR ALONG	24-HOUR CROSS	NUMBER OF FORECASTS	48-HOUR TRACK	48-HOUR ALONG	48-HOUR CROSS
1981	226	48	190	165	103	106	140	315	204	201
1982	275	38	238	144	98	86	176	274	188	164
1983*	191	35	163	130	88	77	126	241	158	145
1984	301	36	252	133	90	79	191	231	159	134
1985*	306	36	257	134	92	79	193	236	169	132
1986*	279	40	227	129	86	77	171	262	169	164
1987*	189	46	138	145	94	90	101	280	153	138
1988*	204	34	99	146	98	83	48	290	246	144
1989*	287	31	242	124	84	73	186	240	166	136
1990*	272	27	228	143	105	74	177	263	178	152
1991*	264	24	231	115	75	69	185	220	152	129
1992*	267	28	230	124	91	64	208	240	177	129
1993*	257	21	225	102	74	57	176	199	142	114
1994*	386	28	345	115	77	68	282	224	147	134
AVERAGE 1981-1993	255	34	209	132	90	57	160	248	170	144

*These statistics are for JTWC forecasts only. NPMOC statistics are not included.

Cross-track and along-track errors were adopted by the JTWC in 1986. Right-angle errors (used prior to 1986) were recomputed as cross-track and along-track errors after-the-fact to extend the data base. See Figure 5-1 for the definitions of cross-track and along-track errors.

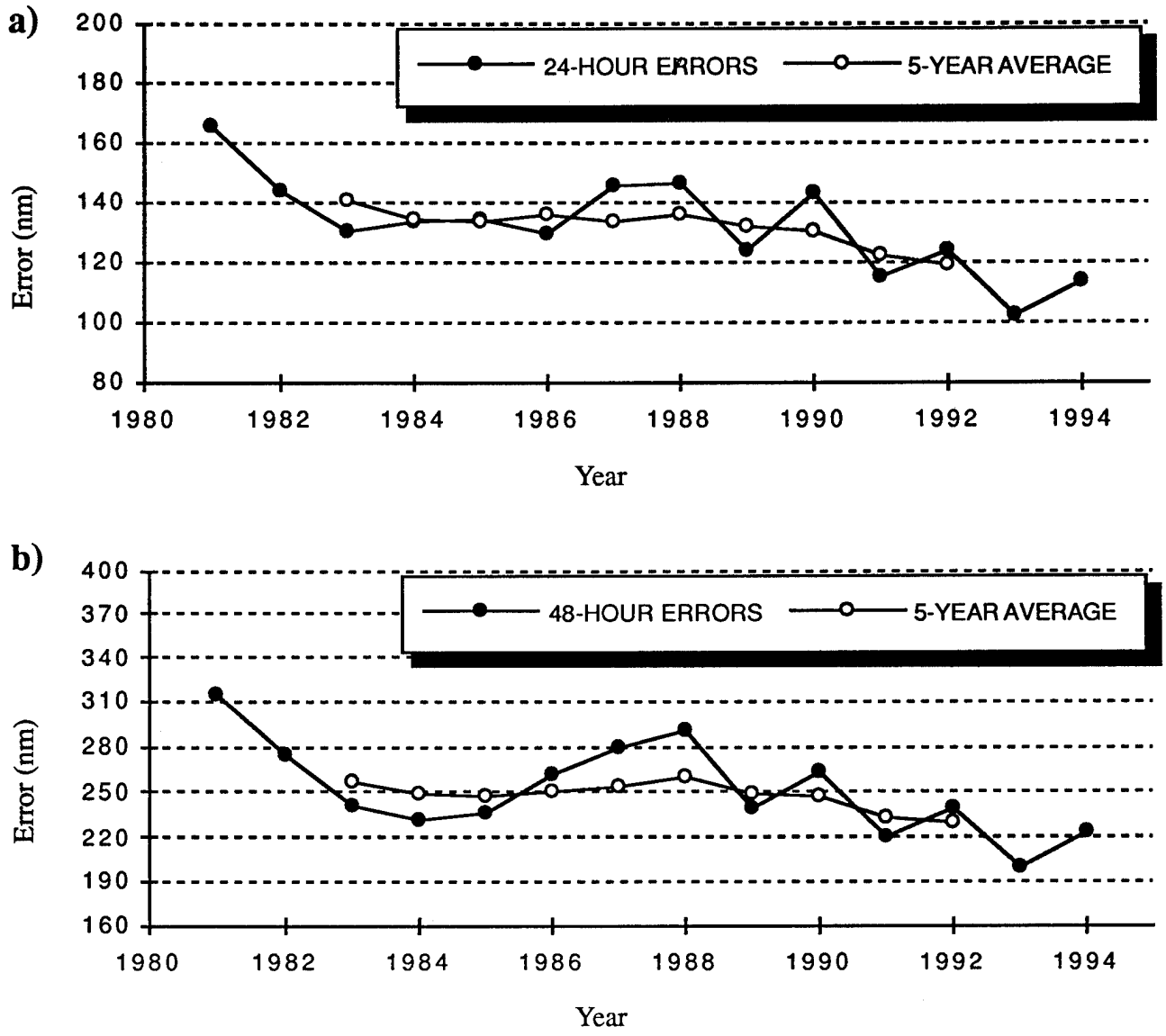

Figure 5-8 Mean track forecast errors (nm) and 5-year running mean for a) 24 hours and b) 48 hours for South Pacific and South Indian Ocean tropical cyclones for the period 1981 to 1994.

5.2 COMPARISON OF OBJECTIVE TECHNIQUES

JTWC uses a variety of objective techniques for guidance in the warning preparation process. Multiple techniques are required, because each technique has particular strengths and weaknesses which vary by basin, numerical model initialization, time of year, synoptic situation and forecast period. The accuracy of objective aid forecasts depends on both the specified position and the past motion of the tropical cyclone as determined by the working best track. JTWC initializes its objective techniques using an extrapolated working best track position so that the output of the techniques will start at the valid time of the next warning initial position.

Unless stated otherwise, all the objective techniques discussed below run in all basins covered by JTWC's AOR and provide forecast positions at 12-, 24-, 36-, 48-, and 72-hours unless the technique aborts prematurely during computations. The techniques can be divided into six general categories: extrapolation, climatology and analogs, statistical, dynamic, hybrids, and empirical or analytical.

5.2.1 EXTRAPOLATION (XTRP) — Past speed and direction are computed using the rhumb line distance between the current and 12-hour old positions of the tropical cyclone. Extrapolation from the current warning position is used to compute forecast positions.

5.2.2 CLIMATOLOGY and ANALOGS

5.2.2.1 CLIMATOLOGY (CLIM) — Employs time and location windows relative to the current position of the storm to determine which historical storms will be used to compute the forecast. The historical data base is 1945-1981 for the Northwest Pacific, and 1900 to 1990 for the rest of JTWC's AOR. A second climatology-based technique exists on JTWC's Macintosh®™ computers. It employs data bases from 1945 to 1992 and from 1970 to 1994. The latter is referred to as the satellite-era data base. Objective intensity forecasts are available from these data bases. Scatter diagrams of expected tropical cyclone motion at bifurcation points are also available from these data bases.

5.2.2.2 ANALOGS — JTWC's analog and climatology techniques use the same historical data base, except that the analog approach imposes more restrictions on which storms will be used to compute the forecast positions. Analogs in all basins must satisfy time, location, speed, and direction windows, although the window definitions are distinctly different in the Northwest Pacific. In this basin, acceptable analogs are also ranked in terms of a similarity index that includes the above parameters and: storm size and size change, intensity and intensity change, and heights and locations of the 700-mb subtropical ridge and upstream midlatitude trough. In other basins, all acceptable analogs receive equal weighting and a persistence bias is explicitly added to the forecast. In the western North Pacific basin, analog weighting is varied using the similarity index, and a persistence bias is implicitly incorporated by rotating the analog tracks so that they initially match the 12-hr old motion of the current storm. In the AOR, a forecast based on all acceptable straight-running analogs called STRT, as well as a forecast based only on historical recurvers called RECR are available.

5.2.3 STATISTICAL

5.2.3.1 CLIMATOLOGY AND PERSISTENCE (CLIPER or CLIP) — A statistical regression technique that is based on climatology, current position and 12-hour and 24-hour past movement. This technique is used as a crude baseline against which to measure the forecast skill of other, more sophisticated techniques. CLIP in

the Northwest Pacific uses third-order regression equations, and is based on the work of Xu and Neumann (1985). CLIPER has been available outside this basin since mid-1990, with regression coefficients recently recomputed by FNOC based on the updated 1900-1989 data base.

5.2.3.2 COLORADO STATE UNIVERSITY MODEL (CSUM) — A statistical-dynamical technique based on the work of Matsumoto (1984). Predictor parameters include the current and 24-hr old position of the storm, heights from the current and 24-hr old NOGAPS 500-mb analyses, and heights from the 24-hr and 48-hr NOGAPS 500 mb prognoses. Height values from 200-mb fields are substituted for storms that have an intensity exceeding 90 kt and are located north of the subtropical ridge. Three distinct sets of regression equations are used depending on whether the storm's direction of motion falls into "below," "on," or "above" the subtropical ridge categories. During the development of the regression equation coefficients for CSUM, the so-called "perfect prog" approach was used, in which verifying analyses were substituted for the numerical prognoses that are used when CSUM is run operationally. Thus, CSUM was not "tuned" to any particular version of NOGAPS, and in fact, the performance of CSUM should presumably improve as new versions of NOGAPS improve. CSUM runs only in the Northwest Pacific, South China Sea, and North Indian Ocean basins.

5.2.3.3 JTWC92 or JT92 - JTWC92 is a statistical-dynamical model for the western North Pacific Ocean basin which forecasts tropical cyclone positions at 12-hour intervals to 72 hours. The model uses the deep-layer mean height field derived from the NOGAPS forecast fields. These deep-layer mean height fields are spectrally truncated to wave numbers 0 through 18 prior to use in JTWC92. Separate forecasts are made for each position. That is, the forecast 24 hour position is not a 12-hour forecast from the forecasted 12-hour position.

JTWC92 uses five internal sub-models which are blended and iterated to produce the final forecasts. The first sub-model is a statistical blend of climatology and persistence, known as CLIPER. The second sub-model is an analysis mode predictor, which only uses the "analysis" field. The third sub-model is the forecast mode predictor, which uses only the forecast fields. The fourth sub-model is a combination of 1 and 2 to produce a "first guess" of the 12-hourly forecast positions. The fifth sub-model uses the output of the "first guess" combined with 1,2, and 3 to produce the forecasts. The iteration is accomplished by using the output of sub-model 5 as though it were the output from sub-model 4. The optimum number of iterations has been determined to be three.

When JTWC92 is used in the operational mode, all the NOGAPS fields are forecast fields. The 00Z and 12Z tropical forecasts are based upon the previous 12-hour old synoptic time NOGAPS forecasts. The 06Z and 18Z tropical forecasts are based on the previous 00Z and 12Z NOGAPS forecasts, respectively. Therefore, operationally, the second sub-model uses forecast fields and not analysis fields.

5.2.4 DYNAMIC

5.2.4.1 NOGAPS VORTEX TRACKING ROUTINE (NGPS) — This objective technique follows the movement of the point of minimum height on the 1000 mb pressure surface analyzed and predicted by NOGAPS. A search in the expected vicinity of the storm is conducted every six hours through 72 hours, even if the tracking routine temporarily fails to discern a minimum height point. Explicit insertion of a tropical cyclone bogus by JTWC began in mid-1990, and has improved the ability of the NOGAPS technique to track the vortex.

5.2.4.2 ONE-WAY (INTERACTIVE) TROPICAL CYCLONE MODEL (OTCM) — This technique is a coarse resolution (205 km grid), three layer, primitive equation model with a horizontal domain of 6400 x 4700 km. OTCM is initialized using 6-hour or 12-hour prognostic fields from the latest NOGAPS run, and the initial fields are smoothed and adjusted in the vicinity of the storm to induce a persistence bias into OTCM's forecast. A symmetric bogus vortex is then inserted, and the boundaries updated every 12 hours by NOGAPS fields as the integration proceeds. The bogus vortex is maintained against frictional dissipation by an analytical heating function. The forecast positions are based on the movement of the vortex in the lowest layer of the model (effectively 850-mb).

5.2.4.3 FNOC BETA AND ADVECTION MODEL (FBAM) — This model is an adaptation of the Beta and Advection model used by NMC. The forecast motion results from a calculation of environmental steering and an empirical correction for the observed vector difference between that steering and the 12-hour old storm motion. The steering is computed from the NOGAPS Deep Layer Mean (DLM) wind fields which are a weighted average of the wind fields computed for the 1000-mb to 100-mb levels. The difference between past storm motion and the DLM steering is treated as if the storm were a Rossby wave with an "effective radius" propagating in response to the horizontal gradient of the coriolis parameter, Beta. The forecast proceeds in one-hour steps, recomputing the effective radius as Beta changes with storm latitude, and blending in a persistence bias for the first 12 hours.

5.2.5 HYBRIDS

5.2.5.1 HALF PERSISTENCE AND CLIMATOLOGY (HPAC) — Forecast positions are generated by equally weighting the forecasts given by XTRP and CLIM.

5.2.5.2 BLENDED (BLND) — A simple average of JTWC's six primary forecast aids: OTCM, CSUM, FBAM, JT92, CLIP, and HPAC.

5.2.5.3 WEIGHTED (WGTD) — A weighted average of the forecast guidance used to compute BLND: OTCM (29%), CSUM (22%), FBAM (14%), JT92 (14%), HPAC (14%), and CLIP (7%).

5.2.5.4 DYNAMIC AVERAGE (DAVE) — A simle average of all dynamic forecast aids: NOGAPS (NGPS), Bracknell (EGRR), Japanese Typhoon Model (JTYM), JT92, FBAM, OTCM, and CSUM.

5.2.6 EMPIRICAL OR ANALYTICAL

5.2.6.1 DVORAK — An estimation of a tropical cyclone's current and 24-hour forecast intensity is made from the interpretation of satellite imagery (Dvorak, 1984). These intensity estimates are used with other intensity related data and trends to forecast short-term tropical cyclone intensity.

5.2.6.2 MARTIN/HOLLAND — The technique adapts an earlier work (Holland, 1980) and specifically addresses the need for realistic 35-, 50- and 100-kt (18-,26- and 51-m/sec) wind radii around tropical cyclones. It solves equations for basic gradient wind relations within the tropical cyclone area, using input parameters obtained from enhanced infrared satellite imagery. The diagnosis also includes an asymmetric area of winds caused by tropical cyclone movement. Satellite-derived size and intensity parameters are also used to diagnose internal steering components of tropical cyclone motion known collectively as "beta-drift".

5.2.6.3 TYPHOON ACCELERATION PREDICTION TECHNIQUE (TAPT) — This technique (Weir, 1982) utilizes upper-tropospheric and surface wind fields to estimate acceleration associated with the tropical cyclone's interaction with the mid-latitude westerlies. It includes guidelines for the duration of acceleration, upper limits and probable path of the cyclone.

5.3 TESTING AND RESULTS

A comparison of selected techniques is included in Table 5-5 for all Northwest Pacific tropical cyclones, Table 5-6 for all North Indian Ocean tropical cyclones and Table 5-7 for the Southern Hemisphere. For example in Table 5-5 for the 12-hour mean forecast error, 762 cases available for a (homogeneous) comparison, the average forecast error at 12 hours was 74 nm (137 km) for JT92 and 78 nm (145 km) for

TABLE 5-5 1994 ERROR STATISTICS FOR SELECTED OBJECTIVE TECHNIQUES IN THE NORTHWEST PACIFIC
(1 JAN 1994 - 31 DEC 1994)

12-HOUR MEAN FORECAST ERROR (NM)

	JTWC		CLIP		OTCM		CSUM		HPAC		JT92		FBAM		NGPS	
JTWC	1009	57														
	57	0														
CLIP	994	58	1023	75												
	74	16	75	0												
OTCM	974	57	1002	73	1003	76										
	75	18	76	3	76	0										
CSUM	991	58	1019	75	1000	76	1020	75								
	74	16	75	0	74	-2	75	0								
HPAC	990	58	1019	75	999	76	1016	75	1019	79						
	78	20	79	4	77	1	79	4	79	0						
JT92	989	57	1017	75	998	76	1015	75	1014	79	1018	69				
	68	11	69	-6	68	-8	69	-6	69	-10	69	0				
FBAM	977	58	1004	75	985	76	1002	75	1001	79	1002	69	1005	70		
	69	11	70	-5	69	-7	70	-5	70	-9	70	1	70	0		
NGPS	679	51	678	65	677	68	677	66	676	69	659	59	666	61	686	88
	87	36	88	23	88	20	88	22	88	19	88	29	88	27	88	0

Number of Cases	X-Axis Technique Error
Y-Axis Technique Error	Error Difference (Y-X)

24-HOUR MEAN FORECAST ERROR (NM)

	JTWC		CLIP		OTCM		CSUM		HPAC		JT92		FBAM		NGPS	
JTWC	933	98														
	98	0														
CLIP	921	99	953	129												
	128	29	129	0												
OTCM	869	96	899	125	900	119										
	117	21	119	-6	119	0										
CSUM	918	99	949	130	897	119	950	130								
	128	29	130	0	127	8	130	0								
HPAC	917	99	949	130	896	119	946	130	949	136						
	134	35	136	6	132	13	136	6	136	0						
JT92	918	99	949	129	897	119	947	130	946	136	950	116				
	115	16	116	-13	114	-5	116	-14	116	-20	116	0				
FBAM	907	99	937	129	885	119	935	129	934	136	936	116	938	115		
	113	14	115	-14	113	-6	115	-14	115	-21	115	-1	115	0		
NGPS	591	91	589	118	573	107	588	117	588	122	587	104	579	104	594	125
	125	34	125	7	126	19	125	8	125	3	125	21	125	21	125	0

Table 5-5 (CONTINUED) 1994 ERROR STATISTICS FOR SELECTED OBJECTIVE TECHNIQUES IN THE NORTHWESTERN PACIFIC (1 JAN 1994 - 31 DEC 1994)

36-HOUR MEAN FORECAST ERROR (NM)

	JTWC		CLIP		OTCM		CSUM		HPAC		JT92		FBAM		NGPS	
JTWC	860	140														
	140	0														
CLIP	850	140	883	190												
	187	47	190	0												
OTCM	777	138	806	183	807	168										
	165	27	168	-15	168	0										
CSUM	847	140	879	190	804	168	880	187								
	183	43	187	-3	183	15	187	0								
HPAC	846	140	879	190	803	168	876	187	879	192						
	189	49	192	2	188	20	192	5	192	0						
JT92	847	140	879	190	804	167	877	187	876	192	880	170				
	167	27	170	-20	165	-2	170	-17	170	-22	170	0				
FBAM	838	140	869	189	795	167	867	186	866	192	868	169	870	172		
	169	29	172	-17	171	4	172	-14	172	-20	172	3	172	0		
NGPS	503	131	500	176	471	151	499	173	499	176	499	155	492	159	504	161
	161	30	161	-15	161	10	161	-12	161	-15	161	6	161	2	161	0

48-HOUR MEAN FORECAST ERROR (NM)

	JTWC		CLIP		OTCM		CSUM		HPAC		JT92		FBAM		NGPS	
JTWC	754	176														
	176	0														
CLIP	745	177	806	251												
	243	66	251	0												
OTCM	657	173	712	244	713	213										
	206	33	213	-31	213	0										
CSUM	742	177	802	252	710	213	803	241								
	229	5	241	-11	235	22	241	0								
HPAC	741	177	802	251	709	213	799	242	802	247						
	238	61	247	-4	242	29	247	5	247	0						
JT92	742	177	802	251	711	213	800	241	799	246	803	228				
	222	45	228	-23	223	10	228	-13	228	-18	228	0				
FBAM	736	175	794	251	703	214	792	241	791	247	793	228	795	232		
	226	49	232	-19	229	15	233	-8	232	15	232	4	232	0		
NGPS	431	166	430	233	398	194	429	223	429	221	430	209	424	215	434	196
	196	30	196	-37	197	3	196	-27	196	-25	196	-13	197	-18	196	0

72-HOUR MEAN FORECAST ERROR (NM)

	JTWC		CLIP		OTCM		CSUM		HPAC		JT92		FBAM		NGPS	
JTWC	609	242														
	242	0														
CLIP	602	242	663	361												
	346	104	361	0												
OTCM	503	237	550	358	551	309										
	294	57	308	-50	309	0										
CSUM	599	242	659	361	548	308	660	343								
	330	88	344	-17	338	30	343	0								
HPAC	598	242	659	361	547	308	656	344	659	348						
	332	90	348	-13	349	41	348	4	348	0						
JT92	529	238	581	363	481	301	579	340	578	349	582	342				
	334	96	342	-21	333	32	342	2	342	-7	342	0				
FBAM	594	244	652	362	543	309	650	343	649	349	577	342	653	345		
	332	88	344	-18	342	33	345	2	344	-5	339	-3	345	0		
NGPS	300	232	298	350	271	278	297	334	297	316	265	322	295	331	300	254
	254	22	254	-96	257	-21	255	-79	253	-63	255	-67	254	-77	254	0

TABLE 5-6 1994 ERROR STATISTICS FOR SELECTED OBJECTIVE TECHNIQUES IN THE NORTH INDIAN OCEAN (1 JAN 1994 - 31 DEC 1994)

12-HOUR MEAN FORECAST ERROR (NM)

	JTWC		CLIP		OTCM		HPAC		FBAM		CLIM		NGPS		STRT	
JTWC	53	57														
	57	0														
CLIP	53	57	53	67												
	67	10	67	0												
OTCM	53	57	53	67	53	61										
	61	4	61	-6	61	0										
HPAC	52	57	52	67	52	61	52	68								
	68	11	68	1	68	7	68	0								
FBAM	52	56	52	64	52	59	51	66	52	62						
	62	6	62	-2	62	3	61	-5	62	0						
CLIM	53	57	53	67	53	61	52	68	52	62	53	72				
	72	15	72	5	72	11	72	4	69	7	72	0				
NGPS	21	53	21	51	21	47	20	55	21	53	26	56	21	120		
	120	67	120	69	120	73	117	62	120	67	77	64	120	0		
STRT	33	52	33	60	33	58	33	64	33	60	33	68	12	96	33	88
	88	36	88	28	88	30	88	24	88	28	88	20	70	-26	88	0

24-HOUR MEAN FORECAST ERROR (NM)

	JTWC		CLIP		OTCM		HPAC		FBAM		CLIM		NGPS		STRT	
JTWC	44	97														
	97	0														
CLIP	44	97	44	106												
	106	9	106	0												
OTCM	44	97	44	106	44	86										
	86	-11	86	-20	86	0										
HPAC	43	98	43	107	43	86	43	108								
	108	10	108	1	108	22	108	0								
FBAM	44	97	44	106	44	86	43	108	44	102						
	102	5	102	-4	102	16	101	-7	102	0						
CLIM	44	97	44	106	44	86	43	108	44	102	44	118				
	118	21	118	12	118	32	118	10	118	16	118	0				
NGPS	16	94	16	87	16	82	15	97	16	91	16	99	16	208		
	208	114	208	121	208	126	209	112	208	117	208	109	208	0		
STRT	27	92	27	91	27	74	27	102	27	98	27	115	8	187	27	150
	150	58	150	59	150	76	150	48	150	52	150	35	113	-74	150	0

36-HOUR MEAN FORECAST ERROR (NM)

	JTWC		CLIP		OTCM		HPAC		FBAM		CLIM		NGPS		STRT	
JTWC	36	134														
	134	0														
CLIP	36	134	36	154												
	154	20	154	0												
OTCM	35	124	35	145	35	123										
	123	-1	123	-22	123	0										
HPAC	35	136	35	155	34	122	35	159								
	159	23	159	4	151	29	159	0								
FBAM	36	134	36	154	35	123	35	159	36	159						
	159	25	159	5	150	27	157	-2	159	0						
CLIM	36	134	36	154	35	123	35	159	36	159	36	193				
	193	59	193	39	184	61	194	35	193	34	193	0				
NGPS	12	110	12	113	12	125	11	131	12	105	12	173	12	313		
	313	203	313	200	313	188	321	190	313	208	313	140	313	0		
STRT	21	121	21	133	21	112	21	151	21	151	21	209	5	279	21	214
	214	93	214	81	214	102	214	63	214	63	214	5	188	-91	214	0

TABLE 5-6 (CONTINUED 1994 ERROR STATISTICS FOR SELECTED OBJECTIVE TECHNIQUES IN THE NORTH INDIAN OCEAN (1 JAN 1994 - 31 DEC 1994)

48-HOUR MEAN FORECAST ERROR (NM)

	JTWC		CLIP		OTCM		HPAC		FBAM		CLIM		NGPS		STRT	
JTWC	28	154														
	154	0														
CLIP	28	154	28	197												
	197	43	197	0												
OTCM	26	148	26	186	26	172										
	172	24	172	-14	172	0										
HPAC	27	156	27	200	25	171	27	219								
	219	63	219	19	216	45	219	0								
FBAM	28	154	28	197	26	172	27	219	28	194						
	194	40	194	-3	182	10	190	-29	194	0						
CLIM	28	154	28	197	26	172	27	219	28	194	28	268				
	268	114	268	71	271	99	268	49	268	74	268	0				
NGPS	9	128	9	173	9	202	8	208	9	137	9	235	9	412		
	412	284	412	239	412	210	437	229	412	275	412	177	412	0		
STRT	15	152	15	184	15	156	15	234	15	200	15	330	2	327	15	288
	288	136	288	104	288	132	288	54	288	88	288	-42	220	-107	288	0

72-HOUR MEAN FORECAST ERROR (NM)

	JTWC		CLIP		OTCM		HPAC		FBAM		CLIM		NGPS		STRT	
JTWC	13	213														
	213	0														
CLIP	13	213	13	345												
	345	132	345	0												
OTCM	12	220	12	347	12	345										
	345	125	345	-2	345	0										
HPAC	12	217	12	353	11	356	12	419								
	419	202	419	66	435	79	419	0								
FBAM	13	213	13	345	12	345	12	419	13	270						
	270	57	270	-75	277	-68	261	-158	270	0						
CLIM	13	213	13	345	12	345	12	419	13	270	13	469				
	469	256	469	124	481	136	463	44	469	199	469	0				
NGPS	6	173	6	357	5	304	5	366	6	219	6	431	6	488		
	488	315	488	131	459	155	574	208	488	269	488	57	488	0		
STRT	6	233	6	325	6	254	6	486	6	342	6	574	1	105	6	453
	453	220	453	128	453	199	453	-33	453	111	453	-121	274	169	453	0

CLIP. The difference of 4 nm (7 km) is shown in the lower right. (Differences are not always exact, due to computational round-off which occurs for each of the cases available for comparison).

TABLE 5-7 1994 ERROR STATISTICS FOR SELECTED OBJECTIVE TECHNIQUES IN THE SOUTHERN HEMISPHERE (1 JUL 1993 - 30 JUN 1994)

12-HOUR MEAN FORECAST ERROR (NM)

	JTWC		CLIP		OTCM		HPAC		FBAM		CLIM		NGPS		STRT	
JTWC	378	67														
	67	0														
CLIP	350	67	493	95												
	103	36	95	0												
OTCM	350	67	493	95	493	92										
	99	32	92	-3	92	0										
HPAC	350	67	493	95	493	92	493	90								
	96	29	90	-5	90	-2	90	0								
FBAM	334	67	474	97	474	93	474	91	474	90						
	96	29	90	-7	90	-3	90	-1	90	0						
CLIM	350	67	493	95	493	92	493	90	474	90	493	100				
	105	38	100	5	100	8	100	10	100	10	100	0				
NGPS	161	64	202	81	202	81	202	78	197	75	202	88	267	116		
	117	53	118	37	118	37	118	40	117	42	118	30	116	0		
STRT	247	69	349	95	349	96	349	92	336	94	349	100	147	120	349	111
	117	48	111	16	111	15	111	19	113	19	111	11	98	-22	111	0

24-HOUR MEAN FORECAST ERROR (NM)

	JTWC		CLIP		OTCM		HPAC		FBAM		CLIM		NGPS		STRT	
JTWC	345	115														
	115	0														
CLIP	324	115	471	154												
	161	46	154	0												
OTCM	309	114	453	153	453	144										
	150	36	144	-9	144	0										
HPAC	324	115	471	154	453	144	471	141								
	145	30	141	-13	140	-4	141	0								
FBAM	309	116	453	155	436	145	453	141	453	146						
	152	36	146	-9	145	0	146	5	146	0						
CLIM	324	115	471	154	453	144	471	141	453	146	471	169				
	172	57	169	15	169	25	169	28	168	22	169	0				
NGPS	145	112	184	138	179	136	184	133	179	133	184	161	244	180		
	176	64	179	41	176	40	179	46	178	45	179	18	180	0		
STRT	232	112	337	145	324	142	337	134	324	146	337	159	132	175	337	175
	176	64	175	30	177	35	175	4 1	177	31	175	16	161	-14	175	0

36-HOUR MEAN FORECAST ERROR (NM)

	JTWC		CLIP		OTCM		HPAC		FBAM		CLIM		NGPS		STRT	
JTWC	315	166														
	166	0														
CLIP	299	168	437	188												
	192	24	188	0												
OTCM	278	166	410	189	410	191										
	191	25	191	2	191	0										
HPAC	299	168	437	188	410	191	437	179								
	178	10	179	-9	181	-10	179	0								
FBAM	285	168	240	188	394	192	420	179	420	201						
	196	28	201	13	198	6	201	22	201	0						
CLIM	299	168	437	188	410	191	437	179	420	201	437	218				
	216	48	218	30	221	30	218	39	217	16	218	0				
NGPS	127	171	164	193	156	200	164	194	159	203	164	230	221	242		
	228	57	240	47	234	34	240	46	239	36	240	10	242	0		
STRT	224	161	326	174	303	176	326	163	314	195	326	200	116	228	326	225
	215	54	225	51	230	54	225	62	226	31	225	25	231	3	225	0

TABLE 5-7 (CONTINUED)

1994 ERROR STATISTICS FOR SELECTED OBJECTIVE TECHNIQUES
IN THE SOUTHERN HEMISPHERE (1 JUL 1993 - 30 JUN 1994)

48-HOUR MEAN FORECAST ERROR (NM)

	JTWC		CLIP		OTCM		HPAC		FBAM		CLIM		NGPS		STRT	
JTWC	282	224														
	224	0														
CLIP	266	226	400	240												
	241	15	240	0												
OTCM	239	222	365	240	365	261										
	256	34	261	21	261	0										
HPAC	266	226	400	240	365	261	400	236								
	232	6	236	-4	237	-24	236	0								
FBAM	256	227	388	241	354	264	388	237	388	276						
	264	37	276	35	270	6	276	39	276	0						
CLIM	266	226	400	240	365	261	400	236	388	276	400	277				
	271	45	277	37	282	21	277	41	277	1	277	0				
NGPS	112	241	143	256	128	279	143	266	140	280	143	297	190	310		
	297	56	307	51	295	16	307	40	305	25	307	10	310	0		
STRT	204	214	303	225	273	240	303	216	294	269	303	259	99	292	303	294
	279	65	294	69	297	57	294	78	296	27	294	35	310	18	294	0

72-HOUR MEAN FORECAST ERROR (NM)

	CLIP		OTCM		HPAC		FBAM		CLIM		NGPS		STRT		RECR	
CLIP	334	334														
	334	0														
OTCM	277	338	277	371												
	371	33	371	0												
HPAC	334	334	277	371	334	335										
	335	1	333	-38	335	0										
FBAM	325	338	269	375	325	339	325	445								
	445	107	425	50	445	106	445	0								
CLIM	334	334	277	371	334	335	325	445	334	374						
	374	40	388	17	374	39	376	-69	374	0						
NGPS	104	363	78	412	104	392	102	438	104	412	135	423				
	427	64	417	5	427	35	430	-8	427	15	423	0				
STRT	259	327	216	350	259	315	252	433	259	362	77	432	259	429		
	429	102	418	68	429	114	431	-2	429	67	484	52	429	0		
RECR	306	333	257	367	306	329	297	441	306	383	97	437	244	413	306	373
	373	40	375	8	373	44	379	-62	373	-10	426	-11	356	-57	373	0

6. TROPICAL CYCLONE WARNING VERIFICATION STATISTICS

6.1 GENERAL

Due to the rapid growth of micro-computers in the meteorological community, tropical cyclone track data (with best track, initial warning, 12-, 24-, 36-, 48-, and 72-hour JTWC forecasts) and fix data (satellite, aircraft, radar and synoptic) are now available as computer files separately upon request. The data will be in ASCII format and can be copied to 3.5 inch diskettes, and will fill two diskettes (or one high density diskette). These data include the western North Pacific Ocean (1 January - 31 December 1994) on one and North Indian Ocean (1 January - 31 December 1994), and western South Pacific and South Indian Oceans (1 July 1993 - 30 June 1994) on the other. Agencies or individuals desiring these data sets should send the appropriate number of diskettes to NAVPACMETOCCEN WEST/JTWC Guam with their request. When the request and your diskettes are received, the data will be copied onto your diskettes and returned with an explanation of the data formats.

6.2 WARNING VERIFICATION STATISTICS

6.2.1 WESTERN NORTH PACIFIC

This section includes verification statistics for each JTWC tropical cyclone warning in the western North Pacific Ocean during 1994.

JTWC BEST TRACK, FORECAST TRACK AND INTENSITY ERRORS BY WARNING

TROPICAL DEPRESSION 01W

	WRN				POSITION ERRORS (NM)						WIND ERRORS (KT)					
DTG (Z)	NO.	LAT	LONG	WIND (KT)	00	12	24	36	48	72	00	12	24	36	48	72
94010106		5.4N	155.8E	20												
94010112		5.7N	153.9E	20												
94010118		6.0N	152.0E	20												
94010200		6.3N	150.1E	20												
94010206		6.6N	148.2E	25												
94010212		6.9N	146.3E	25												
94010218		7.2N	144.4E	25												
94010300		7.5N	142.5E	25												
94010306		7.8N	140.6E	25												
94010312		8.1N	138.8E	25												
94010318		8.4N	137.0E	25												
94010400		8.7N	135.2E	25												
94010406	1	9.0N	133.4E	25	66	112	127	210			0	5	5	10		
94010412		9.4N	131.7E	25												
94010418	2	9.8N	130.0E	25	215	208	234	348			0	0	5	15		
94010500		10.3N	128.5E	25												
94010506	3	10.9N	127.0E	25	141	242	380				0	5	10			
94010512		11.6N	125.8E	25												
94010518	4	12.4N	124.8E	20	52	50					5	10				
94010600		13.2N	124.1E	15												
94010606	5	14.0N	123.5E	15	117						5					
94010612		14.7N	122.9E	15												
		AVERAGE			119	154	247	279			2	5	7	13		
		# CASES			5	4	3	2			5	4	3	2		

TYPHOON OWEN (02W)

DTG(Z)	WRN NO.	LAT	LONG	WIND (KT)	POSITION ERRORS(NM) 00	12	24	36	48	72	WIND ERRORS(KT) 00	12	24	36	48	72
94032818		8.5N	147.7E	15												
94032900		8.9N	146.5E	15												
94032906		9.3N	145.3E	15												
94032912		9.6N	144.1E	15												
94032918		9.9N	142.9E	15												
94033000		10.1N	141.7E	20												
94033006		10.3N	140.5E	20												
94033012		10.5N	139.3E	20												
94033018		10.7N	138.1E	20												
94033100		10.9N	136.9E	25												
94033106		11.1N	135.9E	25												
94033112		11.2N	135.1E	25												
94033118		11.3N	134.3E	30												
94040100	1	11.4N	133.5E	30	42	64	85	126	170	267	5	-5	-15	-15	-25	-40
94040106	2	11.4N	132.7E	35	41	85	134	192	238	262	0	-10	-15	-25	-30	-40
94040112	3	11.4N	131.9E	40	89	135	188	224	274	249	-5	-5	-10	-25	-35	-25
94040118	4	11.4N	131.2E	45	72	84	136	183	216	176	0	0	-5	-20	-35	-20
94040200	5	11.3N	130.5E	50	47	63	94	137	149	90	0	0	-10	-20	-30	-15
94040206	6	11.3N	129.9E	50	8	29	59	89	118	209	0	-5	-10	-25	-25	-10
94040212	7	11.2N	129.3E	55	25	53	88	106	96	105	0	-10	-10	-25	-15	-5
94040218	8	11.0N	128.7E	60	25	51	74	81	66	77	0	-5	-15	-20	-10	-10
94040300	9	10.8N	128.1E	65	0	8	21	73	129	218	0	-5	-15	-5	-5	-10
94040306	10	10.6N	127.6E	65	5	11	46	85	129	181	0	-10	-10	0	-5	-10
94040312	11	10.4N	127.0E	70	6	31	84	135	177	175	-5	-10	0	5	-5	-5
94040318	12	10.3N	126.3E	75	31	91	147	207	248	194	0	-5	5	5	-5	0
94040400	13	10.2N	125.5E	75	11	47	94	123	145	261	-5	5	5	0	-10	-10
94040406	14	10.1N	124.5E	70	13	50	83	132	200	260	0	10	5	-5	-10	-5
94040412	15	10.2N	123.4E	60	59	106	162	231	304	298	5	5	0	-10	-20	-20
94040418	16	10.4N	122.3E	55	84	109	154	217	246	246	10	5	-5	-10	-15	-15
94040500	17	10.7N	121.2E	50	8	18	75	126	186	322	0	-5	-10	-15	-10	-10
94040506	18	11.0N	120.1E	50	17	50	92	115	172	338	0	-10	-15	-10	-10	-10
94040512	19	11.3N	119.0E	50	13	54	92	121	169	321	0	-10	-15	-10	-10	-10
94040518	20	11.6N	118.0E	55	41	102	151	200	261	363	-5	-10	-10	-5	-5	-5
94040600	21	11.8N	117.2E	55	32	37	93	147	221	383	0	0	10	20	30	50
94040606	22	12.0N	116.5E	55	5	63	138	215	303		0	5	15	25	35	
94040612	23	12.5N	116.1E	55	24	91	178	263	348		0	10	20	25	35	
94040618	24	13.0N	116.0E	50	47	121	196	291	383		5	10	25	30	40	
94040700	25	13.6N	115.9E	50	37	69	109	150	168		-5	0	5	5	10	
94040706	26	14.2N	116.0E	45	5	37	69	109			0	10	15	15		
94040712	27	14.8N	116.1E	45	32	45	37	43			0	10	15	20		
94040718	28	15.4N	116.3E	40	68	122	163				5	10	10			
94040800	29	16.0N	116.5E	40	5	45	77				-5	-5	0			
94040806	30	16.6N	116.8E	35	5	12					5	5				
94040812	31	17.2N	117.1E	35	0	6					0	5				
94040818	32	17.7N	117.5E	30	5						0					
94040900		18.1N	117.8E	25												
94040906		18.4N	118.2E	20												
			AVERAGE		29	61	108	153	205	238	2	6	10	15	19	15
			# CASES		32	31	29	27	25	21	32	31	29	27	25	21

TYPHOON PAGE (03W)

DTG(Z)	WRN NO.	LAT	LONG	WIND (KT)	POSITION ERRORS(NM) 00	12	24	36	48	72	WIND ERRORS(KT) 00	12	24	36	48	72
94050800		4.0N	155.4E	15												

TYPHOON PAGE (03W) (CONTINUED)

DTG(Z)	WRN NO.	LAT	LONG	WIND (KT)	POSITION ERRORS (NM) 00	12	24	36	48	72	WIND ERRORS (KT) 00	12	24	36	48	72
94050806		4.2N	154.3E	15												
94050812		4.4N	153.2E	15												
94050818		4.6N	152.1E	15												
94050900		4.9N	151.1E	15												
94050906		5.3N	150.1E	15												
94050912		5.8N	149.1E	20												
94050918		6.4N	148.1E	20												
94051000		7.1N	147.1E	20												
94051006		7.8N	146.1E	20												
94051012		8.5N	145.1E	20												
94051018		9.1N	144.1E	20												
94051100		9.6N	143.0E	25												
94051106		10.1N	142.0E	25												
94051112		10.6N	141.1E	25												
94051118	1	11.1N	140.1E	25	69	59	114	174	225	432	0	0	-5	-5	-5	-15
94051200	2	11.7N	139.2E	30	34	34	95	150	200	452	0	0	0	-5	-10	-20
94051206	3	12.3N	138.4E	30	21	43	91	128	187	429	0	-5	-5	-10	-15	-20
94051212	4	13.0N	137.7E	35	37	18	29	59	181	452	0	-5	-10	-10	-10	-15
94051218	5	13.7N	137.1E	40	8	56	78	112	233	502	-5	-10	-15	-15	-15	-15
94051300	6	14.4N	136.5E	45	29	51	53	121	239	492	-5	-10	-15	-20	-20	-10
94051306	7	15.0N	135.8E	50	34	62	119	177	217	305	-5	-10	-15	-10	-5	-15
94051312	8	15.6N	135.3E	55	18	85	177	242	278	369	0	-5	-10	-10	-5	-15
94051318	9	16.1N	135.0E	60	18	103	210	289	353	576	-5	-10	-15	-10	-5	-10
94051400	10	16.5N	135.1E	65	29	114	213	293	370	607	-5	-10	-15	-15	0	0
94051406	11	16.9N	135.5E	70	23	87	158	239	353	654	0	5	5	0	0	10
94051412	12	17.6N	136.0E	75	34	94	171	231	300	604	0	0	0	5	5	15
94051418	13	18.4N	136.5E	80	58	111	175	227	298	536	-5	-5	-5	0	-5	10
94051500	14	19.3N	137.0E	85	20	53	58	30	83	239	0	0	5	5	5	10
94051506	15	20.3N	137.4E	90	17	25	16	64	116		5	0	0	-5	10	
94051512	16	21.3N	137.9E	90	8	22	70	118	149		0	5	0	0	5	
94051518	17	22.3N	138.5E	90	16	45	106	154	211		0	-5	0	10	5	
94051600	18	23.3N	139.4E	85	20	67	138	203	238		0	0	5	15	10	
94051606	19	24.3N	140.6E	85	24	73	132	206			0	5	15	20		
94051612	20	25.4N	141.9E	80	8	21	58	80			0	10	15	15		
94051618	21	26.6N	143.4E	75	48	97	143				0	15	15			
94051700	22	27.9N	144.9E	65	13	52	111				0	0	5			
94051706	23	29.2N	146.6E	55	6	15					0	0				
94051712	24	30.6N	148.4E	50	15	23					5	10				
94051718	25	32.1N	150.3E	45	5						0					
94051800		33.5N	152.5E	40												
94051806		35.0N	155.0E	40												
		AVERAGE			25	59	115	165	236	475	2	5	8	9	8	13
		# CASES			25	24	22	20	18	14	25	24	22	20	18	14

TROPICAL DEPRESSION 04W

DTG(Z)	WRN NO.	LAT	LONG	WIND (KT)	POSITION ERRORS (NM) 00	12	24	36	48	72	WIND ERRORS (KT) 00	12	24	36	48	72
94051400		5.1N	161.0E	15												
94051406		5.2N	160.3E	15												
94051412		5.2N	159.6E	15												
94051418		5.2N	158.8E	15												
94051500		5.1N	157.9E	15												
94051506		5.1N	157.0E	15												
94051512		5.1N	156.1E	15												
94051518		5.2N	155.1E	15												
94051600		5.3N	154.1E	15												
94051606		5.4N	153.2E	15												

TROPICAL DEPRESSION 04W (CONTINUED)

94051612		5.7N	152.3E	15												
94051618		6.2N	151.3E	15												
94051700		6.6N	150.5E	15												
94051706		7.1N	149.2E	15												
94051712		7.7N	148.6E	15												
94051718		8.3N	147.9E	15												
94051800		9.0N	147.2E	15												
94051806		9.8N	146.5E	15												
94051812		10.3N	146.0E	15												
94051818		10.8N	145.9E	15												
94051900		11.0N	145.3E	15												
94051906		11.0N	144.7E	15												
94051912		11.0N	143.8E	15												
94051918		11.0N	142.7E	15												
94052000		10.7N	141.2E	15												
94052006		10.3N	140.4E	15												
94052012		9.6N	137.9E	15												
94052018		9.0N	136.7E	15												
94052100		8.5N	135.5E	15												
94052106		7.9N	134.5E	15												
94052112		7.6N	133.3E	15												
94052118		7.7N	132.2E	15												
94052200		7.9N	131.3E	15												
94052206		8.1N	130.8E	15												
94052212		8.3N	130.3E	15												
94052218		8.8N	129.7E	15												
94052300		9.2N	129.3E	15												
94052306		9.7N	128.7E	15												
94052312		10.2N	128.3E	20												
94052318		10.7N	127.6E	25												
94052400		11.1N	126.8E	25												
94052406	1	11.5N	124.8E	25	135	247	361	468	574		5	15	30	35	35	
94052412	2	11.9N	123.4E	30	101	186	272	383	486		0	15	20	30	35	
94052418	3	12.3N	121.9E	30	134	230	342	445	553		0	15	20	30	35	
94052500	4	12.7N	120.4E	25	65	84	146	209			0	0	5	10		
94052506	5	13.1N	118.9E	25	67	110	159	221			0	5	10	15		
94052512	6	13.6N	117.3E	25	5	34	82				0	5	5			
94052518	7	14.1N	115.7E	25	46	117	205				0	5	5			
94052600	8	14.6N	114.1E	25	35	110					5	5				
94052606	9	15.0N	112.5E	25	39	81					5	5				
94052612	10	15.4N	110.9E	25	47						5					
94052618	11	15.7N	109.3E	25	83						0					
94052700		16.0N	107.5E	20												
		AVERAGE			69	134	224	346	538		2	8	14	24	35	
		# CASES			11	9	7	5	3		11	9	7	5	3	

TROPICAL STORM RUSS (05W)

	WRN				POSITION ERRORS (NM)						WIND ERRORS (KT)					
DTG (Z)	NO.	LAT	LONG	WIND (KT)	00	12	24	36	48	72	00	12	24	36	48	72
94060206		19.0N	112.5E	20												
94060212		19.1N	112.8E	20												
94060218		19.2N	113.2E	20												
94060300		19.3N	113.6E	25												
94060306		19.4N	114.0E	25												
94060312		19.5N	114.5E	25												
94060318		19.7N	115.1E	25												
94060400		19.9N	115.7E	30												

TROPICAL STORM RUSS (05W) (CONTINUED)

94060406	1	20.1N	116.2E	30	20	45	117	249			-5	-10	-15	-15		
94060412	2	20.1N	116.7E	35	8	57	131	230	337		-5	-5	-10	-15	-25	
94060418	3	20.0N	117.0E	35	18	65	139	246	353		0	-10	-5	-20	-25	
94060500	4	20.0N	117.1E	40	0	66	159	295	440	643	-5	-5	-5	-15	-15	-20
94060506	5	20.0N	117.0E	45	16	87	208	349	476	661	-10	-5	-10	-15	-15	-20
94060512	6	19.9N	116.9E	45	8	61	138	224	271	340	0	0	-5	0	-5	-10
94060518	7	19.8N	116.6E	45	0	46	111	157	216	300	0	-5	-5	-5	-5	0
94060600	8	19.7N	116.1E	50	11	45	91	152	213	275	-5	-5	5	5	5	5
94060606	9	19.5N	115.5E	55	6	36	52	82	136	195	-10	-5	5	5	5	10
94060612	10	19.4N	114.8E	55	5	12	45	92	139	156	-5	5	5	5	-10	5
94060618	11	19.4N	113.9E	55	22	30	39	84	120		-5	0	0	-5	10	
94060700	12	19.5N	113.2E	50	0	18	53	88	96		0	0	0	-10	-5	
94060706	13	19.6N	112.6E	50	0	8	0	39	56		0	5	5	0	0	
94060712	14	19.7N	112.0E	50	18	17	42	39	28		0	5	-10	5	5	
94060718	15	20.0N	111.4E	50	28	60	77	71			5	5	0	0		
94060800	16	20.5N	110.8E	50	13	45	72	90			5	10	5	5		
94060806	17	21.0N	110.3E	50	16	30	48				5	5	5			
94060812	18	21.8N	110.0E	45	0	24	82				0	-5	-5			
94060818	19	22.5N	109.9E	35	8	53					0	0				
94060900	20	23.2N	110.1E	30	17	55					0	0				
94060906		23.7N	110.3E	25												
94060912		24.2N	110.8E	20												
		AVERAGE			11	44	90	156	222	368	3	5	6	8	10	10
		# CASES			20	20	18	16	13	7	20	20	18	16	13	7

TROPICAL STORM SHARON (06W)

	WRN				POSITION ERRORS (NM)						WIND ERRORS (KT)					
DTG (Z)	NO.	LAT	LONG	WIND (KT)	00	12	24	36	48	72	00	12	24	36	48	72
94061800		6.0N	152.0E	15												
94061806		6.2N	150.6E	15												
94061812		6.4N	149.2E	20												
94061818		6.6N	147.8E	20												
94061900		6.8N	146.3E	20												
94061906		7.0N	144.8E	20												
94061912		7.3N	143.3E	20												
94061918		7.7N	141.8E	20												
94062000		8.2N	140.3E	20												
94062006		8.8N	138.9E	20												
94062012		9.5N	137.5E	20												
94062018		10.2N	136.1E	20												
94062100		10.8N	134.7E	20												
94062106		11.3N	133.3E	25												
94062112		11.8N	131.9E	25												
94062118	1	12.2N	130.4E	25	48	78	164	263			0	5	5	-5		
94062200		12.6N	128.9E	20												
94062206	2	13.0N	127.2E	20	36	54					0	0				
94062212		13.5N	125.3E	20												
94062218	3	14.1N	123.3E	20	21	49	104	159	216		0	-10	-15	-5	5	
94062300	4	14.9N	121.3E	25	58	74	122	169	217		-5	-10	-10	5	15	
94062306	5	15.7N	119.4E	30	33	77	110	156	188		-10	-15	-5	5	15	
94062312	6	16.4N	117.6E	35	23	56	120	149			0	-5	10	20		
94062318	7	17.3N	116.1E	45	46	82	123	143			0	5	20	25		
94062400	8	18.2N	114.9E	45	43	81	81				5	15	35			
94062406	9	19.1N	113.9E	45	25	18	30				5	10	15			
94062412	10	20.0N	113.1E	40	39	60					10	20				
94062418	11	20.9N	112.4E	40	71	75					5	10				
94062500	12	21.7N	111.8E	30	101						5					

TROPICAL STORM SHARON (06W) (CONTINUED)

94062506	13	22.6N	111.3E	25	45					5						
94062512		23.6N	110.9E	20												
94062518		24.8N	110.6E	15												
			AVERAGE		46	64	107	174	207		4	10	14	11	12	
			# CASES		13	11	8	6	3		13	11	8	6	3	

TROPICAL DEPRESSION 07W

	WRN				POSITION ERRORS (NM)						WIND ERRORS (KT)					
DTG (Z)	NO.	LAT	LONG	WIND (KT)	00	12	24	36	48	72	00	12	24	36	48	72
94062912		16.6N	136.6E	15												
94062918		16.9N	135.1E	15												
94063000		17.2N	133.6E	15												
94063006		17.5N	132.1E	15												
94063012		17.8N	130.6E	15												
94063018		18.1N	129.1E	15												
94070100		18.3N	127.6E	20												
94070106		18.5N	126.1E	20												
94070112		18.7N	124.6E	20												
94070118		18.8N	123.1E	20												
94070200		18.9N	121.6E	20												
94070206		19.0N	120.1E	20												
94070212		19.1N	118.6E	25												
94070218		19.2N	117.1E	25												
94070300	1	19.4N	115.7E	25	45	47	75	147			0	0	5	10		
94070306	2	19.6N	114.5E	25	67	95	173	266			0	0	10	15		
94070312	3	19.8N	113.5E	30	35	39	64				0	5	0			
94070318	4	20.0N	112.6E	30	34	81	116				0	5	5			
94070400	5	20.5N	112.0E	30	8	20					0	0				
94070406	6	21.1N	111.6E	30	8	28					0	5				
94070412	7	21.6N	111.3E	30	0						0					
94070418		22.2N	111.1E	25												
94070500		22.8N	110.9E	20												
94070506		23.4N	110.7E	15												
			AVERAGE		29	52	107	207			0	3	5	13		
			# CASES		7	6	4	2			7	6	4	2		

TYPHOON TIM (08W)

	WRN				POSITION ERRORS (NM)						WIND ERRORS (KT)					
DTG (Z)	NO.	LAT	LONG	WIND (KT)	00	12	24	36	48	72	00	12	24	36	48	72
94070500		9.0N	139.0E	15												
94070506		9.5N	137.9E	15												
94070512		10.0N	136.8E	20												
94070518		10.5N	135.7E	20												
94070600		11.0N	134.6E	20												
94070606		11.5N	133.6E	20												
94070612		12.0N	132.7E	25												
94070618		12.6N	132.0E	25												
94070700	1	13.2N	131.4E	25	35	13	13	18	12	102	0	-5	-10	-20	-35	-60
94070706	2	13.8N	130.9E	30	57	54	62	95	141	299	0	-5	-10	-20	-45	-65
94070712	3	14.4N	130.5E	35	34	78	92	114	124	156	-5	-10	-20	-35	-50	-35
94070718	4	15.0N	130.1E	40	42	58	72	79	82	234	-5	-15	-25	-45	-45	-5
94070800	5	15.6N	129.7E	45	13	29	65	84	104	290	-10	-20	-35	-50	-40	35
94070806	6	16.1N	129.2E	55	0	13	18	34	84	272	-5	-10	-25	-30	-20	45
94070812	7	16.7N	128.6E	65	12	36	69	58	114	312	-10	-20	-35	-25	-20	85

TYPHOON TIM (08W) (CONTINUED)

94070818	8	17.3N	127.9E	75	18	41	75	127	211		-10	-30	-35	-30	10	
94070900	9	17.9N	127.0E	90	11	20	24	109	202		-15	-25	-20	-15	50	
94070906	10	18.5N	126.2E	105	12	25	66	150	168		-5	-5	0	25	65	
94070912	11	19.2N	125.3E	115	13	38	115	191	233		0	5	10	70	100	
94070918	12	19.9N	124.4E	120	5	21	126	195			0	5	35	80		
94071000	13	20.8N	123.5E	120	18	68	135	178			5	0	60	75		
94071006	14	21.9N	122.5E	125	6	48	100				0	25	55			
94071012	15	23.2N	121.5E	125	17	107	213				0	50	70			
94071018	16	24.4N	120.1E	100	12	105					15	45				
94071100	17	25.2N	118.3E	65	21	52					10	5				
94071106	18	26.0N	116.8E	55	6						0					
94071112		26.9N	115.4E	35												
94071118		27.6N	114.1E	20												
94071200		28.2N	112.8E	15												
		AVERAGE			19	48	83	111	135	238	5	16	30	40	44	47
		# CASES			18	17	15	13	11	7	18	17	15	13	11	7

TROPICAL STORM VANESSA (09W)

	WRN				POSITION ERRORS (NM)						WIND ERRORS (KT)					
DTG (Z)	NO.	LAT	LONG	WIND (KT)	00	12	24	36	48	72	00	12	24	36	48	72
94070800		15.7N	117.0E	20												
94070806		15.9N	116.6E	20												
94070812		16.1N	116.2E	25												
94070818		16.1N	115.8E	30												
94070900	1	16.1N	115.6E	35	0	41	130	255	412		0	5	5	15	25	
94070906	2	16.0N	115.4E	35	6	54	141	254	388		0	5	0	15	20	
94070912	3	15.8N	115.2E	35	8	57	185	343			0	0	10	20		
94070918	4	15.3N	115.3E	35	63	236	414	588			0	-5	15	25		
94071000	5	15.1N	116.2E	40	58	47	135				-5	5	15			
94071006	6	15.5N	117.5E	45	21	92	222				0	15	20			
94071012	7	16.5N	118.7E	35	18	122					10	20				
94071018	8	17.7N	119.7E	30	23	47					15	15				
94071100	9	19.4N	120.5E	25	96						15					
94071106	10	21.0N	121.0E	20	55						10					
		AVERAGE			35	87	205	360	400		6	9	11	19	23	
		# CASES			10	8	6	4	2		10	8	6	4	2	

SUPER TYPHOON WALT (10W)

	WRN				POSITION ERRORS (NM)						WIND ERRORS (KT)					
DTG (Z)	NO.	LAT	LONG	WIND (KT)	00	12	24	36	48	72	00	12	24	36	48	72
94071100		5.4N	138.6E	15												
94071106		5.7N	137.6E	15												
94071112		6.0N	136.6E	15												
94071118		6.3N	135.6E	20												
94071200		6.6N	134.6E	20												
94071206		7.0N	133.6E	20												
94071212		7.4N	132.7E	20												
94071218		7.9N	131.8E	20												
94071300		8.4N	130.9E	20												
94071306		8.9N	130.2E	20												
94071312		9.4N	129.5E	20												
94071318		9.9N	128.9E	20												
94071400		10.4N	128.3E	20												
94071406		10.9N	127.7E	20												
94071412	1	11.5N	127.1E	25	18	11	43	107			0	0	0	-5		

SUPER TYPHOON WALT (10W) (CONTINUED)

94071418	2	12.1N	126.5E	25	48	49	8	112			0	0	0	-10		
94071500	3	12.7N	125.9E	25	30	11	68	160			0	0	-5	-15		
94071506	4	13.3N	125.3E	25	51	49	138	231			0	0	-10	-25		
94071512	5	13.8N	124.8E	30	48	92	191	295			-5	-5	-15	-30		
94071518	6	14.5N	124.6E	30	44	139	225	318			0	-10	-25	-40		
94071600	7	15.0N	125.0E	35	23	17	8	13	62	156	0	-5	-10	-20	-25	-55
94071606	8	15.2N	125.5E	40	18	33	36	82	128	209	-5	-10	-15	-25	-30	-75
94071612	9	15.4N	126.0E	45	29	75	132	203	279	429	-5	-10	-20	-25	-35	-70
94071618	10	15.6N	126.6E	50	34	74	141	224	288	448	-5	-10	-15	-25	-40	-70
94071700	11	15.9N	127.2E	55	21	54	109	159	194	320	-10	-10	-10	-15	-30	-40
94071706	12	16.2N	127.8E	60	18	54	98	123	143	174	-10	-10	-10	-20	-40	-30
94071712	13	16.6N	128.6E	65	23	78	139	192	241	322	-10	-15	-20	-30	-40	-25
94071718	14	17.2N	129.4E	70	45	98	167	234	290	386	-10	-15	-30	-50	-40	-15
94071800	15	17.9N	130.2E	75	8	5	13	13	52	157	-5	-20	-35	-50	-40	-10
94071806	16	18.6N	131.0E	80	12	28	61	74	147	195	5	-15	-30	-25	-30	-5
94071812	17	19.4N	131.5E	90	21	45	77	149	217	229	0	-15	-25	-25	-25	0
94071818	18	20.1N	132.0E	100	25	64	111	169	207	184	-10	-35	-25	-20	-15	10
94071900	19	20.8N	132.6E	110	22	65	115	154	166	141	-15	-35	-25	-15	-10	15
94071906	20	21.6N	133.2E	130	28	78	114	151	163	143	0	0	5	0	5	20
94071912	21	22.4N	133.9E	130	22	47	103	153	161	212	0	0	10	5	10	25
94071918	22	23.1N	134.7E	130	16	37	48	70	104	211	0	5	20	15	20	25
94072000	23	23.8N	135.5E	130	5	12	35	76	142	290	0	10	20	25	25	10
94072006	24	24.6N	136.4E	125	8	12	43	87	180	317	0	15	25	30	30	20
94072012	25	25.4N	137.1E	120	5	27	77	145	243	339	5	20	30	35	35	20
94072018	26	26.2N	137.6E	110	16	69	129	228	328	340	0	10	15	20	20	15
94072100	27	26.9N	137.9E	105	22	72	148	253	327	338	0	5	15	20	15	-10
94072106	28	27.6N	137.8E	95	21	58	138	222	253	221	0	10	20	20	20	-5
94072112	29	28.3N	137.5E	90	15	63	145	199	194	181	0	15	20	15	15	-5
94072118	30	28.9N	137.1E	80	33	85	142	153	164	227	0	0	-5	-5	-10	-10
94072200	31	29.2N	136.3E	75	12	41	62	39	57	228	0	-5	-15	-15	-15	-15
94072206	32	29.4N	135.4E	70	0	15	26	78	154	267	0	0	-5	-15	-10	-15
94072212	33	29.5N	134.4E	65	5	5	62	149	241	299	-5	-10	-15	-20	-20	-10
94072218	34	29.6N	133.5E	65	7	36	116	202	283	280	-10	-10	-15	-20	-30	-15
94072300	35	29.7N	132.8E	65	18	43	123	201	275	235	-10	-5	-5	-5	-5	10
94072306	36	29.9N	132.4E	60	31	95	163	241	284	233	-5	-5	0	-5	0	15
94072312	37	30.1N	132.3E	60	33	98	178	248	267	260	-5	-5	0	-5	10	20
94072318	38	30.4N	132.4E	60	30	70	135	167	168	154	-5	0	-5	0	10	15
94072400	39	30.7N	132.5E	60	5	11	39	74	112	149	-5	0	0	15	15	5
94072406	40	31.0N	132.7E	55	18	36	66	116	145		0	0	5	20	20	
94072412	41	31.3N	132.9E	55	19	41	120	192	228		0	0	15	20	20	
94072418	42	31.7N	133.1E	55	31	83	158	216	239		0	5	20	25	20	
94072500	43	32.2N	133.1E	55	7	50	102	165	255		0	5	0	0	-5	
94072506	44	32.8N	132.6E	50	18	57	131	213			0	5	0	0		
94072512	45	33.4N	131.8E	40	31	99	171	239			0	0	5	0		
94072518	46	33.7N	130.9E	35	66	155	240				0	-5	-5			
94072600	47	33.9N	130.1E	35	7	14	16				0	5	0			
94072606	48	34.0N	129.4E	30	13	13					0	0				
94072612	49	34.0N	128.8E	25	11	18					0	-5				
94072618	50	34.1N	128.2E	25	12						0					
94072700		34.1N	127.7E	25												
94072706		34.0N	127.3E	20												
94072712		33.9N	127.1E	20												
94072718		33.8N	127.0E	20												
94072800		33.7N	127.3E	15												
94072806		33.8N	127.8E	15												
		AVERAGE			23	53	105	162	200	251	3	8	13	18	21	21
		# CASES			50	49	47	45	37	33	50	49	47	45	37	33

TROPICAL STORM YUNYA (11W)

DTG(Z)	WRN NO.	LAT	LONG	WIND (KT)	POSITION ERRORS(NM) 00	12	24	36	48	72	WIND ERRORS(KT) 00	12	24	36	48	72
94071606		13.8N	114.5E	15												
94071612		14.1N	115.2E	15												
94071618		14.5N	115.8E	20												
94071700		14.9N	116.4E	20												
94071706		15.3N	116.9E	20												
94071712		15.6N	117.4E	25												
94071718		15.9N	117.9E	25												
94071800	1	16.2N	118.4E	30	33	71	128	198	280	461	-5	-10	-10	10	10	10
94071806	2	16.5N	118.9E	35	25	58	120	187	266	446	-10	-15	0	-5	0	15
94071812	3	16.9N	119.3E	40	29	78	124	187	260	462	-10	-15	-10	-15	-5	15
94071818	4	17.4N	119.8E	45	37	120	225	347	471		-5	10	15	30	35	
94071900	5	18.0N	120.4E	45	33	133	233	371	500		0	15	10	15	30	
94071906	6	18.6N	121.2E	35	18	96	191	276	368		10	5	15	25	35	
94071912	7	19.1N	122.2E	35	73	189	288	373	446		10	5	10	20	30	
94071918	8	19.5N	123.4E	40	92	167	241	310			10	20	30	40		
94072000	9	19.8N	124.6E	40	5	56	119	153			0	5	15	20		
94072006	10	20.0N	125.9E	35	34	66	87				0	5	10			
94072012	11	20.1N	127.2E	35	53	105	150				0	5	10			
94072018	12	20.2N	128.5E	30	30	12					0	5				
94072100	13	20.3N	129.8E	30	13	41					0	5				
94072112	14	20.6N	132.4E	25	5						0					
94072118		20.8N	133.5E	20												
		AVERAGE			35	92	174	267	371	457	4	9	12	20	21	13
		# CASES			14	13	11	9	7	3	14	13	11	9	7	3

TYPHOON ZEKE (12W)

DTG(Z)	WRN NO.	LAT	LONG	WIND (KT)	POSITION ERRORS(NM) 00	12	24	36	48	72	WIND ERRORS(KT) 00	12	24	36	48	72
94071000		7.9N	140.5E	10												
94071006		8.0N	140.0E	10												
94071012		8.1N	139.5E	10												
94071018		8.2N	139.0E	10												
94071100		8.3N	138.5E	10												
94071106		8.4N	138.0E	15												
94071112		8.5N	137.5E	15												
94071118		8.6N	137.0E	15												
94071200		8.7N	136.5E	15												
94071206		8.8N	136.0E	15												
94071212		8.9N	135.5E	15												
94071218		9.1N	135.0E	15												
94071300		9.3N	134.5E	15												
94071306		9.6N	134.1E	15												
94071312		9.9N	133.7E	15												
94071318		10.2N	133.3E	15												
94071400		10.6N	133.0E	15												
94071406		11.1N	132.8E	15												
94071412		11.8N	132.9E	15												
94071418		12.6N	133.1E	15												
94071500		13.5N	133.2E	15												
94071506		14.3N	133.4E	15												
94071512		15.1N	133.6E	15												
94071518		15.9N	133.8E	15												
94071600		16.7N	134.0E	15												
94071606		17.5N	134.3E	20												

TYPHOON ZEKE (12W) (CONTINUED)

94071612		18.4N	134.6E	20												
94071618		19.4N	135.1E	20												
94071700		20.5N	135.6E	20												
94071706		21.6N	136.2E	20												
94071712		22.6N	137.1E	20												
94071718		23.5N	138.2E	20												
94071800		24.4N	139.7E	25												
94071806	1	25.1N	141.4E	25	118	230	301	337	390	480	0	10	10	15	15	20
94071812	2	25.6N	143.0E	25	149	190	199	198	177	159	0	0	0	5	5	-5
94071818	3	26.1N	144.3E	25	119	105	73	64	144	264	0	0	0	0	5	-10
94071900	4	26.4N	145.5E	30	68	61	141	242			-5	-10	-10	-10		
94071906	5	26.6N	146.5E	30	24	134	196	284			0	-5	-10	-10		
94071912	6	26.7N	147.4E	35	43	105	190	255			-10	-10	-15	-20		
94071918	7	26.7N	148.2E	35	24	24	70	120	138	145	0	0	5	-5	-20	-35
94072000	8	26.8N	148.9E	35	12	26	41	41	44	87	5	5	0	-10	-25	-35
94072006	9	26.8N	149.4E	40	17	5	12	29	53	141	0	0	0	-15	-30	-35
94072012	10	26.8N	149.8E	40	27	48	36	24	19		0	-5	-10	-25	-35	
94072018	11	26.8N	150.4E	40	44	65	34	10	51		-5	-10	-20	-35	-30	
94072100	12	26.9N	150.9E	45	16	30	60	43	31		-10	-15	-25	-30	-30	
94072106	13	27.0N	151.5E	45	20	20	43	23	20		-5	-15	-25	-25	-30	
94072112	14	27.2N	152.3E	50	44	53	48	49	39		-15	-25	-35	-35	-35	
94072118	15	27.5N	153.2E	55	60	96	78	36	34		-20	-30	-30	-35	-35	
94072200	16	27.9N	154.0E	60	12	44	113	163	215		-15	-25	-25	-25	-25	
94072206	17	28.6N	154.5E	65	15	36	70	121	164		0	5	-5	-10	-15	
94072212	18	29.3N	154.6E	65	12	13	30	79	132		-5	-5	-5	-15	-15	
94072218	19	30.1N	154.6E	60	6	18	43	83			0	-5	-5	-10		
94072300	20	31.1N	154.6E	60	12	73	99	114			0	0	-5	-5		
94072306	21	32.2N	154.5E	60	12	46	81				0	0	0			
94072312	22	33.4N	154.3E	55	17	35	55				5	0	0			
94072318	23	34.7N	154.2E	55	30	43					0	0				
94072400	24	36.1N	154.2E	55	24	54					0	0				
94072406	25	37.6N	154.5E	50	12						5					
94072412	26	39.0N	155.5E	50	18						5					
94072418		40.2N	157.6E	50												
94072500		41.5N	160.3E	45												
94072506		43.6N	163.6E	45												
94072512		46.6N	167.2E	40												
		AVERAGE			37	65	92	116	111	213	4	8	11	17	23	23
		# CASES			26	24	22	20	15	6	26	24	22	20	15	6

TROPICAL DEPRESSION (13W)

	WRN				POSITION ERRORS (NM)						WIND ERRORS (KT)					
DTG (Z)	NO.	LAT	LONG	WIND (KT)	00	12	24	36	48	72	00	12	24	36	48	72
94072312		12.7N	148.4E	15												
94072318		12.8N	148.2E	15												
94072400		12.9N	148.0E	15												
94072406		13.1N	147.8E	20												
94072412		13.3N	147.6E	20												
94072418		13.7N	147.3E	20												
94072500		14.4N	146.9E	20												
94072506	1	15.6N	146.3E	25	104	217					5	10				
94072512	2	17.2N	146.2E	25	111	211					5	15				
94072518	3	19.0N	146.7E	25	145						5					
94072600	4	20.7N	147.0E	20	169						5					
		AVERAGE			133	214					5	13				
		# CASES			4	2					4	2				

TROPICAL STORM BRENDAN (14W)

DTG(Z)	WRN NO.	LAT	LONG	WIND (KT)	POSITION ERRORS(NM) 00	12	24	36	48	72	WIND ERRORS(KT) 00	12	24	36	48	72
94072506		13.9N	130.6E	10												
94072512		14.0N	130.0E	10												
94072518		14.1N	129.4E	15												
94072600		14.1N	128.8E	15												
94072606		14.2N	128.2E	15												
94072612		14.5N	127.7E	15												
94072618		14.9N	127.2E	15												
94072700		15.3N	126.7E	15												
94072706		15.7N	126.3E	20												
94072712		16.2N	126.0E	20												
94072718		16.7N	125.9E	20												
94072800		17.2N	126.0E	20												
94072806		17.7N	126.2E	20												
94072812		18.2N	126.6E	20												
94072818		18.8N	126.9E	25												
94072900	1	19.4N	127.3E	30	66	71	94	127			-5	-5	0	-5		
94072906		20.2N	127.8E	30												
94072912	2	21.2N	128.1E	30	34	37	84	172	251	356	-5	-5	-5	-5	-5	20
94072918	3	22.2N	128.4E	30	47	31	121	158	233	186	0	5	5	-5	-15	-10
94073000	4	23.3N	128.6E	30	13	90	97	125	141		0	0	0	-10	-10	
94073006	5	24.4N	128.7E	30	31	53	101	123	98		0	0	-5	-10	0	
94073012	6	25.6N	128.3E	35	34	87	119	144	170		0	0	-10	0	10	
94073018	7	26.8N	127.3E	35	32	82	144	181	248		0	-10	-10	5	5	
94073100	8	28.3N	126.5E	40	96	96	140	179			-5	-15	-5	10		
94073106	9	29.9N	125.9E	45	63	127	190	277			-10	-10	0	10		
94073112	10	31.7N	125.5E	50	18	42	108				-10	0	0			
94073118	11	33.5N	125.5E	50	13	42	82				-5	5	0			
94080100	12	35.3N	126.1E	45	27	113					0	0				
94080106	13	36.8N	127.6E	40	25	61					0	0				
94080112	14	38.0N	129.6E	35	12						0					
94080118	15	39.0N	131.9E	35	15						0					
94080200		39.9N	134.5E	35												
94080206		40.4N	137.3E	40												
94080212		40.7N	139.9E	45												
94080218		40.9N	142.2E	35												
94080300		40.8N	144.2E	30												
94080306		40.8N	145.9E	25												
		AVERAGE			35	72	117	166	191	272	3	4	4	7	8	15
		# CASES			15	13	11	9	6	2	15	13	11	9	6	2

TROPICAL STORM AMY (15W)

DTG(Z)	WRN NO.	LAT	LONG	WIND (KT)	POSITION ERRORS(NM) 00	12	24	36	48	72	WIND ERRORS(KT) 00	12	24	36	48	72
94072700		20.4N	112.0E	15												
94072706		20.5N	111.4E	15												
94072712		20.6N	110.8E	15												
94072718		20.5N	110.3E	15												
94072800		20.4N	109.8E	20												
94072806		20.2N	109.3E	20												
94072812		19.9N	108.8E	25												
94072818		19.5N	108.4E	25												
94072900		19.2N	108.2E	30												
94072906	1	19.0N	108.0E	30	5	26	36	45			5	5	0	10		
94072912	2	18.9N	107.8E	30	5	6	16	41			5	0	5	10		

TROPICAL STORM AMY (15W) (CONTINUED)

DTG(Z)	WRN NO.	LAT	LONG	WIND (KT)	POSITION ERRORS (NM) 00	12	24	36	48	72	WIND ERRORS (KT) 00	12	24	36	48	72
94072918	3	18.8N	107.6E	35	17	54	94				0	0	10			
94073000	4	18.9N	107.3E	40	23	49	95				-5	5	15			
94073006	5	19.1N	106.9E	40	43	79					0	10				
94073012	6	19.3N	106.5E	35	33	46					0	10				
94073018	7	19.5N	106.0E	30	30						5					
94073100	8	19.7N	105.4E	25	57						5					
94073106		19.8N	104.7E	15												
94073112		19.8N	103.9E	10												
		AVERAGE			27	44	61	43			3	5	8	10		
		# CASES			8	6	4	2			8	6	4	2		

TROPICAL STORM CAITLIN (16W)

DTG(Z)	WRN NO.	LAT	LONG	WIND (KT)	POSITION ERRORS (NM) 00	12	24	36	48	72	WIND ERRORS (KT) 00	12	24	36	48	72
94072900		15.5N	143.5E	10												
94072906		16.0N	142.5E	10												
94072912		16.5N	141.5E	10												
94072918		17.0N	140.5E	15												
94073000		17.3N	139.5E	15												
94073006		17.6N	138.5E	15												
94073012		17.9N	137.5E	15												
94073018		18.1N	136.5E	15												
94073100		18.3N	135.5E	15												
94073106		18.5N	134.5E	15												
94073112		18.7N	133.5E	20												
94073118		18.8N	132.5E	20												
94080100		18.9N	131.5E	20												
94080106		19.0N	130.5E	20												
94080112		19.2N	129.5E	20												
94080118		19.4N	128.5E	25												
94080200		19.6N	127.5E	25												
94080206	1	19.9N	126.5E	30	33	71	122	179	198		-5	-5	-15	0	25	
94080212	2	20.4N	125.4E	35	6	16	73	114	154		-5	-10	0	10	40	
94080218	3	21.0N	124.3E	40	13	60	95	118	182		-5	-15	0	25	40	
94080300	4	21.7N	123.1E	50	26	135	237	335			-10	-5	0	25		
94080306	5	22.5N	121.9E	60	26	89	130	207			-10	5	25	35		
94080312	6	23.3N	120.6E	50	8	29	32				-5	-5	0			
94080318	7	23.7N	119.2E	55	21	66	39				-10	-10	-5			
94080400	8	24.0N	117.8E	50	45	109					-10	-5				
94080406	9	24.4N	116.6E	40	24	73					-10	0				
94080412		25.2N	115.5E	30												
94080418		26.1N	114.3E	25												
94080500		27.0N	113.0E	20												
		AVERAGE			23	72	105	191	178		8	7	6	19	35	
		# CASES			9	9	7	5	3		9	9	7	5	3	

SUPER TYPHOON DOUG (17W)

DTG(Z)	WRN NO.	LAT	LONG	WIND (KT)	POSITION ERRORS (NM) 00	12	24	36	48	72	WIND ERRORS (KT) 00	12	24	36	48	72
94073000		12.0N	151.7E	15												
94073006		12.3N	151.1E	15												
94073012		12.6N	150.5E	15												
94073018		12.8N	149.8E	15												
94073100		13.0N	149.1E	15												
94073106		13.2N	148.4E	15												

SUPER TYPHOON DOUG (17W) (CONTINUED)

94073112		13.4N	147.7E	15												
94073118		13.7N	146.9E	15												
94080100		14.0N	146.0E	15												
94080106		14.3N	145.1E	15												
94080112		14.6N	144.2E	15												
94080118		14.9N	143.2E	20												
94080200		15.1N	142.3E	20												
94080206		15.2N	141.5E	25												
94080212		15.3N	140.8E	30												
94080218	1	15.4N	140.2E	35	13	11	52	96	128	189	-5	-10	-20	-30	-40	-50
94080300	2	15.4N	139.5E	40	8	58	140	204	266	458	0	-10	-25	-35	-40	-55
94080306	3	15.3N	138.8E	45	5	39	81	126	185	349	0	-15	-30	-40	-50	-60
94080312	4	15.2N	138.0E	55	13	42	83	121	161	222	0	-5	-5	-15	-20	-10
94080318	5	15.1N	137.1E	65	23	47	80	108	135	165	0	0	0	-5	-5	-5
94080400	6	15.0N	136.2E	75	8	18	42	60	75	88	5	-5	-10	-10	-5	0
94080406	7	15.0N	135.2E	85	8	5	18	46	69	81	5	0	-10	-5	-5	5
94080412	8	15.0N	134.2E	95	13	29	29	18	53	82	-15	-20	-15	-5	0	0
94080418	9	15.1N	133.2E	105	0	13	21	30	37	50	-20	-25	-20	-5	0	-10
94080500	10	15.3N	132.1E	115	11	58	104	111	106	71	-10	-15	-15	-5	5	0
94080506	11	15.7N	130.9E	125	13	49	72	99	87	76	0	-5	0	5	0	15
94080512	12	16.2N	129.7E	130	13	37	36	42	42	39	-5	-5	-5	5	0	15
94080518	13	16.8N	128.5E	140	5	20	28	33	21	101	-5	0	5	10	0	25
94080600	14	17.5N	127.4E	140	8	26	39	29	20	132	0	0	10	10	10	40
94080606	15	18.2N	126.4E	140	13	39	61	54	40	72	0	5	15	5	10	25
94080612	16	19.0N	125.4E	140	16	30	45	31	32	61	0	10	10	15	25	25
94080618	17	20.0N	124.6E	135	6	24	32	12	28	109	5	5	-5	5	15	15
94080700	18	21.0N	123.9E	130	6	18	18	24	70	181	5	0	0	15	20	15
94080706	19	22.2N	123.4E	125	13	11	12	46	87	138	5	-10	5	15	15	5
94080712	20	23.3N	122.9E	125	18	48	80	132	177	328	0	0	20	25	15	10
94080718	21	24.4N	122.4E	125	26	62	135	190	204	325	-30	-10	-5	0	-5	-5
94080800	22	25.5N	122.1E	115	45	87	167	191	206	351	-35	-10	5	0	-5	-5
94080806	23	26.5N	121.8E	100	8	53	83	80	31	137	-20	0	5	0	5	0
94080812	24	27.5N	122.0E	85	24	71	115	157	187	209	-10	0	-10	-10	-5	-5
94080818	25	28.4N	122.4E	75	39	86	147	197	234	263	-5	-5	-15	-10	-10	-5
94080900	26	29.2N	122.8E	65	75	136	192	243	276	295	-10	-15	-15	-10	-10	-5
94080906	27	30.0N	123.2E	65	23	49	102	114	96	90	-10	-15	-10	-10	-10	-5
94080912	28	30.9N	123.5E	65	7	44	72	101	147	81	-10	-10	-5	-5	-5	0
94080918	29	31.7N	123.7E	65	16	32	30	59	109	84	-5	0	0	0	0	0
94081000	30	32.5N	123.8E	60	27	51	112	186	229	350	0	5	5	5	5	5
94081006	31	33.2N	123.9E	55	26	66	141	204	270	477	5	5	5	5	5	15
94081012	32	33.7N	124.1E	50	28	87	151	223	330		-5	0	0	0	5	
94081018	33	34.0N	124.6E	50	14	41	77	157	291		-5	-5	0	0	5	
94081100	34	34.2N	125.0E	45	7	17	87	238	400		0	5	5	5	5	
94081106	35	34.3N	125.3E	45	19	73	221	368	430		-5	-5	-5	-5	10	
94081112	36	34.3N	125.5E	40	25	86	249	402			-5	0	0	0		
94081118	37	34.2N	125.3E	40	64	185	341	489			-5	-5	-5	10		
94081200	38	34.0N	124.6E	35	19	104	175				0	0	0			
94081206	39	33.5N	123.5E	35	7	23	90				0	0	10			
94081212	40	32.9N	122.3E	30	11	19					0	5				
94081218	41	32.3N	121.1E	30	13	64					0	10				
94081300	42	31.7N	119.9E	25	0						0					
			AVERAGE		18	50	97	126	143	169	6	6	8	9	11	14
			# CASES		42	41	39	37	35	31	42	41	39	37	35	31

TYPHOON ELLIE (18W)

DTG(Z)	WRN NO.	LAT	LONG	WIND (KT)	POSITION ERRORS(NM) 00	12	24	36	48	72	WIND ERRORS(KT) 00	12	24	36	48	72
94080300		30.3N	148.7E	15												
94080306		30.1N	148.5E	15												
94080312		30.0N	148.3E	15												
94080318		29.8N	148.1E	15												
94080400		29.7N	147.9E	15												
94080406		29.5N	147.7E	15												
94080412		29.3N	147.5E	15												
94080418		29.1N	147.3E	15												
94080500		28.9N	147.2E	20												
94080506		28.7N	147.0E	20												
94080512		28.5N	146.9E	20												
94080518		28.3N	146.8E	20												
94080600		28.0N	146.6E	25												
94080606		27.4N	146.5E	25												
94080612		26.8N	146.5E	25												
94080618		26.3N	146.3E	25												
94080700		25.9N	146.1E	30												
94080706		25.6N	145.8E	30												
94080712		25.4N	145.3E	30												
94080718		25.2N	144.8E	30												
94080800	1	25.1N	144.3E	35	45	64	84	120			-10	-15	-20	-25		
94080806		25.0N	143.6E	35												
94080812	2	24.9N	142.9E	40	29	81	146	230	363	413	0	0	0	0	-5	-20
94080818	3	24.8N	142.2E	45	16	45	97	216	336	400	0	5	10	10	5	-10
94080900	4	24.6N	141.5E	50	24	64	100	133	210	300	-5	0	5	5	0	-10
94080906	5	24.4N	140.7E	50	12	42	119	214	289	236	-5	0	5	5	0	-10
94080912	6	24.1N	139.9E	55	32	77	204	271	284	216	0	5	5	5	0	-10
94080918	7	23.9N	139.2E	55	31	93	175	218	209	183	0	5	5	5	0	-10
94081000	8	23.5N	138.7E	60	24	121	203	245	241	228	-5	0	0	0	0	-10
94081006	9	23.1N	138.7E	60	28	93	151	208	258	331	-5	0	0	0	5	0
94081012	10	23.0N	138.9E	65	29	65	156	266	335	380	-10	-5	-5	0	0	5
94081018	11	23.4N	139.0E	65	21	107	212	307	392	461	-10	-5	-5	0	0	5
94081100	12	24.1N	138.9E	70	13	56	109	144	170	203	-10	-10	-5	-5	0	10
94081106	13	24.9N	138.3E	70	8	36	80	103	135	176	-5	-5	0	0	5	10
94081112	14	25.7N	137.5E	75	5	20	37	64	85	113	-10	-5	-5	0	10	15
94081118	15	26.5N	136.5E	75	12	26	63	106	157	218	-10	-5	-5	0	0	-5
94081200	16	27.3N	135.3E	75	5	17	56	104	169	228	-5	-5	0	0	-5	-15
94081206	17	28.0N	134.1E	75	0	15	26	65	136	219	-5	-5	0	0	-5	-10
94081212	18	28.7N	132.8E	80	5	36	72	116	160	202	-10	-5	5	5	0	-10
94081218	19	29.4N	131.4E	80	7	11	62	148	226	171	-10	-5	0	0	-5	-5
94081300	20	30.0N	130.0E	80	0	19	61	124	171	141	-5	0	5	0	-10	-5
94081306	21	30.7N	128.6E	80	0	23	80	127	214	367	-5	0	0	-5	-10	5
94081312	22	31.2N	127.2E	75	13	54	102	133	177	206	0	5	5	-5	-10	15
94081318	23	31.7N	125.8E	75	5	43	96	158	229		-5	-5	-5	-5	-10	
94081400	24	32.0N	124.5E	70	17	47	96	138	232		0	5	0	-5	-5	
94081406	25	32.3N	123.4E	70	6	15	45	48	119		0	0	0	-5	5	
94081412	26	32.9N	122.6E	65	7	29	37	69	113		5	0	0	5	15	
94081418	27	33.5N	122.1E	65	5	27	26	27			0	0	0	10		
94081500	28	34.3N	121.9E	65	30	92	145	196			0	-5	5	20		
94081506	29	35.3N	122.0E	60	35	66	103				5	0	15			
94081512	30	36.5N	122.1E	60	28	65	175				5	10	20			
94081518	31	37.9N	122.3E	55	15	80					0	10				
94081600	32	39.5N	122.6E	45	51	118					5	20				
94081606	33	41.4N	123.2E	35	36						10					
94081612		43.5N	124.7E	25												

TYPHOON ELLIE (18W) (CONTINED)

AVERAGE	18	55	104	154	217	257	5	5	5	4	4	9
# CASES	33	32	30	28	25	21	33	32	30	28	25	21

TROPICAL STORM LI (08E)

	WRN				POSITION ERRORS (NM)						WIND ERRORS (KT)					
DTG (Z)	NO.	LAT	LONG	WIND (KT)	00	12	24	36	48	72	00	12	24	36	48	72
94073018		11.4N	120.4W	25												
94073100		11.7N	121.4W	25												
94073106		12.1N	122.6W	25												
94073112		12.5N	123.8W	25												
94073118		13.0N	125.3W	25												
94080100		12.9N	127.0W	25												
94080106		12.7N	128.7W	25												
94080112		12.6N	130.3W	25												
94080118		12.5N	132.0W	25												
94080200		12.4N	133.6W	25												
94080206		12.2N	135.0W	25												
94080212		12.1N	136.5W	25												
94080218		11.7N	137.8W	30												
94080300		11.3N	139.1W	30												
94080306		11.1N	140.0W	25												
94080312		11.0N	140.8W	30												
94080318		10.9N	142.0W	25												
94080400		10.7N	143.5W	25												
94080406		10.5N	145.1W	25												
94080412		10.3N	146.4W	25												
94080418		10.1N	147.8W	25												
94080500		9.7N	149.2W	25												
94080506		9.7N	150.9W	25												
94080512		9.9N	152.7W	25												
94080518		10.5N	154.2W	25												
94080600		11.0N	155.3W	25												
94080606		11.6N	155.9W	25												
94080612		12.2N	156.5W	25												
94080618		12.6N	157.5W	25												
94080700		13.0N	158.4W	25												
94080706		13.4N	159.2W	25												
94080712		13.5N	160.0W	25												
94080718		13.5N	161.1W	25												
94080800		13.5N	162.3W	25												
94080806		13.5N	163.5W	30												
94080812		13.5N	164.8W	40												
94080818		13.5N	166.3W	45												
94080900		13.6N	167.5W	50												
94080906		13.6N	168.2W	50												
94080912		13.6N	169.1W	45												
94080918		13.6N	170.0W	45												
94081000		13.5N	171.0W	45												
94081006		13.6N	171.6W	45												
94081012		13.7N	172.2W	45												
94081018		13.9N	172.7W	50												
94081100		13.9N	173.3W	50												
94081106		13.8N	174.2W	45												
94081112		13.6N	175.1W	45												
94081118		13.3N	176.0W	50												
94081200		13.0N	176.9W	55												
94081206		12.7N	177.9W	60												
94081212		12.6N	178.9W	65												

TROPICAL STORM LI (08E) (CONTINUED)

94081218		12.6N	180.0W	60												
94081300	1	12.9N	178.9E	55	5	89	109	96	43	142	0	5	5	10	5	10
94081306	2	13.3N	177.9E	50	5	16	13	21	34	182	5	10	10	10	5	10
94081312	3	13.8N	177.0E	45	13	29	29	18	18	177	0	5	10	10	5	15
94081318	4	14.2N	176.1E	40	39	65	73	84	74	45	0	5	5	10	15	15
94081400	5	14.7N	175.1E	40	18	48	60	60	77	216	0	0	-5	-5	5	15
94081406	6	15.1N	174.2E	35	13	30	55	63	101	290	0	0	-5	0	5	15
94081412	7	15.6N	173.3E	35	5	18	34	61	108	267	0	0	0	5	15	15
94081418	8	16.0N	172.5E	35	13	37	55	75	124	312	0	0	5	5	15	15
94081500	9	16.5N	171.7E	35	33	72	127	180	240	435	0	0	5	10	15	20
94081506	10	17.0N	170.9E	35	42	72	78	90	129		0	5	5	10	10	
94081512	11	17.5N	170.3E	35	78	126	180	228	281		0	5	10	10	5	
94081518	12	17.9N	169.8E	30	77	133	198	278	357		5	5	5	5	5	
94081600	13	18.1N	169.5E	30	77	103	134	168			0	5	5	5		
94081606	14	18.3N	169.2E	30	145	220	293	344			0	5	5	5		
94081612	15	18.5N	169.0E	25	41	54	107	209			5	5	5	10		
94081618	16	18.7N	168.9E	25	33	54	119				5	5	0			
94081700	17	18.8N	168.8E	25	0	38	122				0	0	10			
94081706	18	19.0N	168.9E	25	11	77					0	5				
94081712	19	19.1N	169.2E	25	0	28					0	5				
94081718	20	19.2N	169.7E	25	0						0					
94081800	21	19.3N	170.2E	20	0						0					
			AVERAGE		31	69	105	132	133	230	1	4	6	7	9	14
			# CASES		21	19	17	15	12	9	21	19	17	15	12	9

SUPER TYPHOON FRED (19W)

	WRN				POSITION ERRORS (NM)						WIND ERRORS (KT)					
DTG (Z)	NO.	LAT	LONG	WIND (KT)	00	12	24	36	48	72	00	12	24	36	48	72
94081200		20.0N	152.0E	15												
94081206		19.8N	151.0E	15												
94081212		19.7N	150.0E	15												
94081218		19.5N	149.1E	20												
94081300		19.3N	148.3E	20												
94081306		19.1N	147.6E	20												
94081312		18.9N	146.9E	20												
94081318		18.6N	146.3E	25												
94081400		18.2N	145.7E	25												
94081406	1	18.0N	145.0E	25	5	45	116	173	192	251	0	0	-5	-10	-10	-15
94081412	2	17.9N	144.2E	30	20	74	141	175	164	198	0	0	-5	-10	-15	-20
94081418	3	18.0N	143.4E	30	46	87	119	129	159	223	0	-5	-5	-5	-5	-10
94081500	4	18.1N	142.5E	35	0	33	99	154	190	168	0	0	0	0	0	0
94081506	5	18.2N	141.5E	40	21	78	127	175	177	217	0	0	0	0	0	0
94081512	6	18.2N	140.4E	45	16	62	115	139	130	114	0	0	0	-5	-5	-10
94081518	7	18.1N	139.3E	50	20	42	78	78	78	26	5	5	5	0	5	-20
94081600	8	17.9N	138.4E	55	16	36	48	29	45	58	5	5	0	0	5	-20
94081606	9	17.7N	137.6E	60	24	42	16	45	68	150	0	0	-5	0	0	-25
94081612	10	17.5N	136.8E	65	8	12	48	42	62	144	0	-5	0	5	0	-20
94081618	11	17.4N	135.9E	70	12	63	103	113	133	81	0	-5	5	5	-5	-20
94081700	12	17.6N	135.0E	80	12	29	70	114	164	167	0	5	15	5	-5	-20
94081706	13	18.0N	134.1E	85	8	37	86	119	151	137	0	10	15	0	-15	-25
94081712	14	18.4N	133.2E	90	11	32	36	55	71	104	0	10	5	-5	-20	-20
94081718	15	18.7N	132.3E	90	11	18	13	32	60	104	0	5	0	-10	-20	-15
94081800	16	19.0N	131.4E	95	5	18	23	49	62	87	0	-5	-5	-15	-15	-5
94081806	17	19.5N	130.6E	100	6	23	69	108	113	64	0	-5	-10	-15	-15	0
94081812	18	20.1N	129.8E	110	16	60	89	113	83	17	0	0	-10	-10	-15	0
94081818	19	20.7N	128.8E	115	21	74	105	104	62	21	0	-5	-10	-10	-10	5
94081900	20	21.2N	127.8E	120	17	16	5	44	28	21	-5	-10	0	5	10	10

SUPER TYPHOON FRED (19W) (CONTINUED)

94081906	21	21.7N	126.9E	125	5	36	72	106	128	114	0	0	5	5	5	20
94081912	22	22.1N	126.1E	130	8	5	61	98	114	153	0	10	10	15	15	35
94081918	23	22.5N	125.5E	130	12	44	108	130	144		0	5	10	20	25	
94082000	24	22.9N	124.9E	125	0	29	60	94	143		5	10	20	25	45	
94082006	25	23.6N	124.6E	125	8	66	129	194	236		0	5	20	35	60	
94082012	26	24.5N	124.5E	120	8	48	82	116	152		5	10	15	40	25	
94082018	27	25.4N	123.9E	115	18	37	49	63			0	5	10	10		
94082100	28	26.2N	123.1E	105	20	31	20	57			0	0	5	15		
94082106	29	26.9N	122.3E	100	12	18	47				0	5	10			
94082112	30	27.5N	121.3E	90	8	36	67				0	-5	10			
94082118	31	28.1N	120.1E	80	19	65					0	5				
94082200	32	28.7N	118.8E	55	0	11					0	5				
94082206	33	29.3N	117.5E	40	0						0					
94082212		29.9N	116.2E	25												
94082218		30.5N	114.9E	20												
			AVERAGE		13	41	74	102	120	120	1	5	7	10	13	14
			# CASES		33	32	30	28	26	22	33	32	30	28	26	22

TYPHOON GLADYS (20W)

	WRN				POSITION ERRORS (NM)						WIND ERRORS (KT)					
DTG (Z)	NO.	LAT	LONG	WIND (KT)	00	12	24	36	48	72	00	12	24	36	48	72
94081900		11.8N	156.7E	15												
94081906		13.0N	156.8E	15												
94081912		14.2N	156.7E	15												
94081918		15.4N	156.5E	15												
94082000		16.6N	156.1E	15												
94082006		17.7N	155.7E	15												
94082012		18.8N	155.5E	20												
94082018		19.8N	155.6E	25												
94082100		20.8N	155.9E	25												
94082106		21.7N	156.3E	30												
94082112		22.4N	156.7E	30												
94082118		23.0N	157.1E	30												
94082200	1	23.5N	157.5E	30	21	65	116	182	271	411	-5	0	5	15	10	-5
94082206	2	23.8N	157.8E	30	18	69	132	211	298	431	-5	0	5	10	10	-10
94082212	3	24.0N	158.1E	30	37	69	166	278	365	505	-5	0	10	5	5	-15
94082218	4	24.2N	158.4E	30	36	101	190	278	371	539	-5	0	5	0	-5	-20
94082300	5	24.3N	158.3E	30	29	122	189	254	296	382	-5	0	-10	-15	-20	-35
94082306	6	24.3N	158.0E	30	8	8	29	45	94	168	-5	-5	-5	-15	-25	-35
94082312	7	24.2N	157.6E	25	16	8	24	36	37	5	0	-10	-10	-15	-20	-25
94082318	8	24.1N	157.1E	30	5	13	28	45	76	180	-5	-10	-15	-20	-25	-20
94082400	9	24.0N	156.6E	35	0	12	36	53	62	82	0	0	-5	-10	-15	0
94082406	10	23.9N	156.1E	35	0	24	40	53	62	101	5	0	-5	-10	-10	10
94082412	11	23.8N	155.6E	40	8	21	28	32	48	126	0	-5	-10	-15	-10	15
94082418	12	23.7N	155.1E	45	24	28	32	20	34	163	0	-10	-15	-15	-5	20
94082500	13	23.7N	154.6E	50	12	16	42	63	87	209	-5	-10	-15	-10	0	20
94082506	14	23.8N	154.1E	55	21	45	69	81	98	172	0	-5	-10	0	5	25
94082512	15	23.9N	153.5E	60	20	45	61	89	132	211	-5	-10	-5	5	20	25
94082518	16	24.0N	152.8E	65	38	54	79	138	209	326	0	0	10	20	25	25
94082600	17	24.2N	152.1E	70	28	53	117	187	257	360	0	5	15	25	25	25
94082606	18	24.4N	151.4E	70	21	50	114	181	265	359	0	10	20	30	30	25
94082612	19	24.5N	150.6E	70	17	63	110	158	197	259	-5	0	15	20	25	20
94082618	20	24.5N	149.6E	65	27	74	129	181	202	245	0	0	15	25	30	20
94082700	21	24.4N	148.4E	65	8	82	147	215	269	339	0	5	5	10	15	10
94082706	22	24.2N	147.2E	60	17	60	116	174	198	212	5	10	15	15	15	10
94082712	23	23.9N	146.0E	55	36	71	120	150	127	150	5	5	10	20	15	10
94082718	24	23.5N	144.8E	50	79	139	192	198	170	171	5	5	10	15	15	10

TYPHOON GLADYS (20W) (CONTINUED)

94082800	25	23.0N	143.7E	50	45	98	143	134	129	127	5	5	10	10	10	0
94082806	26	22.5N	142.6E	45	57	122	157	164	151	113	5	10	10	10	10	-10
94082812	27	22.0N	141.7E	45	65	104	135	161	167	110	0	0	-10	-15	-25	-55
94082818	28	21.6N	140.7E	40	81	108	128	117	89	177	-5	-10	-15	-25	-35	-75
94082900	29	21.3N	139.7E	40	21	86	126	138	133	158	-5	-10	-20	-25	-40	-75
94082906	30	21.4N	138.6E	40	11	37	63	76	110	210	-5	-10	-20	-30	-50	-60
94082912	31	21.6N	137.4E	45	8	23	44	88	133	174	-10	-15	-25	-35	-60	-40
94082918	32	21.8N	136.1E	45	13	45	77	115	132	203	-10	-10	-15	-30	-55	-10
94083000	33	21.9N	134.7E	50	6	45	76	111	168	290	-10	-15	-20	-40	-65	5
94083006	34	22.0N	133.2E	50	6	24	42	96	156		-5	-15	-30	-50	-45	15
94083012	35	22.1N	131.7E	55	16	44	71	120	164		-5	-10	-30	-50	-20	20
94083018	36	22.2N	130.1E	60	16	42	81	128	185		-5	-15	-30	-20	5	
94083100	37	22.4N	128.4E	65	11	22	36	77	179		-5	-20	-40	0	20	
94083106	38	22.6N	126.7E	75	12	30	88	142			-5	-30	-30	0	20	
94083112	39	23.0N	125.1E	85	8	45	72	138			-5	-20	5	10	5	
94083118	40	23.5N	123.6E	95	6	50	92				-5	-15	5	5		
94090100	41	24.2N	122.3E	105	18	29	78				-15	5	20	10		
94090106	42	24.9N	121.0E	85	11	24					0	20	15			
94090112	43	25.4N	119.7E	65	0	73					5	10	5			
94090118	44	26.4N	118.7E	45	24						0					
94090200	45	27.5N	117.8E	30	56						5					
94090206		28.8N	117.2E	20												
94090212		30.2N	116.9E	15												
94090218		31.5N	116.7E	10												
			AVERAGE		23	56	95	134	171	238	4	8	14	17	22	23
			# CASES		45	43	41	39	37	37	45	43	41	39	37	33

TROPICAL STORM HARRY (21W)

	WRN				POSITION ERRORS (NM)						WIND ERRORS (KT)					
DTG (Z)	NO.	LAT	LONG	WIND (KT)	00	12	24	36	48	72	00	12	24	36	48	72
94082000		10.0N	143.5E	10												
94082006		10.5N	142.5E	10												
94082012		11.0N	141.5E	10												
94082018		11.5N	140.5E	10												
94082100		12.0N	139.5E	10												
94082106		12.5N	138.5E	10												
94082112		12.9N	137.4E	10												
94082118		13.3N	136.3E	10												
94082200		13.7N	135.2E	10												
94082206		14.0N	134.0E	15												
94082212		14.3N	132.8E	15												
94082218		14.6N	131.6E	15												
94082300		14.9N	130.4E	15												
94082306		15.2N	129.2E	15												
94082312		15.6N	128.0E	15												
94082318		16.0N	126.8E	15												
94082400		16.4N	125.6E	20												
94082406		16.8N	124.3E	20												
94082412		17.2N	123.0E	20												
94082418		17.6N	121.7E	20												
94082500		18.0N	120.5E	25												
94082506		18.3N	119.3E	30												
94082512	1	18.6N	118.1E	30	37	55	90	96	96	107	0	0	0	0	5	15
94082518	2	18.9N	117.0E	35	34	43	72	81	85	117	-5	-5	-5	-5	0	15
94082600	3	19.1N	116.0E	35	54	102	132	151	174	216	-5	-10	-10	-5	0	20
94082606	4	19.4N	115.0E	40	23	53	57	53	55		-5	-10	-15	-5	-10	
94082612	5	19.8N	114.0E	45	11	5	18	37	49		-5	-5	-10	-10	-10	

TROPICAL STORM HARRY (21W) (CONTINUED)

94082618	6	20.0N	113.1E	50	8	8	26	45	41		-5	-10	-10	-10	-10	
94082700	7	20.2N	112.2E	55	13	5	25	43	21		-5	-10	-10	-5	5	
94082706	8	20.3N	111.4E	60	12	11	11	34			0	0	-5	5		
94082712	9	20.4N	110.6E	60	12	5	17	28			0	-5	-5	10		
94082718	10	20.5N	109.9E	55	12	39	39				0	-5	0			
94082800	11	20.6N	109.2E	55	16	30	34				0	0	15			
94082806	12	20.7N	108.5E	55	20	45					-5	0				
94082812	13	20.9N	107.7E	50	28	64					5	20				
94082818	14	21.0N	106.7E	40	8						5					
94082900		21.0N	105.7E	25												
94082906		21.0N	104.6E	15												
94082912		21.0N	103.4E	10												
			AVERAGE		22	36	48	63	75	147	3	6	8	6	6	17
			# CASES		14	13	11	9	7	3	14	13	11	9	7	3

TYPHOON IVY (22W)

	WRN				POSITION ERRORS (NM)						WIND ERRORS (KT)					
DTG (Z)	NO.	LAT	LONG	WIND (KT)	00	12	24	36	48	72	00	12	24	36	48	72
94082418		24.3N	166.7E	20												
94082500		24.1N	166.4E	25												
94082506		23.9N	166.1E	25												
94082512		23.7N	165.8E	25												
94082518		23.5N	165.4E	25												
94082600		23.3N	165.0E	25												
94082606		23.1N	164.6E	25												
94082612		22.9N	164.2E	25												
94082618		22.6N	163.8E	25												
94082700		22.3N	163.4E	30												
94082706		22.1N	163.1E	30												
94082712		21.9N	162.8E	30												
94082718		21.8N	162.6E	30												
94082800	1	22.0N	162.7E	35	69	135	200	249			-10	-15	-15	-20		
94082806	2	22.3N	162.8E	35	61	121	190	226	248	331	0	0	-5	-5	-5	-15
94082812	3	22.7N	162.8E	40	71	84	122	129	115	185	0	0	0	0	-10	-10
94082818	4	23.2N	162.7E	40	69	78	97	118	101	110	5	-5	-5	-5	-10	-5
94082900	5	23.8N	162.5E	45	40	81	122	123	93	145	0	-5	-5	-10	-15	0
94082906	6	24.5N	162.1E	50	36	55	72	58	75	239	5	5	5	0	0	10
94082912	7	25.2N	161.4E	50	34	92	120	137	169	217	5	5	0	-10	-10	-5
94082918	8	25.7N	160.7E	55	54	93	99	115	140	222	0	0	-5	-15	-15	-15
94083000	9	26.2N	160.0E	55	29	53	95	147	188	269	0	-5	-10	-15	-10	-10
94083006	10	26.7N	159.5E	60	12	26	69	124	192	258	-10	-20	-25	-25	-20	-5
94083012	11	27.1N	159.2E	65	8	16	43	90	124	139	-15	-25	-25	-20	-15	0
94083018	12	27.6N	159.0E	70	18	54	97	128	164	222	-15	-15	-5	0	0	15
94083100	13	28.1N	158.9E	75	13	42	91	125	147	237	-10	-5	5	5	10	20
94083106	14	28.7N	158.8E	75	0	31	71	85	85	199	-5	0	5	5	10	20
94083112	15	29.3N	158.9E	75	5	44	81	90	107	222	-5	5	5	5	10	10
94083118	16	30.0N	159.1E	70	0	13	49	112	180		-5	-5	-5	0	5	
94090100	17	30.7N	159.4E	65	11	28	12	54	75		0	0	0	5	5	
94090106	18	31.2N	159.9E	65	7	12	42	68	87		-5	-5	0	5	5	
94090112	19	31.8N	160.3E	60	6	41	106	145	99		0	5	10	15	15	
94090118	20	32.4N	160.6E	60	19	26	45	68			0	5	15	15		
94090200	21	33.0N	160.7E	55	19	65	88	122			0	5	10	10		
94090206	22	33.6N	160.7E	50	42	51	69				5	15	15			
94090212	23	34.2N	160.8E	45	24	38	75				0	0	5			
94090218	24	34.9N	161.1E	40	26	49					0	5				
94090300	25	35.7N	161.6E	40	17	96					0	5				
94090306	26	36.7N	162.4E	35	15						0					

TYPHOON IVY (22W) (CONTINUED)

94090312	38.0N	163.4E	35
94090318	39.5N	164.4E	30
94090400	41.1N	165.3E	30
94090406	42.7N	166.1E	30

AVERAGE	28	57	90	120	133	214	4	6	8	9	9	10
# CASES	26	25	23	21	18	14	26	25	23	21	18	14

TYPHOON JOHN (10E)

	WRN				POSITION ERRORS (NM)						WIND ERRORS (KT)					
DTG (Z)	NO.	LAT	LONG	WIND (KT)	00	12	24	36	48	72	00	12	24	36	48	72
94081006		10.6N	93.1W	25												
94081012		10.4N	94.1W	25												
94081018		10.5N	95.1W	25												
94081100		10.8N	96.1W	25												
94081106		11.1N	97.1W	30												
94081112		11.2N	98.2W	30												
94081118		11.2N	99.4W	35												
94081200		11.3N	100.6W	40												
94081206		11.5N	101.7W	45												
94081212		11.8N	102.8W	45												
94081218		12.0N	103.8W	50												
94081300		12.3N	104.8W	55												
94081306		12.5N	105.8W	55												
94081312		12.9N	106.5W	55												
94081318		13.3N	106.9W	55												
94081400		13.7N	107.2W	50												
94081406		13.9N	107.8W	45												
94081412		13.9N	108.5W	40												
94081418		13.9N	109.3W	40												
94081500		13.8N	110.1W	45												
94081506		13.8N	111.0W	50												
94081512		13.7N	111.9W	45												
94081518		13.6N	112.8W	45												
94081600		13.6N	113.8W	45												
94081606		13.6N	114.7W	45												
94081612		13.7N	115.6W	45												
94081618		13.6N	116.4W	45												
94081700		13.8N	117.2W	50												
94081706		14.2N	118.0W	50												
94081712		14.6N	118.8W	50												
94081718		15.0N	119.8W	45												
94081800		15.3N	120.9W	45												
94081806		15.3N	122.3W	40												
94081812		15.3N	124.0W	40												
94081818		15.3N	125.7W	40												
94081900		15.3N	127.5W	45												
94081906		15.2N	129.2W	50												
94081912		15.1N	130.9W	55												
94081918		15.1N	132.5W	60												
94082000		15.0N	134.0W	65												
94082006		15.0N	135.6W	75												
94082012		15.0N	137.2W	85												
94082018		15.0N	138.9W	95												
94082100		15.0N	140.6W	105												
94082106		14.8N	142.2W	115												
94082112		14.6N	143.8W	120												
94082118		14.4N	145.5W	125												

TYPHOON JOHN (10E) (CONTINUED)

94082200		14.2N	147.2W	130												
94082206		14.1N	148.9W	130												
94082212		14.0N	150.5W	135												
94082218		13.9N	152.1W	140												
94082300		13.9N	153.7W	145												
94082306		14.1N	155.2W	150												
94082312		14.3N	156.6W	150												
94082318		14.5N	158.0W	145												
94082400		14.6N	159.3W	140												
94082406		14.9N	160.5W	135												
94082412		15.1N	161.6W	130												
94082418		15.2N	162.7W	125												
94082500		15.4N	163.8W	120												
94082506		15.7N	165.0W	110												
94082512		16.0N	166.3W	100												
94082518		16.4N	167.6W	90												
94082600		16.8N	168.8W	85												
94082606		17.2N	169.9W	80												
94082612		17.6N	171.0W	75												
94082618		18.0N	172.2W	80												
94082700		18.5N	173.5W	85												
94082706		19.1N	174.7W	90												
94082712		19.8N	175.9W	95												
94082718		20.4N	177.1W	95												
94082800		20.9N	178.4W	100												
94082806		21.6N	179.6W	100												
94082812	1	22.2N	179.2E	105	8	30	72	115	165	270	-10	-10	-10	-10	-5	0
94082818	2	22.8N	178.1E	105	18	54	97	154	192	300	-10	-15	-15	-10	-5	0
94082900	3	23.3N	177.1E	100	11	28	72	120	153	327	-10	-10	-10	-5	0	0
94082906	4	23.7N	176.2E	100	16	44	101	123	168	364	10	15	15	20	25	15
94082912	5	24.1N	175.4E	95	20	50	79	121	168	342	15	15	15	15	10	10
94082918	6	24.5N	174.8E	95	8	36	60	96	150	294	5	10	10	10	5	0
94083000	7	24.9N	174.3E	90	30	72	96	126	187	320	0	5	5	0	-5	-10
94083006	8	25.3N	173.9E	85	24	37	66	138	225	372	5	10	10	5	-5	-10
94083012	9	25.8N	173.6E	80	5	36	59	108	176	309	-5	0	0	0	-5	-10
94083018	10	26.3N	173.3E	75	24	42	47	49	70	137	0	5	5	0	-5	-5
94083100	11	26.7N	173.0E	70	16	19	39	62	79	144	0	0	5	5	0	-5
94083106	12	27.1N	172.8E	65	18	58	110	145	174	246	0	5	0	0	0	-5
94083112	13	27.5N	172.9E	65	13	58	102	141	198	366	-5	0	0	5	0	-5
94083118	14	27.6N	173.2E	60	18	52	89	138	196	363	0	-5	-5	-5	-5	-20
94090100	15	27.6N	173.4E	60	24	42	66	108	175	331	0	0	0	-5	-5	-20
94090106	16	27.6N	173.7E	60	41	83	125	161	204	308	0	0	0	0	-5	-20
94090112	17	27.6N	174.1E	55	47	71	108	143	175	222	-5	-5	-5	-5	-5	-20
94090118	18	27.6N	174.4E	55	43	58	75	114	157	243	-10	-5	-5	-5	-15	-20
94090200	19	27.6N	174.8E	50	36	54	78	112	143	239	-10	-10	-10	-15	-25	-35
94090206	20	27.5N	175.2E	50	36	54	78	112	129	212	-10	-5	-10	-20	-25	-40
94090212	21	27.4N	175.7E	50	5	31	60	89	116	239	-15	-10	-15	-25	-30	-40
94090218	22	27.3N	176.2E	45	17	31	53	60	93	146	-15	-15	-20	-25	-30	-35
94090300	23	27.1N	176.6E	45	6	20	40	68	132	175	-15	-15	-20	-30	-30	-35
94090306	24	26.9N	177.0E	45	40	84	109	159	216	246	-15	-20	-20	-30	-35	-35
94090312	25	26.7N	177.3E	45	60	103	154	177	185	125	-15	-20	-25	-30	-35	-35
94090318	26	26.5N	177.6E	50	12	32	49	84	106	142	-15	-15	-25	-30	-30	-25
94090400	27	26.4N	178.0E	50	26	43	17	60	73	103	-15	-20	-25	-30	-30	-25
94090406	28	26.3N	178.4E	50	38	34	24	58	73	86	-15	-20	-30	-30	-30	-25
94090412	29	26.2N	178.6E	55	24	56	97	133	164	82	-20	-20	-25	-30	-30	-25
94090418	30	26.1N	178.5E	55	34	89	121	170	200	67	-20	-25	-25	-30	-25	-25
94090500	31	26.2N	178.2E	55	48	91	142	204	215	92	-20	-25	-25	-30	-25	-30
94090506	32	26.3N	177.9E	60	40	63	114	161	147	115	-25	-25	-30	-25	-25	-30
94090512	33	26.4N	177.6E	60	0	28	59	65	10	132	-10	-10	-15	-10	-10	-25

TYPHOON JOHN (10E) (CONTINUED)

94090518	34	26.7N	177.3E	60	6	35	59	47	36	153	-10	-10	-10	-10	-10	-30
94090600	35	27.1N	176.8E	60	8	42	72	66	49	152	-10	-10	-10	-10	-15	-30
94090606	36	27.6N	176.2E	60	43	91	90	80	67	200	-10	-5	-10	-10	-20	-25
94090612	37	28.0N	175.7E	60	7	36	90	129	163	207	-10	-5	-10	-15	-25	-25
94090618	38	28.3N	175.2E	55	5	41	108	149	114	240	-5	-10	-10	-15	-30	-20
94090700	39	28.8N	175.1E	55	7	63	128	145	95	295	-5	-10	-15	-20	-30	-15
94090706	40	29.2N	175.3E	55	41	96	148	190	210		-5	-5	-15	-25	-20	
94090712	41	29.5N	175.8E	55	13	51	94	67	189		-10	-15	-20	-30	-25	
94090718	42	29.8N	176.5E	55	23	35	43	144	327		-15	-20	-35	-30	-25	
94090800	43	30.2N	177.5E	60	13	23	69	175	264		-15	-20	-35	-30	-20	
94090806	44	30.5N	178.7E	60	7	35	92	227			-5	-20	-20	-15		
94090812	45	31.0N	179.8E	65	13	66	219	328			-10	-20	-20	-10		
94090818		31.7N	178.9W	70												
94090900		32.7N	177.6W	70												
94090906		34.4N	175.9W	65												
94090912		37.1N	174.0W	65												
94090918		39.4N	172.5W	60												
94091000		41.5N	171.0W	55												
			AVERAGE		22	51	87	125	152	224	10	12	14	16	17	20
			# CASES		45	45	45	45	43	39	45	45	45	45	43	39

TROPICAL STORM JOEL (23W)

	WRN				POSITION ERRORS (NM)						WIND ERRORS (KT)					
DTG (Z)	NO.	LAT	LONG	WIND (KT)	00	12	24	36	48	72	00	12	24	36	48	72
94083000		11.9N	112.1E	10												
94083006		12.0N	112.4E	10												
94083012		12.1N	112.7E	10												
94083018		12.2N	113.0E	10												
94083100		12.3N	113.3E	10												
94083106		12.4N	113.6E	10												
94083112		12.5N	114.0E	10												
94083118		12.7N	114.5E	15												
94090100		12.8N	115.1E	15												
94090106		13.0N	115.6E	15												
94090112		13.2N	116.1E	15												
94090118		13.4N	116.6E	15												
94090200		13.7N	116.9E	15												
94090206		14.1N	117.0E	20												
94090212		14.6N	117.0E	20												
94090218		15.1N	116.6E	20												
94090300		15.5N	115.9E	20												
94090306		15.9N	115.0E	20												
94090312		16.3N	114.0E	20												
94090318		16.7N	113.0E	25												
94090400		16.9N	112.1E	25												
94090406	1	16.8N	111.3E	25	25	41	72	37	51	134	5	5	10	15	10	0
94090412	2	16.7N	110.7E	30	17	72	84	82	66	66	5	5	10	10	0	5
94090418	3	16.5N	110.1E	30	32	62	54	85	92	134	5	5	10	5	0	10
94090500	4	16.4N	109.6E	35	24	20	93	161	189		0	5	10	-5	-15	
94090506	5	16.4N	109.1E	35	13	37	128	183	230		10	10	10	-10	-20	
94090512	6	16.7N	108.9E	35	6	26	66	72	94		0	0	-5	-5	5	
94090518	7	17.1N	108.8E	35	13	45	72	86	109		0	-5	-5	0	10	
94090600	8	17.6N	109.0E	35	59	99	108	132			0	-5	0	0		
94090606	9	18.3N	109.0E	40	45	13	67	123			0	-5	0	10		
94090612	10	19.0N	108.7E	45	33	71	89				-5	-5	-5			
94090618	11	19.5N	108.2E	45	8	16	30				-5	-5	0			
94090700	12	20.0N	107.7E	45	16	37					-5	0				

TROPICAL STORM JOEL (23W) (CONTINUED)

94090706	13	20.5N	107.1E	45	11	22					0	5				
94090712	14	21.0N	106.5E	40	24						0					
94090718	15	21.5N	105.8E	30	16						5					
94090800		22.1N	105.1E	20												
94090806		22.8N	104.4E	15												
94090812		23.6N	103.8E	10												
			AVERAGE		23	44	79	107	119	112	3	5	6	7	9	5
			# CASES		15	13	11	9	7	3	15	13	11	9	7	3

TYPHOON KINNA (24W)

	WRN				POSITION ERRORS (NM)						WIND ERRORS (KT)					
DTG (Z)	NO.	LAT	LONG	WIND (KT)	00	12	24	36	48	72	00	12	24	36	48	72
94090100		7.0N	150.5E	15												
94090106		7.9N	149.8E	15												
94090112		8.7N	149.1E	15												
94090118		9.4N	148.3E	15												
94090200		10.0N	147.5E	15												
94090206		10.3N	146.5E	15												
94090212		10.6N	145.5E	15												
94090218		11.0N	144.7E	15												
94090300		11.5N	143.9E	15												
94090306		12.2N	143.2E	15												
94090312		12.9N	142.5E	15												
94090318		13.9N	142.0E	15												
94090400		15.0N	141.6E	20												
94090406		16.1N	141.5E	20												
94090412		17.1N	141.4E	20												
94090418		18.1N	141.3E	25												
94090500		19.1N	141.2E	25												
94090506	1	20.1N	141.1E	30	57	37	113	207	306	525	0	0	0	0	10	5
94090512	2	21.0N	141.0E	30	26	105	181	261	341	537	0	0	0	5	10	10
94090518	3	21.9N	140.9E	35	35	93	141	172	177	200	0	0	5	15	15	10
94090600	4	22.7N	140.8E	35	56	81	131	182	229	332	5	0	5	10	15	0
94090606	5	23.4N	140.6E	40	88	162	252	348	429	582	0	-5	5	10	10	-10
94090612	6	24.0N	140.4E	40	24	45	60	78	116	231	0	0	0	5	10	-5
94090618	7	24.4N	140.3E	45	22	29	36	64	111	219	-5	0	5	5	5	-5
94090700	8	24.7N	140.1E	45	11	28	56	100	182	311	5	5	10	10	5	-5
94090706	9	25.1N	140.0E	45	30	56	84	131	199	271	5	5	5	5	0	-10
94090712	10	25.5N	139.8E	50	28	44	73	139	222	266	0	5	5	0	-5	-10
94090718	11	25.9N	139.6E	50	56	79	84	96	110	241	0	0	0	-5	-5	-10
94090800	12	26.3N	139.5E	50	5	27	74	128	147	322	0	0	-5	-10	-10	-10
94090806	13	26.8N	139.5E	55	13	41	75	94	86	249	-5	0	0	5	0	5
94090812	14	27.3N	139.5E	55	8	7	35	31	36	259	-5	-5	-5	-5	-5	0
94090818	15	27.7N	139.6E	60	0	19	20	26	16	324	0	-5	-5	-10	-5	5
94090900	16	28.1N	139.7E	65	6	6	26	16	77	279	0	0	0	-5	-5	0
94090906	17	28.5N	139.9E	70	6	10	36	21	130		0	5	-5	-5	0	
94090912	18	28.9N	140.0E	75	5	36	33	58	162		0	0	-5	-5	0	
94090918	19	29.4N	139.8E	75	5	31	31	101	223		0	-5	-5	0	5	
94091000	20	29.9N	139.5E	80	5	26	96	148	188		0	-5	-5	-10	-10	
94091006	21	30.5N	139.2E	85	7	54	133	168			-5	-5	0	-15		
94091012	22	31.1N	139.4E	85	10	103	154	137			-5	-5	0	-10		
94091018	23	31.8N	140.0E	85	21	100	173				-5	0	5			
94091100	24	32.7N	141.0E	85	23	48	102				-5	-10	-10			
94091106	25	33.7N	142.1E	80	11	33					0	-10				
94091112	26	35.2N	143.6E	80	24	65					0	0				
94091118	27	37.1N	145.5E	75	17						-5					
94091200		39.4N	148.0E	65												

TYPHOON KINNA (24W) (CONTINUED)

DTG(Z)	LAT	LONG	WIND (KT)
94091206	42.3N	151.7E	55
94091212	45.5N	156.5E	45
94091218	48.0N	162.5E	40

	POSITION ERRORS (NM)						WIND ERRORS (KT)					
	00	12	24	36	48	72	00	12	24	36	48	72
AVERAGE	23	53	92	123	175	322	2	3	4	7	7	6
# CASES	27	26	24	22	20	16	27	26	24	22	20	16

TROPICAL STORM LUKE (25W)

DTG(Z)	WRN NO.	LAT	LONG	WIND (KT)	POSITION ERRORS (NM) 00	12	24	36	48	72	WIND ERRORS (KT) 00	12	24	36	48	72
94090606		12.4N	135.8E	15												
94090612		12.4N	135.3E	20												
94090618		12.4N	134.7E	20												
94090700		12.4N	134.0E	20												
94090706		12.5N	133.2E	25												
94090712		12.7N	132.3E	25												
94090718		13.0N	131.3E	25												
94090800		13.4N	130.3E	30												
94090806		14.0N	129.2E	30												
94090812		14.7N	128.2E	30												
94090818		15.4N	127.2E	25												
94090900		16.2N	126.3E	25												
94090906	1	16.8N	125.4E	25	12	58	113	155			0	0	0	0		
94090918	2	17.9N	123.6E	25	16	87	150	209			0	0	0	-5		
94091006	3	18.9N	121.8E	30	0	17	24	56	105	122	0	5	5	5	-5	10
94091012	4	19.4N	120.9E	30	26	54	42	67	102	105	0	5	5	0	0	10
94091018	5	19.9N	120.0E	30	53	72	70	101	117	133	0	0	0	-5	5	15
94091100	6	20.3N	119.0E	30	60	53	81	113	119	112	0	0	-10	-5	5	20
94091106	7	20.4N	117.9E	35	12	65	135	160	160		0	-5	-10	0	10	
94091112	8	20.3N	116.6E	35	16	57	111	117	106		0	-10	-5	0	10	
94091118	9	20.1N	115.1E	40	21	53	69	78	66		-5	-15	0	5	10	
94091200	10	19.8N	113.6E	45	11	21	29	41	57		0	5	10	15	10	
94091206	11	19.5N	112.2E	50	13	33	49	83			5	15	15	15		
94091212	12	19.2N	111.0E	45	8	16	36	58			5	5	5	10		
94091218	13	19.1N	109.9E	40	12	24	50				-5	0	5			
94091300	14	19.0N	108.9E	40	22	40	57				0	10	10			
94091306	15	19.0N	107.9E	35	12	24					5	10				
94091312	16	19.1N	107.0E	35	20	41					0	5				
94091318	17	19.2N	106.1E	30	45						0					
94091400	18	19.3N	105.2E	25	0						0					
94091406		19.5N	104.2E	20												
94091412		19.8N	103.2E	15												
94091418		20.2N	102.2E	10												
AVERAGE					20	45	73	104	105	119	1	6	6	5	7	14
# CASES					18	16	14	12	8	4	18	16	14	12	8	4

SUPER TYPHOON MELISSA (26W)

DTG(Z)	WRN NO.	LAT	LONG	WIND (KT)	POSITION ERRORS (NM) 00	12	24	36	48	72	WIND ERRORS (KT) 00	12	24	36	48	72
94090800		10.0N	179.9E	10												
94090806		9.9N	178.5E	10												
94090812		9.8N	177.0E	10												
94090818		9.7N	175.4E	15												
94090900		9.6N	173.8E	15												
94090906		9.5N	172.2E	15												
94090912		9.4N	170.6E	15												

SUPER TYPHOON MELISSA (26W) (CONTINUED)

DTG(Z)	WRN NO.	LAT	LONG	WIND (KT)	POSITION ERRORS(NM) 00	12	24	36	48	72	WIND ERRORS(KT) 00	12	24	36	48	72
94090918		9.3N	169.0E	20												
94091000		9.3N	167.4E	20												
94091006		9.4N	165.8E	20												
94091012		9.5N	164.3E	25												
94091018		9.6N	162.8E	25												
94091100		9.7N	161.4E	30												
94091106	1	9.8N	160.2E	35	11	37	108	230	360	577	0	0	5	15	20	30
94091112	2	10.0N	159.2E	35	41	99	205	318	434	656	5	0	5	10	20	20
94091118	3	10.3N	158.2E	40	58	158	286	444	596	837	5	10	15	15	20	10
94091200	4	10.8N	157.5E	45	8	54	132	235	357	595	5	5	10	15	15	0
94091206	5	11.4N	157.1E	45	17	82	181	279	381	580	5	5	5	10	5	-10
94091212	6	11.9N	157.0E	50	29	93	180	274	384	588	0	0	5	0	-5	-15
94091218	7	12.3N	157.2E	50	52	122	199	283	368	487	0	-5	0	-10	-20	-10
94091300	8	12.7N	157.5E	55	29	75	125	175	232	326	0	5	0	-5	-10	-5
94091306	9	13.2N	157.9E	60	37	63	104	147	194	281	0	5	-5	-10	-5	5
94091312	10	13.7N	158.2E	60	16	37	66	116	167	264	0	-10	-20	-30	-30	10
94091318	11	14.3N	158.5E	65	11	37	50	52	101	267	0	-10	-25	-30	-20	20
94091400	12	14.9N	158.8E	75	0	33	65	80	110	240	-5	0	5	5	20	40
94091406	13	15.5N	159.1E	85	8	40	72	98	121	241	0	0	5	15	25	45
94091412	14	16.1N	159.4E	95	13	30	55	92	133	287	0	5	5	20	25	50
94091418	15	16.9N	159.7E	110	11	49	71	103	163	313	0	5	15	25	25	50
94091500	16	17.9N	159.8E	120	6	36	48	10	63	275	0	5	20	30	40	55
94091506	17	19.0N	159.7E	130	5	16	21	62	130	360	0	15	30	35	45	55
94091512	18	20.2N	159.5E	135	5	28	74	147	236	397	5	20	35	45	55	50
94091518	19	21.5N	159.1E	130	16	44	108	191	282		15	30	40	55	60	
94091600	20	22.8N	158.5E	125	11	52	118	203	276		15	25	40	55	55	
94091606	21	24.1N	157.7E	115	18	63	124	195	235		0	5	20	30	35	
94091612	22	25.5N	156.7E	110	13	41	91	167	216		0	15	30	35	35	
94091618	23	27.0N	155.7E	100	26	75	145	218			5	15	20	20		
94091700	24	28.5N	154.6E	90	21	42	102	133			-15	-5	-5	-10		
94091706	25	30.0N	153.5E	80	31	53	45				-15	-10	-10			
94091712	26	31.6N	152.4E	70	39	113	161				-5	-5	-10			
94091718	27	33.2N	151.2E	65	58	145					-10	-10				
94091800	28	34.8N	150.1E	60	7	38					-10	-10				
94091806	29	36.3N	149.1E	55	0						-5					
94091812		37.7N	148.6E	55												
94091818		39.1N	148.5E	50												
94091900		40.4N	148.6E	50												
94091906		41.7N	148.7E	45												
94091912		43.1N	149.1E	45												
94091918		44.4N	149.7E	40												
		AVERAGE			21	63	113	178	252	421	4	8	15	22	27	27
		# CASES			29	28	26	24	22	18	29	28	26	24	22	18

TROPICAL STORM NAT (27W)

DTG(Z)	WRN NO.	LAT	LONG	WIND (KT)	POSITION ERRORS(NM) 00	12	24	36	48	72	WIND ERRORS(KT) 00	12	24	36	48	72
94091400		12.5N	139.2E	25												
94091406		12.8N	139.7E	25												
94091412		13.1N	140.3E	30												
94091418		13.4N	141.0E	30												
94091500		13.7N	141.8E	35												
94091506		13.9N	142.7E	35												
94091512	1	14.0N	143.7E	35	18	66	92	150	282		-10	-10	-5	-15	-25	
94091518	2	14.2N	144.8E	35	18	51	79	106	178		-5	-10	-5	-15	-25	
94091600	3	14.4N	146.2E	40	11	26	49	45	230		-10	-10	-10	-15	-20	
94091606	4	14.7N	147.8E	40	49	153	224	223	216		-10	-5	-10	-15	-20	

TROPICAL STORM NAT (27W) (CONTINUED)

94091612	5	15.2N	149.6E	40	62	126	154	145	206	454	-5	0	10	15	5	-10
94091618	6	15.7N	151.4E	40	83	103	43	94	237	490	0	0	10	15	5	-5
94091700	7	16.3N	153.2E	45	29	130	267	426	588	774	0	5	15	20	20	25
94091706	8	17.2N	154.7E	45	5	59	131	259	386	536	0	0	10	10	10	15
94091712	9	18.4N	155.7E	45	12	61	167	321	434	521	0	5	10	10	10	10
94091718	10	19.6N	156.2E	45	56	69	125	216	264	276	0	5	5	0	-5	-5
94091800	11	20.8N	156.3E	40	20	99	213	276	285	240	0	-5	-10	-10	-10	-5
94091806	12	21.9N	156.0E	40	24	98	181	235	280	230	0	-5	-10	-10	-10	-5
94091812	13	22.9N	155.3E	40	42	142	222	268	308	201	0	-5	-5	-5	-5	0
94091818	14	23.7N	154.2E	40	37	72	120	147	136	72	0	-5	0	-5	0	0
94091900	15	24.3N	153.1E	45	12	60	99	135	106	108	0	-5	0	-5	0	0
94091906	16	24.9N	152.1E	45	37	21	26	86	186	342	0	5	10	15	20	30
94091912	17	25.4N	151.2E	45	58	83	84	35	66	149	0	5	10	15	10	10
94091918	18	25.9N	150.5E	40	66	69	44	48	117		5	5	15	15	15	
94092000	19	26.4N	149.9E	40	0	18	75	145	185		0	0	5	0	0	
94092006	20	26.9N	149.4E	40	24	60	122	179	216		0	5	5	5	5	
94092012	21	27.6N	149.0E	40	5	52	127	154	147		0	5	0	0	0	
94092018	22	28.4N	149.1E	35	5	72	111	117			5	5	5	5		
94092100	23	29.2N	149.6E	35	16	67	99	108			10	10	15	10		
94092106	24	29.7N	150.3E	35	20	44	68				5	5	5			
94092112	25	30.1N	151.0E	35	18	50	120				0	5	5			
94092118	26	30.4N	151.6E	30	26	74					5	10				
94092200	27	30.7N	152.0E	30	7	6					0	5				
94092206	28	30.9N	152.4E	25	11						5					
94092212	29	31.1N	152.7E	25	31						0					
94092218		31.4N	152.9E	20												
94092300		31.7N	153.0E	15												
			AVERAGE		28	72	122	171	241	339	3	5	8	10	10	9
			# CASES		29	27	25	23	21	13	29	27	25	23	21	13

SUPER TYPHOON ORCHID (28W)

	WRN				POSITION ERRORS (NM)						WIND ERRORS (KT)					
DTG (Z)	NO.	LAT	LONG	WIND (KT)	00	12	24	36	48	72	00	12	24	36	48	72
94091600		12.0N	128.0E	15												
94091606		12.0N	129.5E	15												
94091612		12.1N	131.0E	20												
94091618		12.1N	132.5E	20												
94091700		12.2N	134.0E	20												
94091706		12.2N	135.4E	25												
94091712		12.2N	136.7E	25												
94091718		12.1N	137.9E	25												
94091800		12.0N	139.1E	25												
94091806	1	11.9N	140.1E	30	72	148	166	198	307	497	0	0	-5	-5	-10	-15
94091812	2	11.8N	141.0E	30	11	13	55	172	292	442	0	0	-5	-5	-10	-15
94091818	3	11.8N	141.8E	30	29	38	112	213	276	320	0	0	-5	-5	-10	-25
94091900	4	12.0N	142.6E	30	24	51	133	245	329	428	0	0	-5	-5	-5	-5
94091906	5	12.4N	143.3E	35	30	128	267	374	445	565	-5	-5	-10	-10	-10	-10
94091912	6	13.1N	143.8E	35	25	118	226	297	366	493	0	0	0	0	0	-5
94091918	7	14.0N	143.8E	40	8	75	120	148	221	382	5	5	5	5	5	-10
94092000	8	14.9N	143.3E	40	34	97	142	183	237	382	5	5	5	5	5	-5
94092006	9	15.7N	142.7E	45	8	41	85	115	214	476	0	0	0	5	5	-10
94092012	10	16.5N	142.2E	45	57	137	176	226	338	567	0	0	0	5	0	-20
94092018	11	17.2N	141.8E	50	18	69	111	202	342	521	5	10	15	20	20	5
94092100	12	17.9N	141.4E	50	18	58	153	262	374	486	5	5	10	10	10	-20
94092106	13	18.5N	141.1E	55	24	107	223	336	413	503	0	-5	-5	-5	-5	-30
94092112	14	18.8N	140.4E	55	56	152	262	347	391	519	5	5	5	5	5	-25
94092118	15	18.7N	139.8E	60	41	117	203	265	285	376	10	15	15	15	5	-20

SUPER TYPHOON ORCHID (28W) (CONTINUED)

94092200	16	18.5N	139.2E	60	36	84	151	222	260	416	15	15	15	15	-5	-30
94092206	17	18.2N	138.6E	65	33	46	70	80	11	132	10	10	10	-10	-25	-35
94092212	18	17.8N	138.3E	70	5	5	47	55	48	170	10	10	5	-5	-15	-30
94092218	19	17.5N	138.1E	75	12	31	82	139	152	286	5	5	-5	-15	-20	-25
94092300	20	17.3N	138.0E	80	5	53	128	162	168	265	0	-5	-15	-15	-30	-25
94092306	21	17.4N	138.0E	85	18	87	155	180	206	274	0	-10	-25	-20	-25	-25
94092312	22	17.7N	137.9E	95	5	41	85	125	222	432	-5	0	10	-5	-15	-20
94092318	23	18.2N	137.7E	105	5	61	99	170	280	487	0	5	10	-5	-10	-20
94092400	24	18.7N	137.3E	115	13	37	57	134	248	510	10	10	5	-5	-10	-15
94092406	25	19.0N	136.9E	125	18	37	45	73	167	406	0	5	5	0	-10	-10
94092412	26	19.4N	136.8E	125	6	16	79	162	285	454	0	0	5	0	-5	-5
94092418	27	19.8N	136.9E	130	11	41	93	153	212	251	0	0	10	0	-5	-5
94092500	28	20.3N	136.8E	135	8	39	77	149	220	295	0	0	10	5	0	-5
94092506	29	20.8N	136.6E	135	5	44	89	164	211	257	0	10	0	-5	5	-5
94092512	30	21.3N	136.3E	135	18	45	80	152	188	191	-10	-10	-10	-10	-5	-10
94092518	31	22.0N	135.9E	130	24	48	106	141	165	131	-5	-10	-10	-5	-5	-5
94092600	32	22.7N	135.5E	130	24	57	111	126	127	84	0	5	5	10	10	5
94092606	33	23.3N	135.0E	130	5	40	64	84	107	96	0	5	10	10	5	0
94092612	34	23.9N	134.3E	125	8	32	73	134	207	231	0	0	5	0	-10	5
94092618	35	24.5N	133.6E	125	6	26	34	62	110	236	0	5	5	0	-5	20
94092700	36	25.1N	133.0E	120	5	16	41	84	89	221	0	5	5	0	-10	-5
94092706	37	25.7N	132.7E	115	10	36	63	90	83	264	0	0	0	-5	-10	-15
94092712	38	26.3N	132.5E	110	8	36	70	93	114		0	0	-5	-10	-5	
94092718	39	26.9N	132.4E	110	8	36	77	92	134		-5	-5	-5	-10	0	
94092800	40	27.5N	132.4E	105	6	32	71	157	295		0	5	0	10	0	
94092806	41	28.1N	132.7E	105	10	36	94	227	377		5	15	10	25	-5	
94092812	42	28.8N	133.1E	105	7	7	19	69			5	5	10	0		
94092818	43	29.7N	133.5E	100	7	15	56	90			5	5	0	-5		
94092900	44	30.9N	134.1E	100	6	16	99				5	20	0			
94092906	45	32.4N	134.8E	95	11	109	165				5	5	-15			
94092912	46	34.3N	135.8E	80	30	55					0	-10				
94092918	47	36.9N	137.1E	65	18	69					-5	-10				
94093000	48	39.5N	138.5E	60	56						-5					
94093006		42.0N	139.7E	60												
94093012		44.2N	140.6E	55												
94093018		46.1N	141.0E	50												
94100100		47.7N	141.4E	45												
94100106		49.1N	142.0E	40												
94100112		50.5N	143.0E	35												
			AVERAGE		19	58	110	167	233	353	3	6	7	7	9	15
			# CASES		48	47	45	43	41	37	48	47	45	43	41	37

TYPHOON PAT (29W)

	WRN				POSITION ERRORS (NM)						WIND ERRORS (KT)					
DTG (Z)	NO.	LAT	LONG	WIND (KT)	00	12	24	36	48	72	00	12	24	36	48	72
94091912		17.4N	170.2E	15												
94091918		17.1N	169.8E	20												
94092000		16.8N	169.4E	20												
94092006		16.5N	169.0E	25												
94092012		16.3N	168.4E	25												
94092018		16.1N	167.8E	30												
94092100		15.9N	167.2E	30												
94092106	1	15.8N	166.6E	35	8	26	77	187	353	529	-5	-10	-20	-30	-35	-10
94092112	2	15.8N	166.0E	40	47	101	178	309	442	581	0	-5	-15	-25	-20	5
94092118	3	15.9N	165.4E	45	85	180	322	496	634	774	-5	-15	-25	-30	-15	10
94092200	4	16.3N	164.8E	50	46	105	245	376	457	516	0	-15	-25	-20	-5	20
94092206	5	16.9N	164.3E	60	29	56	133	171	206	205	0	-15	-20	-5	10	30

TYPHOON PAT (29W)

94092212	6	17.8N	163.9E	70	29	68	137	176	186	226	-5	-15	-10	0	10	35
94092218	7	19.0N	163.4E	80	18	8	26	24	36	176	-10	-5	10	25	30	50
94092300	8	20.5N	163.0E	90	5	26	20	20	34	72	-15	-15	-5	10	20	40
94092306	9	22.0N	162.6E	95	5	28	65	67	122	76	-15	-10	0	15	30	40
94092312	10	23.2N	162.2E	95	8	40	102	100	211	320	0	0	0	0	5	0
94092318	11	24.3N	161.6E	90	0	36	75	90	313	369	0	0	0	10	10	0
94092400	12	25.2N	161.0E	90	5	34	77	198	205	331	-5	0	5	15	10	-5
94092406	13	25.9N	160.1E	85	8	61	174	232	62	258	0	0	5	10	10	-5
94092412	14	26.5N	159.1E	85	16	43	124	181	261	614	0	5	10	10	-5	-10
94092418	15	27.2N	157.8E	80	8	59	199	191	314	643	0	10	10	5	-5	-10
94092500	16	28.0N	155.9E	75	10	109	215	212	334	635	0	5	5	0	-5	-10
94092506	17	28.3N	153.4E	65	31	221	266	295	376	460	0	0	0	0	-5	-5
94092512	18	27.9N	151.5E	60	13	102	252				-10	-20	-30			
94092518	19	27.3N	150.5E	55	13	210	272				-10	-20	-25			
94092600	20	28.5N	151.5E	50	88	229	158	83			5	-5	-10	-15		
94092606	21	30.5N	151.3E	50	80	108	113	169			5	5	0	5		
94092612	22	31.7N	149.2E	50	102	83					0	5				
94092618		32.4N	149.0E	45												
94092700		33.3N	149.3E	45												
94092706		34.2N	149.9E	45												
94092712		35.1N	150.6E	40												
94092718		36.1N	151.5E	40												
94092800		37.2N	152.5E	40												
94092806		38.2N	154.0E	35												
94092812		38.9N	155.5E	35												
94092818		39.4N	156.7E	35												
94092900		39.7N	157.7E	30												
94092906		39.8N	158.8E	30												
94092912		40.0N	160.0E	30												
		AVERAGE			30	88	154	189	268	399	4	8	11	12	14	17
		# CASES			22	22	21	19	17	17	22	22	21	19	17	17

TROPICAL STORM RUTH (30W)

	WRN				POSITION ERRORS (NM)						WIND ERRORS (KT)					
DTG (Z)	NO.	LAT	LONG	WIND (KT)	00	12	24	36	48	72	00	12	24	36	48	72
94092200		16.1N	149.3E	15												
94092206		16.3N	150.1E	15												
94092212		16.6N	150.9E	15												
94092218		17.0N	151.7E	15												
94092300		17.5N	152.4E	20												
94092306		18.1N	153.0E	20												
94092312		18.7N	153.5E	20												
94092318		19.4N	154.0E	25												
94092400		20.1N	154.5E	25												
94092406	1	20.8N	154.9E	30	5	49	150	326	507	488	0	-5	-5	-5	5	0
94092412	2	21.6N	155.4E	30	18	94	230	443	518	468	0	0	-5	0	5	5
94092418	3	22.6N	156.0E	35	58	156	320	497	510	444	-5	-5	-5	0	5	5
94092500	4	23.7N	156.4E	35	48	176	417	526	515	431	-5	-10	-5	0	5	5
94092506	5	25.2N	156.5E	40	34	225	436	400	254	219	-5	-10	-5	0	-5	0
94092512	6	26.9N	155.7E	45	36	181	186	130	72	102	0	10	5	0	0	-5
94092518	7	28.9N	154.1E	45	65	168	129	92	170		0	0	-5	-5	-5	
94092600	8	30.4N	151.8E	45	13	102	80	75	75		0	0	-5	0	-5	
94092606	9	30.9N	149.4E	45	7	139	189	169	99		0	0	0	5	0	
94092612	10	31.7N	149.2E	45	21	64	72	91	133		0	0	5	5	0	
94092618	11	32.4N	149.0E	45	13	55	96	131			0	0	0	0		
94092700	12	33.3N	149.3E	45	5	56	86	109			-5	0	-5	0		
94092706	13	34.2N	149.9E	45	23	77	82				-5	-5	0			

TROPICAL STORM RUTH (30W) (CONTINUED)

94092712	14	35.1N	150.6E	40	15	68	100				0	0	0			
94092718	15	36.1N	151.5E	40	24	85					0	5				
94092800	16	37.2N	152.5E	40	19	28					5	5				
94092806	17	38.2N	154.0E	35	52						5					
94092812	18	38.9N	155.5E	35	70						0					
94092818		39.4N	156.7E	35												
94092900		39.7N	157.7E	30												
94092906		39.8N	158.8E	30												
94092912		40.0N	160.0E	30												
			AVERAGE		30	108	184	250	286	359	2	3	4	2	4	3
			# CASES		18	16	14	12	10	6	18	16	14	12	10	6

TROPICAL DEPRESSION 31W

	WRN				POSITION ERRORS (NM)						WIND ERRORS (KT)					
DTG (Z)	NO.	LAT	LONG	WIND (KT)	00	12	24	36	48	72	00	12	24	36	48	72
94092800		25.1N	168.7E	15												
94092806		25.6N	166.8E	15												
94092812		26.1N	165.0E	20												
94092818		26.6N	163.3E	20												
94092900		27.2N	161.8E	20												
94092906	1	27.8N	160.6E	25	8	100	230	355	457	608	0	5	5	10	15	35
94092912	2	28.3N	159.9E	25	5	57	154	236	301	470	5	5	5	10	10	5
94092918	3	28.8N	159.4E	25	21	95	183	257	339	523	5	5	5	10	10	5
94093000	4	29.2N	159.1E	25	16	61	106	148			5	0	0	0		
94093006		31.8N	159.0E	30												
94093012	5	30.0N	158.9E	30	11	28	24	66			0	0	0	0		
94093018		30.3N	158.7E	30												
94100100	6	30.6N	158.4E	30	18	31	49	95			0	0	0	-5		
94100106		30.9N	158.1E	30												
94100112	7	31.1N	157.7E	30	11	23	49	95			-5	-5	-5	-10		
94100118		31.2N	157.2E	30												
94100200	8	31.3N	156.7E	30	31	82	172	269			-5	-5	-5	-5		
94100206		31.4N	156.4E	30												
94100212	9	31.5N	156.1E	30	23	120	226	224			0	0	5	0		
94100218		31.6N	156.3E	30												
94100300	10	31.7N	156.8E	30	5	30	35				0	5	0			
94100306		31.8N	157.8E	30												
94100312	11	32.0N	159.2E	25	7	79					5	5				
94100318		32.2N	160.6E	25												
94100400		32.4N	162.1E	25												
94100406		32.4N	163.4E	25												
94100412		32.2N	164.4E	20												
94100418		31.9N	165.0E	20												
94100500		31.5N	164.9E	20												
94100506		31.1N	164.3E	20												
94100512		30.7N	163.3E	15												
94100518		30.3N	161.8E	15												
94100600		30.1N	160.2E	15												
94100606		30.0N	158.5E	15												
			AVERAGE		15	65	123	194	366	534	3	3	3	6	12	15
			# CASES		11	11	10	9	3	3	11	11	10	9	3	3

TYPHOON SETH (32W)

DTG(Z)	WRN NO.	LAT	LONG	WIND (KT)	POSITION ERRORS(NM) 00	12	24	36	48	72	WIND ERRORS(KT) 00	12	24	36	48	72
94093006		7.6N	175.6E	10												
94093012		7.6N	173.9E	15												
94093018		7.7N	172.2E	15												
94100100		7.9N	170.5E	15												
94100106		8.1N	168.8E	15												
94100112		8.3N	167.1E	20												
94100118		8.6N	165.3E	20												
94100200		8.9N	163.5E	20												
94100206		9.2N	161.7E	25												
94100212		9.5N	159.9E	25												
94100218	1	9.8N	158.1E	30	88	79	46	26	18	59	0	0	5	10	15	20
94100300	2	10.1N	156.3E	30	70	50	34	37	76	213	5	10	15	20	25	25
94100306	3	10.3N	154.5E	35	71	52	42	54	88	188	10	15	20	30	35	30
94100312	4	10.5N	152.7E	35	0	47	111	188	247	296	5	10	15	20	25	30
94100318	5	10.8N	151.0E	40	23	76	140	217	275	323	0	5	10	15	20	25
94100400	6	11.1N	149.3E	40	33	37	62	126	168	221	5	5	10	10	15	15
94100406	7	11.4N	147.7E	45	21	37	75	123	152	212	5	10	15	15	15	10
94100412	8	11.7N	146.1E	45	13	67	140	185	203	217	5	10	10	10	10	-5
94100418	9	12.0N	144.4E	50	8	29	66	111	138	157	5	10	10	10	10	-5
94100500	10	12.3N	142.7E	50	13	18	59	91	138	149	5	5	5	5	0	-5
94100506	11	12.6N	141.0E	55	8	35	64	94	144	174	0	0	0	0	-10	0
94100512	12	12.9N	139.3E	60	17	49	99	161	206	182	-5	-5	-10	-15	-30	0
94100518	13	13.3N	137.6E	65	11	32	72	127	155	106	0	0	0	-10	-15	5
94100600	14	13.8N	135.9E	70	6	26	36	58	87	158	5	10	10	-5	0	10
94100606	15	14.4N	134.4E	75	13	52	82	104	108	156	5	5	0	-5	5	15
94100612	16	15.0N	132.9E	80	18	47	69	90	102	197	0	-5	-15	-5	5	15
94100618	17	15.6N	131.4E	85	8	8	43	61	82	192	-5	-15	-15	0	10	20
94100700	18	16.3N	129.9E	95	18	0	8	17	55	82	-5	-20	-5	15	15	10
94100706	19	16.9N	128.6E	105	8	41	82	114	122	71	0	5	20	20	10	5
94100712	20	17.6N	127.4E	120	0	16	46	74	83	92	0	10	25	20	15	15
94100718	21	18.4N	126.4E	120	8	28	50	88	97	155	0	15	25	20	15	5
94100800	22	19.1N	125.6E	120	6	24	61	102	100	170	-5	-5	-5	-5	-10	-10
94100806	23	19.8N	125.0E	115	0	18	27	30	50	98	0	0	0	-5	-5	-10
94100812	24	20.5N	124.5E	115	13	32	22	26	53	223	-10	-15	-15	-15	-15	-5
94100818	25	21.2N	124.1E	110	18	30	16	24	73	319	-10	-10	-15	-15	-15	-10
94100900	26	22.1N	123.9E	110	18	42	56	58	67	20	0	0	0	-5	-10	-15
94100906	27	23.0N	123.8E	105	12	61	96	91	98		0	0	0	-5	-10	
94100912	28	24.0N	123.5E	105	18	89	166	246	314		-15	-15	-15	-15	-20	
94100918	29	24.8N	123.1E	100	43	92	138	193	228		-15	-15	-15	-15	-25	
94101000	30	25.7N	122.8E	95	13	42	73	105	160		-10	-10	-10	-15	-20	
94101006	31	26.5N	122.7E	90	6	36	72	120			-10	-10	-10	-20		
94101012	32	27.4N	123.0E	85	11	36	61	72			-10	-10	-10	-15		
94101018	33	28.4N	123.3E	80	5	42	23				-15	-15	-20			
94101100	34	29.5N	123.7E	75	6	13	71				-15	-15	-15			
94101106	35	30.6N	124.4E	70	16	49					-15	-15				
94101112	36	32.0N	125.3E	65	16	62					-20	-20				
94101118	37	33.7N	126.7E	65	16						-25					
94101200		36.3N	128.8E	60												
94101206		39.2N	131.1E	60												
94101212		42.1N	133.5E	55												
94101218		45.0N	136.0E	55												
94101300		47.0N	140.0E	50												
			AVERAGE		19	42	68	101	130	171	7	9	11	12	14	12
			# CASES		37	36	34	32	30	26	37	36	34	32	30	26

TYPHOON VERNE (33W)

DTG(Z)	WRN NO.	LAT	LONG	WIND (KT)	POSITION ERRORS (NM) 00	12	24	36	48	72	WIND ERRORS (KT) 00	12	24	36	48	72
94101312		7.5N	175.5E	15												
94101318		7.9N	174.7E	15												
94101400		8.3N	173.9E	15												
94101406		8.7N	173.0E	15												
94101412		9.0N	172.0E	15												
94101418		9.2N	170.9E	20												
94101500		9.4N	169.7E	20												
94101506		9.6N	168.4E	20												
94101512	1	9.8N	167.1E	25	69	41	37	109	170	231	0	5	10	15	20	30
94101518	2	10.0N	165.7E	25	53	24	109	196	262	309	0	5	10	10	15	25
94101600	3	10.3N	164.1E	25	38	130	224	303	371	429	0	5	10	10	10	10
94101606	4	10.7N	162.4E	25	30	91	168	227	265	308	0	5	0	0	5	0
94101612	5	11.2N	160.6E	25	11	52	99	146	193	267	0	5	5	5	5	-5
94101618	6	11.7N	158.7E	25	13	38	55	96	117	164	0	0	0	0	0	-5
94101700	7	12.2N	156.8E	25	8	8	11	8	29	47	0	0	0	0	-5	-10
94101706	8	12.6N	155.0E	30	13	18	5	5	17	52	0	-5	-5	-5	-10	-10
94101712	9	13.0N	153.3E	30	42	48	51	61	72	80	0	-5	-5	-10	-15	-15
94101718	10	13.4N	151.6E	35	36	43	55	61	84	124	5	5	5	0	5	0
94101800	11	13.7N	150.0E	35	18	30	51	64	66	101	0	0	-5	-10	-5	0
94101806	12	13.9N	148.5E	40	24	46	54	66	79	170	0	0	-5	-5	0	10
94101812	13	14.1N	147.1E	40	30	42	60	72	84	157	0	-5	-10	-10	-5	10
94101818	14	14.3N	145.8E	45	11	40	81	104	120	30	0	-5	-5	-5	-5	5
94101900	15	14.5N	144.5E	50	21	39	75	103	101	116	0	0	5	15	20	15
94101906	16	14.7N	143.1E	55	17	31	52	80	79	202	5	5	10	20	20	15
94101912	17	14.9N	141.7E	60	13	50	92	115	124	231	0	0	5	10	10	-5
94101918	18	15.1N	140.2E	60	18	42	64	46	53	173	0	5	10	10	5	-10
94102000	19	15.4N	138.7E	65	0	18	48	143	258	569	0	5	10	30	15	-10
94102006	20	15.7N	137.3E	65	23	54	117	226	336	617	0	5	10	25	15	-15
94102012	21	16.1N	135.9E	70	8	8	38	103	161	265	0	5	20	25	15	-5
94102018	22	16.5N	134.6E	70	0	29	67	107	157	288	0	5	10	25	15	-20
94102100	23	16.9N	133.6E	75	16	36	49	79	136	252	0	5	10	20	5	-30
94102106	24	17.3N	132.9E	75	18	33	41	69	114	240	0	0	10	15	0	-30
94102112	25	17.6N	132.4E	75	18	45	83	141	166	111	0	-5	-5	-10	-25	-35
94102118	26	17.9N	132.0E	80	6	37	94	141	155	88	0	0	-10	-15	-40	-35
94102200	27	18.1N	131.6E	80	11	6	67	88	98	119	0	-5	-10	-25	-40	-35
94102206	28	18.3N	131.3E	80	18	36	85	104	86	120	0	-10	-15	-40	-40	-35
94102212	29	18.4N	131.0E	85	11	40	49	74	98	141	0	0	-15	-20	-20	-15
94102218	30	18.5N	130.7E	90	23	43	62	90	115	151	-5	-5	-25	-20	-15	-15
94102300	31	18.5N	130.4E	90	21	49	50	77	108	144	-5	-25	-35	-35	-30	-25
94102306	32	18.4N	130.3E	95	24	41	64	103	142	187	-5	-30	-35	-30	-30	-25
94102312	33	18.2N	130.2E	105	5	18	49	83	103	150	-15	-20	-10	-5	5	15
94102318	34	18.1N	130.1E	115	6	30	66	98	115	153	-20	-20	-5	-5	5	20
94102400	35	17.8N	130.0E	115	13	37	74	92	114	155	0	10	15	20	15	20
94102406	36	17.5N	129.9E	115	12	24	53	60	78	65	0	15	15	20	15	25
94102412	37	17.1N	129.8E	110	8	26	59	87	124	77	5	15	20	25	20	30
94102418	38	16.7N	129.7E	105	8	47	81	121	133	130	10	10	10	10	10	10
94102500	39	16.3N	129.6E	105	5	29	70	99	125	170	0	-5	-5	0	5	20
94102506	40	16.0N	129.5E	105	13	41	70	96	130	178	0	-5	-5	5	10	25
94102512	41	15.8N	129.4E	100	18	31	45	98	166	258	5	0	0	10	15	25
94102518	42	15.6N	129.3E	100	13	23	29	93	168	274	0	0	5	10	15	15
94102600	43	15.4N	129.2E	95	5	24	53	125	197	324	0	5	10	15	20	25
94102606	44	15.2N	129.1E	95	13	47	102	163	228	332	0	10	15	20	25	25
94102612	45	15.1N	129.2E	90	23	11	33	34	37	26	5	10	20	25	30	25
94102618	46	15.2N	129.4E	85	46	26	33	30	47	13	5	15	20	30	30	25
94102700	47	15.5N	129.7E	80	8	24	64	93	135	270	5	15	20	20	25	20

TYPHOON VERNE (33W) (CONTINUED)

94102706	48	15.9N	129.9E	75	5	18	50	87	113	200	10	20	25	25	25	20
94102712	49	16.4N	130.1E	70	13	18	26	24	12	52	0	5	5	10	5	5
94102718	50	16.9N	130.4E	65	11	22	28	30	35	97	0	5	10	5	5	5
94102800	51	17.5N	130.7E	60	5	30	53	57	39	18	-15	-15	-15	-15	-15	-20
94102806	52	18.0N	131.0E	55	6	8	21	30	37	104	-10	-10	-15	-15	-15	-20
94102812	53	18.6N	131.3E	55	13	32	60	110	158	226	-10	-10	-15	-10	-15	-20
94102818	54	19.2N	131.6E	50	22	56	100	143	168	264	-5	-10	-15	-10	-15	-20
94102900	55	19.8N	131.9E	50	36	72	122	179	197	244	5	-5	-5	-10	-15	-20
94102906	56	20.4N	132.3E	50	38	60	90	103	92	226	0	-10	-10	-15	-15	-20
94102912	57	21.1N	132.8E	50	13	57	114	161	196		0	0	-5	-10	-15	
94102918	58	21.8N	133.6E	50	6	40	91	124	203		0	0	-5	-10	-15	
94103000	59	22.7N	134.5E	45	16	21	60	84	164		0	-5	-5	-10	-15	
94103006	60	23.5N	135.4E	45	18	32	40	80	99		-5	-5	-10	-15	-15	
94103012	61	24.3N	136.4E	45	10	30	45	124			-5	-5	-10	-15		
94103018	62	25.0N	137.3E	45	30	58	116	159			-5	-5	-10	-10		
94103100	63	25.5N	138.3E	45	16	49	124				-5	-5	-10			
94103106	64	25.8N	139.3E	45	24	60	98				-5	-5	-10			
94103112	65	26.1N	140.4E	45	108	177					-10	-10				
94103118	66	26.7N	141.9E	45	20	67					-10	-10				
94110100		27.4N	143.3E	45												
94110106		27.9N	144.0E	45												
94110112		28.4N	144.7E	45												
94110118		29.2N	145.7E	45												
94110200		30.6N	147.5E	45												
94110206		32.2N	149.5E	50												
94110212		33.9N	151.3E	55												
94110218		35.5N	153.6E	60												
94110300		36.7N	155.2E	60												
94110306		37.7N	156.7E	60												
94110312		38.7N	158.2E	60												
94110318		39.8N	159.7E	60												
94110400		41.7N	161.7E	60												
			AVERAGE		20	40	69	102	131	188	3	6	10	14	15	17
			# CASES		66	66	64	62	60	56	66	66	64	62	60	56

TYPHOON TERESA (34W)

	WRN				POSITION ERRORS (NM)						WIND ERRORS (KT)					
DTG (Z)	NO.	LAT	LONG	WIND (KT)	00	12	24	36	48	72	00	12	24	36	48	72
94101400		14.2N	156.4E	15												
94101406		14.3N	155.2E	15												
94101412		14.4N	154.0E	15												
94101418		14.5N	152.8E	15												
94101500		14.6N	151.6E	15												
94101506		14.7N	150.4E	20												
94101512		14.8N	149.2E	20												
94101518		14.9N	148.0E	20												
94101600		15.1N	146.7E	20												
94101606		15.3N	145.3E	25												
94101612		15.5N	143.9E	25												
94101618		15.7N	142.5E	25												
94101700	1	15.9N	141.1E	30	0	11	41	87	124	178	0	-5	-10	-5	0	5
94101706	2	16.1N	139.7E	35	5	24	64	113	142	171	0	0	5	10	15	10
94101712	3	16.2N	138.4E	40	21	45	72	96	116	168	0	0	5	10	15	10
94101718	4	16.2N	137.1E	45	16	66	116	145	174	223	0	0	5	10	10	5
94101800	5	16.0N	135.8E	50	13	42	57	55	31	49	0	5	10	15	15	5
94101806	6	15.8N	134.4E	50	8	28	40	29	6	83	0	5	10	10	5	5
94101812	7	15.7N	132.9E	55	44	68	76	95	125	189	0	0	5	5	-5	10

TYPHOON TERESA (34W) (CONTINUED)

94101818	8	15.6N	131.5E	55	18	26	42	67	79	84	0	0	0	0	-10	15
94101900	9	15.6N	130.1E	60	5	23	57	98	164	336	-5	-5	-5	-10	-5	15
94101906	10	15.5N	128.8E	60	6	21	47	106	176	360	-5	-10	-10	-10	0	5
94101912	11	15.5N	127.6E	65	13	13	11	60	128	307	0	0	5	10	20	0
94101918	12	15.4N	126.5E	70	16	49	81	133	205	357	-5	5	10	20	20	-5
94102000	13	15.4N	125.5E	75	16	21	54	116	194	322	-5	5	10	20	5	5
94102006	14	15.3N	124.5E	80	8	25	70	148	223	332	0	5	20	15	-5	5
94102012	15	15.2N	123.6E	80	8	26	67	133	205	310	0	0	0	5	0	5
94102018	16	15.0N	122.7E	80	5	18	66	134	197	255	0	0	5	5	5	5
94102100	17	14.7N	121.8E	75	21	79	140	198	239	281	0	5	5	-5	0	0
94102106	18	14.3N	120.9E	65	21	62	130	167	190	185	5	5	0	-5	0	0
94102112	19	13.9N	120.0E	55	18	46	84	114	136	132	0	5	0	5	5	10
94102118	20	13.5N	119.0E	50	30	56	93	126	145	144	0	0	0	5	10	10
94102200	21	13.1N	118.0E	50	29	67	82	104	102	159	0	-5	0	0	10	-5
94102206	22	12.7N	117.0E	55	8	37	110	149	221	311	0	-5	0	0	-10	-25
94102212	23	12.2N	116.1E	60	8	30	45	54	87	176	0	5	5	10	5	-20
94102218	24	11.7N	115.3E	60	21	42	54	76	119	219	5	10	10	5	0	-25
94102300	25	11.3N	114.6E	60	29	52	95	155	197	250	10	5	10	5	0	-20
94102306	26	10.9N	114.0E	60	25	38	64	101	119	193	10	5	10	10	5	-10
94102312	27	10.7N	113.3E	65	24	24	21	42	77	180	0	5	5	5	0	0
94102318	28	10.6N	112.7E	65	13	13	18	36	74		0	5	10	10	5	
94102400	29	10.7N	112.2E	65	8	16	32	55	90		5	5	10	10	10	
94102406	30	10.7N	111.7E	65	30	61	88	119	152		5	10	10	0	-5	
94102412	31	10.8N	111.3E	65	25	34	56	88	133		10	10	10	15	10	
94102418	32	10.8N	110.9E	60	39	47	67	100			15	15	15	25		
94102500	33	10.9N	110.5E	60	18	13	21	67			15	15	20	5		
94102506	34	10.9N	110.1E	55	41	113	176				15	-20	-10			
94102512	35	10.9N	109.7E	55	39	84	135				5	-15	0			
94102518	36	10.8N	109.3E	50	46	69					0	-5				
94102600	37	10.7N	108.8E	45	51	84					-5	0				
94102606		10.6N	108.3E	35												
94102612		10.5N	107.7E	25												
94102618		10.6N	107.0E	20												
94102700		10.7N	106.2E	15												
		AVERAGE			21	43	71	103	141	221	3	5	6	7	6	8
		# CASES			37	37	35	33	31	27	37	37	35	33	31	27

TYPHOON WILDA (35W)

	WRN				POSITION ERRORS (NM)						WIND ERRORS (KT)					
DTG (Z)	NO.	LAT	LONG	WIND (KT)	00	12	24	36	48	72	00	12	24	36	48	72
94101800		12.0N	170.0E	15												
94101806		12.5N	169.0E	15												
94101812		12.9N	168.1E	15												
94101818		13.2N	167.1E	20												
94101900		13.4N	166.2E	20												
94101906		13.6N	165.3E	20												
94101912		13.7N	164.4E	25												
94101918		13.8N	163.6E	25												
94102000		13.8N	162.9E	30												
94102006	1	13.9N	162.2E	30	54	72	100	137	158	131	-5	-10	-10	-15	-25	-50
94102012	2	13.9N	161.5E	35	53	81	125	157	173	117	-5	-5	-5	-10	-20	-45
94102018	3	14.0N	160.8E	40	17	34	44	70	87	98	-5	-5	-10	-20	-30	-50
94102100	4	14.1N	160.1E	40	0	26	47	61	74	88	5	0	-10	-25	-35	-50
94102106	5	14.3N	159.5E	45	13	36	78	117	133	128	0	-5	-20	-35	-45	-50
94102112	6	14.6N	158.9E	50	18	48	85	112	126	146	0	-5	-15	-25	-30	-30
94102118	7	14.9N	158.1E	55	24	56	95	124	139	152	0	-10	-20	-30	-30	-25
94102200	8	15.3N	157.3E	65	36	79	95	124	121	128	0	-10	-25	-35	-30	-25

TYPHOON WILDA (35W) (CONTINUED)

94102206	9	15.7N	156.4E	75	17	63	114	153	197	263	-5	-20	-35	-40	-30	-20
94102212	10	16.1N	155.3E	85	11	29	92	161	200	146	-5	-10	-15	-15	-10	-10
94102218	11	16.4N	154.2E	95	13	29	58	109	149	191	-15	-30	-35	-30	-20	-20
94102300	12	16.6N	153.0E	105	11	44	79	150	224	263	-20	-30	-35	-25	-20	-20
94102306	13	16.7N	151.8E	115	8	48	108	175	242	327	-20	-30	-25	-15	-20	-15
94102312	14	16.6N	150.7E	120	26	83	151	231	274	325	-25	-25	-15	-10	-10	-15
94102318	15	16.4N	149.7E	125	12	37	95	178	245	288	-25	-20	-5	-10	-10	-15
94102400	16	16.2N	148.8E	125	13	36	81	159	237	319	-5	5	15	25	20	15
94102406	17	15.9N	148.1E	125	5	40	104	184	252	329	0	10	15	25	25	15
94102412	18	15.7N	147.6E	120	0	21	80	155	188	210	5	15	25	25	25	10
94102418	19	15.6N	147.3E	115	6	34	100	160	172	152	15	20	25	25	10	5
94102500	20	15.6N	147.1E	115	0	55	150	231	241	202	20	30	30	25	20	10
94102506	21	15.8N	147.2E	115	13	91	191	261	278	221	15	15	15	5	5	-10
94102512	22	16.1N	147.5E	110	6	41	78	86	71	71	15	10	10	5	-5	-20
94102518	23	16.6N	147.9E	110	6	32	48	48	20	124	15	15	10	5	-5	-15
94102600	24	17.2N	148.4E	110	18	32	36	26	33	173	10	10	10	5	0	-15
94102606	25	17.9N	148.9E	105	12	46	86	152	223	359	5	5	5	-5	-10	-15
94102612	26	18.6N	149.4E	105	18	50	103	190	286	617	0	0	-5	-10	-20	-40
94102618	27	19.3N	149.8E	105	24	42	84	152	289	539	0	0	-5	-10	-15	-35
94102700	28	19.9N	150.2E	100	16	40	58	60	116	277	0	0	0	-10	-15	-35
94102706	29	20.5N	150.6E	100	8	16	6	49	118	233	-5	-5	-5	-10	-15	-35
94102712	30	21.1N	151.0E	100	12	23	49	95	157	217	-5	-5	-10	-15	-25	-35
94102718	31	21.6N	151.3E	100	6	30	61	100	149	94	-10	-10	-10	-20	-25	-30
94102800	32	22.2N	151.5E	95	13	35	66	120	152	69	-5	-10	-10	-20	-25	-25
94102806	33	22.9N	151.5E	95	0	20	60	108	146	78	-5	-5	-10	-15	-25	-20
94102812	34	23.6N	151.4E	95	6	54	124	203	256	171	-5	-10	-15	-20	-25	-15
94102818	35	24.2N	151.2E	90	8	36	84	107	127	168	-5	-10	-10	-20	-20	-10
94102900	36	24.7N	151.0E	90	10	48	78	80	57	374	-5	-10	-10	-15	-15	-5
94102906	37	25.1N	150.7E	90	12	36	60	80	86	270	-5	-5	-10	-15	-15	-10
94102912	38	25.5N	150.3E	90	8	13	31	109	237		-5	-5	-5	-10	-10	
94102918	39	25.9N	150.0E	85	8	51	113	224	371		5	0	5	0	-5	
94103000	40	26.4N	149.9E	85	16	80	162	281	422		5	5	10	5	0	
94103006	41	27.0N	150.0E	85	28	83	156	249	343		5	10	15	10	5	
94103012	42	27.8N	150.2E	80	24	65	169	348			5	10	15	10		
94103018	43	28.9N	150.7E	75	6	23	142	319			5	10	10	10		
94103100	44	30.3N	151.5E	70	13	111	275				5	10	15			
94103106	45	32.0N	152.8E	65	54	210	363				5	10	15			
94103112	46	33.8N	154.8E	60	83	259					0	5				
94103118	47	35.6N	157.7E	55	61	208					0	10				
94110100	48	37.4N	161.5E	50	53						0					
94110106	49	39.2N	165.3E	45	42						0					
94110112		40.9N	169.3E	40												
94110118		42.5N	173.4E	40												
			AVERAGE		19	61	115	164	193	223	7	10	14	16	17	21
			# CASES		49	49	47	45	43	39	49	49	47	45	43	39

TROPICAL STORM YURI (36W)

	WRN				POSITION ERRORS (NM)						WIND ERRORS (KT)					
DTG (Z)	NO.	LAT	LONG	WIND (KT)	00	12	24	36	48	72	00	12	24	36	48	72
94102112		25.3N	172.2W	15												
94102118		25.0N	173.5W	20												
94102200		24.7N	175.1W	20												
94102206		24.3N	177.0W	20												
94102212		24.1N	179.3W	25												
94102218		23.9N	178.2E	25												
94102300		23.8N	175.7E	25												
94102306		23.9N	173.2E	30												

TROPICAL STORM YURI (36W) (CONTINUED)

94102312	1	24.0N	170.7E	30	52	121	198	214	178	195	0	0	5	10	15	20
94102318	2	24.3N	168.1E	35	28	65	70	63	120	118	0	5	10	20	15	15
94102400	3	24.4N	165.6E	35	5	56	26	80	167		0	5	10	20	20	
94102406	4	24.8N	163.2E	35	24	119	135	163	228		5	5	15	20	20	
94102412	5	25.2N	161.3E	35	5	5	72	181	244		10	10	20	25	20	
94102418	6	25.6N	159.7E	35	16	64	159	268	332		10	15	15	20	15	
94102500	7	25.9N	158.4E	35	5	30	55	65			0	5	10	10		
94102506	8	26.0N	157.2E	30	12	30	63	76			5	5	10	10		
94102512	9	25.9N	156.1E	30	12	12	64				-5	0	-5			
94102518		26.0N	155.0E	30												
94102600		26.3N	154.2E	25												
94102606		26.8N	153.7E	25												
94102612		27.6N	153.4E	25												
94102618		28.6N	153.4E	25												
94102700		29.8N	153.4E	20												
94102706		31.1N	153.6E	20												
		AVERAGE			18	56	94	139	212	157	4	6	11	17	18	18
		# CASES			9	9	9	8	6	2	9	9	9	8	6	2

SUPER TYPHOON ZELDA (37W)

	WRN				POSITION ERRORS (NM)						WIND ERRORS (KT)					
DTG (Z)	NO.	LAT	LONG	WIND (KT)	00	12	24	36	48	72	00	12	24	36	48	72
94102500		24.5N	160.6E	15												
94102506		24.1N	161.4E	15												
94102512		23.7N	162.2E	15												
94102518		23.3N	162.9E	15												
94102600		22.9N	163.7E	15												
94102606		22.4N	164.4E	15												
94102612		21.9N	165.1E	20												
94102618		21.3N	165.8E	20												
94102700		20.7N	166.6E	20												
94102706		20.0N	167.2E	20												
94102712		19.3N	167.5E	25												
94102718		18.6N	167.4E	25												
94102800		17.9N	167.0E	25												
94102806	1	17.2N	166.4E	25	36	81	125	160			0	-5	-5	-10		
94102812		16.5N	165.8E	30												
94102818	2	15.8N	165.1E	30	79	115	134	156			0	-5	-10	-15		
94102900		15.2N	164.4E	30												
94102906	3	14.6N	163.8E	35	8	37	35	48	104	174	0	5	0	0	-5	-10
94102912	4	14.1N	163.2E	35	40	95	106	119	170	181	0	0	0	0	-5	-15
94102918	5	13.6N	162.5E	40	45	92	162	229	271	221	-5	-5	-5	-5	-5	-15
94103000	6	13.1N	161.8E	40	34	97	180	239	267	235	-5	-10	-10	-15	-10	-25
94103006	7	12.6N	160.9E	45	48	110	189	248	284	240	-10	-15	-15	-20	-15	-30
94103012	8	12.0N	159.8E	45	46	96	155	194	203	157	-5	-5	-10	-10	-20	-30
94103018	9	11.4N	158.6E	50	54	88	140	183	200	251	-10	-10	-10	-15	-20	-35
94103100	10	10.8N	157.3E	50	23	38	33	21	80	256	-10	-10	-10	-20	-25	-35
94103106	11	10.3N	156.1E	55	8	0	18	40	111	296	-10	-10	-15	-20	-30	-35
94103112	12	9.9N	154.8E	55	33	64	56	63	109	141	-10	-10	-15	-25	-25	-40
94103118	13	9.8N	153.6E	60	30	25	21	78	148	235	-5	-10	-20	-25	-30	-50
94110100	14	9.9N	152.4E	60	8	38	78	145	223	297	-5	-15	-20	-25	-25	-60
94110106	15	10.1N	151.3E	65	26	61	131	194	255	309	-5	-10	-20	-25	-25	-65
94110112	16	10.4N	150.3E	70	21	81	144	204	223	203	-5	-5	5	0	0	-15
94110118	17	10.9N	149.6E	75	38	88	145	206	226	211	-5	-10	0	0	5	-5
94110200	18	11.6N	149.0E	80	26	63	109	154	164	202	-5	0	10	5	-5	-5
94110206	19	12.4N	148.5E	85	0	24	58	55	41	51	-10	-5	5	-5	-15	-5
94110212	20	13.3N	147.9E	85	18	85	125	121	106	127	-5	-5	-5	-15	-15	-5

SUPER TYPHOON ZELDA (37W) (CONTINUED)

94110218	21	14.3N	147.3E	90	8	11	18	47	92	99	-5	0	-10	-20	-10	-5
94110300	22	15.3N	146.6E	90	18	29	18	48	79	68	-5	-10	-20	-20	-10	0
94110306	23	16.2N	145.6E	95	6	6	43	79	82	103	-5	-15	-25	-15	-10	-5
94110312	24	17.0N	144.7E	105	8	56	96	106	79	47	-15	-25	-25	-15	-10	0
94110318	25	17.6N	143.7E	115	13	58	94	120	125	121	-10	-20	-10	-10	-10	15
94110400	26	18.0N	142.6E	125	8	36	80	112	155	281	-5	-5	0	5	10	40
94110406	27	18.3N	141.4E	135	0	36	71	125	176	400	-5	0	5	5	10	45
94110412	28	18.6N	140.1E	135	12	41	111	186	246	552	-5	0	5	10	15	55
94110418	29	18.9N	138.8E	135	21	53	103	164	250	615	0	0	5	10	20	65
94110500	30	19.4N	137.5E	135	18	64	117	176	278	605	5	5	5	10	30	70
94110506	31	20.0N	136.3E	135	13	62	126	226	384	640	5	5	5	15	40	75
94110512	32	20.9N	135.3E	135	8	42	97	225	422	613	5	5	10	30	45	75
94110518	33	21.8N	134.3E	135	8	18	97	247	430		0	5	20	45	55	
94110600	34	22.8N	133.6E	130	0	43	129	287	411		0	5	25	45	55	
94110606	35	23.8N	133.2E	130	0	67	202	355	396		0	10	30	40	50	
94110612	36	24.8N	133.5E	125	17	120	287	405	419		-5	10	25	35	40	
94110618	37	25.9N	134.0E	115	24	143	283	330			0	20	30	35		
94110700	38	27.2N	134.9E	100	13	67	108	124			-5	10	15	15		
94110706	39	28.5N	136.3E	85	36	73	174				0	5	10			
94110712	40	29.6N	138.1E	75	39	119	326				10	15	10			
94110718	41	30.5N	139.7E	65	46	191					5	10				
94110800	42	30.9N	141.1E	55	11	74					5	5				
94110806	43	30.7N	142.0E	45	47						5					
94110812	44	30.5N	142.6E	40	82						5					
94110818		30.2N	142.8E	40												
94110900		30.0N	142.7E	35												
94110906		30.1N	142.5E	30												
94110912		30.2N	142.7E	30												
94110918		30.3N	143.2E	25												
94111000		30.4N	144.1E	25												
94111006		30.6N	145.5E	20												
		AVERAGE			25	67	119	164	213	265	5	8	12	17	21	32
		# CASES			44	42	40	38	34	30	44	42	40	38	34	30

TYPHOON AXEL (38W)

	WRN				POSITION ERRORS (NM)						WIND ERRORS (KT)					
DTG (Z)	NO.	LAT	LONG	WIND (KT)	00	12	24	36	48	72	00	12	24	36	48	72
94121018		5.9N	164.6E	15												
94121100		6.0N	163.5E	15												
94121106		6.1N	162.4E	15												
94121112		6.2N	161.3E	20												
94121118		6.3N	160.2E	20												
94121200		6.4N	159.1E	20												
94121206		6.5N	158.1E	20												
94121212		6.6N	157.1E	20												
94121218		6.7N	156.1E	25												
94121300		6.2N	155.1E	25												
94121306		6.1N	154.2E	25												
94121312		6.1N	153.3E	25												
94121318	1	6.0N	152.4E	25	17	16	29	46	87	144	0	5	10	15	25	30
94121400	2	6.0N	151.5E	25	30	29	29	42	51	158	0	0	5	5	10	10
94121406	3	6.1N	150.6E	25	98	154					0	-5				
94121412		6.2N	149.8E	25												
94121418		6.4N	149.0E	25												
94121500		6.7N	148.2E	25												
94121506		6.9N	147.4E	30												
94121512		7.1N	146.6E	30												

TYPHOON AXEL (38W) (CONTINUED)

94121518	4	7.5N	145.8E	30	84	66	56	29	16	94	0	0	0	-5	-5	-20
94121600	5	7.8N	144.9E	30	72	97	131	139	142	138	0	0	-5	-5	-10	-25
94121606	6	8.0N	144.0E	30	79	101	112	116	127	130	0	0	0	-5	-10	-30
94121612	7	8.3N	143.1E	35	64	59	49	84	159	246	0	-5	-5	-5	-10	-25
94121618	8	8.6N	142.2E	35	17	5	29	53	71	97	5	0	0	-10	-15	-30
94121700	9	8.9N	141.4E	40	56	51	53	58	53	91	0	0	-5	-10	-20	-35
94121706	10	9.2N	140.6E	40	45	76	119	150	178	194	0	0	-10	-15	-25	-45
94121712	11	9.5N	139.8E	45	31	54	82	98	105	117	0	0	-5	-15	-20	-55
94121718	12	9.8N	139.0E	45	41	70	101	125	129	153	5	-5	-10	-20	-25	-55
94121800	13	10.1N	138.2E	50	37	59	72	74	77	115	0	-10	-15	-25	-30	-45
94121806	14	10.4N	137.4E	55	24	24	23	21	32	40	-5	-15	-20	-30	-45	-40
94121812	15	10.7N	136.6E	60	24	31	24	24	30	69	-5	-15	-20	-30	-50	-35
94121818	16	11.0N	135.7E	65	5	21	56	74	60	71	-5	-10	-20	-35	-45	-25
94121900	17	11.2N	134.7E	70	16	54	96	112	120	94	0	-5	-5	-25	-20	-10
94121906	18	11.3N	133.7E	75	26	77	109	123	116	63	0	-5	-15	-20	-15	-5
94121912	19	11.3N	132.6E	80	18	47	71	110	128	25	-5	-10	-25	-10	-10	-5
94121918	20	11.2N	131.5E	85	5	11	21	37	33	61	-5	-15	-15	-5	-5	-5
94122000	21	11.1N	130.5E	90	11	18	26	26	5	85	-5	-25	-10	-5	0	-5
94122006	22	11.1N	129.5E	100	11	13	38	37	76	223	-15	-20	-5	5	5	-5
94122012	23	11.1N	128.5E	115	8	36	54	50	105	250	-10	-5	0	0	-5	-15
94122018	24	11.0N	127.6E	115	18	43	30	41	111	225	-5	0	5	0	-5	-20
94122100	25	10.9N	126.7E	105	0	21	54	117	178	312	0	5	10	0	-5	-15
94122106	26	10.8N	125.9E	95	13	62	123	183	246	376	5	15	15	5	-5	-5
94122112	27	10.9N	125.1E	85	13	43	85	112	136	165	5	10	0	-5	-15	0
94122118	28	11.2N	124.2E	75	18	47	84	131	146	192	10	5	0	-5	-15	5
94122200	29	11.5N	123.2E	70	24	46	106	129	150	197	10	5	0	-15	-15	5
94122206	30	11.9N	122.1E	65	6	37	73	88	128	169	5	0	-5	-20	-10	5
94122212	31	12.3N	121.0E	65	16	45	58	55	58	152	0	0	-10	-10	0	10
94122218	32	12.7N	120.0E	60	26	31	40	40	20	238	0	-5	-15	0	5	10
94122300	33	13.2N	119.0E	60	8	24	61	77	82	217	0	-10	-10	5	10	10
94122306	34	13.7N	118.1E	60	13	24	48	60	68		0	-5	5	5	5	
94122312	35	14.3N	117.4E	65	8	13	34	56	139		0	5	10	10	10	
94122318	36	15.0N	116.9E	65	8	41	61	79	155		-5	5	10	10	10	
94122400	37	15.7N	116.6E	60	18	43	56	45	145		0	10	15	15	10	
94122406	38	16.4N	116.2E	50	5	24	29	49			5	10	15	15		
94122412	39	17.0N	115.8E	45	34	74	65	16			0	5	10	5		
94122418	40	17.5N	115.3E	40	0	41	132				-5	0	0			
94122500	41	17.9N	115.0E	35	8	59	154				-5	5	0			
94122506	42	18.3N	114.9E	30	6	38					0	0				
94122512		186.N	115.1E	25												
94122518		18.8N	115.4E	25												
94122600		18.9N	115.8E	25												
94122606		19.0N	116.2E	20												
94122612		19.1N	116.6E	20												
		AVERAGE			26	46	67	77	102	154	3	6	9	11	15	20
		# CASES			42	42	40	38	36	32	42	42	40	38	36	32

STORM BOBBIE (39W)

	WRN				POSITION ERRORS (NM)						WIND ERRORS (KT)					
DTG (Z)	NO.	LAT	LONG	WIND (KT)	00	12	24	36	48	72	00	12	24	36	48	72
94121400		4.0N	175.0E	15												
94121406		4.1N	174.7E	15												
94121412		4.2N	174.4E	15												
94121418		4.3N	174.1E	15												
94121500		4.4N	173.8E	20												
94121506		4.5N	173.5E	20												
94121512		4.6N	173.1E	20												

STORM BOBBIE (39W) (CONTINUED)

94121518		4.7N 172.7E	20												
94121600		4.8N 172.3E	20												
94121606		4.9N 171.9E	25												
94121612		5.0N 171.5E	25												
94121618		5.1N 171.0E	25												
94121700		5.2N 170.4E	25												
94121706		5.3N 169.7E	25												
94121712		5.4N 168.9E	30												
94121718	1	5.5N 168.0E	30	151	216	268	298			-5	-10	-10	-10		
94121800		5.7N 167.0E	30												
94121806	2	5.8N 165.9E	35	98	81	43	18			-10	-10	-10	-10		
94121812		5.9N 164.8E	35												
94121818	3	5.9N 163.7E	35	167	185	166	88	151	200	-5	-5	0	0	5	10
94121900	4	6.1N 162.6E	40	40	66	168	321	369	410	-5	0	0	5	15	15
94121906	5	6.4N 161.5E	40	34	96	233	340	375	404	-5	0	0	5	15	15
94121912	6	6.9N 160.5E	40	55	148	272	343	378	427	-5	-10	-5	5	10	20
94121918	7	7.6N 159.7E	40	32	141	235	250	260	288	-5	-5	0	5	5	20
94122000	8	8.7N 159.4E	45	54	147	169	183	206	251	-10	-5	0	0	5	20
94122006	9	9.8N 159.4E	45	18	77	114	164	201	252	-10	-5	0	5	15	30
94122012	10	11.0N 159.1E	45	24	37	64	94	123	130	-10	-10	-5	5	15	30
94122018	11	11.9N 158.3E	45	13	41	89	128	144	143	-10	-10	-5	5	20	30
94122100	12	12.5N 157.1E	45	24	53	83	117	133	167	-10	-15	-5	5	20	35
94122106	13	13.1N 155.9E	45	18	30	54	71	90	162	-10	-5	5	15	20	35
94122112	14	13.6N 154.6E	50	54	74	108	135	172	255	-5	0	5	20	30	60
94122118	15	14.1N 153.3E	50	29	30	53	105	154	230	-5	0	10	20	30	65
94122200	16	14.6N 152.0E	50	76	91	108	143	199	248	5	10	20	30	45	65
94122206	17	15.0N 150.6E	50	69	87	120	167	211	278	5	15	20	30	45	60
94122212	18	15.4N 149.3E	50	69	84	98	124	151	228	0	5	5	15	15	30
94122218	19	15.7N 148.0E	45	60	79	133	177	200	224	5	5	5	15	20	30
94122300	20	16.0N 146.7E	45	24	17	37	58	74	119	5	5	10	15	20	35
94122306	21	16.3N 145.5E	45	0	55	85	111	127	127	5	5	15	25	35	40
94122312	22	16.6N 144.3E	45	42	101	154	191	214	248	5	10	15	25	35	40
94122318	23	17.0N 143.2E	45	33	66	99	136	145		5	10	20	30	35	
94122400	24	17.4N 142.1E	40	8	11	23	51	54		10	15	20	25	20	
94122406	25	17.8N 141.0E	40	11	32	53	72	132		10	15	20	15	15	
94122412	26	18.2N 139.8E	40	32	66	90	120	214		5	10	10	15	10	
94122418	27	18.6N 138.6E	35	37	60	103	183			5	10	5	5		
94122500	28	19.0N 137.4E	35	12	6	22	121			0	0	5	0		
94122506	29	19.4N 136.3E	30	33	78					0					
94122512		19.8N 135.3E	30												
94122518		20.2N 134.6E	30												
94122600		20.7N 134.4E	25												
94122606		21.4N 134.5E	25												
94122612		22.4N 134.8E	25												
		AVERAGE		46	78	116	154	187	240	6	7	8	13	21	34
		# CASES		29	29	28	28	24	20	29	29	28	28	24	20

6.2.2 NORTH INDIAN OCEAN

This section includes verification statistics for each warning in the North Indian Ocean during 1994.

JTWC BEST TRACK, FORECAST TRACK AND INTENSITY ERRORS BY WARNING

TROPICAL CYCLONE 01B

	WRN				POSITION ERRORS (NM)						WIND ERRORS (KT)					
DTG (Z)	NO.	LAT	LONG	WIND (KT)	00	12	24	36	48	72	00	12	24	36	48	72
94031818		6.3N	96.1E	15												
94031900		6.3N	95.5E	15												
94031906		6.4N	94.8E	15												
94031912		6.7N	94.2E	15												
94031918		7.0N	93.6E	15												
94032000		7.4N	93.1E	20												
94032006		7.9N	92.7E	20												
94032012		8.3N	92.3E	20												
94032018		8.8N	92.0E	20												
94032100		9.3N	91.7E	25												
94032106		9.8N	91.4E	25												
94032112		10.3N	91.1E	25												
94032118		10.8N	90.9E	25												
94032200		11.3N	90.7E	25												
94032206		11.8N	90.5E	30												
94032212	1	12.2N	90.4E	30	8	24	29	91	152	273	0	0	0	5	5	10
94032218	2	12.6N	90.3E	35	18	50	47	106	161		-5	-5	5	10	5	
94032300	3	13.0N	90.4E	35	34	35	120	210	303		-5	-5	-5	0	0	
94032306	4	13.3N	90.3E	40	60	29	77	166	299		-5	0	0	0	0	
94032312	5	13.3N	90.1E	40	26	136	253	376	539		0	0	5	5	5	
94032318	6	13.1N	89.8E	35	60	183	318	484			0	5	0	5		
94032400	7	12.6N	89.6E	35	32	104	189	316			0	0	5	5		
94032406	8	12.2N	89.5E	30	30	78	144				0	0	5			
94032412	9	11.7N	89.3E	30	78	132	232				0	5	10			
94032418	10	11.3N	89.2E	30	42	119					0	5				
94032500	11	10.7N	88.9E	25	59	104					0	5				
94032506		10.0N	88.4E	25												
94032512		9.2N	87.5E	20												
			AVERAGE		41	91	157	251	291	273	1	3	4	4	3	10
			# CASES		11	11	9	7	5	1	11	11	9	7	5	1

TROPICAL CYCLONE 02B

	WRN				POSITION ERRORS (NM)						WIND ERRORS (KT)					
DTG (Z)	NO.	LAT	LONG	WIND (KT)	00	12	24	36	48	72	00	12	24	36	48	72
94042618		7.4N	95.5E	15												
94042700		7.6N	95.0E	15												
94042706		7.8N	94.5E	15												
94042712		8.0N	94.0E	20												
94042718		8.2N	93.5E	20												
94042800		8.4N	93.0E	20												
94042806		8.6N	92.5E	25												
94042812		8.8N	92.0E	25												
94042818		9.1N	91.5E	30												
94042900	1	9.4N	91.1E	30	0	13	35	40	68	141	5	10	10	10	0	-25
94042906	2	9.7N	90.7E	35	13	52	85	140	203	354	5	5	5	0	-10	-35

TROPICAL CYCLONE 02B (ONTINUED)

94042912	3	10.2N	90.6E	35	8	16	29	46	96	171	5	0	0	-10	-20	-20
94042918	4	10.7N	90.5E	40	36	54	67	58	74	135	5	0	0	-15	-30	10
94043000	5	11.3N	90.4E	45	21	43	80	101	133	169	5	0	-10	-20	-30	50
94043006	6	11.9N	90.3E	50	30	66	117	162	180	231	5	-5	-20	-30	-40	70
94043012	7	12.6N	90.2E	55	8	36	94	135	176	256	0	-10	-25	-40	-25	80
94043018	8	13.4N	90.2E	65	13	11	46	70	83		0	-10	-25	-40	10	
94050100	9	14.4N	90.3E	75	5	61	116	145	176		-5	-15	-25	-5	55	
94050106	10	15.4N	90.5E	85	21	40	79	83	129		-10	-15	-20	35	45	
94050112	11	16.5N	90.7E	95	25	78	102	132	170		-15	-25	-5	65	55	
94050118	12	17.6N	91.0E	105	25	59	80	138			-20	-30	30	55		
94050200	13	18.7N	91.3E	115	6	32	80	135			-15	0	60	60		
94050206	14	19.7N	91.7E	125	11	35	94				-5	55	80			
94050212	15	20.7N	92.1E	110	5	29	63				25	55	75			
94050218	16	21.7N	92.6E	80	13	49					30	50				
94050300	17	22.4N	93.5E	50	5	12					30	35				
94050306	18	23.0N	94.5E	30	20						30					
94050312		23.5N	95.6E	20												
		AVERAGE			15	41	78	107	136	209	12	19	26	30	29	41
		# CASES			18	17	15	13	11	7	18	17	15	13	11	7

TROPICAL CYCLONE (03A)

	WRN				POSITION ERRORS(NM)						WIND ERRORS(KT)					
DTG(Z)	NO.	LAT	LONG	WIND (KT)	00	12	24	36	48	72	00	12	24	36	48	72
94060512		17.7N	74.4E	20												
94060518		17.7N	73.2E	20												
94060600		17.9N	72.1E	25												
94060606		18.2N	70.6E	25												
94060612		18.5N	68.9E	30												
94060618		18.7N	67.7E	30												
94060700		18.8N	66.3E	35												
94060706	1	18.8N	65.0E	40	20	38	73	112	146		5	10	25	40	5	
94060712	2	18.8N	63.9E	40	36	62	97	86	80		5	10	25	45	10	
94060718	3	18.9N	62.9E	45	40	90	124	124	95		10	25	40	5	0	
94060800	4	19.1N	62.2E	45	57	93	107	122			15	25	45	10		
94060806	5	19.3N	61.6E	40	33	41	62	71			10	15	10	5		
94060812	6	19.6N	60.9E	40	28	62	78				0	5	10			
94060818	7	19.8N	60.2E	35	11	24	49				0	5	5			
94060900	8	20.0N	59.5E	30	13	39					0	0				
94060906		20.2N	58.9E	30												
94060912		20.4N	58.2E	25												
94060918		20.6N	57.5E	25												
		AVERAGE			30	57	85	104	108		6	12	23	21	5	
		# CASES			8	8	7	5	3		8	8	7	5	3	

TROPICAL CYCLONE 04B

	WRN				POSITION ERRORS(NM)						WIND ERRORS(KT)					
DTG(Z)	NO.	LAT	LONG	WIND (KT)	00	12	24	36	48	72	00	12	24	36	48	72
94102812		11.0N	85.5E	15												
94102818		11.2N	85.2E	20												
94102900		11.4N	84.9E	20												
94102906		11.5N	84.5E	25												
94102912		11.6N	84.0E	25												
94102918		11.7N	83.4E	25												
94103000		11.8N	82.8E	30												
94103006		11.9N	82.1E	30												

TROPICAL CYCLONE 04B (CONTINUED)

94103012	1	12.1N	81.4E	35	8	60	130			0	-10	10
94103018	2	12.4N	80.7E	40	5	24	85			-5	5	10
94103100	3	12.8N	80.1E	45	24	78				-10	5	
94103106	4	13.3N	79.6E	30	8	81				5	10	
94103112		13.9N	79.2E	20								
94103118		14.6N	79.0E	15								
			AVERAGE		12	61	108			5	8	10
			# CASES		4	4	2			4	4	2

TROPICAL CYCLONE 05A

	WRN				POSITION ERRORS (NM)						WIND ERRORS (KT)					
DTG (Z)	NO.	LAT	LONG	WIND (KT)	00	12	24	36	48	72	00	12	24	36	48	72
94111300		7.5N	69.5E	15												
94111306		8.0N	69.2E	15												
94111312		8.5N	68.9E	15												
94111318		8.9N	68.5E	15												
94111400		9.3N	68.1E	15												
94111406		9.6N	67.6E	20												
94111412		9.9N	67.1E	20												
94111418		10.1N	66.6E	20												
94111500		10.2N	66.2E	25												
94111506		10.1N	65.8E	25												
94111512	1	9.9N	65.4E	30	6	24	66	83	103	155	0	0	0	5	5	-5
94111518	2	9.7N	65.0E	30	11	37	70	94	114	184	0	-5	0	0	5	-5
94111600	3	9.5N	64.6E	30	18	46	59	81	99	160	0	0	0	0	0	-10
94111606	4	9.2N	64.2E	35	45	58	66	78	90	168	0	0	0	5	0	-5
94111612	5	9.0N	63.7E	35	46	59	95	118	154	270	0	5	5	5	5	5
94111618	6	8.9N	63.1E	35	30	53	83	118	154	273	0	0	5	5	0	0
94111700	7	8.8N	62.5E	35	50	80	115	167	231	352	0	0	0	0	-5	15
94111706	8	8.7N	61.8E	40	56	76	106	151	203	321	-5	0	0	0	-5	30
94111712	9	8.6N	61.0E	40	43	38	62	113	178		-5	-5	-5	-5	0	
94111718	10	8.5N	60.2E	40	13	18	71	135	190		0	0	0	-5	0	
94111800	11	8.4N	59.3E	45	11	42	88	152	218		0	-5	-5	-5	15	
94111806	12	8.3N	58.2E	45	18	56	109	175	221		0	-5	-10	0	20	
94111812	13	8.2N	57.0E	50	29	53	107	137			-10	-15	-15	0		
94111818	14	8.1N	55.7E	50	41	71	107	136			-5	-10	-5	10		
94111900	15	8.0N	54.3E	55	71	137	178				-5	0	10			
94111906	16	7.9N	52.8E	55	18	23	29				0	5	15			
94111912	17	7.8N	51.2E	50	0	8					5	5				
94111918	18	7.7N	49.7E	45	5	13					5	10				
94112000	19	7.6N	48.2E	30	0						5					
94112006		7.5N	46.7E	15												
			AVERAGE		27	50	89	125	163	236	2	4	5	3	5	9
			# CASES		19	18	16	14	12	8	19	18	16	14	12	8

Intentionally left blank

7. TROPICAL CYCLONE SUPPORT SUMMARY

7.1 TROPICAL CYCLONE FORECASTER'S REFERENCE GUIDE

C.R. Sampson and J.-H. Chu
Naval Research Laboratory, Marine
Meteorology Division, Monterey, CA

The Tropical Cyclone Forecasters Reference Guide consists of seven chapters. Chapters 1,2,3 and 5 have been published as four Naval Research Laboratory Publications since 1992. The remaining chapters, entitled tropical cyclone motion, intensity and structure, will be published in 1995.

There will also be a CD-ROM version of the guide. The paper version of the guide will be revised and put in an electronic format for browsing.

7.2 AUTOMATED TROPICAL CYCLONE FORECASTING SYSTEM (ATCF) 3.0

T.L. Tsui, A.J. Scrader and C.R. Sampson
Naval Research Laboratory, Marine
Meteorology Division, Monterey, CA

The ATCF has been used operationally at JTWC since 1988. The current system runs on an IBM-DOS operating system. NRL, Monterey is adapting the ATCF to the UNIX operating system. The new system will become a part of the Tactical Environmental Support System (TESS) and is expected at JTWC in June of 1996.

7.3 PROTOTYPE AUTOMATED TROPICAL CYCLONE HANDBOOK (PATCH)

C.R. Sampson and R.A. Jeffries
Naval Research Laboratory, Marine
Meteorology Division, Monterey, CA

PATCH is an expert system designed to provide tropical cyclone forecast and training guidance for the western North Pacific Ocean to JTWC. The scope of the project has expanded to include expertise pertaining to tropical cyclone formation, motion, intensification and dissipation, and structure and structure change. The expert system is an integral part of the ATCF upgrade. Initially PATCH will be in a basic stand-alone mode. Ultimately, it will be interactive with the ATCF.

7.4 NEW TROPICAL CYCLONE RELATED WIND DATA SETS

Jeff Hawkins and Chris Velden
Naval Research Laboratory, Marine
Meteorology Division, Monterey, CA

Earth Remote-Sensing Satellite (ERS)-1 scatterometer data during the 1994 season proved valuable, although untimely (delayed 8-24 hours) . The 500 km swath highlighted the feast or famine nature of this narrow swath sensor. Excellent depiction of tropical cyclone circulation is possible when TC overflights occur and are especially relevant to TC wind radii warnings and thus TC numerical model bogus vortexes. ERS-2 (just launched) and more importantly the NASA Scatterometer (NSCAT) sensor (1200 km swath) on (Japanese) Advanced Earth Observing Satellite (ADEOS) (1996) will dramatically increase the coverage of this surface wind vector data set (note: scatterometer winds are typically valid up to a limit of 20-25 m/sec) .

Water vapor tracked winds from consecutive geostationary water vapor channel images are now under development by the University of Wisconsin (Velden) to supply upper-level winds. The advantages are 1) clouds need not be present and 2) Winds are produced from 200-

400 mb and thus fill a substantial data void. Accurate upper-level winds are sorely needed both by NOGAPS and by analysts trying to ascertain the synoptic pattern and it's impact of track motion and intensity.

GMS-5 completes a near global coverage of water vapor imagery when combined with the existing data sets from GOES-7/8 and METEOSAT. TC applications for real time will be coming online with automated tracking algorithms within the next 9-12 months.

7.5 SATELLITE IMAGERY ANALYSIS UPGRADES

Jeff Hawkins and Chris Velden
Naval Research Laboratory, Marine
Meteorology Division, Monterey, CA

Current Dvorak method results indicate distinct problems when applied to tropical cyclones (TC) falling within certain categories. Midget TC's forming within monsoon gyres, landfalling TC's and those that rapidly change intensity are difficult to adequately handle using the present rules. These intensity problems can be attributed to the fact these cases were not adequately covered in the original data set used to develop the method, difficulty in applying the method consistently and the generic limitations inherent in using visible and/or infrared digital data.

This effort will focus on studying a large sample of digital GMS visible/infrared images that will specifically include numerous examples from the problem cases noted above. Operational centers are being surveyed to list TC's which caused problems using the Dvorak technique. Particular attention will be placed on those storms that contain any validation data (aircraft, island, buoys, etc) that will assist in our evaluating the impact of any upgrades. This task will attempt to identify specific deficiencies in the current methods and test proposed modifications and/or new techniques aimed at improving the results and automating them to the extent possible.

A parallel effort will be designed to analyze whether SSM/I brightness temperature images can be evaluated by themselves or in tandem with visible/infrared imagery. Eighty-five GHz imagery depicts the rainband features of TCs extremely well and often include detail not evident in visible/infrared data. A cursory analysis indicates promise for this task, but this effort will need to examine hundreds of available SSM/I images.

7.6 SATELLITE MULTI-SENSOR STRUCTURE AND INTENSITY APPLICATIONS

Jeff Hawkins, Kim Richardson, Joe Turk,
Doug May, Nita Chase, Glenn Sandlin,
Gene Poe and Chris Velden
Naval Research Laboratory, Marine
Meteorology Division, Monterey, CA

No single satellite channel or sensor is capable of measuring all the features and parameters required by operational centers to accurately locate and specify the structure and intensity of tropical cyclones (TC). Thus, a multispectral multi-sensor combination that takes advantage of the inherent benefits of each can likely lead to improved satellite analysis results. This study will include digital data from imagery (visible, infrared and passive microwave), sounders (SSM/T1 & SSM/T2 and the MSU) and scatterometer sensors.

The SSM/I will be the initial focus of this study since it measures parameters ideally suited in depicting the TC and its surrounding environment (e.g., surface wind speed, rainrate, total precipitable water and cloud liquid water). Earlier efforts have shown that individual brightness temperatures (Tbs) and derived parameters are correlated with TC intensity and can help in TC positioning.

Our initial results reveal that remapping SSM/I data to the OLS infrared resolutions can be successfully done using the method of Poe (1990). Direct comparisons with OLS data not only show a one-to-one correlation with rainband features, but also indicate detail not available in either infrared or visible data. In addition, we have found that multi-channel combinations of SSM/I channels using normalized differences highlights features and brings out more storm structure. Information on rain structure, maturity, and phase (ice, liquid) can be extracted and potentially help in understanding current intensity.

Initial work on intensity correlation has been positive, but additional cases involving a wider variety of TC types and environmental conditions are required before definitive accuracies can be determined. Thus, a data base with hundreds of SSM/I TC cases is being created with coincident OLS infrared data. In addition to regression type correlations, a neural network approach is being applied to the SSM/I data sets. All SSM/I Tbs will be put into a training data set and then applied to an independent data set for accuracy analysis. This automated approach could augment and/or provide increased confidence in Dvorak-type estimates.

Microwave sounder data has proven reliable by Velden (1991) in depicting upper-level warm anomalies that are highly correlated with storm intensity. We are working on methods to incorporate this automated technique operationally so that the TDO has this additional tool in real time. The multi-sensor task will also review how to bring this important piece of upper-level atmospheric information into the broader picture of a unified intensity estimate.

7.7 DEVELOPMENT OF THE SYSTEMATIC APPROACH TO TROPICAL CYCLONE TRACK FORECASTING

L.E. Carr, III and R.L. Elsberry
Naval Postgraduate School
Monterey, California

A Systematic and Integrated Approach to Tropical Cyclone Track Forecasting (hereafter the Systematic Approach) is being developed that helps forecasters to more insightfully and consistently: (i) interpret the TC motion ramifications of evolving global model fields; and (ii) anticipate errors in the tropical cyclone (TC) forecast tracks provided by the global model and by other objective track forecast aids that depend on the numerical model. The Systematic Approach is based on the premise that under certain circumstances forecasters can formulate TC track forecasts that improve upon numerical model and objective aid forecasts, if the forecasters are equipped with two key knowledge bases. The first knowledge base is a set of TC-Environmental conceptual models that may be used to associate a wide variety of TC motion patterns with a relatively few recurring combinations of TC structure, environment structure, and interactions between the TC and its environment. The second knowledge base is a set of TC track forecast traits for the numerical model and associated objective aids that is organized around the meteorological knowledge base. Development of the overall framework of the Systematic Approach and the TC-Environment conceptual models knowledge base has been completed (Carr and Elsberry 1994).

The TC-Environment knowledge base enabled the forecaster to develop a comprehensive mental picture of the TC-Environmental situation. This picture consists of conceptual models of Environment structure, TC structure, and TC-Environment transformations by which the structure of the environment and/or the TC may be changed as they interact. The structure of the environment surrounding the TC is assigned to one of four Synoptic Patterns, which are comprised of one or more smaller areas

called Synoptic Regions. A Pattern and Region specification together characterizes the contribution of environmental steering to TC motion.

The wind field structure of the TC is characterized in terms of an Intensity and a Size. The Intensity categories (Exposed Low-level, Tropical Depression/Storm, Typhoon, Intense Typhoon) serve primarily to determine the best steering level at which to make the Pattern and Region characterization of environment structure. The Size categories (Midget, Small, Average, and Large) are assigned according to the maximum B-effect propagation (BEP) speed that would be exhibited by an equivalent size vortex in a nonlinear barotropic model integration. To facilitate such a determination of BEP speed, a TC tangential wind distribution model based on angular momentum conservation is developed, and techniques for adjusting parameters of this model to be consistent with the wind distribution of the actual TC are provided.

A key aspect of the TC-Environment conceptual model knowledge base is that various combinations of Environment structure and TC structure may initiate certain TC-Environment transformations, which include:

- Beta Effect Propagation (BEP);
- Vertical Wind Shear (VWS);
- Ridge Modification by Large TC (RMT);
- Monsoon Gyre-TC Interaction (MTI); and
- Multiple Tropical Cyclone Interactions (TCIs).

The TCIs transformation model represents a significant departure from the conventional practice of attributing most centroid-relative rotations between two TCs as arising from the Fujiwhara effect, i.e., the mutual advection by the cyclonic circulations of the two TCs. Rather, a set of six distinct modes of binary TC interactions, which include both direct and indirect influences, are defined and illustrated via case studies (Carr and Elsberry 1994).

The result of the TC-Environment transformations is to cause various motion-affecting alterations to the Environment Structure and/or TC Structure combination that initiated the transformation. The impact on TC Structure is a rather straightforward change in Intensity (which affects steering level) and Size. In terms of the effect on Environmental Structure, the transformations function as "traditional mechanisms" that cause the environment of the TC to transition either from one Synoptic Region to another within a persistent Synoptic Pattern, or from one Pattern/Region combination to another. It is this second type of transition that usually results in late changes in TC track that may not be well forecast by numerical models or other objective track forecast techniques.

7.8 DEVELOPMENT OF A HIGH CONFIDENCE TROPICAL CYCLONE INTENSITY DATA BASE

C. P. Guard and M. A. Lander
University of Guam
Mangilao, Guam

A close investigation of the tropical cyclone intensity data bases of JTWC reveals that the quality of the data bases may not be sufficient for tropical cyclone intensity studies and validation. A "high confidence" intensity data base is being developed that reevaluates the raw data, makes changes to the intensity data base where warranted, then places a confidence level on the intensity depending on the quality of the raw data on which the near-surface intensity was based. Weighting values are developed for the confidence levels. An important input to the reevaluation is the maximum intensity from land falling tropical cyclones. These data are not routinely available to warning centers out-

side the country of occurrence. In conjunction with this initiative is a proposal to the WMO for the sharing of landfall data among tropical cyclone warning centers and a proposal to include the peak gust and its time of occurrence into the synoptic code.

7.9 AN INVESTIGATION OF THE RELATIONSHIPS BETWEEN CYCLONIC CELLS IN THE TUTT AND THE INTENSITY CHANGE OF TROPICAL CYCLONES.

C. P. Guard
University of Guam
Mangilao, Guam

Tropical cyclone intensity change is correlated with the relative proximity of the TUTT and cyclonic cells within it. Synoptic models are developed that indicate the most favorable patterns for tropical cyclone intensification, rapid intensification, and explosive deepening. Favorable locations, movements, and separation distances are identified. Thumb rules for forecasters are developed from the synoptic models, and the synoptic models will also be shared with modelers to try to better understand the dynamics that occur during the identified relationships between the tropical cyclone and the TUTT.

7.10 THE NATURAL VARIATION IN THE RELATIONSHIP BETWEEN MAXIMUM WIND AND MINIMUM CENTRAL PRESSURE IN TROPICAL CYCLONES.

M. A. Lander and C. P. Guard
University of Guam
Mangilao, Guam

A three-year investigation of the relationships between maximum wind and minimum central pressure in tropical cyclones is culminating in the development of a set of universal wind-pressure relationships that are basin independent. The study reveals the physical parameters that contribute to the relationship, and weights the importance of the various parameters. The radius of maximum winds (RMW) (basically eye size) and the rate of "fall-off" of the winds between the RMW and the outside of the circulation (basically storm size) are found to be the most important. The natural variability between observed maximum wind speed and minimum central pressure is explained in terms of the identified parameters.

7.11 A STUDY OF THE CHARACTERISTICS OF VERY SMALL (MIDGET) TROPICAL CYCLONES.

C. P. Guard and M. A. Lander
University of Guam
Mangilao, Guam

A special case of the study of the relationship between maximum wind and minimum central pressure in tropical cyclones addresses the very small or "midget" tropical cyclone in which the central pressure is frequently observed to be 20 hPa higher for a specific maximum wind than it is in larger tropical cyclones. The study identifies the unique characteristics of these cyclones and presents some proposed mechanisms for their development and rapid intensification at minimal tropical storm intensity. A basin-independent wind-pressure relationship is derived for midget tropical cyclones.

7.12 A SAFFIR-SIMPSON-LIKE HURRICANE SCALE FOR THE TROPICAL WESTERN PACIFIC.

C. P. Guard and M. A. Lander
University of Guam
Mangilao, Guam

The Saffir-Simpson Hurricane Scale (Simpson 1974) has been adapted for use in the tropical western Pacific. After five years of modification and testing, the scale has been fine-tuned and implemented for use in the western North Pacific. The Scale incorporates the basic Saffir-Simpson Scale, but modifies it for tropical building materials, building practices, considers the detrimental effects of termites, wood rot, and sea salt spray, integrates the damage to tropical vegetation and agricultural products, and factors in the affects of coral reefs on storm surge and inundation. The Scale should be applicable in the global tropics.

7.13 NOGAPS TROPICAL CYCLONE FORECAST PERFORMANCE

J.S. Goerss
Naval Research Laboratory
Monterey, California

The tropical cyclone forecast performance of the NOGAPS T159 global spectral model in the North Pacific for July-September 1994 was examined and compared with that for the NOGAPS T79 forecast model. The impact of the assimilation of synthetic tropical cyclone observations upon the NOGAPS T79 analyses and forecasts for the North Pacific was determined along with the impact of incorporating storm motion information into the synthetic observations. The results of this research were presented at the 1995 U.S. PACOM Tropical Cyclone Conference and appear in the conference proceeding report. A paper on the impact of the assimilation of the synthetic observations was presented at the 21st Conference on Hurricanes and Tropical Meteorology. The incorporation of storm motion information into the synthetic tropical cyclone observations was made operational at FNMOC in March 1995.

BIBLIOGRAPHY

Atkinson, G. D. and C. R. Holliday, 1977: Tropical cyclone minimum sea-level pressure and maximum sustained wind relationship for the western North Pacific. *Mon.Wea. Rev.*, **105**, pp 421-427 (also Fleet Weather Central/JTWC Technical Note 75-1).

Brand, S., 1970: Interaction of binary tropical cyclones in the western North Pacific Ocean. *J. Appl. Meteor.*, **9**, pp 433-441.

Brand, S., 1972: Very Large and Very Small Typhoons of the Western North Pacific Ocean. *J. Meteor. Soc. Japan*, **50**, pp 332-341.

Carr, L.E. , and R.L. Elsberry, 1994: Monsoonal interactions leading to sudden tropical cyclone track changes. *Mon. Wea. Rev.*, **123**, pp 265-289.

Carr, L.E., and R.L. Elsberry, 1994: Systematic and integrated approach to tropical cyclone track forecasting, Part I: description of basic approach. Naval Postgraduate School publication NPS-MR-002. Naval Postgraduate School, Monterey, CA 93943. 65 pp. plus figs. and append.

Climate Analysis Center, 1994: Climate Diagnostics Bulletin. Dept of Commerce, Washington, D.C. month by bulletins.

Diercks, J. M., R. C. Weir and M. K. Kopper, 1982: Forecast Verification and Reconnaissance Data for Southern Hemisphere Tropical Cyclones (July 1980 through June 1982). NOCC/JTWC Technical Note 82-1, 77 pp.

Dong, K. and C. J. Neumann, 1983: On the relative motion of binary tropical cyclones. *Mon. Wea. Rev.*, **111**, pp 945-953.

Dunnavan, G. M., 1981: Forecasting Intense Tropical Cyclones Using 700 mb Equivalent Potential Temperature and Central Sea-Level Pressure. NOCC/JTWC Technical Note 81-1, 12 pp.

Dvorak, V. F., 1975: TC Intensity Analysis and Forecasting from Satellite Imagery. *Mon. Wea. Rev.*, **103**, pp 420-430.

Dvorak, V. F., 1984: Tropical Cyclone Intensity Analysis Using Satellite Data. NOAA Technical Report NESDIS 11, 46 pp.

Fujiwhara, S., 1921: The natural tendency towards symmetry, etc. *Quart. J. Roy. Meteor. Soc.*, **47**, pp 287-293.

Fujiwhara, S., 1923: On the growth and decay of vortical systems. **Quart. J. Roy. Meteor. Soc., 49**, pp 75-104.

Fujiwhara, S., 1931: Short note on the behavior of two vortices. *Proc. Phys. Math. Soc. Japan*, Ser. 3, 13, pp 106-110.

Glass, M., and G.W. Felde, 1990: Tropical storm structure analysis using SSM/I and OLS data. 5th Intl. Conf. on Interactive and Info. Processing Systems for Meteor., Oceanogr. and Hydrol., Aneheim, CA, Amer. Meteor. Soc., 432-437.

Gray, W.M., 1968: Global view of the origin of tropical disturbances and storms. *Mon. Wea. Rev.*, **96**, pp 669-700.

Guard, C.P., 1983: A Study of Western North Pacific Tropical Storms and Typhoons that Intensify after Recurvature. First Weather Wing Technical Note-83/002, 28 pp.

Harr, P.A., and R.L. Elsberry, 1991: Tropical cyclone track characteristics as a function of large-scale circulation anomalies. *Mon. Wea. Rev.*, **119**, pp 1448-1468.

Harr, P.A., and R.L. Elsberry, 1995: Large-scale circulation variability over the tropical western North Pacific. Part I: Spatial patterns and tropical cyclone characteristics. *Mon. Wea. Rev.*, **123**, pp 1225-1246.

Hebert, P. H. and K. O. Poteat, 1975: A Satellite Classification Technique for Subtropical Cyclones. NOAA Technical Memorandum NWS SR-83, 25 pp.

Holland, G. J., 1980: An analytical model of wind and pressure profiles in hurricanes. *Mon.Wea. Rev.*, **108**, pp 1212-1218.

Holland, G.J., 1987: [Tropical cyclone] mature structure and structure change. A Global View of Tropical Cyclones. R.L. Elsberry, Ed. (Limited edition publication sponsored by the U.S. Navy, Office of Naval Research.)

Holliday, C. R. and A. H. Thompson, 1979: Climatological characteristics of rapidly intensifying typhoons. *Mon.Wea. Rev.*, **107**, pp 1022-1034.

Japan Meteorological Agency, 1976: Manual for Typhoons. (English Version), Japan Meteorological Agency, 1-3-4 Ote-machi, Chiyoda-ku, Tokyo, 277 pp.

Keen, R.A. 1982: The role of cross-equatorial tropical cyclone pairs in the Southern Oscillation. *Mon.Wea. Rev.*, **110**, pp 1405-1416.

Kepert, J.D., 1993: Research rapporteur report on oceanography and air-sea interaction. Annex to Topic Rapporteur Reports of the Third WMO/ICSU International Workshop on Tropical Cyclones (JTWC-III), Huatulco, Santa Cruz, Mexico, 22 November -1 December 1993. WMO/TD No. 573. Secretariat of the WMO, Geneva, Switzerland.

Kurihara, Y., 1992: Surface conditions in tropical cyclone models. In Modeling Severe Weather: Papers presented at the Fourth BMRC Modeling Workshop.Bureau of Meteorology Research Centre, Melbourne, Australia.

Lander, M. A., 1990: Evolution of the cloud pattern during the formation of tropical cyclone twins symmetrical with respect to the equator. *Mon. Wea. Rev.*, **118**, pp 1194-1202.

Lander, M.A., and G.J. Holland, 1993: On the interaction of tropical-cyclone scale vortices. I: Observations. *Quart. J. Roy. Meteor. Soc.*, **119**, pp 1347 - 1361.

Lander, M.A., 1994a: Description of a monsoon gyre and its effects on the tropical cyclones in the western North Pacific during August 1991. *Weather and Forecasting*, **9**, pp 640-654.

Lander, M.A., 1994b: An exploration of the relationships between tropical storm formation in the Western North Pacific and ENSO, *Mon. Wea. Rev.*, **122**, pp 636-651.

Lander, M.A., 1995a: Specific tropical cyclone track types and unusual tropical cyclone motions associated with a reverse-oriented monsoon trough in the western North Pacific. (Submitted to Weather and Forecasting.)

Lander, M.A., 1995b: The merger of two tropical cyclones. *Mon. Wea. Rev.*, (July issue).

Luther, D.S., D.E. Harrison and R.A. Knox, 1983: Zonal winds in the Central Equatorial Pacific and El Nino. *Science*, **222**, pp 327-330.

Matsumoto, C. R., 1984: A statistical method for one- to three-day tropical cyclone track prediction. Colorado State University Department of Atmospheric Science, Paper 379, 201 pp.

Merrill, R.T., 1984: A comparison of large and small tropical cyclones. *Mon. Wea. Rev.*, **112**, pp 1408-1418.

Mundell, D.B., 1990: Prediction of Tropical Cyclone Rapid Intensification Events. Thesis for fulfillment of Master's degree submitted to Colorado State University, 186 pp.

OFCM, 1993: National Hurricane Operations Plan, U.S. Dept. of Commerce, Washington, D.C., p E-1.

Price, J.F., 1981: Upper ocean response to a hurricane. *J. Phys. Oceanogr.*, **11**, 153-175.

Ramage, C.S., 1986: El Nino. *Scientific American*, June Issue, pp 77-84

Sadler, J.C., 1967: The tropical upper tropospheric trough as a secondary source of typhoons and a primary source of trade wind disturbances. Final Report, contract No. AF 19(628)-3860, HIG Report 67-12, Hawaii Institute of Geophysics, University of Hawaii, Honolulu, HI, 44 pp.

Sadler, J.C., 1976: A role of the tropical upper tropospheric trough in early season typhoon development. *Mon. Wea. Rev.*, **104**, pp 1266-1278.

Sadler, J.C., M.A. Lander, A.M. Hori, and L.K. Oda, 1987: Tropical marine climatic Atlas, Vol II, Pacific Ocean. UHMET 87-02, University of Hawaii, Department of Meteorology, 14 pp.

Sandgathe, S. A., 1987: Opportunities for tropical cyclone motion research in the Northwest Pacific region. Technical Report NPS 63-87-006, Naval Postgraduate School, Monterey, CA 93943, 36 pp.

Shoemaker, D.N., 1991: Characteristics of Tropical Cyclones Affecting the Philippine Islands. NOCC/JTWC Technical Note 91-01, 35 pp.

Simpson, R.H., 1974: The hurricane disaster potential scale. *Weatherwise*, **27**, pp 169-186.

Weatherford, C.L. and W.M. Gray, 1985: Typhoon Structural Variability. Colorado State University Department of Atmospheric Science, Paper No. 391, 77 pp.

Weir, R. C., 1982: Predicting the Acceleration of Northward-moving Tropical Cyclones using Upper-Tropospheric Winds. NOCC/JTWC Technical Note 82-2, 40 pp.

Willoughby, H.E., J.A. Clos, and M.G., 1982: Concentric eye walls, secondary wind maxima, and the evolution of teh hurricane vortex. *J. Atmos. Sci.*, **39**, pp 395-411.

Willoughby, H.E., 1990: Temporal changes in the primary circulation in tropical cyclones. *J. Atmos. Sci.*, **47**, pp 242-264.

Wirfel, W. P. and S. A. Sandgathe, 1986: Forecast Verification and Reconnaissance Data for Southern Hemisphere Tropical Cyclones (July 1982 through June 1984). NOCC/JTWC Technical Note 86-1, 102 pp.

Xu, Y. and C. J. Neumann, 1985: A Statistical Model for the Prediction of Western North Pacific Tropical Cyclone Motion. NOAA Technical Memorandum NWS NHC 28, 30 pp.

APPENDIX A
DEFINITIONS

BEST TRACK - A subjectively smoothed path, versus a precise and very erratic fix-to-fix path, used to represent tropical cyclone movement, and based on an assessment of all available data.

CENTER - The vertical axis or core of a tropical cyclone. Usually determined by cloud vorticity patterns, wind and/or pressure distribution.

EPHEMERIS - Position of a body (satellite) in space as a function of time; used for gridding satellite imagery. Since ephemeris gridding is based solely on the predicted position of the satellite, it is susceptible to errors from vehicle wobble, orbital eccentricity, the oblateness of the Earth, and variation in vehicle speed.

EXPLOSIVE DEEPENING - A decrease in the minimum sea-level pressure of a tropical cyclone of 2.5 mb/hr for at least 12 hours or 5 mb/hr for at least six hours (Dunnavan, 1981).

EXTRATROPICAL - A term used in warnings and tropical summaries to indicate that a cyclone has lost its "tropical" characteristics. The term implies both poleward displacement from the tropics and the conversion of the cyclone's primary energy source from the release of latent heat of condensation to baroclinic processes. It is important to note that cyclones can become extratropical and still maintain winds of typhoon or storm force.

EYE - The central area of a tropical cyclone when it is more than half surrounded by wall cloud.

FUJIWHARA EFFECT - A binary interaction where tropical cyclones within about 750 nm (1390 km) of each other begin to rotate about a common midpoint (Brand, 1970; Dong and Neumann, 1983).

INTENSITY - The maximum sustained 1-minute mean surface wind speed, typically within one degree of the center of a tropical cyclone.

MAXIMUM SUSTAINED WIND - The highest surface wind speed averaged over a 1-minute period of time. (Peak gusts over water average 20 to 25 percent higher than sustained winds.)

MEI-YU FRONT - The Term "mei-yu" is the Chinese expression for "plum rains". The mei-yu front is a persistant east-west zone of disturbed weather during spring which is quasi - stationary and stretches from the east China coast, across Taiwan, and eastward into the Pacific south of Japan.

MONSOON DEPRESSION - A tropical cyclonic vortex characterized by: 1) its large size, the outer-most closed isobar may have a diameter on the order of 600 nm (1000 km); 2) a loosely organized cluster of deep convective elements; 3) a low-level wind distribution which features a 100-nm (200-km) diameter light-wind core which may be partially surrounded by a band of gales; and, 4) a lack of a distinct cloud system center. Note: most monsoon depressions which form in the western North Pacific eventually acquire persistent central convection and accelerated core winds marking its transition into a conventional tropical cyclone.

MONSOON GYRE - A mode of the summer monsoon circulation of the western North Pacific characterized by: 1) a very large nearly circular low-level cyclonic vortex that has an

outer-most closed isobar with diameter on the order of 1200 nm (2500 km); 2) a cloud band rimming the southern through eastern periphery of the vortex/surface low; 3) a relatively long (two week) life span - initially, a subsident regime exists in its core and western and northwestern quadrants with light winds and scattered low cumulus clouds; later, the area within the outer closed isobar may fill with deep convective cloud and become a monsoon depression or tropical cyclone; and, 4) the large vortex cannot be the result of the expanding wind field of a preexisting monsoon depression or tropical cyclone. Note: a series of small or very small tropical cyclones may emerge from the "head" or leading edge of the peripheral cloud band of a monsoon gyre (Lander, 1993).

RAPID DEEPENING - A decrease in the minimum sea-level pressure of a tropical cyclone of 1.75 mb/hr or 42 mb for 24-hours (Holliday and Thompson, 1979).

RECURVATURE - The turning of a tropical cyclone from an initial path toward the west and poleward to east and poleward, after moving poleward of the mid-tropospheric subtropical ridge axis.

REVERSE-ORIENTED MONSOON TROUGH - The distinguishing characteristics of a reverse-oriented monsoon trough are a SW-NE (i.e., reverse orientation of the trough axis with respect to the normal NW-SE orientation of the trough axis, and the penetration of the trough axis into subtropical areas normally the province of easterly flow.

SIGNIFICANT TROPICAL CYCLONE - A tropical cyclone becomes "significant" with the issuance of the first numbered warning by the responsible warning agency.

SIZE - The areal extent of a tropical cyclone, usually measured radially outward from the center to the outer-most closed isobar. Based on an average radius of the outer-most closed isobar, size categories in degrees of latitude follow: 1° to 2° = very small, 3° = small, 4° to 5° = medium (average), 6° to 9° = large, and 10° or greater = very large (Brand, 1972 and a modification of Merrill, 1982).

STRENGTH - The average wind speed of the surrounding low-level wind flow, usually measured within one to three degrees of the center of a tropical cyclone (Weatherford and Gray, 1985).

SUBTROPICAL CYCLONE - A low pressure system that forms over the ocean in the subtropics and has some characteristics of a tropical circulation, but not a central dense overcast. Although of upper cold low or low-level baroclinic origins, the system can transition to a tropical cyclone.

SUPER TYPHOON - A typhoon with maximum sustained 1-minute mean surface winds of 130 kt (67 m/sec) or greater.

TROPICAL CYCLONE - A non-frontal, migratory low-pressure system, usually of synoptic scale, originating over tropical or subtropical waters and having a definite organized circulation.

TROPICAL DEPRESSION - A tropical cyclone with maximum sustained 1-minute mean surface winds of 33 kt (17 m/sec) or less.

TROPICAL DISTURBANCE - A discrete system of apparently organized convection, generally 100 to 300 nm (185 to 555 km) in diameter, originating in the tropics or subtropics, having a non-frontal, migratory character and having maintained its identity for 12- to 24-hours. The system may or may not be associated with a detectable perturbation of the low-level wind or pressure field. It is the basic

generic designation which, in successive stages of development, may be classified as a tropical depression, tropical storm, typhoon or super typhoon.

TROPICAL STORM - A tropical cyclone with maximum 1-minute mean sustained surface winds in the range of 34 to 63 kt (17 to 32 m/sec), inclusive.

TROPICAL UPPER-TROPOSPHERIC TROUGH (TUTT) - A dominant climatological system and a daily upper-level synoptic feature of the summer season, over the tropical North Atlantic, North Pacific and South Pacific Oceans (Sadler, 1979). Cold core lows in the TUTT are referred to as cells, or TUTT cells.

TYPHOON (HURRICANE) - A tropical cyclone with maximum sustained 1-minute mean surface winds of 64 to 129 kt (33 to 66 m/sec). West of 180° E longitude they are called typhoons and east of 180° E longitude hurricanes.

WALL CLOUD - An organized band of deep cumuliform clouds that immediately surrounds the central area of a tropical cyclone. The wall cloud may entirely enclose or partially surround the center.

WESTERLY WIND BURST - A short-duration low-level westerly wind event along and near the equator in the western Pacific Ocean (and sometimes in the Indian Ocean) (Luther et al. 1983). Typically, a westerly wind burst (WWB) lasts several days and has westerly winds of at least 10 kt (5 m/sec) (Keen 1988). Most WWBs occur during the monsoon transition months of April-May, and November-December. They show some relationship to the ENSO phenomenon (Luther et al. 1983; Ramage 1986). Some WWBs are even more energetic, with wind speeds of 30 kt (15 m/sec) observed during well-developed systems. These intense WWBs are associated with a large cluster of deep-convective cloud along the equator. An intense WWB is a necessary precursor to the formation of tropical cyclone twins symmetrical with respect to the equator (Keen 1982; Lander 1990).

APPENDIX B

NAMES FOR TROPICAL CYCLONES IN THE WESTERN NORTH PACIFIC OCEAN AND SOUTH CHINA SEA
(Through 31 December 1995)

Column 1		Column 2		Column 3		Column 4	
ANGELA	*AN-gel-ah*	**ABE**	*ABE*	**AMY**	*A-mee*	**AXEL**	*AX-ell*
BRIAN	*BRY-an*	**BECKY**	*BECK-ee*	**BRENDAN**	*BREN-dan*	**BOBBIE**	*BOB-ee*
COLLEEN	*COL-leen*	**CECIL**	*CEE-cil*	**CAITLIN**	*KATE-lin*	**CHUCK**	*CHUCK*
DAN	*DAN*	**DOT**	*DOT*	**DOUG**	*DUG*	**DEANNA**	*dee-AN-na*
ELSIE	*ELL-see*	**ED**	*ED*	**ELLIE**	*ELL-ee*	**ELI**	*EE-lye*
FORREST	*FOR-rest*	**FLO**	*FLO*	**FRED**	*FRED*	**FAYE**	*FAY*
GAY	*GAY*	**GENE**	*GEEN*	**GLADYS**	*GLAD-iss*	**GARY**	*GAR-ee*
HUNT	*HUNT*	**HATTIE**	*HAT-ee*	**HARRY**	*HAR-ee*	**HELEN**	*HELL-en*
IRMA	*IR-ma*	**IRA**	*EYE-ra*	**IVY**	*EYE-vee*	**IRVING**	*ER-ving*
JACK	*JACK*	**JEANA**	*JEAN-ah*	**JOEL**	*JOLE*	**JANIS**	*JAN-iss*
KORYN	*ko-RIN*	**KYLE**	*KYE-ell*	**KINNA**	*KIN-na*	**KENT**	*KENT*
LEWIS	*LOU-iss*	**LOLA**	*LOW-lah*	**LUKE**	*LUKE*	**LOIS**	*LOW-iss*
MARIAN	*MAH-rian*	**MANNY***	*MAN-ee*	**MELISSA***	*meh-LISS-ah*	**MARK**	*MARK*
NATHAN	*NAY-than*	**NELL**	*NELL*	**NAT**	*NAT*	**NINA**	*NEE-nah*
OFELIA	*oh-FEEL-ya*	**OWEN**	*OH-en*	**ORCHID**	*OR-kid*	**OSCAR***	*OS-car*
PERCY	*PURR-see*	**PAGE**	*PAGE*	**PAT**	*PAT*	**POLLY**	*PA-lee*
ROBYN	*ROB-in*	**RUSS**	*RUSS*	**RUTH**	*RUTH*	**RYAN**	*RYE-an*
STEVE	*STEEV*	**SHARON**	*SHAR-on*	**SETH**	*SETH*	**SIBYL**	*SIB-ill*
TASHA	*TA-sha*	**TIM**	*TIM*	**TERESA***	*teh-REE-sah*	**TED**	*TED*
VERNON	*VER-non*	**VANESSA**	*vah-NES-ah*	**VERNE**	*VERN*	**VAL**	*VAL*
WINONA	*wi-NO-nah*	**WALT**	*WALT*	**WILDA**	*WILL-dah*	**WARD**	*WARD*
YANCY	*YAN-see*	**YUNYA**	*YUNE-yah*	**YURI**	*YOUR-ee*	**YVETTE**	*ee-VET*
ZOLA	*ZO-lah*	**ZEKE**	*ZEEK*	**ZELDA**	*ZELL-dah*	**ZACK**	*ZACK*

---

* Name changes: MANNY replaced MIKE in 1991; MELISSA replaced MIREILLE, TERESA replaced THELMA in 1992, and OSCAR replaced OMAR in 1993.

NOTE 1: Names are assigned in rotation and alphabetically. When the last name in Column 4 (ZACK) has been used, the sequence will begin again with the first name in Column 1 (ANGELA).

NOTE 2: Pronunciation guide for names is italicized.

SOURCE: CINCPACINST 3140.1V

APPENDIX B
(Continued)

NAMES FOR TROPICAL CYCLONES IN THE WESTERN NORTH PACIFIC OCEAN AND SOUTH CHINA SEA
(Effective 01 January 1996)

Column 1		Column 2		Column 3		Column 4	
ANN	*AN*	**ABEL**	*A-bel*	**AMBER**	*AM-ber*	**ALEX**	*AL-x*
BART	*BART*	**BETH**	*BETH*	**BING**	*BING*	**BABS**	*BABS*
CAM	*KAM*	**CARLO**	*KAR-lo*	**CASS**	*KASS*	**CHIP**	*CHIP*
DAN	*DAN*	**DALE**	*DAY-l*	**DAVID**	*DAY-vid*	**DAWN**	*DAWN*
EVE	*EEV*	**ERNIE**	*ER-nee*	**ELLA**	*EL-lah*	**ELVIS**	*EL-vis*
FRANKIE	*FRANK-ee*	**FERN**	*FERN*	**FRITZ**	*FRITZ*	**FAITH**	*FAITH*
GLORIA	*GLOR-ee-uh*	**GREG**	*GREG*	**GINGER**	*JIN-jer*	**GIL**	*GIL*
HERB	*HERB*	**HANNAH**	*HAN-ah*	**HANK**	*HANK*	**HILDA**	*HIL-dah*
IAN	*EE-an*	**ISA**	*EE-sah*	**IVAN**	*I-van*	**IRIS**	*I-ris*
JOY	*JOY*	**JIMMY**	*JIM-ee*	**JOAN**	*JOAN*	**JACOB**	*JAY-kob*
KIRK	*KIRK*	**KELLY**	*KEL-ee*	**KEITH**	*KEETH*	**KATE**	*KATE*
LISA	*LEE-sah*	**LEVI**	*LEE-vi*	**LINDA**	*LIN-dah*	**LEO**	*LEE-o*
MARTY	*MAR-tee*	**MARIE**	*ma-REE*	**MORT**	*MORT*	**MAGGIE**	*MAG-ee*
NIKI	*NI-kee*	**NESTOR**	*NES-tor*	**NICHOLE**	*nik-KOL*	**NEIL**	*NEEL*
ORSON	*OR-son*	**OPAL**	*O-pel*	**OTTO**	*OT-tow*	**OLGA**	*OL-gah*
PIPER	*PI-per*	**PETER**	*PEE-ter*	**PENNY**	*PEN-ee*	**PAUL**	*PAUL*
RICK	*RICK*	**ROSIE**	*RO-zee*	**REX**	*REX*	**RACHEL**	*RAY-chel*
SALLY	*SAL-lee*	**SCOTT**	*SCOTT*	**STELLA**	*STEL-lah*	**SAM**	*SAM*
TOM	*TOM*	**TINA**	*TEE-nah*	**TODD**	*TODD*	**TANYA**	*TAHN-yah*
VIOLET	*VI-uh-let*	**VICTOR**	*vik-TOR*	**VICKI**	*VIK-ee*	**VIRGIL**	*VER-jil*
WILLIE	*WIL-lee*	**WINNIE**	*WIN-ee*	**WALDO**	*WAL-doh*	**WENDY**	*WEN-dee*
YATES	*YATES*	**YULE**	*YOU-lee*	**YANNI**	*YAN-nee*	**YORK**	*YORK*
ZANE	*ZANE*	**ZITA**	*ZEE-tah*	**ZEB**	*ZEB*	**ZIA**	*ZEE-uh*

NOTE 1: Assign names in rotation, alphabetically, starting with (ANN) for first tropical cyclone of 1996. When the last name in Column 4 (ZIA) has been used, the sequence will begin again with the first name in Column 1 (ANN).

NOTE 2: Pronunciation guide for names is italicized.

SOURCE: CINCPACINST 3140.1W (Draft)

APPENDIX C
CONTRACTIONS

A-track	Along-track
AB	Air Base
ABW	Air Base Wing
ABIO	Significant Tropical Weather Advisory for the Indian Ocean
ABPW	Significant Tropical Weather Advisory for the Western Pacific Ocean
ACCS	Air Control Center Squadron
ACFT	Aircraft
ADP	Automated Data Processing
AFB	Air Force Base
AFGWC	Air Force Global Weather Central
AIREP	Aircraft (Weather) Report
AJTWC	Alternate Joint Typhoon Warning Center
AMOS	Automatic Meteorological Observing Station
AOR	Area of Responsibility
ARC	Automated Remote Collection (system)
ARGOS	(International Service for Drifting Buoys)
ATCF	Automated Tropical Cyclone Forecast (system)
AUTODIN	Automated Digital Network
AWDS	Automated Weather Distribution System
AWN	Automated Weather Network
BLND	Blended (Hybrid Aid)
CDO	Central Dense Overcast
CI	Current Intensity
CIV	Civilian
CLD	Cloud
CLIM	Climatology
CLIP or CLIPER	Climatology and Persistence Technique
CM	Centimeter(s)
C-MAN	Coastal-Marine Automated Network
CMOD	Compact Meteorological and Oceanographic Drifter
COMNAVMETOCCOM	Commander Naval Meteorology and Oceanography Command
CPA	Closest Point of Approach
CPHC	Central Pacific Hurricane Center
CSC	Cloud System Center
CSUM	Colorado State University Model
DAVE	Name of a Hybrid Aid
DDN	Defense Data Network
DEG	Degree(s)
DFS	Digital Facsimile System
DMSP	Defense Meteorological Satellite Program
DOD	Department of Defense
DSN	Defense Switched Network
DTG	Date Time Group
EGRR	Bracknell Model
ERS	European Space Agency (ESA) Remote Sensing satellite
FBAM	FNOC Beta and Advection Model
FI	Forecast Intensity (Dvorak)
FLENUMETOCCEN	Fleet Numerical Meteorology andOceanography Center
FT	Foot/Feet
GMS	Geostationary Meteorological Satellite
GMT	Greenwich Mean Time
GOES	Geostationary Operational Environmental Satellite
GSRS	Geostationary Satellite Receiving System
GTS	Global Telecommunications System

hPa	Hectopascal
HPAC	Mean of XTRP and CLIM Techniques (Half Persistence and Climatology)
HF	High Frequency
HR	Hour(s)
HRPT	High Resolution Picture Transmission
ICAO	International Civil Aviation Organization
INIT	Initial
INST	Instruction
IR	Infrared
JTWC	Joint Typhoon Warning Center
JTWC92 or JT92	Statistical-Dynamical Objective Technique
JTYM	Japanese Typhoon Model
KM	Kilometer(s)
KT	Knot(s)
LAN	Local Area Network
LAT	Latitude
LLCC	Low-Level Circulation Center
LONG	Longitude
LUT	Local User Terminal
LVL	Level
M	Meter(s)
MAX	Maximum
MB	Millibar(s)
MBAM	Medium Beta and Advection Model
MCAS	Marine Corps Air Station
MCS	Mesoscale Convective System
MET	Meteorological
MIDDAS	Meteorological Imagery, Data Display, and Analysis System
MIN	Minimum
MINI-MET	Mini-Meteorological
MISTIC	Mission Sensor Tactical Imaging Computer
MM	Millimeter(s)
MOVG	Moving
MSLP	Minimum Sea-level Pressure
NARDAC	Naval Regional Data Automation Center
NAS	Naval Air Station
NASA	National Aeronautics and Space Administration
NCTAMS	Naval Computers and Telecommunications Area Master Station
NEDN	Naval Environmental Data Network
NESDIS	National Environmental Satellite, Data, and information Service
NESN	Naval Environmental Satellite Network
NEXRAD	Next Generation (Doppler Weather) Radar
NHC	National Hurricane Center
NM	Nautical Mile(s)
NMC	National Meteorological Center
NOAA	National Oceanic and Atmospheric Administration
NODDES	Naval Environmental Data Network Oceanographic Data Distribution and Expansion System
NODDS	Navy/NOAA Oceanographic Data Distribution System
NOGAPS or NGPS	Navy Operational Global Atmospheric Prediction System
NAVPACMETOCCEN	Naval Pacific Meteorology and Oceanography Center (Hawaii)
NAVPACMETOCCEN WEST	Naval Pacific Meteorology and Oceanography Center (Guam)
NPS	Naval Postgraduate School
NR	Number
NRL	Naval Research Laboratory
NRPS or NORAPS	Navy Operational Regional Atmospheric Prediction System
NSDS-G	Naval Satellite Display System - Geostationary

NTCC	Naval Telecommunications Center
NWP	Northwest Pacific
NWS	National Weather Service
OBS	Observations
OLS	Operational Linescan System
ONR	Office of Naval Research
OSS	Operations Support Squadron
OTCM	One-Way (Interactive) Tropical Cyclone Model
PACAF	Pacific Air Force
PACMEDS	PacificMeteorological Data System
PACOM	Pacific Command
PCN	Position Code Number
PDN	Public Data Network
PIREP	Pilot Weather Report(s)
RADOB	Radar Observation
RECON	Reconnaissance
RECR	Recurve (Forecast Aid)
ROCI	Radius of outer-most closed isobar
SAT	Satellite
SEC	Second(s)
SDHS	Satellite Data Handling System
SFC	Surface
SGDB	Satellite Global Data Base
SLP	Sea-Level Pressure
SPAWRSYSCOM	Space and Naval Warfare Systems Command
SSM/I	Special Sensor Microwave/Imager
SST	Sea Surface Temperature
STNRY	Stationary
ST	Subtropical
STR	Subtropical Ridge
STRT	Straight (Forecast Aid)
STY	Super Typhoon
TAPT	Typhoon Acceleration Prediction Technique
TC	Tropical Cyclone
TCFA	Tropical Cyclone Formation Alert
TD	Tropical Depression
TDA	Typhoon Duty Assistant
TDO	Typhoon Duty Officer
TESS	Tactical Environmental Support System
TIROS-N	Television Infrared Observational Satellite-Next Generation
TOGA	Tropical Ocean Global Atmosphere
TOVS	TIROS Operational Vertical Sounder
TS	Tropical Storm
TUTT	Tropical Upper-Tropospheric Trough
TY	Typhoon
TYAN	Typhoon Analog (Forecast Aid)
ULCC	Upper-Level Circulation Center
US	United States
USAF	United States Air Force
USCINCPAC	Commander-in-Chief Pacific (AF - Air Force, FLT - Fleet)
USN	United States Navy
VIS	Visual
WESTPAC	Western (North) Pacific
WGTD	Weighted (Hybrid Aid)
WMO	World Meteorological Organization
WNP	Western North Pacific
WRN or WRNG	Warning(s)
WSD	Wind Speed and Direction
X-track	Cross-track
XTRP	Extrapolation
Z	Zulu time (Greenwich Mean Time/Universal Coordinated Time)

APPENDIX D

PAST ANNUAL TROPICAL CYCLONE REPORTS

Copies of the past Annual Tropical Cyclone Reports for DOD agencies or contractors can be obtained through:

Defense Technical Information Center
ATTN:FDAC
Cameron Station
Alexandria, VA 22304-6145

Phone: (703)-274-7633
Fax: (703)-274-9307

Copies for non-DOD agencies or users can be obtained from:

National Technical Information Service
5285 Port Royal Road
Springfield, VA 22161

Phone: (703)-487-4650
Fax: (703)-321-8547

Refer to the following numbers when ordering:

Year	Acquisition Number	Year	Acquisition Number	Year	Acquisition Number
1959	AD 786147	1971	AD 768333	1983	AD A137836
1960	AD 786148	1972	AD 768334	1984	AD A153395
1961	AD 786149	1973	AD 777093	1985	AD A168284
1962	AD 786128	1974	AD 010271	1986	AD A184082
1963	AD 786208	1975	AD A023601	1987	AD A191883
1964	AD 786209	1976	AD A038484	1988	AD A207206
1965	AD 786210	1977	AD A055512	1989	AD A232469
1966	AD 785891	1978	AD A070904	1990	AD A239910
1967	AD 785344	1979	AD A082071	1991	AD A251952
1968	AD 785251	1980	AD A094668	1992	AD A274464
1969	AD 785178	1981	AD A112002	1993	AD A285097
1970	AD 785252	1982	AD A124860		

APPENDIX E
DISTRIBUTION LIST

1 COPY

ACCU-WEATHER, INC.
AEROMET, INC.
ANALYSIS & PROCESSING CENTER, INDONESIA
ARNOLD ASSOCIATES
ASIAN DISASTER PREPAREDNESS CENTER, BANGKOK, THAILAND
ATMOSPHERIC DIV LIBRARY, NEW ZEALAND
BARRETT CONSULTING GROUP
BRUNEI SHELL PETROLEUM CO
CATHOLIC UNIVERSITY OF AMERICA
CAF WEATHER CENTRAL, TAIWAN
CENTRAL MET OBSERVATORY, BEIJING
CENTRAL METEOROLOGICAL OFFICE, SEOUL
CHULALONGKORN UNIVERSITY, BANGKOK
CHUNG CHENG INSTITUTE, TAIWAN
CITY POLYTECHNIC OF HONG KONG
CIUDAD UNIVERSITARIA, MEXICO
CIVIL DEFENSE, CHUUK
CIVIL DEFENSE, MAJURO
CIVIL DEFENSE, PALAU
CIVIL DEFENSE, POHNPEI
CIVIL DEFENSE, SAIPAN
CIVIL DEFENSE, YAP
CINCPACFLT
CNN, ATLANTA, GA
CNO, WASHINGTON, D.C.
COMNAVMETOCCOM
COLORADO STATE UNIVERSITY LIBRARY
COMMONWEALTH NORTHERN MARIANA ISLANDS
COMNAVMAR
COMNAVSURFPAC, SAN DIEGO
COMPATRECFOR
COMPHIBGRU ONE
COMSCWESTPAC GU
COMSEVENTHFLT
COMSPAWARSYSCOM
COMSUBGRU SEVEN
COMTHIRDFLT
COMUSNAVCENT
CONGRESSIONAL INFORMATION SERVICE, MD
DCA GUAM
DET 2, 5WS CAMP HUMPHREYS, KOREA
DET 3, 5WS CAMP CASEY, KOREA
DISASTER CONTROL OFFICE, SAIPAN
ECONOMIC COUNCIL SAIPAN
EDMUNDS COLLEGE SOCIAL SCIENCE DEPT
ENVIRONMENTAL QUALITY PROTECTION BOARD, PALAU
FAIRECONRON ONE
FEDERAL EMERGENCY MANAGEMENT AGENCY, GUAM
FIJI METEOROLOGICAL SERVICE
GEOLOGICAL FLUID DYNAMICS LAB, PRINCETON, NJ
GEOLOGICAL SURVEY, GUAM
GEOPHYSICS LAB/LYS
GIFU METEOROLOGICAL OFFICE, JAPAN
GODDARD SPACE FLIGHT CENTER
GUAM COMMUNITY COLLEGE
GUAM POWER AUTHORITY
GUAM PUBLIC LIBRARY
HORIZON MARINE, INC
HQ AIR COMBAT COMMAND/OSW
HQ AWS
HQ AWS GROUP, ATC & WX WING JASDF, TOKYO
HQ US STRATCOM/J3615
HQ USAF/XOW
INDIA METEOROLOGICAL DEPT.
INDIAN INSTITUTE OF TROPICAL MET
INSTITUO DE GEOFISICA, MEXICO
INTERNATIONAL CENTER FOR DISASTER MITIGATION, TOKYO
JAPAN AIR LINES
JCS ENV SERVICES DIV, PENTAGON
JET PROPULSION LAB, PASADENA
KOREAN METEOROLOGICAL ADMIN FORECAST BUREAU
LEND FOUNDATION
LISD CAMP SPRINGS CENTER, MD
LOS ANGELES PUBLIC LIBRARY
MARATHON OIL CO, TX
MAURITIUS METEOROLOGICAL SERVICE
MASS INST OF TECH
MCAS FUTENMA
MCAS IWAKUNI
MCAS KANEOHE BAY, HI
MERCANTILE AND GENERAL REINSURANCE, AUSTRALIA
METEOROLOGICAL DEPARTMENT, PAKISTAN
METEOROLOGICAL OFFICE, BRACKNELL
METEOROLOGICAL SERVICE, MADAGASCAR
METEOROLOGICAL SERVICE, MAURITIUS
METEOROLOGICAL SERVICE, REUNION
MIL ASST ENV SCI (R & AT / E &LS)
MOBIL OIL GUAM, INC
NASA
NATIONAL CLIMATIC DATA CENTER LIBRARY, ASHEVILLE,NC
NATIONAL METEOROLOGICAL CENTER
NATIONAL METEOROLOGICAL LIBRARY,

BRACKNELL, UK
NATIONAL TAIWAN UNIVERSITY
NATIONAL TECHNICAL INFORMATION SERVICE
NATIONAL WEATHER SERVICE, CHUUK
NATIONAL WEATHER SERVICE, MAJURO
NATIONAL WEATHER SERVICE, PALAU
NATIONAL WEATHER SERVICE, PAPUA NEW GUINEA
NATIONAL WEATHER SERVICE, POHNPEI
NATIONAL WEATHER SERVICE, SAIPAN
NATIONAL WEATHER SERVICE, YAP
NAVAL CIVIL ENG LAB PORT HUENENE, CA
NAVAL POSTGRADUATE SCHOOL LIBRARY
NAVAL RESEARCH LAB
NAVEURMETOCCEN, ROTA
NAVHISTCEN
NAVICECEN, SUITLAND
NAVLANTMETOCCEN, NORFOLK
NAVLANTMETOCDET, ASHEVILLE
NAVLANTMETOCFAC, JACKSONVILLE
NAVOCEANO
NAVPACMETOCDET, ATSUGI
NAVPACMETOCDET, BAHRAIN
NAVPACMETOCDET, KADENA
NAVPACMETOCDET, SASEBO
NAVPACMETOCFAC, SAN DIEGO
NAVPACMETOCFAC, YOKOSUKA
NEW ZEALAND ATMOSPHERIC DIV LIBRARY
NEW ZEALAND INSURANCE
NOAA/ACQUISITION SECTION, ROCKVILLE, MD
NOAA/AOML, HRD, MIAMI, FL
NOAA/HYDROMETEOROLOGY BR, SILVER SPRINGS, MD
NOAA/NESDIS, HONOLULU, HI
NOAA/PMEL, SEATTLE, WA
NOAA ENVIRONMENTAL RESEARCH LAB
NOAA LIBRARY, SEATTLE, WA
NOBEL DENTON
NRL ATMOSPHERIC DIRECTORATE
OCEANROUTES, INC, JOLIMENT, WEST AUSTRALIA
OCEANROUTES, INC, SINGAPORE
OCEANROUTES, INC, SUNNYVALE, CA
OCEANWEATHER, INC
OFFICE OF FEDERAL COORDINATOR MET
OFFICE OF NAVAL RESEARCH
OFFICE OF THE NAVAL DEPUTY, NOAA
ONR
PACIFIC STARS & STRIPES
PACNAVFACENGCOM
PAGASA FORECAST SECTION
PAGASA LIBRARY
PENNSYLVANIA STATE UNIVERSITY
QUEENS COLLEGE, DEPT OF GEOLOGY
REUNION METEOROLOGICAL SERVICE
RUCH WEATHER SERVICE, INC
SAINT LOUIS UNIVERSITY
SAT APPL LAB, NOAA/NESDIS, WASHINGTON, DC
SHANGHAI TYPHOON INSTITUTE
SOUTHSIDE WEATHER SERVICE AUSTRALIA
SRI LANKA METEOROLOGICAL SOCIETY
SRI LIBRARY
TAO PROJECT OFFICE
TEXAS A & M UNIVERSITY
UNIV OF COLORADO, ATMOS SCIENCE
UNIVERSITY OF CHICAGO
UNIVERSITY OF GUAM, BIOLOGY DEPT
UNIVERSITY OF HAWAII LIBRARY
UNIVERSITY OF WASHINGTON
USAFETAC/DN
USCINCPAC
USCINCPAC REP GUAM
USNA (OCEANOGRAPHY DEPT/LIBRARY)
USS AMERICA (CV 66)
USS BELLEAU WOOD (LHA 3)
USS BLUE RIDGE (LCC 19)
USS CARL VINSON (CVN 70)
USS CONSTELLATION (CV 64)
USS EISENHOWER (CVN 69)
USS INDEPENDENCE (CV 62)
USS J. F. KENNEDY (CV 67)
USS KITTY HAWK (CV 63)
USS LINCOLN (CVN 72)
USS NEW ORLEANS (LPH 11)
USS NIMITZ (CVN 68)
USS PELELIU (LHA 5)
USS SARATOGA (CV 60)
USS TARAWA (LHA 1)
USS TRIPOLI (LPH 10)
USS T. ROOSEVELT (CVN 71)
USS WASP (LHD 1)
VANUATU METEOROLOGICAL SERVICE
WORLD DATA CENTER B1, MOSCOW
AFGWC/WFM
607WS WS/CC YONGSAN AIN KOREA
8 0SS/OSW KUNSAN AB, KOREA
15WS HICKAM AFB, HI
18 OSS/OSW KADENA AB, JAPAN
60 OSS/OSW TRAVIS AFB, CA
334 TTS/TTMV KEESLER AFB, MS
374 OSS/DOW YOKOTA AB, JAPAN
375 OG/WXF SCOTT AFB, IL
432 OSS/OSW MISAWA AB, JAPAN
603 ACCENS/WE OSAN AB, KOREA
633 OSS/OSW ANDERSEN AFB, GU
652 ABG/DOW MCCLELLAN AFB, CA
815 WS (AFRES), KEESLER AFB, MS

2 COPIES

AFGWC/WFMP
AWS TECH LIBRARY
BUREAU OF METEOROLOGY, BRISBANE
BUREAU OF METEOROLOGY, DARWIN
BUREAU OF METEOROLOGY LIBRARIAN, MELBOURNE
BUREAU OF METEOROLOGY, PERTH
BUREAU OF PLANNING, GUAM
CIVIL DEFENSE, GUAM
DEFENSE TECHNICAL INFORMATION CENTER
DEPARTMENT OF COMMERCE
ECMWF, BERKSHIRE, UK
ESCAP LIBRARY, BANGKOK
FLENUMETOCCEN MONTEREY
FLORIDA STATE UNIVERSITY
INSTITUTE OF PHYSICS, TAIWAN
MARINERS WEATHER LOG
MET RESEARCH INST LIBRARY, TOKYO
MICRONESIAN RESEARCH CENTER UOG, GUAM
NATIONAL CLIMATIC DATA CENTER
NATIONAL DATA BUOY CENTER
NATIONAL HURRICANE CENTER, MIAMI
NATIONAL WEATHER SERVICE, HONOLULU
NAVPACMETOCCEN
NAVPACMETOCDET DIEGO GARCIA
NAVPACMETOCDET MISAWA
NOAA GUAM
NORA 1570 DALLAS, TX
OKINAWA METEOROLOGY OBSERVATORY
SAT APPL LAB, NOAA/NESDIS, CAMP SPRINGS, MD
TYPHOON COMMITTEE SECRATARIAT, MANILA
UNIVERSITY OF PHILIPPINES
US ARMY, FORT SHAFTER
WORLD DATA CENTER A, NOAA
73 WEATHER GROUP, ROK AF

3 COPIES

BUREAU OF METEOROLOGY, DIRECTOR, MELBOURNE, AUSTRALIA
CENTRAL WEATHER BUREAU, TAIWAN
INDIA METEOROLOGICAL DEPT
INOSHAC, DDGM (WF)
JAPAN METEOROLOGICAL AGENCY
KOREAN METEOROLOGY ADMINISTRATION PLANNING BUREAU
NAVPGSCOL DEPT OF METEOROLOGY
NOAA CORAL GABLES LIBRARY
PACAF/DOW
UNIVERSITY OF HAWAII, METEOROLOGY DEPT
WEATHER CENTRAL, CAF
COLORADO STATE UNIVERSITY
METEOROLOGY DEPT, BANGKOK
R & D UNIT, NHC, MIAMI
ROYAL OBSERVATORY HONG KONG
NRL WEST
NATIONAL WEATHER ASSOCIATION

UNCLASSIFIED
SECURITY CLASSIFICATION OF THIS PAGE

REPORT DOCUMENTATION PAGE

Form Approved
OMB No. 0704-0188

1a. REPORT SECURITY CLASSIFICATION UNCLASSIFIED	1b. RESTRICTIVE MARKINGS
2a. SECURITY CLASSIFICATION AUTHORITY	3. DISTRIBUTION/AVAILABILITY OF REPORT AS IT APPEARS IN THE REPORT/ DISTRIBUTION UNLIMITED
2b. DECLASSIFICATION/DOWNGRADING SCHEDULE	
4. PERFORMING ORGANIZATION REPORT NUMBER(S)	5. MONITORING ORGANIZATION REPORT NUMBER(S)
6a. NAME OF PERFORMING ORGANIZATION NAVPACMETOCCENWEST/JTWC 6b. OFFICE SYMBOL (*If applicable*)	7a. NAME OF MONITORING ORGANIZATION NAVPACMETOCCENWEST/JTWC
6c. ADDRESS (*City, State, and ZIP Code*) PSC 489, BOX 12 FPO AP 96536-0051	7b. ADDRESS (*City, State, and ZIP Code*) PSC 489, BOX 12 FPO AP 96536-0051
8a. NAME OF FUNDING/SPONSORING ORGANIZATION NAVPACMETOCCENWEST/JTWC 8b. OFFICE SYMBOL (*If applicable*)	9. PROCUREMENT INSTRUMENT IDENTIFICATION NUMBER
8c. ADDRESS (*City, State, and ZIP Code*) PSC 489, BOX 12 FPO AP 96536-0051	10. SOURCE OF FUNDING NUMBERS PROGRAM ELEMENT NO. / PROJECT NO. / TASK NO / WORK UNIT ACCESSION NO.
11. TITLE (*Include Security Classification*) 1994 ANNUAL TROPICAL CYCLONE REPORT	
12. PERSONAL AUTHOR(S)	
13a. TYPE OF REPORT ANNUAL 13b. TIME COVERED FROM JAN 94 TO DEC 94	14. DATE OF REPORT (*Year, Month, Day*) 1994 15. PAGE COUNT 337 plus i - vi
16. SUPPLEMENTARY NOTATION	

17. COSATI CODES		
FIELD	GROUP	SUB-GROUP
04	02	

18. SUBJECT TERMS (*Continue on reverse if necessary and identify by block number*)
TROPICAL CYCLONES — TROPICAL STORMS
TROPICAL DEPRESSIONS — TYPHOONS/SUPER TYPHOONS
TROPICAL CYCLONE RESEARCH — METEOROLOGICAL SATELLITES

19. ABSTRACT (*Continue on reverse if necessary and identify by block number*)

ANNUAL PUBLICATION SUMMARIZING TROPICAL CYCLONE ACTIVITY IN THE WESTERN NORTH PACIFIC, BAY OF BENGAL, ARABIAN SEA, WESTERN SOUTH PACIFIC AND SOUTH INDIAN OCEANS. A BEST TRACK IS PROVIDED FOR EACH SIGNIFICANT TROPICAL CYCLONE. A BRIEF NARRATAIVE IS GIVEN FOR ALL TROPICAL CYCLONES IN THE WESTERN NORTH PACIFIC AND NORTH INDIAN OCEANS. ALL FIX DATA USED TO CONSTRUCT THE BEST TRACKS ARE PROVIDED UPON REQUEST ON DISKETTES. FORECAST VERIFICATION DATA AND STATISTICS FOR THE JOINT TYPHOON WARNING CENTER (JTWC) ARE SUBMITTED.

20. DISTRIBUTION/AVAILABILITY OF ABSTRACT ☒ UNCLASSIFIED/UNLIMITED ☒ SAME AS RPT. ☐ DTIC USERS	21. ABSTRACT SECURITY CLASSIFICATION UNCLASSIFIED
22a. NAME OF RESPONSIBLE INDIVIDUAL FRANK H. WELLS	22b. TELEPHONE (*Include Area Code*) (671)-349-5286 22c. OFFICE SYMBOL JTWC

DD Form 1473, JUN 86 *Previous editions are obsolete.*

BLOCK 18 (CONTINUED)

RADAR
AUTOMATIC METEOROLOGICAL OBSERVING STATIONS
SYNOPTIC DATA
TROPICAL CYCLONE INTENSITY
TROPICAL CYCLONE BEST TRACK
TROPICAL CYCLONE FORECASTING
TROPICAL CYCLONE RECONNAISSANCE
TROPICAL CYCLONE STEERING MODELS
OBJECTIVE FORECASTING TECHNIQUES
TROPICAL CYCLONE FIX DATA
MICROWAVE IMAGERY
DRIFTING BUOYS

BACK COVER: From its location on Guam, JTWC monitors an area of responsibility that stretches from 180° east longitude westward across the Western Pacific and Indian Oceans to the eastern coast of Africa.

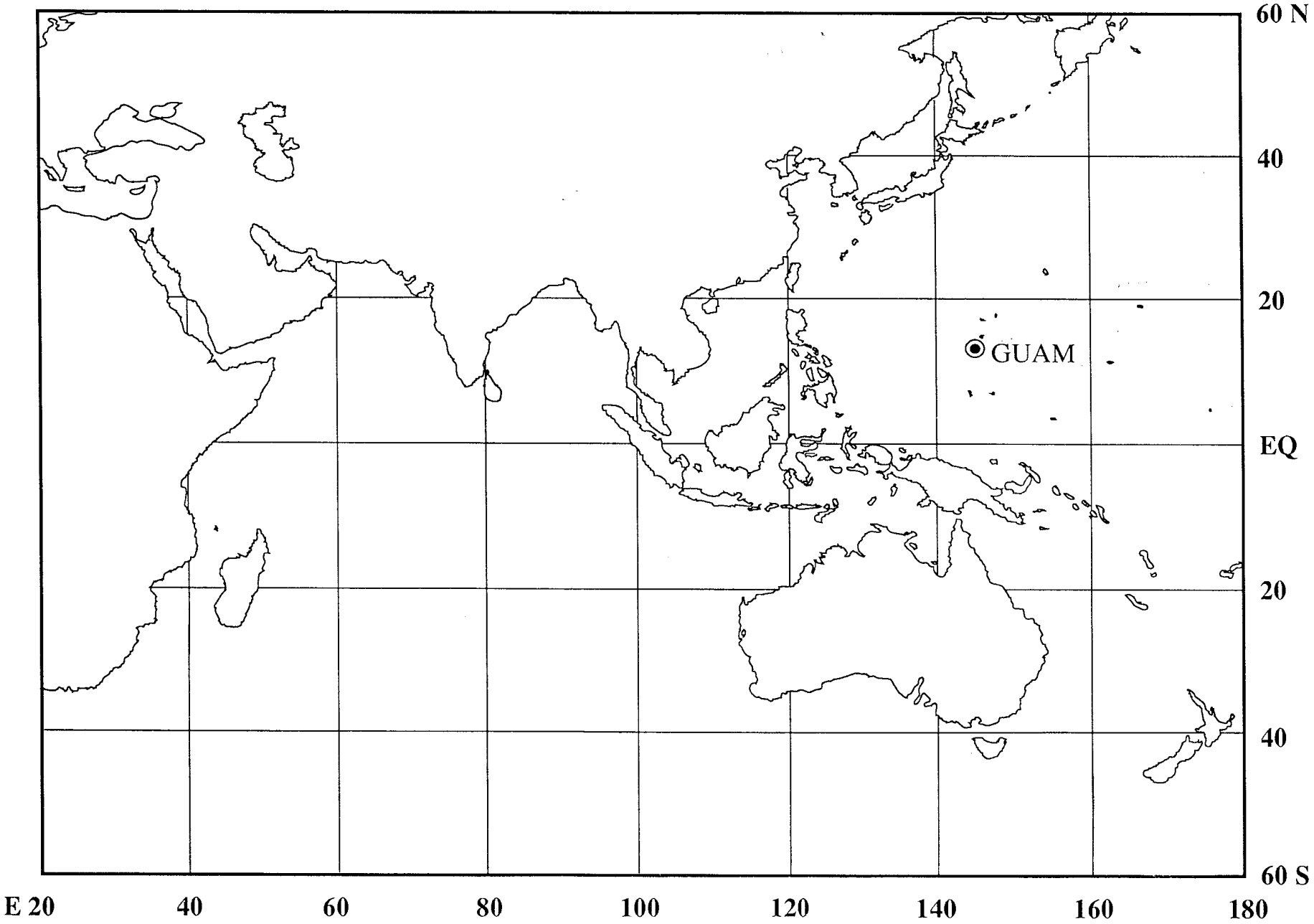
60 N
40
20
GUAM
EQ
20
40
60 S
E 20
40
60
80
100
120
140
160
180